Dissecting humoral immune responses in melanoma and the design of antibody immunotherapy

Karagiannis, Panagiotis

Awarding institution:
King's College London

Dissecting humoral immune responses in melanoma and the design of antibody immunotherapy

A thesis submitted to the Faculty of Medicine of King's College London for the degree of Doctor of Philosophy

by

Panagiotis Karagiannis

at the

St. John's Institute of Dermatology
Division of Genetics and Molecular Medicine
School of Medicine
King's College London

July 2013

Declaration

The work presented is my own and all experiments, except where acknowledged in the text, were performed by myself.

Panagiotis Karagiannis

E-Declaration

Panagiotis Karagiannis

Acknowledgements

It is with immense gratefulness that I acknowledge the endless support, mentorship and help of my primary supervisor Dr. Sophia N. Karagiannis. Her guidance has made it possible for me to understand science and her advice was instrumental to the quality of my work. I would also like to thank my secondary supervisor Professor Frank O. Nestle for his continuous support and my third supervisor Dr. James F. Spicer for advice and guideance. My special thank go to all the member of the Karagiannis Group and Nestle Lab who kept my spirit high, guided me and became friends shapping my life. This moments of unity during endless hours of labratory work will truely be unforgetable for me. Further, I would like to thank Ms Barbara Egger, Dr. Pooja Nakra-Takhar, Dr. Isabel Correa, Ms. Isabella Tosi, Dr. Barry Flutter and Dr. Louise Saul for proof reading my thesis and helping me to identify the mistakes I would have never found. I would also like to thank Mr Philippe Dufour-Feronce for his great assitance with the illustration and Dr. Richard Brunner, who has thaught me how to use Latek. At the end I would like to thank my family.

Panagiotis Karagiannis

ABSTRACT

Antibodies against melanoma antigens have been detected in patients but, despite known regulatory and activatory functions attributed to humoral immunity, the roles of B cells in solid tumours such as melanoma are inadequately understood. Insights into humoral responses and mechanisms of tumour-induced immune escape may inform the design of more effective antibodies.

The aims of this thesis are three-fold: a) to gain insights into regulatory mechanisms in tumour microenvironments that influence antibody expression; b) to examine whether humoral immune responses are associated with clinical outcomes with a view of defining biomarkers for melanoma; and c) to design antibody therapeutic strategies that may be less prone to tumour-induced immunomodulatory mechanisms.

Th2-biased microenvironments favour production of IgG_4 subclass antibodies, mainly through local expression of IL-10. Since IL-10 is expressed locally in melanoma tumours, B cell infiltration, IgG expression, cytokine production and IgG subclass distribution in melanoma tissues (n=57) were investigated and compared to samples from health volunteers (n=26). Consistent with Th2-biased inflammation, $CD22^+$ and $IgG_4{}^+$ B cells infiltrated melanoma lesions. When cultured together ex vivo, B cells secreted increased VEGF and IgG_4, while tumour cells enhanced IL-10 secretion. Two antibodies (IgG_1, IgG_4) against the tumour-associated antigen CSPG4 were engineered to examine the functional significance of IgG_4 subclass. Despite accumulation in tumours, anti-CSPG4 IgG_4, in contrast to anti-CSPG4 IgG_1, did not trigger effector cells to kill tumours *in vitro* and *in vivo*. IgG_4 mediated IgG_1 blockade through the reduction of FcγRI activatory signalling, reducing immune effector

cell capacity, and significantly impairing the potency of IgG_1 in a humanised mouse model of cutaneous melanoma.

Since IgG_4 may impair anti-tumoural immunity, correlations between IgG_4 serum levels and clinical outcomes were studied. Increased IgG_4/IgG_{total} ratios (G4-levels) in melanoma patient sera (n=173) were seen compared to those of healthy volunteers (n=104). G4-levels were predictive of disease progression (ROC Curve analysis z=0.62; p=0.0065). Using 0.034 as a cut-off for G4-levels (Youden Index) higher expression correlated with decreased progression-free survival (median 694 days; hazard ratio 2.559; 95% CI 1.555 to 4.211; p=0.0004) and overall survival (median 879 days; hazard ratio 1.871; 95% CI 1.0.45 to 3.349; P=0.035). These findings suggest that IgG_4 may be further evaluated as a putative biomarker in sera of patients with melanoma.

Tumour immune evasion may be overcome by employing antibodies less prone to Fcγ-mediated blockade, such as those of the IgE class. Two antibodies, anti-CSPG4 IgG_1 and anti-CSPG4 IgE induced significant tumor cell death by differential mechanisms: antibody-dependent cell-mediated phagocytosis and antibody-dependent cell-mediated cytotoxicity, respectively, by human monocytes *in vitro*. Anti-CSPG4 IgE was however superior to IgG_1 ($p<0.05$) in restricting subcutaneous human melanoma tumour growth in a humanized mouse model. IgE efficacy was confirmed in an orthotropic patient tumour in mice populated with autologous patient PBMCs. In summary, this thesis reports a novel pathway of tumour evasion through melanoma favouring production of IgG_4 subclass antibodies; provides evidence that IgG_4 can be considered as a putative biomarker in melanoma and demonstrates a possible strategy to overcome Fcγ-mediated blockade by designing an IgE antibody against a melanoma-associated antigen and demonstrating its superiority to IgG_1.

Contents

1 Introduction

1.1 Cancer and melanoma: facts and figures

1.1.1 Incidence and epidemiology

Cancer is a generic term for over one hundred different diseases, characterised by uncontrolled growth of malignantly transformed cells, invasion of adjacent tissues and metastasis to other organs and sites in the body through the lymphatic system and blood circulation. The incidence of cancer has been steadily increasing in the past decades and reached a rate of 175.5/100000 in 2008. It accounted for 13% of all deaths worldwide in 2008 [WHO, 2013] and for 28% of all deaths in the United Kingdom [CRUK, 2013]. Epidemiological studies have shown that approximately 30% of all cancers are caused by external factors such as the consumption of tobacco, dietary conditions like obesity or infectious agents [Jemal et al., 2010]. Public health campaigns are therefore aimed at influencing population behaviour. For instance, in the case of the skin cancer, melanoma, intensive sun exposure increases the likelihood of its occurrence and therefore campaigns aimed at triggering behavioural adjustment can lead to preventive benefits. While screening for the detection of cancers at early stages has had positive impact on clinical outcomes and reduced mortality,

many forms of cancer including malignant melanoma remain "global killers" as limited effective therapies are available. Projections by the World Health Organisation (WHO) indicate that deaths from cancer will continue to rise reaching an estimated 13.1 million by 2030 [Globocan, 2013]. Malignant melanoma is the most lethal form of skin cancer and despite accounting for only 5% of all types of skin cancers it is responsible for the majority of skin cancer-related deaths [Lens and Dawes, 2004]. Also being the fastest rising cancer in the UK, melanoma is a major therapeutic challenge and effective treatments are urgently needed. This introductory section sets out to give a general overview of cancer and melanoma in discussing melanoma incidence and epidemiology (herein, 1.1.1), elaborating on melanoma pathophysiology, incidence and epidemiology (1.1.2), and ultimately introducing therapeutic concepts (1.1.3) and specific forms of therapy in melanoma (1.1.4).

1.1.2 Melanoma pathophysiology, incidence and epidemiology

1.1.2.1 Pathophysiology

Melanoma develops from melanocytes, skin cells originating from neural crest progenitor cells. Since melanocytes produce melanin they are morphologically highly pigmented. Having a dendritic shape they are found primarily in the basal layer of the epidermis but can also be present in other epithelial sites including the eye. Melanocytic dendrites are used to transport melanin to adjacent keratinocytes. In taking up melanin, keratinocytes protect themselves against DNA damage induced by intensive sun exposure. The main risk factor for neoplastic changes causing the occurrence of melanoma is exposure to UV sunlight. DNA changes triggering malignancy are predominantly caused by UV light exposure in the wavelength of 290–320nm (UVB), which induces the incorporation of dipyrimidine into the DNA. These changes occur in melanoma more frequently in oncogenes such as CDK4, CDKN2a, BRAF, KIT, PTEN, RAS, Rb, p16. Pale skin is a major risk factor for melanoma, but also multiple melanocytic naevi, sun sensitivity, immunosuppression, atypical mole syndrome and giant congenital melaocytic naevi add to the risk. Since only 10% of all melanoma cases have positive family history [Yeh and Bastian, 2009] malignant melanoma appears to be largely an acquired rather than an inherited disease.

1.1.2.2 Incidence and epidemiology

The incidence rates of melanoma are rising constantly. Especially in the Caucasian population, melanoma has risen faster than any other malignancy over the last two decades [Gilbert et al., 2011]. Currently melanoma has an incidence rate of 12.4/100,000 and a mortality rate of 3/100,000 in the UK (worldwide ASR 3.1/10000 and 0.8/10000 respectively) (CRUK, 2012). Higher reported incidence rates most likely reflect better surveillance and early diagnosis programmes. Further improved early detection would permit identifying more patients at earlier disease stages, allowing for surgical intervention and thus translating into enhanced overall survival rates [Verdecchia et al., 2009]. Currently 20% of patients diagnosed with melanoma develop metastatic disease for which prognosis remains extremely poor with a median survival ranging from 8 to 18 months [Balch et al., 2009]. Treatment options for these patients are limited despite recently discovered promising therapies [Chapman et al., 2011, Hodi et al., 2010].

1.1.2.3 Classification and staging

Cutaneous melanoma is classified in a clinical context into four types: 1) lentigomaligna melanomas with a papula or nodular structure; 2) superficial spreading (malignant) melanomas with large flat irregular pigmented lesions that grow laterally before invading the dermis; 3) nodular (malignant) melanomas with rapidly growing nodules that tend to ulcerate and bleed; 4) acral lentigo (malignant) melanomas mainly present at sites of friction in the body, e.g. sole, palm. Similarly, staging of melanoma is determined according to defined criteria (TMN Classification). These parameters include the extent of dermal invasion (Breslow and Clarke scores); the presence of blisters and ulceration on the surface of the skin, the mitotic rate of melanoma cells in lesions and the presence of local or distant metastases. Although a more advanced disease stage correlates with worse prognosis and chances of survival, there have been reported cases of spontaneous melanoma lesion regressions and remissions of systemic disease attributed to immunological responses in patients with melanoma [Balch et al., 2009].

1.1.3 Therapeutics

Conventional therapies for most cancers include surgery, chemotherapeutic and radiation treatments, which kill tumour cells, but also damage healthy cells and tissues. As a result of significant advances in our understanding of cancer cell biology, and through identification of an array of tumour-associated antigens (TAA), and specific melanoma-associated antigens, targeted therapies designed to selectively destroy melanoma cells have been emerging, and such agents include small molecule therapies. Melanoma-associated antigens, which could serve as suitable targets for therapies have been identified and are classified in three groups [Fritsch, 2003]:

- Differentiation antigens that are involved in the differentiation of the cell, cell proliferation or cell migration e.g. gangliosides, tyrosinase, Melan-A/MART-1, gp100, TRP-1, TRP2, High-Molecular Weight Melanoma Associated Antigen (CSPG4).

- Cancer testis antigens are a category of immumogenic cancer antigens with restricted expression to the male germ cells in the testis e.g. NY-ESO1, MAGE-1, MAGE-2, BAGE, GAGE [Scanlan et al., 2002].

- Mutated melanoma antigens: BRAF, NRAS, c-kit, GNA11, GNAQ CDK4, MUM-1

Novel therapies against some of these can differentiate between malignant and non-malignant cells more effectively compared to conventional chemotherapeutic treatments. Some of these drugs build on differences in cell cycle regulation between healthy and malignant cells, whereas others specifically inhibit tumour cell-associated protein kinases, and others interfere with DNA replication that may induce disruption of the cell cycle of tumour cells and trigger apoptosis. An alternative focus of targeted therapies is the disruption of tumour-associated vasculature and inhibition of angiogenesis aiming at depriving tumours of vital blood supply and restricting potential escape routes of metastatic cells. Antibodies offer an important emerging treatment modality that is increasingly used to target different types of cancers. Antibodies have been called "magic bullets" since they are designed to recognise antigens with strong specificity and high affinity, targeting only cells that express these targets and ultimately selectively destroying cancer cells. Antibodies kill tumours through a variety of mechanisms. These include direct effects such as downstream

signalling to block vital growth signals, disrupting cell surface antigen association with growth factors, blocking intracellular signalling cascades regulating cell proliferation and engender apoptosis. Antibodies could also activate various components of the immune system with potent tumour killing capacity including recruitment and activation of immune effector cells, by activating either arm of the complement system. Antibodies could also directly act by modulating regulatory mechanisms by targeting immune cells such as T_{regs} or cell surface molecules that are important checkpoints restricting T cell activation. Other types of antibodies include those conjugated to radionuclides and bi-specific antibodies, engineered to recognise more than one target molecule. Bi-specific antibodies are examples of agents with enhanced immune cell activatory functions. They comprise of two variable regions with different specificities and a Fc region recognising Fc receptors. This characteristic enhances the contact between a T cell, a cell that expresses Fc receptors and a tumour cells (i.e. catumaxomab). This established link between two immune cells and a tumour cell can induce tumour cell death [Staerz et al., 1985]. Approximately 920 anti-cancer therapeutic candidates entered commercially-sponsored clinical studies between 1990 and 2006 [Reichert and Wenger, 2008] (Figure 1.1). Of these candidates 44% were small molecule drugs, 14% natural products [Butler, 2008], and 21% gene therapy approaches, recombinant proteins and synthetic peptides. Finally, and of greatest relevance to this thesis, monoclonal antibodies (mAbs) comprised 21% of this new generation of anti-cancer therapeutics [Reichert and Wenger, 2008] (Figure 1.1).

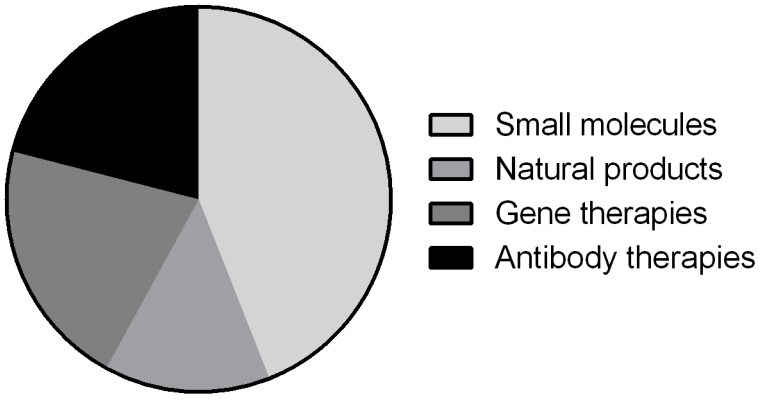

Figure 1.1: Composition of anti-tumour therapeutics in studies from 1990–2006. Data was taken from [Reichert and Valge-Archer, 2007].

1.1.4 Current therapies for melanoma

1.1.4.1 Treatment of localised disease

Localized disease in melanoma is currently treated through surgical removal, using safety margins of 0.5 cm for tumour *in situ* and 2 cm for tumour with a Breslow thickness up to 2 mm or thicker [Thompson et al., 2005]. Routine elective lymphadenectomy is currently not a standard of care because it has not been proven to be efficacious in comparison to observation alone [Morton et al., 2006]. However, sentinel lymph node biopsy has been suggested by several groups to be of benefit for patients with melanoma lesions >1 mm in size with or without ulceration, allowing for more accurate staging and therefore clearer information on prognosis. In contrast, complete dissection of regional lymph nodes after positive sentinel lymph node biopsy has not proven to be effective in improving overall survival (OS) [Morton et al., 2006]. New European guidelines recommend the use of radiotherapy for localized disease if the tumour cannot be fully dissected [Dummer et al., 2012]. In terms of systemic intervention, adjuvant pegylated IFNα-2b (5 years) or high dose IFNα-2b (1 year) have been approved by the FDA for patients with positive lymph nodes and low disease burden (micrometastasis). These adjuvant treatments have shown improved disease free survival (DFS), relapse free survival (RFS) and ambiguous success for OS [Dummer et al., 2012,Mocellin et al., 2010,Eggermont et al., 2008]. Adjuvant chemotherapy, mistletoe extract, viscum album and hormone therapies did not prove to be beneficial in localized disease [Dummer et al., 2012, Kleeberg et al., 2004]. Vemurafenib, an inhibitor for a mutant form of the kinase BRAF, found in approximately half of melanomas did not appear efficacious for localized disease, as treatment has been associated with an enhanced risk of keratoakanthomas, squamous cell carcinomas (SCC) and the development of new melanomas [Oberholzer et al., 2012, Su et al., 2012, Zimmer et al., 2012].

1.1.4.2 Treatment of loco-regional disease

In cases of loco-regional disease with high tumour burden (stage IIIc), surgical removal of the tumour lesion and lymph nodes with additional guidance provided for

the subsequent choice of treatment from additional imaging such as Positron Emission Tomography (PET) and computed tomography (CT) have been collectively proven to help treatment decisions [Dummer et al., 2011]. In contrast, treatment with radiotherapy or restricted area perfusion with melphalan and/ or with the cytokine tumour necrosis factor α (TNF-α) did not improve survival outcomes [Burmeister et al., 2012, Hong and Fogarty, 2012].

1.1.4.3 Treatment of systemic metastasis

1.1.4.4 Approved treatments

Historically standard treatments for patients include cytotoxic drugs such as dacarbazine (DITC), a reference drug in metastatic melanoma that was never tested in a prospective phase III trial. Other chemotherapeutic agents are temozolomide, taxanes, fotemustine and platin derivatives as single agents or in combination with immune-modulators such as IFNα-2b or IL-2 [Petrella et al., 2007]. However, no survival benefits have been demonstrated for treatment with polychemotherapy [Dummer et al., 2012]. In 2011 the FDA and EMA approved two therapies for the treatment of metastatic melanoma, namely vemurafenib, a kinase inhibitor and ipilimumab, an anti-checkpoint blockade antibody (anti-CTLA-4). Vemurafenib inhibits the mutated form of the BRAF kinase, detected in 50% of all melanomas [Tsai et al., 2008, Flaherty et al., 2010, Chapman et al., 2011]. Although vemurafenib was designed to block the V600E (glutamate for valine) mutated form of BRAF it has also been described to inhibit other mutations such as the V600K (lysine for valine) mutation [Turajlic et al., 2013]. Although recent studies show prolonged progression free survival (12.5 vs. 9.5 months) and overall survival (13.6 vs. 9.7 months in comparison to dacarbazine (DITC) (Chapman JCO 2012) the majority of treated patients develop secondary resistance to the drug [Flaherty et al., 2010]. This resistance is associated both with mechanisms overcoming the blockade of BRAF kinase inhibitors as well as with alternative activation of the MAP kinase pathway [Khattak et al., 2013a, Khattak et al., 2013b, Mao et al., 2013, Long et al., 2013], which together with enhanced risk of keratoakanthomas and squamous cell carcinomas (SCC) suggest that combination therapies using different kinase inhibitors to overcome these

shortcomings are worthy of study and are currently being evaluated (experimental therapy described in section below). Ipilimumab is an IgG_1 monoclonal antibody that recognises the ckeckpoint cell surface molecule CTLA-4 on T cells and blocks the binding between CTLA-4 and CD80/CD86, thereby activating the numerous T cells present in melanoma. This can result in universal activation of all T cells, including those against the tumour. Ipilimumab has shown efficacy in several phase III clinical trials in untreated and treated metastatic patients in combination with a range of therapies such as peptide vaccines and also as a mono-therapy [Hodi et al., 2010, Robert et al., 2011]. Subsequent trials using combination therapy such as IL-2 and ipilimumab [Prieto et al., 2012] have indicated some promising outcomes, but are still under evaluation. Moreover, Khattak et al. showed in an initial study that ipilimumab restricted tumour volume in metastatic uveal melanoma, indicating this as a suitable treatment of different subtypes of melanoma [Khattak et al., 2013b]. In summary ipilimumab is now approved by the regulatory authorities in metastatic melanoma. Suggested combination therapy of the two clinically approved agents ipilimumab and vemurafenib are being evaluated but some drawbacks due to hepatotoxicity have been reported [Ribas et al., 2013].

1.1.4.5 Experimental treatments

Therapeutic approaches using alternative CLTA-4 inhibitory antibodies other than ipilimumab, and novel selective inhibitors for mutant forms of BRAF such as dabrafenib as well as c-kit and MARK/ERK kinase (MEK) inhibitors have individually shown impressive outcomes in prospective randomised trials. Furthermore, antibodies against alternative immune cell regulatory proteins such as PD-1, PD-L1, CD137, OX40 or CD40 are being investigated [McArthur and Ribas, 2013]. For example, administration of the anti-PD-1 antibody nivolumab demonstrated objective responses in approximately 30% of individuals treated in a phase I trial [Topalian et al., 2012]. Furthermore, combination therapy with nivolumab and ipilimumab in a dosing study demonstrated clinical safety and showed enhanced efficacy that appeared to be superior compared to that published on either antibody alone [Wolchok et al., 2013]. In a more recent study, Hamid et al. report that the monoclonal antibody lambrolizumab (anti-PD-1) triggered sustained tumour regressions in patients that had refractory disease after ipilimumab treatment, while only displaying minor toxic effects (grade

1 and grade 2) [Hamid et al., 2013]. Likewise, the identification of new mutations in melanoma such as alternative BRAF, NRAS, c-kit, GNA11 and GNAQ mutations has led to the development of different kinase inhibitors. The kinase inhibitors debrafenib and tremetenib improved response rate and survival in patients carrying the appropriate mutation in randomised phase III trials [Chapman et al., 2011, Flaherty et al., 2012, Ascierto et al., 2011]. In conclusion, a new generation of agents, such as kinase inhibitors and immune-modulatory agents, especially antibodies, are paving the way for a higher therapeutic benefit with enhanced quality of life during treatment for patients. Antibody immunotherapy is highly associated with the immunological response in the tumour; and the success or failure of treatments may be related to the immunological status of patients, including the specific immune bias in tumour microenvironments. Thus, a better understanding of the immunomodulatory and immunosuppresive forces at play in tumours may inform treatment design and patient stratification.

1.2 Relationship between the immune response and cancer cells

The immune system is believed to play a crucial role in the development of cancer. This section elaborates on how tumours interact with the immune system and specifically with the humoral arm of adaptive immunity, and how cancer cells may evade immune responses (1.2.1); how signals such as cytokines polarize and downregulate components of the humoral immune response generally in diseases (1.2.2) and how immunoediting occurs in melanoma (1.2.1). This discussion is the basis for the subsequent exploration of designing more effective antibodies, specifically for the treatment of cancer (1.3).

1.2.1 Cancer immunoediting

Cancer cells are involved in a network of interactions with their environment, including surrounding healthy stromal cells, extracellular matrix components and im-

portantly, immune cells. These interactions impact on the ability of tumour cells to survive, divide, shape their microenvironment and also metastasize to distant sites in the body. To date, considerable attention has been focused on understanding the relationship between cancer cells with immune cells both *in situ* and systemically, from the perspective that cancer cells can modulate or even suppress effective immune responses [Waldmann, 2003, Waldmann and Morris, 2006]. The hypothesis of tumour-induced editing of the immune response (immunoediting) is based on the inference that tumour and anti-tumoural immune defences interact in different stages: in the first instance, the immune system detects the presence of aberrated cells and immune cells home into the tumour to eliminate it (Elimination); if elimination is not achieved, tumour and immune system reach a state of equilibrium (Equilibrium); subsequently the tumour may overcome this equilibrium and evade immune clearance by triggering the release of an array of mediators by tumour cells as well as by inflammatory and stromal cells that promote tumour growth and metastasis (Evasion) [Schreiber et al., 2011, Vesely and Schreiber, 2013] (Figure 1.2). Investigating different aspects of these interactions between host immunity and cancer has informed the development of numerous strategies to activate the immune responses to target and eradicate cancer cells.

1.2.2 Immune cells and cytokines influenced by tumours

Influenced by tumour cells tumour associated lymphocytes such as dendritic cells, macrophages and monocytes alter their phenotypes, immune activatory status, tumouricidal or tumour-promoting capacities, together with their immune polarization (Th_1/ Th_2) and Fc receptor expression in the tumour microenvironment. Elucidating the nature of these alterations has formed the focus of extensive study, not only in the tumour microenvironment but also in patients' circulation. Numerous mechanisms, mostly associated with Th_2-type inflammation, have been reported to play major roles in promoting tumour development. For instance, the immunomodulatory cytokine IL-10 acts in different ways such as promoting T regulatory cells (T_{regs}), which are associated with poorer patient prognosis (Nicholaou 2009; Wang 2012). T_{regs} in turn, may suppress maturation of antigen-presenting cells and can modulate the functions of NK cells or macrophages [Terabe et al., 2004, Rabinovich

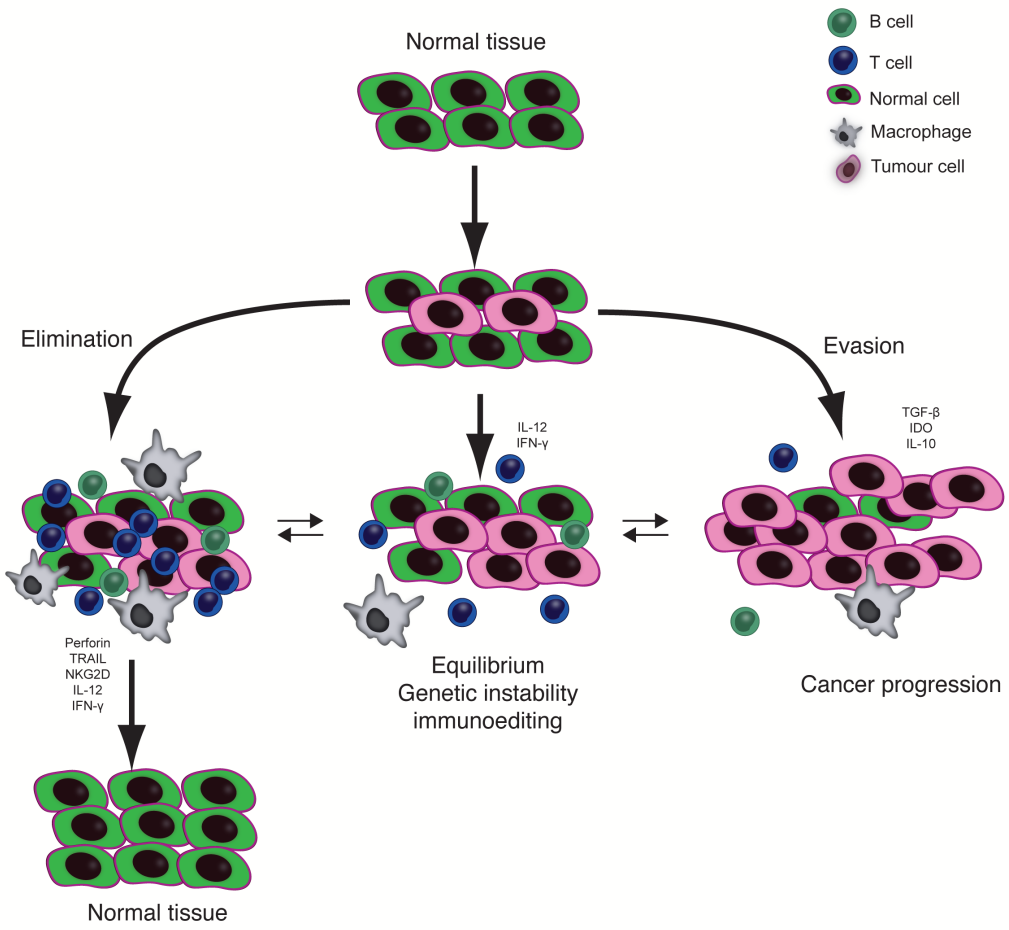

Figure 1.2: There are three stages of cancer immunoediting. Cancer immunoediting is the result of different stages that function either independently or in sequence to control and modulate cancer. Once normal cells are transformed by acquiring mutations preferentially in oncogenes and failed intrinsic tumour suppression, the immune system may function as an extrinsic tumour-suppressor. In the first stage, elimination, immune cells and molecules such as antibodies recognize transformed cells and destroy them, resulting in a return to normal physiological tissue. However, if the immune system is unable to completely eliminate the tumour cells, surviving tumour may enter into the equilibrium stage, where immune cells are still able to prevent tumour outgrowth. The acquisition of further mutations may subsequently result in the evasion of tumour cell recognition, killing, or control by immune cells and leads to clinically detectable malignancies in the escape stage.

et al., 2007, Couper et al., 2008, Emmerich et al., 2012, Gerlini et al., 2004]. It has been repeatedly shown that particularly tumour-associated macrophages (TAMs) are polarized towards an alternatively activated M2-phenotype in the tumour microenvironment, that is induced by cytokines such as IL-4, IL-13 and IL-10. These

M2-macrophages are thought to promote tumour growth and invasion by tissue remodelling via the release of stromal remodelling agents such as matrix metalloproteinases or by secreting suppressive mediators such as prostaglandins, IL-10 and indoleamine dioxygenase (IDO-1) [Mantovani and Sica, 2010, Sica and Mantovani, 2012]. Another myeloid cell type that is known to induce dysfunction in immune cells is the myeloid derived suppressor cell (MDSC). MDSCs are known to produce nitric oxide, which induces apoptosis in T cells and limits availability of the essential amino acid cysteine leading to the production of suppressive cytokines such as IL-10 [Poschke et al., 2011, Kerkar and Restifo, 2012, Pietra et al., 2012]. Furthermore, "alternative activation" of several types of TH cells such as TH_1 cells that would normally provide immune activatory signals by secreting IFNγ. In tumours, TH_1 cells functions are modulated by the induction of programmed cell death receptor (PD-1) on (cytotoxic) T cells [Tanchot et al., 2012, Sharpe et al., 2007] or TH_{17} cells that can induce angiogenesis and recruitment of neutrophils that secrete elastase, a tumour promoting mediator [Coussens et al., 2013]. In addition to the secretion of cytokines, tumour cells protect themselves against directly induced toxicity by expressing decoy molecules such as FcγRIIb or PD-L1 on their surface to avoid immune cell targeting [Cassard et al., 2008, Dong et al., 2002, Iwai et al., 2002]. A thorough evaluation of the cellular constituents in tumours and of the key cytokines such as the pro-angiogenic vascular endothelial growth factor (VEGF) or the pleotropic immunomodulatory cytokine IL-10, can help decipher the processes of tumour cell-led immunosuppression and provide a better understanding of the initiation of evasion and inform the design of better immunotherapeutic approaches [Hicklin and Ellis, 2005]. It is now well established that a chronic inflammatory environment can support tumour progression. Coussens and colleagues have provided insights into the role of the humoral response in this context. The group describes auto-antibodies that build immune complexes with complement or Fc receptors on immune cells such as mast cells or macrophages, promoting vascularisation and immunosuppression [de Visser et al., 2005, Tan and Coussens, 2007, Andreu et al., 2010]. Likewise, B cells that produce IL-10 and/or TNFα have been reported to induce myeloid derived suppressor cells [Schioppa et al., 2011]. In a more recent publication a novel B cell subtype with a regulatory phenotype (B_{regs}), which is activated by IL-21 was described. These B_{regs} induce suppression in a T_{reg}-like manner via granzyme B and could therefore play a pivotal role in tumour evasion [Lindner et al., 2013]. On the contrary, several studies reported that the number of infiltrating $CD20^+$ B cells

correlated with increased disease survival [Nielsen et al., 2012, Ladányi et al., 2011]. These seminal reports indicate that modulation of humoral immunity could lead to suppression or promotion of anti-tumour responses in cancer. On the other hand, histologically-detected tumour infiltrating lymphocytes (TIL) in different cancers generally correlates with better clinical prognoses. Extensive studies have been performed in colorectal cancer showing that T cell subsets such as $CD8^+$ cells are highly predictive of disease progression [Angell and Galon, 2013, Pagès et al., 2009, Mlecnik et al., 2011, Galon et al., 2006]. These findings are now paving the way for prospective-retrospective studies in other cancers where similar observations are already being made. These findings may suggest that despite immunosuppression, the immune response may harbour the potential to mount a substantial defence against tumours. This can be translated into better clinical outcomes, providing the basis for the design of immunoactivatory therapies.

1.2.3 Modulation of immune responses in melanoma

Spontaneous tumour regressions and remissions reported in patients with melanoma, along with clinical features of vitiligo-like depigmentation, halo naevi in a small cohort of patients and increased prevalence of melanoma in immunosuppressed individuals all point to important and potentially clinically-significant interactions between melanoma and immune responses. Although the immune system appears to recognise melanoma cells there are several escape mechanisms by which the tumour is able to circumvent immune-mediated clearance. These include a) modulation of immune cell mechanisms such as suppressing immune cell activation and maturation, b) recruitment and induction of immune regulatory cells (e.g. T_{regs}) and pro-inflammatory cells (e.g. alternatively-activated macrophages), c) up-regulation of immunomodulatory molecules (e.g. CTLA4, PD-1), d) promoting production of immunosuppressive cytokines (e.g. IL-10, TGF-β) [Urosevic and Dummer, 2003, Beck et al., 2001] and e) regulating the migration and differentiation of stromal cells in the tumour micro-environment (e.g. metalloproteinases) [Lin et al., 2004, Mantovani et al., 2005]. Analysis of immune cell subsets such as FoxP3 (T_{regs}), $CD11c^+$ (conventional dendritic cells) and $CD86^+$ (mature dendritic cells) in primary tumours (n=54) and/or sentinel lymph nodes (n=84) revealed that FoxP3 infiltrates had a

negative impact on anti-tumour immunity, whereas conventional dendritic cells were down-regulated. These findings imply that the immune cell profiles correlate with primary tumour >2.0 mm and with disease progression in sentinel lymph nodes, as well as with clinical outcomes [Ma et al., 2012]. Interestingly, $CD20^+$ infiltrate increase among the immune cell infiltrates correlated positively with survival [Ladányi et al., 2011, Erdag et al., 2012], suggesting that humoral immunity may exert both anti-tumoural and tumour-promoting effects in melanoma. Additionally, cytotoxic T-lymphocytes specific for melanoma-associated antigens have been reported in the blood of patients with advanced disease. These T cells can target and kill tumour cells, cause apoptosis of melanoma cells and activate other immune cells such as macrophages and NK-cells that can then also seek out and kill tumour cells by a number of mechanisms [Fritsch, 2003, Palucka et al., 2007]. The recruitment of immune inflammatory cells may also oppose tumour development and it is considered an attempt by the host to suppress tumour growth. Clinical and scientific observations suggest that activating the immune response may hold promise for the treatment of melanoma. This premise has formed the focus of many studies and has given rise to various systemic immune therapies for melanoma such as IFNα-2b, IL-2 and also more recently, anti-CTLA4 antibodies, which have found clinical applications. Despite these promising developments and reported anti-tumoural immune responses in patients, some of the above tumour-induced immunomodulatory mechanisms may explain why, immunotherapeutic strategies aimed at producing a more efficient host immune response have shown only partial efficacy in subsets of patients. The challenge in cancer immunotherapy is to redress the fine balance between tumour-promoting and tumour-suppressing immune inflammatory elements in order for the immune system to mount an effective response against cancer.

1.3 Antibodies and B cells

Antibodies and B cells are involved in immune protection from pathogens, but on the other hand, they could participate in the pathogenesis of diseases (1.2). To understand this complex process it is essential to elaborate on what is an antibody (1.3.1), how an antibody mediates immune response through Fc receptors on immune cells (1.3.2), how B cells produce antibodies in the first place (1.3.3), how different

classes of antibodies are created through class switch recombination (1.3.4) and how antibody classes are polarized by cytokines such as IL-10 (1.3.5). The description of these aspects is the basis for the subsequent discussion of IgG_4 polarization in the context of disease (1.4).

1.3.1 Antibody Structure

In 1890, Behring and Kitasato discovered the presence of "something" in the blood that was able to neutralize diphtheria toxin, reporting that transfusing sera already containing the antitoxin activity protected the recipient animal from infection with the same toxin (Behring E, 1890). This was further elucidated by Paul Ehrlich' description of the interaction between the antitoxin and diphtheria toxin that lead to the introduction of the term "antibody" (Antikörper) in 1891 [Ehrlich, 1891]. More than 100 years since the discovery of antibodies, these molecules demonstrate a diverse range of applications. One example of application is their use as treatment modalities for a range of diseases including a number of human malignancies. There are nine different identifiable antibody (immunoglobulin) classes and subclasses in the human proteome: IgM, IgG_1, IgG_2, IgG_3, IgG_4, IgD, IgA_1, IgA_2 and IgE (Figure 1.3).

All antibody molecules share the same basic structure of a heterodimeric protein, but display remarkable variability in the regions that bind antigens. Every antibody has a symmetric core structure consisting of two identical light chains (L chains, each about 24 kD) and two identical heavy chains (H chains, each ∼55 or 70 kD) (Figure 1.4).

One light chain is covalently attached to one heavy chain by a disulfide bond (with the exeption of IgA2m(1) antibodies) and the two heavy chains are covalently attached to each other by disulfide bonds. The heavy chain consists of one amino terminal (N-terminus) variable (V) region and contains four or three carboxy terminal (C-terminus) constant (C) regions. The light chain consists of only one V region and one C region [Putnam, 1969].

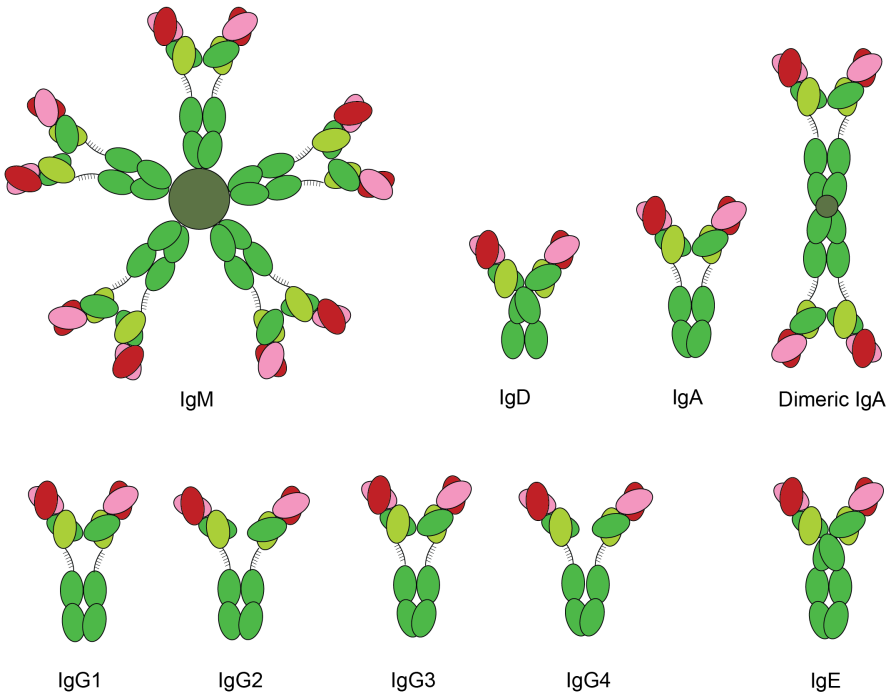

Figure 1.3: Representation of the five immunoglobulin classes, distinguished by their heavy chain structure: IgM, IgD, IgA, IgG and IgE. Heavy chains consist of one variable domain (VH)(red) and multiple constant domains (dark green), three for IgA, IgG and IgD (CH1,CH2, and CH3) and four for IgE and IgM (CH1, CH2,CH3, and CH4). The light chains are composed of one variable domain (VL) (pink) but have a single constant domain (CL) (pale green) for all antibody classes.

Variable regions are named so for containing regions of variability in amino acid sequences that define the specificity and affinity of antibody binding to its target antigen. The V region of one heavy chain (VH) is juxtaposed with the V region of one light chain (VL) to form an antigen-binding site; each antibody has two sets of these pairs (Figure 1.4). The heavy chain C regions do not participate in antigen recognition but components of C regions interact with other effector cells of the immune system by recognising specific receptors (FcR) on the surface of these cells and mediating many of the biological functions of antibodies (Figure 1.4) [Murphy and Walport, 2005]. Antibodies can have one of two types of light chains, κ or λ, distinguished by their carboxy terminal regions. An antibody has either two identical κ light chains or λ light chains. In humans about 60% of antibodies have κ light chains and about 40% have λ light chains. The diversity of antigen receptor

-multiportein complexes (the antigen receptor shares the same antigen recognition side as the antibody that will develop from the B cell) on the surface of B cells made up by the heavy and light immunoglobulin chains- repertoire and its ability to induce cell differentiation upon specific antigen contact is a key component of the adaptive immune response. The gene locus for the variable region of antibodies combines 44 Variable, 27 Diverse, and 6 Joining gene segments (VDJ for the heavy chain and VJ for the light chains) to generate an enormous antibody repertoire based on nearly random recombination of the single gene segments on chromosom 14 [Bassing et al., 2002]. Therefore VDJ recombination contributes to the diversity of antigen recognition sites (variable regions) on antibodies. Assembly of different antigen receptor genes form arrays of gene segments achieved through the recombination at the complementarity-determining region 3 (CDR3), CDR3 being one of the main genomic regions forming the interaction sites between antigen receptor and antigen. This rearrangement is initiated mainly by two genes recombination activating gene 1 and 2 (RAG1, RAG2) [Schatz et al., 1989, Oettinger et al., 1990]. RAG1 and RAG2 recognize and bind to recombination signal sequences (RSS) and induce double-stranded breaks. The described mechanism of coordinated gene rearrangements enables human B cells to generate a hugely diverse repertoire (7128 combinations) of antibody specificities. Antibodies activate the immune cells through eliciting the interaction of the Fc regions of the antibody and Fc receptors on immune cells, also known as cross linking of Fc receptors. Therefore the functions of antibodies can be highly dependent on immune cell-mediated mechanisms induced by the interaction between Fc regions with Fc-receptors.

1.3.2 Fc receptors on immune cells

Fc receptors are proteins that recognise Fc regions of immunoglobulins. They are mainly expressed on the surface of immune cells and help mediate antibody functions, including antibody dependent cell-mediated cytotoxicity (ADCC) and antibody dependent cell-mediated phagocytosis (ADCP). Additionally they are able to induce complement-dependent cytotoxicity (CDC) [Scott et al., 2012]. These activities can be directed against microbes, viruses and also against neoplastic cells [Weng and Levy, 2003, Weng et al., 2004]. As this thesis focuses on IgG and IgE antibodies,

this section elucidates the functional characteristics and distribution of their cognate (Fcγ and Fcϵ) receptors.

1.3.2.1 Fcγ receptors (FcγRs)

FcγRs are a group of transmembrane glycoproteins that bind the constant region of IgG antibodies. Crystallographic analysis suggests that there is a 1:1 stoichiometry interaction between IgG and FcγR [Nimmerjahn and Ravetch, 2008]. According to their structure and biological properties, FcγRs are subdivided in 3 major classes: FcγRI, FcγRII and FcγRIII. These receptors have an immunoreceptor tyrosine-based activation motif (ITAM) with the exception of FcγRIIb, which hosts an immunoreceptor tyrosine inhibition motif (ITIM). Monocytes, macrophages, dendritic cells, basophils and mast cells all have distinct repertoires of activating (FcγRI, FcγRIIa and FcγRIII) and inhibitory (FcγRIIb) FcγRs. In contrast, natural killer cells (NK cells) express only the activating receptor FcγRIIIa and B cells express only the inhibitory receptor FcγRIIb during certain stages of their development. Although NK cells express only the activation receptor FcγRIIIa, NK infiltration into tumour does not always correlate with a positive prognosis. This apparent oxymoron was partially resolved by Aloulou and colleagues describing in their manuscript that ITAM domains are also capable of inducing inhibitory functions (ITAMi) and blocking immune cell activation [Aloulou et al., 2012]. With the exception of FcγRIIa, FcγRIIb and FcγRIIc all other FcγRs depend on a ligand binding the α-chain and a signal-transduction adaptor molecule that contains ITAMs (Figure 1.5).

Their activation is triggered by the phosphorylation of ITAMs by kinases of the SRC family and leads to downstream activation of major pathways such as the RAS-RAF-MAPK [Nimmerjahn and Ravetch, 2008]. The diversity in receptor distribution is also reflected in the heterogeneous function that IgG might play during physiological processes or pathogenesis. For instance, macrophages/monocytes could be engaged in different ways by different IgG subclasses, promoting or inhibiting pathological processes. These aspects are subject to further investigation in the context of melanoma, and form part of this thesis.

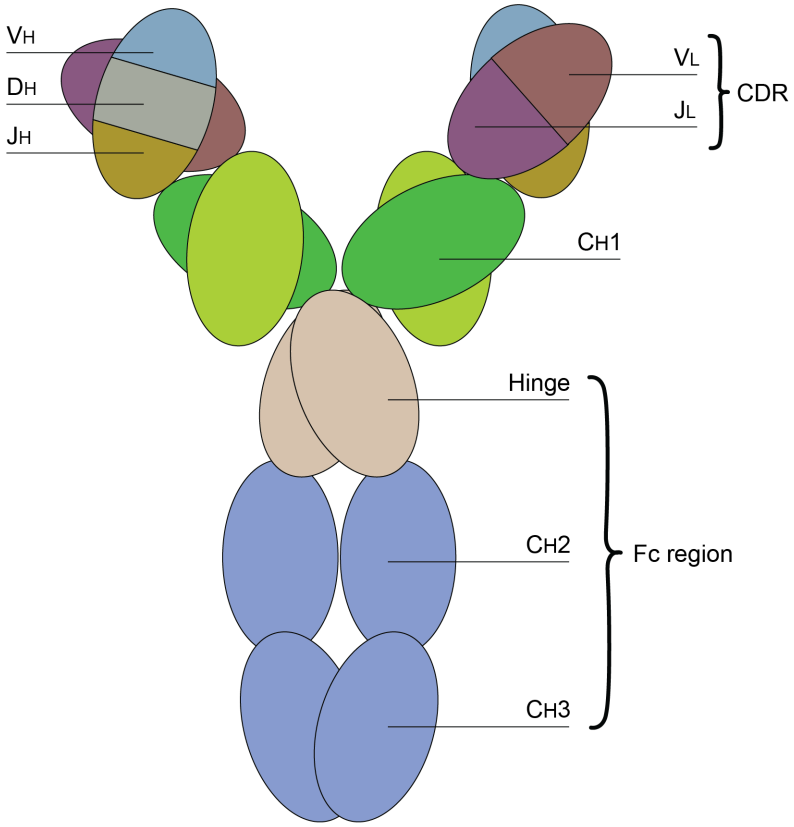

Figure 1.4: Variable regions have been given their name because they contain regions of variability in amino acid sequences that define the specificity and affinity of antibody binding to its target antigen. The V region of one heavy chain (VH) is juxtaposed with the V region of one light chain (VL) to form an antigen-binding site; each antibody has two sets of these pairs. The C region domains do not participate in antigen recognition. The heavy chain C regions interact with other effector cells of the immune system by recognising specific receptors (FcR) on the surface of these cells and mediate many of the biological functions of antibodies. Antibodies can have one of two types of light chains, κ or λ, distinguished by their carboxy terminal regions. An antibody has either two identical κ light chains or λ light chains. In humans about 60% of antibodies have κ light chains and about 40% have λ light chains.

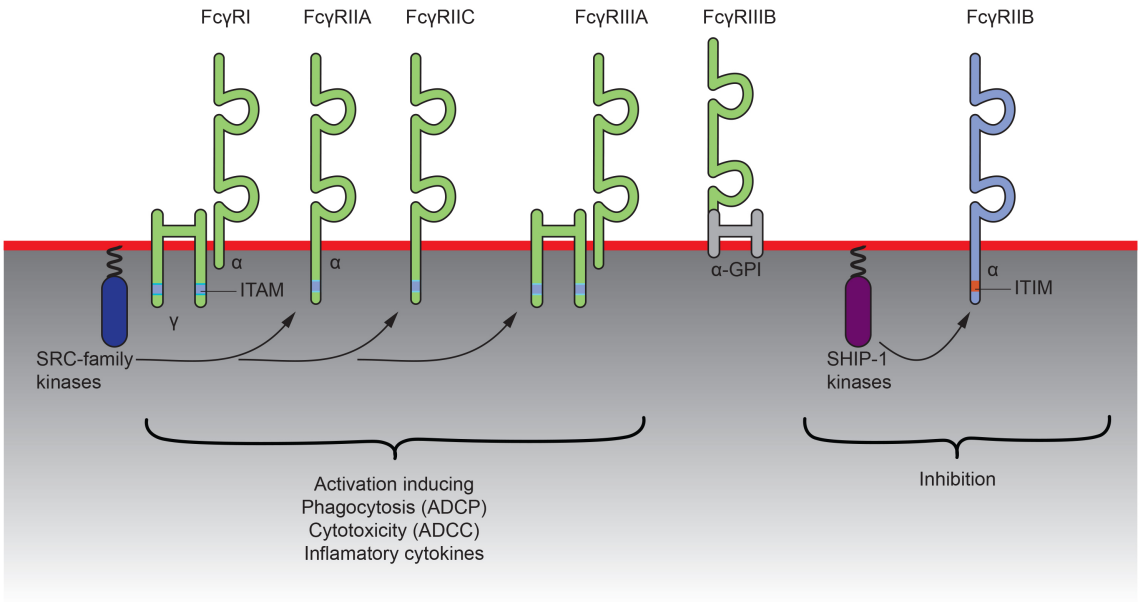

Figure 1.5: Humans have one high-affinity Fcγ receptor (FcγRI) and several Fcγ receptors with low to medium affinity for the antibody Fc fragment. With respect to the type of signals triggered by FcR crosslinking, there is one single-chain inhibitory receptor, FcγRIIb, signalling through an immunoreceptor tyrosine based inhibitory motif (ITIM) in its cytoplasmic domain. With the exception of human FcγRIIa and FcγRIIc, signalling of the other FcR is usually mediated by a ligand-binding immunoreceptor tyrosine based activating motifs (ITAMs). In addition, humans have a glycosyl-phosphatidylinositol (GPI)-linked receptor (expressed by neutrophils), called FcγRIIIb.

	FcαR $10^7 M^{-1}$	**FcϵRI** 10^9–10^{11} M^{-1}	**FcϵRII** 10^8–10^9 M^{-1}	**FcγRI** 10^8–10^9 M^{-1}	**FcγRII** 10^7 M^{-1}	**FcγRIII** 10^5 M^{-1}
Macrophage	•	•	•	•	•	•
Eosinophil	•	•	•	•	•	•
Neutrophil	•			•	•	•
Basophil		•				
Mast cell		•			•	•
Dendritic cell		•	•	•	•	•
B cell		•		•		
NK cell						•

Affinity displayed below receptors indicates Ka

Table 1.1: Binding affinities of immunoglobulins to Fc receptors on immune cells. FcαR binds IgA; FcϵR binds IgE and FcγR binds IgG

1.3.2.2 Fcϵ receptors (FcϵRs)

The two known Fcϵ receptors on the surface of specialised immune cells are FcϵRI (also known as the high-affinity receptor) and CD23 (otherwise known as FcϵRII or the low affinity receptor) [Gould and Sutton, 2008]. Every IgE antibody binds only one FcϵRI (1:1 stoichiometry interaction) [Dhaliwal et al., 2012]. FcϵRI exists in two forms: the $\alpha\beta\gamma 2$ tetramer and $\alpha\gamma 2$ trimer [Kraft and Kinet, 2007]. FcϵRI and FcγRs share the same γ subunit and therefore share some signalling properties like the immunoreceptor tyrosine-based activation motif (ITAM). The high affinity IgE receptor (FcϵRI) has a nanomolar affinity (Ka = 10^9–$10^{11}\mathrm{M}^{-1}$) and is expressed on a variety of immune cells including basophils, mast cells, Langerhans cells, myeloid DCs, plasmacytoid DCs, monocytes, macrophages and eosinophils. Crosslinking of FcϵRI receptors by antigen engagement between two different antibodies activates a signalling cascade mediating immune cell activity. Moreover, FcϵRI has been identified on intestinal epithelial cells, were the receptor is believed to play a role in immunosurveillance or protein trafficking [Untersmayr et al., 2010]. The low affinity receptor CD23 has a micromolar affinity (Ka = 10^7–$10^8\mathrm{M}^{-1}$) for IgE and is mainly expressed or up-regulated on activated immune cells, including B cells, monocytes and macrophages, eosinophils, natural killer T cells, T cells, follicular DCs and platelets [Gould and Sutton, 2008]. CD23 can also be found on non-immune cells including airway epithelial cells [Dullaers et al., 2012]. There are two variants of CD23 that are induced by splicing differences. CD23a is found on activated B cells and is thought to play key roles in antigen-IgE complex endocytosis, antigen processing and presentation to T cells [Gould and Sutton, 2008]. CD23b is inducible by IL-4 on a variety of immune cells such as monocytes and B cells. Engagement of CD23b by IgE antibody-antigen complexes on immune cells such as monocytes and macrophages prompts production and release of modulatory or cytotoxic mediators including nitric oxide and TNFα. Furthermore, this receptor has been described to induce antibody depended phagocytosis, especially in the context of parasitic infections [Vouldoukis et al., 2011].

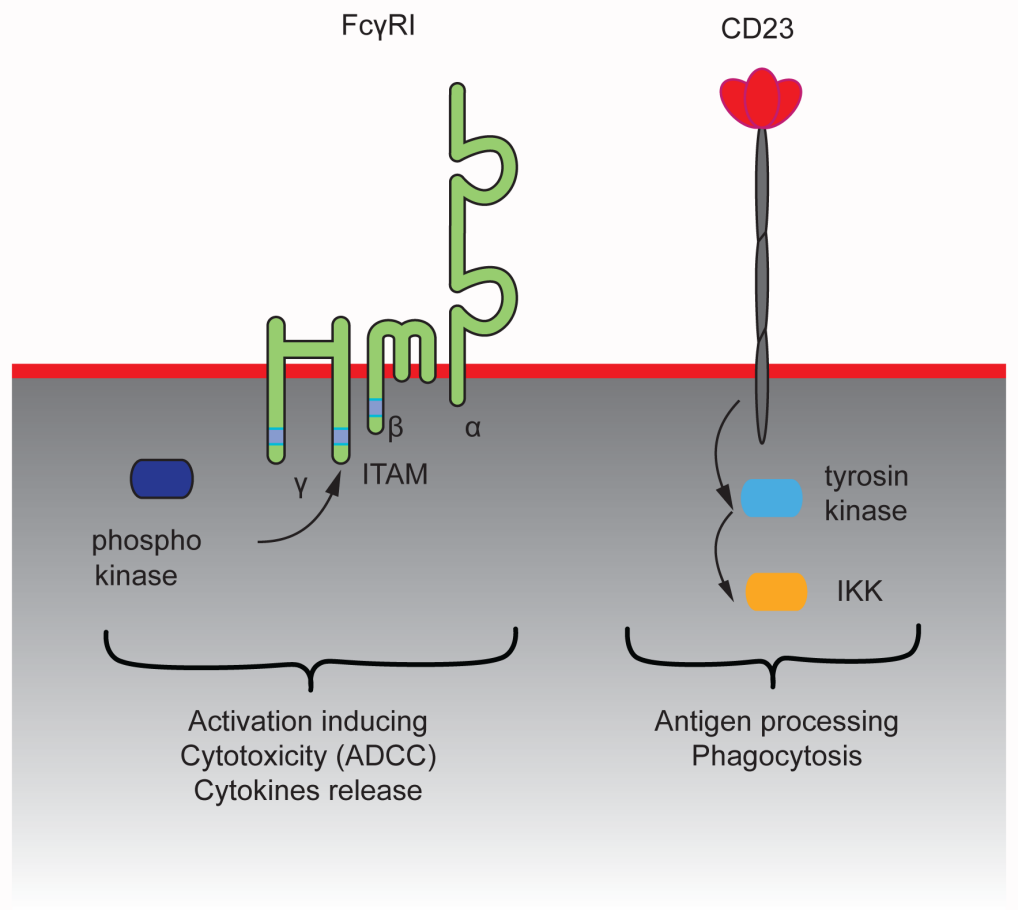

Figure 1.6: Diagram of the proposed down stream singalling events accruing while FcϵRI and FcϵRII (CD23) are activated. Cross-linking of FcϵRI leads to activation of ITAM domain and phosphorylation of different downstream kinases, whereas activation of CD23 leads to the downstream signalling through tyrosine kinases and Iκk.

1.3.3 B cells: development, activation and antibody production

B lymphocytes producing antibodies are primarily responsible for the humoral arm of the adaptive immune response. Their principle functions are those of antigen-presenting cells (APCs) and their capacity to eventually develop into memory B cells or antibody-secreting plasma cells after activation by antigen interaction. There are several stages in B lymphocyte differentiation, each representing key genetic changes in the antibody loci. These changes are important for the evolution of B cells expressing antibodies with high affinities to a wide range of antigens, including those

expressed on the surface of pathogens but also those on the surface of tumour cells. B cell development starts in the bone marrow with formation of lymphoid progenitor cells, which undergo rearrangement of their variable regions (immunoglobulin heavy chain and light chain genes are rearranged). These eventually give rise to immature and mature resting B1 cells that both express surface-bound immunoglobulin complexes (IgM^+) also termed B Cell Receptors (BCR). IgM (BCR)-expressing immature B cells migrate to the spleen (transitional B cells), where some differentiate into mature B lymphocytes, while others that fail to receive adequate stimulatory signals undergo apoptosis in a process termed clonal deletion [Honjo and Neuberger, 2004] (Figure 1.7).

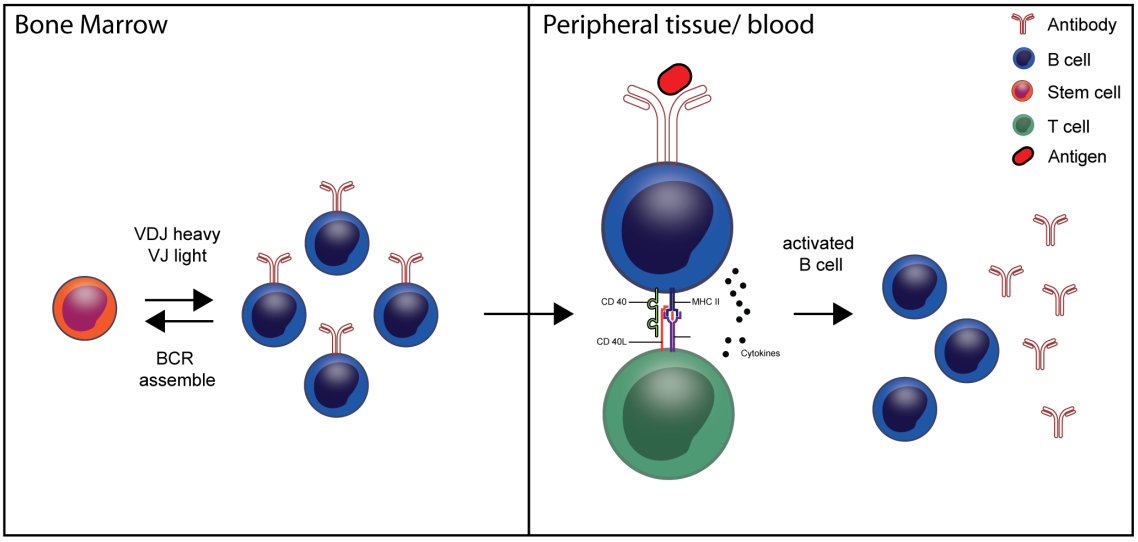

Figure 1.7: Development of B cells from progenitor cells to activated antibody-secreting B cells. In the bone marrow progenitor cells are matured to unique B cell receptor expressing cell by recombination of the variable, diversity and joining (VDJ) regions. After these cells have moved out of the bone marrow, they can be activated through interactions with T cells. This activation works by signalling between the TCR-MHCII, CD40-CD40L and interleukin receptor on the B cell.

B lymphocytes entering the peripheral blood express different cell surface proteins throughout their lifespan. These include CD40, CD19, CD20, CD22 and CD27; some of these molecules can function as co-stimulatory or inhibitory molecules. Late pro-B cells in the bone marrow through to mature B cells, express CD19 and CD20 (Honjo,

2004), but these markers are not expressed on early pro-B cells or plasma cells. Mature B cells but not plasma cells express CD22 [O'Keefe et al., 1999, Depoil et al., 2008]. Mature memory B cells are known to express a combination of CD22, CD27, CD40 and CD79. In addition to antigen-specific signals other antigen-independent (polyclonal) activation signals have been described which induce activation, maturation and/or differentiation of B cells in tissue and blood. B cell activation occurs among others through toll-like receptor (TLR-7, TLR-9) engagement by specific nucleotide patterns or through the interaction between CD40 on B cells and CD40L expressed on T helper cells. This is a crucial co-stimulatory signal leading to B lymphocyte proliferation and differentiation to antibody-producing plasma cells. Although the impact of the above-mentioned stimulatory elements on B lymphocyte differentiation and antibody production is still being elucidated, studies have shown that B lymphocytes can respond to one or a combination of these signals while antigen recognition alone may not be adequate or necessary for B cell activation [Murphy and Walport, 2005].

1.3.4 Signals triggering class switching in B cells

Immunoglobulin class switching or class switch recombination (CSR) occurs in maturing B cells in response to antigen and co-stimulatory signals. Mature B cells expressing a μ constant (μC) or δ constant (δC) immunoglobulin constant region can switch to another antibody isotype triggered by an interchromosomal recombination event. This occurs mostly after activation through antigen cross-presented to B cells by an antigen presenting cell, and additional signals including CD40 (a member of the TNF-receptor superfamily responsible for T cell-dependent immunoglobulin class switch) as well as CD19 (a cell surface protein that assembles with the BCR to decrease the threshold of activation). The accompanied cytokine environment (modulated by T helper cells) leads to a switch towards a particular antibody class or subclass e.g. IgG (1-4), IgA (1-2) or IgE antibodies (Figure 1.8) [Murphy and Walport, 2005, Pieper et al., 2013]. CSR involves only the constant region of the immunoglobulin heavy chain while the variable region and therefore antigenic specificity is maintained. However, as maturation of the variable regions is closely associated with CSR, these two processes can also happen simultaneously. It is also

possible that CSR leads to the production of different immunoglobulin isotypes (e.g. IgG_1, IgG_2 etc), recognising the same antigen (Figure 1.8).

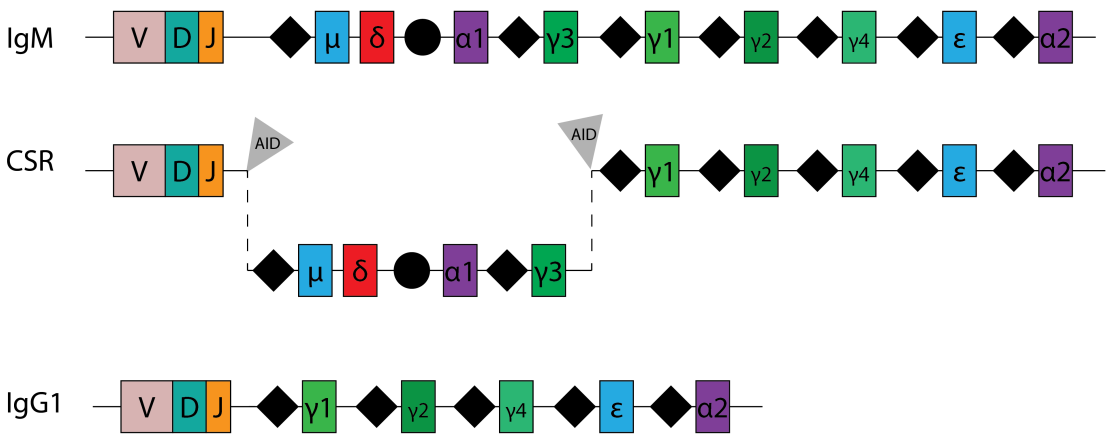

Figure 1.8: Schematic representation of the mechanism of class switch recombination in activated B cells. The black symbols between the constant regions represent the s-regions

Both short-lived plasma cells and high affinity memory B-lymphocytes require high-affinity class-switched antibodies. Deletion of the switch regions (S regions being the tandem repeats of pentametric nucleotides that flank each constant region and are rich in Guanine) is a key event for initiation of CSR. Although several proteins are involved in CSR, the enzyme Activation-Induced Cytidine Deaminase (AID) [Muramatsu et al., 2000, Revy et al., 2000] is essential, and it is responsible for initiating the process by converting cytosine to uracil. The uracil is excised by the uracil DNA glycosylase UNG resulting in single strand DNA breaks. Subsequent mismatch repair proteins then convert the resulting single-strand DNA breaks to double-strand breaks with DNA ends appropriate for end-joining recombination. Interestingly, at least two full rounds of cell proliferation seem to be required for CSR of IgG and IgA antibodies [Rush et al., 2005]. Moreover AID mRNA is actively regulated by Stat6 and NfKB induction, triggered by synergistic signalling of IL-4, CD40 and PAX5. As these proteins provide very rapid signals, they are considered to be responsible for the short expression of AID mRNA. Interaction between CD40L (CD154) on

T helper cells and CD40 on B cells is required for antibody class switching from IgM to one of the mature antibody classes [Armitage et al., 1993, Spriggs et al., 1992, Banchereau et al., 1994]. The absence of this interaction is thought to lead to hyper-IgM syndrome in humans, which is associated with immunodeficiency [DiSanto et al., 1993]. Other signals such as those from the B cell activation factor (BAFF), produced by myeloid cell, antigen presenting cells as well as T cells can also play a role in antibody class switching in humans by signalling through its receptors TACI and BAFF-R [Darce et al., 2007a, Darce et al., 2007b]. The enzyme AID is also involved in a subsequent process of programmed mutation in the variable regions of the human immunoglobulin locus, and specifically in "hypervariable regions" of CDRs. This process leads to affinity-matured antibodies in the tissue and is defined as Somatic Hypermutation (SHM). SHM mainly in the form of single base substitutions gives rise to clones with different affinities, and allows for selection of B cells that express immunoglobulins with high affinity for a specific target antigen [Di Noia and Neuberger, 2007].

1.3.5 Cytokines influencing class switching and production of antibodies by B cells

A number of cytokines and growth factors also contribute to and regulate class switching of B cells from IgM/IgD- to IgG/IgA/IgE-expressing cells. For instance, research on animal models has revealed that interleukin-4 (IL-4) and interferon gamma (IFNγ) are common regulatory cytokines of IgE and IgG_1 class-switching respectively, since animals missing IL-4 or Stat-6 (a kinase involved in the IL-4 signalling pathway) have substantially low levels of IgG_1 and no IgE class antibodies [Takeda et al., 1996, Ozaki et al., 2002]. In a murine model, tumour growth factor β (TGFβ) induced class-switching to IgA, while IL-2 and IL-5 promoted IgA secretion [Cazac and Roes, 2000]. In contrast IL-6 may support IgG_2a and IgG_2b [Kopf et al., 1998]. The cytokine interleukin-13 (IL-13) is particularly interesting as it is thought to be involved in Th2-mediated allergic inflammation. IL-13 along with IL-4 can induce expression of IgE and IgG_4 antibodies, and can also promote activation of inflammatory cells such as macrophages [Wynn, 2003]. IL-13 can signal through its own receptors (IL13-Ra/b) but also via the IL-4 receptor [Wynn, 2003], and can stimulate

the spontaneous secretion of IgE and IgG_4 in the blood of patients with nephrotic syndrome, indicating that IL-13 alone can modulate immune responses, without the involvement of IL-4 (Kimata et al., 1995). In the context of melanoma it has been reported that patient lymph nodes infiltrated by melanoma cells have higher expression levels of IL-13 mRNA when compared to lymph nodes with no tumour cell metastases [Torisu-Itakura et al., 2007]. This might indicate that IL-13 is involved in mechanisms of immune modulation in melanoma.

1.3.5.1 The role of IL-10 in class switching towards IgG_4

One of the most interesting cytokines in immune regulation is interleukin 10 (IL-10) with its pleiotropic activities in T-, B-, NK-cells and macrophages. As one of the strongest suppressors of immune activation, IL-10 was first described as cytokine synthesis inhibitory factor (CSIF) for down-regulating IFN-γ in T- and NK-cells. The involvement of IL-10 with B cells and the alteration of their antibody repertoires were investigated in the last decade. Analysing the modulatory potential of artificially generated T cell clones with different IL-10 profiles on $CD19^+$ B cells, Satoguina et al. showed that IgG_4 production correlated with IL-10 and that adding recombinant IL-10 to IL-10-deprived co-cultures induced IgG_4 polarisation [Satoguina et al., 2005]. As these correlations were modest (r^2=0.352) the authors postulated that IL-10 is not the only causal factor. In a subsequent study the same group showed that cell-cell contact involving the glucocorticoid-induced tumour necrosis factor and its ligand in the presence of IL-10 but not TGF-β were instrumental in IgG_4 production [Satoguina et al., 2008]. These two studies suggested that IL-10 is a key factor contributing to polarisation of B cells to produce IgG_4. Research into allergen immunotherapy in patients with seasonal allergies revealed that an early induction of IL-10 and late production of IgG_4 antibodies occurs in patient circulation as a result of these treatments, giving rise to the idea that these antibodies could be partly inhibitory when competing with other antibodies for recognition of the allergen [Francis et al., 2008, James et al., 2012]. In a more recent study, van de Veen et al. confirmed that allergen tolerance has two essential features, one being the aforementioned IL-10 producing B-cells and IgG_4 expressing B cells [van de Veen et al., 2013]. Also in cancer, pioneering work by Daveau and colleagues reporting an IgG_4 increase in the sera of melanoma patients compared to healthy volunteers is

indicative of potential roles of IL-10 and IgG$_4$ in cancer. The above-discussed studies suggest that there may be various immune modulatory mechanisms at play in different disease settings and possibly in melanoma, which may determine the nature, specificity and strength of the humoral response against cancer antigens. IL-10 is one component of the immune response likely to be involved, and therefore its role and impact in redirecting antibody responses in cancer are investigated as part of this thesis.

1.4 IgG$_4$ antibodies in inflammatory diseases, allergy and cancer

This section describes the characteristics of the antibody subclass IgG$_4$ (1.4.1) and explores its role across three different disease entities - inflammatory diseases (1.4.2), allergy (1.4.3) and cancer (1.4.4) - to understand its biological involvement in these diseases. This is the basis for the subsequent discussion of antibody and B cell responses in melanoma (1.5).

1.4.1 IgG$_4$ antibody structure and functional implications

There are four subclasses of IgGs (1-4) and IgG$_4$ has been discovered fourth in serum, hence the name. The concentration of IgG$_4$ ranges from 10 μg/ml to 1 mg/ml, accounting normally for 2 - 3% of the total concentration of IgG (10 mg/ml)antibodies in the blood [Aucouturier et al., 1984, French, 1986]. IgG$_4$ is distinct from the other IgG subclasses for its low or negligible immune cell activation potential. It only mediates reduced or no ADCC via Fcγ receptors. Moreover it is unable to bind C1q protein complexes and consequently cannot activate the classical complement pathway. Although IgG$_4$ shares 95% structural homology with IgG$_1$, its affinity to FcγRI and FcγRII is reduced mostly due to the K_{off} (dissociation from the receptor). Structural differences between IgG$_1$ and IgG$_4$ have been localized to a few amino acid differences. In particular the amino acid position 331 (P331S; Proline→Serine) is important for the binding of the antibody to C1q while L234F (Leucine→Phenylalanine) as well

as P331S are important amino acids for the affinity to Fcγ receptor I [Bruhns et al., 2009, Tao et al., 1993, Brekke et al., 1994, Canfield and Morrison, 1991]. However, the most striking difference between IgG$_1$ and IgG$_4$ lies in the hinge regions involving two proline residues in the IgG$_1$ and a proline and serine residue in the IgG$_4$ sequences at the core of the hinge. These changes establish equilibrium between inter-heavy chain disulphide bonds (classical disulphide) and intra-chain disulphide bonds (non-classical disulphide) giving IgG$_4$ its unique ability to exist as a "half molecule". This initial form ("half molecule") is ultimately responsible for the reported bi-specificity of IgG$_4$ antibodies [Bloom et al., 1997, Schuurman et al., 2001, Angal et al., 1993] (Figure 1.9).

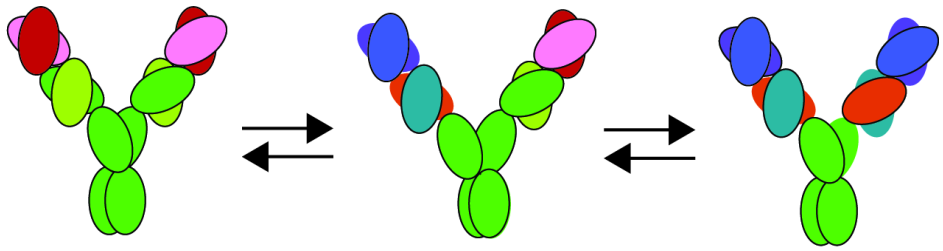

Figure 1.9: IgG$_4$ Fab-arm exchange occurs between two IgG antibodies by the exchange of a heavy chain-light chain pair. The resulted molecule does acquire two distinct Fab arms and therefore become bispecific.

	FcγRI	**FcγRIIa**	**FcγRIIb**	**FcγRIIc**	**FcγRIIIa**	**FcγRIIIb**	**FcRn**
IgG_1	650	52	1.2	1.2	20	2.0	80
IgG_2	–	4.5	0.2	0.2	0.7	–	NA
IgG_3	610	8.9	1.7	1.7	98	10	NA
IgG_4	340	1.7	2.0	2.0	2.5	–	NA

Affinity constant of Fcγ receptors (x $10^5 M^{-1}$) [Balch et al., 2009]

– indicates no binding and NA indicates not analysed

Affinities for FcγRIIa variant H_{131} and for FcγRIIIa variant V_{158} are displayed

Table 1.2: Affinity of IgG subclasses for Fcγ receptors

Bi-specific IgG$_4$ antibodies were found *in vitro* in the presence of reducing reagents and developed spontaneously *in vivo* by injecting equal amounts of two recombinant IgG$_4$ antibodies. This process is presumably unique to IgG$_4$ antibodies was termed "Fab-arm exchange" [van der Neut Kolfschoten et al., 2007]. More recent studies have reported that a change in residue 409 (Lysine→Arginine) in the CH_3 region is a key component of "Fab-arm exchange", making CH_3 a second domain on which "Fab-arm exchange" depends [Davies et al., 2013, Labrijn et al., 2011, Rose et al., 2011]. Class switching and physiological IgG$_4$ responses can be induced by prolonged or repeated antigen exposure in combination with a Th2 cytokine environment. Especially the cytokines IL-10, IL-13 and IL-21 have been reported to favour IgG$_4$ over IgE [Satoguina et al., 2008, Maehara et al., 2012].

1.4.2 IgG$_4$ antibodies in inflammatory diseases

The cutaneous blistering diseases pemphigus vulgaris and pemphigus foliaceus were among the first diseases where IgG$_4$ antibodies were first reported to mediate an immune reaction against desmoglein 1. Destruction of the junction protein desmoglein 1 leads to the milder form of the disease [Rock et al., 1989, Warren et al., 2003]. Additionally, IgG$_4$ autoantibodies against the M-type phospholipase A2 receptor or the metalloproteinase ADAMTS13 were reported to play a major role in idiopathic membranous glomerulonephritis [Beck and Salant, 2010] and thrombocytopenic purpura [Ferrari et al., 2009] respectively. The identification of a newly recognised condition termed IgG$_4$-related disease adds to the IgG$_4$-associated pathologies. This fibro-inflammatory condition can be characterized by several features: a tendency to form sclerotic lesions at multiple body sites; a dense lymphocytic infiltrate rich in T cells and IgG$_4$ producing plasma cells; and optional elevated serum IgG$_4$ concentrations. The disease was initially discovered in the pancreas leading to the classification of Type 1 and Type 2 autoimmune pancreatitis, whereby Type 1 is used as a synonym for IgG$_4$-related autoimmune pancreatitis [Hamano et al., 2001]. As IgG$_4$-related pancreatitis is frequently observed in associated extrapancreatic fibro-inflammatory lesions harbouring IgG$_4$ cells, the term IgG$_4$-related diseases was expanded to include conditions in other organ systems like the biliary tree, salivary glands, periorbital tissues, kidneys, lungs, lymph nodes, meninges, aorta, breast, prostate, thyroid, peri-

cardium and skin. The common characteristics shared by IgG$_4$ across different sites are found to be the histopathological features described above as the features of fibro-inflammatory condition. Moreover IgG$_4$-related disease features a high number of infiltrating IgG$_4$ positive cells in various organs accompanied by a diffuse T cell infiltrate that includes activated T_{regs}, distinguishing it from other autoimmune diseases. Additionally, these infiltrating cells do not appear to form part of any organised structure resembling a classical germinal centre-like formation [Stone et al., 2012,Zen and Nakanuma, 2010,Deshpande et al., 2011,Deshpande et al., 2012,Cornell et al., 2007, Kasashima et al., 2008]. Unrelated disorders like Mikulicz's syndrome (benign lymphoepithelial lesion), Küttner's tumour (chronic sclerosing sialadenitis), multifocal fibrosclerosis and eosinophilic angiocentric fibrosis are now also considered to belong to IgG$_4$-related disease group [Geyer et al., 2010, Deshpande et al., 2011]. As the disease location and pathophysiology has a high variability, the main diagnostic criteria remain the histopathological assessment. Three features have been defined for the diagnosis of IgG$_4$-related disease: 1) Dense lymphoplasmacytic infiltrate with IgG$_4$ positivity, 2) Fibrosis arranged at least focally in a storiform pattern and 3) Obliterative phlebitis.

1.4.3 Increased IgG$_4$ levels in allergic patients receiving immunotherapy

Specific immunotherapy (SIT) involves the administration of allergens to achieve clinical tolerance with the aim of easing the symptoms in patients with allergic conditions. Long-term clinical benefits of SIT persist even after discontinuation of therapy, indicating the involvement of a cellular memory component to this therapy. The mechanism behind the therapy has been extensively studied, but still remains a focus of research and debate. Research on SIT has to-date focused on altered T lymphocyte responses and induction of allergen specific IgG$_4$ antibodies. Two individual patterns of change, which may occur sequentially, have been described. The first event is induced within 1-4 weeks and entails the generation of regulatory T cells secreting IL-10 and TGFβ, accompanied by suppression of allergen-induced late cutaneous responses. Subsequently, around week 10 post-challenge, elevated serum titres of allergen-specific IgG$_4$ and IgA are observed. While these titres appear pro-

portional to the dose of administered antigen rather than to clinical improvements, some reports suggest that the capacity of IgG_4 antibodies to block IgE functions correlate with clinical responses [Canonica et al., 2009, Shamji et al., 2012]. These events coincide with a decrease of allergen-specific IgE antibodies and a shift in the allergen specific T cell response from predominantly a Th_2 to Th_1 type [Canonica et al., 2009]. Serum obtained from patients following SIT has been shown to inhibit allergen-IgE binding to B cells, thus affirming the effect mediated largely by IgG_4 antibodies in patient sera. This *in vitro* system introduced the idea that SIT triggers production of "blocking antibodies" that inhibit IgE functions such as IgE-facilitated antigen presentation (FAP) on B cells. Similarly, basophil histamine release assays or basophil activation assays have demonstrated the functional ability of IgG_4 to inhibit IgE-dependent activation and mediator release either by competing with IgE for the antigen and/or by stimulation of surface IgG-inhibitory receptors present on basophils and mast cells [Shamji et al., 2012, James et al., 2012]. Interestingly, IgA antibodies could not block allergen-IgE binding to B cells. The contribution of IgA in the responses to SIT may lie in engagement of surface IgA receptors and release of the inhibitory cytokine IL-10, which may participate in the induction of immune tolerance to allergens [Pilette et al., 2007]. The mechanisms triggering elevated IgE-neutralizing antibodies following SIT are not completely understood, although it is known that prolonged exposure to antigenic stimuli can direct production of IgG_4 by B cells. B cells can switch from IgG_4 to IgE but not vice versa, as these sections of the gene are spliced out during class switching recombination. Thus, it is assumed that IgG_4 must be produced by switching from IgM, IgG_{1-3} or IgA1, or by proliferation of pre-existing $IgG_4{}^+$ B cells during SIT. It has been suggested that Th2 cytokine environments with elevated levels of IL-10 can drive the differentiation of IgG_4-switched B cells to IgG_4-secreting plasma cells [Satoguina et al., 2005]. In addition to IL-10, the immunoregulatory cytokine IL-21 has been found to increase IgG_4 production *in vitro* [Wood et al., 2004]. The IgE-neutralizing and tolerogenic properties of IgG_4 may be partly due to competing with allergen-specific IgE for antigen specificity. However, since only a fraction of IgG_4 antibodies are allergen specific after immunotherapy, other mechanisms may be involved. Van der Neut Kolfschoten and colleagues used recombinant IgG_4 antibodies against grass and cat allergens, which when co-injected in a mouse graft, became bi-specific by "Fab-arm exchange" [van der Neut Kolfschoten et al., 2007]. The resulting bi-specific IgG_4 antibodies might reduce binding of IgE antibodies for allergens and interrupt IgE-FcϵRI-multivalent allergen

complex formation on the surface of immune effector cells. These properties could therefore moderate IgE-mediated inflammatory cascades, consistent with the observations that IgE effector cells such as eosinophils, mast cells or basophils are reduced after SIT against house dust mite and grass pollen [Passalacqua et al., 1999]. An additional mechanism by which SIT can tolerize allergic immune responses may be due to the ineffective Fc-mediated functions of IgG$_4$. Lacking complement activator properties and mediating ineffective FcR signals, IgG$_4$ antibodies could have reduced capacity to trigger cytotoxicity or phagocytosis and may thus fail to activate immune responses.

1.4.4 IgG$_4$ and cancer

Although IgG$_4$ has recently been associated with a group of fibro-inflammatory conditions termed IgG$_4$-related disease, the presence of IgG$_4$ antibodies or IgG$_4$+ B cells in cholangiocarcinoma, pancreatic cancer, lymphoma and squamous cell carcinoma have previously been described [Harada et al., 2012, Stone et al., 2012, Strehl et al., 2011]. IgG$_4$ has attracted interest in pancreatic cancer as initial studies postulate that this antibody subclass could be used to distinguish between autoimmune pancreatitis and pancreatic cancer [Raina et al., 2008, Kasashima et al., 2008, Kamisawa et al., 2008, Kawa et al., 2012]. Furthermore, a study in extrahepatic cholangiocarcinoma demonstrated abundant IgG$_4^+$ immune cell infiltration and postulated that cancer cells that expressed HLA-DR and secreted IL-10 could act in a similar capacity to regulatory T cells and modulate the humoral response in favour of IgG$_4$ [Harada et al., 2012]. In a preliminary study, squamous cell carcinoma has been reported to have an IgG$_4$ immune infiltrate component; however the roles of these infiltrates was not further investigated [Strehl et al., 2011]. While IgG$_4$ has been intensely investigated in allergen immunotherapy, its role in the pathogenesis of cancers remains poorly understood. Different association studies indicate the presence or involvement of this antibody class in various cancers including melanoma, thus suggesting the merit of further investigating the potential contributions of IgG$_4$ in redirection of immune responses and tumour-induced immune escape.

1.5 Antibody and B cell responses in melanoma

Although immunological research in melanoma has focused mainly on T cells, the immune cell infiltrate comprises an array of different stromal as well as immune inflammatory cells such as macrophages, neutrophils, NK cells and also B cells [Clemente et al., 1996, Erdag et al., 2012]. In general, the antigen-specific B cell response is not yet fully explored in melanoma. This section describes what is known about humoral responses and specifically IgG_4 in circulation (1.5.1) and in tumour lesions of patients with melanoma (1.5.2 - 1.5.3).

1.5.1 Circulating B cell and antibody responses in patients with melanoma

Attempts to study the humoral response in melanoma have focused on circulating antibodies in patient sera [Stockert et al., 1998, Trefzer et al., 2006]. These studies reported a humoral response against specific tumour-associated antigens (TAA) such as the cancer-testis antigen NY-ESO-1 as well as against autologous tumour cells. Moreover, they demonstrated that a tumour-antigen specific response takes place in the context of melanoma at least in the temporal setting. Interestingly, Sittler et al. demonstrated that whole-cell vaccine therapy that triggers antibodies directed against auto-antigens does not induce autoimmunity, indicating that even though some tumour antigens might be also expressed by normal somatic cells the vaccine-induced autoantibodies are neither lethal nor cause toxicity [Sittler et al., 2008]. The presence of tumour cell-reactive B cells in the peripheral blood of patients indicates that these cells might mature in the tumour microenvironment or could also be the product of adaptive immune responses occurring elsewhere in the body such as in draining lymph nodes [Yamaguchi et al., 1987, Kirkwood and Robinson, 1990]. Until recently, it was not clear whether serum autoantibodies in melanoma signified a local or systemic memory response. Our group reported the presence of a tumour-reactive mature memory B cell response in the circulation of 21 patients with melanoma. This reactivity was found against a multitude of cell-surface antigens expressed across different melanoma cell lines, but less so against antigens on the surface of primary

human melanocytes. We also observed appreciable frequency of tumour cell reactive antibodies expressed by mature memory B cells in human melanoma against cell surface antigens on allogeneic melanoma cells studied by limiting dilution analysis. We furthermore established that tumour-reactive B cell frequency was higher in early disease stage patients (stage II) and decreased in late stage disease patients (stages III - IV). These data are in agreement with reports of a collapsed memory B cell compartment in the circulation of patients with advanced melanoma [Carpenter et al., 2009]. In our study, we also demonstrated that a patient derived IgG monoclonal antibody can activate human monocytic cells to kill tumour cells by cytotoxicity, while a non-reactive monoclonal antibody derived from the same patient did not display any tumour killing activity [Gilbert et al., 2011]. Taken together, our data suggested that although a tumour-reactive memory B cell compartment exists in the circulation of patients with melanoma and patient-derived antibodies harbour the potential to activate effector functions against cancer, this memory B cell compartment diminishes with disease progression. We reasoned that humoral immunity is not oblivious to the presence of melanoma, however, B cell responses might be subject to suppressive signals, most likely orchestrated though numerous inflammatory mediators in tumours and the circulation which may be triggered by the presence of melanoma

1.5.2 B cell infiltrates in melanoma lesions

As mentioned above, a number of studies analysed the presence and prognostic significance of B cell infiltrates in the tumour microenvironment of colorectal cancer, breast cancer and melanoma. Maletzki *et al.* showed that B cells infiltrating colorectal cancer produce cancer cell specific antibodies. Mahmoud and colleagues correlated the number of infiltrating $CD20^+$ cells with overall survival benefit in breast cancer patients, while Erdag showed that the immune cell infiltrates containing a bigger proportion of $CD20^+$ cell have better clinical outcome in melanoma [Maletzki et al., 2012, Mahmoud et al., 2012, Punt et al., 1994, Erdag et al., 2012]. An initial study analysing the outcome of a bioengineered GM-CSF tumour cell vaccine reported that higher titres of IgG antibodies against the H^+-ATPase (ATP6S1) correlates with tumour destruction and prolonged patient survival [Hodi et al., 2002]. This study

suggests that potent humoral responses can induce immune cell mediated tumour cell destruction. Despite this limited evidence of the benefit of B cell infiltrates in cancer, the roles of melanoma-specific antibody-producing B cells are not yet fully elucidated and similarly to T cells, B cells may also be subject to tumour-induced modulatory signals which may impair their capacity to trigger effective anti-tumoural functions.

1.5.3 Impairment of immune responses by antibodies through alternatively activated B cells and antibodies

Dysregulation of the immune response has been described in metastatic melanoma and other cancers with $CD4^+$ T helper cells primed towards a more dominant TH_2 phenotype producing cytokines such as IL-4, IL-5, IL-6, IL-10 and IL-13 [Tan and Coussens, 2007]. In addition, it is believed that infiltrating T_{regs} and B_{regs} may induce immune suppressive conditions independently of TH_1 TH_2 or TH_{17} environments by means of secreting cytokines such as TGF-β, granzyme B and IL-10 [Lindner et al., 2013]. It has been suggested that the humoral arm of the immune response may be biased by the immunoregulatory cytokine IL-10, which polarizes B cells to produce IgG_4 antibodies, but until recently, this was not demonstrated in any cancer including melanoma [Platts-Mills et al., 2004, Satoguina et al., 2005]. However, descriptive evidence that the humoral immune responses may be redirected in the context of melanoma was published a number of years ago by Daveau *et al.* who reported dysregulation of IgG_4 levels in the sera of melanoma patients compared to sera of healthy volunteers [Daveau et al., 1977]. Ten years later, in a comprehensive study, Neuberger and colleagues compared the effectiveness of a matched set of chimeric antibodies with different subclasses showing that IgG_4 mediated ineffective complement activation and antibody dependent cytotoxicity [Brüggemann et al., 1987]. These poor effector functions were thought to be solely attributable to the very low affinity of IgG_4 to its cognate Fcγ receptors and its poor ability to bind complement [van der Zee et al., 1986]. However, Bruhns et al. have shown in a recent study that IgG_4 has a comparatively high affinity to FcγRI, one of the main activatory receptors of IgG (for affinity of IgG_4 see Table 1.2) [Bruhns et al., 2009]. The discovery of "Fab arm exchange" by van der Neut Kolfschoten et al. revolu-

tionised the field of antibody-antibody interaction research as the authors confirmed that IgG_4 has the unique capacity to exchange Fabs with other antibodies, reducing those antibodies' affinity to their target antigens and significantly reducing the biological functions of those antibodies' [van der Neut Kolfschoten et al., 2007]. The "Fab arm exchange", unique to IgG_4, may contribute to the anti-inflammatory activities attributed to this antibody subclass. New interest in IgG_4 emerged following the recognition of a new group of fibro-inflammatory conditions termed IgG_4-related disease [Stone et al., 2012]. As this condition is associated with sclerotic diseases, several studies have been conducted to investigate if IgG_4 could be used as a predictive marker for autoimmune pancreatitis (AIP) [Ghazale et al., 2008, Oseini et al., 2011, Choi et al., 2007, Hirano et al., 2006, Hamano et al., 2001]. The control cohorts of these studies included patients with pancreatic cancer, but while AIP samples were distinct from pancreatic cancer samples, it is notable that serum IgG_4 is elevated in pancreatic cancer compared to healthy controls. These findings suggested that IgG_4 might be of importance in malignant conditions. A more recent study confirmed the functional relevance of IL-10 in inducing $IgG_4{}^+$ plasma cells in extrahepatic cholangiocarinoma [Harada et al., 2012]. A follow-up study showed a positive correlation between the presence of $IgG_4{}^+$ cells with $FoxP3^+$ cells but no correlation between $IgG_4{}^+$ cells with $CD8^+$ cells, suggesting that alternatively-activated humoral immune responses are associated with other regulatory elements in the tumour microenvironment [Kimura et al., 2012]. Taken together, the above studies confirm that IgG_4 production represents a biologically significant mechanism that contributes to reducing the potency of immune responses and this may be a mechanism found in some malignancies. Therefore this antibody subclass is of special interest to the work presented in this thesis.

1.6 Discovering novel antibodies for cancer treatment

Antibodies recognising cancer antigens were originally derived from immunizing mice with tumour cell lysates, proteins or epitopes of tumour-associated proteins. The first antibodies were produced using hybridoma technology, which for the first time

yielded sufficient amounts of antibody for further investigations of antibody efficacy in cancer therapy. The first mAbs had some drawbacks: derived from mice upon administration in patients, the human immune system mounted a brisk human anti-mouse antibody (HAMA) response with production of host antibodies that neutralised the on-target therapeutic effects of these antibodies and cleared them from the circulation; thereby vastly-reducing their therapeutic effects against cancer and causing toxicities. The advent of recombinant DNA technology enabled the construction of chimaeric (mouse variable and human constant regions) [Sahagan et al., 1986], humanized [Jones et al., 1986, Carter et al., 1992] and human antibodies. All these types of antibodies can trigger neutralising antibody responses [Winter and Harris, 1993, Jakobovits et al., 2007, Lanzavecchia et al., 2007]. Indeed, HACA (human anti-chimeric antibody) and HAHA (human anti-human antibody) responses have been reported in patients. Phage display is an *in vitro* technology established for the discovery of fully-human antibodies. It is designed to mimic the natural immune process of antibody affinity maturation in an *in vitro* setting. This process uses filamentous bacteriophages that display single-chain variable region antibody fragments (scFv) on their surface. Immune selection is then mimicked by direct binding of the phage to a specific antibody or antigen. The phagemids bound to the antigen are eluted after removal of unbound phages in a series of panning steps. Panning can enrich the most specific phage by 20-10,000 fold per round, eventually leading to the selection of the variable region sequences with the highest affinity to the target antigen. Similarly to the equivalent *in vivo* immune process, the V gene in this phage can also be subject to random mutations allowing for the selection of mutants with high affinity for the antigen. A limitation of this technique is that to obtain a fully "affinity matured" antibody, the produced antibody heavy chains must be matched with random light chains [Winter and Harris, 1993]. Recently technologies using human transgenic mice such as the Xenomouse© were introduced to produce fully-human antibodies through a process of immunizing animals *in vivo*. These mice express the human immunoglobulin gene loci and secrete human antibodies, which are subsequently immortalized by standard hybridoma technology *in vitro* [Jakobovits et al., 2007]. More recent developments include the use of humanised mice (HIS-mice) that have been injected with human $CD38^+$ lymphocyte progenitors and subsequently immunized with antigen. As these mice develop a human immune system, it is thought that this approach better mimics the antigen processing and antibody maturation leading to a more "natural" antibody response [Becker et al., 2010]. Following speci-

ficity screening, positive antibodies from the HIS-mouse are recombinantly produced using a novel transfection and expression system allowing for a quicker evaluation of the discovered agent [Kwakkenbos et al., 2010]. The approach to derive antibodies from human B lymphocytes is also of interest in this context. Although the idea and attempts to implement it dates back over four decades, maintaining and immortalising B cells *ex vivo* has proven challenging. In 2004, Traggiai *et al.* proposed a new method to obtain fully-human antibodies by isolating B cells from human blood, growing them in culture, immortalizing them with Epstein Barr virus (EBV), while simultaneously activating them with the toll-like receptor 9 (TLR-9) agonist CpG 2006 ODN. Supernatants from these B cell cultures were screened against the SARS virus to select B cells, which secreted antibodies specific to virus envelope proteins. Using this approach, the team was able to screen and generate 35 neutralizing monoclonal antibodies against the SARS coronavirus from a convalescent patient. From these results it was concluded that the B cell pool of a patient can be interrogated at any time after priming with the only limiting factor being the large number of cells, which need to be screened to access specific antibodies [Traggiai et al., 2004,Lanzavecchia et al., 2006]. These technologies, together with recombinant protein expression platforms have allowed for the development of many strategies to engineer, examine and apply antibodies as therapeutic agents in cancer and other diseases.

1.6.1 Monoclonal antibody approaches for cancer therapy

Most monoclonal antibodies used in immunotherapy of cancer patients recognise epitopes of tumour-associated antigens (TAA) on the surface of tumour cells therefore binding to tumour cells rather than somatic cells with high specificity and affinity. These interactions result in tumour cell destruction by a number of mechanisms. There are more than 15 approved antibodies for the treatment of cancers such as non-Hodgkin lymphoma, leukaemia, breast and colorectal carcinomas (Table 1.3). Moreover, 165 novel antibody candidates (54% in Phase I; 39% in Phase II and 7% in Phase III) are being tested in clinical trials for various indications [Reichert and Dhimolea, 2012,Reichert, 2011,Weiner et al., 2010,Scott et al., 2012]. Only about half of the candidates are full-length IgG antibodies, while the others comprise antibody drug conjugates (ADC), multi-specific or otherwise engineered forms of antibodies.

These numbers indicate that non-canonical antibodies are currently being developed at fast pace. Furthermore, efforts to enhance efficacy by improving Fc Receptor affinity, specificity and effector functions are receiving increased attention [Woof, 2012].

1.6.2 Antibody modalities in clinical use for cancer therapy

Most of the antibodies now in clinical use target surface proteins highly expressed on cancerous cells (TAA) with the most targeted antigens including the epithelial cell adhesion molecule (EpCAM), mucin-1 (MUC1), epidermal growth factor receptor (EGFR), carcinoembryonic antigen (CEA), CD20, CD33, CD52, CD22, Lewis Y, prostate-specific membrane antigen (PSMA), human epidermal growth factor receptor 2 (HER2/neu), as well as elements found in tumour-associated vasculature such as the vascular endothelial growth factor (VEGF). The anti-CD20 mAb Rituximab was the first mAb to be approved for cancer therapy. The United States Food and Drug Administration (FDA) approved it for the treatment of B cell lymphomas in 1997. Today, anti-CD20 antibodies are integrated into standard treatment regimes and can significantly improve patient survival for CD20-positive B cell malignancies [Fisher et al., 2005, Swenson et al., 2005, Cheson and Leonard, 2008]. Trastuzumab, which is licensed for the treatment of HER2/neu-positive breast carcinomas, constitutes a milestone for the potential efficacy of antibody therapies for the treatment of solid tumours [Reichert and Valge-Archer, 2007]. In a review article, Reichert *et al.* reported that antibodies that are currently clinically evaluated target 92 distinct antigens. Only one antibody is tested for each of 65 antigens while the remaining 27 antigens are targeted by an average of three antibodies each. Despite a growing interest in novel TAAs, well-validated targets such as EGFR, HER2/neu and CD20 are among the top five most frequently selected targets for antibody immunotherapies (targeted by 33 mAbs in clinical studies). Presently more than 15 antibodies are licensed for the treatment of different malignancies [Reichert and Dhimolea, 2012]. Notwithstanding the mentioned successes, there are still no effective approved antibodies for the treatment of many tumours, suggesting that antibody therapeutics have not yet reached their full potential. Therefore an unmet clinical need persists

for more effective antibodies that can recognise and kill tumour cells, especially in the context of solid tumours such as melanoma.

1.6.3 Antibody-mediated mechanisms of action against cancer cells

Antibodies can mediate tumour cell death and inhibit tumour progression by a number of mechanisms. These include direct effects blocking vital growth signals, disrupting cell surface antigen association with growth factors, blocking intracellular signalling cascades to reduce tumour cell proliferation and engendering apoptosis. Antibodies are also capable of activating various components of the immune system with potent tumour killing capacity. These include: 1) recruitment and activation of effector cells (T-lymphocytes, dendritic cells, granulocytes, NK cells and monocytes) through recognition of Fc receptors on these cells; some of these cells may kill tumour cells by cytotoxicity and/or phagocytosis (Figure 1.10); 2) modulation of regulatory mechanisms by targeting regulatory immune cells such as T_{regs} (e.g. anti-CD25) or by targeting cell surface molecules that are important checkpoints restricting T cell activation (e.g. anti-CTLA4 blockade).

Antibodies can also exert anti-tumoural functions by activating the classical pathway of the complement system [Brüggemann et al., 1987, Christiansen and Rajasekaran, 2004, Nestle, 2006, Schadendorf et al., 2006]. Monoclonal antibodies licensed for the treatment of cancer are known to kill tumour cells by one or more of the above mechanisms.

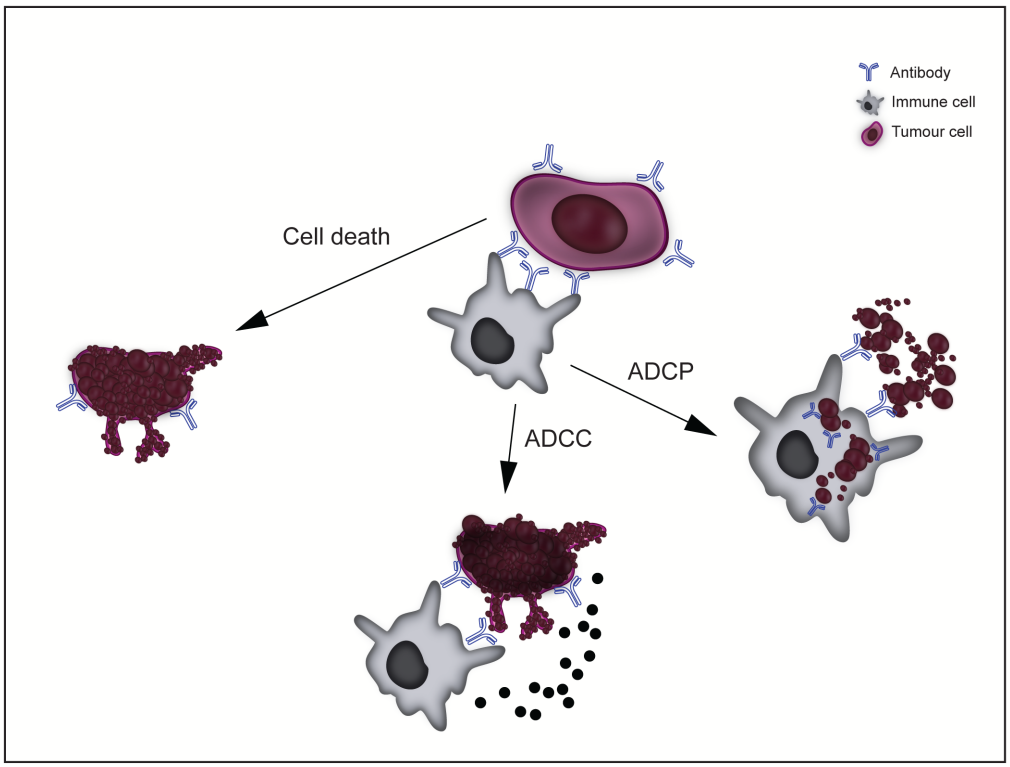

Figure 1.10: Different antibody dependent/induced mechanisms against cancer cells. Indicating three of the most important antibody mediated mechanisms antibody dependent immune effector cell mediated cytotoxicity (ADCC), antibody dependent immune effector cell mediated phagocytosis (ADCP) and induction of direct cell death (e.g. apoptosis/ growth arrest) by cell signaling activation.

Generic name (trade name)	Target	Specification	FDA or EMA approval date (indication)	Mechanisms of action
Alemtuzumab (Campath)	CD52	humanized IgG_1	2001 (Chronic lymphocytic leukemia)	Direct induction of apoptosis and CDC
Bevacizumab (Avastin)	VEGF	humanized IgG_1	2004 (colorectal cancer)	Inhibition of VEGF signalling
Brentuximab vedotin (Adcetris)	CD30	chimeric IgG_1	2011 (anaplastic large cell lymphoma; Hodgkin lymphoma)	Delivery of toxin payload (auristatin toxin)
Cetuximab (Erbitux)	EGFR	chimeric IgG_1	2004 (colorectal cancer; head and neck cancer)	Inhibition of EGFR signalling and ADCC
Catumaxomab (Removab)	CD3 and EpCAM	rat-mouse bispecific	2009 approved by EMA (malignant ascites in EpCAM+ ptients)	Immune cell engagement
Denosumab (Xgeva)	RANKL	human IgG	2010 (tumour bone metastasis)	Inhibition of RANKL
Gemtuzumab (Mylotarg)	CD33	humanized IgG_4	2000 (acute myelogenous leukemia)	Delivery of toxic payload (calicheamicin toxin)
Ibritumomab tiuxetan (Zevalin)	CD20	murine IgG_1	2002 (non-Hodgkins lymphoma)	Delivery of radioisotope ^{90}Y
Ipilimumab (Yervoy)	CTLA-4	human IgG_1	2011 (melanoma)	Inhibition of CTLA4 signalling
Ofatumumab (Arzerra)	CD20	human IgG_1	2009 (chronic lymphoid leukemia)	ADCC and CDC
Panitumumab (Vectibix)	EGFR	human IgG_2	2006 (colorectal cancer)	Inhibition of EGFR signalling
Pertuzumab (Perjeta)	HER2/neu	humanized IgG_1	2012 (breast cancer)	Inhibition of HER2 dimerisation
Rituximab (Rituxan)	CD20	chimeric IgG_1	1997 (non-Hodgkin lymphoma)	ADCC, CDC, and induction of apoptosis
Tositumomab (Bexxar)	CD20	murine IgG_2	2003 (non-Hodgkin lymphoma)	Delivery of radioisotope ^{131}I, ADCC and direct induction of apoptosis
Trastuzumab (Herceptin)	HER2/neu	humanized IgG_1	1998 (breast cancer)	Inhibition of HER2\neu signalling, ADCC and ADCP
Ado trastuzumab emtansine (Kadcyla)	HER2/neu	humanized IgG_1	2013 (breast cancer)	Delivery of toxin payload (emtansine)

Table 1.3: Monoclonal antibodies currently approved by FDA and EMA

The mechanisms employed by antibodies to target and kill cancer cells are important measures of potential efficacy in cancer therapy. Hence, implementation of appropriate assays to elucidate the mechanisms by which antibody candidates exert anti-tumoural effects as well as functional assays to evaluate their mechanisms of action and potency are highly desirable and expected to inform the design and evaluation of effective future therapies for cancer. This work has therefore also focused on evaluating the effector functions of antibodies and on developing strategies to design antibodies with improved efficacy. A number of functional assays to characterise and evaluate the mechanisms of action and anti-tumoural efficacy of these antibodies engineered with Fc regions of different antibody classes and subclasses are employed and described herein (Chapter 5).

1.6.4 Identifying antibodies for the treatment of melanoma

Potential targets for antibody therapeutics include known surface melanoma-associated antigens for example MART-1/MelanA, which are commonly overexpressed by melanoma cells but may also be expressed by melanocytes. Targeting these cell surface antigens has resulted in manifestations of autoimmune-like responses in patients such as vitiligo (Boon and van der Bruggen, 1996; Schneeberger et al., 2000). Other targets of antibody immunotherapies have in the past included the cancer testis family of antigens MAGE, BAGE, RAGE or NY-ESO 1 [Boon and van der Bruggen, 1996, Schneeberger et al., 2000]. Although antibody immunotherapy for melanoma has had some success in pre-clinical models and showing promising clinical outcomes [Pedicord et al., 2011,Curran et al., 2010,Chapman et al., 2011,Wolchok et al., 2013], none of the above antigens have served as targets for therapeutics that achieved regulatory approval for clinical use. The strategies for antibody therapies described below have reached clinical trials in patients with melanoma, with the first antibody against one of these now approved for clinical use.

1.6.4.1 Antibodies targeting melanoma vasculature

Antibodies targeting tumour-associated vasculature in order to deprive the tumour of vital nutrients have been developed. The monoclonal antibody bevacizumab that recognises the human vascular endothelial growth factor-A (VEGF-A) is an example of this type of treatment. Bevacizumab inhibits the biological activity of VEGF-A by preventing vascularisation of tumours. This antibody has been tested in combination with the alkylating chemotherapeutic agent fotemustine or with IFN-α2b as a first line treatment for advanced melanoma in randomised phase II trials. Despite reporting early data on suppression of angiogenesis and lymphangiogenesis, the authors highlighted that a high proportion of the patients (5/20) had to discontinue treatment due to toxicity [Del Vecchio et al., 2010].

1.6.4.2 Checkpoint molecule blockade approaches

Antibodies targeting negative regulators of immune activation have had striking successes in recent years. Blocking the negative regulation of T cells these antibodies enable tumour-cell specific T cells to target cancer cells, thus aiming to overcome the immunosuppressive effects of tumour microenvironments. Examples of these checkpoint blockade antibodies are those targeting CTLA 4 and PD-1.

1.6.4.3 Anti-CTLA 4

Antibodies recognising the cytotoxic T lymphocyte-associated antigen 4 (anti-CTLA4) are now promising agents for the treatment of melanoma, they target a key element in T cell immune regulation (CTLA4), which is a main negative regulator for T cell immunity . Anti-CTLA4 antibodies (e.g. tremelimumab, ipilimumab) interfere with CD28-B7.1 (CD80) co-stimulatory signals provided to T cells during antigen presentation competing with CD28 for B7.1 recognition. A recent double-blind phase III study showed that ipilimumab with or without a gp100 peptide improved patient survival [Hodi et al., 2010]. However, adverse events, mostly resembling autoimmune-like reactions are associated with this treatment (e.g. colitis, diarrhoea,

pruritus, dermatitis and fatigue) that can be severe but are mostly reversible with appropriate treatment [Ribas et al., 2005, Kirkwood et al., 2008, Weber et al., 2008]. An additional mechanism of anti-CTLA4 antibody (ipilimumab) function is IgG_1 mediated ADCC against T_{regs}, which are cells shown to overexpress CTLA-4 antigen on their surface. By eliminating T_{regs} in proximity to tumour cells, the tumour microenvironment shifts from being suppressive to becoming more inflammatory. This shift may enhance the potential of cytotoxic $CD8^+$ T cells to eradicate tumour cells [Curran et al., 2010].

1.6.4.4 Co-inhibitory ligands and receptors

Research interest has also focused on other co-inhibitory ligands/ receptors such as 4-1BB (CD137), OX40 (CD134) and PD-1. These molecules are expressed upon activation of immune cells such as T and B cells, and are thought to modulate immune responses in cancer [Pollok et al., 1993, Weinberg et al., 2000, Greenwald et al., 2005, Watts, 2005]. Monoclonal antibodies against PD-1 have so far met with limited success (approximately 30% of melanomas treated with nivolumab had a partial response) while some are currently being further evaluated in clinical trials [Brahmer et al., 2010, Topalian et al., 2012]. More recent studies report that concurrent therapy with nivolumab and ipilimumab provided superior clinical activity compared to that induced by ipilimumab alone. Treatment with the anti-PD-1 antibody lambrolizumab (anti-PD-1) included patients who had disease progression during treatment with ipilimumab and treatment resulted in high rate of sustained tumour regressions [Hamid et al., 2013, Wolchok et al., 2013].

1.6.5 Why directly targeting a tumour associated antigen with a monoclonal antibody may provide benefits for the treatment of melanoma

Anti-CTLA4 therapeutics paved the way for the first successful antibody agent to be used for the treatment of metastatic melanoma. Yet, this therapy is directed against a checkpoint blockade molecule (CTLA4), which is expected to activate all

T cells expressing CTLA4 irrespective of whether they are directed against tumour cells or not. Thus, autoimmune-like toxicities are inevitable. Furthermore, by not selectively targeting immune responses against only cancer cells, such antibodies may not be as efficient as possible. For instance, specific targeting of tumour cells that overexpress the tumour-associated antigen HER2/neu in breast cancer is thought to be efficacious for a number of reasons: a) because of the exquisite specificity against tumour cells, b) the longevity of the anti-tumour effects in restricting proliferation and survival of tumour cells c) focusing effector cells specifically against tumour cells and triggering ADCC and ADCP, d) because the target antigen, HER2/neu, is also thought to be expressed by breast cancer cells with stem cell characteristics, providing a unique opportunity for an antibody to directly target this cell subset normally resistant to most treatments including chemotherapies, and e) treatment with trastuzumab is also thought to trigger adaptive immune response against the target antigen, offering the opportunity to develop a memory response against HER2/neu-expressing tumour cells [Hudis, 2007, Marcucci et al., 2013]. Melanoma is thought to be a highly immunogenic tumour due to naturally occurring immune cell infiltrates, which include cells producing melanoma reactive antibodies and cytotoxic T cells against melanoma antigens in patients. Also, the enhanced prevalence of melanoma in immune compromised patients implies its immunogenic nature of melanoma [Lacy et al., 2012]. Despite this active natural immune response in melanoma, immune cells do not impede tumour development or growth, suggesting that the immune system may be redirected and possibly not sufficiently activated, not least because most tumour antigens are also self-antigens. Nonetheless, not only antibodies reactive to melanoma-associated antigens have been found in the blood of melanoma patients, but also a mature memory B cell compartment expressing antibodies that recognise tumour cells exists in these patients [Gilbert et al., 2011, Zippelius et al., 2007]. Importantly, the presence of these naturally occurring antibodies is not associated with any toxicity or autoimmunity, suggesting that passive immunotherapy targeting self-antigens can be applied to treat melanoma. Thus, developing strategies to directly target tumour-associated antigens holds considerable promise, expected to benefit from tumour cell targeting and expected favourable toxicity profiles.

1.6.5.1 CSPG4: a tumour-associated antigen with multiple functional roles in melanoma

The chondroitin sulphate proteoglycan 4 (CSPG4) also called high molecular weight melanoma-associated antigen (HMW-MAA) or melanoma-associated chondroitin sulphate proteoglycan (MCSP) is a known cell-surface tumour-associated antigen and promising target for antibody therapy. This 280kDa cell-surface proteoglycan was discovered more than three decades ago, it is overexpressed by more than 80% of melanomas and is also thought to be highly immunogenic [Wilson et al., 1981] (Figure 1.11). CSPG4 plays a central role in cancer pathogenesis and progression of melanoma cells by linking multiple oncogenic pathways required for malignant progression. These properties make it an attractive target for therapies, including monoclonal antibodies: (i) CSPG4 expression promotes epithelial to mesenchymal transition at the radial growth phase of melanoma, facilitating progression to the vertical growth phase, this is associated with distant tumour metastases and significantly worse prognosis [Yang et al., 2009]. (ii) CSPG4 interacts with integrins (mostly $\alpha 4\beta 1$) and promotes adhesion, motility and survival of tumour cells, aiding metastasis through focal adhesion kinase (FAK) activation of Src, as well as triggering activation of PI3K/AKT and NFκB pathways, which promotes enhanced survival, chemoresistance, cell motility and migration of melanoma tumour cells [Yang et al., 2004, Chekenya et al., 2008]. (iii) CSPG4 promotes MAPK signalling through receptor tyrosine-dependent and independent pathways, triggering activation of the ERK 1,2, which provide migration, proliferation and epithelial to mesenchymal transition all of which promote tumour cell progression and metastasis. Activation of the MAPK/ ERK 1,2 signalling pathway by CSPG4 also synergises with the effects of constitutively active mutant $BRAF^{V600E}$ on the same signalling cascade. Although $BRAF^{V600E}$ alone is not sufficient to maintain high constitutive activation of ERK 1,2, the combination of CSPG4 expression and $BRAF^{V600E}$ provide an important additional trigger that drives cancer progression through constitutive activation of the MAPK/ ERK 1,2, signalling cascade [Satyamoorthy et al., 2003, Yang et al., 2009]. (iv) CSPG4 is also present on angiogenesis-associated pericytes, which can activate endothelial cell to enhance vessel formation. Thus, anti-CSPG4 antibodies may inhibit another central component that may promote tumour survival and metastasis in the tumour microenvironment [Burns et al., 2010]. (v) CSPG4 plays also similar roles in facilitating disease progression in other cancers (oligodendrocytomas,

gliomas, triple-negative breast carcinomas and squamous cell carcinomas), providing opportunities to develop anti-CSPG4 treatments that may be further applied to other indications. (vi) Recent studies report expression of CSPG4 in BRAF inhibitor-resistant tumours, claiming that anti-CSPG4 therapy prolongs tumour growth inhibition of the clinically approved BRAF inhibitor vemurafenib [Chekenya et al., 2008, Yu et al., 2011]. This may provide an opportunity to target BRAF-resistant tumours with anti-CSPG4 therapies, including monoclonal antibodies. (vii) In several clinical trials, CSPG4 specific antibodies alone or conjugated to radioisotopes or toxins were administered [Larson et al., 1985, Schroff et al., 1985, Spitler et al., 1987], and although there were only modest clinical responses observed, none of the patients in the trials experienced major adverse events [Ferrone et al., 1993, Reisfeld and Cheresh, 1987]. Furthermore, in a group of 300 patients that had been enrolled in an immuno-scintigraphy trial, patients that had received multiple injections of CSPG4-specific antibody displayed significant survival benefits [Bender et al., 1997]. A study by Hamby *et al.* investigated the propensity of sera from different human melanoma patients, immunized monkey or immunized rabbits to inhibit the binding of anti-CSPG4 antibodies to melanoma cells expressing CSPG4. While sera from rabbits as well as from monkeys inhibited binding of some antibody clones, human sera did not inhibit binding of the CSPG4 antibodies to the cell line. This indicated that immunogenicity of human CSPG4 in rodents is different from that in human patients [Hamby et al., 1987].

1.6.5.2 Strategies using CSPG4 as a therapeutic target

Several studies in patients and in animal models have evaluated treatment with either monoclonal antibodies coupled to toxins, or anti-idotype antibodies to mount an immune response against CSPG4. A clinical trial reported that patients treated with anti-idiotypic antibodies and who subsequently developed an adaptive immune response against CSPG4 including anti-CSPG4 antibodies, had statistically significant survival benefits [Mittelman et al., 1992]. These suggested the potential of anti-CSPG4 antibodies to mediate tumour cell death and anti-tumoural immune responses. Likewise, several preclinical studies show that antibodies isolated from rodents immunised with CSPG4 mimotopes and injected into recipient tumour xenograft-challenged mice conferred protection against growth of the xenograft tu-

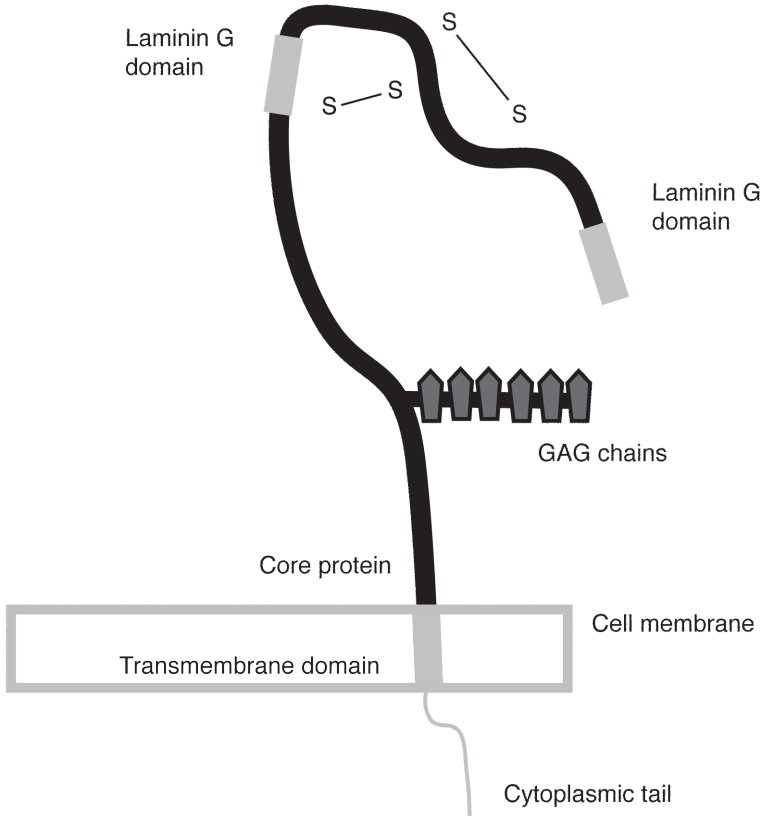

Figure 1.11: CSPG4: schematic representation of chondroitin sulphate proteoglycyan 4. Adapted from [Campoli et al., 2010]

mours [Luo et al., 2005, Wagner et al., 2005, Wagner et al., 2008]. Moreover, anti-idiotypic antibodies mimicking the epitope defined by the anti-CSPG4 antibody clone 225.28s were reported to induce HLA class 1-restricted CSPG4-specific cytotoxic T cells [Murray et al., 2004]. This study infers that immunotherapy against CSPG4 can result in T cell activation and protection from melanoma tumours. Further supporting this hypothesis is the finding that adoptive transfer of cytotoxic T cells engineered to express receptors against CD20 and CSPG4 can block tumour growth and promote regression in animal models of CSPG4-expressing melanoma [Schmidt et al., 2011]. More recent reports show that monoclonal antibodies against CSPG4 inhibit constitutive activation of the MAPK/ ERK 1,2, signalling pathway and enhance the effects of $BRAF^{V600E}$ -specific inhibitors [Wang et al., 2010b, Yang et al., 2009, Yu et al., 2011]. All these attributes and preliminary findings make CSPG4 an attractive target for antibody-mediated immunotherapy.

1.6.5.3 The anti-CSPG4 antibody clone 225.28s

The monoclonal antibody 225.28s was initially generated from mice immunized with the human melanoma cell line M21 COLO38 by hybridizing mouse splenocytes with murine myeloma cells and developing a mouse hybridoma [Ng et al., 1982]. The specific mouse clone was originally used as part of a panel of antibodies to help identify CSPG4 in histological sections with the aim of enabling better diagnosis of melanoma. It was considered necessary to use a variety of antibodies for the detection of melanoma, as CSPG4 was reported to have different determinants with variable expressions during tumour development [Giacomini et al., 1984, Ziai et al., 1987, Neri et al., 1996]. Multiple dosing with the mouse 225.28s antibody conjugated to methotrexate (MTX) showed efficacy at 5 mg/kg doses in a M21 xenograft nude mouse model. Interestingly, isolated tumours from these animals did not show any refractory against the antibody or MTX indicating that this therapy could overcome tumour evasion [Ghose et al., 1991]. The 225.28s antibody was also used in several anti-idiotypic studies to analyse whether the induced antibody response in human sera was CSPG4 specific and could therefore inhibit the binding of the antibody to the antigen [Mittelman et al., 1990, Chattopadhyay et al., 1991]. Likewise the antibodies were used to select mimotopes for vaccination against melanoma since the induced antibodies restrict growth and induce lysis of the melanoma cell line *in vitro* [Wagner et al., 2005]. Mouse anti-CSPG4 225.28s furthermore was shown to inhibit the constitutive activation of MAPK/ ERK 1,2, signalling pathway and to enhance the effects of $BRAF^{V600E}$ -specific inhibitors [Wang et al., 2010a, Yang et al., 2009, Yu et al., 2011]. In a recent study reporting CSPG4 to be an antigen expressed by triple-negative breast cancer, the 225.28s antibody induced growth arrest by restricting colony formation *in vitro* and partly inhibited tumour cell migration of MDA-MB-231 triple negative breast cancer cells *in vitro* [Wang et al., 2010a]. These studies imply that the 225.28s clone recognises an epitope on CSPG4 that is involved in promoting tumour growth, motility and metastasis. The above pre-clinical and clinical studies for clone 225.28s demonstrate promise for this and potentially other antibody therapies that directly target antigens such as CSPG4 on the surface of melanoma cells. However none of these have conclusively demonstrated immune activation. Thus engineering an antibody of this specificity with human Fc regions to also perform effector functions may improve efficacy and clinical translation.

1.7 Using IgE antibodies to target tumours

1.7.1 Rationale for examining the relationship between antibody class and efficacy

Solid tumours such as melanoma are frequently highly refractory to treatment with IgG antibodies. Possible explanations for the partial success of IgG antibodies may be their low affinity for its receptors, resulting in circumscribed capacity to recruit, focus and activate effector cells against cancer cells. Other reasons may include inhibitory mechanisms employed by tumours such as the expression of inhibitory and decoy receptors such as FcγRIIb on effector cells and expression of FcγRIIb receptors by melanoma tumour cells [Andreu et al., 2010]. Efforts to design more efficacious antibodies for cancer have so far either focused on developing conjugates to toxins, cytokines and radioisotopes or concentrated on structural modifications of antibody Fc regions to render them more potent against tumours. The latter involves for instance glycoengineering of antibodies, which has been reported to enhance effector functions [Woof, 2012, Okazaki et al., 2004, Kircheis et al., 2012] and to extend their half-life in the circulation and improve their bioavailability [Kaneko and Niwa, 2011]. A concrete example is the drug-conjugated antibody trastuzumab emtansine-1 (T-DM1) that improved survival of trastuzumab-resistant tumours in a phase III trial [Verma et al., 2012], thus demonstrating not only its efficacy but also superiority to the native antibody. In contrast, an alternative modification uses natural immune surveillance and immune activatory properties of the constant regions of different classes and subclasses of antibodies. This approach potentially leads to a significant enhancement in the abilities of antibodies to function in the context of cancer at different anatomical sites. The human immune system employs nine classes and subclasses of antibodies that differ in Fc regions to combat disease. At present, only IgG (most often IgG_1) is used in immunotherapy of cancers, while antibodies belonging to non-IgG antibody classes such as IgE and IgA have yet not been tested in patients [Woof, 2012]. The use of alternative antibody classes could be of potential benefit as each antibody class operates in different anatomic compartments and functions through unique Fc-receptors and immune effector cells with diverse capabilities to target specific antigens in the body [Reali et al., 2001, Vange-

lista et al., 2005, Karagiannis et al., 2012]. In humans, IgA antibodies comprise two subclasses, IgA1 and IgA2 [Woof, 2011]. IgA is the most hydrophilic antibody class (a characteristic it gains most likely from its glycosylation pattern), thus offering a highly useful and efficacious alternative to IgG immunotherapy for the treatment of mucosal cancers. Studies examining IgA-mediated effector functions, report a role of IgA in maintenance of the mucosal barrier by opsonising pathogens or by inducing immune cell mediated responses in the context of against microbes and parasites [Balu et al., 2011, Bakema et al., 2011]. Likewise, initial investigations demonstrate that IgA mediates efficient tumour cell killing [Bakema et al., 2011, Lohse et al., 2011]. These promising findings need to be further investigated in order to elucidate the full potential of IgA class antibodies in the context of cancer therapy. A number of disparate studies suggest that antibodies of the IgE class can activate immune effector cells to target and kill tumour cells more effectively than the equivalent IgG antibodies [Karagiannis et al., 2009, Karagiannis et al., 2009, Karagiannis et al., 2007]. Antibodies of the IgE class are known for their role in the allergic response and in protection against parasites, naturally residing in tissues where they exert immunological surveillance. Comparative studies examining the efficacy of IgE antibodies include research conducted at King's College London on the chimaeric monoclonal antibody MOv18 IgE [Gould et al., 1999, Karagiannis et al., 2008, Karagiannis et al., 2007, Karagiannis et al., 2009]. MOv18 IgE recognises the tumour-associated antigen Folate Receptor α (FRα) that is expressed by ovarian cancers, mesotheliomas and other solid tumours. In these studies the IgE antibody demonstrated superior efficacy compared to the corresponding IgG_1 in two *in vivo* models of cancer [Gould et al., 1999, Karagiannis et al., 2007]. Thus, the mechanisms by which antibodies of different isotypes influence the nature of the immune response harnessed to combat cancer cells informs and may potentially benefit the design of future effective therapies [Kershaw et al., 1998, Turner et al., 2006, Jensen-Jarolim et al., 2008]. Antibodies of the IgE class primarily mediate allergic responses; thus, in an effort to understand whether IgE antibodies play a role in natural immune surveillance against cancer, researchers have for a number of years explored epidemiological associations between allergy and cancer.

1.7.2 Epidemiological associations between IgE allergy and cancer

Several associations between allergic conditions and cancers have been reported. In the late 1960s, Ure and MacKay described a negative correlation between atopy and cancer in studies based on patient history records [Ure, 1969]. Subsequently, a study by Jacobs et al., conducted in a larger population measuring IgE by two independent techniques, confirmed prior findings of an association between low IgE titres and neoplasms [Jacobs et al., 1972], thus increasing the credibility of prior findings. Following the described studies and further epidemiologic observations, recent meta-analyses indicate a more complex association between allergy and cancer and reported segregation between cancers with strong inverse correlations with cancers like glioma [Van Hemelrijck et al., 2010]. Yet all these studies have limitations, one being that they investigate overall levels of IgE irrespective of any specificity, and do not measure specific IgE reactivity to tumour cells. It may therefore be more relevant to evaluate tumour antigen-specific IgE for tumour cell reactivity rather than to measure total IgE levels.

1.7.3 Why design IgE antibodies for cancer therapy

A number of attributes of the IgE antibody class may support its potential study as an anti-cancer modality. Unlike IgG, IgE antibodies lack an inhibitory receptor. Andreau *et al.* reported that the IgG inhibitory receptor FcγRIIb is overexpressed on tumour cells indicating a potential mechanism of tumour cell evasion from immune attack. The absence of such a receptor for IgE suggests that this potential escape mechanism can be overcome if IgE antibodies are used as a therapeutic tool [Gould et al., 2003, Gould and Sutton, 2008]. In addition, the difference in serum and tissue half-lives of IgE antibodies compared to IgG might also confer an advantage to IgE in the treatment of solid tumours. IgE has 1.5 days clearance from the serum [Ravetch and Kinet, 1991, Gould et al., 2003, Gould and Sutton, 2008], while the half-life of IgE antibodies in tissues can exceed two weeks [Hellman, 2007]. The opposite is true for IgG. IgE is mainly bound with exceedingly high affinity to FcϵRI bearing cells assuring longer tissue immune surveillance, which can be beneficial in the con-

text of tissue-resident cancer cells. It is therefore possible that tumour-specific IgE immunotherapy can overcome immune suppression by triggering long-lived powerful effector functions in tissues, and, unlike IgG, it is not subject to inhibitory signals in tumours. The following section elaborates on the mechanism of immune suppression and FcϵR bearing cells which may reveal the "hidden" potential of the IgE antibody subclass. In order to eradicate tumour cells IgE mediates effector cell activation through its receptors FcϵRI and CD23 [Karagiannis et al., 2008]. Activation of this signalling cascade can result in 1) degranulation of pro-inflammatory mediators and cytokines, 2) antibody dependent cytotoxicity (ADCC) induced by mediators such as nitric oxid that results in target cell lysis, and 3) antibody dependent phagocytosis (ADCP) by natural phagocytes such as macrophages naturally residing in the tumour microenvironment. However, cytokine signalling is subject to influences from the tumour microenvironment composed of stromal cells (e.g. fibroblasts, endothelial cells) and immune cell infiltrates. The latter group includes cells that express Fcϵ receptors such as macrophages, DCs, mast cells, B cells and eosinophils; these cells are thought to provide a tumour promoting environment through tissue remodelling, suppressing effective immune responses and promoting metastasis by release of inflammatory cytokines and chemokines. The main hypothesis in the field of Allergo-Oncology, the emerging discipline advocating that IgE-mediated functions may be harnessed against cancers, is that treatment with a tumour antigen-specific IgE antibody either directly administered or triggered by vaccination, can stimulate Fcϵ receptor-expressing cells enabling the cells to overcome the immune suppression and to mount a response against the tumour. Three key Fcϵ receptor bearing cells, mast cells, eosinophils and macrophages have been proposed to play a major role as described below.

1.7.3.1 Mast cells

The early presence of mast cells in a variety of solid tissues and in tumours like melanoma, characterises their role as tissue-resident "sentinels" prone to initiate a rapid response to pathogens and immunogenic antigens [Galli et al., 1999, Ribatti et al., 2003, Molin et al., 2002]. However, mast cells have also been described to exert immune suppression by secreting modulatory cytokines such as IL-10 and TNF-α; while their presence in tumours has been associated with poor prognosis [Gulubova

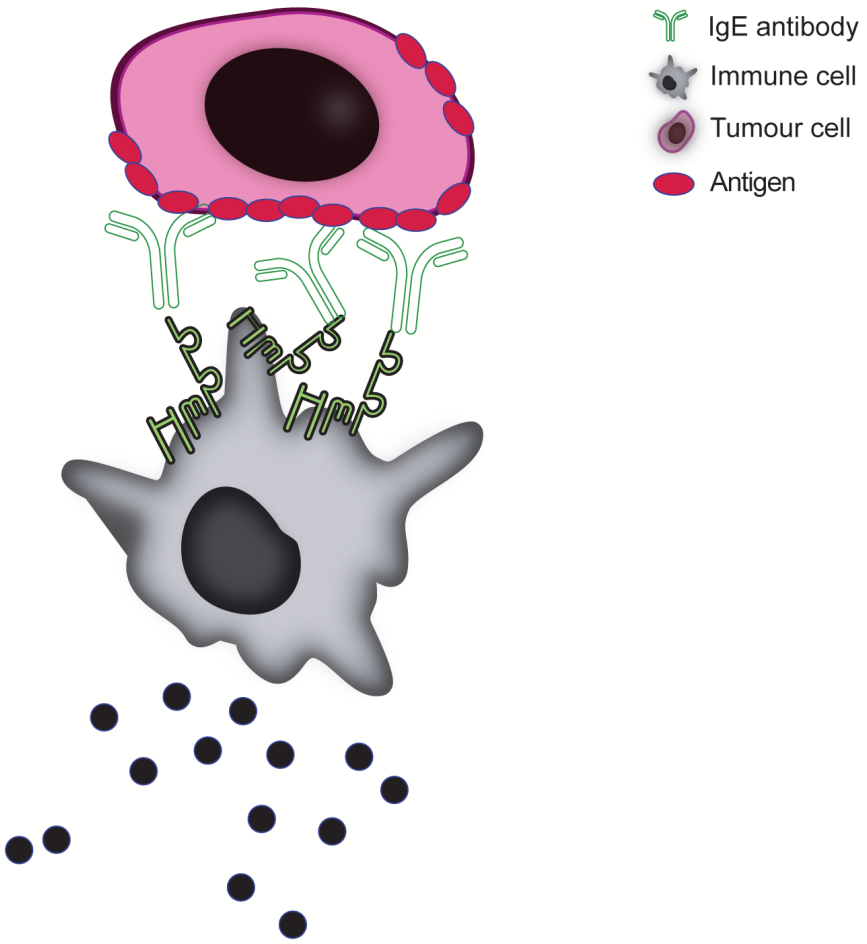

Figure 1.12: IgE cross-linking of FcεRI induced degranulation.

and Vlaykova, 2009, Cai et al., 2011]. Investigating the biological mechanisms of mast cells revealed that they contribute to tumour invasion and angiogenesis by secreting VEGF [Coussens et al., 1999, Soucek et al., 2007, Gounaris et al., 2007], and by promoting T_{regs} development. VEGF and T_{regs} can in turn suppress immune response and impair cross-presentation by dendritic cells, thereby mediating tolerance [de Vries et al., 2011]. Using a mouse allograft model, Noelle and colleagues demonstrated that triggering intra-graft or systemic mast cell degranulation by cross-linking of IgE resulted in the transient loss of the suppressive activities of T_{regs} [de Vries et al., 2009]. This model illustrates the transient breakdown of pe-

ripheral tolerance induced by IgE thus proposing a therapeutic mechanism against tumours directly based on specific IgE immunotherapy.

1.7.3.2 Eosinophils

Eosinophils were long regarded as Fcϵ receptor-expressing cells in allergic diseases and parasitic infections. In 1981 eosinophils were first observed in peri-tumoural infiltrates of several types of cancers including solid tumours, and thereafter termed tumour-associated tissue eosinophilia (TATE) [Lowe et al., 1981, Munitz and Levi-Schaffer, 2004]. Traditionally referred to as effector cells, eosinophils are now recognised as multifunctional cells capable of initiating and regulating inflammatory responses as well as activating the adaptive immune response by antigen presentation to T cells [Gatault et al., 2012]. Several studies have reported TATE to be a positive prognostic indicator in solid tumours such as bladder cancer, colorectal cancer, laryngeal carcinoma and squamous cell carcinoma [Fernández-Aceñero et al., 2000, Dorta et al., 2002, Ishibashi et al., 2006]; with the exception of Hodgkin's lymphoma [Gatault et al., 2012, vonWasielewski et al., 2000]. Despite TATE's heightened prognostic capacity, the exact mechanisms underlying this anti-tumour immune response are not yet elucidated. Studying the presence and status of eosinophils during IL-2 therapy in renal cancer and melanoma showed that systemic IL-2 treatment induced eosinophil degranulation and the subsequent tumour cell death [Huland and Huland, 1992, Cormier et al., 2006, Simson et al., 2007]. In several *in vivo* studies eosinophil infiltration into tumours of wild-type mice was shown to induce an early and persistent response [Cormier et al., 2006]. Analysis of the role of eosinophils in IL-5 transgenic mice demonstrated a significant increase of eosinophils into the tumour resulting in reduction of tumour establishment and growth [Simson et al., 2007]. The common IL-5-rich environments found in allergy and also in this cancer model may suggest that an "allergic-like" response involving activated eosinophils can induce eradication of tumours. This concept was further investigated by Legrand *et al.* analysing the cytotoxic potential of eosinophils from allergic donor (n=4) and non-allergic donors (n=6) against the colon cancer cell line Colo-205 [Legrand et al., 2010].

1.7.3.3 Macrophages

Macrophages are the major Fc-bearing cell type in tissues. They express all three classes of Fcγ receptors and also both Fcϵ receptors. Therefore these cells can be potentially activated by either immunoglobulin class. Most observations of tumour-associated macrophages (TAMs) described TAMs to foster tumour progression [Qian and Pollard, 2010]. TAMs were reported to mediate a pro-tumour microenvironment by: 1) producing VEGF [Lin et al., 2007]; 2) remodelling the tissue matrix via MMPs; 3) supporting tumour cell proliferation, survival and invasion by secreting chemokines and cytokines such as CXCL3, TNF-α, TGF-β, EGFR ligand or IL-6 [Mantovani et al., 2008]; and 4) maintaining immunosuppressive microenvironments that inhibit cytotoxic T cell activities by secreting IL-10 and promoting T_{regs} [Ojalvo et al., 2009](Ojalvo 2009; Deodens 2010). Monocytes/macrophages can be differentially polarised under different stimuli: M1 macrophages are inducible via lipopolysaccharide and produce IFNγ, IL-2 and TNFα; and M2 macrophages secrete mediators such as IL-4, IL-13 and IL-10 [Biswas and Mantovani, 2010] thought to have suppressive effects. High plasticity of those cells in the tumour microenvironment allows for both phenotypes to co-exist. This model may provide new attractive therapeutic opportunities such as strategies to block the immunosuppressive functions, or limit their recruitment in tumours, or reprogram TAMs or prevent their polarisation towards M2. In this context, DeNardo *et al.* showed in a murine model that inhibition of macrophage colony-stimulating factor 1 or its receptor diminished macrophages and promoted cytotoxic therapies in a $CD8^+$ T cell-dependent manner [DeNardo et al., 2011]. Furthermore, repolarisation of macrophages through the TNF-α receptor superfamily member, CD40, leads to anti-tumour effects and depletes tumour stroma, thus enabling access of other immune cells resulting in pancreatic tumour regression [Beatty et al., 2011]. This thesis puts forward the hypothesis that tumour-specific IgE antibodies activate TAMs triggering their activation and repolarisation, leading to anti-tumoural functions (Chapter 5).

1.7.4 Immunotherapeutic approaches aimed at activating IgE-mediated immunity against tumours

Different attempts have been made to harness allergic and IgE reactions against cancer and to investigate their potential benefits. These studies have utilised immunological strategies such as the deployment of IgE as an adjuvant [Reali et al., 2001], development of IgE-coated cellular vaccines [Reali et al., 2001, Nigro et al., 2009, Nigro et al., 2012], production of oral mimotope vaccination strategies with the aim of inducing tumour-specific IgE antibodies [Riemer et al., 2007], or the production of recombinant IgE antibodies targeting tumour-associated antigens [Nagy et al., 1991, Daniels et al., 2012, Kershaw et al., 1996, Kershaw et al., 1998, Teo et al., 2012, Karagiannis et al., 2012].

1.7.4.1 IgE adjuvant model

In the IgE adjuvant model, aimed at inducing specific tumour responses, IgE is coupled to the surface of tumour cells through a three-step biotin-avidin bridge strategy, these IgE coated tumour cells are then used to immunise immunocompetent mice. In these experimental models tumour growth was significantly reduced in IgE treated animals and they show prolonged survival compared with controls and also with IgG treated animals. Interestingly, disintegration of the antibody-Fc regions as well as depletion of eosinophils, $CD8^+$, or $CD4^+$ cells abolishes the anti-cancer effects of the treatment [Reali et al., 2001] implying the importance of IgE effector cells and also of adaptive immunity in this process. Experiments in either FcϵRI or CD23 knockout mice were conducted to further explore the properties of IgE as an adjuvant [Nigro et al., 2009]. These showed that IgE-coated tumour cells in FcϵRI knockout animals did not restrict tumour growth, whereas those in CD23 knockout animals retained the anti-tumour effect, thus linking efficacy to FcϵRI [Nigro et al., 2009]. Human FcϵRIα transgenic mice immunised with a different alternatively developed IgE adjuvant vaccine (from the above explained) also showed significant anti-tumour properties, thereby confirming the key role of human FcϵRI in IgE anti-tumour adjuvanticity [Nigro et al., 2012].

1.7.4.2 Mimotope vaccine model inducing IgE antibodies

An independent study made use of the phage display technology to define peptide structures mimicking natural epitopes of HER2/neu recognised by trastuzumab (mimotopes). Selected mimotopes were used to induce an immune response consisting of tumour antigen-specific IgE antibodies, by immunising BALB/c mice via the oral route under simultaneous neutralisation of gastric acid [Riemer et al., 2007]. This applied immunisation regime resulted in serum IgE antibodies recognising HER2/neu which were capable of mediating cytotoxicity of the HER2/neu overexpressing cell line SKBR3 *in vitro*. Although these results suggest that oral administration of mimotopes can lead to the production of cytotoxic IgE antibodies, it remains unclear whether these antibodies mediated these anti-tumour effects *in vivo* [Riemer et al., 2007].

1.7.4.3 Passive IgE immunotherapy

Advances in the production of recombinant antibodies have allowed for quick development, assessment and evaluation of passive IgE immunotherapy. Two decades ago, Nagy *et al.* conducted a study showing that a murine IgE antibody specific to the major envelope glycoprotein (gp36) of the mouse mammary tumour virus (MMTV) overexpressed in syngeneic H2712 cells improved the survival of immunocompetent mice [Nagy et al., 1991]. Further development of this model used both a murine anti-Ly-2 IgE in an immunocompetent mouse populated with murine cytotoxic T cells (CTLs), which expressed a chimeric FcϵRI-ζ receptor (human FcϵRIα and the human CD3ζ) and immunosuppressed animals utilising primary human T cells retrovirally-transduced with a chimeric FcϵRI receptor linked to the cytoplasmic domains of the human co-stimulatory molecule CD28. This resulted in improved survival of mice when compared to controls [Kershaw et al., 1996]. Moreover, testing a murine IgE antibody specific to the 30.6 antigen, expressed by human colorectal carcinomas (COLO205) in an immunosuppressed mouse model showed superior efficacy at a lower concentration than its IgG_1 counterpart. It is however noteworthy that these antibodies were never tested simultaneously [Kershaw et al., 1998, Mount et al., 1994]. Furthermore, the efficacy of the first mouse/human chimeric IgE anti-

body was demonstrated in immunosupressed animals populated by human immune cells. This was the ovarian cancer-associated anti-folate receptor α (FRα) antibody termed MOv18 IgE. In order to allow for comparison of the IgE antibody to its IgG_1 counterpart, MOv18 IgE was engineered using chimeric MOv18 IgG_1 by exchanging first the Fc of the heavy chain and subsequently the κ-light chain [Gould et al., 1999]. After a series of comparison experiments *in vitro*, both antibodies were tested in immunodeficient mice (*in vivo*) using two separate human xenograft models. One model was an ovarian carcinoma model using the human FRα-overexpressing cell line IGROV-1 grown subcutaneously in SCID mice. The second model was an orthotopic human ovarian carcinoma ascites model grown intraperitoneally in nude mice which expressed moderate levels of FRα. Since the human IgE Fc regions are not recognised by mouse Fcϵ receptors, and unlike in humans, mouse FcϵRI is only expressed on mast cells and basophils, both of these mouse model systems entailed antibody administration together with human PBMCs in order to provide the relevant effector cells [Gould et al., 1999,Karagiannis et al., 2003,Karagiannis et al., 2007,Karagiannis et al., 2008]. In both of these model systems, MOv18 IgE was shown to be superior to its IgG_1 counterpart in restricting tumour growth over time and in enhancing survival of IgE treated mice, respectively. Histological analysis of the cell line derived tumours revealed large areas of tumour necrosis in mice treated with MOv18 IgE compared to controls, further suggesting that anti-tumour effector cell functions are activated in response to MOv18 IgE treatment [Karagiannis et al., 2003,Karagiannis et al., 2007,Karagiannis et al., 2008]. These studies also demonstrated that monocytes/macrophages are important immune effector cells in the context of tumour antigen-specific IgE immunotherapy, since depletion of monocytes from the human PBMCs administered in the orthotopic patient-derived ovarian carcinoma model abolished the anti-tumoural effects of IgE; and reconstitution of depleted PBMCs with monocytes restored the survival advantage conferred by IgE immunotherapy. Furthermore, human macrophages infiltrated tumours from the IgE-treated animal cohort in the orthotopic patient-derived xenograft model, further supporting a role for monocytes/macrophages in IgE immunotherapy. In support of the findings with MOv18 IgE, two separate studies by Daniels-Wells et al. showed that in immunocompetent human FcϵRIα transgenic mice, an anti-HER2/neu IgE and an anti-PSA IgE antibody did not display any toxicity, while each antibody conferred survival benefits, in each model system. In the anti-PSA IgE study, the IgE antibody was compared to its IgG_1 counterpart and displayed superior efficacy [Daniels et al., 2012,Daniels-

Wells et al., 2013]. All of the above-mentioned mechanisms of IgE antibodies are described in protection from parasitic infections, further supporting the possibility that they may also be harnessed against tumour cells [Jensen-Jarolim et al., 2008]. Furthermore, Fcϵ receptors are also present on antigen presenting cells such as DCs, B cells and macrophages, and may also trigger possible cross-presentation, potentially inducing adaptive immune responses against tumours. This could increase the potent as well as longevity of protection against tumours conferred by IgE antibodies. Mounting evidence thus supports the notion that the potent immune responses of IgE can be harnessed against cancer and this may include developing recombinant IgE antibodies recognising tumour antigens. The IgE concept as a therapy has not been examined in melanoma and merits investigation.

	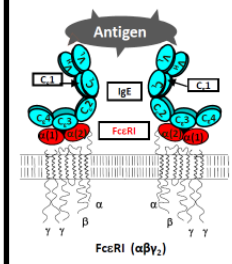	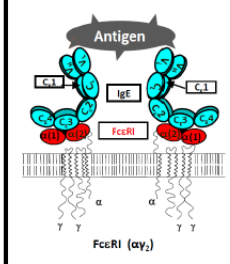	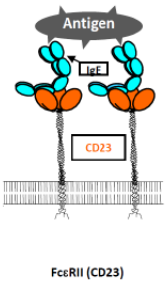
Affinity for IgE (K_a)	$10^9 - 10^{11}$ M^{-1}	$10^9 - 10^{11}$ M^{-1}	$10^6 - 10^8$ M^{-1}
Key receptor expressing immune effector cells	Mast cells Basophils	Eosinophils / Monocytes	Monocytes
Expression density (molecules/cell)	130,000-150,000	>2,000 / 2,000 - 5,000	0-20,000
Immune Mechanisms	Degranulation	ADCC / ADCC/ ADCP	ADCP

Figure 1.13: Interaction of IgE with Fcϵ receptors mediate effector cell functions in response to cancer cells. Schematic of IgE binding to FcϵRI tetrameric ($\alpha\beta\gamma_2$) (left) and FcϵRI trimeric ($\alpha\gamma_2$)(middle) through extracellular alpha (α) chain and interaction with the low-affinity receptor CD23 trimer is through recognition of the lectin domain (right). Expression affinities for IgE and expression densities of IgE receptors of key effector cells and immune mechanisms each mediates.The presence of the β chain on the FcϵRI tetramer is responsible for high cell surface expression densities on mast cells and basophils and is associated with induction of degranulation. In the presence of IgE, FcϵRI trimers are known to induce ADCC, while CD23 expression on monocytes and macrophages can trigger ADCP of parasites. Figure reproduced from [Karagiannis et al., 2012]

1.8 Biomarkers in melanoma

The quest for disease-relevant biomarkers for many disease pathologies including malignant diseases is receiving great attention with the advent of novel screening technologies and our enhanced understanding of disease pathways. In the context of cancer, molecules associated with tumour inflammation and possibly with tumour-promoting or tumour-eradicating mechanisms locally and systemically could be candidate biomarkers. New reliable biomarkers are indeed needed in the growing field of oncology to assist with diagnosis, early detection, staging of patients, prognosis of disease progression and also to stratify patients for particular treatments or to help predict responses to specific therapies. One can foresee that the discovery of specific disease-relevant biomarkers could potentially help us harness the full therapeutic benefits of drug interventions before terminal endpoints. Clinically validated biomarkers could for example be used to evaluate a therapy in phase III trials before the terminal endpoint is reached, thus allowing for quicker assessment and better health care provision.

1.8.1 Definition of a clinically relevant biomarker

Several definitions and guidelines have been proposed to define biomarkers. These include specifications that a biomarker should be objectively measured and evaluated as an indicator of a pathological process, or of a pharmacological response to a therapeutic intervention. Henry and Hayes were among the first to propose criteria that a candidate biomarker must fulfil in order to qualify for clinical application: 1) there must be a clear difference between readouts from each of the analysed groups; 2) the rationale and utility of the test used to measure the biomarker must be well-defined; 3) the results measured must be reliable and reproducible. Following these guidelines, Hunter et al. distinguished between different "validation steps" for biomarkers: 1) validity of the test; 2) clinical validity and 3) clinical utility [Henry and Hayes, 2012]. In 2000, at the First International Meeting on Cancer Diagnostics (NCI-EORTC) the "Reporting Recommendations for Tumour Marker Prognostic Studies" (REMARK) was developed. This guideline was implemented to overcome the widespread deficiencies in the reporting of putative biomarkers during prospec-

tive trials. The guideline consists of a checklist of 20 items including full description of the research and hypotheses, patient sample selection and recruitment, marker evaluation and measurement techniques, statistical design and analysis of study results [McShane et al., 2005, Altman et al., 2012]. This collaborative effort among clinicians, laboratory scientists, statisticians and journal editors has the potential to drastically improve the implementation of novel biomarkers into common clinical practice. There have been extensive efforts in the field to define biomarkers in patient blood and melanoma lesions and the most commonly examined are discussed below.

1.8.2 Serological biomarkers in cancer

1.8.2.1 LDH

The enzyme Lactate dehydrogenase (LDH) is the most used serological biomarker in melanoma. It remains to date the strongest prognostic biomarker found to increase with tumour burden [Solassol et al., 2011]. LDH is mostly released upon cell damage or death with both phenomena indicating higher tumour burden and disease progression. It is however noteworthy that release of LDH in the sera does not exclusively occur in neoplasia but also in other disease settings such as hemolysis, hepatitis, myocardial infarction and infectious diseases. Therefore LDH presence in the blood of patients with melanoma may result in false-positive readouts. Recent studies have shown that LDH is less sensitive in early stage disease with low predictive value for metastatic relapse [Hofmann et al., 2009]. It is nonetheless at present a useful and clinically-available tool for indication of tumour progression in patients at later disease stages.

1.8.2.2 Tyrosinase

Tyrosinase is part of the biosynthesis process of melanin and constitutively expressed in melanocytes and melanoma cells. Tyrosinase mRNA levels are detectable in the blood of melanoma patients with advanced metastatic disease detected by nested RT-PCR [Quaglino et al., 2007, Visús et al., 2007]. Initial evaluations revealed that

tyrosinase is an independent prognostic marker for tumour progression [Schmidt et al., 2005, Visús et al., 2007, Quaglino et al., 2007]. Samija et al demonstrated that tyrosine mRNA is associated with a decrease in overall survival [Samija et al., 2010]. However, high variability in the readouts of serum tyrosinase have been reported, most likely due to difficulties in sample processing and the transient presence of metastasising tumour cells in the blood [Visús et al., 2007]. Therefore it is not surprising that several studies could not confirm a significant prognostic utility of tyrosinase [Garbe et al., 2003, **?**]. This includes a recent study that showed no differences in tyrosinase serum levels when comparing patient to healthy volunteer blood [Zhang et al., 2011].

1.8.2.3 VEGF

Growth factors in combination with interleukins are major regulators of inflammatory conditions in the tumour microenvironment. VEGF is known to support tumour-associated angiogenesis, and to contribute to inflammatory conditions which promote immunosuppression and redirection of effective anti-tumoural immunity. Ugurel et al. reported that vascular endothelial growth factor was an independent prognostic marker for overall and progression-free survival in their cohort (125 stage I-IV patients) [Ugurel et al., 2001]. Unfortunately, several subsequent studies could not confirm this finding. Although associations between VEGF and the disease were found, no correlation with disease progression was attained [Osella-Abate et al., 2002, Pelletier et al., 2005, Vihinen et al., 2007].

1.8.2.4 Osteopontin

Osteopontin, a secreted integrin-binding glycophosphoprotein, has been described to reduce apoptosis, enhance tumour growth and be a major component for the recruitment of tumour promoting stromal cells from the bone marrow [Perrotta et al., 2011, McAllister et al., 2008]. In a recent study, Maier et al. demonstrated that osteopontin in combination with S100B can help to differentiate patients who are likely to subsequently relapse and develop metastatic disease from those who do not

. Yet, the presence of osteopontin is also associated with other medical conditions such as autoimmune diseases and might therefore be associated with increased false-positive readouts in patients with melanoma [Maier et al., 2012].

1.8.2.5 YKL-40

YKL-40 is a glycoprotein secreted by many cells including cancer cells and by immune cells such as macrophages and activated neutrophils [Volck et al., 1998, Johansen, 2006]. The physiological functions of YKL-40 are yet not fully understood and reports of its functionality as an independent prognostic marker vary [Schmidt et al., 2006, Díaz-Lagares et al., 2011, Egberts et al., 2012]. More importantly, YKL-40 expression is influenced by immunomodulatory drugs such as IL-2 and IFN-α2b and therefore its use as a biomarker can yield in false-negative readouts during treatment [Krogh, 2013].

1.8.2.6 Melanoma inhibitory activity

The small protein Melanoma inhibitory activity (MIA) is secreted by melanoma cells and is involved in cell-cell contact by interacting with the extracellular matrix. It is also thought that MIA promotes tumour cell invasion and metastasis [Palmer et al., 2011]. Equally it was reported that MIA has a high sensitivity and specificity compared to other clinically-relevant biomarkers such as LDH [Hofmann et al., 2009, Díaz-Lagares et al., 2011]. Elevated levels of MIA correlated with more advanced disease stages, poorer prognosis and decreased disease-free survival [Hofmann et al., 2009, Díaz-Lagares et al., 2011, Perrotta et al., 2011, Juergensen et al., 2001]. However, different studies using multivariate analysis demonstrated higher rates of false positive readouts in women, suggesting an alternative source of MIA may exist and that this protein may participate in and be influenced by other biological processes unrelated to malignancy [Essler et al., 2011, Bosserhoff et al., 2004, Hofmann et al., 2009].

1.8.2.7 Cell adhesion molecules

Cancer associated cell adhesion proteins are proteins that adhere to different cells, show altered expression levels in cancer, and impact cell tumour migration, immune cell evasion and angiogenesis [Sapoznik et al., 2012]. Past studies have associated serum levels of cell adhesion molecules with the development of metastasis [Ebrahimnejad et al., 2004, Franzke et al., 1998, Hirai et al., 1997]. An example from this group of proteins is carcino-embryonic antigen-related cell adhesion molecule 1 (CEACAM1), which is recognised as an independent predictive maker for the risk of metastasis [Thies et al., 2002]. Moreover, it was shown that CEACAM expression correlates with disease stage and with overall survival (OS) [Sivan et al., 2012].

1.8.2.8 S100

The family of S100 proteins has been of special interest as diagnostic markers in melanoma over the last decade since the expression and secretion of these proteins is much higher in malignant compared to healthy tissues [Davey et al., 2000, Hsieh et al., 2002, Petersson et al., 2009]. S100 proteins and in particular S100B were recently found to be elevated in the serum of melanoma patients with these elevated levels being associated with poorer prognosis [Beyeler et al., 2006, Oberholzer et al., 2008], disease free-survival and overall survival [Kruijff et al., 2009]. In a more recent prognostic study of patients treated with IFN-α2b versus observation in stage II and III patients, investigators showed that S100B is associated with worse OS and distant metastasis free survival (DMFS). Interestingly, S100B in patients' sera correlated over time with disease progression, increasing further in parallel to increases in disease burden [Bouwhuis et al., 2011]. False positive results can occur during brain, liver or renal injuries as well as infectious diseases [Molina et al., 2002, Tsoporis et al., 2011, Michetti et al., 2012]. However, data acquired, to date point to the merits of further evaluations of S100 as a potential clinical tool.

1.8.3 Tissue specific biomarkers for melanoma

Tissue specific biomarkers are molecules demonstrated to be over-represented in cancer lesions, and may facilitate diagnosis, early detection, prognosis of disease progression and patient stratification.

1.8.3.1 BRAF

Approximately 50% of all melanoma patients have an activating mutation in the $BRAF^{V600}$ gene on the long arm of chromosome 7 [Davies et al., 2002, Long et al., 2011]. This change results in the constitutive activation of BRAF kinase, which is likely to promote the RAS—RAF—MEK—ERK pathway-induced proliferation and extensive tumour cell growth. Recently two type I RAF inhibitors, vemurafenib and dabrafenib, have shown to improve survival in phase III clinical trials in patients with advanced-stage disease. These drugs are now standard of care [Hauschild et al., 2012, Chapman et al., 2011,Flaherty et al., 2014]. Although progression—free survival with each drug is only 5—7 months, this treatment option are far superior from historical agents [Chapman et al., 2011, Flaherty et al., 2010, Sosman et al., 2012, Falchook et al., 2012]. The disease recurrence during BRAF kinase inhibtor treatment may be induced by different mechanisms such as the alternative splice variants of BRAF or de novo mutations in the NRAS or MEK kinases [Mao et al., 2013]. Taken together, screening of the BRAF mutation in melanoma patients allows for the stratification of treatment with effective agents and is therefore a curial biomarker in melanoma.

1.8.3.2 Cyclooxygenase-2

Cyclooxygenases (COX1-3) are a group of proteins that are important modulators in the human body, affecting essential pathways such as the catabolic metabolism. COX1-3 also converts arachidonic acid into prostaglandin. Of this group COX-2 can be induced in tumour cells [Meyer et al., 2009, Bosserhoff, 2006]. Becker et al. showed a correlation between COX-2 staining intensity and Breslow thickness in melanoma [Becker et al., 2009]. Furthermore, Kuzbicki et al. reported a higher

COX-2 staining intensity in melanoma lesions compared to benign nevi [Kuzbicki et al., 2012].

1.8.3.3 Galectin-3

The Galectin-3 molecule is mainly secreted by inflammatory cells and is associated with both tumour progression and metastasis in melanoma [Buljan et al., 2011]. However, using a multifactorial Cox regression analysis, Brown et al. showed an inverse association between galectin-3 with tumour size (thin tumours had more galectin-3) and improved OS [Brown et al., 2012].

1.8.4 Matrix Metalloproteinases

Matrix metalloproteinases play an important role in remodelling the tumour tissue microenvironment as they are responsible for proteolytically breaking components of the local tissue architecture, promoting tissue remodelling and facilitating tumour cell migration (reviewed in [Stamenkovic, 2003]). For these reasons the proteins are over-represented in tumour tissues. Nikkola and colleagues showed that MMP-1 and MMP-3 positive melanoma metastases correlate with decreased disease-free survival (DFS) [Nikkola et al., 2002]. Furthermore, Rotte et al. confirmed a higher expression of MMP-2 in melanoma when compared to normal and dysplastic nevi. In this study, the levels of MMP-2 expression positively correlated with tumour progression and worse survival [Rotte et al., 2012]. It is however noteworthy that this study was conducted using tumour tissue microarrays through the application of peroxidase developed with 3,3'-Diaminobenzidine (DAB - a brown substrate), making the assessment of MMP-2 difficult to distinguish from melanoma cells in pigmented lesions.

1.8.4.1 Cell adhesion molecules

Cell adhesion molecules are linker proteins that connect cells. Some among them,such as the carcinoembryonic antigen-related cell adhesion molecule 1 (CEACAM-1), foster interactions between somatic cells and immune cells. It was demonstrated that expression of CEACAM on tumour cells inhibits immune responses and leads to tumour progression (reviewed in Clin and Develop Immunol 2012). Investigation of CEACAM1 expression suggested it to be an independent factor for the risk of metastasis [Thies et al., 2002].

1.8.4.2 The Chondroitin sulphate proteoglycan 4 (CSPG4) as a biomarker

The Chondroitin sulphate proteoglycan 4 (CSPG4), also known as the High Molecular Weight Melanoma Associated Antigen (HMW-MAA) or the Melanoma-associated chondroitin sulphate proteoglycan (MCSP) is a glycoprotein-proteoglycan complex expressed on the surface of melanoma, glioma, neuroblastoma, certain breast cancinomas and acute leukaemias [Ross et al., 1983]. CSPG4 is thought to play crucial roles in cell adhesion, melanoma migration and metastasis (see Section 1.6.5.1) (reviewed in [Campoli et al., 2010]). Although CSPG4 is over-expressed in over 80% of all melanomas, it is found at all disease stages and data so far have not yielded any correlations with disease progression [Vergilis et al., 2005]. However, a recent study reported that a cytoplasmic form of the protein appears to correspond with response to therapy of a melanoma vaccine, indicating that CSPG4 may potentially be evaluated as a marker of disease progression [Reynolds et al., 2006].

Biomarker	Study	Correlation	Methodology	Reference
LDH	50 patients stage I-II and 61 patients stage IV before and after treatment	Tumour stage; prognosis	Photometric assay	Egberts (2012)
LDH	30946 patients stage I-III and 7972 stage IV	survival rate	Meta-analysis	Balch (2009)
Tyrosine	200 patients stage IV	Poor prognosis	Nested RT-PCR	Quaglino (2007)
Tyrosine	85 patients stage IV	survival rate	RT-PCR	Schmidt (2005)
Tyrosine	114 patients stage I-IV and 20 healthy volunteers	survival rate	RT-PCR	Visus (2007)
Tyrosine	201 patients stage I-IV and 40 healthy volunteers	overall survival	RT-PCR	Samija (2010)
COX-2	63 human melanytic skin tumours (17 nevi; 36 primary cutaneous melanomas; 11 lymph node metastatis)	Tumour progression	IHC	Kuzbicki (2006)
COX-2	101 primary melanomas and 28 metastatic	Breslow thickness	IHC	Becker (2009)
MMP-1 & MMP-3	70 melanomas	Disease-free survival	IHC	Nikkola (2002)
MMP-9	71 patients stage IV and 8 healthy volunteers	Poor prognosis	ELISA	Nikkola (2005)
MMP-2	482 melanoma (330 primary and 152 metastatic); 149 nevi (49 normal and 100 dyslpastic)	Tumour progression	IHC	Rotte (2012)
VEGF	125 blood samples from patients and 30 healthy volunteers	Tumour stage; survival	ELISA	Ugurel (2001)
VEGF	155 melanoma blood samples	Tumour progression	RT-PCR	Osella-Abate (2002)
VEGF	324 melanoma blood samples	Tumour stage	ELISA	Pelletier (2005)
VEGF-C & VEGFR-3	75 melanoma blood samples (stage IV) and 30 healthy volunteers	Tumour burden	ELISA	Mouawad (2005)
Osteopontin	345 melanoma patient blood samples	Breslow thickness and survival	IHC	Rangel (2008)
Osteopontin	34 invasive growing melanomas	Poor prognosis	IHC	Alonso (2007)
Osteopontin	106 patient blood samples	Tumour stage	ELISA	Maier (2012)
Gal-3	21 melanomas and 20 begine leasions	Poor prognosis	IHC	Abdou (2010)
Gal-3	104 melanoma (71 superficial spreading; 33 nodular melanoma)	Tumour progression	IHC	Buljan (2011)
Gal-3	53 bengine nevi; 31 dysplastic nevi; 59 in-situ melanoma; 314 primary melanoma; 69 metastatic melanoma	Tumour progression	IHC	Brown (2012)
Gal-3	83 patient samples (stage III-IV)	Poor prognosis	ELISA	Vereecken (2009)
YKL-40	110 melanoma patient blood samples (stage IV) and 245 healthy volunteers	Tumour progression	ELISA	Schmidt (2006)
YKL-40	234 melanoma blood patient samples (stage I-II)	Poor prognosis	ELISA	Schmidt (2006)
YKL-40	50 melanoma patient blood (stage I-II) & 61 (stage IV)	Tumour stage	ELISA	Egberts (2012)
MIA	110 with advanced disease and 66 disease free and 65 healthy controls	survival rate	ELISA	Diaz-Lagares (2011)
MIA	125 melanoma patient blood sample	Poor prognosis	ELISA	Essler (2011)
CEACAM	49 melanoma patient blood (stage III-IV)	Tumour stage; survival	ELISA	Sivan (2012)
S100B	221 melanoma patient blood (stage II-III)	survival rate	LIA	Bouwhuis (2011)
S100B	20 melanoma patient blood	Metastasis detection	ELISA	Oberholzer (2008)
S100B	192 melanoma patient blood	Poor prognosis	ELISA	Beyeler (2006)

Table 1.4: List of biomarker studies in melanomas

1.8.5 Statistical methods to evaluate the importance and predictive value of a biomarker including combination analysis

The identification and development of novel biomarkers is very important in evidence-based medicine. Not only could early disease detection or patient stratification guide the selection of therapies for individual patients and patient subpopulations, but also it could permit defining new endpoints during prospective drug studies that would allow quicker access to novel beneficial treatments. Due to natural variability of different measured substances, it has proven difficult to identify single biomarkers that provide such information with high accuracy. Choosing threshold points for binary markers has multiple dimensions such as detecting cases and detecting controls. Any threshold proposing reduction to a single (dimensional) decision involves making a value judgment about the relative importance of these two dimensions (i.e. detecting cases and controls). William John Youden has suggested the use of the following calculation to make this judgement call: Y (Youden Index) = sensitivity + specificity - 1. The Youden Index still implies a judgement, albeit a conscious one. While in some contexts it is more important to detect cases with high probability (defined as sensitivity), in others, it is more important to detect controls with high probability (defined as specificity). In the example of population screening, only small percentages of people constitute cases, while prediction of the cases depends on the threshold value picked. Thus, an incorrect threshold value based on high sensitivity in the Youden Index may detect too many cases in the population. On the other hand, in clinical studies one might elect to replace the existing gold standard test since it is very important to detect as many cases as practically possible by choosing a threshold of high sensitivity at the expense of low specificity. As an alternative to single biomarker analysis, it has been suggested that a strategy entailing multiple measurements could be adopted to increase the diagnostic accuracy by combining biomarkers that are already clinically-validated. For this improved approach, quantitative measures of performance (accuracy) for various collections of diagnostic tests need to be compared with different combinations of available diagnostic tests or techniques. For this purpose, adaptive mathematical methods are required to be operationalized. In the past, various statistical methods were used to identify markers with diagnostic or prognostic capability; some of the most important ones are

linear discriminant analysis, regression trees, binary regression and artificial neural networks [Lin et al., 2012]. All of these methods are designed to calculate hazard ratios or (in other words) likelihoods, assuming linear effects across one of the variables in the logistic regression. However, in cases with a curvilinear relationship, a quadratic term in the marker over and above the linear term would provide an improved fit and ultimately yield a better analysis. McIntosh and Pepe suggest that modification of linear binary regression in terms of optimising the function through maximisation of the receiver operating characteristic curve (ROC) [McIntosh and Pepe, 2002] would lead to a better analysis and prediction. A more recent report by Lin et al. compares likelihood approaches for the evaluation of medical diagnostic systems by applying a multiple binary test. The authors conclude that modification and further development of the method published by Pepe and colleagues leads to an improvement in accuracy [Lin et al., 2012]. Taken together, the validity of a biomarker does not only depend on its biological function and measurement but also on the subsequent calculation and evaluation of it.

1.8.6 Immunoglobulins: promising biomarkers for early disease

The development of novel biomarkers capable of diagnosis at early stages of the disease would improve therapy. From the 100,000 biomarkers reported in the literature [Amur et al., 2008] only 43 are approved by the FDA [FDA, 2013] in clinical settings. In the context of cancer, one of the biggest challenges is the undetectable levels of potential biomarkers at early disease stages. Early stages are characterized by mostly minimal disease manifestation with no more than $1x10^6$ tumour cells that release approximately 1,000 molecules into five litres of blood volume at steady state. Therefore, the concentrations of the biomarker would only amount to $3x10^{-14}$ M, which would make the detection of relevant biomarkers quite challenging. Delectability, sensitivity and specificity in the circulation are all important and desirable for assessing the potential clinical utility of a biomarker. High concentration of antibodies and thus vast amplification of a specific signal is achieved through the activation of B cells. Each B cell can produce 5,000-20,000 antibodies/minute and B cells can go through mitosis every 3 days, which may maintain or enhance

antibody production [Sulzer et al., 1994, Cenci and Sitia, 2007, Forster and Rajewsky, 1990, Cooperman et al., 2004]. These features might render the study of B cells and antibody responses in cancer an attractive proposition. A new technologies termed "immunosignaturing" features protein-coated chips which are used to screen for reactive antibodies against specific proteins. The "signatures" resulting from this process allow for the identification and prediction of the course of the disease. This relatively new method was described to have a diagnostic utility in Alzheimer's disease [Restrepo et al., 2013] and in brain cancers [Hughes et al., 2012]. Preliminary evaluations suggest that IgG_4, subclass antibodies, known to be associated with "alternative" Th_2 immune environments (discussed in sections 1.3.5.1, 1.4 and 1.5.3 above) may be used in the diagnosis of pancreatic cancer to help distinguish between autoimmune pancreatitis and pancreatic cancer. This finding indicates that higher levels of IgG_4 may be present in autoimmune diseases compared to cancer [Kawa et al., 2012]. The presence of IgG_4 in relation to pathologies has been examined in the context of allergies and chronic exposure to antigens or allergens. Increased serum levels of IgG_4 antibodies were observed in bee keepers associated with chronic occupational exposure to bee venom. Furthermore, numerous studies point to elevated levels of IgG_4 antibodies associated with allergic individuals undergoing allergen immunotherapies. Patients are exposed to melanoma-associated antigens in the context of long-lived IL-10-driven inflammatory conditions that may favour IgG_4 antibodies and the latter is supported by an early report of dysregulated levels of IgG_4 in patients with melanoma. For the above reasons, the IgG_4 antibody subclass is of interest as a component of melanoma-associated inflammation (Chapter 3). By extension, and based on reports evaluating IgG_4 as an indicator of pathology or response to stimuli in different disease settings, including some malignancies, Chapter 4 is focusing on examining the presence of circulating and tissue-associated IgG_4^+ B cells and IgG_4 antibodies and their significance in disease pathology and prognosis.

1.9 Aims and Hypothesis

In light of the importance of understanding the complexity of the immune response in melanoma and to inform the design of effective immunotherapies, the overarching goal of this thesis is to dissect the humoral responses in melanoma and to derive and

evaluate an immunotherapeutic approach using an antibody agent recognising the melanoma surface antigen CSPG4. The primary objectives are threefold:

1) To dissect the humoral response by analysing antibody B cell infiltration, antibody subclasses expression, and antibody class and subclass modulation of the humoral immune response in melanoma and eventually to examine the functional implications of these findings (i.e. impairment of the immunological reaction); 2) To evaluate the propensity of antibodies and components of the redirected humoral immune compartment in melanoma as putative biomarkers; 3) To explore efficacy and mechanisms of a class of antibodies that may be less prone to tumour-induced humoral immune blockade in melanoma, namely antibodies of the IgE class. In this thesis, an IgE antibody recognising the tumour cell surface antigen, CSPG4 was engineered and compared to its IgG counterpart *in vitro* and in two independent humanised mouse models of melanoma.

Chapter 3 describes findings relating the modulation of humoral immunity, specifically of B cell and antibody responses, by immunosuppressive cytokines such as IL-10, secreted in the tumour microenvironment. This Th2-biased microenvironment in melanoma may trigger altered immune responses [Satoguina et al., 2005, Jeannin et al., 1998], inducing antibodies of the less activatory IgG_4 subclass. This impairing mechanism was evaluated *in vitro* and in a humanised mouse model, by developing and implementing a range of new and improved functional assays. Based on the relevance of redirected humoral responses in melanoma, Chapter 4 reports on the investigation into the use of immunoglobulin IgG_4 as a putative biomarker in melanoma. Antibodies of the IgG_4 subclass are produced at elevated levels in different cancers (section 1.4) and in Chapter 3, it is demonstrated that they exert functional immunomodulatory roles in melanoma (Chapter 3). Therefore, the potential of IgG_4 to predict the risk of disease progression was investigated. Chapter 5 examines the activity and efficacy of the engineered anti-CSPG4 IgE class antibody. Using established *in vitro* techniques and novel *in vivo* models, anti-CSPG4 antibodies (IgG_1 and IgE) were compared. Experiments investigate tumour antigen epitope recognition on patient specimens, confirming the relevance of this agent in the treatment of many patient lesions. Experiments reported here also evaluated the potency and mechanisms of action of the novel anti-CSPG4 IgE confirming its functional activity and its capacity to mediate tumour cell death. The anti-CSPG4 IgE

was examined in two independent humanised mouse models, comparing its efficacy against its IgG_1 counterpart and against isotype control antibodies. Ultimately, gene expression analysis from xenograft tumours demonstrated IgE specific gene expression patterns providing insights into the antibody's mechanisms of action.

2 Material & Methods

2.1 Human sample collection

All human samples, including healthy skin, tumour samples, lymph nodes and blood, were collected with written informed consent. The study was approved by the Guy's Research Ethics Committee, Guy's and St. Thomas' NHS Trust for all experiments described (Title: "Molecular and Immunopathogenesis of Melanoma", REC reference number 08/H0804/139, approval date 15/10/2008).

2.2 Sterile culture of cell lines

All cells were maintained in a 5% CO_2 humidified incubator at 37 °C. All tissue culture reagents were from Gibco, unless otherwise indicated. The human monocytic cell line U937 [Sundström and Nilsson, 1976] and the melanoma cell line A2058 (CRL-1593.2; CRL-11147, ATCC, Manassas, USA) were grown in RPMI 1640 medium, 10% (FCS), 2 mM L-glutamine, penicillin (5000 U/ml) and streptomycin (100 μg/ml). The melanoma cell lines A375 (CRL-1619, ATCC, Manassas, VA), SK-MEL28 (HTB-

72, ATCC) and MALM-3M (CCL-185, ATCC) naturally expressing Chondroitin sulfate proteoglycan 4 (CSPG4) also known as High Molecular Weight Melanoma Associated Antigen (HMW-MAA) were grown in Dulbecco's Modified Eagles Media (DMEM) (Gibco, Eugene, USA), 10% FCS, 2 mM L-glutamine, penicillin (5000 U/ml) and streptomycin (100 μg/ml). The melanoma cell lines wm-115 (CRL.1675, ATCC) and SK-MEL2 (HTB-68, ATCC) naturally expressing CSPG4 were grown in Modified Eagles Media (MEM) (Gibco, Eugene, USA), 10% FCS, 2 mM L-glutamine, penicillin (5000 U/ml) and streptomycin (100 μg/ml). The melanoma cell line G-361 (CRL-1424, ATCC) naturally expressing CSPG4 was grown in Modified Eagles Media (MEM) (Gibco, Eugene, USA), 10% FCS, 2 mM L-glutamine, penicillin (5000 U/ml) and streptomycin (100 μg/ml). Primary human melanocytes (ATCC, PCS-2000-012, ATCC) were grown in Dermal Cell Basal Medium (ATCC) and supplemented with the Melanocyte Growth Kit (ATCC). The rat basophilic leukemia mast cell line, RBL SX-38 (Wiegand et al., 1996) (a gift by Prof. JP Kinet, Harvard University, USA) is transfected to express the tetrameric form of the human FcϵRI receptor ($\alpha\beta\gamma 2$) and was maintained in DMEM supplemented with 10% FCS, 500 μg/ml with 1.2 mg/ml G418, 2 mM L-glutamine, penicillin (5000 U/ml) and streptomycin (100 μg/ml) (all by Gibco).

2.3 Biotinylation of anti-CSPG4 IgE antibody

The amount of biotin used to biotinylate a protein is dependent on its size and distribution of amino groups on the protein. For antibodies one can use a 20-fold molar excess of biotin reagent to label 1-10mg/ml of antibody, which would lead to binding of 4-6 biotin groups/ antibody. Calculation for the use of Sulfo-NHS-LC-Biotin were performed according to the instructions provided by Thermo Scientific using the EZ-Link Sulfo-NHS-LC-Biotinylation kit (Thermo Scientific). Following the calculation, the vial containing Sulfo-NHS-LC-Biotin (Biotin) was allowed to equilibrate to room temperature and subsequently dissolved in PBS according to calculation. Subsequently, biotin was mixed to CSPG4 IgE antibody and incubated at 4 °C for two hours. Shortly before the incubation period ended Thermo Scientific Zebra Spin Desalting Column were prepared by washing (spin columns at 1,000g for 2 minutes) the column 3x with 2.5 ml of PBS. The antibody biotin mix was pipetted

onto the resin and allowed to be absorbed. 100 μl of ultrapure water were added and the column was subsequently spun at 1,000g for 2 minutes to collect the biotinylated antibody.

2.4 Immunohistochemistry

Paraffin sections were cut at 6 μm thickness on a microtome (Leica) and dried overnight at 37 °C. Prior to staining, sections were deparaffinised with a 20 min incubation in Xylene and then re-hydrated by serial incubations in alcohol (95% $\rightarrow$ 70% $\rightarrow$ 50% $\rightarrow$ 30% ethanol). Heat-induced antigen retrieval was performed in a 95 °C water bath, using Citric Acid (10mM Citric Acid, 0.05% Tween 20, pH 6.0). Section were then blocked with blocking buffer containing 2.5% goat serum and 0.1% bovine serum albumin (BSA) in PBS 0.05% Tween (PBST) for 35 minutes at room temperature. Subsequently, sections were stained overnight at 4 °C using the following commercial antibodies: mouse anti-human CD22 (Abcam; 1:200); rabbit anti-human FoxP3 (eBioscience; 1:50); mouse anti-humanCD45 (eBioscience; 1:250); and mouse anti-human IgG_4 (BD Bioscience; 1:50-1:100). On the following morning slides were washed 3x with PBST. Primary antibodies were then detected using biotinylated goat anti-rabbit IgG (1:400, Vector labs, USA) (incubating for 1 hour at room temperature). Sections were subsequently washed 3x in PBST and incubated for 30 minutes with VECTASTAIN © ABC-AP Reagent containing Levamisole (Vector Labs) to block endogenous alkaline phosphatase. Following another wash, slides were incubated in alkaline phosphatase substrate buffer and left to develop for a maximum of 30 minutes at room temperature. Washing the slides in tap water stopped the reaction. Hematoxylin counterstaining was performed by dipping the slides into Mayer's hematoxylin solution (Sigma Aldrich). After a final wash in tap water, slides were de-hydrated by serial incubations in alcohol and xylene (30%$\rightarrow$50%$\rightarrow$70%$\rightarrow$95%$\rightarrow$xylene) and mounted using DPX mounting media. All components used to visualise the biotinylated antibodies are part of the VECTOR Red Alkaline Phosphatase Substrate Kit (Vector Labs). Analysis was performed on a Zeiss Axiophot microscope using 10x and 20x magnification lenses (Carl Zeiss) and NIS-Elements imaging software (Nikon) or a tissue image analyser (Hamamatsu).

2.4.1 Immunohistochemistry assessment

Expression of CSPG4 on tissue microarray sections was evaluated analysing high power fields (7.5x) using the following criteria: "negative" = no intensity; "low"= low intensity; "intermediate"= intermediate intensity; "high"= high intensity. Cell density of sections stained for IgG_4+ cell infiltration was evaluated analysing high power fields (10x) using the following criteria: "negative"=0% infiltration; "low"<25% infiltration; "high">25% infiltration.

2.5 Immunofluoresence

Freshly-frozen tissue sections embedded in OCT were cut at 4 μm-8 μm thickness using a cryostat (Leica, Wetzlar, Germany), sections were air-dried and stored at $-80\,^{\circ}C$ until further use. Prior to staining, slides were equilibrated at room temperature for 10 minutes, followed by fixation in acetone for 20 minutes. Section were then blocked with blocking buffer containing 2.5% goat serum and 0.1% bovine serum albumin (BSA) in PBS 0.05% Tween (PBST) for 35 minutes at room temperature. Subsequently, sections were stained overnight at $4\,^{\circ}C$ using the following commercial antibodies: mouse anti-human CD22 mAb (eBioscience; 1:200); goat anti-human IgG (DakoGlostrup; 1:500); mouse anti-human IgG_4 (BD Bioscience; 1:50-1:100); mouse anti-human CD64 (Biolegend; 1:250); mouse anti-human CD32 (Abcam; 1:250); mouse anti-human CD16 (Abcam; 1:200); goat anti-mouse IgG, biotinylated (DAKO); rabbit anti-human S100. Alkaline phosphatase staining was conducted as described in immunohistochemistry section. Fluorescent staining was performed as followed: donkey anti-mouse Alexa 555 and donkey anti-goat Alexa 488 (both Life Technologies; 1:250) were incubated for 45 minutes and slides were then subsequently washed 3x in PBST. Following the wash slides were mounted with ProlongGold antifade containing DAPI (LifeTechnologies). Images were captured using a Zeiss Axio Observer.Z1/ Axiophot microscope using AxioVision (10x, 20x and 63x magnification lenses (Carl Zeiss)).

2.6 Gene expression analysis

2.6.1 Specimen collection for mRNA analysis

Primary melanoma tumour lesions, melanoma skin metastases, lymph nodes and healthy skin were collected with informed written consent. For gene expression studies, all primers and all probes used are listed in the Appendix (Supplements). Samples were freshly placed in RNAlater solution (Qiagen, Crawley, UK) and stored at $-70\,^{\circ}\mathrm{C}$ until use.

2.6.2 RNA isolation form patient-derived samples

RNA isolation was performed using a Qiagen Homogenizer II and an RNeasy kit. All reagents were from Qiagen unless otherwise indicated. Tissues were removed from RNAlater and placed in a 2 ml microfuge tube. Tissues were immersed in 600 μl lysis buffer, placed in Qiagen Homogenizer II and blended until liquidised. After homogenisation, the sample was spun at 14000 rpm for 3 min. Following centrifugation, supernatants were aspirated and pipetted into gDNA Eliminator spin columns and spun for 30 sec at $\geq$ 10,000 rpm. To each flow-through, 600 μl (1 volume) of 70% ethanol was added and samples were mixed immediately by pipetting, transferred to RNeasy spin columns and spun for 30 sec at 14,000 rpm. Spin columns were then washed with 700 μl of buffer RW1 and 500 μl buffer RPE (centrifuged for 15 sec at 14,000 rpm). After columns were air dried by centrifugation (2 min at 14,000 rpm), RNA was eluted with 50 μl of RNAase-free water into RNAse-free microfuge tubes. The quality of the RNA was assessed by recording absorbance at A260/A280 using a NanoDrop ND-1000 Spectrophotometer, and the Agilent 2100 RNA kit and Bioanalyser platform (Agilent Technologies, Wokingham, UK). Samples with A260/A280 ratios >1.8 or a RNA Integrity Number (RIN) >5.0 were used.

2.6.3 cDNA production

For production of cDNA, 500 ng RNA per reaction was used as a template for reverse transcription as follows: 12 μl reactions containing 0.5 μg/μl OLIGO dT primer and 1 μl RNA in nuclease free water were prepared and denatured at 70 °C for 10 min. The reverse transcription reaction was performed using 1 μl SuperScript II Reverse Transcriptase (Invitrogen), 4 μl 5x 1st strand buffer, 2 μl 0.1M DTT, 1 μl 10 mM dNTPs and 12 μl RNA OLIGO dT primer mix. The cDNA was amplified by the following thermal cycling steps: 42 °C for 5 min, 45 °C for 50 min, 70 °C for 10 min. For reverse transcription of flow cytometically-sorted cells, High Capacity cDNA Reverse Transcription Kit (Life Technologies) was used as follows: a master mix consisting of 2μl of 10x RT Buffer, 0.8 μl of 25x dNTP Mix, 2 μl of 10x RT random primers was prepared. Subsequently, 14.2 μl of isolated RNA was added to 9 μl of master mix. Finally 1 μl of MultiScribe Reverse Transcriptase was added and placed into a BioRad thermal cycler (Biorad). cDNA was produced using the following thermal cycling steps: 37 °C for 30 min, 95 °C for 5 min, 4 °C on hold.

2.6.4 cDNA quality control

Successful production of cDNA was analysed by a PCR reaction to detect the ubiquitously-expressed gene GAPDH. Briefly, 30 μl of PCR reaction per sample was prepared with 2 μl cDNA, 3 μl 10x PCR buffer, 3 μl 25 mM MgCl2, 1 μl 10 mM dNTPs, 0.5 μl 20 μM GAPDH forward primer, 0.5 μl 20 μM GAPDH reverse primer, 0.5 μl Taq DNA polymerase (2.5 U/rxn) and 19.5 μl H2O. Reaction mixtures were denatured at 95 °C for 5 mins followed by 32 thermal cycles of: 94 °C 1 min; 59 °C, 1 min; and 72 °C, 1 min; additional final extension at 72 °C for 4 min. PCR products were analysed by gel electrophoresis (1.5% agarose gel with 1x TBE plus Ethidium Bromide (EthBr), voltage of 125V) and DNA bands were visualized using UV light. PCR products showing a band at 400 kB were selected for further assessments.

2.6.5 Immunoglobulin and cytokine mRNA analysis of patient specimens/ Real-time gene expression Taqman assays

CD22, mature IgG, IL-4, IL-10, IFNγ and VEGF mRNA expression were assessed by multiplex real-time quantitative RT-PCR using TaqMan® Gene Expression Assays (primers and probes from Life Technologies) according to the manufacturers' instructions. Primers and probes for the quantification of mature IgG mRNA were designed in-house using Primer Express (Life Technologies) as follows: Probe: 5' FAM CATCGGTCTTCCCC-MGB 3'; J segment primer: 5'ACCCTGGTCACCGTCTCCTCA 3'; Mature IgG reverse primer: 5' TGCAGCAGCGGGTCAAG 3'. For each sample, mRNA abundance was normalized against the amount of human GAPDH mRNA (VIC) for the cytokine TaqMan® Gene Expression Assays or against β2-microglobulin mRNA (VIC) for CD22 and mature IgG mRNA. Data analysis was performed using either a ΔCt method and subsequently, comparing it to an arbitrary number, or a $\Delta\Delta$Ct method comparing it to freshly isolated cells from blood. Results were expressed as relative mRNA expression units or $\Delta\Delta$Ct.

2.7 Antibody and cytokine analysis

2.7.1 Isolation of primary human cells from peripheral blood

B cells or monocytes from human peripheral blood were isolated by negative selection using RosetteSep enrichments kits (StemCell) according to the manufacturer's instruction. Briefly, human blood was incubated with RosetteSep for 20 minutes at room temperature, then mixed with an equal amount of PBS containing 2% FCS and layered carefully on a 15 ml Ficoll-PaquePLUS (GE Healthcare) gradient. Following a centrifugation at 1200g for 20 minutes (increase 3; break 0) at room temperature, enriched cells were removed with a Pasteur pipette from the density media and washed (1400rpm for 6 minutes at room temperature) in PBS 2% FCS to remove any remaining contaminating Ficoll-PaquePLUS. Where necessary, an additional red blood cell lysis was performed using Red Cell Lysis buffer (Biosciences). Subsequently cells were counted on a Haemocytometer and resuspended in appropri-

ate buffers or media as needed for down stream applications. Monocytes were kept in PBS 2% FCS with the addition of 1mM EDTA to prevent aggregation.

2.7.2 *Ex vivo* cultures of B cells from melanoma lesions

Single cell suspensions were derived from patient tissues (lymph nodes or melanoma skin lesions) using a GentleMACs tissue dissociator (Miltenyi, Bergisch Gladbach, Germany) and filtered through a 100 μm strainer. Subsequently, cell were grown *ex vivo* in RPMI 1640 media supplemented with 10% FCS, 2 mM L-glutamine, penicillin (5000 U/ml) and streptomycin (100 μg/ml), Epstein Bar Virus and CpG (as described in the PhD thesis of Dr. Amy Gilbert, King's College London, 2013).

2.7.3 *Ex vivo* co-cultures with allogeneic tumour cell and peripheral blood mononuclear cell enriched with B cells

In *ex vivo* culture and stimulation experiments, human peripheral blood B cells were co-cultured in 96-well plates for 5 days together with irradiated peripheral blood mononuclear cells (PBMCs) and tumor cells at 1:5:10 ratios in RPMI 1640 medium, 10% FCS, 2 mM L-glutamine, penicillin (5000 U/mL), streptomycin (100 μg/mL) (all Life Technologies) and 2.5 ng/ml CpG 2006 ODN (InVivogen, California, USA) in a 5% CO_2 humidified incubator at 37 °C.

2.7.4 Co-cultures of allogeneic human melanoma cells or melanocytes with human peripheral blood B cells

B lymphocytes freshly isolated from human blood using RosetteSep (StemCell) and Ficoll-PaquePlus (GE Healthcare) were plated at 2 x 10^3 cells/well on U-bottom microplates (Nunc) along with 1 x 10^4 irradiated A375 (48 Gy) melanoma cells or primary human melanocytes. Co-cultures were incubated in RPMI 1640 medium, 10% FCS, 1% penicillin-streptomycin. After 5 days, total IgG secreted or cytokines

in B cell culture supernatants were measured using a sandwich ELISA or Milliplex for cytokines assay kit. Cells were also harvested and stained for cell sorting using the anti-MCSP-APC (Miltenyi) and anti-CD45-PeCy7 (BD Bioscience) antibodies.

2.8 Quantification of Immunoglobulins in patient sera

Luminex bead array assay kits, Milliplex for cytokines (Millipore) or Bioplex for IgG subclasses (Biorad), were used according to the manufacturers' instructions and data were acquired and analyzed using a FlexMap3D or Bio-Plex200, luminex bead analyser, respectively. Serum and isotyping standards were thawed and diluted in serum matrix (provided by supplier) and left on ice 30 min prior to each assay. Anti-isotype conjugated beads were vortexed for 3 minutes and then diluted in assay buffer to adjust to a final volume of 50 μl. 96-well plates were pre-wetted with 100 μl of assay buffer/well, vacuumed using a Vacuum manifold (Millipore), and 50 μl multiplex bead working solution was added per single well. Subsequently, wells were vacuumed, washed using 100 μl wash buffer per well, and standards or samples were added to the appropriate wells (resuspending the beads), before a further 30 minutes incubation at room temperature on an orbital shaker. Following 3 washes with 100 μl wash buffer, 25 μl of detection antibodies mix were added to the wells and samples were incubated for 30 minutes. This step was then followed by 3 washes with 100 μl wash buffer and treatment with 50 μl Strepavidin-PE for 15 minutes. After a final 3 washes with wash buffer (3x 100 μl), the wells were resuspended in 125 μl PBS and analysed on a Bioplex200 or FlexMap3D.

2.8.1 Evaluation of IgG_4/IgG_{total} levels

Elevated serum levels of IgG_4 antibody in patient compared to healthy volunteer sera correlate with risk of disease progression and survival. Blood samples were centrifuged for 15 minutes at 1500x g (4 °C) and subsequently stored at −80 °C prior to analysis. Milliplex IgG subclass luminex bead array assay kits (Millipore) were used as described above. Data were acquired and analyzed using a FlexMap3 (Luminex

Cooperation). IgG_4/IgG_{total} was calculated by dividing the concentration of IgG_4 by the total concentration of IgG measured (concentration in pg/ml). LDH serum levels were measured at the central laboratories of the associated hospital. Patients were segregated into those with stable disease (SD, neither progressive disease nor subsequent relapse during study period) and those with progressive disease (PD, either active progressing disease or subsequent relapse patients being up-staged during study period). Patients with co-morbidities that may have influenced IgG_4/IgG_{total} (IgG_4 levels) (e.g. lymphoma), or patients who missed their follow-up appointments, were excluded.

2.9 Flow cytometric cell sorting

Cells for downstream mRNA or protein analysis were sorted on a FACSAriaII^{TM} or a FACSAriaII^{TM} (special order) cytometer (Figure 2.1). Briefly, cells were prepared as described in the appropriate sections of this Chapter. Cytometer settings were optimized for the specific sample and drop delay was calculated using AccuDrop^{TM} (BD Bioscience) technology. A sorting layout, defining cell number and position was generated. Sorting strategies for each cell type are depicted in the Supplementary Figures of Chapters 3 and 5.

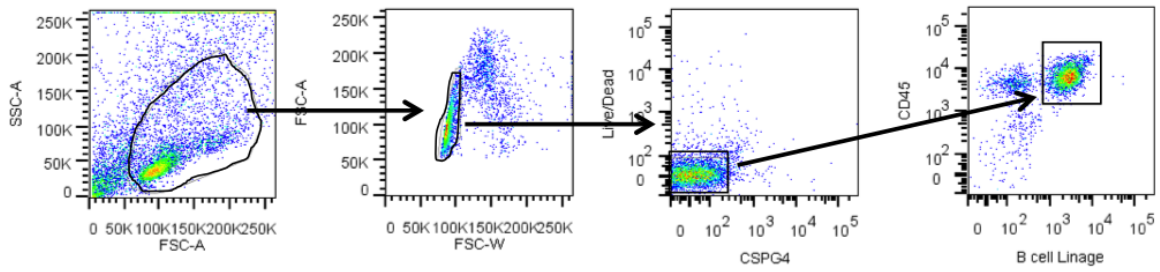

Figure 2.1: Flow cytometric sorting strategy to isolate A375 tumor cells and PBMCs from co-culture experiments.

2.10 Western blot assays to examine signalling pathways

Protein lysates were separated by SDS-PAGE using 4-15% polyacrylamide minigels (Bio-Rad) and transferred onto 0.2 μm PVDF membranes (BioRad Trans-Blot Turbo single use packages) using a BioRad Trans-Blot Turbo Transfer system (Bio-Rad). Membranes were blocked with 5% skimmed milk in PBS-Tween for 1.5 hours on an orbital shaker at room temperature. Subsequently, blots were incubated overnight on an orbital shaker with the primary antibodies against unphosphorylated and phosphorylated forms of Src, Akt, MEK(1/2) and SHIP-1 (all from Cell Signaling) diluted in 1% skimmed milk-PBS-Tween (PBST) according to manufacturer's recommendations. On the following day, membranes were washed 3x in 5 ml PBST and then incubated with goat anti-rabbit-HRP (Cell Signaling, 1:5000) for 1.5 hours at room temperature on an orbital shaker. After three washes in PBST, antibodies were visualized with an ECL detection kit (GE Healthcare) on a Hyperfilm (Amersham) using a film developer.

2.11 Cell-based ELISA detection subclass antibodies

Tumour cell-reactive antibodies were detected using cell-based ELISA as previously described [Gilbert et al., 2011]. Briefly, A375 tumor cells were plated at 3-6 x 10^5 cells on 96-well flat-bottom tissue culture plates (Corning). Cells were lightly fixed in 0.5% formaldehyde / Hank's Buffered Salt Solution. Plates were then wrapped in foil and placed in a $-80\,^{\circ}$C freezer until the day of the assay. On the day of the assay, plates were thawed for 30 minutes, washed 3 times with PBS and then blocked with a 5% non-fat milk/PBS solution for 2 hours. After removal of the blocking solution, 100 μl of supernatants from *ex vivo* B cell cultures, or non-specific IgG control (125 μg / 100 μl) or tumour-specific IgG_1 or IgG_4 antibodies (0.05 μg / 100 μl) were added, and plates were incubated for 90 minutes at room temperature on an orbital shaker. Plates were subsequently washed, and bound tumour cell-reactive antibodies from B

cell culture supernatants were detected using a mouse anti-human IgG_1 (AbSerotec, 1:400) or mouse anti-human IgG_4 (BD Bioscience, 1:50) antibody. This was followed by a 45 minute incubation with a goat anti-mouse IgG PE-labelled $F(ab)_2$ Fc-specific antibody (Jackson ImmunoResearch, 1:350). After a final wash in PBS, fluorescence intensities, describing the tumour cell reactivity for each sample, were measured on an ELISA reader (BMG Labtech, excitation 488, emission 540). All samples were measured in duplicates and median fluorescence intensities (MFI) were corrected against background and normalized against the MFI of the equivalent non-tumour cell reactive isotype control antibody. Antibodies were defined as reactive against tumor cells when the measured MFI was two standard deviations above the MFI of the non-specific isotype control antibody.

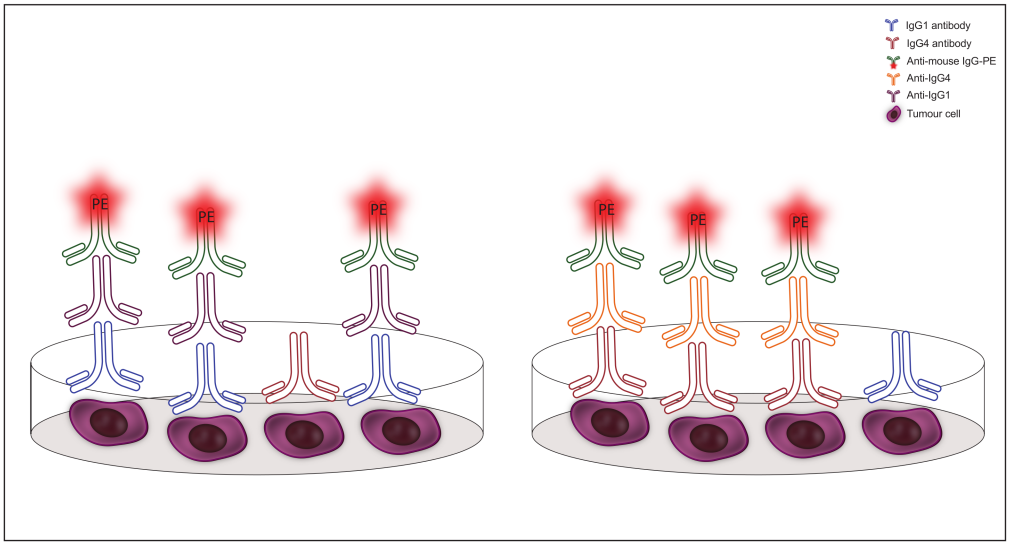

Figure 2.2: Experimental design depicting a cell-based ELISA to detect tumour-reactive antibodies of different IgG subclasses

2.12 *In vitro* analysis of anti-CSPG4 antibodies

2.12.1 Flow cytometric assessments of antibody binding to antigen/ cell surface receptors

To assess antibody binding to the tumour associated antigen CSPG4 on tumour cells or to Fc receptors on monocytic U937 and on human primary immune effector cells, cells were incubated with 10 μg/ml of mAb for 30 minutes at 4 °C and washed twice in PBS, 5% normal goat serum (FACS buffer). Cells were then incubated with mouse anti-human IgG-FITC or IgE-FITC antibodies (Jackson ImmunoResearch, Suffolk, UK) (10 μg/ml) for 30 minutes at 4 °C. Cells were finally washed again in FACS buffer prior to acquisition and analysis on a FACSCantoTM (BD Biosciences San Diego, California, USA).

2.12.2 *In vitro* assays of antibody mechanisms of action/Flow cytometric ADCC/ADCP assay

We adapted a modified three-colour flow cytometric assay to simultaneously measure tumour cell cytotoxicity (ADCC) and phagocytosis (ADCP) (Bracher et al., 2007; Karagiannis et al., 2007; Karagiannis et al., 2008a; Karagiannis et al., 2008b) to assess killing of CSPG4 expressing cells by human effector cells. Prior to assays, A375 cells were labelled with 5.0 μM CFSE (5-(and-6-) carboxyfluoresceindiacetate-succinimidyl ester, (Molecular Probes, Eugene, Oregon, USA) in PBS for 10 min at 37 °C. Cells were then washed in DMEM medium, 10% FCS, 2 mM L-glutamine and returned to normal culture conditions overnight (5% CO_2 humidified incubator at 4 °C). The following day, CFSE-labelled tumour cells were washed, mixed with effector cells at E:T ratio of 3:1 with or without antibodies, and incubated for 3 h at 37 °C (all antibodies were tested at a concentration of 10 μg/ml). Subsequently, cells were washed in PBS supplemented with 5% BSA (FACS buffer) and incubated for 20 min at 4 °C with an anti-CD89-PE (BD Bioscience, San Diego, California, USA) (10 μg/ml) (BD Bioscience). Following a further wash, dead cells were labelled for 2 min at 4 ∘C with DAPI (LifeTechnologies 1:10000). After a final wash, cells were

mixed thoroughly to interrupt cell-cell contact, re-suspended in 300 μl FACSbuffer and acquired on a FACS Canto (BD Biosciences). CFSE-labelled tumour cells were detected in the FITC channel (530/30 nm band pass filter and a 502 long pass filter), CD89-PE-labelled monocytic effector cells in the PE channel (585/42 nm band pass filter and a 556 long pass filter) and $DAPI^+$ dead cells in the PacificBlue channel (345/20 nm band pass filter), while single fluorochrome-labelled control samples were included in each experiment for compensation adjustments between channels. Two dual colour flow cytometric dot plots were generated to calculate ADCC and ADCP as previously described [Bracher et al., 2007, Karagiannis et al., 2009]. Briefly, one dot plot depicted $CFSE^+$ tumour cells on the x-axis and $DAPI^+$ cells on the y-axis, allowing quantification of % double positive events ($CFSE^+/DAPI^+$ cells) indicating tumour targets killed by effector cells by antibody-dependent cell mediated cytotoxicity (ADCC, cytotoxicity). The second dot plot depicted $CFSE^+$ tumour cells on the x-axis and CD89-PE^+ effector cells on the y-axis in order to quantify total $CFSE^+$ tumour cell events for each experimental condition and the % of tumour cells present within PE^+ effector cells, indicating antibody-dependent cell mediated phagocytosis (ADCP, phagocytosis) by effector cells ($CFSE^+/PE^+$ cells) (Figure 2.3).

The proportions of tumour cells killed by cytotoxicity and phagocytosis were derived using the following formulas:
Percentage of tumour cells killed by cytotoxicity (ADCC):
R1 SL control - R1 = X; [(X + R3)/R1 SL Control] x 100
Percentage of tumour cells phagocytosed (ADCP): [R2/R1 SL Control] x 100
Control samples were either given no antibody, or incubated with chimaeric MOv18 (IgE and IgG_1) antibodies against the tumour antigen Folate Receptor α, which is not expressed on A375 tumour cells, and is therefore not expected to mediate tumour cell death. Each assay condition was tested in triplicate.

2.12.3 *In vitro* flow cytometric ADCC/ADCP assay using kinase inhibitors to block IgE mediated mechanism

The previously described ADCC/ADCP assay was performed with the addition of an incubation step. Prior to the co-incubation of effector and target cells, primary

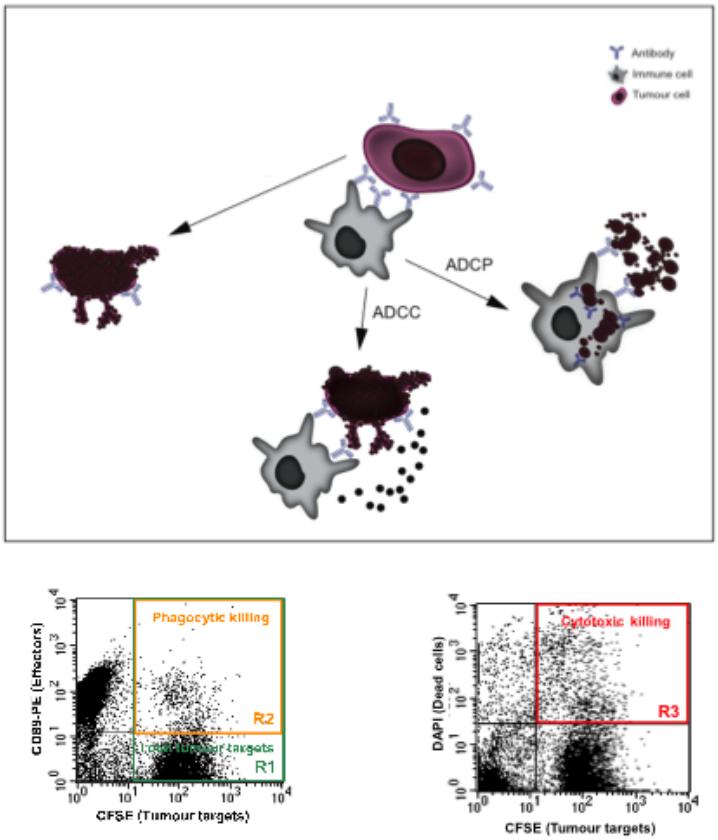

Figure 2.3: Diagram of ADCC/ADCP mechanisms. Below are two examples of flow cytometic dot plots to quantify ADCP and/or ADCC. ADCP was calculated from dot plot with cancer cells stained by CFSE and immune cells stained in PE (Left). Phagocytosed cells are double positive CFSE-PE depicted in R2. Cytotoxicity was calculated using dot plots with DAPI and CFSE (right). Double positve cells R3 along with loss of total number in R1 compared to control allows for the calculation of total ADCC.

monocytes were incubated with the kinase inhibitor PF-431396 (Sigma Aldrich) for 20 minutes to inhibit PTK2 activity. Subsequently monocytes were washed in RPMI 1640 medium, 10% FCS, 2 mM L-glutamine (1200rpm for 5 minutes at room temperature) and co-incubation with A375 melanoma cells at a 3:1 ratio. Following a 3 hour incubation cells were handled as previously described and analysed on a FACSCantoTM.

2.12.4 Imagestream analysis of receptor binding

For assessments of antibody binding to CSPG4 on a panel of human melanoma cell lines A375 primary human melanocytes, U937 monocytes or human primary monocytes, cells were incubated with 10 μg/mL CSPG4-IgG$_1$ or CSPG4-IgG$_4$ for 30 minutes at 4 °C, followed by two washes in FACSbuffer. Cells were then treated with goat anti-human IgG (Fab')2-FITC antibody on an ImageStreamX (Amnis Corporation, Seattle, WA). ImageStreamX quantitative analyses were based on the acquisition of 20,000 cell events, and median fluorescence intensities (MFI) were measured and calculated using an object mask to detect surface staining only (method described in ImageStreamX users manual).

2.12.5 Imagestream analysis of IgG$_1$ and IgG$_4$ binding competition assay

To investigate the competition between IgG$_4$ and IgG$_1$ in binding to the cells surface Fcγ receptors on primary monocytes, increasing concentrations of IgG$_4$ were added together with a defined concentration of IgG$_1$. Specifically, CSPG4-IgG$_1$ (10 μg/ml) was co-incubated with increasing concentrations of CSPG4-IgG$_4$ (at 1:1; 1:3; 1:6, 1:10 ratios of IgG$_1$ to IgG$_4$). Each incubation was performed for 30 minutes at room temperature, followed by two washes in PBS with 5% normal goat serum (FACS buffer). Cells were then treated with goat anti-human IgG$_1$-PE (10 μg/mL) (MiltenyiBiotec) to detect IgG$_1$ binding only for 30 minutes at 4 °C, and cells were washed in FACS buffer prior to acquisition and analysis on an ImageStreamX (Amnis Corporation, Seattle, WA). As above, ImageStreamX quantitative analyses constituted acquisition of 20,000 cell events and median fluorescence intensity (MFI) measurements using an object mask to detect cell surface staining only.

2.12.6 Cell viability assay (MTS)

The direct effects of antibodies on cell viability were measured by the MTS assay (tetrazolium compound 3-(4,5-dimethylthiazol-2-yl)-5-(3-carboxyphenyl)-2-(4-sulfophenyl)-2H-tetrazolium inner salt) using phenazinemethosulfate (PMS) as a reducing agent (CellTiter 96© Aqueous One Solution Cell Proliferation Assay, Promega Southampton, UK). During the experiment, MTS/PMS tetrazolium compound is bioreduced by cells into a colored formazan (orange) product that is soluble in tissue culture medium and can be measured on an absorbance plate reader. The absorbance does then correlate directly with proliferation. To assess the anti-proliferative potential of the CSPG4-IgE antibody, cells were seeded on 96-well plates in grown in DMEM, 10% FCS, 2 mM L-glutamine, penicillin (5000 U/ml) and streptomycin (100 μg/ml) and allowed to adhere before treatment with 10 μg/ml of anti-CSPG4-IgE, trastuzumab IgG_1, anti-NIP-IgE control antibody (final concentration 10 μg/ml, 200 μl per well) or no additives. Cells were returned to culture, and cell viability was assessed at 24 hours and 72 hours. Following cell cultures, MTS/PMS reagent was added at 20 μl per well to cell cultures, and cells were incubated for 2 hours before analysis on a absorbance plate reader (all components for these assay were from the CellTiter 96® AQueous Non-Radioactive Cell Proliferation Assay kit (Promega, Wisconsin, USA)). The quantity of formazan product (as measured by recording absorbance at 490 nm, and following subtraction of background absorbance at 650nm) was considered directly proportional to the number of live cells in culture.

2.12.7 *in vitro* mast cell degranulation assays

The engineered IgE antibody against the melanoma-associated antigen CSPG4-IgE was evaluated in a potency assay for its capacity to engage its congnate Fc receptors and activate effector cells to degranulate *in vitro*. The rat basophilic leukemia mast cell line RBL SX-38 expresses the human form of the FcϵRI receptor as a $\alpha\beta\gamma 2$ tetramer, which is naturally expressed on the surface of human mast cells and basophils. RBL SX-38 [Linko-Lopponen and Makinen, 1985, Bodinier et al., 2008] cells were seeded at a concentration of 2 x 10^4 cells/well in 100 μl media onto 96-well round bottom plates (Nunc, Roskilde, Denmark) and incubated in a 5% CO2

humidified incubator at 37 °C overnight. The following day, cells were sensitized with 100 ng/ml of CSPG4- IgE or control hapten specific IgE (NIP) antibody for 2 hrs at 37 °C in a humidified incubator. Cells were then washed twice with stimulation buffer (Hank's Buffered Salt Solution, HBSS supplemented with 1% BSA) and stimulated with either 1 x 10^5 A375 tumour cells per well, 100 ng/ml of polyclonal rabbit anti human-IgE (Dako, Ely, UK) antibody, or stimulation buffer alone for 30 mins at 37 °C in a humidified incubator. Controls were: untreated wells, to measure background degranulation; or HBSS containing 0.1% Triton-X100 (Sigma), to measure total mediator release. Degranulation was terminated by placing samples on ice and 50 μl of supernatant was transferred to 96-well polystyrene black MicroWellTM Plates (Nunc). Degranulation was quantified by measuring release of the mediator β-hexosaminidase using a fluorogenic substrate (4-methylumbelliferyl-N-acetyl-β-D-glucosaminide) prepared according to a standard protocol (Linko-Lopponen and Makinen, 1985; Casal et al., 2003). Supernatants were incubated with an equal amount of fluorogenic substrate at 37 °C in the dark for 2 hrs and then quenched using 0.5M tris (hydroxymethyl) aminomethane buffer (Tris) (pH=9.0) (Sigma, St. Louis, Missouri, USA). Fluorescence was measured on an Omega micro-plate reader (BMG Labtech, Aylesbury, UK), using excitation and emission filters at 360nm and 405nm. Degranulation was calculated as % relative to that measured with addition of Triton X-100, and compared with unstimulated cells ($< 10\%$).

2.12.8 FcγR inhibition assays and functional analysis of IgG_1 and IgG_4

To investigate which FcγR family on the surface of monocytes is responsible for the tumouricidal functions of the engineered anti-CSPG4 IgG_1 antibody, an *in vitro* ADCC/ADCP tumour killing experiment was conducted using either anti-CSPG4 antibodies alone or in combination with antibodies that are known to block individual Fcγ receptor families. The above-mentioned ADCC/ADCP assay was utilized for this purpose. The cells were incubated simultaneously with the appropriate CSPG4-IgG_1/IgG_4 antibodies alone or in combination with mouse anti-human FcγRI (Biolegend, used at 5μg per test; [Bruhns et al., 2009]; mouse anti-human FcγRII (Abcam, used at 10μg per test); and mouse anti-human FcγRIII (Abcam,

used at 5μg per test), which have been previously described to block the antibody Fc-mediated functions of different FcγR family members [Bruhns et al., 2009, Bunk et al., 2010]. Blocking experiments with specific or non-specific IgG_4 antibodies were conducted using a 3:1 (IgG_4:IgG_1) ratio and the appropriate concentrations of the blocking antibodies were used as reported.

2.12.9 Cell sorting of human monocytes and protein isolation

Primary monocytes were isolated by flow cytometric cell sorting following ADCC/-ADCP assays in order to assess the downstream signalling signatures associated with specific antibody treatments. Following ADCC/ADCP assays, cells were incubated with mouse anti-human CD14-PECy7 (Miltenyi) for 30 min at 4 °C, followed by two washes in PBS, 1% BSA/DAPI (Sigma; LifeTechnologies). Cells were then filtered and sorted on a FACSAriaII (BD Biosciences) for $CD14^+$ viable cells into a mammalian cell lysis buffer (Cell Signaling) containing PMSF (Sigma Aldrich).

2.13 Antibody analysis *in vivo*

2.13.1 Animal models

Male and female NOD/scid/ IL-2Rγ-/- mice (NOD.cg-Prkdcscid Il2rg tm1Wjl /SzJ [NSG]; The Jackson Laboratory, Bar Harbor MA) were used between 6 and 10 weeks of age. Mice were maintained under specific pathogen-free conditions and handled in accordance with the Institutional Committees on Animal Welfare of the UK Home Office (The Home Office Animals Scientific Procedures Act, 1986).

2.13.2 Allo-immunity xenograft model

NSG mice were injected subcutaneously with 5 x 10^5 A375 melanoma cells in 150 μl PBS. On day 5, mice received intravenous injections of 10 x 10^6 human peripheral blood lymphocytes (PBL, derived from whole human blood by lysis of red blood cells) and 10 mg/kg of appropriate antibody. Subsequent injections of antibody treatments were given either three more times (on days 12, 18 and 25) or once more (on day 13) at doses of 10 mg/kg each in 150 μl PBS each. A control group was treated with 10 x 10^6 human PBLs on day 5 and injected with 150 μl of PBS on treatment days. Tumor growth was monitored and measured using calipers. Tumor size (mm^3) was calculated using the following formula: $mm^3 = d^2$ x (D/2) [d= small diameter of tumor; D= large diameter of tumor]. Experiments were terminated once the first animal was measured with a subcutaneous tumour size no greater than 750 mm^3. Spleen engraftment of 40-70% human $CD45^+$ cells was confirmed by flow cytometry for each animal and in all experiments.

2.13.3 Humanized mouse model of an orthotropic patient tumour with autologous PBMCs

NSG mice were transplanted with equal sizes of original patient-derived skin melanoma tumour obtained by surgical procedure. In brief, mice were anaesthetised with Isoflurane (Baxter, 2%-0.5%) using a routine vaporiser. Subsequently, the surgical area was cleared of hair and disinfected with Povidon-Iodide solution (Betaisodona, Mundipharm). A 1 cm incision above the abdomen was performed. Whilst avoiding perforating the peritoneum, the subcutis was explored and the tumour was placed between the dermis and peritoneum. The incision was then closed using Vetbond tissue adhesive (3M) and bandaged. At the same time, mice were injected intravenously with 10 x 10^6 human peripheral blood lymphocytes (PBL, derived from whole human blood by lysis of red blood cells) and 10 mg/kg of antibody or control saline. Subsequent injections of antibody were given every 7 days. Tumour growth was monitored and measured using calipers. Tumor size (mm^3) was calculated using the following formula: $mm^3 = d^2$ x (D/2) [d= small diameter of tumor; D= large

diameter of tumor]. Mice were sacrificed when their tumour reached a size no greater than 750 mm^3.

2.14 Quality control and quantification for cRNA production

The agilent 2100 bioanlyser is a microfluidics-based platform used of the sizing, quantification and quality control of nucleic acids, protein and cells. The RNA Nano kit (Agilent Technology) allowed for the quantification and analysis of the integrity of total RNA as to detect possible rRNA impurities. The RNA Integrity Number (RIN) was set at 9 and any sample that showed a value below was excluded from further analyses. RNA that was of good enough quality was further processed using the IlluminaTotalPrep RNA Amplification kit (Ambion) as following: RT-PCR with T7 oligodT primers was used to produce first strand cDNA. The cDNA then underwent second strand synthesis using DNA polymerase and enzymatic RNA degradation. *in vitro* transcription technology, along with biotin UTP, was employed to generate multiple copies of biotinylated cRNA. The labelled cRNA was purified via filter cartridges and quantified using a Qubit RNA assay kit (LifeTechnolgy) on a Qubitfluorometer (LifeTechnolgy). The KCL Genomics Centre performed the hybridization and microarray data acquisition. Chrysanthi Ainali (PhD student, KCL) in collaboration with Jananan S. Pathmanathan (MSc student, KCL) conducted subsequent data analysis.

2.15 Statistical analyses

All statistical test where performed using GraphPad Prism Version 6 with the exception of cross-table calculations, Fisher Exact Test and binary logistic regressions which were performed using IBM SPSS software. Results were initially assessed for Gaussian distribution. Subsequent statistical analysis was chosen according to the distribution.

2.15.1 *In vitro* and *in vivo* data statistical evaluations

All statistical analyses were performed using GraphPad Prism software (version 5 or 6 GraphPad). Comparative quantitative RT-PCR analyses in human skin specimens were conducted using a Kruskal-Wallis analysis with a Dunn post-test. Comparative analyses of immunohistochemical staining were performed using a Mann-Whitney-U-test. One-way ANOVA with Bonferoni post-test was employed to compare ADCC/ADCP of tumor cells by human monocytes, triggered by antibodies. Two-way ANOVA with Bonferoni post-test was employed to compare restriction of tumor cell growth *in vivo*. Prior to any analysis data points in each cohort were tested for normal distribution using the D'Agostino-Pearson normality test. P values were indicated as follows: * $P<0.05$, ** $P<0.01$, *** $P<0.001$; ns = not significant $P>0.05$. Box plots in real-time RT-PCR expression experiments represent mean and whiskers indicate Min/Max values. Error bars in all *in vitro* figures represent standard deviation (SD). Error bars in all *in vivo* figures and histological analyses represent standard error of mean (SEM).

2.15.2 Statistical tests used for IgG_4 biomarker evaluation

Significant increases between the IgG_4 fraction (IgG_4/IgG_{total}) measurements in healthy volunteer sera and breast cancer sera were calculated using the Kruskal-Wallis one-way analysis of variance with post-hoc Dunn's test. ROC analysis was performed using the build-in method in GraphPad Prism Version 6. The Youden Index (specificity + sensitivity -1) was used to calculate the cut-off point for IgG_4 used to evaluate differences in overall survival and disease-free progression between groups. The sensitivity and specificity was calculated via the ROC analysis. Significant differences in progression free survival and overall survival for IgG_4 levels and LDH were calculated using Mantel-Cox analysis. Statistical differences in circulating B cells between healthy volunteer blood and blood form patients with melanoma were calculated using a Mann-Whitney-U-test.

2.16 List of reagents

Product name	Catalogue No.	Supplier
BupH™ Carbonate-Bicarbonate Buffer Packs, 0.2M carbonate-bicarbonate, pH 9.4	28382	Pierce
Maxisorp™ 96 Well Plates	442404	Nunc
O-Phenylene Diamine Dihydrochloride (OPD) Tablet	P6912	Sigma Aldrich
Stable Peroxidase Substrate Buffer 10x	34062	Pierce
Streptavidin-Horseradish Peroxidase (HRP) Conjugate	21130	Pierce
Tween® 20	P1379	Sigma Aldrich
Phosphate Buffered Saline 1x pH 7.2, Non-sterile	20-7400-10	Severn Biotech
Phosphate Buffered Saline 1x pH 7.2, sterile	20012	LifeTechnologies
Dimethyl Sulfoxide (DMSO)	472301	Sigma Aldrich
FluoroNunc™ Black 96 Well Plates	MPA-560-040A	Fisher Scientific
Hanks' Balanced Salt Solution (HBSS) with Calcium, Magnesium, no Phenol Red	14025050	LifeTechnologies
Triton X-100	X100	Sigma Aldrich
4-methylumbelliferyl-N-acetyl-D-glucosaminide (β-N-acetylhexosaminidase substrate) C18H21NO8	M2133	Sigma Aldrich
HCl 1 M	H1758	Sigma Aldrich
6 Well Tissue Culture Plates	3516	Corning
CellTracker™ Blue Dye (7-Amino-4-Chloromethylcoumarin)	C211	LifeTechnologies
LIVE/DEAD Viability/Cytotoxicity Kit for mammalian cells containing Calcein AM and Ethidium homodimer-1	L3224	LifeTechnologies
MatTek 12 Well Glass Bottomed Culture Plates	P12G-1.0-10	MatTek Corporation
Carboxy Fluorescein Diacetate Succinimidyl Ester (CFSE)	21888	Sigma Aldrich
Vacuum Stericup® Filter Units (0.22 μm pore size)	FDR-120-090W	Millipore
Sodium Azide	S-2002	Sigma Aldrich
β-mercaptoethanol 50 mM	M6250	Sigma Aldrich
TaqMan® Universal PCR Master Mix	4326708	Applied Biosystems
Oligo dT	AM5730G	LifeTechnology
Superscript II	18064022	LifeTechnology
10x Lysis Buffer	9803	BioLabs
PMSF	P7626	Sigma
HBSS	14025050	LifeTechnology
Ficoll Paque Plus	17144003	GE Healthcare
TBE 10x	T8935	Sigma Aldrich
Agarose	A4679	Sigma Aldrich
Ethanol	45-986-6	Sigma Aldrich
Neutral Buffered Formalin (10%)	PRC/R/4/200ml	Pioneer Research Chem.
MicroAmp® Optical 96 Well Reaction Plate	N8010560	LifeTechnologies
MicroAmp® Optical Adhesive	4311971	LifeTechnologies
% (v/v) formaldehyde in PBS	361367L	Pioneer Research Chem.
ProLong® Gold antifade reagent with DAPI	P36931	LifeTechnologies
4–15% Mini-PROTEAN® TGX™ Precast Gel	456-1083	BioRad
Trans-Blot® Turbo™ Midi PVDF Transfer Packs	170-4157	BioRad
Precision Plus Protein™ Kaleidoscope Standards	161-0375	BioRad
LDS Sample Buffer, Non-Reducing (4X)	84788	Pierce
RNAlater	AM7021	LifeTechnologies
O-Phenylene Diamine Dihydrochloride (OPD) Tablet	P6912	Sigma Aldrich
Stable Peroxidase Substrate Buffer 10x	34062	Pierce
Streptavidin-Horseradish Peroxidase (HRP) Conjugate	21130	Pierce
Tween® 20	P1379	Sigma Aldrich
Phosphate Buffered Saline 1x pH 7.2, Non-sterile	20-7400-10	Severn Biotech
Phosphate Buffered Saline 1x pH 7.2, sterile	20012	LifeTechnologies
Dimethyl Sulfoxide (DMSO)	472301	Sigma Aldrich
FluoroNunc™ Black 96 Well Plates	MPA-560-040A	Fisher Scientific
Hanks' Balanced Salt Solution (HBSS) with Calcium, Magnesium, no Phenol Red	14025050	LifeTechnologies
Triton X-100	X100	Sigma Aldrich
4-methylumbelliferyl-N-acetyl-D-glucosaminide (β-N-acetylhexosaminidase substrate) C18H21NO8	M2133	Sigma Aldrich
HCl 1 M	H1758	Sigma Aldrich
6 Well Tissue Culture Plates	3516	Corning
CellTracker™ Blue Dye (7-Amino-4-Chloromethylcoumarin)	C211	LifeTechnologies
LIVE/DEAD Viability/Cytotoxicity Kit for mammalian cells containing Calcein AM and Ethidium homodimer-1	L3224	LifeTechnologies
MatTek 12 Well Glass Bottomed Culture Plates	P12G-1.0-10	MatTek Corporation
Carboxy Fluorescein Diacetate Succinimidyl Ester (CFSE)	21888	Sigma Aldrich
Vacuum Stericup® Filter Units (0.22 μm pore size)	FDR-120-090W	Millipore
Sodium Azide	S-2002	Sigma Aldrich
β-mercaptoethanol 50 mM	M6250	Sigma Aldrich
TaqMan® Universal PCR Master Mix	4326708	Applied Biosystems
Oligo dT	AM5730G	LifeTechnology
Superscript II	18064022	LifeTechnology
10x Lysis Buffer	9803	BioLabs
PMSF	P7626	Sigma
HBSS	14025050	LifeTechnology
Ficoll Paque Plus	17144003	GE Healthcare
TBE 10x	T8935	Sigma Aldrich
Agarose	A4679	Sigma Aldrich
Ethanol	45-986-6	Sigma Aldrich
Neutral Buffered Formalin (10%)	PRC/R/4/200ml	Pioneer Research Chem.
MicroAmp® Optical 96 Well Reaction Plate	N8010560	LifeTechnologies
MicroAmp® Optical Adhesive	4311971	LifeTechnologies
4% (v/v) formaldehyde in PBS	361367L	Pioneer Research Chem.
ProLong® Gold antifade reagent with DAPI	P36931	LifeTechnologies
4–15% Mini-PROTEAN® TGX™ Precast Gel	456-1083	BioRad
Trans-Blot® Turbo™ Midi PVDF Transfer Packs	170-4157	BioRad
Precision Plus Protein™ Kaleidoscope Standards	161-0375	BioRad
LDS Sample Buffer, Non-Reducing (4X)	84788	Pierce
RNAlater	AM7021	LifeTechnologies

Table 2.1: List of reagents

Antibody	Supplier	Host Species	Conjugate	Catalogue No.
anti-human CD14	Biolegend	mouse	PE-Cy7	325618
anti-human CD22	BD Bioscience	mouse	APC	333145
anti-human CD19	BD Bioscience	mouse	FITC	555412
anti-human IgG	Jackson Immuno-Research	goat	FITC	109-095-098
anti-human IgG	AbDSerotec	goat	unconjugated	204001
anti-human CD89	BD Bioscience	mouse	PE	555686
Anti-human HER2/neu Trastuzumab (Herceptin®)	Roche	human	unconjugated	
anti-mouse IgG	Invitrogen	goat	Alexa 488	A11017
anti-human IgE	Vector	goat	FITC	FI-3040
anti-human CD3	DAKO	mouse	PE	R0910
anti-human CSPG4 IgG_1 (high-molecular weight melanoma associated antigen)	In house	human chimaeric	unconjugated	Clone: 225.28s
anti-human CSPG4 IgG_4 (high-molecular weight melanoma associated antigen)	In house	human chimaeric	unconjugated	Clone: 225.28s
anti-human CSPG4 IgE (high-molecular weight melanoma associated antigen)	In house	human chimaeric	unconjugated	Clone: 225.28s
anti-human FRα (Folate Receptor α) IgG	In house	human chimaeric	unconjugated	Clone: MOv18
anti-human FRα (Folate Receptor α) IgE	In house	human chimaeric	unconjugated	Clone: MOv18
isotype control	DAKO	mouse	unconjugated	X0931
anti-rabbit IgG	Invitrogen	goat	Alexa 647	A21245
anti-human IgG Fc-specific antibody	Sigma	goat	HRP	A0293
anti-human IgG Fc-specific F(ab)'2 antibody	Jackson Immuno-Research	goat	HRP	109-036-098
anti-human CD27	eBioscience	mouse	PE	12-0279-73
anti-human CD27	BD Bioscience	mouse	APC	337169
anti-human CD20	BD Bioscience	mouse	APC	340908
anti-human CD20	BD Bioscience	mouse	PerCP-Cy5.5	332781
anti-human CD3	Invitrogen	mouse	Pe-Cy5.5	MHCD0318
anti-NIP IgE	AbDSerotec	human chimaeric	unconjugated	MCA3335
anti-human IgE	Dako	rabbit	unconjugated	A0094
anti-human MCSP (high-molecular weight melanoma associated antigen)	Invitrogen	mouse	unconjugated	412000
anti-goat IgG	Invitrogen	donkey	Alexa 555	A21432
anti-human CD22	eBioscience	rabbit	unconjugated	14-0229-80
anti-human CD64	Biolegend	mouse	unconjugated	305015
anti-human CD32	Abcam	mouse	unconjugated	ab41899
anti-human CD16	Abcam	mouse	unconjugated	ab46679
anti-human CD27	BD Bioscience	mouse	V450	560448
anti-human CD19	BD Bioscience	mouse	BV605	562653
anti-human CLA	BD Bioscience	rat	FITC	555947
anti-human CD14	BD Bioscience	mouse	AlexaFluor 700	557923
anti-human CD45	BD Bioscience	mouse	V500	560777
anti-human CD3	BD Bioscience	mouse	APC-H7	641397
anti-human IgG_1	Miltenyi Biotec	mouse	PE	130-093-188
anti-human IgG_4	BD Bioscience	mouse	unconjugated	555881
human IgG_4	Sigma	human	unconjugated	I4639
human IgG3	Sigma	human	unconjugated	I5654
IgG, F(ab')2 fragment Fcγ	Jackson Immuno-Research	goat	unconjugated	109-036-098
anti-mouse CD45	eBioscience	rat	APC-Fluor 700	47-0451
anti-human CD68	DAKO		unconjugated	

Table 2.2: List of antibodies

Product Name	Catalogue No.	Supplier
Dermal Cell Basal Medium	PCS-200-030	ATCC
Dimethylsulfoxide (DMSO)	472301	Sigma
Ethanol; CH3OH	45-983-6	Sigma
EDTA dissodium salt C10H14N2ONa2O82xH20	E0399	Sigma
RPMI 1640	31870-025	LifeTechnology
Dulbecc's Modified Eagle's Medium (DMEM)	21980-032	LifeTechnology
Dimethylsulfoxide (DMSO)	D2650	Sigma
Eagle's Minimum Essential Medium with Earle's Salts	E15-825	PAA
Foetal Calf Serum (FCS)	10106-169	LifeTechnology
Penicillin; Streptomycin; Glutamine (PSG)	10378-016	LifeTechnology
Geneticin (G418)	10131-027	LifeTechnology
Goat Serum (non specific)	16210-072	LifeTechnology
Phosphate buffered saline sterile	14190-094	LifeTechnology
recombinant human IL-4	204-IL	R&D Systems
Trypsin EDTA Solution	35400-027	LifeTechnology
Trypan Blue Solution	T8154	Sigma
Bovine Serum Albumin	5497	Sigma
HBSS with Phenol	24020-133	LifeTechnology
IgG from human	I2511	Sigma
RosetteSep CD14 monocyte enrichment	15068	StemCell Technologies
RosetteSep HLA B cell enrichment	15064HLA	StemCell Technologies
Trizma	T1503	Sigma
Ficoll Paque Plus	17144003	GE Healthcare
TBE 10x	T8935	Sigma
Agarose	A4679	Sigma
Corning® cell culture flasks (175cm)	CLS431079	Corning
Corning® cell culture flasks (75cm)	CLS430720	Corning
U 96 well plate; Cell Culture; clear with lid; Sterile	168136	Thermo Fischer

Table 2.3: Cell culture material

Name	Supplier	Catalogue No.
High Capacity RNA-to-cDNA Kit	LifeTechnologies	4387406
RNeasyPLUS Mini Kit	Qaigen	74104
Illumina® TotalPrep™ RNA Amplification Kit	LifeTechnologies	AMIL1791
MILLIPLEX® MAP Human Isotyping Magnetic Bead Panel	Millipore	HGAMMAG-301K
Bio-Plex Pro™ Human Isotyping Assays	BioRad	171-A3100M
MILLIPLEX MAP Human Cytokine/Chemokine Magnetic Bead Panel	Millipore	HCYTOMAG-60K

Table 2.4: List of kits

3 IgG4 SUBCLASS ANTIBODIES IMPAIR ANTITUMOR IMMUNITY IN MELANOMA

Chapter 3 Paper 1: IgG4 subclass antibodies impair antitumour immunity in melanoma

The following figures from paper 1 were contributed by myself:

Figure 1: All data

Figure 2: 2A in collaboration with Dr. Amy E. Gilbert, the rest of Figure 2 all data

Figure 3: 3A in collaboration with Dr. Amy E. Gilbert, the rest of Figure 3 all data

Figure 4: All data

Figure 5: All data

Figure 6: All data

Figure 7: 3B in collaboration with Mr Alexander Koers, the rest of Figure 3 all data

Figure 8: All data

IgG4 subclass antibodies impair antitumor immunity in melanoma

Panagiotis Karagiannis,[1] Amy E. Gilbert,[1] Debra H. Josephs,[1] Niwa Ali,[1] Tihomir Dodev,[2] Louise Saul,[1] Isabel Correa,[1] Luke Roberts,[3] Emma Beddowes,[3] Alexander Koers,[4] Carl Hobbs,[5] Silvia Ferreira,[3] Jenny L.C. Geh,[6] Ciaran Healy,[6] Mark Harries,[7] Katharine M. Acland,[3] Philip J. Blower,[4] Tracey Mitchell,[3] David J. Fear,[2] James F. Spicer,[8] Katie E. Lacy,[1] Frank O. Nestle,[1] and Sophia N. Karagiannis[1]

[1]National Institute for Health Research (NIHR) Biomedical Research Centre at Guy's and St. Thomas' Hospitals and King's College London, Cutaneous Medicine and Immunotherapy Unit, St. John's Institute of Dermatology, Division of Genetics and Molecular Medicine, King's College London School of Medicine, Guy's Hospital, King's College London, London, United Kingdom. [2]Division of Asthma, Allergy and Lung Biology, Medical Research Council and Asthma UK Centre in Allergic Mechanisms of Asthma, King's College London, Guy's Campus, London, United Kingdom. [3]Skin Tumour Unit, St. John's Institute of Dermatology, Guy's Hospital, King's College London, and Guy's and St. Thomas' NHS Foundation Trust, London, United Kingdom. [4]Division of Imaging Sciences, Rayne Institute, King's College London School of Medicine, St. Thomas' Hospital, and King's College London, London, United Kingdom. [5]Wolfson Centre for Age-Related Diseases, King's College London, London, United Kingdom. [6]Department of Plastic Surgery at Guy's, King's, and St. Thomas' Hospitals, London, United Kingdom. [7]Clinical Oncology, Guy's and St. Thomas' NHS Foundation Trust, London, United Kingdom. [8]Department of Academic Oncology, Division of Cancer Studies, King's College London, Guy's Hospital, London, United Kingdom.

Host-induced antibodies and their contributions to cancer inflammation are largely unexplored. IgG4 subclass antibodies are present in IL-10–driven Th2 immune responses in some inflammatory conditions. Since Th2-biased inflammation is a hallmark of tumor microenvironments, we investigated the presence and functional implications of IgG4 in malignant melanoma. Consistent with Th2 inflammation, $CD22^+$ B cells and $IgG4^+$-infiltrating cells accumulated in tumors, and IL-10, IL-4, and tumor-reactive IgG4 were expressed in situ. When compared with B cells from patient lymph nodes and blood, tumor-associated B cells were polarized to produce IgG4. Secreted B cells increased VEGF and IgG4, and tumor cells enhanced IL-10 secretion in cocultures. Unlike IgG1, an engineered tumor antigen-specific IgG4 was ineffective in triggering effector cell–mediated tumor killing in vitro. Antigen-specific and nonspecific IgG4 inhibited IgG1-mediated tumoricidal functions. IgG4 blockade was mediated through reduction of FcγRI activation. Additionally, IgG4 significantly impaired the potency of tumoricidal IgG1 in a human melanoma xenograft mouse model. Furthermore, serum IgG4 was inversely correlated with patient survival. These findings suggest that IgG4 promoted by tumor-induced Th2-biased inflammation may restrict effector cell functions against tumors, providing a previously unexplored aspect of tumor-induced immune escape and a basis for biomarker development and patient-specific therapeutic approaches.

Introduction

Despite numerous reports investigating the clinical significance of immune cells in the circulation and in tumor lesions, the nature of local B cell responses and functional contributions of antibodies produced in cancer are largely unexplored (1–4). Recent studies have mainly focused on the immunoregulatory roles of B cells in mouse models of cancer through mechanisms such as effector cell engagement of Fcγ receptors and production of cytokines such as TNF-α and IL-10 (5, 6).

B cells respond to a variety of local stimuli to differentiate, undergo class switching, and produce antibodies of specific classes and subclasses. Human B cells are known to produce 4 subclasses of IgG (IgG1, IgG2, IgG3, IgG4), with each subclass having different biological functions (7, 8). These antibody types vary in their ability to activate immune system components, including the formation of the complement complex or the engagement of Fc receptors on the surface of effector cells (9). However, whether IgG subclasses and their effector functions are of significance in cancer inflammation is relatively unknown.

IgG4 is considered a "weak" subclass due to its poor ability to bind complement and Fc receptors and to activate effector cells. IgG4 production is normally associated with prolonged exposure to antigens and has been reported to interact with antibodies of the IgG and IgE classes through their Fc domains, potentially influencing antibody-mediated functions (10, 11). In healthy adult serum, IgG1, IgG2, IgG3, and IgG4 represent 65%, 25%, 6%, and 4% of the total IgG pool, respectively, but these proportions may be altered in certain disease contexts (8, 12). Associations of IgG4 antibodies are reported in a range of chronic inflammatory and autoimmune conditions that feature infiltration of target organs by IgG4-expressing cells (13, 14). Despite association with inflammatory pathologies, in allergy, elevated serum IgG4 antibody titers correlate with a reduction of allergic symptoms and successful allergen immunotherapy (15, 16). In this context, IgG4 antibodies are thought to interfere with IgE-mediated effector cell activation. This indirectly implies a functional significance of IgG4 in modulating antigen-specific antibody-mediated effector mechanisms and in inducing clinical tolerance (17, 18).

Authorship note: Frank O. Nestle and Sophia N. Karagiannis contributed equally to this work.

Conflict of interest: The authors have declared that no conflict of interest exists.

Citation for this article: *J Clin Invest.* 2013;123(4):1457–1474. doi:10.1172/JCI65579.

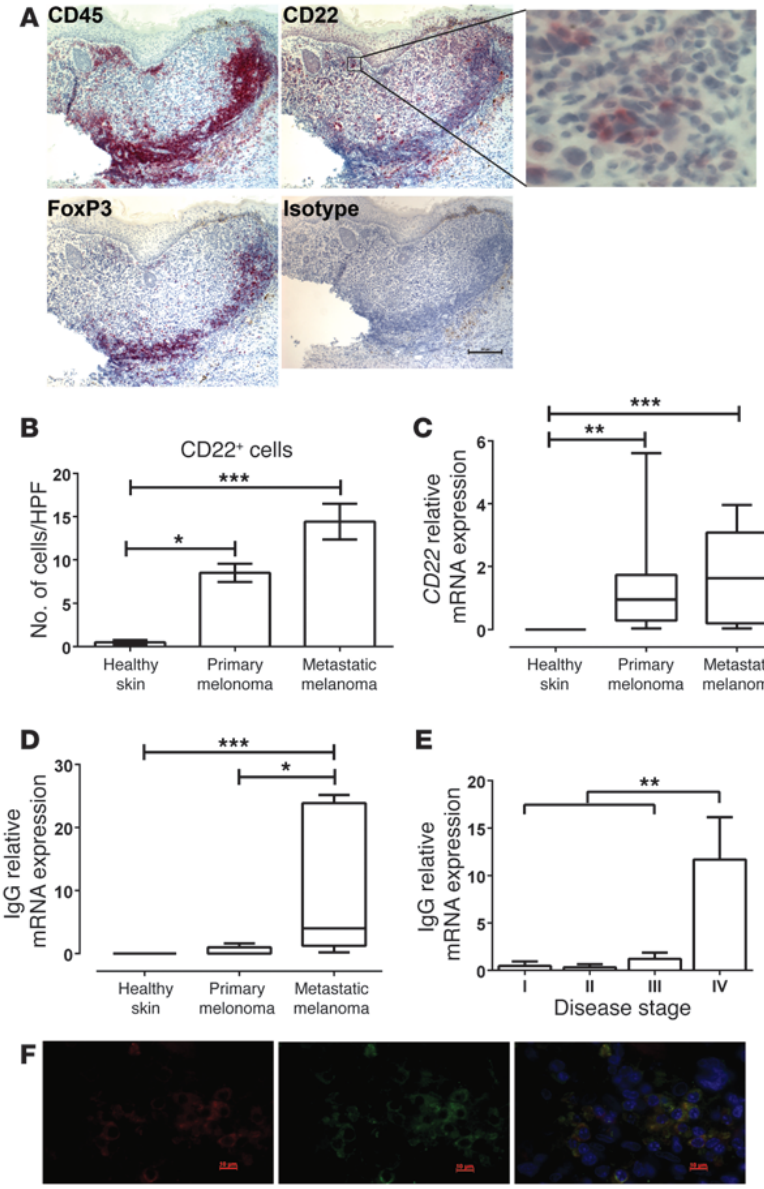

Figure 1
B cells (CD22⁺) infiltrate melanoma lesions and produce IgG. (**A**) Immunohistochemistry showing the presence of lymphocytes (CD45⁺), mature B cells (CD22⁺), activated lymphocytes (FoxP3⁺) (alkaline phosphatase [red], hematoxylin [blue]), and colocalization of all 3 within cutaneous metastases (scale bar: 100 μm; original magnification, ×10). CD22⁺ cells in melanoma are shown at higher magnification (original magnification, ×40). (**B**) Significantly increased CD22⁺ B cell infiltration was measured in primary (n = 6) and metastatic (n = 7) melanoma lesions compared with healthy skin (n = 8). HPF, high-powered microscope field. (**C**) Comparative real-time PCR showed significantly elevated CD22 expression in primary (n = 10) and metastatic (n = 10) melanomas compared with healthy skin (n = 9). (**D**) Increased expression of mature IgG mRNA in metastatic melanoma lesions (n = 10) compared with primary melanomas (n = 10) and healthy skin (n = 9) measured by comparative real-time PCR analysis. (**E**) IgG expression (by comparative real-time RT-PCR) is elevated in melanoma lesions of stage IV patients compared with lesions of stage I–III patients. (**F**) Immunofluorescent evaluations of IgG⁺ B cells in human metastatic melanoma lesions (CD22⁺ B cells in red; left) (IgG⁺ cells in green; middle) and CD22⁺IgG⁺ B cell infiltrates (right). Scale bar: 10 μm; original magnification, ×63. (**B** and **E**) $^{*}P < 0.01$, $^{**}P < 0.01$, $^{***}P < 0.001$, Mann-Whitney U test. (**C** and **D**) $^{*}P < 0.05$, $^{**}P < 0.01$, $^{***}P < 0.001$, Kruskal-Wallis 1-way ANOVA with Dunn's post-hoc test. Horizontal lines in box plots represent the mean, and whiskers indicate minimum and maximum values

The relationship between IgG4 and malignancy is largely unexplored. Infiltrating IgG4⁺ cells in lesions of patients with extrahepatic cholangiocarcinomas and pancreatic cancers were recently reported (19, 20), and early studies have indicated abnormalities in serum titers of IgG4 in patients with melanoma (21). Both the presence and potential biological role of IgG4 subclass antibodies in melanoma tumor lesions remain largely unknown. Th2-mediated immune responses represent the classical hallmarks of local inflammation in solid tumors such as melanomas (22). The immunoregulatory cytokine IL-10 has been shown to trigger "a modified Th2 response" by inducing differentiation of IgG4⁺ B cells and, in the presence of IL-4, to direct antibody class switching of B cells to secrete IgG4 (23, 24).

The association between induction of IL-10 and production of IgG4 antibodies has been shown in IgG4-related diseases and also in allergic individuals undergoing allergen immunotherapy (25). Th2-type inflammation in tumor tissues is dominated by IL-10–producing cells, such as Tregs and M2-type macrophages (26, 27). We therefore reasoned that these Th2-type tumor inflammatory microenvironments may favor "alternatively activated" humoral immunity and local expression of IgG4 antibodies.

In this study, we show mature B cells and IgG4 antibodies in melanoma lesions in the presence of key Th2-type cytokines that may trigger IgG4 production. Using engineered IgG1 and IgG4 antibodies of the same specificity against a tumor-associated antigen, we demonstrate the capacity of IgG4 to counteract antitumor immunity in vivo.

Results

CD22⁺ B cells infiltrate melanoma lesions and IgG antibodies are expressed in situ. The presence of mature CD22⁺ B cells was observed in melanoma lesions by immunohistochemistry (Figure 1A). CD22⁺ cell infiltrates were found both within tumor lesions and in surrounding stroma areas rich in CD45⁺ cells, indicating that this population is part of the immune inflammatory infiltrate in tumors. Furthermore, CD22⁺ cells were also seen in close proximity to FoxP3⁺

Table 1
Pathological evaluations of IgG4, CD22, and FoxP3 of melanoma lesions, with corresponding clinical parameters

Patient ID	Gender	Breslow	Stage	Date of diagnosis	Date of biopsy	Infiltrating CD22	Infiltrating IgG4	Infiltrating FoxP3	Status
M72	F	3.12	IV	12/12/2003	01/26/2011	–	–	–	Alive
M78	M	1.07	IV	03/02/2009	05/14/2009	+	+	–	Deceased
M109	M	1.86	IV	02/19/2007	09/13/2009	+	+	–	Deceased
M141	M	9.7	IV	10/23/2006	11/27/2009	+	–	+	Alive
M173	F	2.2	IIIB	10/23/1998	02/12/2010	++	+	+	Deceased
M248	F	NA	IIIB	06/01/2004	07/30/2010	+	–	+/–	Alive
M430	F	6.75	IIC	11/29/2011	01/27/2012	++	–	++	Alive
M525	F	2.2	IIC	06/29/2012	08/02/2012	++	++	+	Alive
M549	F	0.45	III	07/02/2010	09/29/2012	+	+/–	++	Alive

Evaluation criteria were as follows: –, 0% infiltration; +/–, <25% infiltration; +, >25% < 50% infiltration; ++, >50% infiltration; +++, >75% infiltration. See also Figures 1 and 2. $n = 9$. NA, not available.

cells, which may imply associations between regulatory elements and B cells in tumors, as reported in the context of cholangiocarcinoma (19). $CD22^+$ cell infiltrates were found in 8 out of 9 melanoma lesions examined, and 6 of these $CD22^+$ tumors were also positive for FoxP3 (Table 1). Quantitative immunohistochemical evaluations also confirmed infiltration of $CD22^+$ B cells, associated with 6 out of 6 primary and 5 out of 7 metastatic tumor lesions, while we detected sporadic $CD22^+$ infiltrates in 2 out of 8 healthy skin specimens (Figure 1B and Supplemental Figure 1, left panel; supplemental material available online with this article; doi:10.1172/JCI65579DS1). Primary and metastatic melanoma tumors had ≥7 $CD22^+$ B cells per high-powered microscope field, compared with very low or absent $CD22^+$ B cell infiltration in healthy skin ($P < 0.05$ and $P < 0.001$, respectively; Figure 1B).

The presence of $CD22^+$ B cells in melanoma lesions was also confirmed by quantitative RT-PCR analyses. *CD22* mRNA expression was determined in healthy skin ($n = 9$), primary melanoma lesions ($n = 10$), and melanoma skin metastases ($n = 10$) (Figure 1C). We detected low to no expression of *CD22* mRNA in healthy skin samples and significantly elevated levels in primary and metastatic melanoma skin lesions ($P < 0.01$ and $P < 0.001$, respectively), suggesting recruitment of mature B cells to tumors (Figure 1C). Levels of mature IgG mRNA were elevated in metastatic melanoma lesions ($n = 10$) compared with those in both primary melanomas ($n = 10$) ($P < 0.05$) and healthy skin samples ($n = 9$) ($P < 0.001$), in which there was little to no expression (Figure 1D and Table 2). When we analyzed IgG4 expression by disease stage, we found significantly higher expression of IgG mRNA in lesions from patients with stage IV disease ($n = 6$) compared with expression in lesions from patients at stages I–III ($n = 14$) (Figure 1E). Local expression of $CD22^+IgG^+$ B cell infiltrates was detected in melanoma lesions, as determined by dual-color immunofluorescence (Figure 1F). These data confirm that mature antibody-expressing B cells infiltrate melanoma lesions and that IgG antibodies are expressed locally in metastatic melanoma.

Tumor-associated B cells are polarized to produce IgG4 antibodies in Th2-biased inflammatory melanoma microenvironments. To examine the proportions of IgG subclasses produced in melanoma, B cells from melanoma skin lesions ($n = 2$, stages III and IV), patient lymph nodes ($n = 3$, stage III), patient blood ($n = 6$, stages III and IV), and healthy volunteer blood ($n = 4$) were cultured ex vivo (Tables 2 and 3 and Supplemental Table 1). IgG subclass titers (IgG1, IgG2, IgG3, IgG4) in culture supernatants were then measured by ELISA. Proportional IgG subclass expression and $IgG4/IgG_{total}$ ratios from healthy volunteer peripheral blood B cells (IgG1: 79.5% ± 8.5%; IgG2: 14.3% ± 7.9%; IgG3: 4.3% ± 1.5%; IgG4: 1.5% ± 1%), patient peripheral blood B cells (IgG1: 76.4% ± 14.3%; IgG2: 15.8% ± 10.2%; IgG3: 4.1% ± 3.2%; IgG4: 3.9% ± 2.2%), and B cells from patient lymph nodes (IgG1: 83.2% ± 3.6%; IgG2: 6.5% ± 0.5%; IgG3: 3.3% ± 1.0%; IgG4: 7.0% ± 2.1%) were consistent with those commonly detected in human sera ($IgG4/IgG_{total}$ ratio range: 0.01–0.083, each condition tested in triplicate) (Figure 2A and ref. 12). However, B cells derived from metastatic melanoma lesions exhibited higher proportional IgG4 subclass production ($IgG4/IgG_{total}$ ratio range: 0.209–0.334) (IgG1: 43.2% ± 1.7%; IgG2: 4.1% ± 1.4%; IgG3: 24.8% ± 3.5%; IgG4: 27.5% ± 5.3%) (Figure 2A).

Using immunohistochemical evaluations, we also detected substantial levels of IgG4-immunopositive cells infiltrating tumor areas in primary and metastatic melanoma lesions, while $IgG4^+$ cells were rarely observed in healthy skin (Figure 2B, left, and Supplemental Figure 1, right panels). These observations were confirmed with quantitative assessments of sections, which showed IgG4 positivity in 9 out of 12 melanomas and sporadic expression in 2 out of 10 healthy skin specimens ($P < 0.001$; Figure 2B, right). Furthermore, immunohistochemical evaluations of $IgG4^+$ infiltrates were examined in relation to clinical parameters for a cohort of 9 patients. Although these observations are limited by the small number of patients, it is noteworthy that 3 patients who are deceased demonstrated IgG4 positivity in the lesions tested (Table 1). Expression of IgG4 was also confirmed by RT-PCR sequence alignments of patient specimens (representative clone in Supplemental Figure 2). These data suggest that IgG4 production occurs in situ in the melanoma microenvironment.

We then asked whether IgG4 antibodies in the tumor microenvironment and in patient circulation may recognize tumor cells. For this, we examined the reactivities against tumor cells of IgG1 and IgG4 antibodies produced by B cells derived from patient blood ($n = 2$, patients in stage III and IV), cutaneous metastases ($n = 3$, 2 patients in stage III and 1 patient in stage IV), and a lymph node metastasis ($n = 1$, a patient in stage III) and cultured ex vivo for 5 days. Tumor cell reactivity evaluations were conducted using a previously described cell-based ELISA (28). We found detectable levels of IgG4 reactivity against A375 metastatic melanoma cells, above background set by human IgG4 antibody controls, in

Table 2
Clinical parameters, pathological evaluations, and IgG expression levels for melanoma lesions

Patient ID	Gender	Age	Stage	IgG expression	Breslow	Clark	Ulceration	Tumor inf. lymphocytes	Classification	TNM classification
M123	M	76	IV	0.5	5.85	IV	Absent	Absent	Primary	T4a;N3;M1a
M125	F	62	IB	0	1.65	III	Absent	Present	Primary	T2a;N0;M0
M127	F	36	IIIC	4.006	N/A	N/A	N/A	N/A	In transit metastasis	T3a;N3;M0
M128	F	82	IB	0	1.08	III	Absent	Present	Primary	T2a;N0;M0
M129	M	63	IV	22	N/A	N/A	N/A	N/A	In transit metastasis	T3a;N3;M1c
M133	M	75	IIC	0.0234	3.3	IV	Absent	Absent	Primary	T4b;N0;M0
M147	F	46	IIIA	1.456	2.1	Unknown	Absent	Unknown	Primary	T3a;N1a;M0
M171	M	48	IIIC	0.00032	N/A	N/A	N/A	N/A	In transit metastasis	T2a;N3;M0
M173	F	87	IIIB	0.00041	N/A	N/A	N/A	N/A	In transit metastasis	T3b;N2c;M0
M192	F	88	IV	4.006	N/A	N/A	N/A	N/A	Dist. subcutaneous metastasis	T4b;N0;M1a
M294	M	80	IIC	0.0041	6.36	IV	Present	Absent	Primary	T4b;N0;M0
M72	F	77	IV	17	N/A	N/A	N/A	N/A	In transit metastasis	T3a;N3;M1c
M80	M	70	IIA	0.0056	2.85	IV	Absent	Absent	Primary	T3a;N0;M0
M172	M	73	IIIB	1.78	N/A	N/A	N/A	N/A	In transit metastasis	T3b;N2c;M0
M141	M	64	IV	0.861	N/A	N/A	N/A	N/A	Dist. skin metastasis	T4a;N3;M1a
M245	M	79	IIB	1.61	3	III	Present	Unknown	Primary	T3b;N0;M0
M284	F	65	IIIC	0.0202	N/A	N/A	N/A	N/A	In transit metastasis	Tx;N3;M0
M149	M	60	IB	1.4	1.11	IV	Absent	Absent	Primary	T2a;NxMx
M269	F	73	IIA	0	2.32	IV	Absent	Present	Primary	T3a;N0;M0
M221	M	52	IV	25	N/A	N/A	N/A	N/A	In transit metastasis	Tx;N0;M1c

See also Figures 1 and 2. $n = 20$. N/A, not assessed; inf., infiltrating; Dist., distant. Numbers in the "Breslow" column indicate the thickness (mm) of the primary melanoma. Values in the "Clark" column (I–V) indicate the level of anatomical invasion of the skin into different skin compartments

1 blood sample and 1 cutaneous metastasis (Figure 2C). In the same specimens, we found no equivalent detectable reactivity of IgG1 antibodies against these tumor cells. In contrast, we detected IgG1 antibody reactivity to melanoma cells in the lymph node sample without detectable equivalent IgG4 reactivity. Additionally, using 2-color immunofluorescence on a cutaneous melanoma lesion, we demonstrated colocalization of IgG4 with the melanoma-associated antigen S100, further supporting the presence of tumor reactive IgG4 antibodies in situ (Figure 2D). These experiments, together with detected IgG4 expression in melanoma lesions by RT-PCR analysis (Supplemental Figure 2), suggest that tumor-reactive antibodies of the IgG4 subclass are expressed by patient B cells situated in both melanoma lesions and the circulation. We reasoned that the polarization of IgG4 in situ may be influenced by local factors, such as production of IL-10 in combination with IL-4, which is known to induce differentiation of $IgG4^+$ B cells, drive class switching, and to maintain polarization of humoral immune responses in favor of IgG4 (29). Accordingly, we found significantly elevated mRNA expression of the Th2 cytokines *IL4* and *IL10* and of the inflammatory cytokine *IFNG*, reported to be involved in tumorigenesis, by quantitative RT-PCR in both primary ($n = 10$) and metastatic ($n = 10$) melanoma skin specimens when compared with healthy skin samples ($n = 9$) ($P < 0.05$; Figure 2E and ref. 30). Secretion of these cytokines was also confirmed in ex vivo cultures of tumor lesions (Figure 2F). These findings indicate a potential association of Th2-biased local expression of IL-10 and IL-4 with IgG4 production at inflammatory tumor sites.

Melanoma tumor cells trigger Th2-driven polarization, inducing B cells to secrete IgG4. To elucidate whether melanoma cells can influence polarized expression of IgG4 by B cells, we attempted to recreate the proximity between B cells and tumor cells in an ex vivo stimulation assay. We cocultured melanoma patient peripheral blood B cells with autologous irradiated PBMCs in the presence or absence of A375 metastatic melanoma cells or human primary melanocytes. Similarly to that in B cells isolated from melanoma lesions, we detected increased $IgG4/IgG_{total}$ ratios from blood B cells cultured with PBMCs in the presence of melanoma cells (IgG1: 35.0% ± 5.6%; IgG2: 23.1% ± 0.9%; IgG3: 30.3% ± 4.6%; IgG4: 20.0% ± 1.1%), while $IgG4/IgG_{total}$ ratios remained low when B cells were cultured with PBMCs in the absence of melanoma cells (IgG1: 54.8% ± 3.5%; IgG2: 29.3% ± 8.6%; IgG3: 9.2% ± 1.3%; IgG4: 6.7% ± 1.2%) ($n = 9$, Figure 3A, left). When we compared IgG4 polarization of B cells plus PBMCs in the absence or presence of melanocytes (IgG1: 51.9% ± 2.9%; IgG2: 21.5% ± 4.2%;

Table 3
Clinical parameters and pathological evaluations for lymph node specimens

Patient ID	Gender	Age	Stage	Nodes sampled	Nodes involved	Metastasis	TNM
M488	F	53	IIIA	2	1	Yes	T2a;N1a;M0
M36	M	69	IIIC	9	1	Yes	T4b;N3;M0
M490	F	54	IIIB	14	2	Yes	T4b;N2a;M0

See also Figures 1 and 2. $n = 3$.

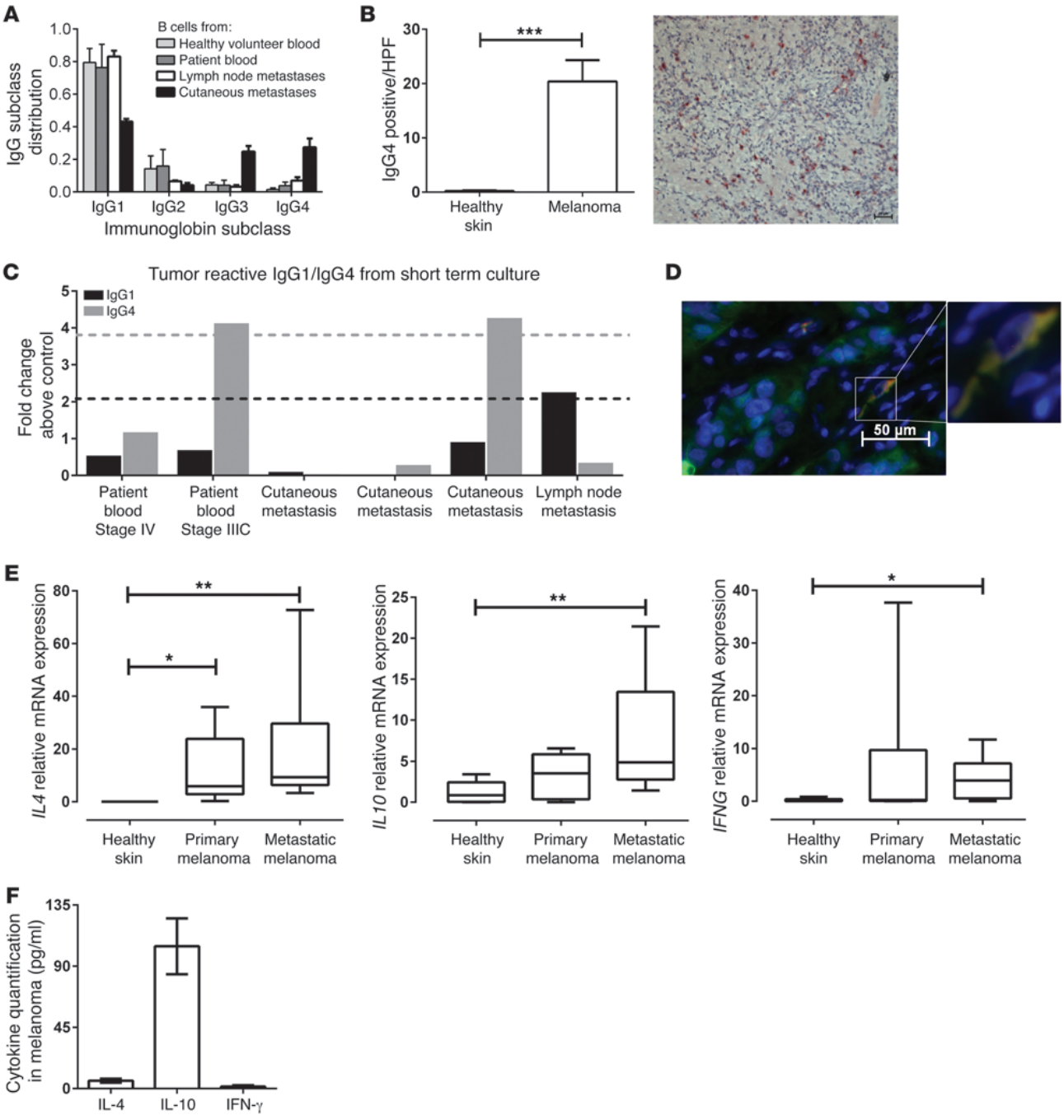

Figure 2

B cells in melanoma lesions are polarized to produce IgG4 antibodies with reactivity against tumor cells. (**A**) Polarization of IgG subclasses in B cells derived from metastatic melanoma skin tumor lesions ($n = 2$), patient lymph nodes ($n = 3$), peripheral blood from patients with melanoma ($n = 6$), and from healthy volunteers ($n = 4$). Cells were cultured ex vivo, and IgG subclass expression profiles were analyzed from culture supernatants by ELISA (mean ± SD; each sample condition tested in triplicate). (**B**) Immunohistological evaluations confirm significantly increased IgG4$^+$ cell infiltration in melanoma lesions ($n = 10$) but not healthy skin ($n = 10$) (***$P < 0.001$), and representative metastatic melanoma depicts IgG4$^+$ cells (red; hematoxylin [blue]) (scale bar: 20 μm; original magnification, ×10). (**C**) Reactivity of patient B cell–derived IgG1 and IgG4 antibodies to A375 tumor cells evaluated using a cell-based ELISA. Dashed black and gray lines indicate cut-off points for IgG1 and IgG4 tumor-reactive antibodies, respectively (lines defined as 2 SDs above isotype control antibodies). (**D**) Immunofluorescent staining of IgG4$^+$ (red) colocalized with S100$^+$ (green) cells in metastatic melanoma (scale bar: 50 μm; original magnification, ×40). (**E**) Increased expression of *IL4*, *IL10* and *IFNG* in metastatic melanomas ($n = 10$) compared with primary melanomas (n = 10) and healthy skin ($n = 9$) by comparative real-time PCR. Horizontal lines in box plots represent mean, and whiskers indicate minimum and maximum values. *$P < 0.05$, **$P < 0.01$, Kruskal-Wallis 1-way ANOVA with Dunn's post-hoc test. (**F**) Cytokines IL-4, IL-10 and IFN-γ are secreted in metastatic melanoma lesion ex vivo cultures.

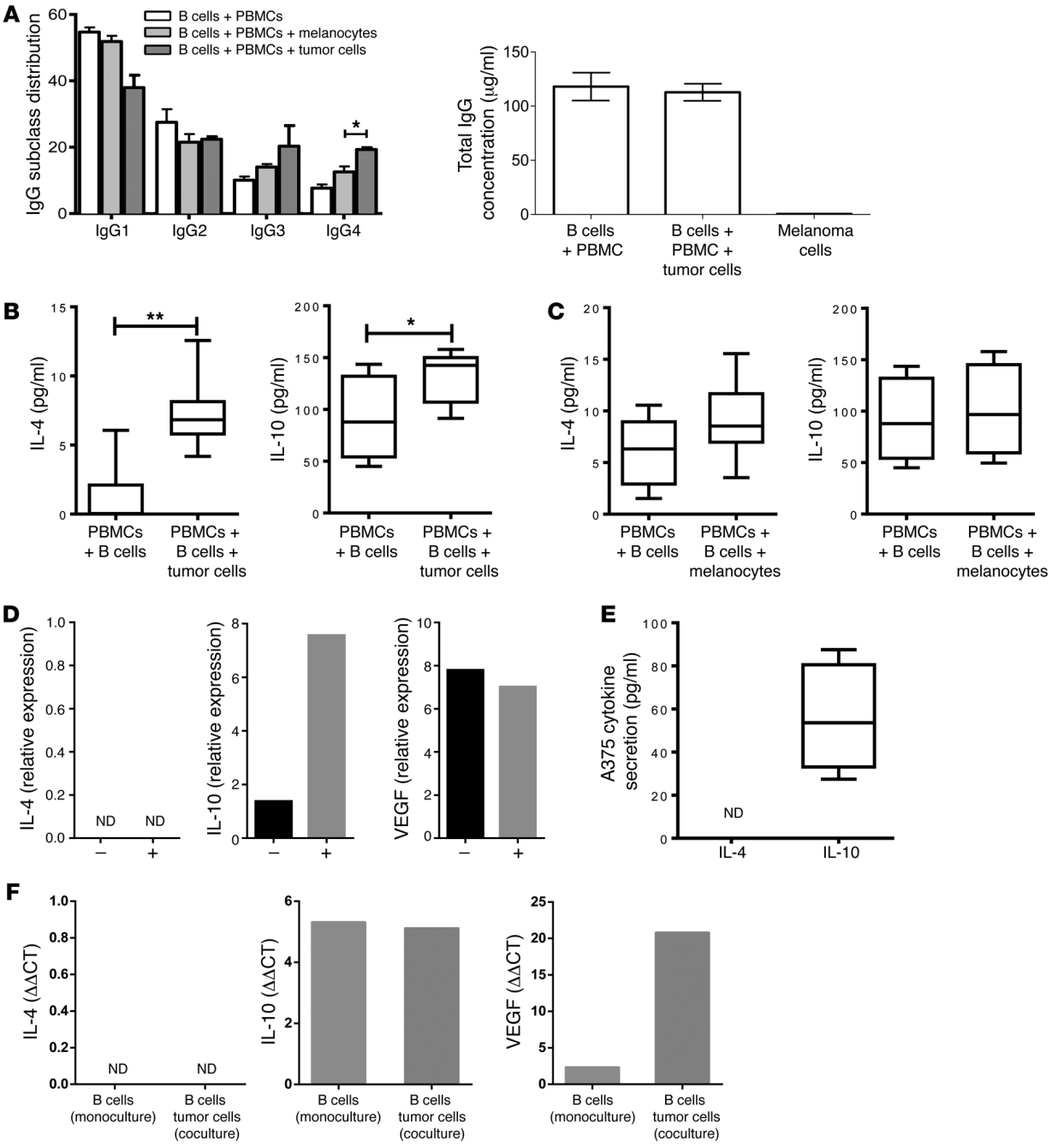

Figure 3

Ex vivo stimulation assays demonstrate that tumor cells polarize B cells to produce IgG4. (**A**) IgG subclass production by patient peripheral blood B cells. Cells were cocultured with irradiated PBMCs with or without metastatic melanoma cells or primary melanocytes for 5 days. Culture supernatants were harvested, and IgG subclass expression profiles were analyzed by IgG subclass ELISA. IgG subclass fractions and total IgG concentrations were illustrated for each sample as mean ± SD of 3 independent experiments (all conditions performed in triplicates). *$P < 0.01$. Secretion of Th2 cytokines IL-10 and IL-4 from B cell cultures treated with or without (**B**) tumor cells or (**C**) primary melanocytes were analyzed by cytokine multiplex assay analysis. Both cytokines were significantly increased in cultures containing tumor cells but not in cocultures with melanocytes (*$P < 0.01$; **$P < 0.01$, Mann-Whitney U test; $n = 9$ replicates per coculture condition). Horizontal lines in box plots represent mean, and whiskers indicate minimum and maximum values. Comparative real-time PCR analysis of IL-4, IL-10, and VEGF expression by A375 melanoma cells isolated by flow cytometric sorting before (–) and after (+) cocultures with B cells and PBMCs shows (**D**) increased IL-10 expression by cocultured melanoma cells and (**E**) confirmation that A375 cells secrete IL-10 but not IL-4 in culture. ND, not detected. (**F**) Comparative real-time PCR analysis of IL-4, IL-10, and VEGF expression by B lymphocytes isolated by flow cytometric sorting from monocultures or from cultures with tumor cells, showing increased expression of VEGF expression by B cells when cocultured with tumor cells.

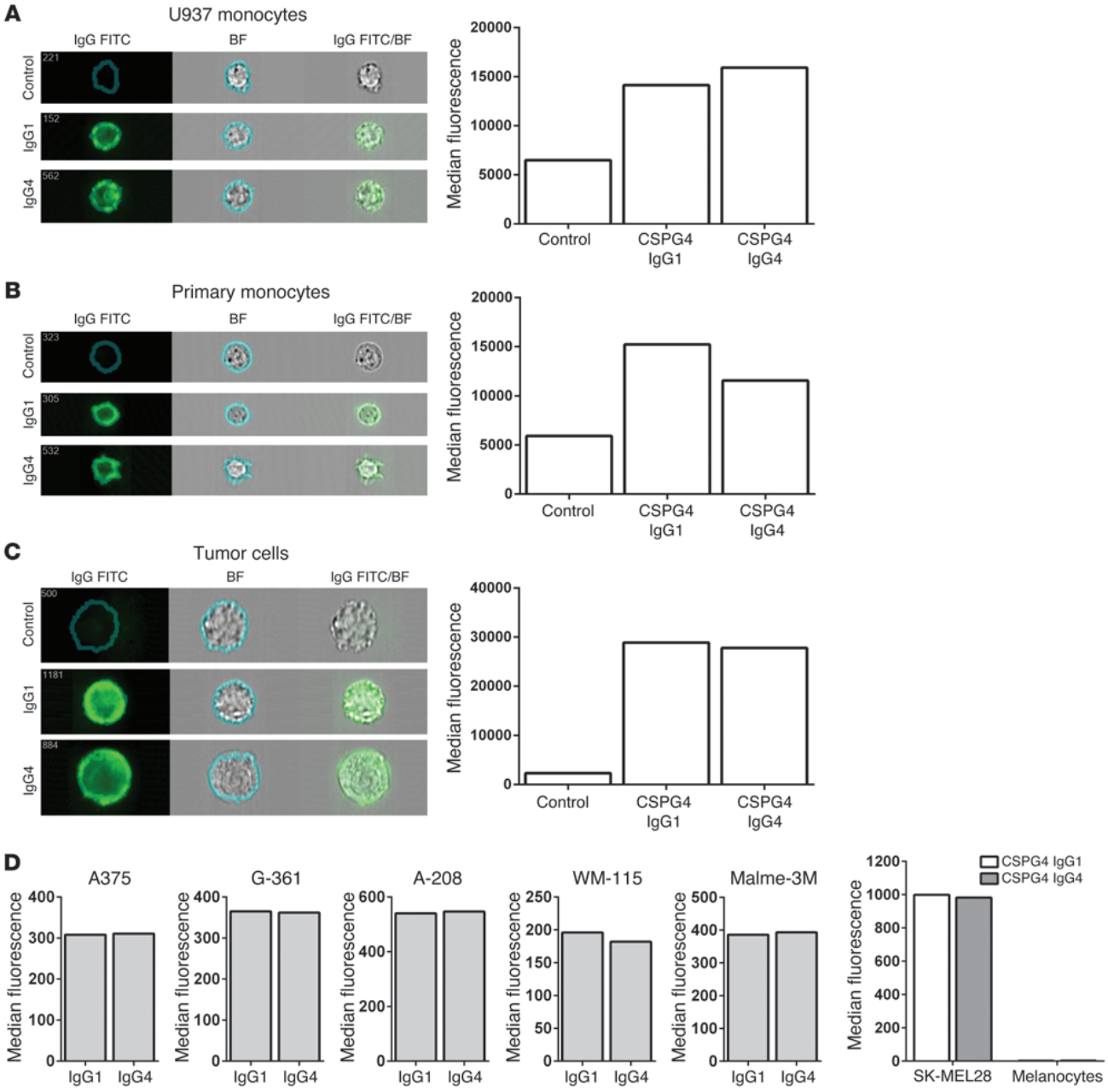

Figure 4

Biological properties of engineered IgG1 and IgG4 antibodies recognizing the melanoma-associated antigen CSPG4. Anti-CSPG4 IgG1 and anti-CSPG4 IgG4 antibodies bind to receptors on the cell surface of (**A**) U937 monocytic cells, (**B**) primary monocytes, and (**C**) tumor cells. ImageStream and flow cytometric evaluations confirm IgG1 and IgG4 antibody binding to Fcγ receptors (top and middle panels) and also to the antigen CSPG4 (bottom panel) expressed on the surface of SK-MEL-28 melanoma cells. ImageStream images are shown on the left. IgG FITC, cell surface (area indicated by circle on top left of each panel) binding of antibodies on cells; BF, bright-field image of cells; IgG FITC/BF, composite image of antibody and bright-field images, confirming anti-CSPG4 antibody binding to the cell surface. Quantitative analyses are based on the acquisition of 20,000 cells. Control samples for U937 and monocytes were incubated with goat anti-human IgG $(Fab')_2$-FITC antibody. Control samples for antibody binding to tumor cells were human IgG1 and IgG4 isotype antibodies of irrelevant specificity. (**D**) Flow cytometric analysis of CSPG4 IgG1 or CSPG4 IgG4 antibody binding to a panel of tumor cell lines or primary human melanocytes. Antibody binding was detected with an anti-human IgG $(Fab')_2$-FITC, and specific binding was depicted by MFI values above isotype control antibody binding.

IgG3: 14.0% ± 1.5%; IgG4: 12.6% ± 2.8%), we observed a small, but not statistically significant, difference in $IgG4/IgG_{total}$ ratios with the addition of melanocytes, indicating that IgG4 polarization may be partly due to an allogeneic HLA mismatch effect in these assays. We demonstrated significant changes in IgG4 polarization (higher $IgG4/IgG_{total}$ ratios) when comparing B cells, PBMCs, and melanocytes with samples of B cells, PBMCs, and melanoma cells ($P < 0.05$). The overall titers of IgG antibodies produced in the presence or absence of melanoma cells in these assays were comparable (Figure 3A, right).

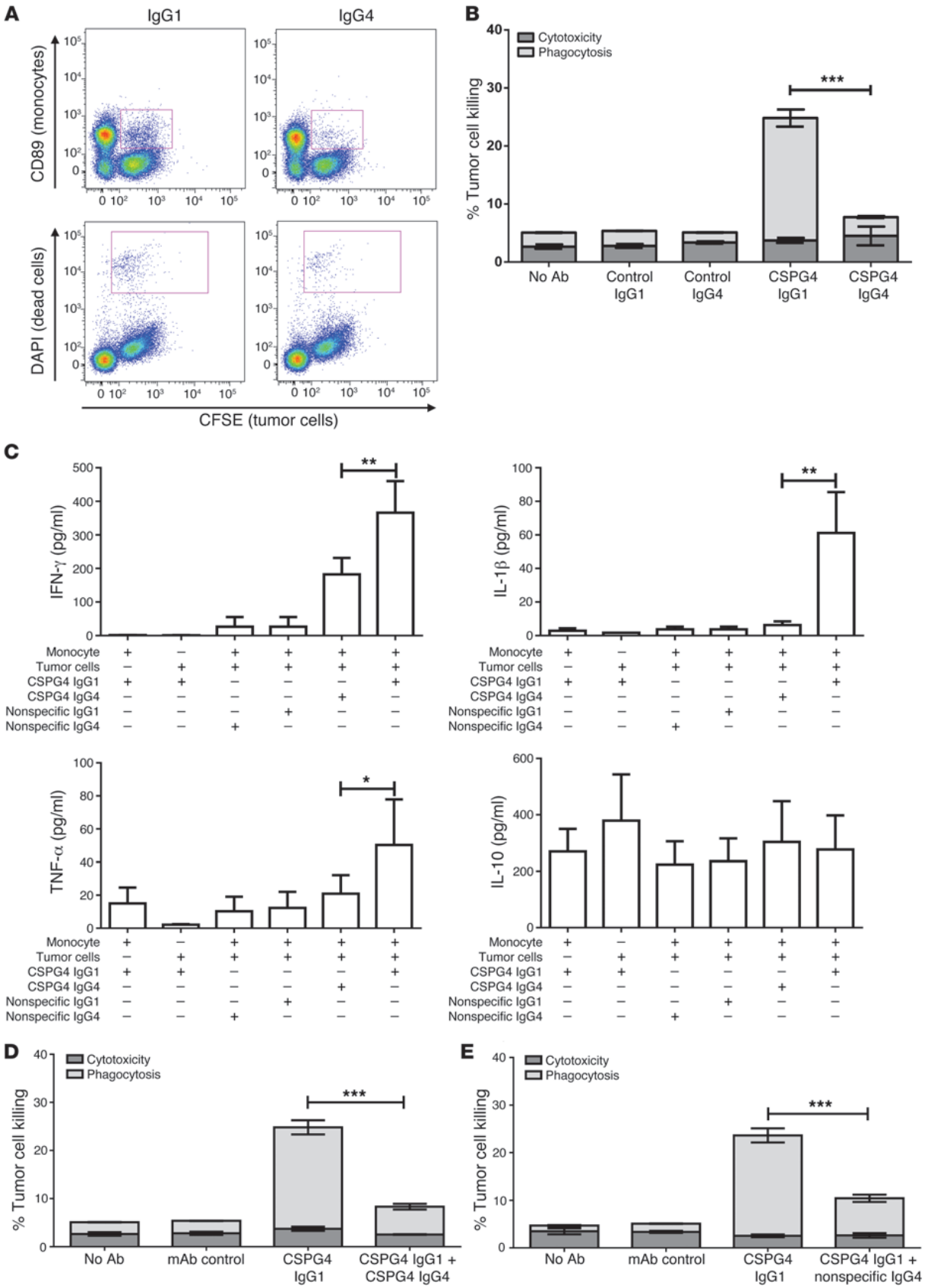

Figure 5
IgG4 irrespective of tumor specificity is ineffective in triggering anti-melanoma effector functions in vitro and prevents IgG1 from mediating tumor cell killing. (**A**) Dot plots depicting $CFSE^+$ tumor cells and CD89-PE^+ monocytes (effector cells) were used to quantify $CFSE^+$ tumor cells present within PE^+ effector cells, indicating phagocytosis (ADCP) ($CFSE^+/PE^+$ cells) (top panel). $CFSE^+/DAPI^+$ double-positive tumor cell events indicate tumor targets killed by cytotoxicity (ADCC, bottom panel) by IgG1 but not IgG4. (**B**) Quantification of tumor antigen-specific IgG1 and IgG4 antibody induced ADCC/ADCP by monocytes. Tumor antigen-specific IgG1 mediated tumor cell killing compared with an unspecific control antibody or cells alone. The corresponding anti-CSPG4 IgG4 antibody induced no tumor cell killing above isotype control levels. (**C**) Titers of secreted IFN-γ, IL-1β, and TNF-α, but not of IL-10, were higher in culture supernatants of monocytes and tumor cells stimulated with anti-CSPG4 IgG1 antibodies compared with those stimulated with anti-CSPG4 IgG4 or controls. All samples were tested in duplicates; mean ± SD (n = 6). (**D**) Tumor antigen-specific IgG1 against the melanoma antigen CSPG4 can induce monocytes to kill tumor cells, but addition of anti-CSPG4 IgG4 blocks the antitumor functions of the same concentrations of IgG1. (**E**) Similar blocking of IgG1-mediated tumor cell killing can be observed when CSPG4 IgG1 is coincubated with a nonspecific human IgG4 antibody. (**B**, **D**, and **E**) All assays were performed in triplicates. Data represent percentage tumor cell killing (mean ± SD) (n = 6). *P < 0.05, **P < 0.01; ***P < 0.001.

We next asked whether ex vivo production of IgG4 in the presence of melanoma cells is associated with Th2-biased inflammatory cytokines. Consistent with our findings in metastatic melanoma lesions, ex vivo stimulation of B cells with metastatic melanoma cells triggered enhanced IL-4 and IL-10 levels, as compared with B cell cultures in the absence of melanoma cells (P < 0.01 and P < 0.05, respectively) (Figure 3B). We also detected increased titers of VEGF, IL-6, and MCP-1, but not IFN-γ, in cocultures with melanoma cells (Supplemental Figure 3A). In contrast, when we compared IL-4 and IL-10 titers in cultures of B cells and PBMCs in the presence or absence of melanocytes, we did not observe any significant increases (Figure 3C). These findings indicate that melanoma cells drive Th2-biased inflammatory environments favoring increased $IgG4/IgG_{total}$ production ratios.

To further investigate the origin of Th2 cytokine production, we harvested A375 melanoma cells before and after coculture assays by flow cytometric cell sorting (strategy for flow cytometric sorting shown in Supplemental Figure 3B). We demonstrated increased expression of IL-10 by these cells following coculture with B cells and PBMCs. Message for IL-4 was not detected, and *VEGF* mRNA was present but was not upregulated following coculture (Figure 3D). When cultured alone under normal culture conditions, melanoma cells did not express or secrete IL-4, but the cells secreted detectable levels of IL-10 (Figure 3E). These assays point at enhanced expression of IL-10 by melanoma cells in these coculture assays. Neither B cells nor tumor cells expressed IL-4 message under these culture conditions, and therefore, IL-4 may be contributed by another cell type in PBMCs (Supplemental Figure 3C) or possibly stromal cells in the tumor microenvironment.

Having shown that tumor cells produce IL-10 in culture, next we investigated the cytokines produced by sorted B cells in these culture conditions (strategy for flow cytometric sorting shown in Supplemental Figure 3D). B cells in coculture experiments upregulated VEGF expression, while expression of IL-10 by these cells was detected but not upregulated following coculture with tumor cells (Figure 3F). These experiments suggest that B cells may contribute to polarized humoral immunity by enhancing production of VEGF.

IgG4 subclass antibodies lack antitumoral effector functions and block IgG1-mediated tumor cell killing by patient monocytes. To explore potential mechanisms by which IgG4 may impact on antitumoral responses, we engineered 2 antibodies, with IgG1 and IgG4 Fc regions, that share identical variable regions recognizing the melanoma-associated antigen CSPG4. With these, we attempted to mimic a clinically relevant situation, in which IgG1 and IgG4 were found alone or together in the presence of tumor antigen-expressing cancer cells and FcγR-expressing immune effector cells, such as patient monocytes/macrophages (5, 19). Both antibodies bound to FcγR-expressing U937 monocytes, to patient monocytes (Figure 4, A–C), and to a panel of melanoma cells (Figure 4D).

First, we examined the ability of each antibody to activate patient-derived monocytes to kill tumor cells in vitro. Patient monocytes incubated with anti-CSPG4 IgG4 and A375 melanoma cells mediated nonsignificant tumor cell killing compared with a nonspecific IgG4 (antibody clone SP211-IgG4) after 3 hours (n = 6). In contrast, the corresponding anti-CSPG4 IgG1 of the same specificity triggered statistically significant increases in phagocytosis (antibody-dependent cellular phagocytosis [ADCP]) (21.1% ± 2.5%) of melanoma tumor cells by monocytes compared with anti-CSPG4 IgG4 (3.2% ± 0.3%) and controls (2.6% ± 0.1%) (P < 0.001; Figure 5, A and B). Consistent with reduced IgG4 antitumor activity, we detected lower levels of IFN-γ (P < 0.01), IL-1β (P < 0.01), and TNF-α (P < 0.05) in supernatants from cultures treated with anti-CSPG4 IgG4 compared with those treated with anti-CSPG4 IgG1 (n = 6) (Figure 5C).

When anti-CSPG4 IgG1 and anti-CSPG4 IgG4 were combined with patient-derived monocytes and melanoma cells, the tumoricidal capacity of anti-CSPG4 IgG1, previously observed in the antibody-dependent cellular cytotoxicity/ADCP (ADCC/ADCP) assays, was significantly reduced in the presence of anti-CSPG4 IgG4 (P < 0.001, Figure 5D). This suggested that anti-CSPG4 IgG4 is not only incapable of triggering effector cell–mediated tumor killing but may additionally suppress tumor cell killing capacity of tumor-specific IgG1. To evaluate whether specificity for the tumor antigen was necessary for an IgG4 antibody to block IgG1 effector cell functions against tumor cells, we performed ADCC/ADCP (cytotoxicity/phagocytosis) assays, incubating tumor cells and patient-derived monocytes with anti-CSPG4 IgG1 in combination with a human IgG4 antibody of irrelevant specificity. Nonspecific IgG4 partly hindered tumor-specific IgG1 tumor cell killing (P < 0.001; Figure 5E), suggesting that tumor cell specificity may only be partly responsible for the antibody modulatory properties of IgG4. These data are in line with known properties of IgG4 interactions with Fc regions of immunoglobulins, and they are also consistent with reports that only a small fraction of IgG4 antibodies are allergen specific in allergic subjects following immunotherapy (31). In summary, IgG4 antibodies lack antitumoral effector functions and impair IgG1-mediated tumor cell killing by patient monocytes.

IgG4 blocks IgG1 tumor cell killing by inhibiting IgG1 binding and activation through FcγRI. In order to elucidate whether IgG4 antibodies could hinder binding of IgG1 on the surface of effector cells, we performed a competition binding assay using monocytic cells. This showed decreased IgG1 binding on the surface of human monocytes with increasing concentrations of IgG4 (Figure 6A), suggesting that IgG4 competes with IgG1 for FcγR binding on the surface of effector cells.

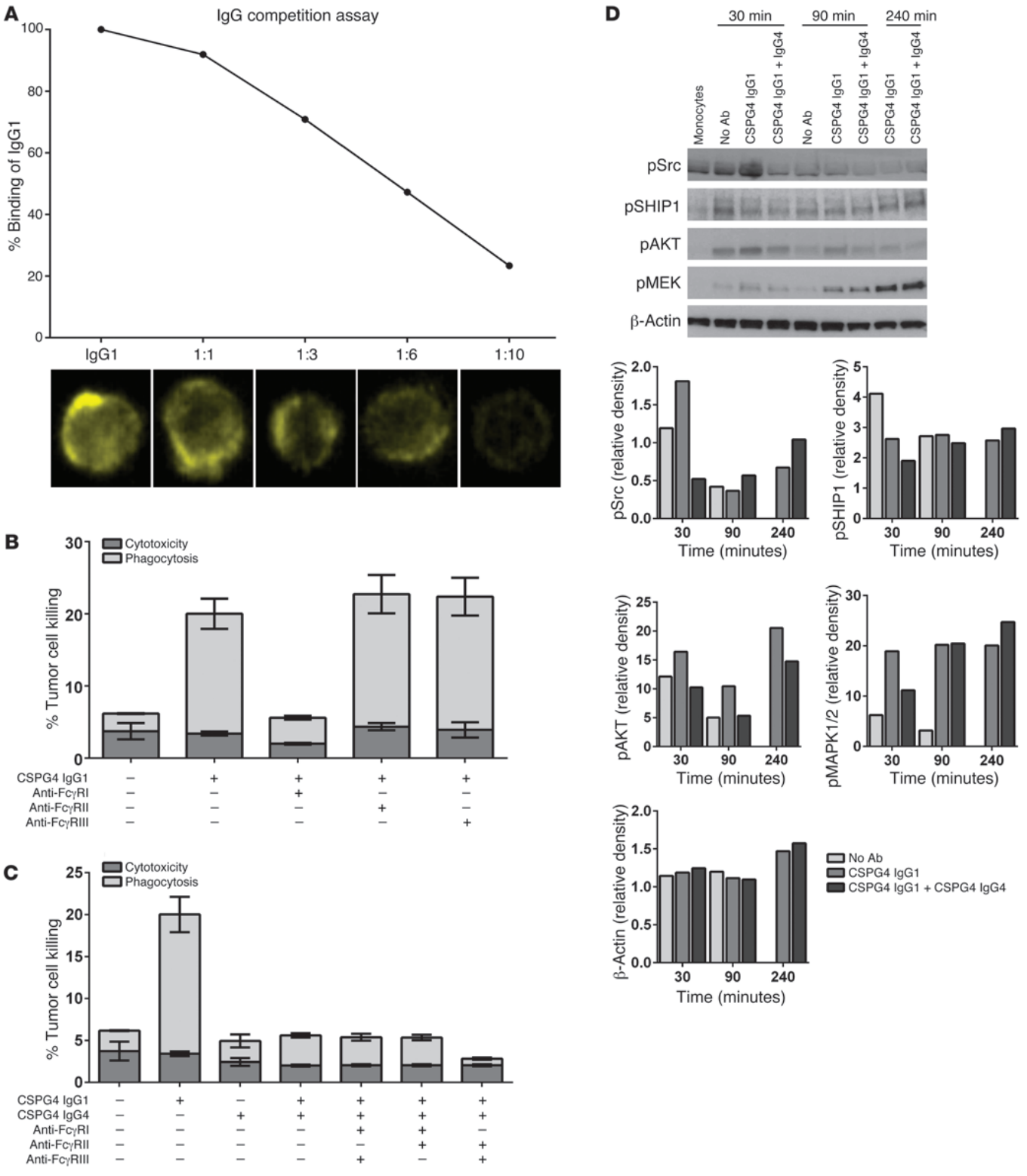

Figure 6
IgG4 blocks IgG1 antibody-dependent tumor cell killing by inhibiting IgG1 binding and activation through FcγRI. (**A**) Competition assay of IgG1 binding on the surface of monocytic cells displaced by addition of increasing concentrations of IgG4 antibody. Proportion of cells binding IgG1 is decreased with increasing concentrations of IgG4, demonstrated by flow cytometric evaluations and representative confocal images (yellow, by ImageStream). (**B**) Anti-CSPG-4 IgG1-mediated tumor cell killing (by flow cytometry) is inhibited by addition of an antibody known to block IgG Fc binding to FcγRI but not with addition of blocking antibodies to FcγRII or to FcγRIII. (**C**) Inhibitory functions of anti-CSPG-4 IgG4 are not lost by blocking FcγRII or FcγRIII with previously described specific FcγR blocking antibodies in flow cytometric antibody-dependent tumor cell killing assays. (**D**) Protein extracts of primary human monocytes isolated by flow cytometric sorting at different times during the antibody-mediated tumor cell killing assay were examined for phosphorylated products of the FcγR signaling pathway. Western blots of phospho-proteins and band density quantifications relative to freshly isolated monocytes demonstrate that IgG4 inhibits the activatory signaling cascades of FcγR (Src, AKT, MEK), while lack of pSHIP implies that FcγRII signaling is not involved in the IgG4 blockade. (**B** and **C**) Data are representative figures of 3 independent experiments.

In order to investigate which FcγR is predominantly responsible for the induction of tumor cell killing via IgG1, we conducted tumor killing assays during which individual FcγR families were blocked with antibodies described in the literature to have an inhibitory capacity for these specific receptor families. We demonstrate that, in this experimental system, blockade of FcγRI, but not of the other 2 receptor families, was responsible for the IgG1-mediated tumor cell killing (Figure 6B). We confirmed the widespread distribution of FcγRI along with the other 2 FcγRs (FcγRII and FcγRIII) in melanoma lesions (1 representative of 4 patient specimens shown in Supplemental Figure 4). Since FcγRs such as FcγRIIb are known to play immunomodulatory roles, we investigated whether specific inhibition of IgG binding to each of these receptor families had any bearing on the killing inhibition mediated by IgG4. In these experiments, we found that inhibition of CD32 is not involved in IgG1 blocking by IgG4 (Figure 6C).

Next, at different time points during in vitro tumor cell killing assays, we harvested monocytes by flow cytometric sorting and assessed phosphorylation of downstream signaling events triggered through engagement of FcγR engagement and activation (32). We observed increased phosphorylation of known members of the FcγR activatory signaling cascades (Src, MEK, and AKT) in the presence of IgG1 compared with the presence of both IgG1 and IgG4 antibodies (33). On the contrary, there were no differences in the levels of phosphorylated SHIP1 in relation to CSPG4 IgG1 or in relation to coincubation with IgG1 and IgG4 antibodies together at any of the time points tested (Figure 6D). These data suggest that inhibition of IgG1-mediated tumor cell killing by IgG4 is attributed to lack of effector cell activation rather than induction of inhibitory signals via FcγRs such as FcγRIIb. We conclude that in this experimental system IgG4 functions by competing with IgG1 for FcγRI binding and therefore blocking the activatory cascades through reduced phosphorylation of Src, MEK, and AKT.

IgG4 impairs antitumor immunity in a human melanoma xenograft model. Next, we compared the efficacies of anti-CSPG4 IgG1 and IgG4 in vivo in a subcutaneous human melanoma xenograft mouse model engrafted with human immune effector cells (Supplemental Figure 5 and ref. 34). Intravenous treatment with anti-CSPG4 IgG1 (3 × 10 mg/kg weekly doses) significantly reduced tumor size compared with treatments with nonspecific mAb or vehicle controls ($n = 6$, $P < 0.05$; Figure 7A). However, tumor size in anti-CSPG4 IgG4–treated mice increased in line with that in controls, suggesting that IgG4 was significantly less effective than IgG1 at restricting tumor growth in vivo ($P < 0.001$). Furthermore, when anti-CSPG4 IgG1 and IgG4 were administered together, tumors grew similarly to vehicle-treated controls ($n = 6$, $P < 0.001$ for IgG1/IgG4 combinations compared with IgG1 treatment alone; Figure 7A), indicating that anti-CSPG4 IgG4 might counteract IgG1 antitumor functions in vivo.

To ascertain that impaired antitumoral functions of anti-CSPG4 IgG4 were not due to inability of IgG4 to localize in CSPG4-expressing tumors in the mice, ^{111}In radio-labeled anti-CSPG4 IgG4 biodistribution was monitored by PET/SPECT imaging of human xenografts ($n = 3$). Accumulation in tumors was observed within 24 hours following antibody treatment (Figure 7B). Furthermore, we observed that subcutaneous human melanoma xenografts from mice treated with anti-CSPG4 IgG1 attracted higher levels of human CD68$^+$ cells (macrophages) compared with mice treated with IgG4 or combinations of IgG1 and IgG4 antibodies (Figure 7, C and D). These findings indicate that macrophages may be recruited and potentially play a role in restricting tumor growth when engaged by CSPG4 IgG1 in situ.

Serum IgG4 antibodies may be predictive of clinical outcomes in melanoma. Having investigated the immunomodulatory potential of IgG4 in melanoma in vitro and in vivo, we then evaluated whether the presence of IgG4 in patient circulation could be used as a possible biomarker. We performed IgG1–IgG4 subclass Luminex bead array assays using sera from 33 patients with stage III and IV melanoma (Figure 8 and Table 4). Spearman correlation analyses were performed to examine any significance among IgG subclass titers in sera in relation to patient survival. We demonstrated a negative correlation only between IgG4 serum titers and patient survival ($r = -0.31$, $P < 0.05$), while no significant correlations were found in relation to the other IgG subclasses (Figure 8A).

Normal IgG4/IgG_{total} ratios in human sera have been reported around 0.025 (35). In this study, we confirmed this (Figure 2A) and additionally found that IgG4/IgG_{total} ratios in patient sera had a median of 0.034 (95% CI of mean, 0.024–0.044). We therefore reasoned that serum IgG4/IgG_{total} ratios above the 75% percentile (IgG4/IgG_{total} = 0.04) may be considered high in patient sera (Supplemental Figure 6). To gain an insight into the significance of IgG4/IgG_{total} ratios in patient sera, we analyzed cumulative survival on a Kaplan-Meier survival plot in our 33 patient cohort. We found that patients with higher serum IgG4/IgG_{total} ratios (>0.04, $n = 13$) had significantly lower survival rates (median survival 8 months; hazard ratio, 0.19; 95% CI, 0.0635–0.5685) compared with patients whose IgG4/IgG_{total} serum ratios were <0.04 ($n = 20$) ($P < 0.01$) (Figure 8B).

Overall, we have shown that IgG4 subclass antibodies are present in tumor lesions and that they are inefficient in restricting melanoma tumor cell growth. In addition, IgG4 suppressed IgG1-mediated melanoma cell killing in vitro and in a clinically relevant humanized mouse engrafted with human melanoma. When examined in relation to clinical outcomes, data presented here suggest that IgG4 is associated with reduced survival and may be evaluated as a prognostic biomarker in melanoma.

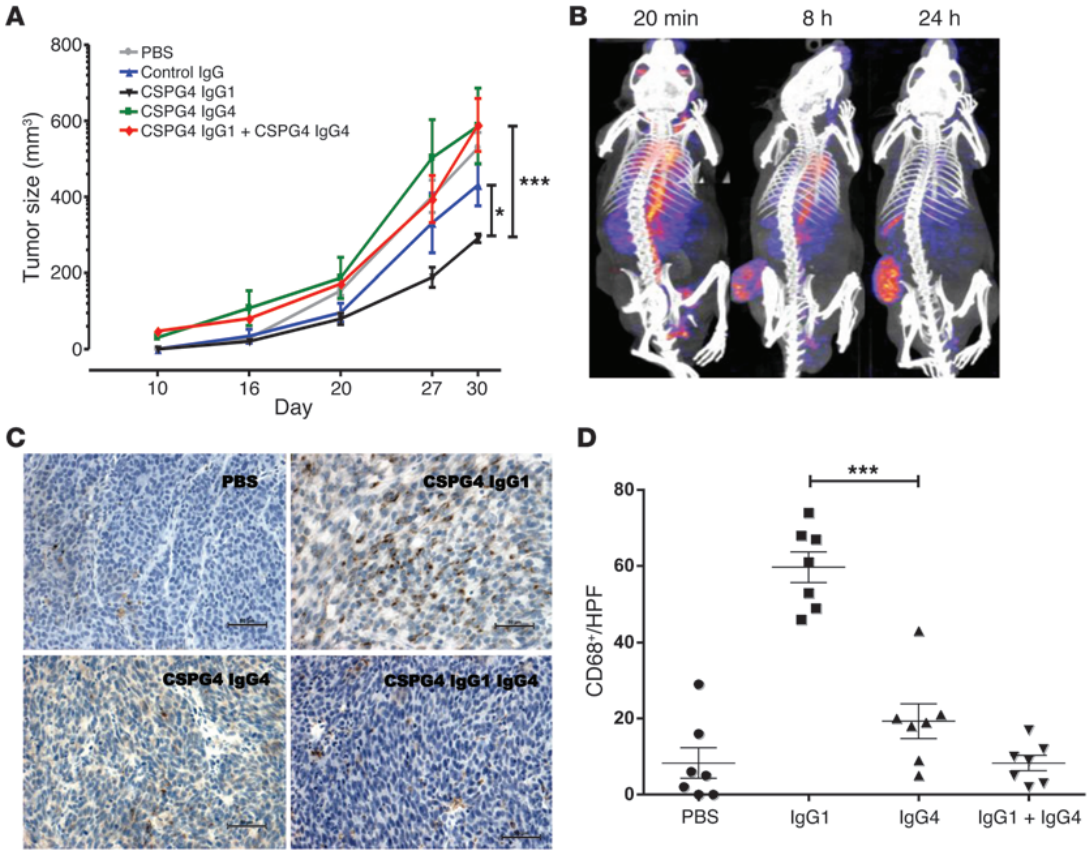

Figure 7

IgG4 has no antitumoral effector functions in vivo and blocks tumor-specific IgG1 function. (**A**) Anti-CSPG4 IgG1 antibody is capable of restricting the growth of subcutaneous melanoma lesions in NSG mice engrafted with human immune effector cells, while tumors in mice treated with an anti-CSPG-4 IgG4 antibody or coadministered with anti-CSPG4 IgG1 and IgG4 antibodies grow similarly to those from mice treated with nonspecific antibody or vehicle alone (n = 7 mice per group; mean ± SEM tumor volume in mm³). *P < 0.05, ***P < 0.001, 2-way ANOVA with Bonferroni post-hoc test. Data are representative of 2 experiments. (**B**) Representative NanoSPECT/CT images of Indium-111–labeled anti-CSPG4 IgG4 antibody (red), demonstrating accumulation of antibody in subcutaneous melanoma lesions at 20 minutes, 8 hours, and 24 hours following intravenous administration (n = 3). (**C**) Representative immunohistological images and (**D**) quantitative analyses of sections from human melanoma tumors grown in NSG mice treated with vehicle alone, anti-CSPG4 IgG1, anti-CSPG4 IgG4, or a combination of anti-CSPG4 IgG1 plus anti-CSPG4 IgG4 antibody, demonstrating elevated levels of human CD68⁺ (brown) immune cell infiltration in human xenograft tumors in animals treated with anti-CSPG4 IgG1 antibody. Horizontal bar indicate the mean, and individual symbols indicate individual tumors. Scale bar: 50 μm; original magnification ×20. ***P < 0.001.

Discussion

Despite the fact that B lymphocytes constitute important sentinels of adaptive immunity and the antibody-mediated immune response, the mechanisms by which they participate in tumor immunity remain only partially understood (2–4, 36–39). We described a hitherto undiscovered aspect of local humoral immunity in melanoma, characterized by B cell infiltration and local expression of IgG4 antibodies, in the context of prominent expression of IgG4 polarizing cytokines IL-10, IL-4, and VEGF. We demonstrated that, in the presence of melanoma cells, production of these cytokines is enhanced and B cells are polarized to produce IgG4 ex vivo. Importantly, we showed that IgG4 antagonizes IgG1-mediated human anti-melanoma immunity in vitro and in vivo and that IgG4 blockade is mediated through competition with IgG1 for FcγR binding and therefore inhibits downstream signaling activation of effector cells (i.e., monocytes).

Previous studies have reported the presence of CD20⁺ cells in melanoma lesions (2, 3), but this pan–B cell marker is also expressed by melanoma stem cells (40, 41). We selected the B cell marker CD22 to differentiate B cells from melanoma stem cells and to study mature B cells that may express class-switched antibodies. We detected CD22 at the mRNA and protein levels in melanoma lesions but at very low levels in normal skin (Figure 1). These cells were observed within tumor lesions and also surrounding stroma areas rich in CD45⁺ cells, indicating that B cells form part of the immune inflammatory infiltrate; however, the significance of CD22⁺ B cell infiltrates in cancer remains unclear. B cell and plasma cell (CD138) infiltration in melanoma have been associated with favorable clinical outcomes, and lymphoid structures containing B cells (CD20) and also plasma cells (CD138) were recently reported (4, 42). Other reports highlight immunomodulatory roles for B cells in cancer, suggesting that their contribution may reflect a balance between effective immunity and tumor-induced inflammation (20, 43).

The presence of mature IgG mRNA in metastatic melanoma lesions and CD22⁺IgG⁺ and IgG4⁺ cells infiltrating tumor cell areas

Table 4
Clinical parameters and disease staging at the time of sampling for peripheral blood donor cohort used for serum detection of IgG subclass and correlations

Patient	Gender	Breslow	Date of sample	Age at date of sample (yr)	Date of death	Stage
M31	F	3.5	03/05/2009	45	01/20/2010	IV
M42	F	4.29	03/19/2009	80	07/20/2009	IIIc
M70	M	9.3	04/23/2009	43	10/05/2009	IV
M72	F	3.12	04/16/2009	76	Alive	IV
M85	M	NA	06/18/2009	53	Alive	IV
M95	F	2.77	12/10/2009	65	06/28/2011	IV
M107	M	6	08/06/2009	63	09/10/2011	IIIC
M109	M	1.86	08/13/2009	74	02/23/2010	IV
M110	F	2.42	08/21/2009	48	Alive	IIIB
M111	M	1.21	08/21/2009	66	12/19/2010	IIIB
M114	F	2.37	09/10/2009	52	Alive	IIIC
M123	M	2.04	10/08/2009	76	05/05/2010	IV
M130	M	3.6	11/05/2009	66	12/31/2009	IV
M137	F	NA	11/26/2009	69	03/18/2010	IV
M138	F	2	11/26/2009	60	Alive	IV
M139	F	2.3	11/26/2009	55	Alive	IV
M146	F	4.2	12/03/2009	80	11/11/2010	IIIC
M147	F	2.3	01/07/2010	46	Alive	IIIA
M150	F	1.6	01/07/2010	32	Alive	IIIA
M154	M	NA	01/14/2010	80	Alive	IIIB
M158	M	NA	02/11/2010	53	Alive	IIIA
M161	F	1.1	02/11/2010	52	Alive	III
M163	M	NA	01/28/2010	75	11/14/2010	IV
M199	M	6.7	04/15/2010	62	04/26/2012	IV
M247	F	2.16	07/29/2010	35	Alive	IV
M122	M	NA	10/15/2009	78	05/05/2010	IV
M134	M	3.45	11/12/2009	81	02/05/2010	IV
M214	M	2.2	05/13/2010	70	Alive	III
M235	F	5.25	06/03/2010	60	Alive	III
M244	M	NA	07/15/2010	34	Alive	IV
M251	M	2.1	08/05/2010	70	Alive	III
M268	M	3.1	10/21/2010	83	12/11/2011	III
M399	M	3.7	10/20/2011	41	Alive	IV

Numbers in the "Breslow" column indicate the thickness (mm) of the primary melanoma. See also Figure 8. $n = 33$.

suggest that B cells may participate in local tumor surveillance through production of antibodies. This study demonstrates the expression of IgG antibodies in situ rather than being sequestered or diffused into tumors from the circulation. This was shown by the detection of mature IgG mRNA, IgG4 clone expression, and $IgG4^+$ infiltrates in melanoma lesions as well as by the production of tumor-reactive IgG4 antibodies by tumor-resident B cells (Figure 2). Recent findings implicate increased IgG4 serum titers and $IgG4^+$ tissue infiltrates in a range of inflammatory conditions triggered by chronic exposure to nonmicrobial antigens (14, 18, 31). Our findings demonstrating increased expression of IgG, the presence of $IgG4^+$ infiltrates in tumors, and tumor-reactive B cells in lesions are consistent with exposure to tumor antigens, as this might allow for antibody class switch recombination (44).

We found a striking polarization in IgG subclass distribution produced by tumor-derived B cells in favor of IgG4 (Figure 2). We directly showed a role for tumor cells in influencing IgG4 production by B cells (Figure 3). Furthermore, ex vivo stimulation of human B cells with melanoma cells also resulted in a similar proportional increase in $IgG4/IgG_{total}$ ratios compared with unstimulated B cells, and we demonstrated that melanoma tumor cells, but not normal human melanocytes, are capable of polarizing B cell responses in favor of IgG4 production. In melanoma tumor lesions, these increased $IgG4/IgG_{total}$ ratios were accompanied by expression of Th2-biased inflammatory cytokines known to drive production of IgG4 by B cells. Tumors circumvent immune-mediated clearance by triggering inflammatory cells with immunoregulatory properties and immunosuppressive mediators (e.g., IL-10, VEGF, TGF-β) in situ (34, 45, 46). The immunoregulatory cytokine, IL-10, can direct "a modified Th2 response" favoring B cell production of IgG4 (23, 25, 47). In support of this, we have found induction of increased IL-10 production by tumor cells cultured with B cells ex vivo. IL-10 has been implicated in modified Th2 responses in the context of IgG4-related diseases (48, 49). Although IgE and IgG4 are triggered by similar Th2-biased signals, IL-10 is thought to divert a classical Th2-type immunity, bypassing IL-4–induced IgE responses in favor of IgG4 (23, 29). Classically, high $IgG4/IgG_{total}$ ratios are considered a natural effort by the immune system to contain immune activation. These alterations, however, have also been documented in individuals chronically exposed to occupational or environmental antigens and are not normally accompanied by development of IgE (50, 51). Consistent with this, we detected *IgE* mRNA in only 2 out of 10 patient lesions that we examined (data not shown), which also points to the involvement of altered Th2 responses in tumor microenvironments (52).

As reported by others in the context of IgG4-related diseases, we detected local expression of tissue-resident IgG4 together with enhanced expression of IL-10 and IL-4 cytokines in tumors (Figure 3 and ref. 49). We also demonstrated that tumor cells are capable of stimulating such modified Th2 responses, featuring production of IL-10 and IL-4 and secretion of IgG4 by B cells. Also consistent with a tumor-associated inflammatory environment, VEGF, known to polarize Th2-biased cytokine production by PBMCs through induction of IL-10–secreting cells such as Tregs (53), along with well-described tumor-induced inflammatory mediators IL-6 and MCP-1 (53–56), was found at significantly increased levels ($P < 0.001$; Supplemental Figure 3A), upregulated by B cells in cultures of B cells with melanoma cells compared with cultures without tumor cells. While tumor cells contributed enhanced expression of IL-10 in coculture assays, neither B cells nor tumor cells expressed IL-4 under these coculture conditions, and it is pos-

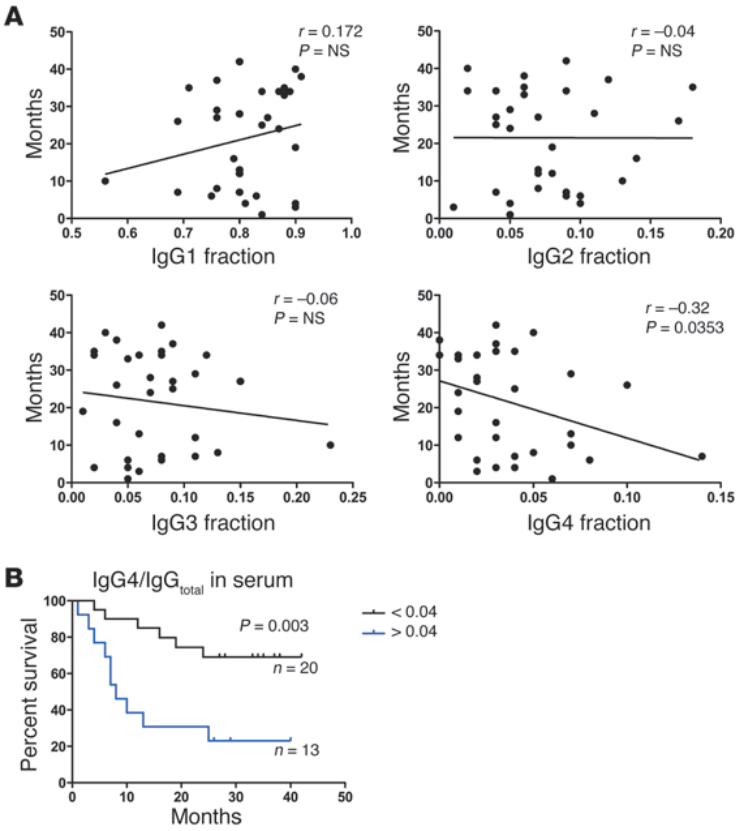

Figure 8
Elevated levels of IgG4 antibodies in patient sera correlate with patient survival. (**A**) IgG subclass ELISA evaluations of sera from 33 patients with stage III and IV melanoma were evaluated using Spearman correlation analyses for $IgG_{subclass}/IgG_{total}$, fractions in relation to patient survival (months), showing a statistically significant negative correlation between IgG4 fraction only ($r = –0.32$; $P = 0.00353$). (**B**) Kaplan-Meier cumulative survival analysis of overall patient survival was compared with respect to $IgG4/IgG_{total}$ fractions (stratified according to fractions above (blue) or below (black) the 75 percentile of the $IgG4/IgG_{total}$ fractions measured from the 33 metastatic melanoma patient cohort), indicating that high $IgG4/IgG_{total}$ ratios in sera are associated with a significantly lower overall survival ($P = 0.003$; hazard ratio 0.19; 95% CI 0.0635–0.5685).

sible that IL-4 production may be contributed by other stromal or immune cells in tumor microenvironments. Our findings therefore identify melanoma tumor cells as potential inducers of IgG4 in tumor microenvironments via B cell–produced VEGF, triggering enhanced IL-10 production by tumor cells.

Insights into how IgG4 antibodies contribute to immune homeostasis and to different disease pathologies are starting to emerge. IgG4 is considered a "nonactivating" subclass associated with chronic inflammation and limited immune activating functions (57). Links between IgG4 and tissue inflammation (14), in the context of well-characterized inflammatory mechanisms at play in tumors, raise the possibility of a key role for this antibody subclass in tumor inflammation. In support of this concept, we have shown the local presence of IgG4 antibodies in melanoma and their contributions to tumor inflammatory responses. In addition, we found that tumor antigen-specific IgG1, but not the corresponding IgG4, could activate patient-derived monocytes to kill tumor cells in vitro (Figure 5). These findings were confirmed by in vivo experiments, since tumor antigen-specific IgG4 was unable to restrict tumor growth, despite accumulating in tumor lesions (Figure 7). Polarizing humoral responses in favor of IgG subclasses with low or no potency in activating effector cells against tumors may therefore represent a mechanism of tumor escape.

Another potential mechanism relates to IgG4 interactions with other IgG antibodies and its capacity to impede IgG functions that would otherwise activate effector cells to eradicate tumors. We observed that a tumor antigen-specific IgG4 antibody hindered the ability of the corresponding IgG1 to induce ADCP of tumor cells by patient monocytes. This may be the outcome of one or more potential scenarios. First, IgG4 may compete with IgG1 for tumor antigen recognition, and, in support of this, we found tumor-reactive IgG4 antibodies associated with melanoma lesions. Second, IgG4 could bind to Fcγ receptors, preventing IgG1 interactions on the surface of effector cells. The implications of the latter mechanism would be that IgG4 of any specificity could neutralize IgG1-FcR–mediated effector functions against tumors through engagement of the main Fcγ receptor families (58). In agreement with this possibility, a nonspecific IgG4 also blocked IgG1-mediated tumor cell ADCP by patient monocytes almost as effectively as the tumor antigen-specific IgG4 (Figure 5). This suggested that antigen specificity may only partly account for the IgG4 antibody-neutralizing properties (31, 59, 60). Furthermore, here we demonstrated that tumor antigen-specific IgG4 inhibited IgG1-dependent tumor cell killing by blocking activatory signal cascades associated with FcγRI effector mechanisms, which would normally lead to functions such as ADCP (Figure 6). One can therefore envisage that if IgG4 antibodies are abundant in tumor microenvironments, their proximity to tumor cells may not only inhibit the effector functions of naturally expressed antibodies, but IgG4 could also impair therapeutic antibody effector functions in situ by one or more mechanisms, as has already been reported following antibody treatments for rheumatoid arthritis (61, 62). Our findings are also consistent with similar reported functional roles of IgG4 in blocking immune responses in atopic individuals receiving allergen immunotherapy (18, 31). While these effects signal the relief of symptoms and successful allergen immunotherapy, the presence of IgG4 in tumor microenvironments and its antibody-neutralizing functions may contribute to evasion of the humoral immune response to cancer.

Further supporting the potential significance of IgG4 in melanoma growth are our findings that elevated levels of IgG4 in patient

sera are associated with poorer survival (Figure 8). Data presented here mandate a closer examination of IgG4 antibodies but also of IgG3 antibodies, which are also proportionally elevated in tumors and possess lower effector cell activatory properties compared with IgG1 antibodies (63), as potentially useful biomarkers in tumor lesions and/or in the circulation. Additionally, data demonstrating VEGF and IgG4 production by B cells in the presence of tumor cells imply that B cells may be "reeducated" through cross-talk with tumor cells and highlight the need to further dissect the mechanisms by which tumors escape humoral immune responses.

In conclusion, we present the first evidence of local IgG4 expression in melanoma, associated with the IgG4-polarizing cytokines IL-10, VEGF, and IL-4. Our data suggest that IgG4 antibodies triggered in the presence of tumor cells participate in local inflammation and may represent one regulatory mechanism by which tumors evade immune attack. Studies in larger cohorts of patients are required to elucidate associations of IgG4 with immunological, molecular, and clinical parameters and patient responses to treatments, paving the way for biomarker development and design of personalized medicine approaches. Future strategies to counteract IgG4 immunoregulatory pathways or to design antibody treatments and derivatives less prone to IgG4 blockade will be of potential therapeutic value.

Methods

Patient data and specimen collection. Melanoma tumor skin lesions, lymph nodes, and blood were collected from a total of 57 patients diagnosed with stage I–IV malignant melanoma (Tables 1–3 and Supplemental Table 1). Patients were staged and classified according to the American Joint Committee on Cancer Melanoma Staging and Classification criteria (64). Samples were used fresh, or placed in OCT for cryosectioning or in RNAlater solution (Life Technologies) and stored at –70°C for subsequent RNA extraction, or fixed in formal saline and embedded in paraffin. Discarded human skin samples were obtained from 18 volunteers undergoing routine plastic surgery. Human peripheral blood lymphocytes (PBLs) and B cells were isolated from a cohort of 8 healthy volunteers. Human samples were collected with informed written consent, in accordance with the Helsinki Declaration, and study design was approved by the Guy's Research Ethics Committee, Guy's and St. Thomas' NHS Foundation Trust.

Human cell isolation and ex vivo stimulation assays. Peripheral blood B cells from patients with melanoma and healthy volunteers were isolated using the B cell enrichment cocktail (Stemcell Technologies) and cultured at a density of 500 cells per well (in 96-well plates) in combination with (3,010 cGy) irradiated autologous PBMCs, Epstein-Barr virus, and the TLR9 agonist CpG 2006, as previously described (28). Single cell suspensions were derived from patient tissues (lymph nodes or melanoma skin lesions) using a Gentle MACs Tissue Dissociator (Miltenyi) and filtered through a 100-μm strainer. In ex vivo stimulation experiments, human peripheral blood B cells were cocultured for 5 days together with irradiated PBMCs and tumor cells at 1:5:10 ratios in RPMI 1640 medium, 10% FCS, 2 mM L-glutamine, penicillin (5,000 U/ml), and streptomycin (100 μg/ml) (all Life Technologies) (65). Primary human monocytes from patients with melanoma were obtained using the monocyte enrichment cocktail (Stemcell Technologies) according to the manufacturer's instructions (66).

Cell culture and reagents. Cell lines were obtained from ATCC. Media for maintaining the melanoma cell lines were as follows: DMEM, 10% FCS for A375 (CRL-1619) and A-2058 (CRL-11147); McCoy's medium, 10% FCS for G-361 (CRL-1424); MEM, 10% FCS for WM-115 (CRL-1675) and SK-MEL-28 (HTB-72); and Iscove's modified Dulbecco's medium, 20% FCS for Malme-3M (HTB-64). Primary human melanocytes (PCS-2000-012) were grown in Dermal Cell Basal Medium (ATCC) and supplemented with the Melanocyte Growth Kit (ATCC). The monocytic cell line U937 (CRL-1593.2) was grown in DMEM, 10% FCS. Cells were grown in 2 mM L-glutamine, penicillin (5,000 U/ml), and streptomycin (100 μg/ml). The B95-8 marmoset blood leukocyte cell line secreting Epstein-Barr virus was grown in RPMI 1640 medium, 10% FCS, 2 mM L-glutamine, penicillin (5,000 U/ml), and streptomycin (100 μg/ml). All cells were maintained in a 5% CO_2 humidified incubator at 37°C.

RNA isolation from patient samples. Specimens placed in RNAlater solution (Life Technologies) were stored at –70°C prior to RNA extraction. RNA isolation was performed using a Qiagen Homogenizer II and an RNeasy Kit (Qiagen). Reagents were from Qiagen unless otherwise indicated. Tissue was removed from RNAlater, placed in a 2-ml microfuge tube with lysis buffer, and homogenized. Total RNA was prepared using the RNeasy Plus Mini Kit (Qiagen) according to the manufacturer's protocol. A total 500 ng of RNA was reverse transcribed into complementary DNA, using SuperScript II Reverse Transcriptase and OLIGO(dT) primer mix (Life Technologies) according to the manufacturers' instructions.

RNA and protein isolation from in vitro assays. Cells used in coculture experiments were labeled either with CSPG4-IgG-APC (Miltenyi) and CD45-PE-Cy7 (BD Biosciences) or with CSPG4-IgG-APC, CD45-PE-Cy7, and B cell lineage (CD19, CD22)-FITC and sorted using an Aria II (BD Biosciences). Cells from the ADCC/ADCP assay were labeled with anti-CD14-PE-Cy7 or CD89-PE. Sorted cells were resuspended either in RLT buffer for RNA isolation following the RNeasy Kit (Qiagen) or in Cell Lysis buffer (Cell Signaling) supplemented with 5 mM PMSF for protein isolation.

Western blot. Protein lysates were separated by SDS-PAGE using 4%–15% polyacrylamide minigels (Bio-Rad) and transferred onto PVDF membranes using a Bio-Rad Trans-Blot Turbo Transfer system (Bio-Rad). Membranes were blocked with 5% skimmed milk in PBS-Tween 20 and incubated with rabbit antibodies specific for the unphosphorylated and phosphorylated forms of Src, Akt, MEK(1/2), and SHIP-1 (all from Cell Signaling) in 1% skimmed milk-PBS-Tween 20 according to manufacturer recommendations. Rabbit antibodies were detected with goat anti-rabbit-HRP (Cell Signaling) and visualized with the ECL Detection Kit (GE Healthcare) on a Hyperfilm (Amersham).

Cell-based ELISA. Tumor cell–reactive antibodies were detected using cell-based ELISA, as previously described (28). Briefly, A375 tumor cells were plated at 3×10^5 to 6×10^5 cells on 96-well flat-bottom tissue culture plates, fixed in 0.5% formaldehyde, and stored at –80°C. On the day of the assay, plates were thawed, blocked with a 5% skimmed milk/PBS solution for 2 hours, and incubated with 100 μl of ex vivo culture supernatants, nonspecific IgG (125 μg/100 μl), or tumor-specific IgG1 or IgG4 antibodies (0.05 μg/100 μl) for 90 minutes at room temperature. Bound tumor cell–reactive antibodies were detected using a mouse anti-human IgG1 (AbD Serotec, 1:400) or mouse anti-human IgG4 (BD Biosciences, 1:250) antibody. This was followed by a 45-minute incubation with a goat anti-mouse IgG PE-labeled F(ab)′2 Fc-specific antibody (Jackson ImmunoResearch, 1:350). Fluorescence intensity depicting tumor cell reactivity was measured on an ELISA reader (BMG Labtech; excitation 488 nm, emission 540 nm). All samples were in duplicates, and MFIs were corrected against background and normalized against the MFI of the isotype control antibody. Antibodies were defined as reactive against tumor cells when the measured MFI was 2 SDs above the MFI of the specific isotype control antibody.

Quantitative real-time RT-PCR analysis. *CD22*, mature IgG, *IL4*, *IL10*, *IFNG*, and *VEGF* mRNA expression were assessed by multiplex real-time quantitative RT-PCR using TaqMan Gene Expression Assays (primers and probes, Life Technologies) according to the manufacturers' instructions. Primers and probes for the quantification of mature IgG mRNA were designed in-house using Primer Express (Life Technologies) as follows: probe,

5′ FAM-CATCGGTCTTCCCC-MGB 3′; J segment primer, 5′ ACCCTGGTCACCGTCTCCTCA 3′; mature IgG reverse primer, TGCAGCAGCGGGTCAAG). For each sample, mRNA abundance was normalized against the amount of human *GAPDH* mRNA (VIC) for the cytokine TaqMan Gene Expression Assays or against β_2-microglobulin mRNA (VIC) for *CD22* and mature IgG mRNA. Data analysis was performed using either a ΔCt method, comparing it to an arbitrary number, or a ΔΔCt method, comparing it to freshly isolated cells from blood. Results were expressed as relative mRNA expression units or ΔΔCt.

Immunohistochemical evaluations of frozen tissue specimens. Freshly frozen tissue sections embedded in OCT were cut at 4-μm to 8-μm thickness using a cryostat (Leica), and sections were air dried and stored at –80°C until further use. Prior to staining, slides were equilibrated at room temperature for 10 minutes, followed by fixation in acetone for 20 minutes. Sections were then air dried and stained using standard operation procedures for immunohistochemistry and immunofluorescence using the following commercial antibodies: mouse anti-human CD22 mAb (eBioscience); goat anti-human IgG (DakoGlostrup); mouse anti-human IgG4 (BD Biosciences); mouse anti-human CD64 (Biolegend); mouse anti-human CD32 (Abcam); mouse anti-human CD16 (Abcam); goat anti-mouse IgG, biotinylated (DAKO); and rabbit anti-human S100. Subsequently, antibodies were detected with the VECTOR Red Alkaline Phosphatase Substrate Kit (Vector Labs) or with donkey anti-mouse Alexa Fluor 555 and donkey anti-goat Alexa Fluor 488 (both Life Technologies). Images were captured using a Zeiss Axio Observer.Z1/ Axiophot microscope using AxioVision (×10, ×20, and ×63 magnification lenses, Carl Zeiss).

Immunohistochemical evaluations of paraffin-embedded tissue specimens. Paraffin sections were cut at 6-μm thickness on a microtome (Leica) and dried overnight at 60°C. Prior to staining, sections were deparaffinized with a 20-minute incubation in Xylene and then rehydrated by serial incubations in alcohol. Heat-induced antigen retrieval was performed in a 95°C water bath, using citric acid. Subsequently, sections were stained using standard operation procedures for immunohistochemistry with the following commercial antibodies: mouse anti-human CD22 (Abcam); rabbit anti-human FoxP3 (eBioscience); mouse anti-human CD45 (eBioscience); and mouse anti-human IgG4 (BD Biosciences). Antibodies were detected with goat/rabbit anti-mouse IgG-biotinylated (DAKO) and visualized using the VECTOR Red Alkaline Phosphatase Substrate Kit, including Levamisole (Vector Labs). All sections were mounted in DPX mounting solution and analyzed on a Zeiss Axiophot microscope using ×10 and ×20 magnification lenses (Carl Zeiss) and NIS-Elements imaging software (Nikon).

IgG subclass ELISA. Immunoglobulin subclasses produced in cell culture supernatants were measured using an IgG1-, IgG2-, IgG3-, and IgG4-specific ELISA. Capture antibodies were from AbD Serotec (IgG1 and IgG3) and BD Biosciences (IgG2 and IgG4). Certified Reference Material 470 (67) (ERM-DA470, Institute for Reference Materials and Measurements) was used as the standard to quantify Ig subclass. Maxisorp 96-well plates were coated with mouse anti-human IgG1, IgG2, IgG3, or IgG4 antibodies in carbonate-bi-carbonate buffer (0.2 M, pH 9.4) overnight, and plates were blocked for 1 hour with 2% nonfat milk and PBS-Tween 20. Plates were incubated with culture supernatants diluted 1:1 in 50% RPMI media, 50% PBS, 0.025% Tween 20 for 3 hours, and subclass antibody binding was detected with goat anti-human IgG $F(ab')_2$-HRP incubated for 2 hours (Jackson ImmunoResearch), followed by a color reaction with 0.5 mg/ml o-phenylenediamine dihydrochloride substrate (Sigma-Aldrich) in peroxide substrate buffer (Pierce). Reactions were stopped with the addition of 1 M HCl. Optical density values were measured at 492 nm (reference wavelength: 650 nm). Standard curve fitting was performed using Graphpad Prism software (Graphpad) with a 4-parameter curve fit using a minimum of 6 points on the standard curve.

Luminex bead array analysis. Luminex Bead Array Assay Kits, Milliplex for cytokines (Millipore) or Bioplex for IgG subclasses (Bio-Rad), were used according to the manufactures instructions, and data were acquired and analyzed using a FlexMap3 (Luminex Cooperation) or Bio-Plex200 (Luminex Cooperation), respectively.

Production of human anti-CSPG4 antibodies. The cDNA of the heavy and light chain variable regions directed against the human CSPG4, a cell surface antigen expressed by >80% of malignant melanomas, were derived from previously published variable region sequences of the murine mAb 225.28S (68–70), and antibodies were subsequently cloned and produced in an method analogous to that previously described (71).

Flow cytometric and ImageStream evaluations of antibody binding. For assessment of antibody binding to CSPG4 on a panel of human melanoma cell lines (A375, A-2058, G-361, WM-115, SK-MEL-28, Malme-3M), primary human melanocytes, U937 monocytes, or human primary monocytes, cells were incubated with 10 μg/ml mAbs for 30 minutes at 4°C, followed by 2 washes in PBS with 5% normal goat serum (FACS buffer). Cells were then treated with goat anti-human IgG $(Fab')_2$-FITC antibody or goat anti-human IgG1-PE (10 μg/ml) (Jackson ImmunoResearch) for 30 minutes at 4°C and washed in FACS buffer prior to acquisition and analysis on a FACSCanto flow cytometer (BD Biosciences) or ImageStreamX (Amnis Corporation). For ImageStreamX, quantitative analyses are based on the acquisition of 20,000 cell events, and MFIs were measured and calculated using an object mask to detect surface staining only.

Cytotoxicity/phagocytosis (ADCC/ADCP) assays. Antibody-dependent cell-mediated killing of CSPG4-expressing cells by anti-CSPG4 antibodies was quantified by a 3-color flow cytometric ADCC/ADCP assay, as previously described (72). Briefly, A375 melanoma cells were stained 24 hours prior to assays with 5.0 μM CFSE (5-[and 6-] carboxyfluorescein diacetate succinimidyl ester, Life Technologies) in PBS for 10 minutes at 37°C; washed in DMEM medium, 10% FCS, 2 mM L-glutamine; and returned to standard culture conditions. The following day, CFSE-labeled tumor cells were washed and then mixed with human monocytes at an E/T cell ratio of 2:1, with or without (5 μg/ml) antibodies, followed by a 3 hours incubation at 37°C. Cells were then washed in PBS with 2% normal goat serum (FACS buffer), incubated for 30 minutes with a mouse anti-human CD89 PE (BD Biosciences), washed again in FACS buffer, and resuspended in PBS supplemented with DAPI (Life Technologies). All assay conditions were tested in triplicates and replicated in 6 independent experiments using peripheral blood monocytes derived from 6 patients with stage II melanoma.

Assessments of receptor function were conducted using blocking antibodies: mouse anti-human FcγRI (Biolegend); mouse anti-human FcγRII (Abcam); and mouse anti-human FcγRIII (Abcam), which have been previously described to block the antibody Fc-mediated functions of different FcγR family members (73–75). Blocking experiments with specific or nonspecific IgG4 antibodies were conducted using a 3:1 (IgG4/IgG1) ratio.

Samples were acquired immediately using a FACSCanto flow cytometer (BD Biosciences). For event acquisition and analysis, CFSE-labeled tumor cells were detected in FITC (530/30-nm band-pass filter and a 502-nm long-pass filter), CD89-PE-labeled primary monocytes were detected in PE (585/42-nm band-pass filter and a 556-nm long-pass filter), and $DAPI^+$ dead cells were detected in Pacific Blue (345/20-nm band-pass filter) channels, while control samples were set for compensation adjustments between CFSE and PE. Two dual-color flow cytometric dot plots were generated to calculate ADCC and ADCP, as previously described (66, 72, 76).

Assessments of antibodies in a subcutaneous human melanoma model in NOD/SCID/Il2rg$^{-/-}$ mice engrafted with human immune cells. Male and female NOD/SCID/*Il2rg*$^{-/-}$ mice (NOD.cg-Prkdc SCID Il2rg tm1Wjl /SzJ [NSG]; The Jackson Laboratory) were used at between 6 and 10 weeks of age. Mice were maintained under specific pathogen–free conditions and handled in accor-

dance with the Institutional Committees on Animal Welfare of the UK Home Office (The Home Office Animals Scientific Procedures Act, 1986). NSG mice were injected subcutaneously with 5×10^5 A375 melanoma cells in 150 μl PBS. On day 5, mice received intravenous injections of 10×10^6 human PBLs (derived from whole human blood by lysis of red blood cells) and 10 mg/kg of antibody. Subsequent injections of antibody treatments were given 3 times on days 12, 18, and 25 at doses of 10 mg/kg each in 150 μl PBS. A control group was treated with 10×10^6 human PBLs on day 5 and injected with 150 μl of PBS on days 12, 18, and 25. Tumor growth was monitored and measured using calipers. Tumor size (mm^3) was calculated using the following formula: $mm^3 = d^2 \times (D/2)$, where d stands for the small diameter of tumor and D stands for the large diameter of tumor.

Experiments were terminated once the first animal was measured with a subcutaneous tumor size no greater than 750 mm^3. Spleen engraftment of 40%–70% human $CD45^+$ cells was confirmed by flow cytometry for all experiments (Supplemental Figure 5).

NanoSPECT/CT imaging of anti-CSPG4 antibody in vivo. NSG mice were injected subcutaneously with 5×10^5 A375 tumor cells on day 0. On day 5 mice were injected intravenously with 10×10^6 human PBLs. Spleen engraftment was analyzed as above (Supplemental Figure 5). Anti-CSPG4 IgG4 (7 mg) was conjugated with the bifunctional chelator CHX-A"-DTPA prior to experiments, and on day 24, the antibody was radiolabeled with 20 MBq of Indium-111 (St. Thomas' and Guy's Trust, KCL, London, Radiopharmacy) and administered intravenously at 10 mg/kg as above. Images were captured under anesthesia after 20 minutes, 8 hours, and 24 hours using a NanoSPECT/CT preclinical imager (Bioscan) equipped with a multipinhole (9 pinholes; aperture 1.0 mm) collimator and reconstructed using the Invivoscope software (Bioscan).

Statistics. Comparative quantitative PCR analyses in human skin specimens were conducted using a Kruskal-Wallis analysis with a Dunn post-hoc test. Comparative analyses of immunohistochemical staining were performed using a Mann-Whitney *U* test. One-way ANOVA with Bonferroni post-hoc test was used to compare ADCC/ADCP of tumor cells by human monocytes, triggered by antibodies. Two-way ANOVA with Bonferroni post-hoc test was used to compare restriction of tumor cell growth in vivo. For correlation and patient survival analyses, Spearman and Mantel-Cox analyses were applied. All statistical analyses were performed using GraphPad Prism software (version 5.03, GraphPad). Error bars in all in vitro figures represent SD. Error bars in all in vivo figures and histological analyses represent SEM.

Acknowledgments

The authors thank Angela Clifford for recruitment of volunteers; Isabella Tosi, Katazryna Grys, Eduardo Calonje, and Tawatchai Suttikoon for help with sample processing and assessments; Rebecca Beavil and Andrew Beavil for expert assistance with antibody engineering and purification; Chung-Ching Chu for assistance with illustrations; and Hannah Gould and Pooja Takhar for advice and discussions. We acknowledge the Biomedical Research Centre Immune monitoring core Facility team at Guy's and St. Thomas' NHS Foundation Trust for assistance. We thank all patients and healthy volunteers who participated in this study. The authors are solely responsible for study design, data collection, analysis, decision to publish, and preparation of the manuscript. The research was supported by the NIHR Biomedical Research Centre based at Guy's and St. Thomas' NHS Foundation Trust and King's College London. The views expressed are those of the author(s) and not necessarily those of the NHS, the NIHR, or the Department of Health. The authors acknowledge support by CR UK/EPSRC/MRC/NIHR KCL/UCL Comprehensive Cancer Imaging Centre (C1519/A10331) (to D.H. Josephs, P.J. Blower, J.F. Spicer, and S.N. Karagiannis); Cancer Research UK (C30122/A11527) (to S.N. Karagiannis, J.F. Spicer, D.H. Josephs, L. Saul); Cancer Research UK (C16736/A8371) (to F.O. Nestle and S.N. Karagiannis); Mary Dunhill Trust (to F.O. Nestle); CR UK/NIHR in England/DoH for Scotland, Wales and Northern Ireland Experimental Cancer Medicine Centre (to F.O. Nestle and J.F. Spicer); BBSRC grant BB/H019634/1 (D.J. Fear); and the Overseas Research Students Award Scheme (to A.E. Gilbert).

Received for publication July 2, 2012, and accepted in revised form January 3, 2013.

Address correspondence to: Sophia N. Karagiannis, Cutaneous Medicine and Immunotherapy Unit, St. John's Institute of Dermatology, Division of Genetics and Molecular Medicine, Kings' College London and NIHR Biomedical Research Centre at Guy's and St. Thomas' Hospitals and King's College London, Guy's Hospital, Tower Wing 9th Floor, London, SE1 9RT, United Kingdom. Phone: 44.0.20.7188.6355; Fax: 44.0.20.7188.8050; E-mail: sophia.karagiannis@kcl.ac.uk.

1. Weide B, et al. Functional T cells targeting NY-ESO-1 or Melan-A are predictive for survival of patients with distant melanoma metastasis. *J Clin Oncol*. 2012;30(15):1835–1841.
2. Watson DB, Burns GF, Mackay IR. In vitro growth of B lymphocytes infiltrating human melanoma tissue by transformation with EBV: evidence for secretion of anti-melanoma antibodies by some transformed cells. *J Immunol*. 1983;130(5):2442–2447.
3. Kirkwood JM, Robinson JE. Human IgG and IgM monoclonal antibodies against autologous melanoma produced by Epstein-Barr-virus-transformed B lymphocytes. *Cancer Immunol Immunother*. 1990; 32(4):228–234.
4. Erdag G, et al. Immunotype and immunohistologic characteristics of tumor-infiltrating immune cells are associated with clinical outcome in metastatic melanoma. *Cancer Res*. 2012;72(5):1070–1080.
5. Andreu P, et al. FcRgamma activation regulates inflammation-associated squamous carcinogenesis. *Cancer Cell*. 2010;17(2):121–134.
6. Schioppa T, et al. B regulatory cells and the tumor-promoting actions of TNF-alpha during squamous carcinogenesis. *Proc Natl Acad Sci U S A*. 2011; 108(26):10662–10667.
7. Jefferis R. Isotype and glycoform selection for antibody therapeutics. *Arch Biochem Biophys*. 2012; 526(2):159–166.
8. Papadea C, Check IJ. Human immunoglobulin G and immunoglobulin G subclasses: biochemical, genetic, and clinical aspects. *Crit Rev Clin Lab Sci*. 1989;27(1):27–58.
9. Steplewski Z, Sun LK, Shearman CW, Ghrayeb J, Daddona P, Koprowski H. Biological activity of human-mouse IgG1, IgG2, IgG3, and IgG4 chimeric monoclonal antibodies with antitumor specificity. *Proc Natl Acad Sci U S A*. 1988;85(13):4852–4856.
10. Aalberse RC, Schuurman J. IgG4 breaking the rules. *Immunology*. 2002;105(1):9–19.
11. Aalberse RC, Stapel SO, Schuurman J, Rispens T. Immunoglobulin G4: an odd antibody. *Clin Exp Allergy*. 2009;39(4):469–477.
12. French M. Serum IgG subclasses in normal adults. *Monogr Allergy*. 1986;19:100–107.
13. Neild GH, Rodriguez-Justo M, Wall C, Connolly JO. Hyper-IgG4 disease: report and characterisation of a new disease. *BMC Med*. 2006;4:23.
14. Stone JH, Zen Y, Deshpande V. IgG4-related disease. *N Engl J Med*. 2012;366(6):539–551.
15. Eifan AO, Shamji MH, Durham SR. Long-term clinical and immunological effects of allergen immunotherapy. *Curr Opin Allergy Clin Immunol*. 2011; 11(6):586–593.
16. Frew AJ. Allergen immunotherapy. *J Allergy Clin Immunol*. 2010;125(2 suppl 2):S306–S313.
17. Garcia BE, Sanz ML, Gato JJ, Fernandez J, Oehling A. IgG4 blocking effect on the release of antigen-specific histamine. *J Investig Allergol Clin Immunol*. 1993;3(1):26–33.
18. Shamji MH, et al. Functional rather than immunoreactive levels of IgG4 correlate closely with clinical response to grass pollen immunotherapy. *Allergy*. 2012;67(2):217–226.
19. Harada K, et al. Significance of IgG4-positive cells in extrahepatic cholangiocarcinoma: molecular mechanism of IgG4 reaction in cancer tissue. *Hepatology*. 2012;56(1):157–164.
20. Cipponi A, et al. Neogenesis of lymphoid structures and antibody responses occur in human melanoma metastases. *Cancer Res*. 2012;72(16):3997–4007.
21. Daveau M, et al. IgG4 subclass in malignant melanoma. *J Natl Cancer Inst*. 1977;58(2):189–192.
22. Ellyard JI, Simson L, Parish CR. Th2-mediated anti-tumour immunity: friend or foe? *Tissue Antigens*. 2007;70(1):1–11.
23. Platts-Mills TA, Woodfolk JA, Erwin EA, Aalberse R. Mechanisms of tolerance to inhalant allergens: the relevance of a modified Th2 response to aller-

gens from domestic animals. *Springer Semin Immunopathol*. 2004;25(3–4):271–279.
24. Satoguina JS, Weyand E, Larbi J, Hoerauf A. T regulatory-1 cells induce IgG4 production by B cells: role of IL-10. *J Immunol*. 2005;174(8):4718–4726.
25. Francis JN, et al. Grass pollen immunotherapy: IL-10 induction and suppression of late responses precedes IgG4 inhibitory antibody activity. *J Allergy Clin Immunol*. 2008;121(5):1120–1125.
26. Robinson DS, Larche M, Durham SR. Tregs and allergic disease. *J Clin Invest*. 2004;114(10):1389–1397.
27. Jeannin P, Lecoanet S, Delneste Y, Gauchat JF, Bonnefoy JY. IgE versus IgG4 production can be differentially regulated by IL-10. *J Immunol*. 1998; 160(7):3555–3561.
28. Gilbert AE, et al. Monitoring the systemic human memory B cell compartment of melanoma patients for anti-tumor IgG antibodies. *PLoS One*. 2011; 6(4):e19330.
29. Punnonen J, de Waal Malefyt R, van Vlasselaer P, Gauchat JF, de Vries JE. IL-10 and viral IL-10 prevent IL-4-induced IgE synthesis by inhibiting the accessory cell function of monocytes. *J Immunol*. 1993;151(3):1280–1289.
30. Zaidi MR, et al. Interferon-gamma links ultraviolet radiation to melanomagenesis in mice. *Nature*. 2011;469(7331):548–553.
31. James LK, et al. Allergen specificity of IgG(4)-expressing B cells in patients with grass pollen allergy undergoing immunotherapy. *J Allergy Clin Immunol*. 2012;130(3):663–670.
32. Nakamura K, Malykhin A, Coggeshall KM. The Src homology 2 domain-containing inositol 5-phosphatase negatively regulates Fcgamma receptor-mediated phagocytosis through immunoreceptor tyrosine-based activation motif-bearing phagocytic receptors. *Blood*. 2002;100(9):3374–3382.
33. van der Poel CE, Spaapen RM, van de Winkel JG, Leusen JH. Functional characteristics of the high affinity IgG receptor, FcgammaRI. *J Immunol*. 2011;186(5):2699–2704.
34. Chu CC, et al. Resident CD141 (BDCA3)+ dendritic cells in human skin produce IL-10 and induce regulatory T cells that suppress skin inflammation. *J Exp Med*. 2012;209(5):935–945.
35. French MA, Harrison G. Serum IgG subclass concentrations in healthy adults: a study using monoclonal antisera. *Clin Exp Immunol*. 1984;56(2):473–475.
36. Anderson KS, et al. Serum antibodies to the HPV16 proteome as biomarkers for head and neck cancer. *Br J Cancer*. 2011;104(12):1896–1905.
37. Hussein MR, Elsers DA, Fadel SA, Omar AE. Immunohistological characterisation of tumour infiltrating lymphocytes in melanocytic skin lesions. *J Clin Pathol*. 2006;59(3):316–324.
38. Yeilding NM, Gerstner C, Kirkwood JM. Analysis of two human monoclonal antibodies against melanoma. *Int J Cancer*. 1992;52(6):967–973.
39. Yamaguchi H, et al. Cell-surface antigens of melanoma recognized by human monoclonal antibodies. *Proc Natl Acad Sci U S A*. 1987;84(8):2416–2420.
40. Schmidt P, Kopecky C, Hombach A, Zigrino P, Mauch C, Abken H. Eradication of melanomas by targeted elimination of a minor subset of tumor cells. *Proc Natl Acad Sci U S A*. 2011;108(6):2474–2479.
41. Zabierowski SE, Herlyn M. Melanoma stem cells: the dark seed of melanoma. *J Clin Oncol*. 2008; 26(17):2890–2894.
42. Ladanyi A, et al. Prognostic impact of B-cell density in cutaneous melanoma. *Cancer Immunol Immunother*. 2011;60(12):1729–1738.
43. Zapata JM, Llobet D, Krajewska M, Lefebvre S, Kress CL, Reed JC. Lymphocyte-specific TRAF3 transgenic mice have enhanced humoral responses and develop plasmacytosis, autoimmunity, inflammation, and cancer. *Blood*. 2009;113(19):4595–4603.
44. Coker HA, Durham SR, Gould HJ. Local somatic hypermutation and class switch recombination in the nasal mucosa of allergic rhinitis patients. *J Immunol*. 2003;171(10):5602–5610.
45. Whiteside TL. Immune suppression in cancer: effects on immune cells, mechanisms and future therapeutic intervention. *Semin Cancer Biol*. 2006; 16(1):3–15.
46. Gerlini G, Tun-Kyi A, Dudli C, Burg G, Pimpinelli N, Nestle FO. Metastatic melanoma secreted IL-10 down-regulates CD1 molecules on dendritic cells in metastatic tumor lesions. *Am J Pathol*. 2004; 165(6):1853–1863.
47. Platts-Mills T, Vaughan J, Squillace S, Woodfolk J, Sporik R. Sensitisation, asthma, and a modified Th2 response in children exposed to cat allergen: a population-based cross-sectional study. *Lancet*. 2001;357(9258):752–756.
48. Nakashima H, et al. An amplification of IL-10 and TGF-beta in patients with IgG4-related tubulointerstitial nephritis. *Clin Nephrol*. 2010;73(5):385–391.
49. Zen Y, Nakanuma Y. Pathogenesis of IgG4-related disease. *Curr Opin Rheumatol*. 2011;23(1):114–118.
50. Krop EJ, Stapel SO, De Vrieze H, Van der Zee JS. Immunoglobulin E and G4 antibody responses in occupational airway exposure to bovine and porcine plasma proteins. *Int Arch Allergy Immunol*. 2006; 139(3):237–244.
51. Matsui EC, et al. Mouse allergen-specific immunoglobulin G and immunoglobulin G4 and allergic symptoms in immunoglobulin E-sensitized laboratory animal workers. *Clin Exp Allergy*. 2005; 35(10):1347–1353.
52. Strid J, Sobolev O, Zafirova B, Polic B, Hayday A. The intraepithelial T cell response to NKG2D-ligands links lymphoid stress surveillance to atopy. *Science*. 2011;334(6060):1293–1297.
53. Nevala WK, Vachon CM, Leontovich AA, Scott CG, Thompson MA, Markovic SN. Evidence of systemic Th2-driven chronic inflammation in patients with metastatic melanoma. *Clin Cancer Res*. 2009;15(6):1931–1939.
54. Deng W, et al. Down-modulation of TNFSF15 in ovarian cancer by VEGF and MCP-1 is a pre-requisite for tumor neovascularization. *Angiogenesis*. 2012; 15(1):71–85.
55. Maeda K, Mehta H, Drevets DA, Coggeshall KM. IL-6 increases B-cell IgG production in a feed-forward proinflammatory mechanism to skew hematopoiesis and elevate myeloid production. *Blood*. 2010;115(23):4699–4706.
56. Hirano H, et al. TLR4, IL-6, IL-18, MyD88 and HMGB1 are highly expressed in intracranial inflammatory lesions and the IgG4/IgG ratio correlates with TLR4 and IL-6. *Neuropathology*. 2012;32(6):628–637.
57. Labrijn AF, Aalberse RC, Schuurman J. When binding is enough: nonactivating antibody formats. *Curr Opin Immunol*. 2008;20(4):479–485.
58. Bruhns P, et al. Specificity and affinity of human Fcgamma receptors and their polymorphic variants for human IgG subclasses. *Blood*. 2009; 113(16):3716–3725.
59. Rispens T, Ooievaar-De Heer P, Vermeulen E, Schuurman J, van der Neut Kolfschoten M, Aalberse RC. Human IgG4 binds to IgG4 and conformationally altered IgG1 via Fc-Fc interactions. *J Immunol*. 2009;182(7):4275–4281.
60. Leyendeckers H, et al. Correlation analysis between frequencies of circulating antigen-specific IgG-bearing memory B cells and serum titers of antigen-specific IgG. *Eur J Immunol*. 1999;29(4):1406–1417.
61. van Schouwenburg PA, et al. IgG4 production against adalimumab during long term treatment of RA patients. *J Clin Immunol*. 2012;32(5):1000–1006.
62. Svenson M, Geborek P, Saxne T, Bendtzen K. Monitoring patients treated with anti-TNF-alpha biopharmaceuticals: assessing serum infliximab and anti-infliximab antibodies. *Rheumatology (Oxford)*. 2007;46(12):1828–1834.
63. Bruggemann M, et al. Comparison of the effector functions of human immunoglobulins using a matched set of chimeric antibodies. *J Exp Med*. 1987;166(5):1351–1361.
64. Balch CM, et al. Final version of 2009 AJCC melanoma staging and classification. *J Clin Oncol*. 2009;27(36):6199–6206.
65. Lapointe R, Bellemare-Pelletier A, Housseau F, Thibodeau J, Hwu P. CD40-stimulated B lymphocytes pulsed with tumor antigens are effective antigen-presenting cells that can generate specific T cells. *Cancer Res*. 2003;63(11):2836–2843.
66. Karagiannis SN, et al. IgE-antibody-dependent immunotherapy of solid tumors: cytotoxic and phagocytic mechanisms of eradication of ovarian cancer cells. *J Immunol*. 2007;179(5):2832–2843.
67. Schauer U, et al. IgG subclass concentrations in certified reference material 470 and reference values for children and adults determined with the binding site reagents. *Clin Chem*. 2003;49(11):1924–1929.
68. Campoli M, Ferrone S, Wang X. Functional and clinical relevance of chondroitin sulfate proteoglycan 4. *Adv Cancer Res*. 2010;109:73–121.
69. Price MA, et al. CSPG4, a potential therapeutic target, facilitates malignant progression of melanoma. *Pigment Cell Melanoma Res*. 2011;24(6):1148–1157.
70. Neri D, et al. Recombinant anti-human melanoma antibodies are versatile molecules. *J Invest Dermatol*. 1996;107(2):164–170.
71. Karagiannis P, et al. Characterisation of an engineered trastuzumab IgE antibody and effector cell mechanisms targeting HER2/neu-positive tumour cells. *Cancer Immunol Immunother*. 2009;58(6):915–930.
72. Bracher M, Gould HJ, Sutton BJ, Dombrowicz D, Karagiannis SN. Three-colour flow cytometric method to measure antibody-dependent tumour cell killing by cytotoxicity and phagocytosis. *J Immunol Methods*. 2007;323(2):160–171.
73. Bunk S, et al. Internalization and coreceptor expression are critical for TLR2-mediated recognition of lipoteichoic acid in human peripheral blood. *J Immunol*. 2010;185(6):3708–3717.
74. Tamm A, Schmidt RE. The binding epitopes of human CD16 (Fc gamma RIII) monoclonal antibodies. Implications for ligand binding. *J Immunol*. 1996;157(4):1576–1581.
75. Hober D, et al. Circulating and cell-bound antibodies increase coxsackievirus B4-induced production of IFN-alpha by peripheral blood mononuclear cells from patients with type 1 diabetes. *J Gen Virol*. 2002;83(pt 9):2169–2176.
76. Karagiannis SN, et al. Role of IgE receptors in IgE antibody-dependent cytotoxicity and phagocytosis of ovarian tumor cells by human monocytic cells. *Cancer Immunol Immunother*. 2008;57(2):247–263.

Supplementary Figure 1

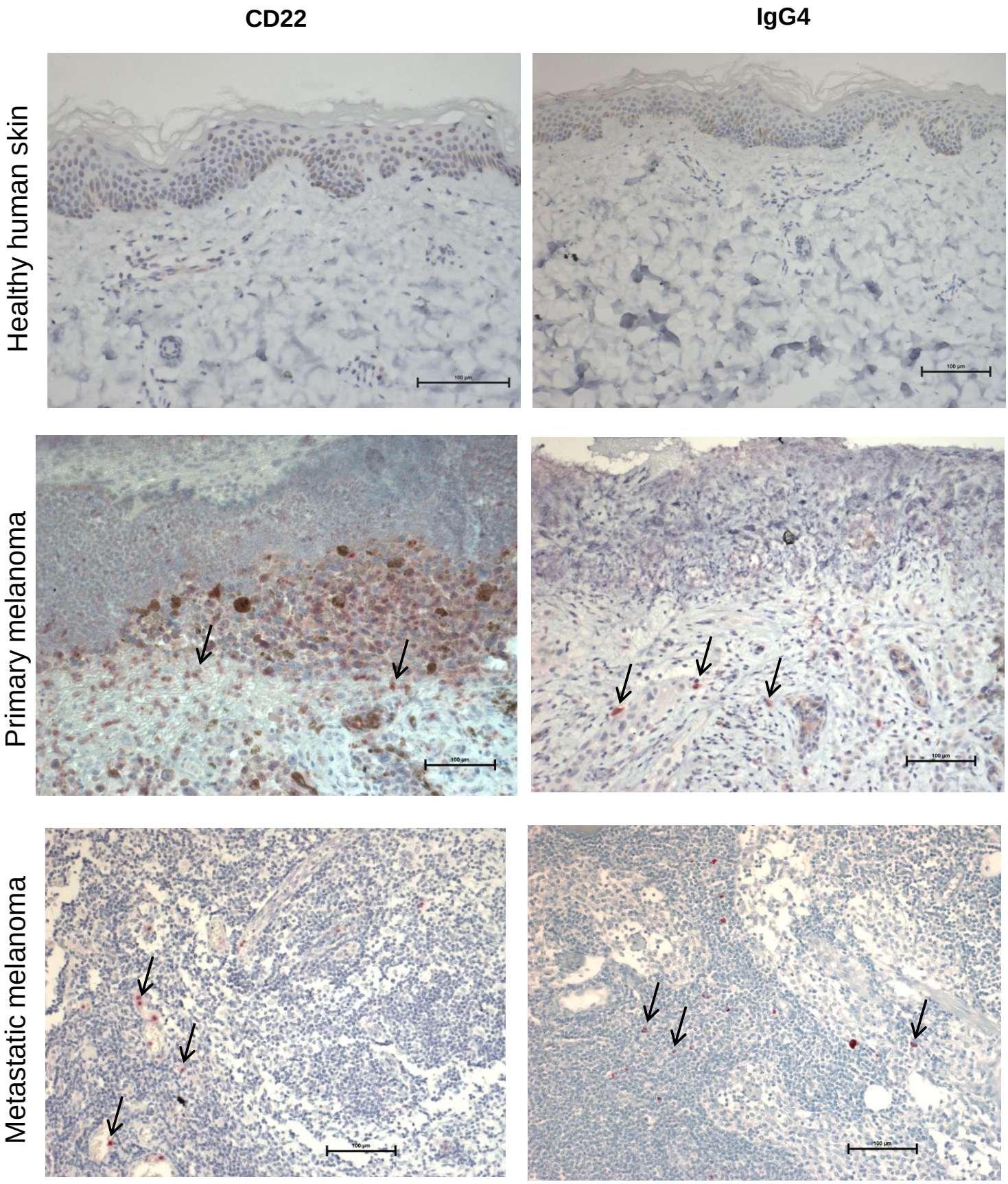

Supplementary Figure 1: Immunohisochemical analysis of CD22+ (left) and IgG4 (right), cells (shown in red and indicated by arrows) in healthy skin, primary and metastatic melanoma lesions. Counterstaining in hematoxylin (blue; Scale bar: 100 μm, magnification 10x).

Supplementary Figure 2

A

FR-1 — CDR-1 — FR-2 — CDR-2 — FR-3 — CDR-3 — FR-4

```
GAGGTGCAGCTGGTGGAGTCTGGGGGAGGCTTGGTACAGCCTGGGGGGTCCCTCAGACTCTCCTGTGCAGCCTCTGGATTCACCTTTAGCATCTATGCCATGAGCTGGG

TCCGCCAGGCTCCAGGGAAGGGGCTGGAGTGGGTCTCAACTATTAGTGGTAGTGCTGATAGCACATACTACGCAGACTCCGTGAAGGGCCGCTTCACCATCTCCAGAGA

CAACTCCAAGAACACGCTGTATTTGCAAATGAACAGCCTGAGAACTGAGGACACGGCTGTGTATTACTGTGCGAAAGGGACACTGGCTACGAAGGGCGGTATGGACGTC

TGGGGCCAAGGGACCACGGTCACCGTCTCCTCA
```

B

γ4

```
                GCC TCC ACC AAG GGC CCA TCC GTC TTC CCC CTG GCG CCC TGC TCC AGG AGC ACC TCC GAG AGC ACA GCC GCC CTG GGC TGC
M173            A   S   T   K   G   P   S   V   F   P   L   A   P   C   S   R   S   T   S   E   S   T   A   A   L   G   C
K01316          -   -   -   -   -   -   -   -   -   -   -   -   -   -   -   -   -   -   -   -   -   -   -   -   -   -   -
P01861          -   -   -   -   -   -   -   -   -   -   -   -   -   -   -   -   -   -   -   -   -   -   -   -   -   -   -

                CTG GTC AAG GAC TAC TTC CCC GAA CCG GTG ACG GTG TCG TGG AAC TCA GGC GCC CTG ACC AGC GGC GTG CAC ACC TTC CCG
M173            L   V   K   D   Y   F   P   I   P   V   T   V   S   W   N   S   G   A   L   T   S   G   V   H   T   F   P
K01316          -   -   -   -   -   -   -   -   -   -   -   -   -   -   -   -   -   -   -   -   -   -   -   -   -   -   -
P01861          -   -   -   -   -   -   -   -   -   -   -   -   -   -   -   -   -   -   -   -   -   -   -   -   -   -   -

                GCT GTC CTA CAG TCC TCA GGA CTC TAC TCC CTC AGC AGC GTG GTG ACC GTG CCC TCC AGC AGC TTG GGC ACC CAG ACC TAC
M173            A   V   L   Q   S   S   G   L   Y   S   L   S   S   V   V   T   V   P   S   S   S   L   G   T   Q   T   Y
K01316          -   -   -   -   -   -   -   -   -   -   -   -   -   -   -   -   -   -   -   -   -   -   -   K   -   -
P01861          -   -   -   -   -   -   -   -   -   -   -   -   -   -   -   -   -   -   -   -   -   -   -   K   -   -

                ATC TGC AAC GTG AAT CAC AAG CCC AGC AAC ACC AAG GTG GAC AAG AGA GTT
M173            I   C   N   V   N   H   K   P   S   N   T   K   V   D   K   R   V
K01316          T   -   -   -   -   -   -   -   -   -   -   -   -   -   -   -   -
P01861          T   -   -   -   -   -   -   -   -   -   -   -   -   -   -   -   -
```

Supplementary Figure 2: V_H-D-J (**A**) and alignment of γ4 constant region (**B**) amplified by RT-PCR from a melanoma patient (M173) indicating that the acquired protein sequence has the highest similarity with IGHG4 (Accession P01861;K01316) analysed using Blast/Uniport (http://www.uniprot.org/blast/uniprot).

Supplementary Figure 3

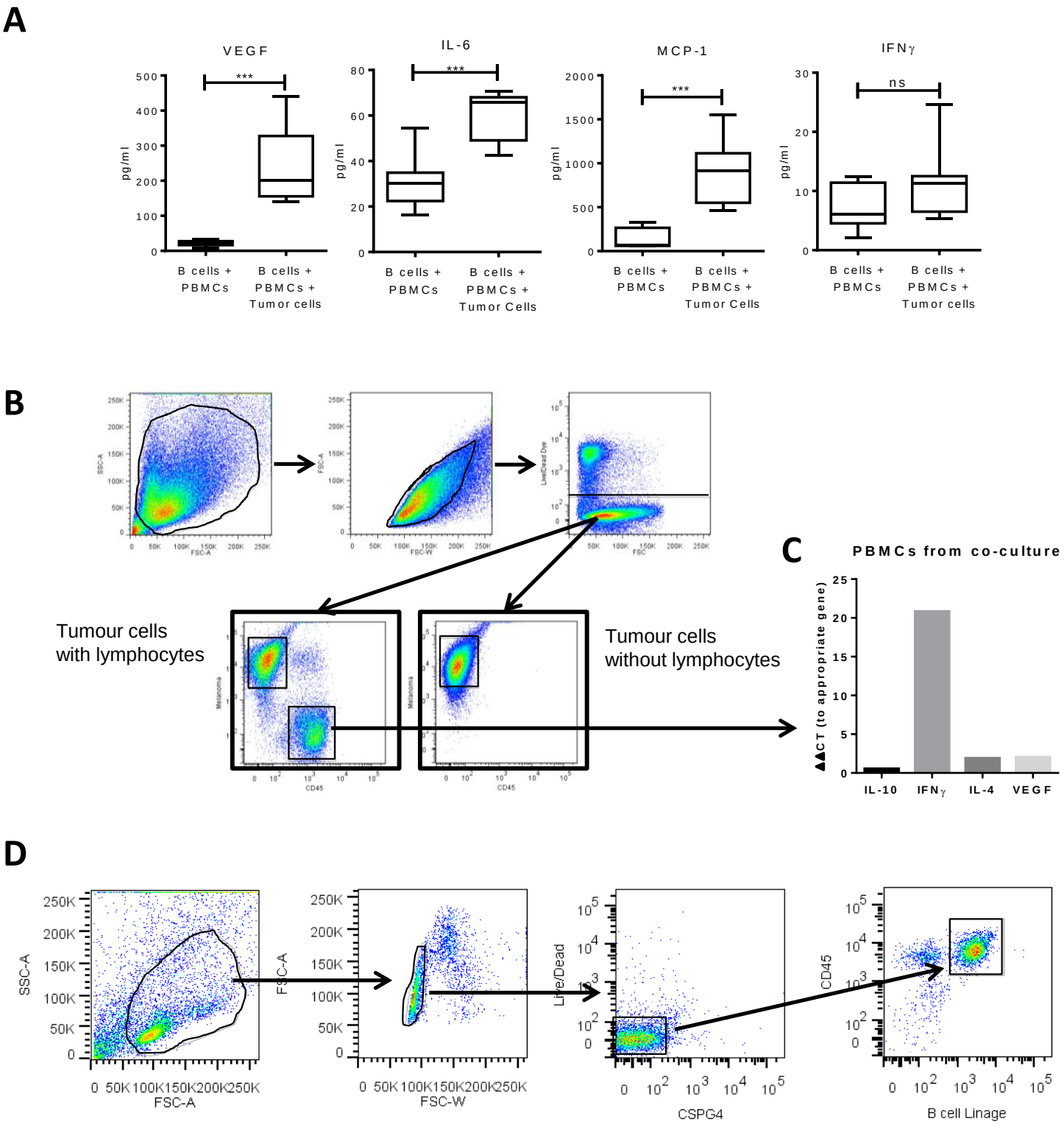

Supplementary Figure 3: (A) Cytokines secreted in culture supernatants of B cells and PBMCs stimulated with or without A375 melanoma tumour cells were analysed by Luminex bead array analysis. Titres of VEGF, IL-6 and MCP-1, but not of IFNγ, were significantly increased in cultures treated with tumour cells (*** $P<0.001$; ns = not significant $P>0.05$, analysed by using Mann-Withney-U-test, n=9). **(B)** Flow cytometric sorting strategy to isolate A375 tumor cells and PBMCs from co-culture experiments; purified cells were used to examine cytokine expression in Figure 3D and expression of cytokines by PBMC in these cultures is depicted in **(C)**. **(D)** Flow cytometric sorting strategy to isolate B cells from co-culture experiments described in Figure 3F.

Supplementary Figure 4

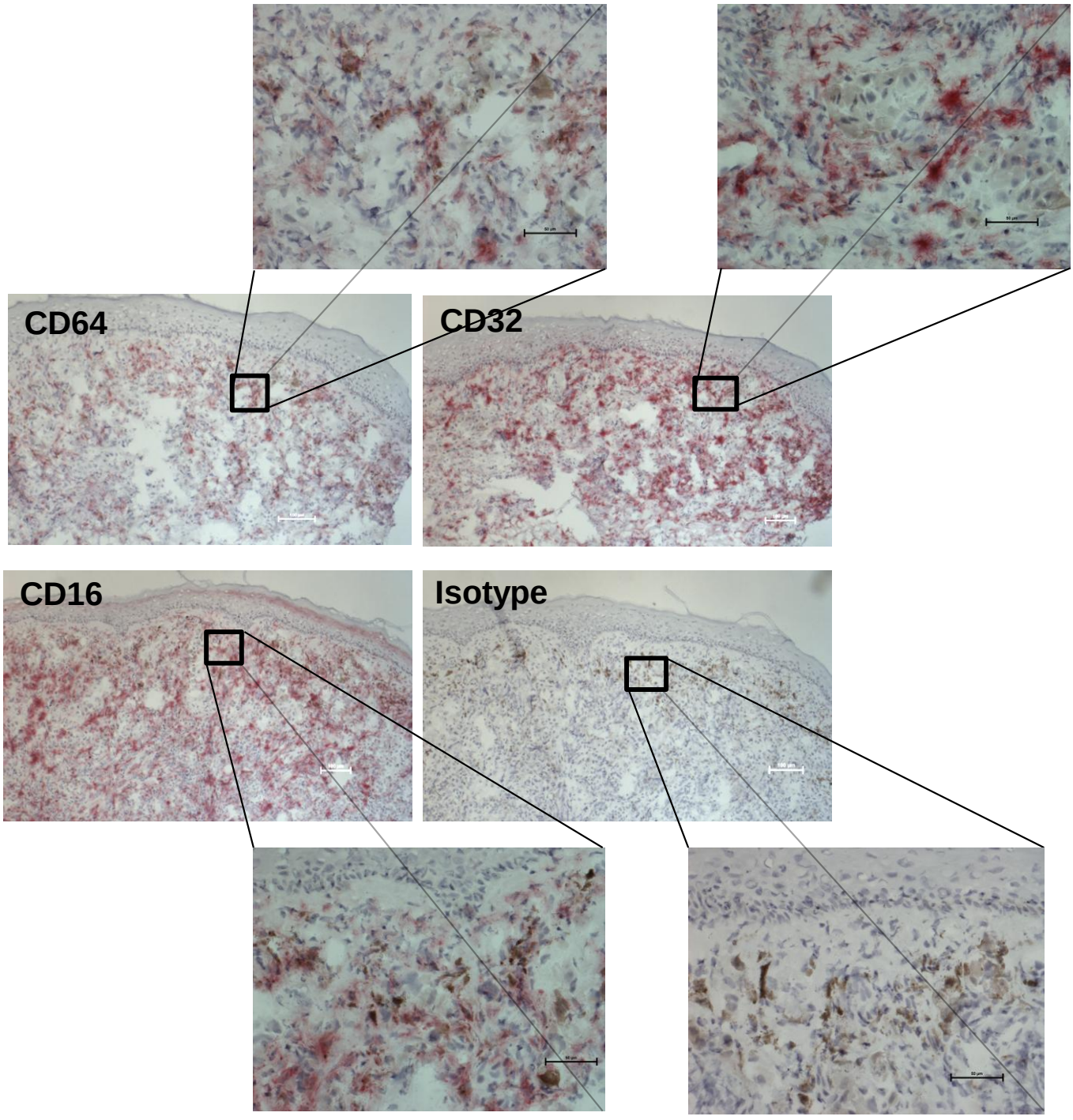

Supplementary Figure 4: Immunohistochemical analysis of FcγR distribution was conducted using fresh-frozen sections of human melanoma lesions and visualized using AP (in red). Representative images demonstrate all three families of FcγRs, i.e. FcγRI (CD64), FcγRII (CD32) and FcγRIII (CD16) widely expressed in melanoma lesions. Main images were captured at 10x magnification (scale bars: 100 μm); magnified images were captured at 20x (scale bars: 50 μm).

Supplementary Figure 5

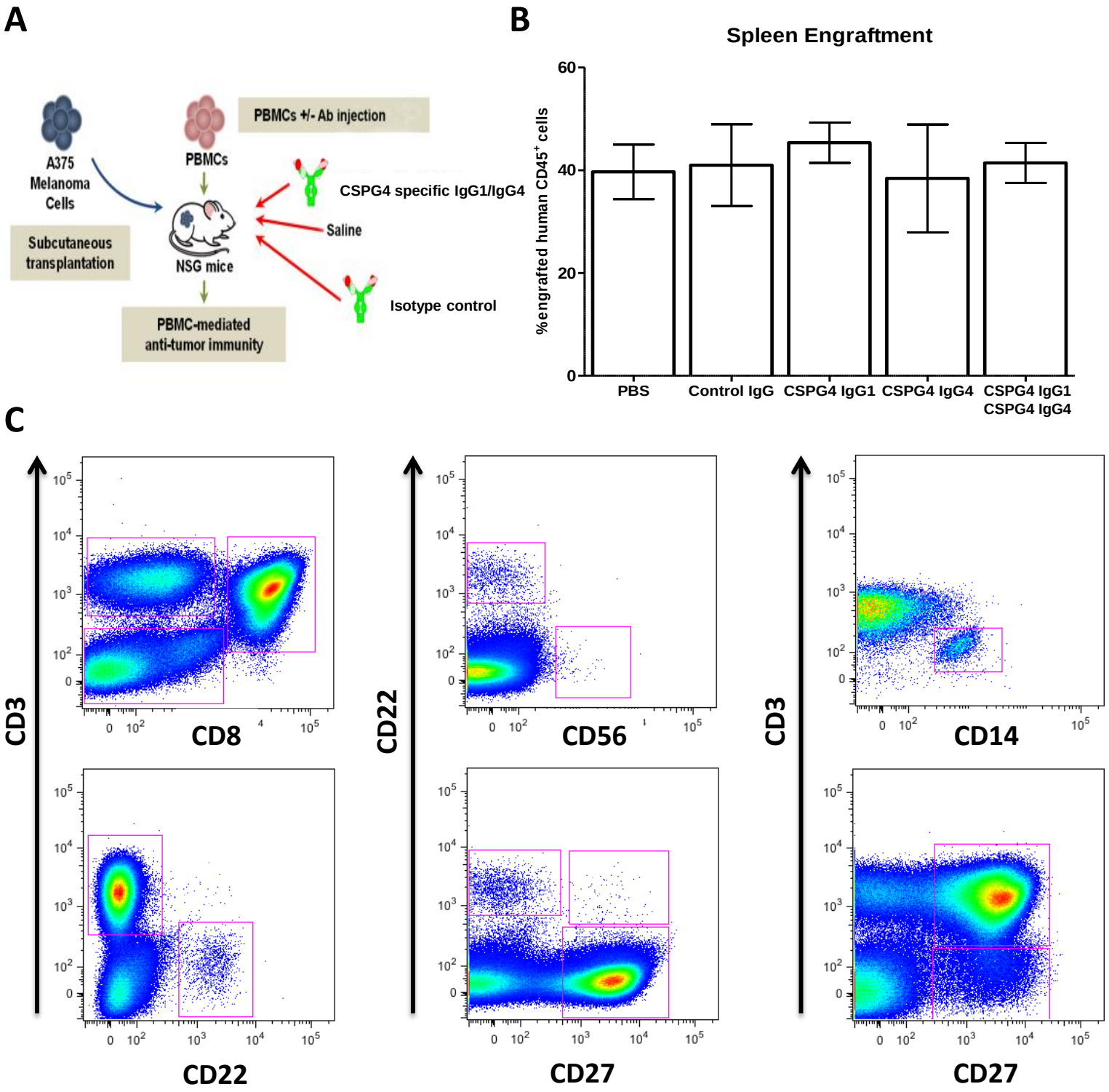

Supplementary Figure 5: (A) Design of in vivo model in NOD/scid/ IL-2Rγ$^{-/-}$ mice to determine antibody-mediated effector functions. (**B)** Engraftment of human CD45+ immune cells in mouse spleens, evaluated by flow cytometry showed no significant difference in human CD45^{+} engraftment across treatment groups. **(C)** Representative flow cytometric gating strategies to identify immune cell subsets within the human CD45^{+} mouse CD45^{-} gates engrafted in mouse spleens.

Supplementary Figure 6

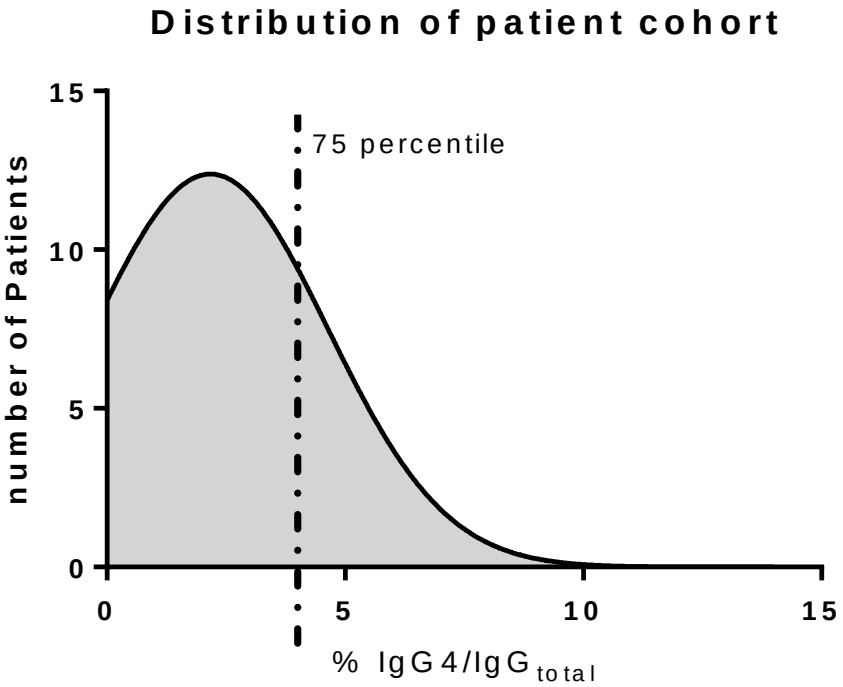

Supplementary Figure 6: Patient distribution based on % IgG4\IgG$_{total}$; black dashed line indicates the 75 percentile, used as cut off point for cumulative survival analysis (Figure 8).

Supplementary Table 1: Clinical parameters and disease staging of peripheral blood donors used for ex vivo B cell cultures at the time of sampling (Figures 2 and 3).

Patient ID	Gender	Age	Stage	TNM
M282	F	43	IB	T2a;N0;M0
M285	M	82	IIA	T2b;N0;M0
M286	F	68	IIB	T4a;N0;M0
M287	F	62	IIIA	T2a;N1a;M0
M338	M	72	IIIB	Tx;N2c;M0
M385	M	67	IIIC	Tx;N3;M0
M380	M	41	IIB	T4a;N0;M0
M381	M	57	IB	T1b;N0;M0
M386	F	64	IIIB	Tx;N2c;M0
M394	M	56	IIB	T4a;N0;M0
M396	M	73	IIC	T4b;N0;M0
M397	F	70	IIB	T3b;N0;M0
M401	F	60	IIIA	T2a;N1a;M0
M402	M	50	IIIB	Tx;N1b;M0
M404	F	65	IB	T2b;N0;M0
M405	M	51	IIC	T4b;N0;M0
M408	F	71	IB	T1a;N0;M0
M409	F	78	IIA	T3a;N0;M0
M430	F	78	IIC	T4b;N0;M0
M433	F	48	IIIB	T3b;N2c;M0
M435	M	45	IB	T2a;N0;M0
M437	M	46	IIA	T3a;N0;M0
M438	F	62	IIA	T2b;N0;M0
M443	M	69	IB	T2a;N0;M0
M318	M	60	IB	T2a;N0;M0
M320	F	71	IIB	T3b;N0;M0
M247	F	37	IV	T3b;N0;M1c
M224	F	76	IIB	T3b;N0;M0
M223	M	35	IB	T2a;N0;M0

4 IgG4: A CANDIDATE BIOMARKER TO PREDICT THE RISK OF DISEASE PROGRESSION IN CUTANEOUS MELANOMA

4.1 Introduction

Approximately 20% of individuals diagnosed with malignant melanoma at early stage go on to develop metastases, yet current serum and histopathological evaluators cannot predict the risk of disease recurrence. Presently, it is difficult to predict which patients will develop metastatic disease and this contributes to malignant melanoma still remaining a lethal skin cancer despite emerging targeted therapies [Hodi et al., 2010, Chapman et al., 2011, Wolchok et al., 2013]. Prognosis still relies on histological evaluation of the primary lesion including Breslow thickness, ulceration and mitotic rate, together with sentinel node involvement, all requiring surgical interventions [de Vries et al., 2011]. Whilst sentinel node biopsy has been demonstrated to provide valuable prognostic information, around 80% of patients have a negative test

and may develop complications of as a result of surgery [de Vries et al., 2006, Morton et al., 2006]. Hence, alternative non-invasive biomarkers would be highly valuable for early disease. Serum readouts such as S-100B and melanoma-inhibitory activity (MIA) have demonstrated some value in predicting poor outcomes; yet, the only serological marker recommended in the American Joint Committee on Cancer guidelines is lactate dehydrogenase (LDH). LDH is the only serum marker routinely used in the clinical management of patients with melanoma [Balch et al., 2009]. Elevated LDH levels indicate active cell necrosis, normally associated with increased disease burden occurring in advanced stages [Tandler et al., 2012]. Hence, novel early disease prognostic serum biomarkers are needed to stratify patients who are most likely to recur and who may benefit from early interventions [Gogas et al., 2009]. Moreover, as emerging immune checkpoint blockade therapies may depend on patients' immunological status, identification of biomarkers associated with immunosuppression could inform treatments. Insights into pathogenic roles of IgG_4 in inflammatory diseases and also in cancers, such as pancreatic cancer, extrahepatic cholangiocarcinomas, squamous cell carcinomas and melanomas [Daveau et al., 1977, Harada et al., 2012, Strehl et al., 2011], include the presence of IgG_4^+ immune cell infiltrates, elevated or dysregulated IgG_4 serum levels and associations with regulatory elements in tumour microenvironments. Additionally, findings presented in Chapter 3 demonstrate not only the presence of IgG_4 infiltrating cells in melanoma tumours, but also functional contributions of IgG_4 in promoting tumour progression by impairing anti-tumoural immunity. Importantly, preliminary assessments of IgG_4 in sera from patients with melanoma reported in Chapter 3 reveal correlations of higher IgG_4 serum levels with less favorable patient survival. Taken together, these data mandate a closer examination of the clinical significance of this antibody subclass and its relevance to prognosis in melanoma, ultimately leading to an assessment of IgG_4 as a disease biomarker.

4.2 IgG_4 serum levels predict the risk of disease progression

Collection of melanoma patient sera and healthy volunteer sera was conducted at a South London melanoma clinic between 2000 and 2012. Samples were anonymised prior to handling and examined for IgG_4 levels (IgG_4/IgG_{total}). Additionally, 80 sera previously collected from patients with stage I-II breast cancer were kindly provided by Prof. Ian S. Fentiman (Guy's Hospital), Prof. Joyce Taylor-Papadimitriou and Prof. Joy Burchell (KCL) and were included in this study. Subsequently collected samples were assayed for IgG_4 levels using a Luminex bead array assay. Collected data were linked to patient information and analysed (Figure 4.1).

	Melanoma	**Breast Cancer**	**Healthy Volunteer**
Mean age (SD)	60 (17)	59 (8)	55 (19)
Sex			
Male (%)	85 (49.70)	0 (0)	42 (40.40)
Female (%)	86 (50.30)	80 (100)	62 (59.60)
Disease Stage			
I	36	46	NA
II	48	34	NA
III	49	0	NA
IV	38	0	NA

Table 4.1: Baseline characteristics of patients and healthy volunteer cohort. SD: standard deviation; NA: not applicable

The analysis of 265 cancer patient (171 melanomas; 80 breast cancers) and 104 healthy volunteer sera (patient baseline characteristics described in Table 4.1), revealed statistically significantly elevated serum IgG_4 levels in melanoma (median

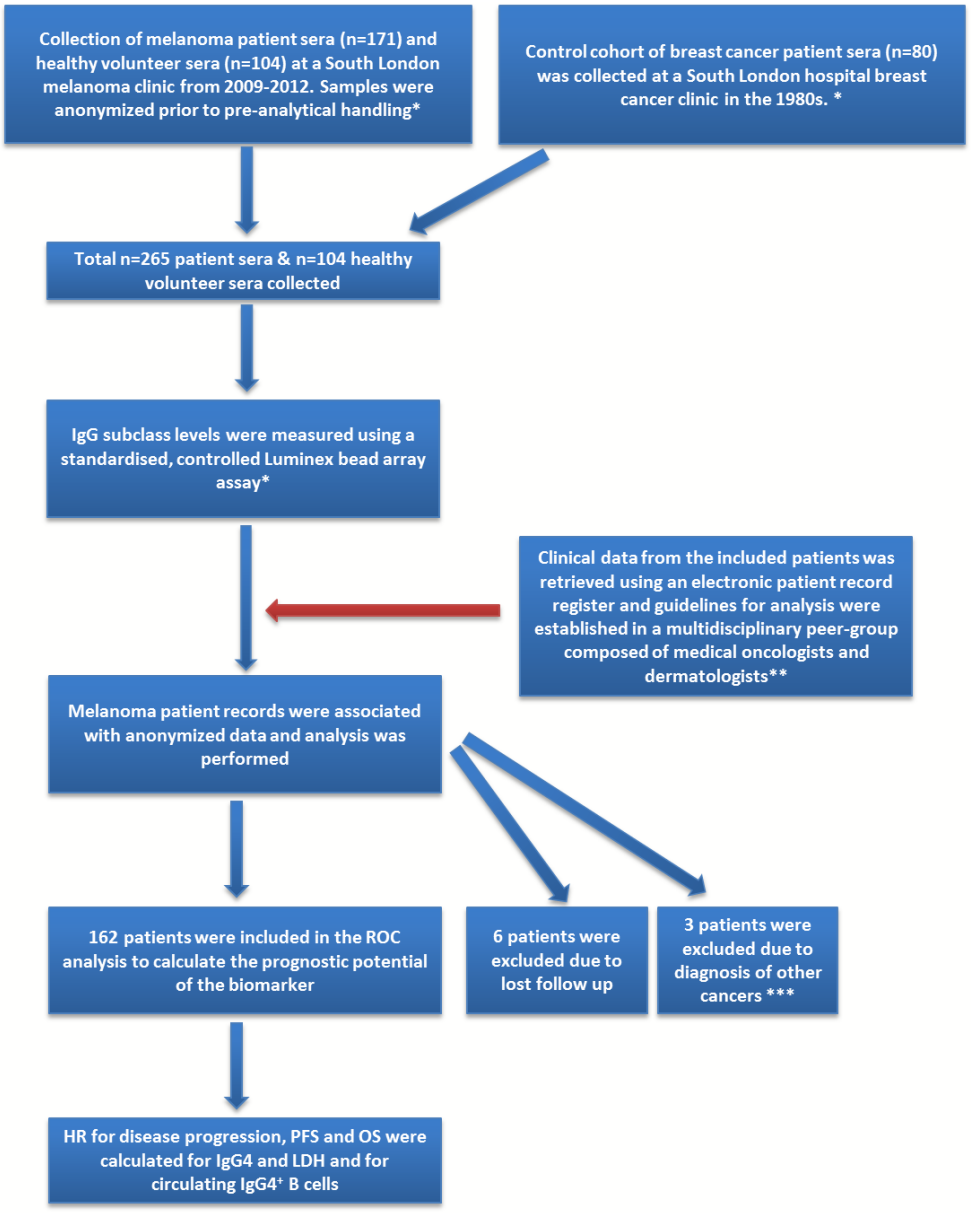

Figure 4.1: Flow diagram depicting study and experimental design as well as collection and processing of clinical samples(*:Researchers working on this study were blinded to prevent bias; **: Two independent medical professionals not involved in the quantification of IgG4 or LDH evaluated patient information; ***: Patients with co-morbidities that may influence IgG4 levels were excluded from the analysis)

0.031; 95%[CI] 0.036-0.051) compared with IgG$_4$ levels in healthy sera (median 0.017; 95%[CI] 0.026-0.042; P<0.05), (Figure 4.2). In contrast, serum IgG$_4$ levels in breast

cancer (median 0.013; 95%[CI] 0.012-0.030) were not significantly elevated compared to those in healthy sera (P<0.05).

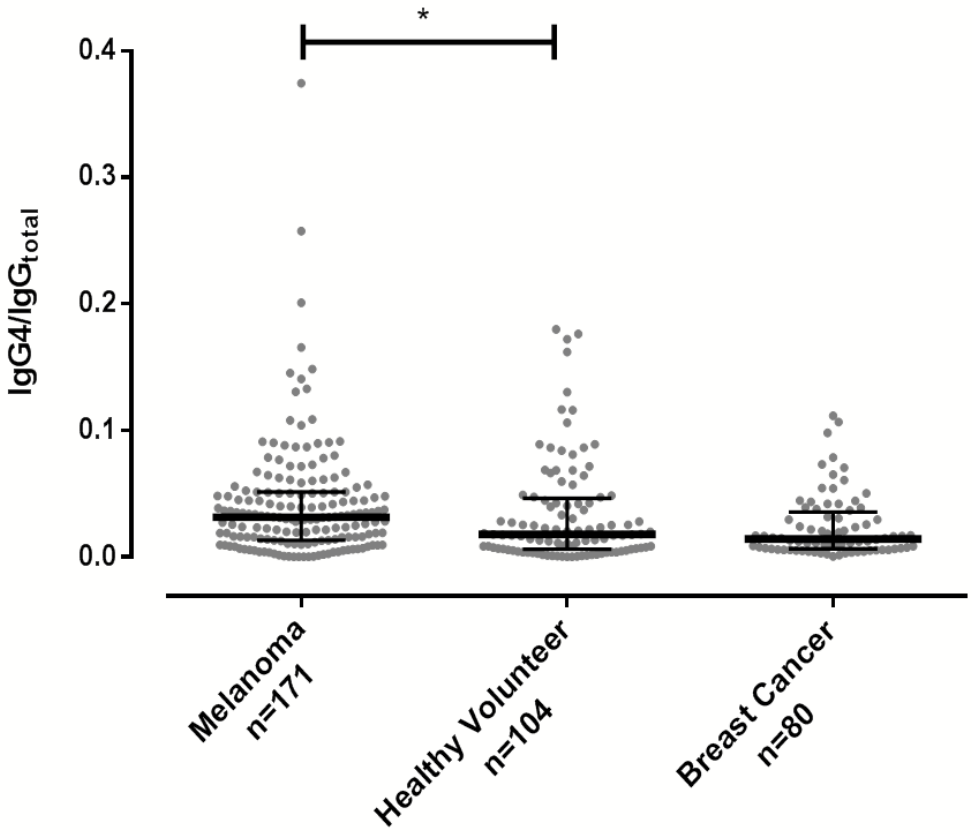

Figure 4.2: Sera from patients with melanoma (n=171) and breast cancer (n=80) were analyzed for circulating IgG$_4$ serum levels and compared to sera from healthy volunteers (n=104). IgG$_4$ levels in the melanoma patient cohort were statistically significantly increased compared to IgG$_4$ levels in healthy volunteer sera, whilst IgG$_4$ levels in breast carcinoma sera were not elevated in comparison to those in healthy sera, indicating that IgG$_4$ may be relevant in melanoma but not in breast carcinomas (Kruskal-Wallis one-way analysis of variance with post-hoc Dunn's test; lines represent medians and error bars indicate interquartile range; *P<0.05).

In order to evaluate IgG$_4$ as a prognostic tool, sera from 162 patients with melanoma were further analysed. From the original cohort of 171, 6 patients were excluded as they did not attend follow-up appointments and 3 patients were excluded due to subsequent diagnosis of other carcinomas which may have affected IgG$_4$ serum lev-

els. Patients were segregated into those with stable disease (SD, neither progressive disease nor subsequent relapse during study period) and those with progressive disease (PD, either active progressing disease or subsequent relapse patients who were up-staged during study period). Here, receiver operating characteristic (ROC) and area under the curve (AUC) analyses were performed [Baker, 2003]. Patients with stable disease (SD) (median 0.023; 95%[CI] 0.026-0.040) displayed significantly lower serum IgG_4 levels (median 0.023; 95%[CI] 0.026-0.040) compared with those who developed progressive disease (PD) (median 0.039; 95%[CI] 0.039-0.066) ($P<0.01$). A mean AUC of 0.64 ($P=0.0021$), 57.14% sensitivity (95%[CI] 45.35-68.37) and 67.78% specificity (95%[CI] 57.10-77.25), demonstrated the value of IgG_4 as a prognostic marker (Figure 4.3).

Since LDH is the only clinically-used serum biomarker to predict metastatic disease, the potential of IgG_4 and LDH to predict the risk of progression-free survival (PFS) and overall survival (OS) was next evaluated in the same patient serum samples. Based on ROC analysis, a threshold of 0.034 for IgG_4 levels was calculated via the Youden's Index [YOUDEN, 1950] (n=90 in IgG_4low, <0.034; n=72 in IgG_4high, $\geq$0.034). For LDH, samples were segregated into normal (240-480 mmol/l, n=137) and abnormal (>480 mmol/l, n=19) concentrations. These cutoffs were subsequently used to compare patient serum IgG_4 and LDH hazard ratios (HR) for the risk of progression-free survival (PFS) and overall survival (OS). Kaplan-Meier Curve evaluations revealed statistically significantly worse PFS (HR 95%[CI] 2.56 (1.58-4.17); log-rank P=0.0001) and lower OS (HR 95%[CI] 2.54 (1.43-4.54); log-rank P=0.0015) in the IgG_4high group compared to the IgG_4low group (Figure 4.4, left). The age- and sex-adjusted HR to predict the risk for PD in the IgG_4high group of patients across all disease stages (I-IV) was 2.23 (95%[CI] 1.36-3.64) (Table 4.2). Patients with abnormal LDH levels (n=19) had lower PFS (HR 95%[CI] 5.60 (15.19-106.2); log-rank P<0.0001) and lower OS (HR 95%[CI] 5.34 (11.11-101.50); log-rank P<0.0001) compared to those in the LDH normal group (Figure 4.4, right). The adjusted HR for PD across all stages in the abnormal LDH group was 6.48 (95%[CI] 3.68-11.37) (Table 4.2). These data support the value of serum LDH and IgG_4 in prognosis of disease outcomes in melanoma.

In stages I-III, each serum marker, IgG_4high and abnormal LDH, independently predicted the risk for PD (IgG_4: HR 95%[CI] 4.01 (1.98-8.11); LDH: HR 95%[CI]

6.65 (2.49-17.72)). However, in regional disease (stages I-II) IgG_4 had a statistically significant (HR 95%[CI] 4.60 (1.73-12.23) for predicting PD, whereas serum LDH was not statistically significant (Table 4.2; ; patient baseline clinical characteristics and correlations with serum IgG_4 and LDH levels are described in Table 4.3 and Table 4.4, respectively). Thus, while these data confirms the prognostic value of LDH in metastatic disease stages only, IgG_4 serum levels provide significant prognostic information in earlier stages (I-II).

	Stage I–II	**Stage I–III**	**Stage I–IV**
	HR$^\wedge$ (95% [CI])	**HR$^\wedge$ (95% [CI])**	**HR$^\wedge$ (95% [CI])**
IgG_4 (IgG_4/IgG_{total})	n=78	n=124	n=162
<0.034	1.00 (Ref)	1.00 (Ref)	1.00 (Ref)
≥0.034	4.60 (1.73–12.23)	4.01 (1.90–8.11)	2.23 (1.36–3.64)
AUC (95% [CI])	0.68 (0.55–0.81)	0.68 (0.58–0.77)	0.64 (0.66–0.72)
P-Value	0.01	0.001	0.002
LDH (mmol/L)	n=74	n=119	n=156
240–480	1.00 (Ref)	1.00 (Ref)	1.00 (Ref)
≥480	non significant*	6.65 (2.49–17.72)	6.48 (3.68–11.37)

$^\wedge$: Age and sex adjusted Hazard Ratio (HR) and 95% Confidence Intervals (CI) for risk of disease progression. Ref: reference value; * non significant as no HR could be calculated due to sample size distribution; calculated values: 13.61 95% [CI] 1.22–151.61

Table 4.2: IgG_4 hazard ratio prediction calculation. IgG_4 had a significant HR to predict the risk of disease progression overall (combined stages I–IV) as well as in subgroups (stages I–II; stages I–III) (P<0.01). In contrast, LDH had a more significant HR to predict the risk of disease progression overall (combined stages I–IV) as well as in the subgroup including patients with lymph node metastasis (stages I–III), but failed to show statistical significance in the early disease patient group (stagesI-II). The analysis of this data was performed by Dr. Mieke Van Hemelrijck (KCL)

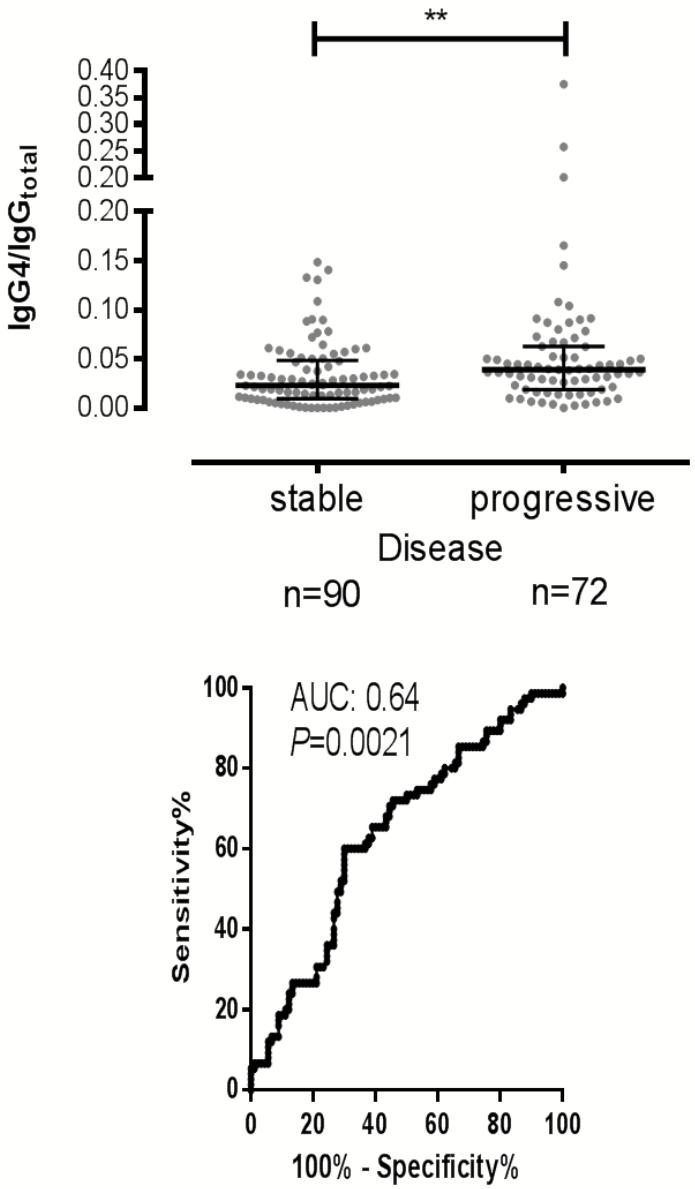

Figure 4.3: Comparative IgG$_4$ serum level analysis among melanoma patients with subsequent stable (SD; n=90) or progressive disease (PD; n=72) demonstrates increased IgG$_4$ levels in patients with subsequent PD compared to patients with SD during the study (as D'Agostino's K-square test for normality did not pass, statistical significance was calculated using the Mann-Whitney-U-test (**P<0.01))(upper panel). Receiver Operating Characteristic (ROC) analysis was performed to assess the potential of IgG$_4$ serum levels to predict the risk for disease progression. The calculated mean AUC= 0.64 and P=0.0021 indicate that IgG$_4$ can predict the risk of melanoma progression (lower panel).

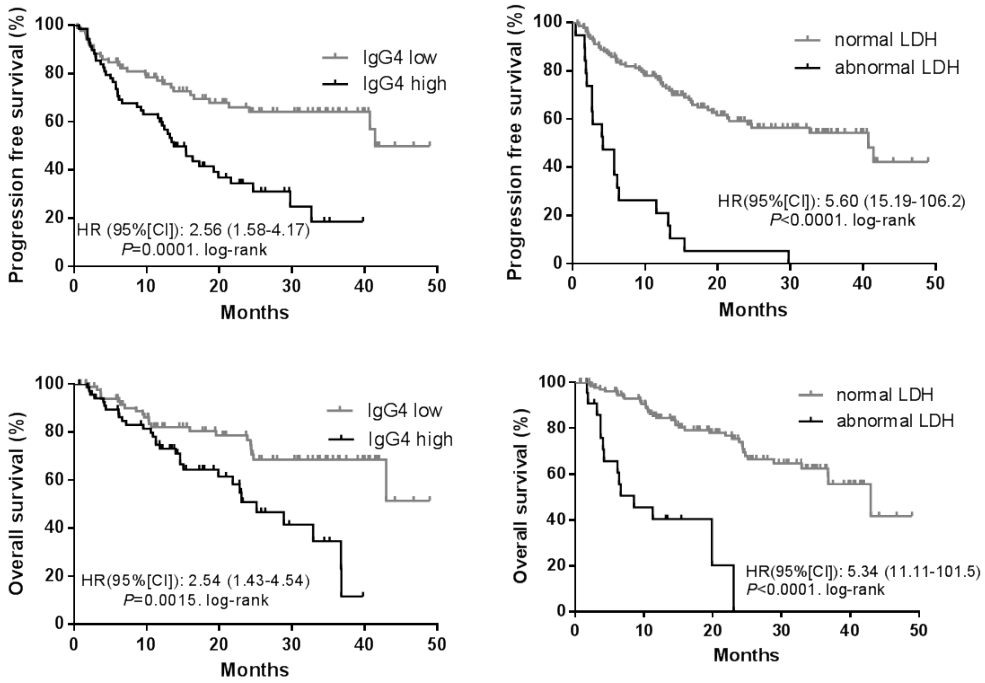

Figure 4.4: Evaluatation of progression free survival (PFS) and overall survival (OS) in a melanoma cohort. Based on ROC analysis, a threshold value of 0.034 for IgG$_4$ (calculated via the Youden's Index) was used to compare patient serum IgG$_4$ and LDH (hazard ratios (HR) for the risk of progression free survival (PFS) and overall survival (OS)). The cohort was analyzed using multivariate analysis. For LDH, samples were segregated into normal (240-480 mmol/l) and abnormal (>480 mmol/l) concentrations. Top row: Kaplan-Meier Curve evaluations of progression free survival (PFS) for IgG$_4$ (HR 95%[CI] 2.56 (1.58-4.17); log-rank P=0.0001) and PFS for LDH (HR 95%[CI] 5.60 (15.19-106.20); log-rank P<0.0001) (n=154 patient sera) confirm that patients with low IgG$_4$ serum levels have an increased PFS compared to patients with high IgG$_4$ levels. Bottom row: Kaplan-Meier Curves of (OS) for IgG$_4$ (HR 95%[CI] 2.54 (1.43-4.54); log-rank P=0.0015) and OS for LDH (HR 95%[CI] 5.34 (11.11-101.50); log-rank P<0.0001) (n=154 patients in both IgG$_4$ and LDH cohorts), demonstrating that elevated IgG$_4$ levels are associated with worse OS and could predict the risk of disease progression.

4.3 Circulating IgG_4^+ B cells predict the risk of disease progression in early stages of melanoma

Since serum IgG_4 levels were predictive of the risk of disease progression in earlier stages of melanoma, the presence of corresponding circulating IgG_4^+ B cells in patients and healthy volunteers was next examined. Increased frequencies of IgG_4^+ B cells in peripheral blood mononuclear cells (PBMC) of melanoma patients compared to those from healthy volunteers were investigated by flow cytometry (Figure 4.5).Flow cytometric analyses were performed using an antibody cocktail to the markers CD45, CD22, CD19, CD3, CD14 and IgG_4 (Figure 4.5). After dead cells were excluded, the frequencies of circulating IgG_4^+ peripheral blood B cells ($IgG_4^+CD45^+CD22^+CD19^+CD3^-CD14^-$) in peripheral blood mononuclear cells (PBMC) of melanoma patients were compared to those from healthy volunteers (Figure 4.5, bottom panel for representative flow cytometric dot plots used to draw comparisons between a healthy volunteer and a patient sample).

The proportion of IgG_4^+ cells in the peripheral blood B cell ($CD45^+CD22^+CD19^+$ $CD3^-CD14^-$) compartment of melanoma patients (n=47) (median 0.50; 95%[CI] 0.47-0.73) was significantly elevated, (median 0.50; 95%[CI] 0.47-0.73) compared to that of healthy volunteers' (n=24) (median 0.2; 95%[CI] 0.13-0.37) (Mann-Whitney-U-test; $P<0.001$) (Figure 4.6, top). Furthermore, statistically significantly higher circulating IgG_4^+ B cell frequencies in stage I-II (median 0.50; 95%[CI] 0.44-0.72) ($P<0.001$) (n=24) and stage III-IV (median 0.40; 95%[CI] 0.41-0.89) ($P<0.01$) (n=23) disease were measured when compared with IgG_4^+ B cell frequencies in healthy volunteer bloods (median 0.2; 95%[CI] 0.13-0.37) (n=24) (Kruskal-Wallis one-way analysis of variance with post-hoc Dunn's test) (Figure 4.6, bottom). These data are consistent with previous reports of dysregulated humoral immunity in melanoma, IgG_4-mediated immune suppression reported in Chapter 3 and also with the serum IgG_4 findings described Section 4.2 above. The frequencies of circulating IgG_4^+ B cells from patients with melanoma diagnosed at different disease stages were further analyzed to examine whether they can predict the risk of disease progression (Mann-Whitney-U-test; significance was indicated where appropriate; lines represent medians and error bars indicate interquartile range) (Figure 4.7) along with corresponding ROC analysis. As with circulating IgG_4 levels, increased IgG_4^+ B cells

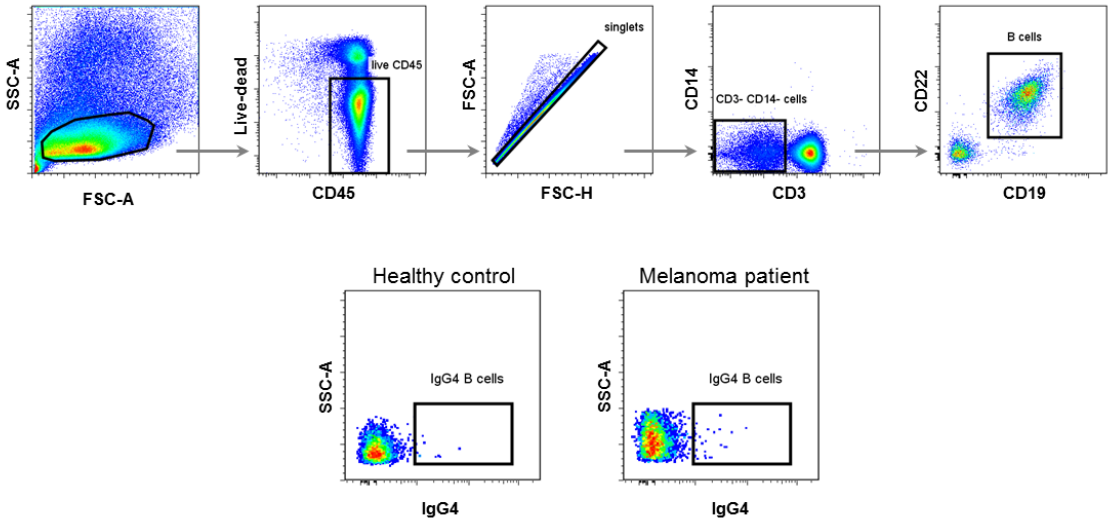

Figure 4.5: Representative flow cytometric dot plots and gating strategy for evaluation of the circulating IgG_4^+ B cell compartment. Lymphoid cells were gated according to their FSC-A and SSC-A properties, viable $CD45^+$ were selected and cell doublets excluded using FSC-A and FSC-H dot plots. $CD3^-CD14^-$ cells were selected and subsequently the B cell compartment was identified as $CD19^+CD22^+$ cells (first row). Representative dot plots depicting IgG_4^+ ($CD45^+CD22^+CD19^+CD3^-CD14^-$) peripheral B cells from PBMCs of a healthy volunteer (left) and of a melanoma patient (right) are shown in the lower panel.

were predictive of the risk of disease progression in regional disease. In the stage I-II patient cohort, patients with stable disease had a statistically significantly lower frequency of IgG_4^+ B cells compared with patients who developed progressive disease (stages I-II; AUC=0.81; P=0.014; (median of SD 0.30; 95%[CI] 0.17-0.56 vs. median of PD 0.70; 95%[CI] 0.50-0.95)). There were no statistically significant differences between SD and PD patient groups in stages I-III; (AUC=0.54; P=0.64; (median of SD 0.30; 95%[CI] 0.28-0.66 vs. median of PD 0.50; 95%[CI] 0.29-0.86) and in stages I-IV (; AUC=0.54; P=0.64; (median of SD 0.30; 95%[CI] 0.30-0.69 vs. median of PD 0.50; 95%[CI] 0.35-0.82)) (Figure 4.7).

Taken together, these data suggest that, similarly to elevated serum IgG_4 levels being prognostic at early stage (I-II) disease, the IgG_4^+ B cell compartment is elevated in the circulation of patients with melanoma and these elevated IgG_4^+ B cell frequencies are predictive of the risk of disease progression. These findings further support the value of IgG_4 as a promising biomarker in melanoma.

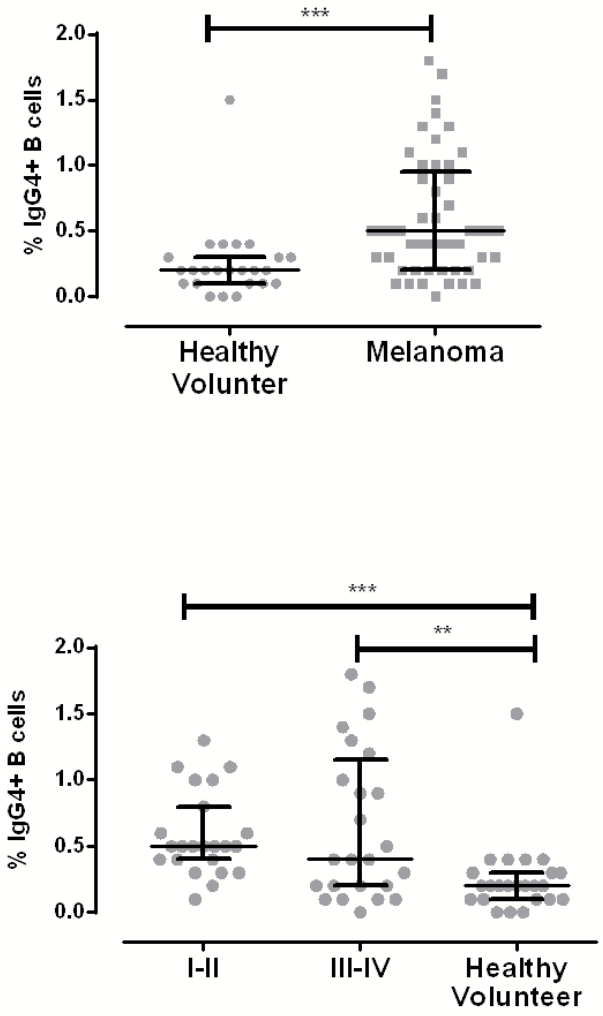

Figure 4.6: Top: Frequency of the IgG_4^+ peripheral B cell ($CD45^+CD22^+CD19^+CD3^-CD14^-$) compartment was compared between 24 healthy control and 47 melanoma patient samples, showing a statistically significant increase in the patient group (Mann-Whitney-U-test; *** $P<0.001$); Bottom: Patient samples were stratified by disease stage (I-IV) and compared with a healthy volunteer cohort (Kruskal-Wallis one-way analysis of variance with post-hoc Dunn's test). IgG_4^+ B cell frequencies were statistically different between stage I-II (n=24; ***$P<0.001$) or stage III-IV (n=23; **$P<0.01$) in comparison to B cells from healthy volunteers. Lines represent medians and error bars indicate interquartile range.

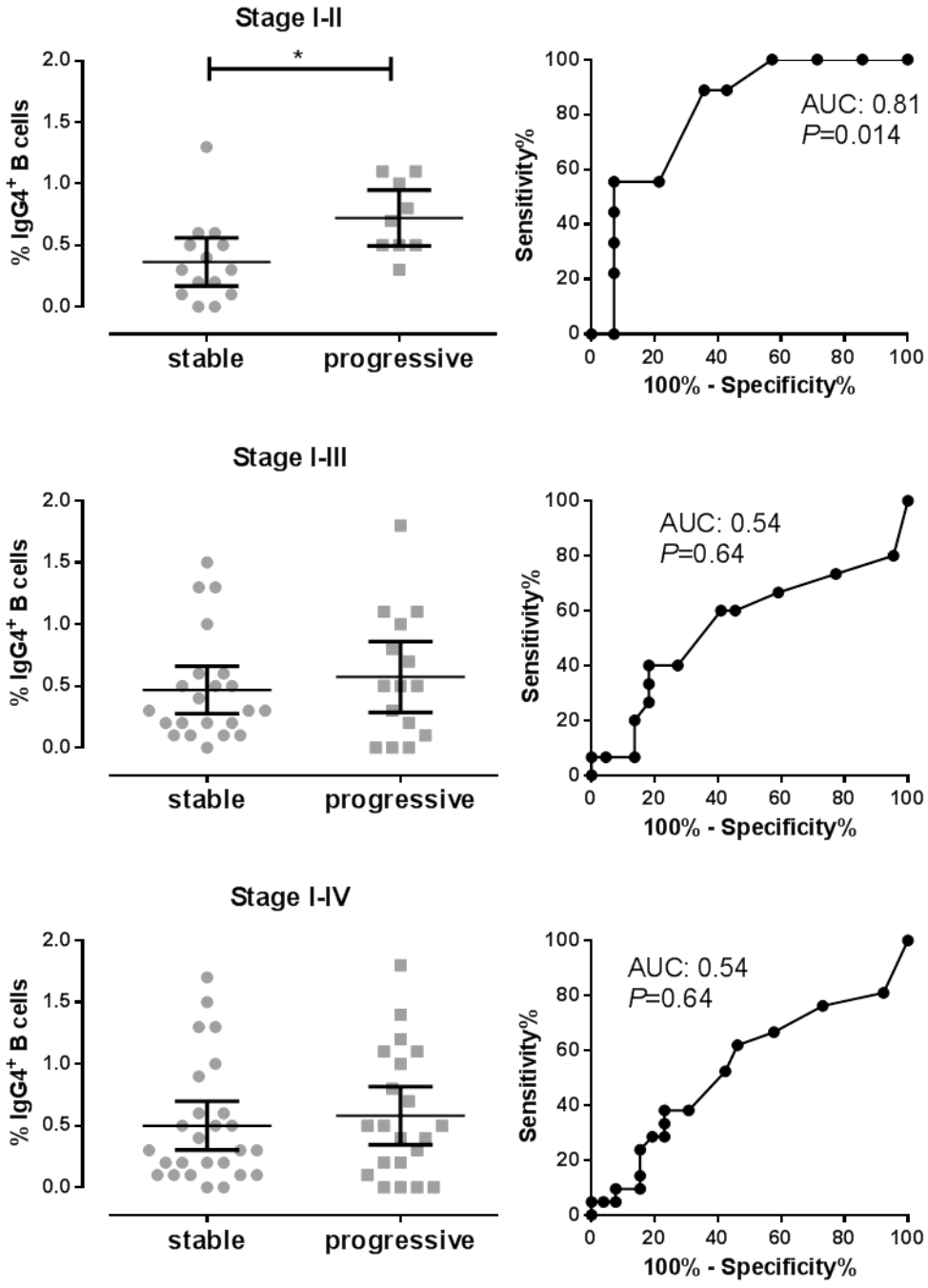

Figure 4.7: Frequency of circulating IgG_4^+ B cells from patients with melanoma diagnosed at different disease stages were analyzed to examine whether they can predict the risk of disease progression (Mann-Whitney-U-test; *P<0.05; lines represent medians and error bars indicate interquartile range). Corresponding ROC analysis is depicted directly next to each column graph. In the stage I-II patient cohort, patients with stable disease had a statistically significantly lower frequency of IgG_4^+ B cells compared to patients with progressive disease (*P<0.05; top panel). For this cohort, a median AUC of 0.81 calculated by ROC analysis further demonstrating the validity of the marker.

4.4 IgG_4 expression in tumours

In order to evaluate whether elevated serum IgG_4 and circulating IgG_4^+ B cells in melanoma were also reflected by tumour IgG_4^+ cell infiltration immunohistochemical analysis of tissue microarrays (n=256) for the presence of IgG_4^+ cells was conducted (Figure 4.8).

IgG_4^+ cell infiltration was detected in melanoma tumours and it was higher in melanoma skin lesions (n=108), melanoma lymph node metastases (n=56) and distant organ metastases (n=60) when compared to healthy skin (n=32) specimens. IgG_4 expression was detected in 42.60% (19.45% high positivity) of melanoma skin lesions, 21.40% (8.90% high positivity) of lymph node metastases and 30% (10% high positivity) of distant metastases. Low-grade positivity was found in 12.25% of healthy skin specimens (n=32) (Figure 4.9). Similarly, IgG_4^+ cells infiltrates were observed across disease stages (stage I-II: 39.43% (16.90% high; 22.53% low); stage III-IV: 40% (6.67% high; 33.33% low)) and in skin tumour lesions of different thicknesses (T1-T2: 38.88% (33.33% high; 5.55% low); T3: 37.29% (27.29% high; 10% low); T4: 46.03% (15.87% high; 15.87% low)) (Figure 4.9, bottom panel). These findings may signify, suggesting that IgG_4-attributed immunosuppression may occur throughout malignant disease and irrespective of skin tumour thickness.

These promising data suggest the merit of further analyses to correlate tissue IgG_4^+ infiltrates with disease outcomes to assess the clinical relevance of IgG_4 as a histological biomarker.

	IgG$_4$<0.034 (n=90)	**IgG$_4$≥0.034 (n=72)**
Mean age (SD)	57 (18)	64 (15)
Sex		
Male (%)	40 (44.44)	41 (56.94)
Female (%)	50 (55.56)	31 (43.06)
Mean Breslow (SD)	2.68 (2.42)	3.20 (2.10)
Disease Stage (%)		
I	27 (30.00)	9 (12.50)
II	19 (21.11)	23 (31.94)
III	23 (25.56)	23 (31.94)
IV	21 (23.33)	17 (23.61)
Ulceration (%)		
None	53 (58.89)	28 (38.89)
Present	19 (21.11)	28 (38.89)
Unknown	18 (20.00)	16 (17.78)

SD: Standard deviation

Table 4.3: Baseline clinical characteristics of melanoma patient cohort and correlations with serum IgG$_4$ levels

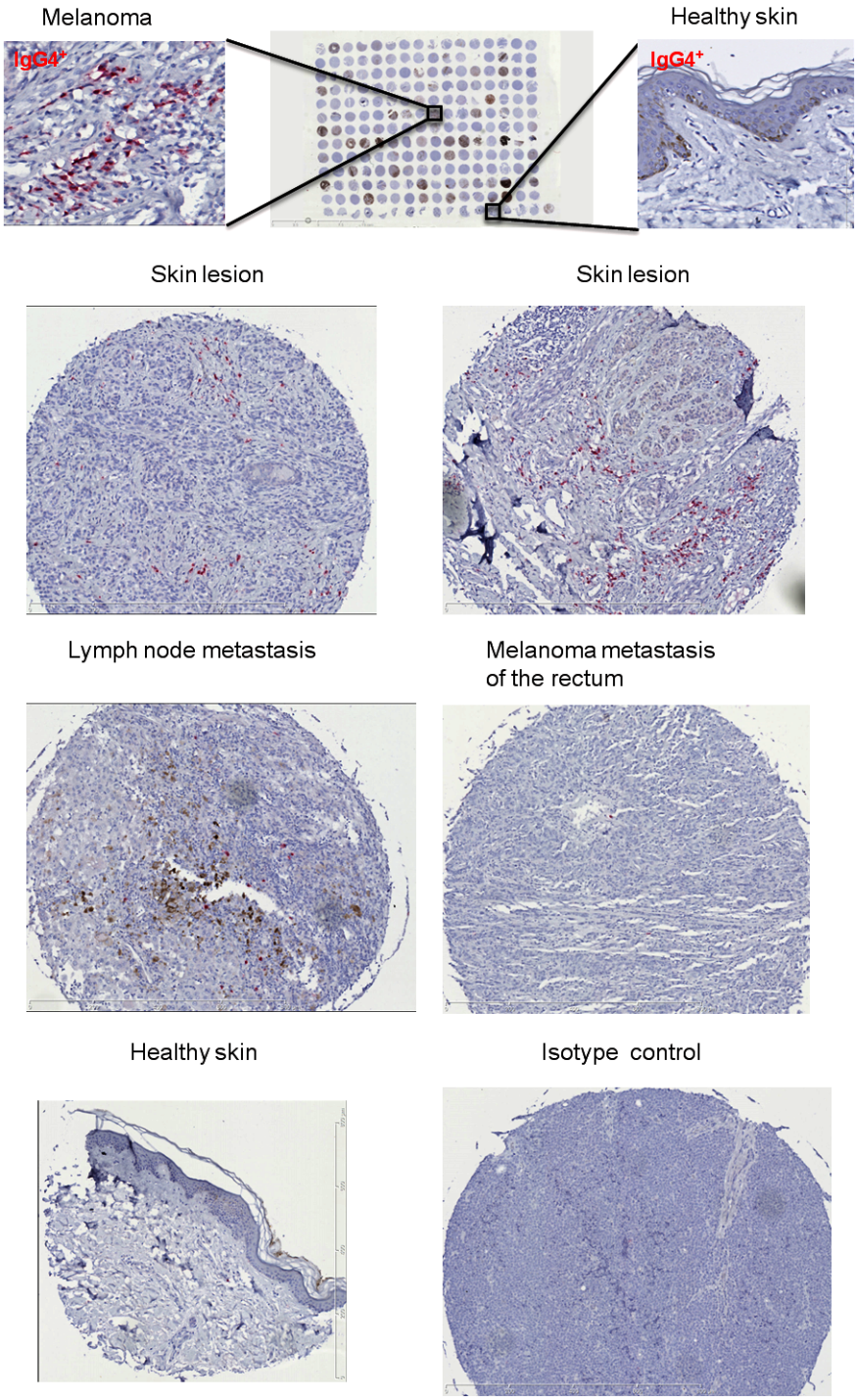

Figure 4.8: Representative images of IgG$_4$ staining on tissue microarray sections (IgG$_4$ is stained by alkaline phosphatase in red, counterstaining in hematoxylin in blue).

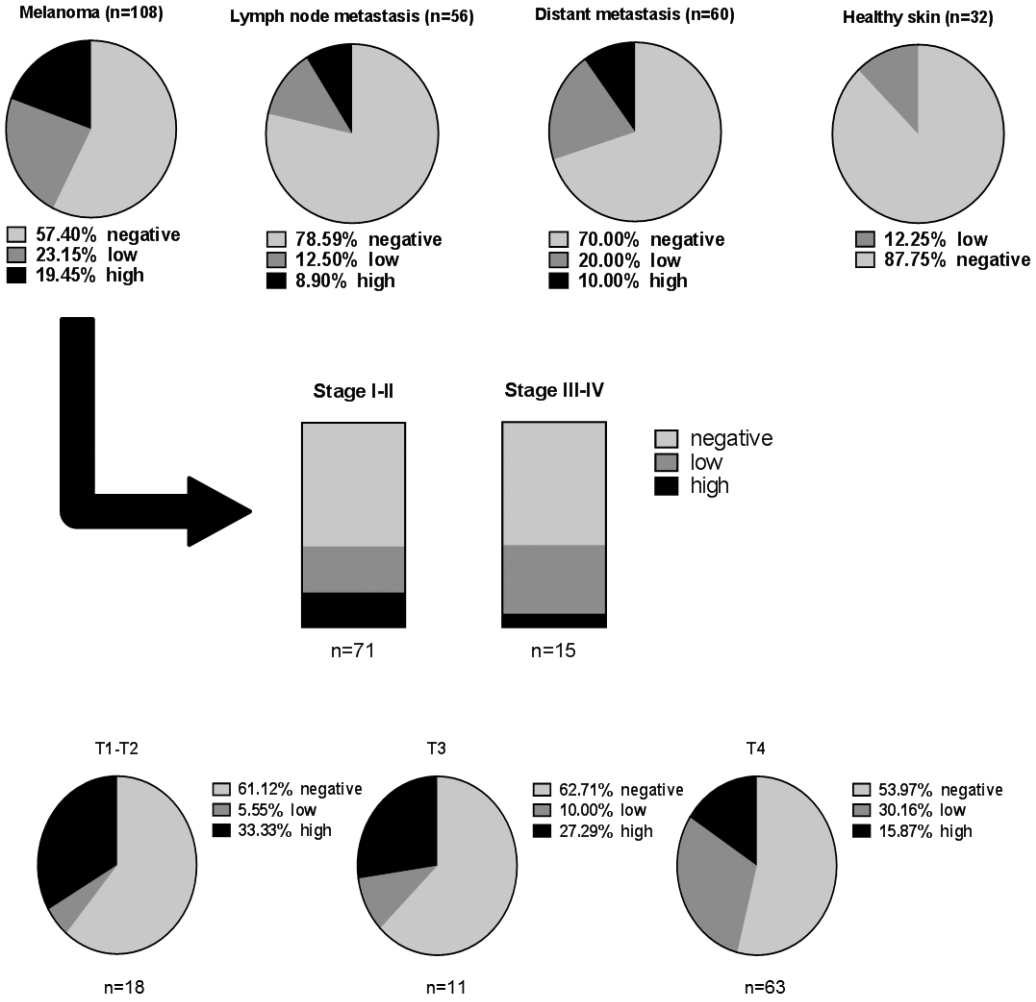

Figure 4.9: Evaluation of TMA sections showed more frequent IgG$_4$$^+$ cell infiltration in melanoma tissues when compared to healthy discarded skin, and infiltration found in early and metastatic skin lesions (Pie charts represent % of total numbers).

	LDH (240–480) (n=137)	**LDH >480 (n=19)**
Mean age (SD)	60 (17)	62 (14)
Sex		
Male (%)	68 (49.64)	11 (57.89)
Female (%)	69 (50.36)	8 (42.11)
Mean Breslow (SD)	2.88 (2.27)	2.73 (2.10)
Disease Stage (%)		
I	34 (24.82)	0 (0)
II	39 (28.47)	1 (5.26)
III	41 (29.93)	4 (21.05)
IV	23 (16.79)	14 (73.68)
Ulceration (%)		
None	73 (52.90)	5 (26.32)
Present	38 (27.54)	7 (36.84)
Unknown	27 (19.56)	7 (36.84)

SD: Standard deviation

Table 4.4: Baseline clinical characteristics of melanoma patient cohort and correlations with serum LDH levels

4.5 Conclusions

Taken together, these findings identify the prognostic value of IgG_4 in early stage melanoma (I-II). In agreement with previous reports [Hofmann et al., 2009, Hofmann et al., 2011, Kluger et al., 2011], the data presented here demonstrate that LDH is an independent predictor with specificity in metastatic melanoma, but lacks predictive value in local disease (stage I-II). This may be because LDH serum levels are proportional to cell necrosis, not commonly present in patients with low disease burden, and this is supported here by observed baseline LDH readouts at early disease stages (I-II) (Table 4.2). A drawback for the use of LDH release as a marker of melanoma progression is the presence of serum LDH as a result of other diseases such as hemolysis, hepatitis, myocardial infarction or infection. Thus, abnormal serum LDH levels are not exclusive to neoplasia, but may indicate underlying pathologies such as hemolysis, hepatitis, myocardial infarction or infection, yielding false-positive results in melanoma [Vereecken et al., 2012]. Similarly, elevated serum IgG_4 is described in autoimmune pancreatitis, indicating that IgG_4 may also be influenced by biological mechanisms unrelated to malignancy [Kawa et al., 2012], albeit for a subset of patients. This issue needs to be further investigated in future studies evaluating the clinical utility of serum IgG_4 as a biomarker in melanoma. Elevated levels of serum IgG_4 in melanoma could predict the risk of disease progression for patients at early disease stages (I-II), and these data were also supported by the significance of an elevated IgG^+ B cell subset in predicting the risk of disease progression at the same early stages of disease (I-II). Taken together, these findings not only support the relevance of serum IgG_4 as a promising biomarker in early disease, but may also signify the presence of an IgG_4-biased mature memory B cell compartment in patient circulation. This suggests that temporal and memory IgG_4-biased immunity is an early indicator of active immunosuppressive mechanisms associated with worse prognosis and lends support to recent evidence of IgG_4 antibodies contributing to the impairment of effective immunity against melanoma. Additionally, the presence of a prominent $IgG_4{}^+$ cell infiltrate in melanoma tumours across patient tumours, tumour thickness and stages of disease indicates that potential immunosuppressive mechanisms are present and most likely active in melanoma at the peripheral and local levels. Although immunohistochemical evaluations demonstrated $IgG_4{}^+$ cell infiltration in melanoma tumours, it was not possible to associate these infiltrates

with patient history or clinical outcome information. However, the findings mandate further examination of IgG_4 as a tissue biomarker in future studies, correlating these $IgG_4{}^+$ cell infiltrates with other immunohistochemical parameters such as ulceration, mitotic rate and potentially other known markers such as S-100B as well as with patient information. In summary, data presented in this Chapter provide the rationale for future evaluations of IgG_4 and potentially other immunoregulatory components of the humoral response as prognostic indicators in melanoma and possibly other malignant diseases. In support of this notion, humoral immune components, including circulating antibodies, are emerging biomarkers for autoimmune, inflammatory, allergic and malignant diseases, strengthened by recent reporting of "immunosignaturing"' a method which predicates that monitoring antibodies could prove more sensitive than screening for specific antigens in early disease [Maecker et al., 2010, Gilbert et al., 2011, Sykes et al., 2013]. IgG_4, here reported to be indicating immunosuppressive mechanisms in melanoma, and to be elevated in the circulation of patients with worse prognosis, is a promising prognostic factor at early stages, where standard markers like LDH lack sensitivity. Larger prospective studies analyzing IgG_4 and LDH will ascertain the clinical significance of IgG_4 and pave the way for improved patient stratification and therapy.

5 IgG1 and IgE antibodies against CSPG4: Investigating a new therapeutic approach

5.1 Introduction

Findings presented in this thesis provide evidence that IgG4 can impair the cytotoxic properties of IgG_1 antibodies in melanoma (Chapter 3), suggesting that therapeutic antibodies of the IgG_1 class may be partly prevented from engaging Fcγ receptors on immune effector cells in tumours and may consequently be less effective in activating these cells to kill cancer cells. This chapter aims to investigate a strategy to design a therapeutic antibody of a class other than IgG that may be less prone to IgG_4 blockade mechanisms. Previous literature demonstrates that antibodies engineered with Fc regions of the IgE class may trigger highly effective Fc-mediated functions against cancer cells and might be superior to those triggered by the equivalent IgG_1 antibodies (Chapter 1, Section 1.7). The rationale for designing an antibody of the IgE class to treat melanoma tumours is also based on a number of reasons:

a) Melanoma tumours are known to comprise substantial immune cell infiltrating components, and the recent clinical success of checkpoint blockade antibody strategies such as ipilimumab (Chapter 1, Section 1.6) indicate that immune responses can be successfully activated against cancer cells by targeted immunotherapies [Hodi et al., 2010]. Yet, there are presently no antibodies in clinical use that directly target antigens expressed on melanoma tumour cells. Therefore, designing a tumour antigen-specific antibody that could direct effective immune responses specifically against melanoma cells may be highly desirable.

b) IgE mediates effector functions by activating a distinct set of cognate receptors (FcϵRI and FcϵRII) on immune effector cells (monocytes, mast cells, eosinophils etc) different to those recognised by IgG Fc. Therefore, an antibody with Fc regions of the IgE class may not be subject to the Fc receptor blockade mechanisms mediated by IgG4 as IgG4 Fc may compete with IgG_1 Fc for FcγRI binding and immune cell activation (Chapter 3).

c) FcϵR-bearing immune effector cells naturally reside in the skin and certain types like monocytes/macrophages and mast cells are also present in melanoma. IgE sequestered into tissue binds with very high affinity to these Fcϵ receptors on potent immune effector cells. These cells retain the antibody through strong IgE Fc-FcϵR interactions resulting in antibody half-life in tissues longer than that of IgG (Chapter 1, section 1.7) [Gould et al., 2003, Clynes et al., 2000, Geha et al., 1985]. IgE antibodies naturally exert immune effector functions in tissues, including the skin, and these functions are reported to occur in Th2-biased inflammatory environments, normally found in tumours, including melanomas.

d) The rationale for studying antibodies of different classes originates from a number of studies dating back over two decades that suggest that antibodies of the IgE class may hold promise for the treatment of solid tumours. This concept has not been tested in melanoma [Kershaw et al., 1996, Jensen-Jarolim et al., 2008]. Therefore, designing melanoma-specific antibodies of the IgE class may be of interest for the development and testing of potentially more efficacious therapeutics for the treatment of melanoma. Based on the above, the potency of an IgE antibody directed against a melanoma associated antigen (the melanoma associated antigen CSPG4 discussed in Chapter 1, section 1.6.8) is a worthwhile novel endeavour. The melanoma-associated

antigen CSPG4 was discovered three decades ago. Its expression was initially thought to be limited to melanocytes, endothelial cells and pericytes. However continuous evaluation of this antigen revealed that it is also expressed on the interfollicular epidermis, the basal layer of normal oral mucosa, chondrocytes in normal and osteoarthritic adult articular cartilage, smooth muscle cells, angiomyolipomas, differentiated myofibers of the sarcolemma and neuromuscular junction of human postnatal skeletal muscle, microglial and mesangial cells of the renal glomerulus. The antigen is also over-expressed in a number of other malignancies such as mesotheliomas, triple negative breast cancer squamous cell carcinomas of the head and neck, and glioblastomas [Campoli et al., 2010, Wang et al., 2010a, Rivera et al., 2012]. The most notable expression of CSPG4 has been shown in stem-like cells of the inter-follicular epidermis of the skin, lower levels of expression by human melanocytes have been reported. However, loss of CSPG4 was found to be not lethal, as knock-out mice for the mouse homologue of CSPG4 survived [Price et al., 2011]. Expression of CSPG4 is also linked to numerous signaling pathways that support tumour growth, adhesion, migration and which support tumour progression and metastasis (Chapter 1, Section 1.6.8), making it a suitable therapeutic target. Indeed, CSPG4-targeted therapies and immunotherapies, including those utilising antibodies have been tested in patients with melanoma, with some success and without overt toxicities [Campoli et al., 2010, Ferrone et al., 1993, Kang et al., 2000, Siccardi et al., 1986]. Therefore harnessing the potent immune activatory potential of IgE class antibodies directed against tumour-associated antigens merits investigation, especially in Th2 biased microenvironments such as those of melanoma tumours, as this may result in effective immune responses against this difficult to treat malignancy.

5.2 Generation of chimeric anti-CSPG4-specific antibodies

For this study, the variable region sequences of the mouse monoclonal antibody clone 225.28s were selected, these were originally published in 1996 by Neri et al. [Neri et al., 1996]. The original 225.28s clone was derived by hybridoma technology in mice and showed efficacy against tumour growth in a number of *in vitro* and *in vivo*

models [Ferrone et al., 1993, Hafner et al., 2005b]. Furthermore, a toxin-conjugated $F(ab)_2$ derivative of this clone reached clinical testing [Imai et al., 1983]. However, to date no molecule of this specificity has been engineered into a chimeric or humanised recombinant format. This modification is important as the mouse antibody clone suffers from two obvious disadvantages: a) mouse sequences are expected to induce HAMA responses in patients, resulting in neutralisation of the antibody and rapid clearance from the circulation, thereby significantly reducing any efficacy against tumour cells, and b) an antibody with Fc regions of mouse origin cannot be used in patients as it will not effectively recognise Fc receptors expressed by human immune effector cells and therefore it is not expected to effectively recruit these cells to target and kill tumour cells by mechanisms such as cytotoxicity and/or phagocytosis. With the exception of an antibody obtained by phage display technology, which did not progress further than preliminary functional evaluations, there does not appear to be any human or chimeric antibody specific for CSPG4 in preclinical or clinical evaluation at present, and therefore the potential therapeutic relevance of a recombinant antibody (with matched heavy and light chains) against this antigen has not yet been fully examined.

5.2.1 Engineering IgG and IgE antibodies of known melanoma antigenic specificity

In order to engineer antibodies using defined variable heavy and light chains of known melanoma tumour specificity, the matched sequences of heavy and light chains were cloned into a single vector system designed at KCL. Vector design is reported in the PhD thesis of Dr. Tihomir Dodev (KCL, 2013). The single vector incorporating the antibody heavy and kappa light chains is depicted in (Figure 5.1), and features two different promoters which take into account that at least twice as many light chains to heavy chains are need for expression and production of recombinant antibodies. To investigate the role of IgG_1 and IgE antibody classes, dedicated vectors with Fcϵ- and Fcγ constant heavy and light chain regions were designed.

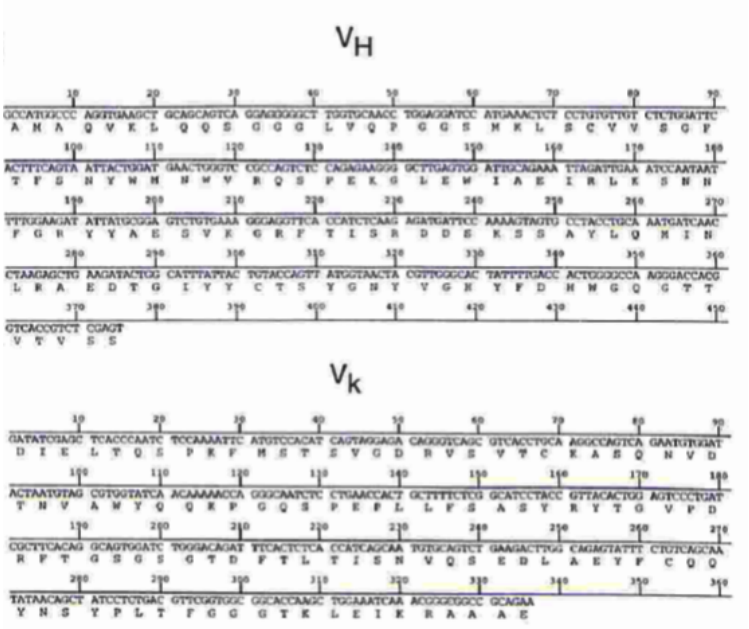

Figure 5.1: Heavy and light variable region sequences of the melanoma antigen CSPG4-specific antibody clone 225.28s derived by immunising mice with melanoma tumour cell lysates, as previously published [Neri et al., 1996]. Murine heavy (V_H) and κ ($V\kappa$) regions cDNA and translated protein sequences are depicted.

5.2.2 Generation and initial testing of anti-CSPG4 IgG and IgE antibodies

The variable sequences of antibody clone 225.28s were inserted into the human IgG_1 and IgE heavy and kappa light chain vectors (Figure 5.2) and these were used to transfect competent HEK293F cells. Supernatants were collected after 4 weeks and antibodies were purified using affinity columns as described in the PhD thesis of Dr. T Dodev; KCL, 2013.

The biophysical properties of the two engineered chimeric antibodies were tested by SDS polyacrylamide gel electrophoresis under non-reduced and reduced conditions and by HPLC size-exclusion chromatography analysis (kindly provided by Dr. T. Dodev). In these assays, the newly engineered antibodies were directly additionally compared to previously produced antibodies engineered as IgG_1 and IgE class molecules with variable domains recognising the tumour-associated antigen FRα, which is expressed by a number of solid tumours including ovarian cancer. The IgG_1

antibody was also compared to clinical-grade trastuzumab (Herceptin®), a humanised IgG_1 antibody in clinical use for the treatment of HER2/neu-expressing breast cancers [Hudis, 2007]. SDS-PAGE chromatography demonstrated that both CPSG4 IgE and IgG_1 antibodies were of the same molecular weight as the isotype control. HPLC analysis confirmed that both antibodies are monomeric of (>95% purity) and only minimum aggregation was detected for both purified antibodies (Figure 5.3).

5.2.3 Binding of antibodies to tumour cells and FcR-expressing immune effector cells

The capacity of the engineered antibodies to recognise their target antigens and Fc receptors on immune effector cells was next examined. Interactions of anti-CSPG4 antibodies with A375 tumour cells were analysed by immunofluorescence and flow cytometry. Both anti-CSPG4 IgE and IgG_1 chimeric antibodies recognized the CSPG4 antigen on A375 melanoma cells since each bound to >99. % of melanoma cells as demonstrated by flow cytometry. The antibodies also bound to Fc receptors on monocytic cells (Figure 5.4).

The IgE antibody bound to cells of the monocytic cell line U937, which also express both IgE receptors, FcϵRI and FcϵRII (CD23) at low densities and also to FcϵR-expressing human primary monocytes (Figure 5.5).

As expected, the IgG_1 antibody also bound to U937 cells which are known to express FcγRI and FcγRII and to FcγR-expressing primary human monocytes (Figure 5.4). We further confirmed the specific binding of the chimeric CSPG4 IgE and IgG_1 antibodies to the surface of the A375 tumour cells by immunofluorescence microscopy, while a hapten-specific isotype control IgE antibody (NIP IgE) and a human IgG_1 antibody isotype control (MOv18 IgG_1) for CSPG4 IgG_1 did not show binding above background. Counterstain was performed using DAPI (Figure 5.6).

In conclusion, the two chimeric antibodies of known specificity were engineered with human Fc regions of the IgE and IgG_1 classes, and these antibodies recognised the

CSPG4 tumour-associated antigen on tumour cells and bound through their Fc regions to immune effector cells.

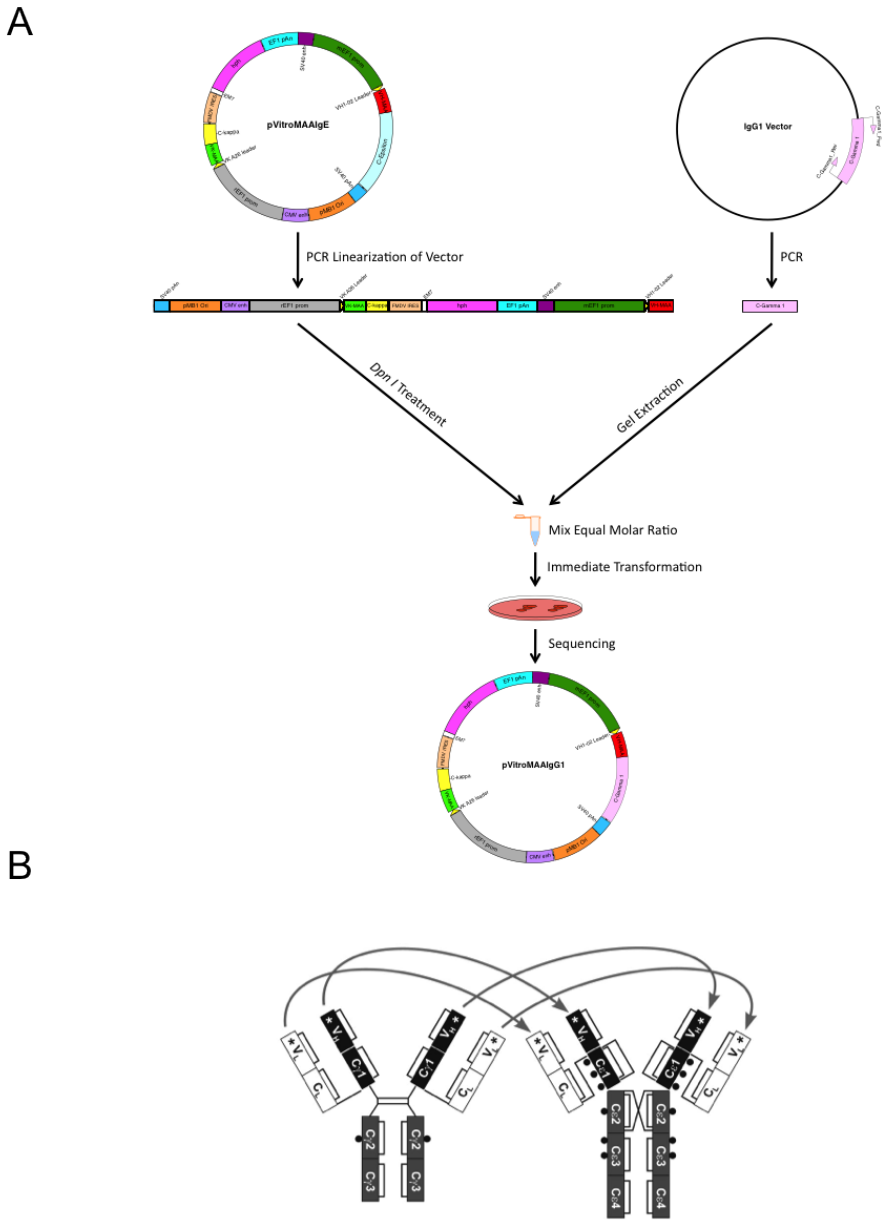

Figure 5.2: A) Schematic representations of the heavy and light chain cloned into the pVitro vector design for cloning and expression of IgG and IgE antibodies. B) Schematic representation of the design of an IgE antibody: the variable heavy and light chains of IgG_1 (left, regions indicated with stars) were inserted into the epsilon heavy chain regions of IgE and the epsilon heavy chain was combined with the kappa light chain domains to produce the corresponding IgE antibody (right). The resulting engineered IgE molecule should recognise the same antigenic epitope and be bound by IgE receptors. Glycosylation sites are depicted by black circles (adopted from [Karagiannis et al., 2009]).

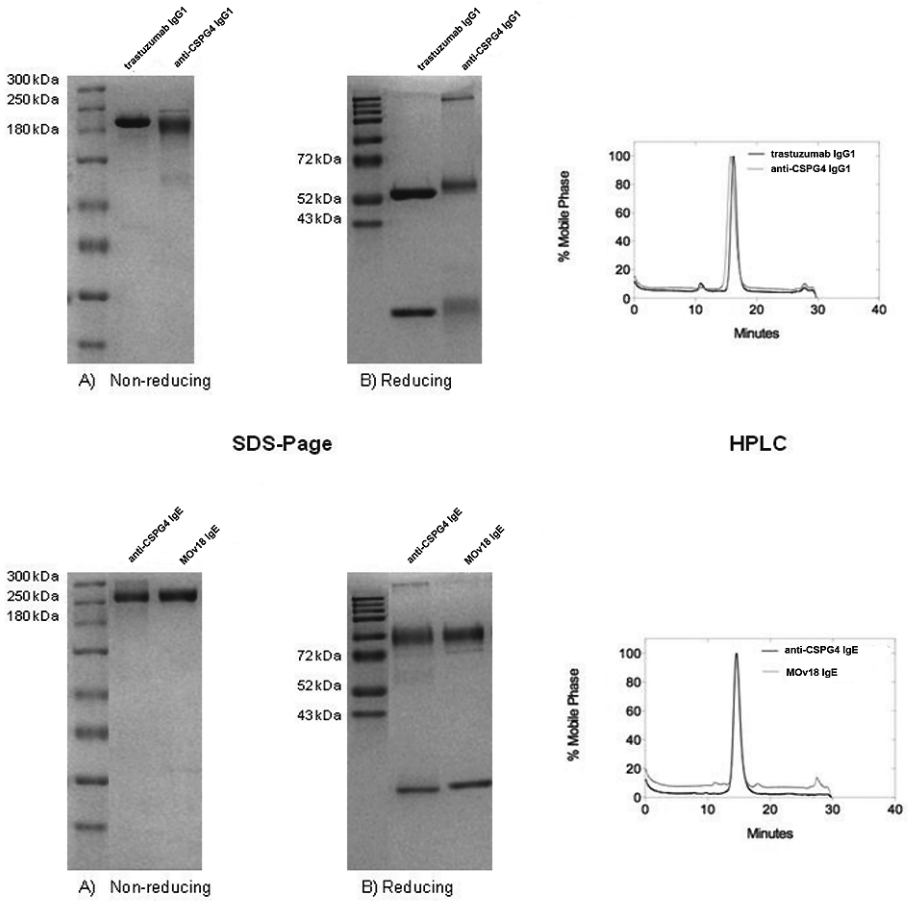

Figure 5.3: Biophysical characterisation of the engineered CSPG4 melanoma antigen-specific IgG_1 (top) and IgE (bottom) antibodies. Nonreduced (left) and reduced (middle) SDS polyacrylamide gel electrophoresis of CSPG4 IgE (bottom) and IgG_1 (top) protein products, compared with the previously-characterised chimeric antibodies MOv18 IgE and trastuzumab IgG_1. Size-exclusion chromatography analysis of purified CSPG4 IgE and IgG_1 antibodies compared to purified chimeric human MOv18 IgE and trastuzumab IgG_1 (right). Figure courtesy of Dr Tihomir Dodev, KCL.

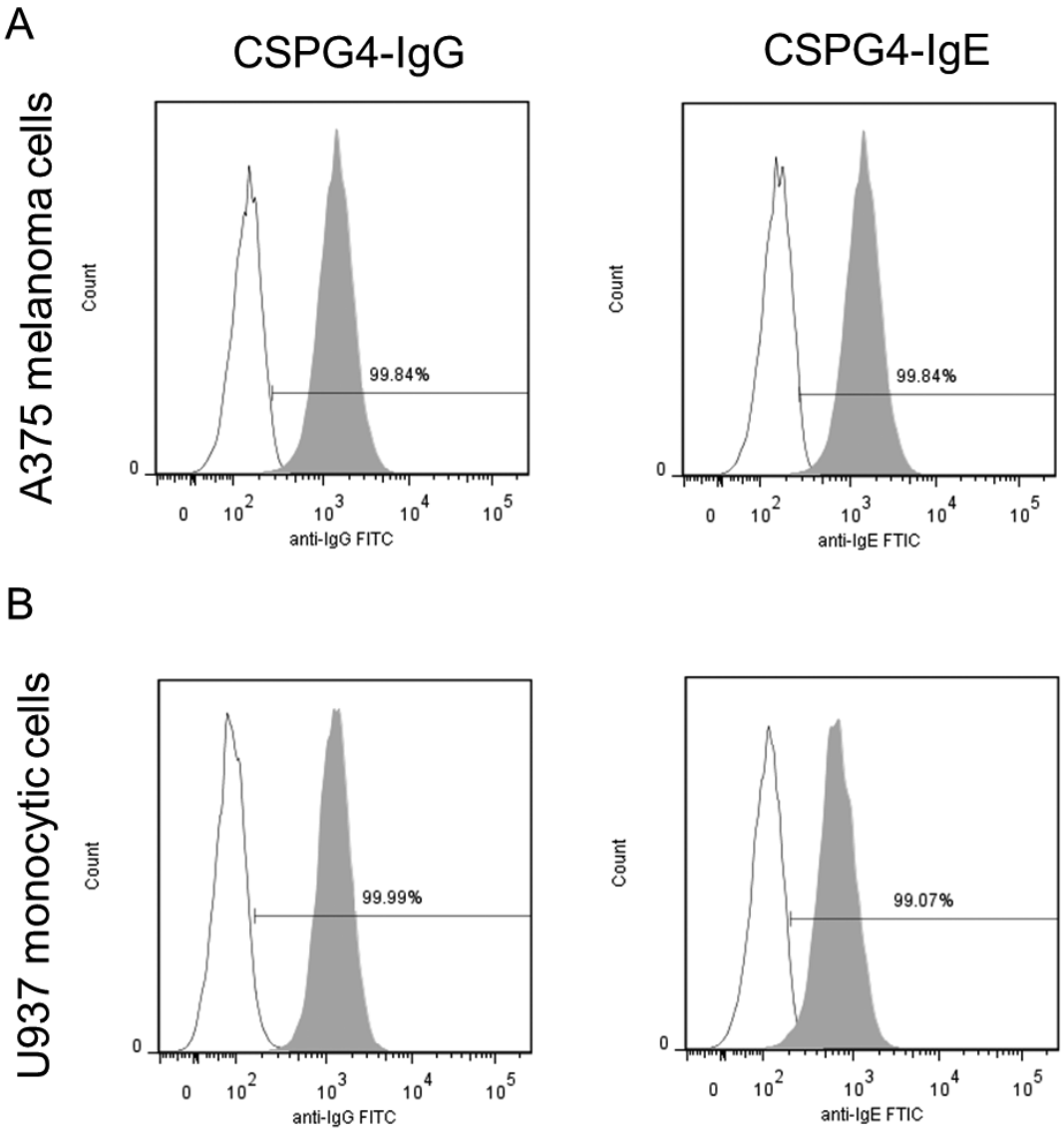

Figure 5.4: Flow cytometric histograms showing CSPG4-IgE and CSPG4-IgG_1 binding. A) Binding of CSPG4 IgG (left) and CSPG4 IgE (right) to A375 melanoma tumour cells. B) Binding of CSPG4 IgG_1 (left) and CSPG4 IgE (right) to U937 monocytic cells. Detection of the primary antibody was performed with goat anti-human IgG or goat anti-human IgE (both in grey), respectively.

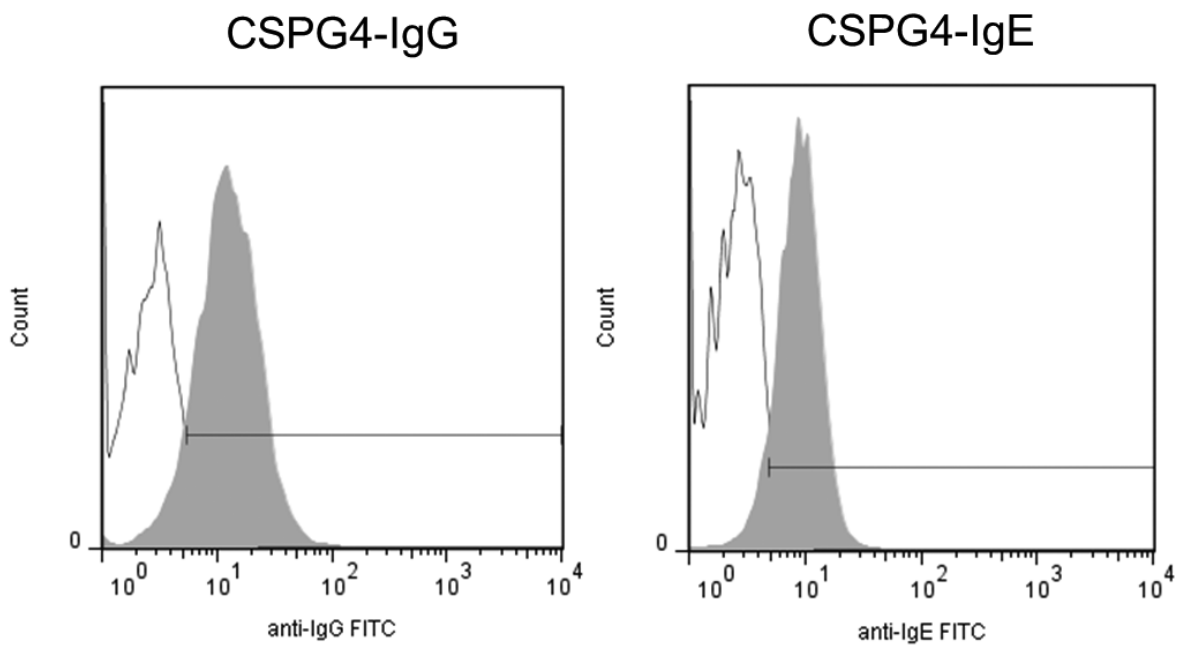

Figure 5.5: Flow cytometric histograms showing CSPG4 IgG_1 and CSPG4 IgE binding on primary monocytes. Detection of the primary antibody was performed with goat anti-human IgG or goat anti-human IgE (both in grey), respectively.

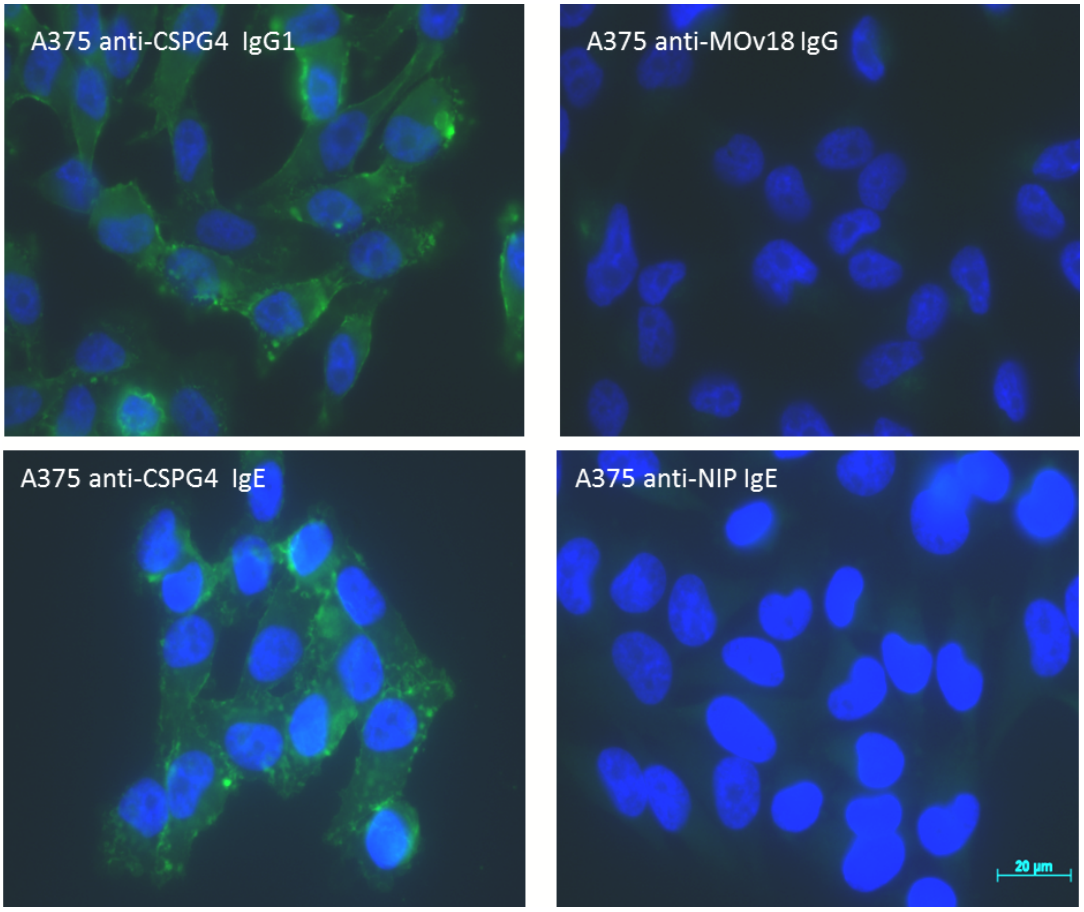

Figure 5.6: Immunofluorescence staining confirming binding of CSPG4 IgE and CSPG4 IgG_1 antibodies to A375 melanoma tumour cells. The depicted isotype control a hapten specific IgE antibody (NIP IgE). Antibodies bound to tumour cells were detected using a goat anti-human IgE-FITC or IgG-FITC antibody. Counterstain was performed using DAPI. Images were captured using a 63x oil objective. Scale bar = 20 μm.

5.2.4 Distribution of CSPG4 in human skin and in melanoma recognised by the engineered antibody

To evaluate the specificity of this engineered antibody clone, a human tissue microarray comprising of 221 melanoma tumour specimens and 16 healthy skin specimens were stained with purified and directly biotinylated CSPG4 IgE antibody. Reactivity with specimens was detected by alkaline phosphatase, which produced a pink/red colour for CSPG4-expressing cells, allowing the distinction between CSPG4 expression and melanin in pigmented melanoma lesions (Figure 5.7).

Immunohistological evaluations confirmed high levels of expression of CSPG4 in cutaneous melanomas, with a total of 93.66% of melanoma lesions testing positive for CSPG4 (17.72% high; 37.97% intermediate; 37.97% low positivity). Further evaluations of disease-involved lymph nodes demonstrated that 85.72% were positive in total (25.00% high; 42.86% intermediate; 17.86% low positivity). Moreover, 72.72% (10.40% high; 25.97% intermediate; 36.36% low positivity) of distant site metastases specimens, such as those of the colon, oesophagus and liver expressed CSPG4. Additionally, CSPG4 expression was detected in different disease stages and also in cutaneous lesions of different thicknesses (T2-4) (Figure 5.7). These findings indicate that CSPG4 may be considered as a target for therapy for most patients with melanoma. These data are also in concordance with previous reports, demonstrating overexpression of CSPG4 across different disease stages [Campoli et al., 2010]. In contrast to expression by tumour lesions, expression of low level CSPG4 was observed in 6.25% of human skin specimens. Thus, tissue microarray (TMA) data demonstrates that this engineered antibody clone (CSPG4 IgE) can recognise its target antigen on patient-derived lesions and that the target epitope is accessible in tissue metastases and throughout different disease stages in patient tumours. Furthermore, data presented here confirm enhanced expression of CSPG4 in melanoma compared to healthy skin specimens, confirming previously published reports.

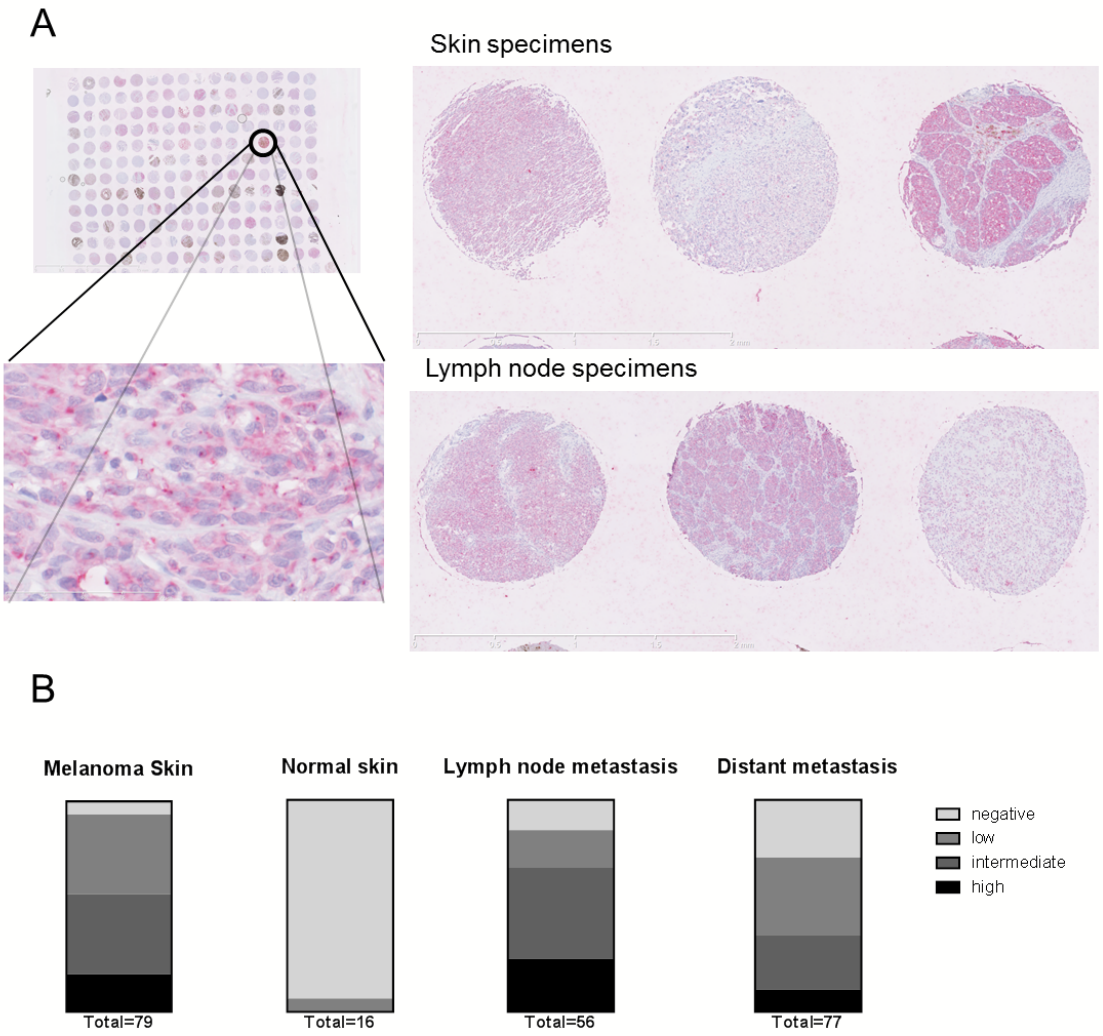

Figure 5.7: Evaluation CSPG4 detected by the anti-CSPG4 IgE antibody in patient melanoma lesions, diseased lymph nodes, distant organ metastases and healthy skin (n=228). The sections are part of tissue microarrays (BioMax®) and detection was conducted using immunohistochemistry (alkaline phosphatase in red, counterstaining with hematoxylin in blue). A) Representative images of melanoma skin and lymph node specimens. B) Evaluation of the TMA sections showing that melanoma related samples have higher expression of CSPG4 compared to healthy skin.

5.3 Functional properties of engineered antibodies

Following engineering and specificity evaluations of the chimeric antibodies, it was essential to examine whether these antibodies were: a) functionally active once they

engaged the antigen on tumour cells, and/or b) capable of activating immune effector cells by signalling through their Fc receptors. Moreover, it was reasonable to ask whether recognition of the target epitope of the antigen on the surface of tumour cells contributes or is necessary for any anti-tumoural functions these agents may confer. The subsequent section discusses the functional properties of the engineered antibodies using established *in vitro* functional assays.

5.3.1 Direct anti-CSPG4 antibody-mediated effects on tumour cells *in vitro*

A non-immunological mechanism by which therapeutic antibodies work is the direct induction or inhibition of essential downstream signals related to the specific epitope of this target antigen. Antibody-antigen engagement may trigger downstream signaling cascades that may eventually lead to tumour cell death. The potential of anti-CSPG4 antibodies to trigger direct tumour cell death or anti-proliferative events in the absence of effector cells was investigated by employing a cell viability assay (MTS). With this assay, the potential of the engineered antibodies to directly mediate reduction of A375 melanoma tumour cell proliferation *in vitro* was examined. Cell viability of cells cultured with different antibodies was measured after 24 and 72 hours. Neither anti-CSPG4 IgE nor IgG_1 appeared to restrict cell proliferation after 24 hours (CSPG4 IgE: 100.3% (SD: 2.4); CSPG4 IgG_1: 102.1% (SD: 10.5)), compared to equivalent isotype control antibodies of the same classes (MOv18 IgE: 102.8% (SD: 6.5); MOv18 IgG_1: 107% (SD: 4.4)) or compared to trastuzumab IgG_1 (105% (SD: 5.8)). Decreased cell proliferation was measured after 72 hours in cells incubated with trastuzumab IgG_1 (18% (SD: 3.6)). This confirmed the known function of trastuzumab in restricting proliferation of HER2/neu-expressing tumour cells over time, and this was expected since A375 melanoma cells express moderate levels of the target antigen for this antibody (Figure 5.8).

However, cell viabilities for the anti-CSPG4 IgE (120.0% (SD: 8.3)) anti-CSPG4 IgG_1 (114.9% (SD: 7.5)) as well as the isotype controls (MOv18 IgE: 102.4% (SD: 9.2) and MOv18 IgG_1 131% (SD: 11.4)) appeared similar, leading to the conclusion that under these culture conditions, antibodies recognising CSPG4 did not induce any

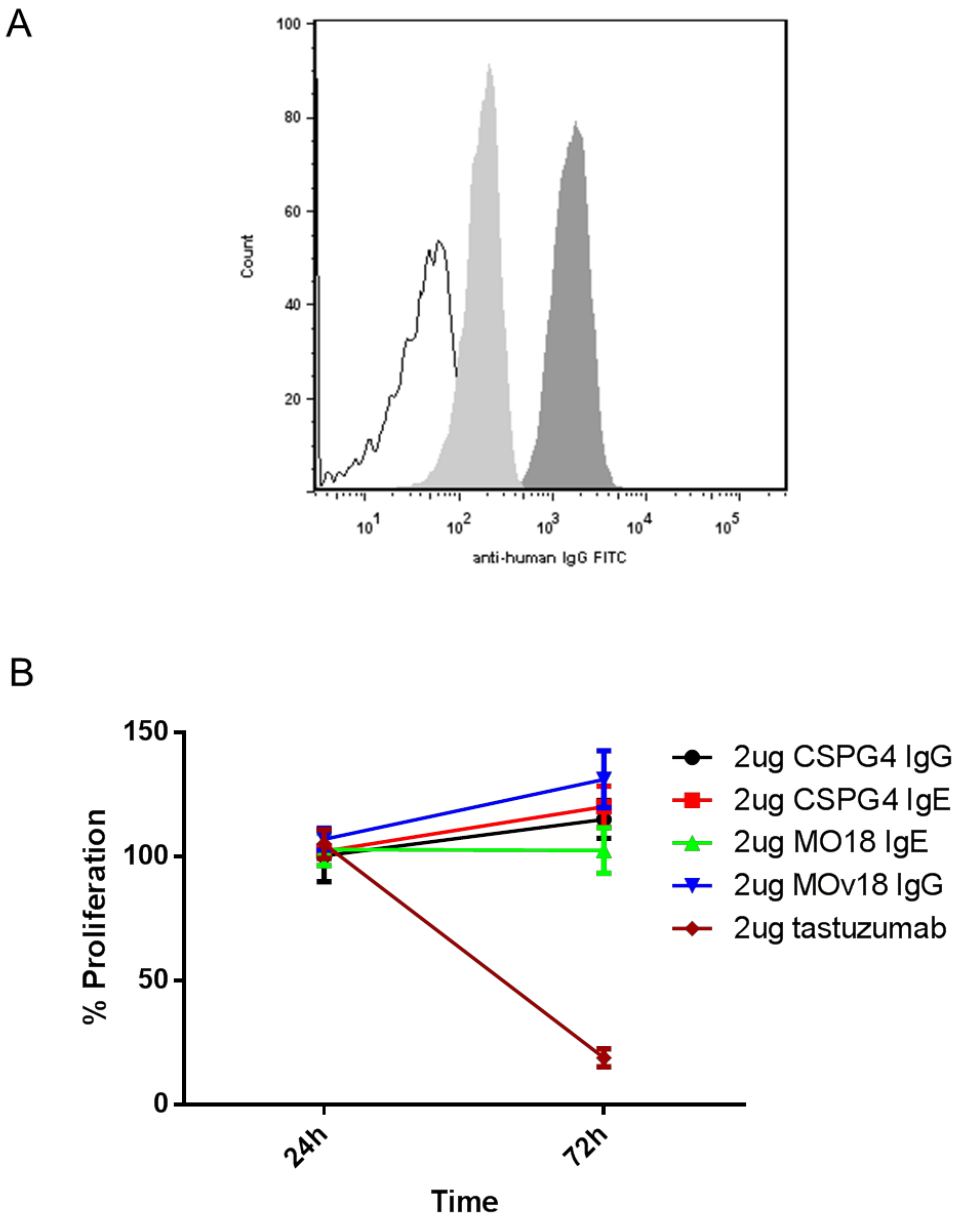

Figure 5.8: A) Light gray: Expression of Her2/neu antigen on A375 tumour cells. Dark gray: Expression of CSPG4 on A375 tumour cells. Unstained histogram represents isotype control. B) MTS cell viability assay examining potential direct effects of the anti-CSPG4 antibodies on melanoma tumour cell proliferation. Effects on proliferation were compared with those of trastuzumab (IgG_1), which is known to reduce tumour cell proliferation.

anti-proliferative effects against melanoma tumour cells (Figure 5.8). This shows that A375 tumour cells were not susceptible to direct anti-proliferative effects by

anti-CSPG4 antibodies, while trastuzumab IgG_1 exerted an anti-proliferative effect on these cells over a period of 72 hours.

5.3.2 Engaging the FcRI receptors on effector cells by antibodies

5.3.2.1 Ability of IgE to engage FcϵRI and trigger mast cell degranulation

The functional properties of IgE in engaging FcϵRI on the surface of mast cells to trigger effector cell activation and to induce a functional degranulation were firstly examined. The engineered anti-CSPG4 IgE antibody could trigger functional degranulation through recognition of human high affinity IgE (FcϵRI) receptors together with cross-linking of these FcϵRI receptors on the surface of effector cells, a process normally not triggered by antibody alone, but which can take place when FcϵRI is cross-linked by antibody-multivalent antigen complexes on the surface of effector cells. These experiments made use of the rat basophilic leukaemia mast cell line RBL SX-38, which was transfected to express the human FcϵRI. This assay is normally used as a functional readout to confirm IgE antibody functional capacity and to evaluate potency. Degranulation was measured by β-hexosaminidase release, depicting mast cell activation (Figure 5.9). Because degranulation requires cross-linking of antibody on the surface of mast cells, mast cells alone 0.0% (SD: 3.54) or mast cells incubated with anti-CSPG4 IgE antibody only (0.6% (SD: 10.03) did not potentiate β-hexosaminidase release. As expected, mast cell lysis yielded high levels of stored β-hexosaminidase enzyme (Triton-X, 100% (SD: 12.58)). On the contrary, the CSPG4 IgE antibody induced significant degranulation of RBL SX-38 cells following stimulation with a polyclonal anti-human IgE antibody (25.44% (SD: 3.41)) which could cross-link FcϵRIs on the cell surface. The CSPG4 IgE antibody could also activate RBL SX-38 cells in an antigen-dependent manner through cross-linking of cell surface bound IgEs by the CSPG4-expressing A375 melanoma cells when added to effector cells in this assay (39.40% (SD: 3.82)). The control antibody NIP IgE could also activate RBL SX-38 cells when added with a polyclonal anti-human IgE antibody (21.31% (SD: 5.75) while minimal degranulation was observed with NIP IgE antibody alone (0.0% (SD: 8.74). These data show that the anti-CSPG4

IgE can function by cross-linking the Fcϵ-receptor via polyclonal antibodies and via multivalent antigen engagement, leading to mast cell activation, degranulation, and potential cytotoxic activity which could be directed against cancer cells in tumours where mast cells may reside.

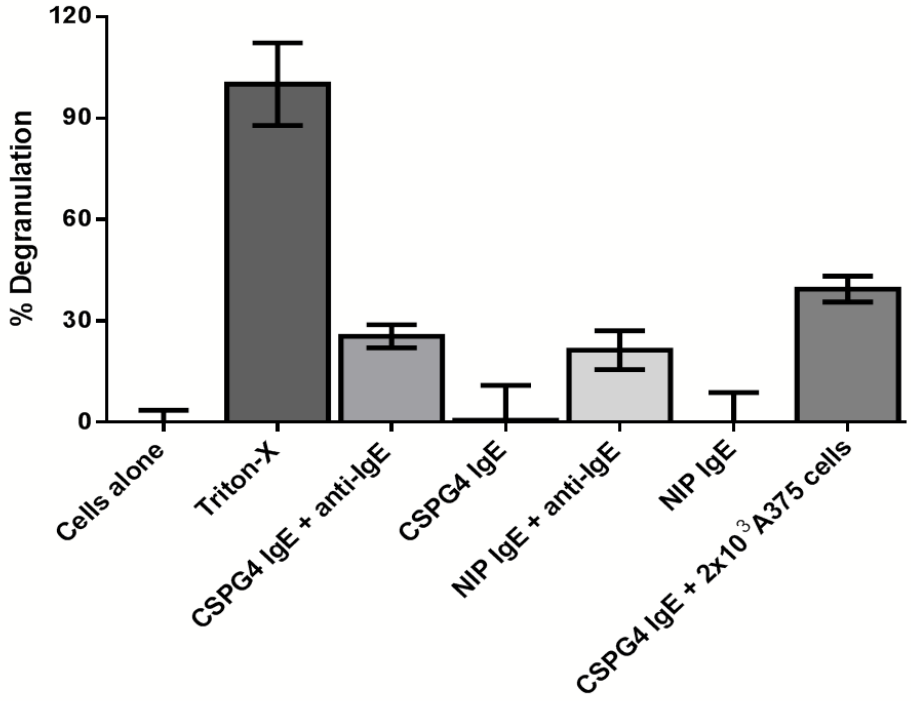

Figure 5.9: Effect of CSPG4 IgE cross-linking the human FcϵRI on RBL SX-38 mast cell leads to degranulation. CSPG4 IgE was cross-linked with a polyclonal anti-human IgE antibody to confirm its degranulation activity. Degranulation was detected by measuring β-hexosaminidase release into the culture supernatant.

5.3.2.2 Antibody-dependent cell-mediated tumour killing mechanisms

To investigate cell-dependent mechanisms (ADCC and ADCP) mediated by anti-CSPG4 IgE and IgG_1 antibodies, a three-colour flow cytometric assay measuring tumour killing (Chapter 2 Section 2.12.2) was employed. In this set of experiments, U937 monocytic cells or primary monocytes were used as effector cells and the CSPG4-expressing A375 metastatic melanoma cells as tumour targets. The as-

say was modified from the one previously published and adapted for the purpose of this experiment [Bracher et al., 2007]. CFSE, a green fluorescent intracellular dye, was used to label A375 tumour cells prior to incubation with U937 monocytic cells or primary monocytes (isolated by RosetteSep Monocytes purification kit) in the presence or absence of antibodies. After the incubation period (3 hours), U937 cells or monocytes were labelled with anti-CD89 PE. Before acquisition and analysis by flow cytometry, these mixed cell cultures were also incubated with DAPI, which was subsequently used to identify dead cells. Quantification of the flow cytometric data (as described in Figure 2.3) demonstrated that after 3 hours in culture, the anti-CSPG4 IgG_1 antibody mediated significant levels of tumour cell death, mostly mediated through ADCP, against A375 tumour cells by monocytic U937 cells. Tumour killing was mediated by ADCP (30.93%) for anti-CSPG4 IgG_1 compared to tumour cell death measured for samples incubated with the control FRα-specific chimeric MOv18 IgG_1 antibody (15.40%) or with cells incubated with no antibody (8.26%) ($p<0.001$, One-way ANOVA, with modified Bonferroni post-test; Figure 5.10). On the other hand, anti-CSPG4 IgE triggered significant levels of melanoma cell death, mostly through ADCC (ADCC: 27.02% for anti-CSPG4 IgE; 5.34% for MOv18 IgE; 6.07% with no antibody ($p<0.001$ Figure 5.10). Incubation with anti-CSPG4 IgE induced only minimal tumour cell ADCP compared to those incubated with control MOv18 IgE (6.65% vs. 7.78%; $p<0.001$, One-way ANOVA, with modified Bonferroni post-test; Figure 5.10).

Moreover, employing the ADCP/ADCC assay and using patient-derived (stage II melanoma, n=9) primary monocytes as effector cells, both anti-CSPG4 IgE (ADCP 20.97% (anti-CSPG4 IgE); 13.50% (MOv18 IgE); 4.42% (no antibody); $p<0.01$ Figure 5.10) and anti-CSPG4 IgG_1 (ADCP: 42.70% (anti-CSPG4 IgG_1); 12.10% (MOv18 IgG_1); 5.68% (no antibody); $p<0.001$ Figure 5.10) antibodies induced tumour cell killing by monocytes *in vitro*. These data demonstrate that both anti-CSPG4 antibodies can activate human monocytic cells as well as patient-derived monocytes and they can direct anti-tumoural functions. The findings suggest that, given appropriate stimuli, patient immune effector cell mechanisms retain the potential to mount effective responses against cancer cells.

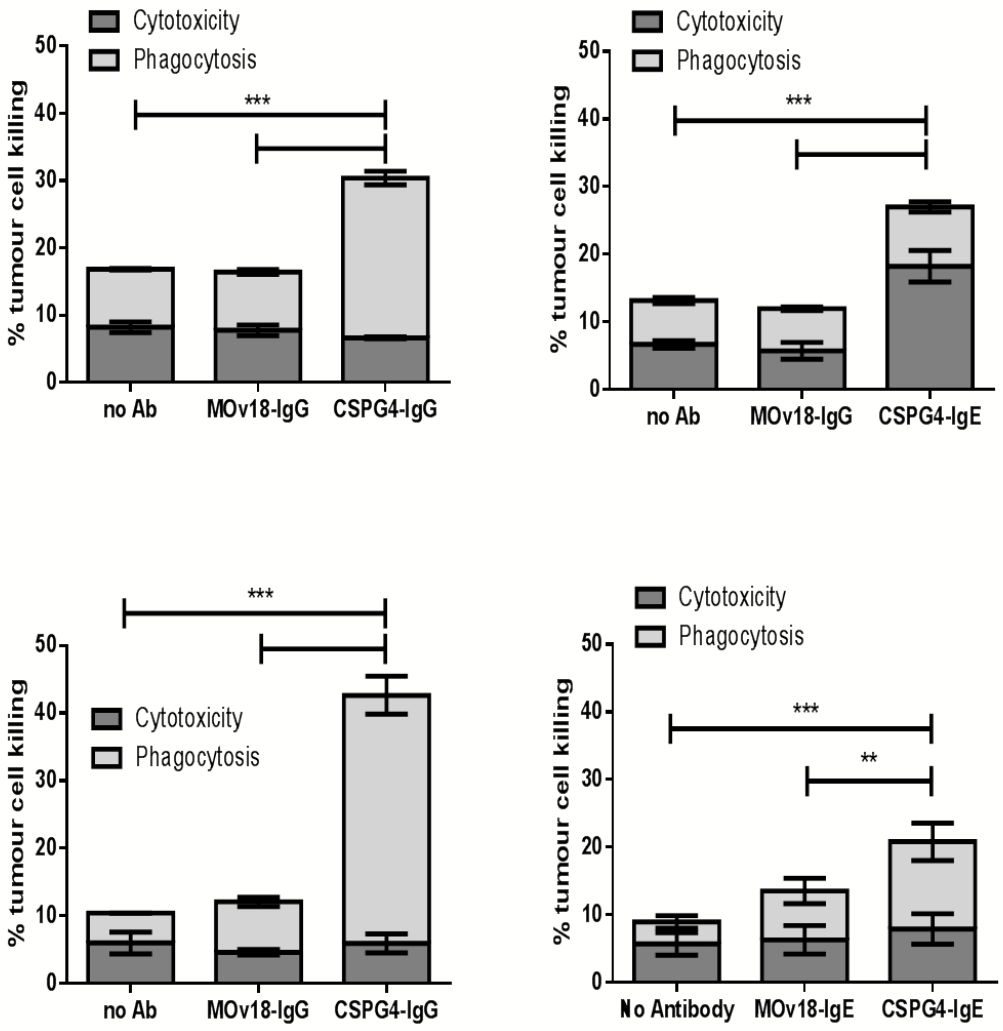

Figure 5.10: Quantification of ADCC/ADCP assay confirmed that anti-CSPG4 IgG_1 and anti-CSPG4 IgE mediated significant ADCP and ADCC of A375 tumour cells by U937 monocytic cells (top panel, n=4). Quantification of ADCC/ADCP assay confirmed that anti-CSPG4 IgG_1 and anti-CSPG4 IgE mediated significant ADCP and ADCC of A375 tumour cells by primary monocytes (bottom panel, n=9). Cytotoxicity: dark grey bars; phagocytosis: light grey bars. Results are means ± SD. (*$p<0.05$; **$p<0.01$; ***$p<0.001$; ns: $p>0.05$).

5.4 *In vivo* functional assays to study antibody efficacy for cancer therapy

Ultimately, all potential therapeutics must be tested for their efficacy using relevant *in vivo* models. It is therefore desirable to design and validate novel translational

assays in order to examine the potential therapeutic efficacy of these agents. In the context of developing translational strategies to examine immune effector-mediated functions of antibodies, *in vivo* models, which can demonstrate these functions are needed. Hence, developing *in vivo* systems with human immune system components can be informative; such as mice humanised for the expression of human Fc receptors; or mouse models amenable to engraftment of human immune cells. Additionally, *in vivo* models akin to the patient disease setting, which may feature patient-derived tumours or patient immune cell components, can provide key information on therapeutic benefits in a patient setting and can contribute to the translational significance of a candidate therapeutic. This section describes the establishment and application of two humanised mouse models of human melanoma that permit investigations of IgG and IgE class antibody efficacy.

5.4.1 Establishment of a human melanoma xenograft model in NOD/SCID γ-/- mice to study efficacy of antibodies for cancer therapy

An immunodeficient mouse model strain NOD/SCID γ-/- mice (NOD.Cg-Prkdcscid Il2rgtm1Wjl/SzJ), lacking T-, B- and NK cells was chosen as their immune system can be reconstituted with human immune cells in spleens and circulation, allowing the investigation of therapeutics in the context of human immunity [Ali et al., 2012]. A375 human melanoma cells (doses 0, 1x10^4, 1x10^5, 5x10^5, or 1x10^6 tumour cells per challenge) were injected subcutaneously in the flank of the mice, and tumour growth was monitored over time (Figure 5.4.1) by calliper measurements as described in Chapter 2 (Section 2.13.2).

Tumours were measured until they reached a maximum of 750mm^3 in size. In pilot experiments, tumours grew exponentially up to 750mm^3 over a period of 4 weeks in a reproducible manner (Figure 5.4.1), two representative experiments, n=4 and n=5 mice per tumour challenge dose). A tumour cell challenge of 5x10^5 melanoma cells per mouse resulted in reproducible tumour growth over a period of 4 weeks and this dose was used in subsequent experiments. Moreover, introduction of peripheral blood mononuclear (PBL) cell into this system did naturally result in significant tumour

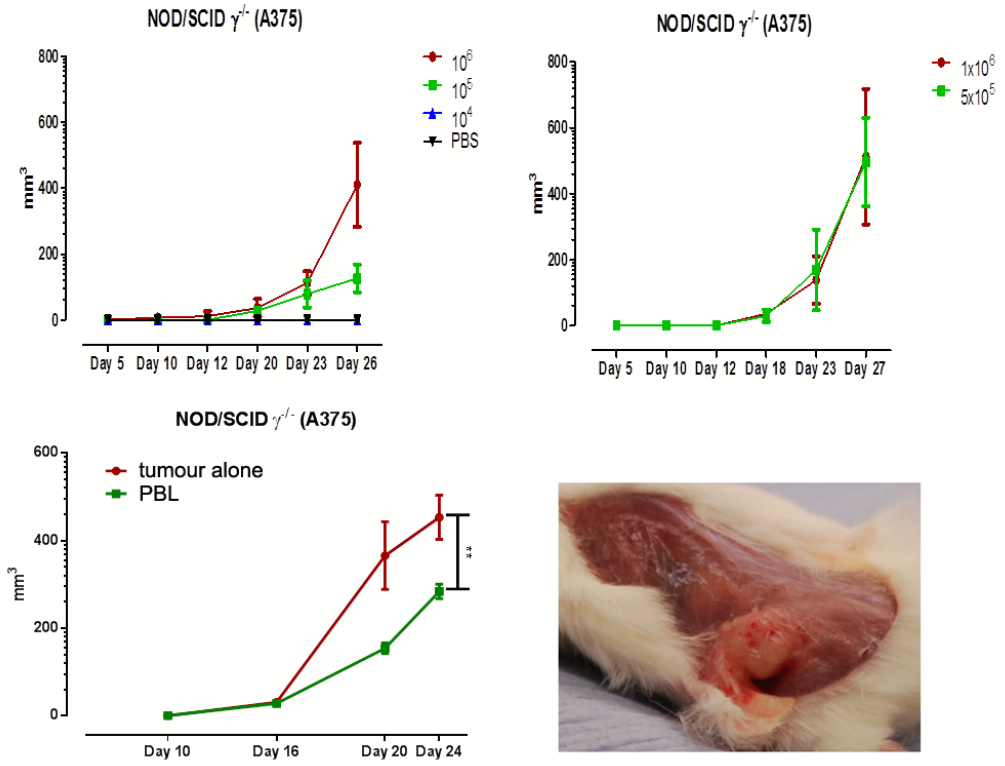

Figure 5.11: Establishment of a subcutaneous melanoma tumour model using A375 metastatic melanoma cells injected on day 0 into NOD/SCID γ-/- mice. Top left: n=4 mice per condition (tumour cells only); Top right: confirmation of initial experiments with n=5 mice per condition (tumour cells only) Bottom left: Comparison between animals with/without engraftment of human peripheral blood leukocytes (PBL). Bottom right: illustration of subcutaneous tumour in NOD/SCID γ-/- (**p<0.01). The y-axis respresents tumour volume in mm^3.

growth restriction compared to engraftment of the tumour cells alone. This finding is expected, as the PBL are not HLA matched with the tumour cells and will therefore induce, to some extend, an immunological response (Figure 5.4.1). Tumours were excised and embedded in paraffin for further macroscopic and microscopic observation of tumour growth and tumour-associated antigen CSPG4 expression by the xenograft was assessed by immunofluorescence staining. These evaluations confirmed that the tumour-associated antigen CSPG4 is expressed in subcutaneous melanoma tumours grown in NOD/SCID γ-/-mice (Figure 5.12).

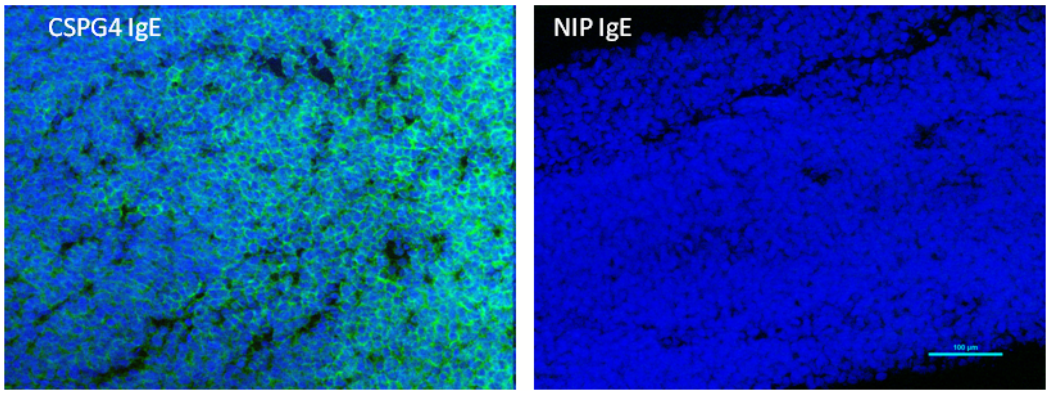

Figure 5.12: Immunofluorescence analysis of subcutaneous tumour model of A375 metastatic melanoma cells. Sections were stained for expression of the melanoma marker CSPG4 (left) and mouse IgG isotype control antibody (right). Images were captured using a 10x objective. Scale bar = 150 μm.

Expression of CSPG4 antigen confirms that the A375 melanoma xenograft model may be used to evaluate the therapeutic potential of monoclonal antibodies recognising this antigen. Investigation of splenic engraftment in this xenograft model (Day 30) revealed that the animals reconstituted with human peripheral blood cells (PBLs) had a detectable human $CD45^+$ compartment distinct from spleen-resident mouse $CD45^+$ cell populations. The human immune cell compartment comprised a range of specialised human immune effector cells such CD3 (T cells), CD22 (B cells), CD14 (monocytes) and CD123 (plasmacytoid dendritic cells or basophilis) (Figure 5.13).

5.4.2 *in vivo* evaluation of anti-CSPG4 antibodies in a subcutaneous melanoma xenograft model

The tumour growth restricting capacities of the engineered human/chimeric antibodies recognising CSPG4 (IgG_1 and IgE) were investigated in the above established subcutaneous human melanoma xenograft model. Following tumour challenge and engraftment of human PBLs to provide human effector cells in this system, antibodies were administered weekly (Figure 5.13) or fortnightly ($p<0.001$; Figure 5.14) at 10 mg/kg doses by the intravenous route. Treatment with weekly doses of CSPG4 IgE resulted in severely-restricted melanoma tumour growth over a period of 30 days ($p<0.01$), while tumours in mice treated with the correspond-

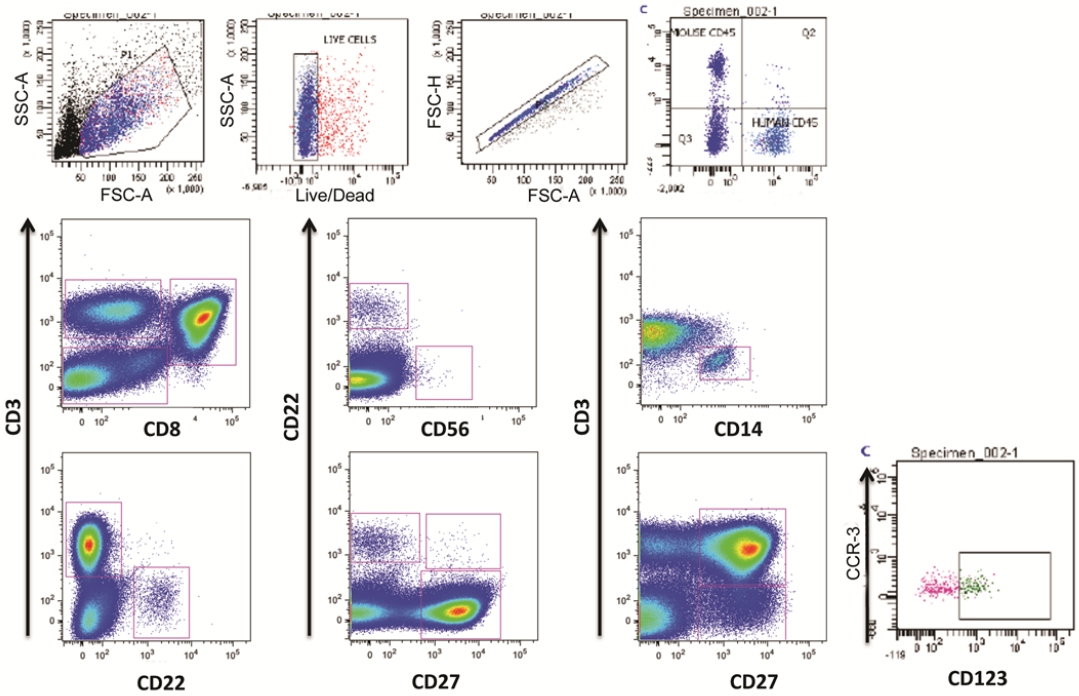

Figure 5.13: Representative flow cytometric dot plots identifying human immune cell subsets within the live singlet human $CD45^+$, mouse $CD45^-$ population engrafted in NOD/SCID γ-/- mouse spleens. Top panel: Lymphoid cells were gated according to their FSC-A and SSC-A properties, viable $CD45^+$ were selected and cell doublets excluded using FSC-A and FSC-H dot plots, subsequently mouse $CD45^+$ were excluded from human $CD45^+$. Bottom panels are representative dot blots of engrafted lymphoid cells including CD3, CD22, CD14, CD27 and CD123 cells indicating that the immune system is partially present after PBL engraftment.

ing CSPG4 IgG_1 antibody were growing significantly larger compared with those in the IgE antibody-treated animals ($p<0.05$). The growth of tumours from animals treated with CSPG4 IgG_1 antibody was significantly restricted compared with those from animals treated with isotype control antibodies MOv18 IgE and IgG_1 against the tumour antigen FRα, which is not expressed on A375 melanoma cells ($p<0.05$; Figure 5.14). Xenografts given vehicile alone grew exponentially up to $750mm^3$ over the same time period (data from 2 independent experiments (2 human PBL donors); n=7 animals per group). These experiments suggest that the tumour antigen-specific chimeric antibody CSPG4 IgE and to a lesser extent, the antibody CSPG4 IgG_1, demonstrated tumour growth restricting functions *in vivo*. Moreover,

dosing fortnightly with CSPG4 IgE resulted in severely restricted melanoma tumour growth over a period of 30 days compared to controls ($p<0.001$; Figure 5.14), while tumours in mice treated with the corresponding CSPG4 IgG_1 antibody grew in a fashion similar to control antibody-treated animals ($p<0.05$). These findings imply that IgE antibodies retain their tumour growth-restricting properties even when dosed less frequently than their IgG_1 antibody counterparts (Figure 5.14).

Immunohistochemical analysis of the extracted tumours revealed that all groups featured human CD45 infiltration into tumours, suggesting that human immune cell engraftment extended beyond the spleen and into the human xenografts, rendering this model more relevant in the context of studying antibody therapeutic efficacy for cancer. Interestingly, tumours from CSPG4 IgE-treated animals had statistically significantly increased CD45 infiltration ($*p<0.05$) and CD68 ($***p<0.001$) infiltration compared to those treated with PBS alone. Furthermore, localization and distribution of human immune cell infiltrates appears disparate between controls and IgE: tumour-associated human $CD68^+$ (macrophage) infiltrates from IgE-treated animals appeared to be located in cell clusters, potentially indicating differences in chemotaxis and function of these cells in response to treatment with IgE. These data are in line with a previous report of human $CD68^+$ infiltrating cells in a patient-derived orthotopic model of ovarian carcinoma in mice treated with the chimeric MOv18 IgE antibody [Karagiannis et al., 2003] (Figures 5.15 and 5.16).

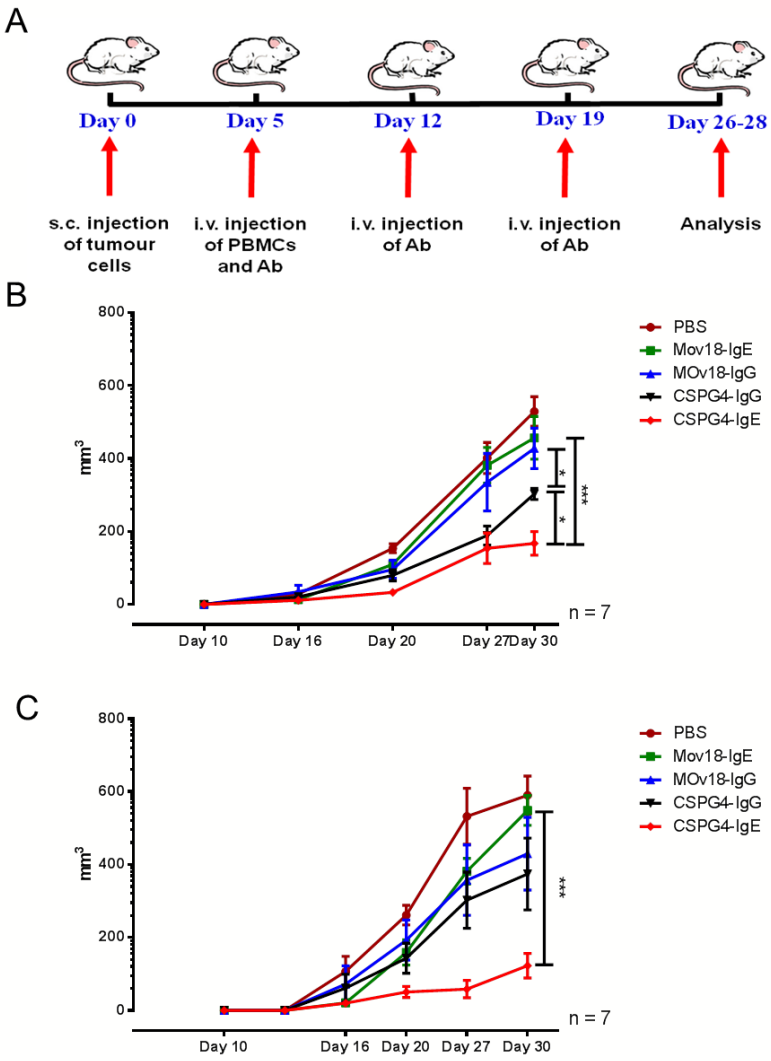

Figure 5.14: Anti-CSPG4 IgE is restricting tumour growth in subcutaneous melanoma tumour model. A) Design of dosing regime in *in vivo* model to determine antibody-mediated effector function. B) Anti-CSPG4 IgE restricts growth of A375 s.c. human melanoma in the humanised mouse compared to anti-CSPG4 IgG_1 (*$p<0.05$) and non-specific antibody controls (***$p<0.001$) when administered intravenously every 7 days following tumour challenge (4x10 mg/kg doses, n=7). C) Anti-CSPG4 IgE restricts s.c. tumour growth when administered every 14 days following tumour challenge (2x10 mg/kg doses) while anti-CSPG4 IgG_1 and control antibodies display no tumour-restricting functions (***$p<0.001$, n=7).

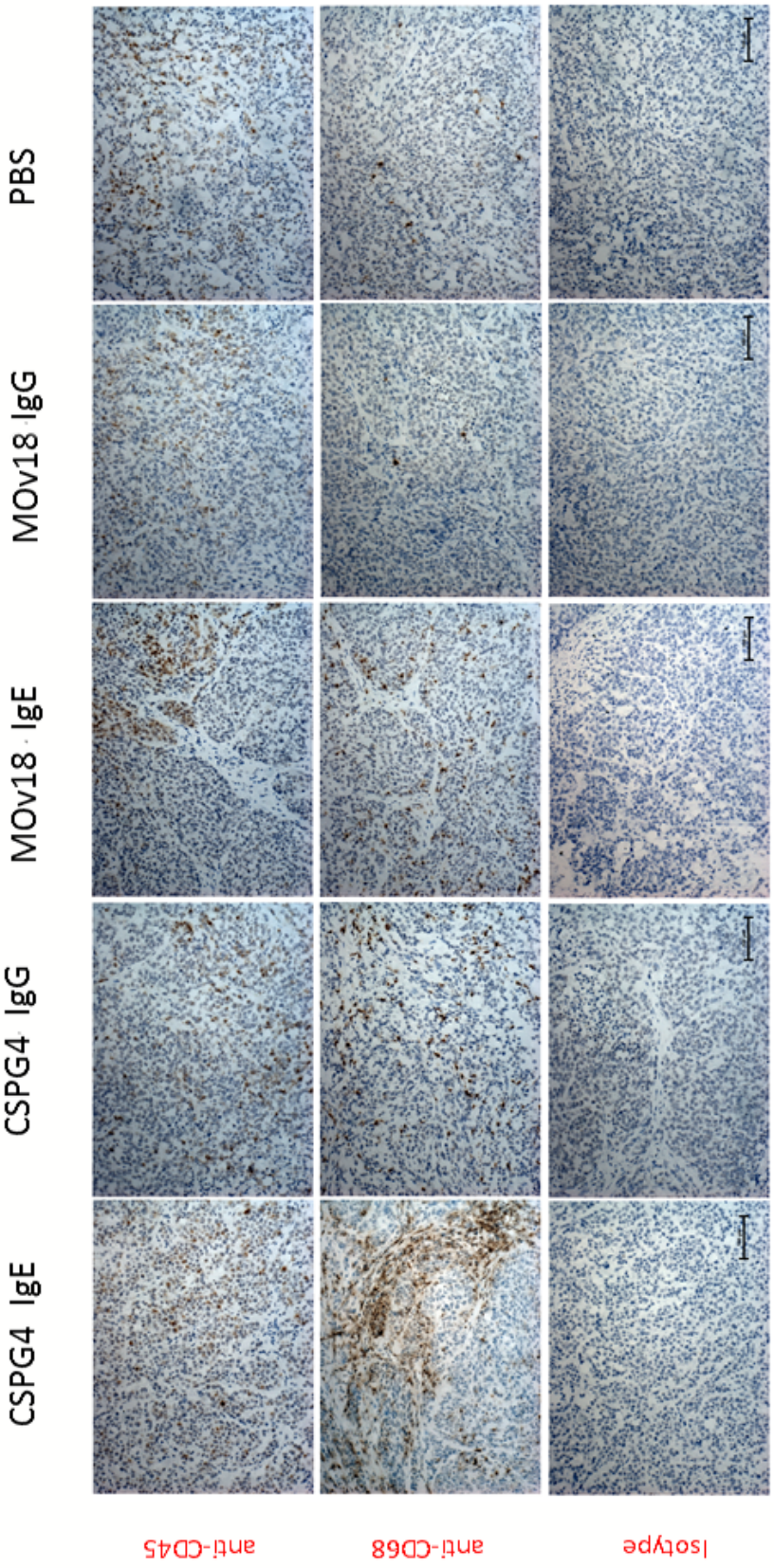

Figure 5.15: IgE is attracting immune cell infiltrates in subcutaneous melanoma tumour model. Immunohistochemical labeling for the presence of leukocytes (CD45) and macrophages (CD68)(all; markers stained with DAB in brown, counterstaining with hematoxylin in blue) show the presence and co-localisation of the markers within the tumours of NSG mice (Scale bar: 100 μm, magnification 10x).

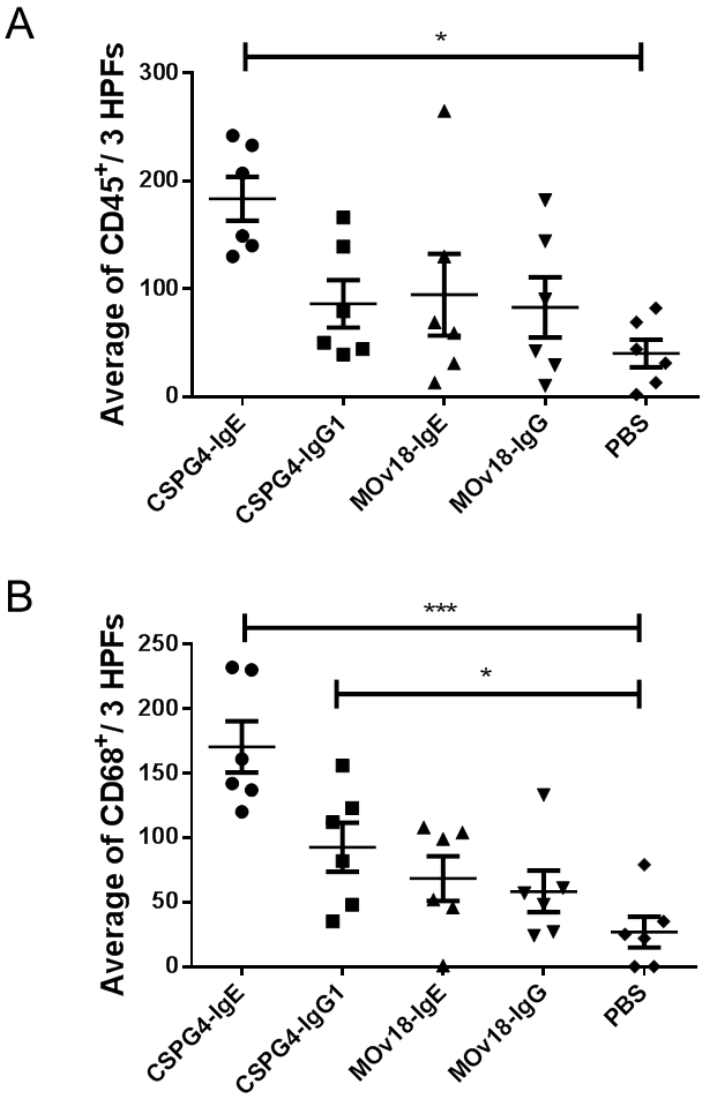

Figure 5.16: Evaluation of immune cells infiltration in subcutaneous melanoma tumour model. A) Human leukocytes (CD45) infiltration is observed in all treatment groups. Anti-CSPG4 IgE treated animals have a statistically significantly increase of CD45 cells compared to PBS treated animals. B) Human macrophages (CD68) infiltration is observed in all treatment groups. Anti-CSPG4 IgE and anti-CSPG4 IgG_1 treated animals have a statistically significant increase compared to PBS treated animals (average number of 3 independent high power fields magnification 10x (HPF); *$p<0.05$; ***$p<0.001$; lines represent mean and error bars standard error).

Analysis of human immune cell populations in the spleens demonstrated comparable engraftment levels in animals treated with PBS (36.66%), CSPG4 IgE (39.67%),

CSPG4 IgG (40.96%), MOv18 IgE (37.58%) and MOv18 IgG_1 (44.35%) antibodies (Figure 5.17.

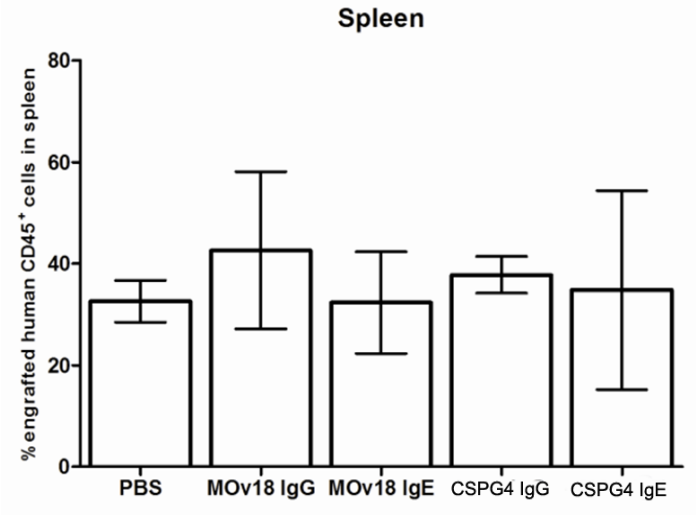

Figure 5.17: Engraftment of human $CD45^+$ immune cells in mouse spleens of NOD/SCID γ-/- mice, showing no significant difference in human $CD45^+$ engraftment across treatment groups.

Since immune responses in this model may be partly due to alloimmunity (human PBLs are not HLA-matched with A375 tumour cells), a novel disease-relevant human skin tumour engraftment model was developed which featured a human patient-derived melanoma tumour engrafted with autologous PBLs.

5.4.3 *In vivo* evaluation of anti-CSPG4 antibodies in a human tumour transplantation model with autologous PBLs

Human metastatic melanoma lesions (n=3 in independent experiments) derived from patients with stage III or IV melanoma were transplanted intraperitoneally into NOD/SCID γ-/- mice and simultaneously engrafted with autologous human lymphocytes (PBLs). Quintana and colleagues have recently reported a similar patient-derived model, and demonstrated correlations between disease progression in animals with disease outcome of the patient. This might indicate that intrinsic differences

in metastatic efficiency among melanoma patient-derived tumours are important determinants of clinical outcome in patients and may be used to mimic natural disease in animal recipients [Quintana et al., 2012]. An advantage of the patient tumour xenograft model developed herein lies with the additional reconstitution of the patient's immune system component, which was not the case in the study by Quintana et al. This additional feature permits examination of immunotherapies and antibody therapeutic candidates in the background of the patient's immune system which may include immunoregulatory components; this may provide a better prediction of this agent's efficacy as a treatment in patients. Transplanted tumours triggered multiple disseminated metastases in the lung, liver and spleen of the animals within seven to nine weeks following tumour implantation in the PBS treated group (Figure 5.18).

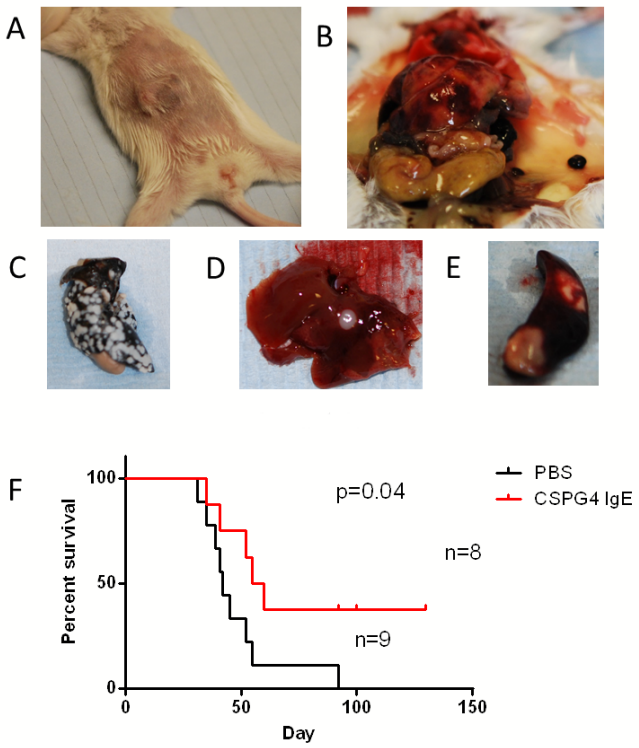

Figure 5.18: Human metastatic melanoma lesion derived from a patient with stage III/IV melanoma was established subcutaneously in NOD/scid/IL-2Rγ-/- mice engrafted with human lymphocytes (A), which triggers multiple disseminated metastases six weeks following tumour implantation (B-E). Treatment with anti-CSPG4 IgE mAb (weekly 10 mg/kg doses) singificantly prolongs survival compared to untreated controls (Mantel-Cox: $p<0.05$; (F)).

Treatment with CSPG4 IgE at 10 mg/kg weekly doses significantly prolonged survival of tumour-bearing animals (median survival 57.5 days; hazard ratio 0.35 confidence interval 0.11-0.90; n=8) compared with those animals treated with PBS (median survival 42 days; hazard ratio 2.79 confidence interval 1.12-9.46; n=9) (Mantel-Cox: $p<0.05$). These data suggest that IgE can prolong survival of mice bearing human melanomas in the context of patients' immune system components.

5.5 Gene expression arrays analysis of tumours from animals treated with antibodies

To gain early insights into active immune pathways associated with improved efficacy of IgE antibody treatments, gene expression analyses were performed using the human melanoma xenografts derived from the different treatment groups (CSPG4 IgE n=5; CSPG4 IgG_1 n=4; PBS n=4). The xenograft samples were retrieved at the end of experiments described in section 5.4.2. After assessing for RNA integrity, Human Ref-6 and Ref-12 BeadChips (Illumina, Ambion) were used to generate RNA expression data from tumours. Each array contains over 50000 probe sets representing approximately 40000 human genes. Data were background-subtracted then log-transformed and quantile-normalized. The expression levels were compared by the limma method (Limma package from the R software), an empirical Bayesian method with a moderated t- statistic implemented in Bioconductor and the Benjamini-Hochberg method was used to correct for multiple testing. A gene was considered as differentially expressed if the q-value (false discoveries) was below 0.02 and fold change (FC) more than 1.2 and less than -1.2 (analysis was performed by Dr. Chrysanthi Ainali and Mr. Jananan S. Pathmanathan). When comparing gene expression between tumours from the PBS group versus those from the CSPG4 IgE-treated group, 797 genes were identified as differentially expressed. For the PBS versus CSPG4 IgG_1-treated group comparisons, 681 genes were found to be differentially expressed. Interestingly, 665 gene signatures were found to be common between the CSPG4 IgE and CSPG4 IgG_1 treatment groups, but differentially expressed in these tumours when compared to the PBS only treatment group. Furthermore, 132 genes were differentially expressed in the CSPG4 IgE cohort com-

pared to all the other groups including the CSPG4 IgG_1, but only 16 genes were specifically differentially expressed in the CSPG4 IgG_1 cohort compared to the others, including the CSPG4 IgE group (these results were generated by Mr. Jananan S. Pathmanathan; Figure 5.19). These findings may indicate a notable impact of CSPG4 IgE when compared to CSPG4 IgG_1 and the other treatments in eliciting immune responses, and these are in line with the improved anti-tumoural functions of the tumour antigen-specific IgE antibody obsereved in these xenograft models.

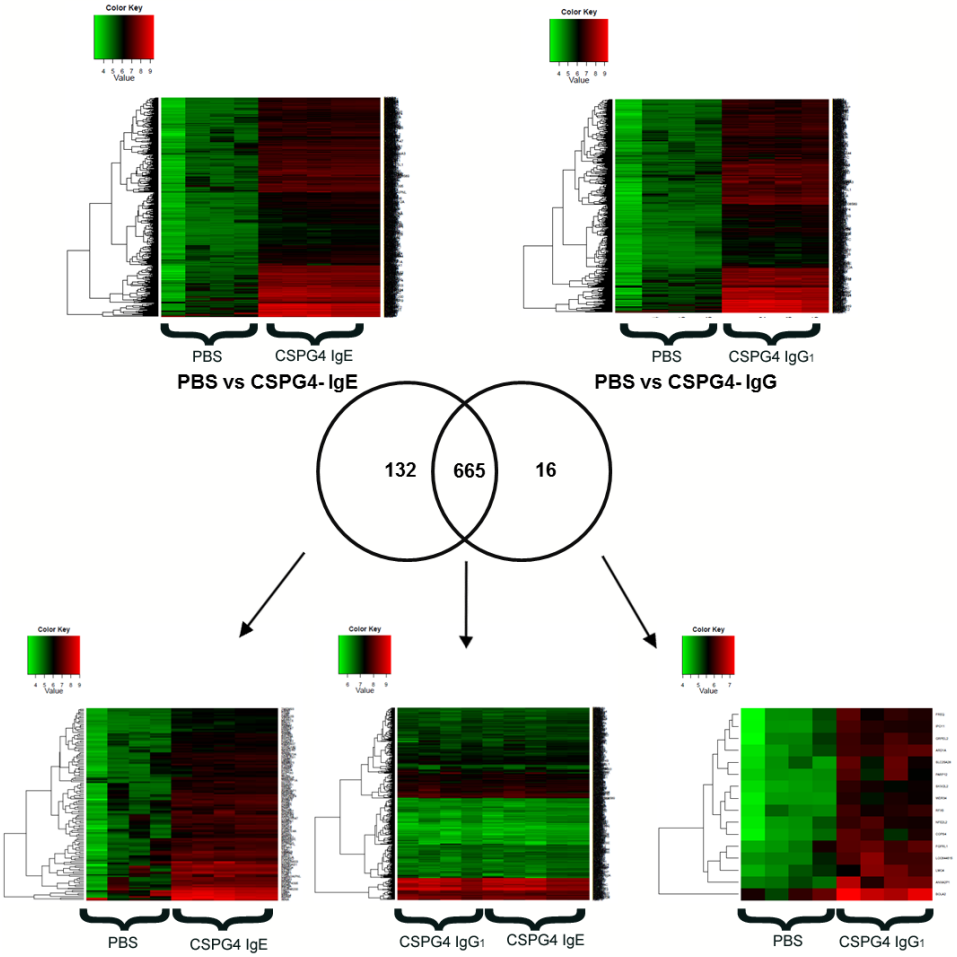

Figure 5.19: Gene expression microarrays from melanoma xenografts indicate differential gene expression profiles associated with anti anti-CSPG4 IgE-treated tumours compared to those treated with anti-CSPG4 IgG_1.

5.6 Signalling pathway evaluation *in vitro* expression and functional validation of differentially expressed genes

Knowledge of all direct and indirect interactions between proteins in a biological system could facilitate the description of cellular mechanisms and functions. Especially gene expression profiles allow us to detect the activation of distinct genes and to provide hints into their biological activities by placing their interactions in the context of larger known networks and signalling pathways in human cells. These evaluations can lead to the discovery of novel signalling pathways, and importantly, they can point at the key signalling cascades involved in biological processes or associated with specific treatments. One useful tool for these analyses, the STRING database, provides available data on protein-protein interactions, also including lower-quality data or computational predictions [Franceschini et al., 2013]. The STRING database was employed in the present study to annotate the differentially expressed genes identified in the experiments and analyses described in section 5.5. For this purpose, the genes identified as uniquely differentially expressed in tumour specimens from the CSPG4 IgE treated group compared to others were plotted against one of the best characterised published downstream IgE signalling pathway cascades (these gene expression analysis results were generated by Mr. Jananan S. Pathmanathan; Figure 5.20). From the transcriptomic analyses, it was clear that a number of signalling molecules which are mapped through STRING analyses as part of the FcϵR downstream signalling pathways were also upregulated in the CSPG4 IgE-treated tumours. From the previously-identified group of differentially upregulated genes and consequential enhanced signalling pathway analyses, the kinase PTK2 (p-value=0.01) which is connected to FcR signalling is up-regulated in IgE-treated mice and accordingly, it is connected with GSK3B, which is thought to directly interacting with NFκB1. Therefore, this kinase is indirectly connected with NFκB1 and can regulate the IgE mediated tumour killing *in vitro*. It is important to note, that PTK2 is also indirectly connected with SOS1 (which is under-expressed in our experiments and involved in FcϵRI signalling pathway) via NCK2, CRK and FYN. The kinase was previously described to be involved in the FcϵRI signalling cascade [Vial et al., 2000]. To study the validity of the transcriptomic findings, the functional roles of

PTK2 were then further evaluated in relation to CSPG4 IgE antibody treatment, in order to confirm not only its role as an important component of IgE-FcϵRI activatory cascades in IgE-treated tumours, but also as a step to validate the activation of the downstream network it belongs to. These data would support that engagement of tumour antigen-specific IgE antibodies with their FcϵRs on the surface of immune effector cells may be part of the activatory network that contributes to IgE-mediated anti-tumoural function. The role of PTK2 in antibody-mediated anti-tumoural effects conferred by CSPG4 IgE was then examined using functional *in vitro* assays. Firstly, an ADCC/ADCP assay was conducted using human monocytic cells as effector cells and A375 melanoma cells as targets. As previously demonstrated, CSPG4 IgE in the presence of human monocytic cells triggered 58.5% tumour cell death, higher than the non-specific isotype control antibody MOv18 IgE (22.15%), or no antibody (22.32%). In the same experiments, when PTK2 activity was blocked in human monocytes with the kinase inhibitor PF-431396 prior to the ADCC/ADCP assay incubations, CSPG4 IgE-mediated tumour cell killing was statistically significantly inhibited (21.85%) down to levels similar to controls (Figure 5.20). These findings indicate that treatment with a tumour antigen specific IgE antibody is crucially associated with enhanced downstream signaling through FcϵRI, which triggers cell activation and it is directly linked to the tumour killing properties conferred by this IgE antibody. These data support the findings of the transcriptomic analyses presented in section 5.5, and point to the importance of IgE-FcϵRI engagement and the downstream FcϵRI activatory cascades all participating in triggering IgE effector functions of monocytes/macrophages by *in vitro* and *in vivo*. In addition to enhanced gene expression, activation of protein kinases such as PTK2 can be examined by their phosphorylation state. In order to examine PTK2 phosphorylation in effector cells when engaged with anti-CSPG4 IgE and tumour cells, monocytes used as effector cells in the ADCC/ADCP assays were isolated by flow cytometric sorting at the end of assays and phosphorylation of PTK2 in primary monocyte lysates was studied by western blotting. These experiments indicated that monocytes isolated after incubation with tumour cells and CSPG4 IgE were associated with higher levels of phosphorylated PTK2 compared to monocytes incubated with the no antibody. These experiments suggested that phosphorylation of PTK2 was associated with increased levels of IgE antibody-mediated tumour cell death in a tumour antigen-specific manner (Figure 5.20).

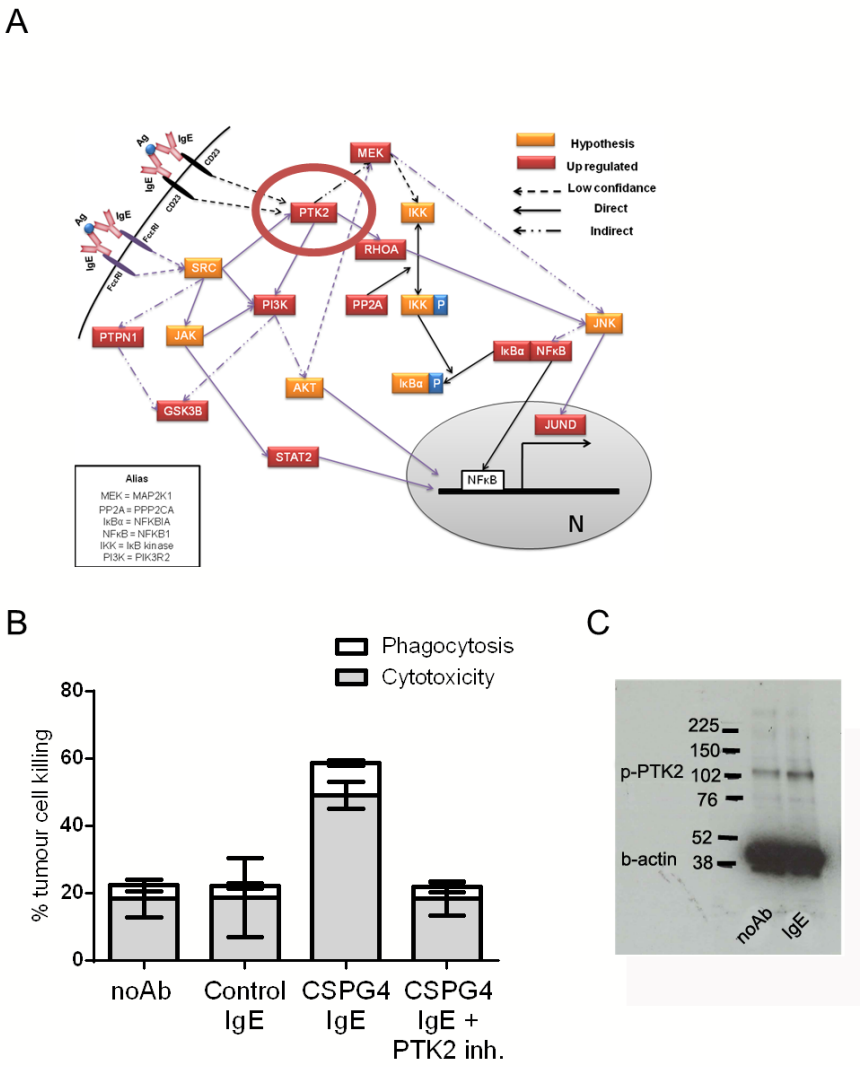

Figure 5.20: A) Integrated signalling pathways for Fcϵ receptor designed by data mining from KEGG and publications including genes that were differentially expressed in the NSG tumour environment. (in red over-expressed genes while yellow genes correspond to hypothetical connectors. B) ADCC/ADCP assay measurements confirmed that anti-gE mediated significant levels of tumour cells killing by U937 monocytic cells. The killing mediated by IgE was inhibited by the specific PTK2 kinase inhibitor PF-431396, indicating the relevance of this kinase in the downstream singalling of IgE. C) Protein extracts from U937 monocytic cells isolated by flow cytometric sorting at the end of a ADCC/ADCP assay. Examination of phophorylated PTK2 by western blot indicated that monocytic cells incubated with anti-CSPG4 IgE had enhanced amounts of phosphorylated PTK2 compared to cell incubated with no antibody.

5.7 Conclusions

Previous studies have presented substantial *in vitro* and *in vivo* evidence that IgE immunotherapy against cancer may be comparable or even superior to that of IgG_1 antibodies and new independent preclinical evidence supports the original findings for the superior efficacy of IgE cancer immunotherapy in a variety of cancers and model systems [Daniels et al., 2012,Daniels-Wells et al., 2013,Gould et al., 1999,Karagiannis et al., 2003,Karagiannis et al., 2007]. However the number of the IgE class candidates for passive immunotherapy, which are suitable for further clinical translation is limited, and the concept remains widely unexplored for a number of solid cancers. Up to now only the anti-folate receptor α specific antibody MOv18-IgE has been tested in several mouse and rat models for its efficacy and safety ([Karagiannis et al., 2007, Karagiannis et al., 2008, Karagiannis et al., 2012]; Josephs KCL PhD thesis). The data in this chapter show for the first time the relevance of the IgE therapeutic concept in the context of melanoma using another engineered chimeric IgE antibody an indication not previously explored with IgE immunotherapy. Anti-CSPG4 IgE antibody is shown to induce melanoma tumour death *in vitro* and in two highly-translational xenograft-bearing humanised mouse models. The anti-CSPG4 IgE a) could be produced under serum-free conditions at high purity, and these characteristics can help its translation for cancer therapy; b) recognised its target antigen on the surface of tumour cells and in different melanoma tumour tissues, illustrating that the epitope is accessible regardless of anatomic location of the tumour and throughout disease stages; c) the antibody could activate mast cells (RBL-SX38) through cross-linking of the Fcϵ-receptor by multivalent antigen, triggering mast cell degranulation; d) the antibody was active in recruiting monocytes to mediate ADCC and ADCP against tumour cells; and e) IgE showed superiority in humanised animal models compared to isotype controls and its IgG_1 counterpart. Analysis of lesions from different treatment groups revealed that tumour lesions from anti-CSPG4 IgE-treated animals had enhanced human $CD68^+$ and $CD45^+$ immune cell infiltrates compared to animals treated with PBS alone. This observation may indicate that macrophages ($CD68^+$), normally reported in the literature to be alternatively activated in the context of cancers, including melanoma, are potentially functionally-active or could be activated in tumours treated with IgE antibodies. This is supported by previous findings with the anti-FRα IgE antibody. Indeed, the activation of the protein kinase

PTK2 demonstrated in this chapter to be associated with the anti-tumoural functions of IgE antibody treatment *in vitro* and *in vivo* is known to be involved in effector cell downstream activation cascades triggered by engagement of IgE receptors (FcϵRs) on immune effector cells such as macrophages and monocytes. These data support the notion that effector cells, and in particular monocytes/macrophages, are important and key effector cells which may be redirected against tumour cells by IgE therapeutics and that these cells participate in anti-tumoural responses. Furthermore, in concordance with these findings several reports indicate that the micro-anatomical location and activation profile of macrophages influences clinical outcomes in certain tumour types [Dai et al., 2010, Movahedi et al., 2010]. Moreover, gene expression analysis of the extracted xenograft tumours from animals treated with anti-CSPG4 antibodies or PBS alone revealed a high number of differentially-expressed genes in anti-CSPG4 IgE-treated animals that allowed for subsequent identification of signalling molecules involved in the Fcϵ signalling cascade. Further *in vitro* phosphoprotein analysis targeting these genes confirmed that the kinase PTK2 is essential for the activation of human monocytes by IgE antibodies in the presence of tumour cells. Although the *in vitro* experiments in this chapter as well as published data demonstrate that PTK2 (also known as FAK1) is phosphorylated in IgE-activated monocytes and mast cells, the functional involvement of PTK2 requires further investigation, since there are reports that expression and functions of this protein can be modulated by anti-CSPG4 antibodies in cancer cells and therefore engagement with CSPG4 IgE with tumour cells may trigger downstream events activating tumour cells with unknown consequences [Vial et al., 2000, Campoli et al., 2010]. The initial work presented in this chapter finally illustrates the promise of interrogating protein-protein interaction networks in translational research. The use of tools such as the STRING database, benefiting from increased coverage and integration by also including lower-quality data and computational predictions, will help generate novel hypotheses to guide research. With regards to anti-cancer immunity, a protein-protein landscape illustrating the potential interactions between tumours and components of immunity can be designed through an immune-scoring system for all human genes, based on literature mining and information theory principles. In summary, this chapter contributes a set of data confirming the promise of an IgE therapeutic candidate in a number of *in vitro* and *in vivo* model systems and provides a combination of transcriptomic, computational and functional analyses which point to activatory mechanisms associated with IgE antibody-mediated activation of key

effector cells such as monocytes/macrophages against tumours. These findings support further research on immunotherapeutic strategies focusing immune responses directly against tumours such as those employing antibodies of the IgE class.

6 Discussion

6.1 Impaired antibody responses against tumours: IgG4

6.1.1 Immunoediting of antibody responses in melanoma

Monoclonal antibodies form a significant addition to the therapies against cancer, with 17 antibodies already approved for oncology indications [Reichert and Dhimolea, 2012]. Although monoclonal antibodies function by a multitude of mechanisms against tumour cells, the Fc-mediated mechanisms by which antibodies engage and activate immune cells play important roles [Woof, 2012, Moore et al., 2010]. In this context, Fc-mediated functions have been observed to have a substantial effect on the efficacy of clinically-applied antibodies and are already associated with oncology treatments such as trastuzumab [Karagiannis et al., 2009, Nahta and Esteva, 2007, Lazar et al., 2006], cetuximab [Jonker et al., 2007] and ipilimumab [Lipson and Drake, 2011]. Whether administered as therapeutics or expressed by host B cells in response to tumour growth, antibodies have the potential to trigger potent anti-tumoural responses by activating effector cells to destroy tumour cells. How-

ever, tumour-induced immunoediting in the tumour microenvironment is known to suppress the anti-tumoural functions of T cells and it would be reasonable to hypothesize that those tumour-induced inflammatory conditions triggering suppression of T cell functions can also lead to immunoediting of humoral responses and substantially impair the potency of B cell and antibody functions against cancer. Until recently, the nature and functional significance of the humoral response in cancer and particularly in melanoma have been insufficiently studied, understood or appreciated. Moreover, whether and how the humoral response is immunoedited or suppressed by the presence of tumours have also remained great unknowns. Our group previously reported the presence of a tumour-reactive mature memory B cell compartment in the circulation of patients with melanoma. By isolating tumour-reactive antibody clones from patients' mature memory B cells, we found that patient-derived antibodies can activate effector cells to destroy tumour cells *ex vivo* in an antigen-specific manner [Gilbert et al., 2011]. These findings suggest that patient humoral immunity is not oblivious to the presence of cancer and additionally harbours the potential to be triggered against tumour cells. However, hints that immune escape mechanisms may operate to suppress tumour-reactive humoral responses came from our findings that this tumour-reactive memory B cell compartment appears more prominent at earlier disease stages and is substantially reduced with disease progression. Findings reported by others and us also demonstrate that both the broad and the tumour-reactive mature memory B cell compartments are reduced in patients with advanced disease [Carpenter et al., 2009]. Taken together, these reports suggest that like T cells, B cells may also be subject to tumour-induced suppressive signals.

6.1.2 Redirection of humoral immunity by tumour-induced Th_2 inflammation

Insights into one immune escape mechanism are provided with findings presented in this thesis which demonstrate that in tumour microenvironments and in the presence of melanoma tumours, B cells are polarized to favour production of IgG_4, an antibody subclass with substantially-restricted effector functions compared to well-known potent IgG1 antibodies; this can translate to severely-impaired anti-tumoural effector cell activation. The biological relevance of IgG_4 subclass antibodies in cancer

disease pathogenesis is a novel discovery and adds to the relatively newly-described roles of IgG_4 subclass in some inflammatory diseases (IgG_4-related disease) [Stone et al., 2012]. In melanoma, early studies have indicated polarization of IgG antibody subclasses in the serum of patients with melanoma, but the biological relevance and functional implications of these findings remained unexplored until recently [Daveau et al., 1977]. The presence of infiltrating IgG_4^+ plasma cells in cholangiocarcinomas [Harada et al., 2012] was also recently reported, sparking new interest in the roles different components of humoral immunity play in cancer. However, beyond this small number of reports, the effects of IgG_4 in cancer have been largely unexplored. Immunohistological analysis of patient specimens demonstrated an increase in IgG_4 positive cell infiltrates in melanoma. Following this observation of IgG_4 polarization, the impact of Th_2 cytokines on the humoral immunity were explored. Mechanisms by which antibody immune responses are influenced by Th_2 cytokine environments have been previously described. In these reports, it was shown that IL-4 could induce class switching to IgE and IgG_4 and that IL-10 could enhance IgG_4 production by switched B cells [Satoguina et al., 2005, Jeannin et al., 1998]. Increased production of Th_2 cytokines such as IL-4 and IL-10 has been described in melanoma and other cancers [Sheu et al., 2001, Agarwal et al., 2006, Nevala et al., 2009]; and IgG_4, rather than IgE antibodies, have been described to be elevated in individuals chronically exposed to known allergic triggers such as bee venom and animal fur [van de Veen et al., 2013]. However until recently, the combination of these conditions, (i.e. IL-10-driven Th_2 inflammatory conditions and chronic exposure to antigens) in relation to their potential to redirect antibody production by B cells was not investigated in the context of cancer. Using tumour specimen and *ex vivo* culture studies, Chapter 3 reports a substantial $CD22^+$ and IgG_4^+ cell infiltrate detected in melanoma tumours and the presence of Th_2 cytokine conditions which can alter IgG subclass production in the tumour microenvironment. When cultured *ex vivo*, B cells from tumours produced a greater proportion of IgG_4 subclass antibodies than B cells in the circulation, hinting at a considerable tumour-associated polarisation of B cells in favour of IgG_4. Additionally, *ex vivo* stimulation experiments showed that IgG_4 levels were increased only in culture conditions that included melanoma cells in combination with peripheral immune cells, and these cultures featured increased levels of inflammatory Th_2-biased mediators IL-4, VEGF and IL-10, which are known to favour polarisation of B cells to produce IgG_4. This skewing of antibody subclasses was not observed in culture conditions where melanoma cells were

absent or substituted with human melanocytes. These latter cultures lacked substantial levels of the key IgG_4-promoting cytokines IL-10 and VEGF [Chen et al., 1994, Sumimoto et al., 2006]. This suggests that key Th_2 mediators such as IL-10, VEGF and IL-4 contribute to IgG_4 polarisation and that melanoma cells could be an important source or trigger of at least some of these inflammatory cytokines. Our additional finding that only a small fraction of patient derived tumours tested positive for IgE antibody expression is consistent with chronic exposure to antigens (possibly tumour antigens) and the alternative (or IL-10-driven) rather than classic (or IL-4-dominant) Th_2-driven inflammatory conditions in tumours, both of which are expected to favour class switching to and enhanced production of IgG_4 rather than IgE. The additional data presented in Chapter 3 demonstrating that IgG_4 antibodies in tumours and patient circulation can also recognise tumour cells, further suggest that humoral immunity recognising cancer cells triggered in patients may be biased towards IgG_4, and not IgE or IgG1. These findings may explain why in the presence of Th_2-biased inflammatory conditions, IgE-driven anti-tumoural responses are not commonly observed in patients. These may support the case that perhaps a "classic", IgE-biased, rather than an "alternative", IgG_4-biased, immunity may tip the balance in favour of anti-tumoural immunity, and they need further consideration and investigation. Thus, findings reported in this thesis reveal for the first time a hitherto undiscovered feature of humoral immunity in melanoma tumours, characterized by B cell infiltration and local expression of IgG_4 antibodies, polarized by cytokines such as IL-10, IL-4 and VEGF. These findings link the presence of melanoma cells with the secretion of these cytokines and with B cell polarization, contributing to enhanced production of IgG_4 subclass antibodies in the presence of tumours.

6.1.3 Impairing antibody effector functions: the roles of IgG_4

Insights into the functional significance of IgG_4 polarisation in tumours come from findings presented in this thesis which demonstrate that not only is IgG_4 itself shown to be ineffective in activating effector cells to destroy tumours, it also antagonizes otherwise cytotoxic IgG1-mediated human anti-melanoma immunity *in vitro* and *in vivo*. An interesting mechanistic insight is provided by evidence that IgG_4 blockade

is mediated through competing with IgG1 for FcγR binding and therefore inhibiting downstream signalling activation of effector cells (i.e. monocytes), rather than by potentiating suppressive triggers through engagement with FcγRIIb. This inhibition of anti-tumoural functions of IgG1, the antibody subclass thought to have the most potent immune effector functional capacity among IgGs, accompanied by the proportional increase in IgG_4, generally thought to have the least potent Fc effector functions among the four IgG subclasses [van der Zee et al., 1986, Brüggemann et al., 1987, Aalberse et al., 2009]. This translates into weakened anti-tumour antibody responses. An obvious consequence would be impairing the capacity of host-induced and therapeutic antibodies to mediate antibody dependent-mechanisms including CDC, ADCC and ADCP. Additional in depth studies are required to dissect the full immunomodulatory mechanisms influencing antibody functions of different classes and subclasses in melanoma and to elucidate whether and how these mechanisms might apply in different cancers. A number of conclusions may be derived from these findings:

1. the importance of activating effector cells against cancer highlighted by data presented in Chapter 3 are in concordance with a growing appreciation for the clinical significance of immune cell infiltrates in tumour microenvironments, their roles in immune surveillance and their utility in predicting disease outcomes and response to treatments;

2. the plastid nature of effector cells to either become activated or suppressed under different conditions in the context of host-induced and therapy-triggered anti-tumoural immunity and in the presence of diverse immunosuppressive conditions;

3. the potential merit of designing targeted therapeutic strategies to sequester and activate these effector functions against cancer cells, and

4. the need to further elucidate mechanisms of immune suppression of humoral immunity is evident and can potentially translate into better-designed therapeutic strategies that perhaps may be less prone to or capable of reversing or overcoming tumour-induced immune blockade mechanisms.

The work presented in this thesis presents the first evidence of local and systemic enhancement of IgG_4 in melanoma. The associated IgG_4-polarization driven by key cytokines such as IL-10 and VEGF suggests that IgG_4 antibodies triggered in the presence of melanoma cells contribute to local inflammation and may represent a regulatory mechanism by which tumours evade clearance by the immune system.

6.1.4 Future directions in dissecting the mechanisms of humoral immune responses by tumours

Data in this thesis demonstrate that IgG_4 promoted by tumour-induced Th_2-biased inflammation restricts anti-tumoural immunity. These insights provide a novel perspective on tumour-induced immune escape, a rationale for further dissecting the cross-talk between different components of humoral immunity with tumours and for studying the implications of these associations on clinical outcomes. Importantly, the present and also future findings will continue to provide translational opportunities by informing the search for better treatments. The humoral response remains only partly investigated in the context of immunoediting [Tan and Coussens, 2007]. Therefore, future work dissecting the role of tumour-specific IgG_4 antibodies, and perhaps also other antibody classes in cancer, may lead to a better understanding of immune impairment in the tumour microenvironment. For instance:

1. Tumour-specific IgG_4 antibodies may both compete for the Fc receptors as well as for tumour antigens with other host-induced and/or therapeutic antibodies, thus blocking antibody-mediated mechanisms in a dual manner.

2. One direction for further exploration also lies with understanding the contributions of different cells in Th_2-biased inflammation. In this study, when co-cultured with B cells, tumour cells enhanced IL-10 expression, while B cells secreted enhanced amounts of VEGF in the presence of tumour cells.

   (a) Firstly, exploring the feedback loops of signalling cascades induced by VEGF in tumour cells and linked events that trigger production of Th_2 cytokines such as IL-10 which polarise the humoral response, would lead to a better understanding of immunoediting. This can inform the design of

novel therapies aiming to reverse immune escape or help stratify patients who may benefit from certain therapies such as anti-VEGF treatments.

(b) Secondly, data in this thesis are in concordance with published findings by Harada and colleagues who report co-localisation of T regulatory cells ($FoxP3^+$) with B cells and in particular with IgG_4 producing cells in tumours. As T_{regs} are also rich sources of IL-10, it is conceivable that the presence of these cells can further contribute to "alternative", Th_2-polarised conditions that favour IgG_4. These findings would also support the idea that B cells are polarized locally in the tumour microenvironment to switch to IgG_4. Furthermore, for the initiation of IgG_4 production, the cytokine IL-4 was reported to be essential [Robinson et al., 2004] and continuous IL-4 production is highly dependent on prior expression of IL-4 (auto-feedback) [Le Gros et al., 1990]. T regulatory cells, which can also produce IL-4, might therefore be of crucial importance to the polarisation of B cells in tumours. Thus, T_{regs} may be a source of this crucial component required to trigger those IgG_4-driven suppressive responses.

3. Moreover, analysis of the anatomical compartment in which class switch recombination takes place, locally or in adjacent lymph nodes, may improve opportunities for interventions aimed at reversing this polarisation. This could be accomplished by repolarising or directing potent immune cells against the tumour and may lead to tumour eradication rather than evasion. Pre-clinical studies reporting that blocking the migratory potential of antigen presenting cells could lead to more potent anti-CD8 effects directed against tumour cells hint towards the potential involvement of antigen presenting cells in immunomodulatory mechanisms through perhaps production of cytokines such as IL-10 that may suppress T cell but also, as presented in this thesis, humoural responses. For example, $CD141^+$ dermal dendritic cells, known for their immunoregulatory roles in immunity may regulate the humoral response through production of IL-10 and prevent tumour eradication [Chu et al., 2012].

6.1.5 IgG$_4$ blockade mechanisms informing future novel therapeutic approaches

Future strategies to counteract IgG$_4$ immunoregulatory pathways such as IL-10 blockade or anti-CD25$^+$ antibodies might lead to an advanced clinical improvement in patients who do not respond to treatments with immune checkpoint blockade antibodies. Curran et al. reported that the combination of anti-CTLA-4 antibodies and anti-PD1 antibodies lead to a proportional increase in T effector cells (such as CTLs), as the antibodies decrease the T regulatory cell compartment by inducing ADCC against them. These data suggest that checkpoint blockade antibodies of the IgG$_1$ class have a bivalent mechanism, namely unblocking CD8 T cell activation and also targeting suppressive T regulatory cells. Therefore, combining checkpoint blockade antibodies with T$_{reg}$ specific antibodies such as anti-CD25 may translate into higher efficacy. In future studies, it may be worth investigating if IgG$_4$ levels in the serum of cancer patients correlate with clinical responses to antibody immunotherapy. Furthermore, longitudinal studies in phase III trials monitoring not only IgG$_4$ protein levels but also IgG$_4$$^+$ cells and their abilities to recognise tumour cells may lead to a better understanding of the systemic memory B cell response in the disease. This may then lead to the development of new therapeutics targeting these cells to counteract IgG$_4$ impairment in melanoma. An alternative approach is to design antibody treatments with engineered Fc regions and antibodies of different classes and derivatives less prone to IgG$_4$ blockade; this may have an increased therapeutic value.

6.2 IgG$_4$: a novel promising biomarker in melanoma

6.2.1 The search for disease-relevant biomarkers for melanoma and the promise of humoral responses

Despite the rise of numerous biomarkers for many malignancies including melanoma, there remains an unmet clinical need in this field. Although currently most biomark-

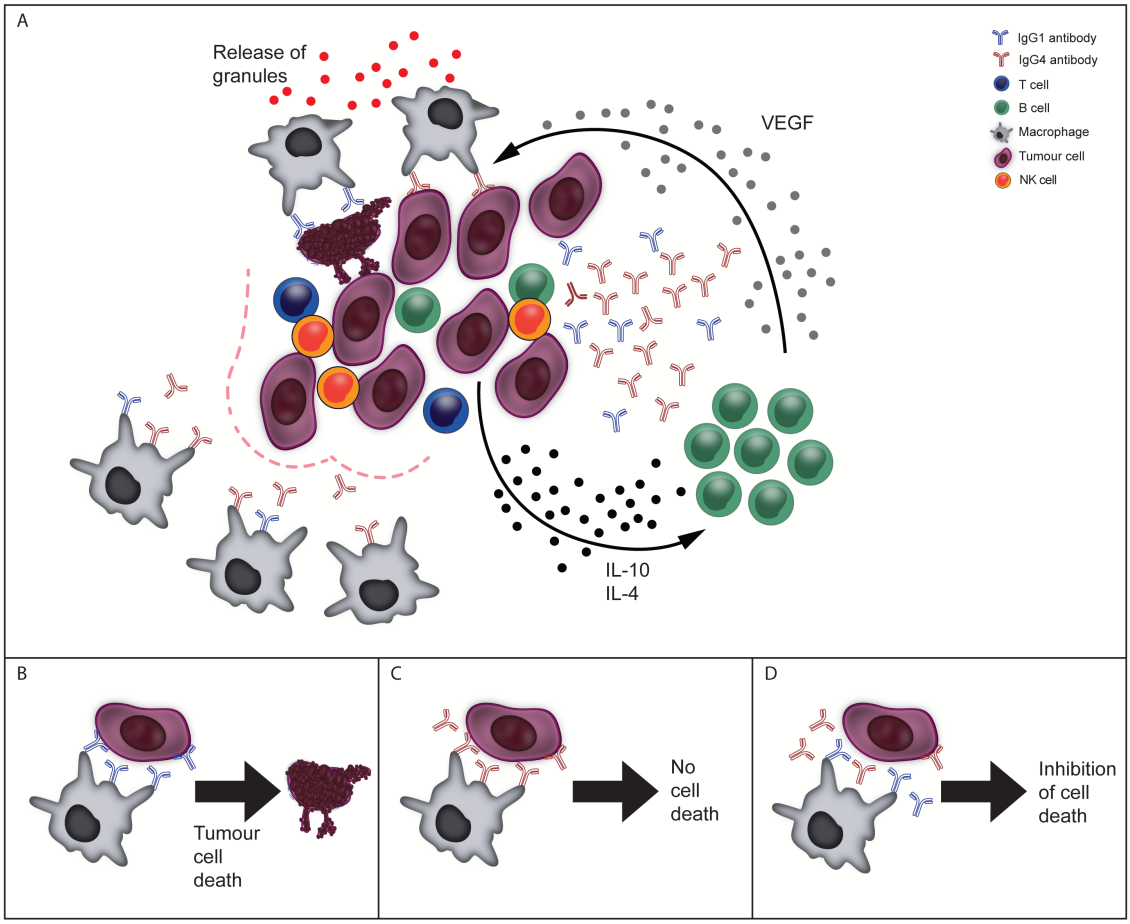

Figure 6.1: IgG$_1$ induces ADCC while IgG$_4$ impairs effector cell function in the tumour microenviroment. A) Tumour cells, aided by immune inflammatory and stromal cells in the tumour microenvironment, can polarise B cells to secrete IgG$_4$ subclass antibodies by secreting Th$_2$ cytokines such as IL-10 and IL-4, and via B cell-produced VEGF, which may favour further production of IL-10 by tumour cells and inflammatory infiltrates. IL-10-VEGF-IL-10 induction may be part of a feedback loop mechanism resulting in class-switching and activation signals for IgG$_4^+$ B cells in tumours. IgG$_4$ antibodies (red) are poor activators of anti-tumoural effector cell functions, while IgG$_1$ antibodies (blue) are effective activators of immune cells. B) Tumour specific IgG$_1$ antibodies can mediate effective antibody-dependent tumour cell killing by immune effector cells (e.g. monocytes/macrophages) through activation of FcγRI (CD64) signalling. C) IgG$_4$ does not activate effector cells to kill tumour cells (through ineffective induction of FcγR signalling upon effector cell engagement). D) IgG$_4$ antibodies can impair IgG$_1$-mediated tumour cell killing by competing for recognition of FcγRI receptors on effector cells.

ers lack sufficient combined sensitivity and specificity, there is wide scope for potential applications for clinically-validated biomarkers [Tandler et al., 2012]. Novel

biomarkers are needed for many applications, such as aiding diagnosis, early detection, staging of patients, prognosis of disease progression, patient stratification for particular treatments or to help predict responses to specific therapies. For instance, a biomarker could in principle be used to assess the superiority of a therapy in phase III trials before the terminal endpoint is reached, thus allowing for quicker assessment and better health care provision. One can foresee that the discovery of specific disease-relevant biomarkers could potentially help us harness the full therapeutic benefits of drug interventions before terminal endpoints. Importantly, markers that are directly linked to the pathogenesis or progression of the disease are desirable. The only serum biomarker in clinical practice for melanoma is LDH. Elevated LDH serum levels are found in patients with progressive disease at later stages of melanoma. The presence of LDH indicates active cell necrosis, which occurs during disease progression in melanoma [Balch et al., 2009]. In this context, it is important to highlight that LDH only indicates enhanced cell death, which normally occurs in advanced disease when patients have high tumour burden, thus this marker is generally useful in late but not in early disease stages [Hofmann et al., 2011]. Furthermore, serum LDH is not exclusively elevated as a result of tumour burden and can be influenced by other conditions such as myocardial infarction. Another promising serum biomarker candidate is S-100B; it has demonstrated high sensitivity and specificity higher than that of LDH in advanced disease, but it is still not applied in clinical routine as the data reported indicate a large variation between patient samples [Tandler et al., 2012]. This latter feature of variation among patients is a common problem in the search for clinically-useful serum biomarkers and generally represents a limitation that has prevented a number of clinically available biomarkers to reach clinical utility. Detection of circulating tumour cells (CTCs) represents an alternative biomarker approach to the analysis of protein and DNA in patient sera. CTCs should be relevant to disease progression, as their presence is expected in the circulation of patients with advancing and metastatic tumours and may signify a worse clinical prognosis. This approach is however limited due to the large inter- and intra-patient variabilities in the cancer cell markers for those cells and large variations in CTC counts between blood draws [Karakousis et al., 2013]. Humoral immune components, including circulating antibodies, are emerging as biomarkers for autoimmune, inflammatory, allergic and malignant diseases. This concept is strengthened by the recent reports on "immunosignaturing", a method which lends merit to the notion that monitoring antibodies could prove more sensitive than screening for specific antigens in early dis-

ease stages (Chapter 1, Section 1.4). Immunosignaturing is conducted using protein arrays to determine whether specific antibody patterns correlate to disease [Hughes et al., 2012]. This technique has two unique advantages: a) antibody responses are occurring at early points of pathogenesis and could be used as a sign of disease occurrence; and b) antibody production is naturally amplified upon B cell activation by antigen recognition and can be measured. The merits of immunosignaturing have been demonstrated in Alzheimer's disease by comparing different cohorts of patients and one can also foresee potential applications in cancer [Restrepo et al., 2013].

6.2.2 The merits of evaluating IgG$_4$ as a biomarker in melanoma

In support to the above principle that antibodies could be useful indicators of disease pathology and outcomes even at early stages, data presented in this thesis indicate that the presence of IgG$_4$ in melanoma is indicative of active immunosuppressive mechanisms. Importantly, preliminary evidence conducted in a 33 patient cohort demonstrates that higher IgG$_4$ serum levels are associated with worse prognosis (Chapter 3). These findings were further dissected in Chapter 4, using a larger cohort of patient sera and blood PBMCs, and it is concluded that circulating IgG$_4$ can be a promising prognostic readout at early stages of melanoma, where standard markers like LDH lack sensitivity. Elucidating the association of IgG$_4$ with clinical outcome can pave the way for biomarker development and implementation for more sensitive markers at early disease stages. Although IgG$_4$ may be a promising candidate marker in prognosis of early disease patients, the important question of whether it could help inform decisions along with or instead of sentinel lymph node biopsy (SNB) still remains. Presently, 80% of SNB samples are histologically tumour cell-negative, and it may be useful to develop novel less intrusive readouts that can provide similar information for patients with local disease whilst avoiding or reducing the risk of potential long-term complications associated with SNB interventions. Further studies must be conducted to compare the predictive values of SNB and serum IgG$_4$ readouts; these evaluations may yield better and less intrusive clinical tools along with improved patient management. Furthermore, the increased numbers of IgG$_4^+$ B cells in the circulation of melanoma patients compared to healthy volunteers may pave the way for a more personalised medicine approach involving

monitoring circulating B cell subsets such as memory class-switched cells. Monitoring B cell subsets associated with immune modulation such as IgG_4^+ B cells may provide useful information with regards to the nature of long-lived memory responses rather than relying on the temporal immune signals through detecting serum proteins and antibodies. Data reported in this thesis (Chapters 3 and 4) also demonstrate IgG_4^+ cell infiltration is enhanced in melanoma tumours compared to healthy skin; although it was not possible with available patient data to correlate these infiltrates with patient outcomes or history; this finding could lead to further studies specifically focused on evaluating IgG_4 positivity in melanoma as a tissue marker, perhaps useful in predicting disease burden or metastatic potential. In summary, findings reported in Chapters 3 and 4 of this thesis demonstrate the potential of IgG_4 as an immunological and serological biomarker, mandating the need for larger longitudinal studies analyzing IgG_4 to ascertain its clinical significance and utility.

6.2.3 Future investigations of IgG_4 as a biomarker and potential clinical benefits

Analysing IgG_4 in the serum of patients has shown to predict the risk of progression in melanoma. The advantages of this minimally invasive test would not only benefit the patient, but could also have positive financial implications for the health service. To date, sentinel lymph node biopsies (SNB) is a tool for staging patients and for predicting the risk of progressive disease in melanoma. However, SNB require a specialized team to conduct the procedure, sterile facilities and instrumentation, which inevitably involves higher costs in comparison to a serological test that can be conducted after a single blood draw. IgG_4 has shown efficacy in predicting the risk of disease progression at early stage of melanoma. In future, it could be assessed whether IgG_4 serum level, together with histopathological assessments such as Breslow thickness, may help to pre-screen patients prior to SNB in order to identify those who may benefit from undergoing this procedure. This pre-screening could not only lower the cost of treatment but, if applied, may also be of benefit since the post-operative complications of SNB such as lymphedema would be avoided for a large majority of patients who gain no benefit from undergoing SNB. However, extensive longitudinal studies comparing simultaneously SNB and IgG_4 will need to investi-

gate any correlations or predictive potential of IgG_4. In the future, monitoring IgG_4 could also help assessment of treatments and treatment-related responses. Including IgG_4 serum level measurements as a surrogate maker to investigate the efficacy of a drug in a randomized clinical trial may prove effective, as this marker might be able to help assess the outcome before the primary endpoint. Moreover, evaluating IgG_4 in immunotherapy with treatments such as ipilimumab may be considered [Downey et al., 2007]. The acquired data could reflect the effects of the tumour environment on the patient immune system and its capacity to respond to specific immune activatory therapies. The reported titres of IgG_4 correlate with the risk of disease progression and support the data demonstrating the immune suppressive functions of IgG_4 in melanoma described in this thesis. Therefore, as IgG_4 is a part of the pathological process in this disease it can be used to monitor changes in the course of the disease. It is noteworthy that similar elevated IgG_4 levels were also observed in pancreatic cancer, extrahepatic cholangiocarcinoma and squamous cell carcinoma, providing evidence that this phenomenon might not be limited to melanoma [Kawa et al., 2012, Harada et al., 2012, Strehl et al., 2011]. On another note, IgG_4 might also be further studied as a biomarker in breast cancer; although in this thesis IgG_4 did not show any potential to predict progression, it is important to point out that the patients involved in this study had only stage I-II disease. In future, assessment of a more heterogeneous population of breast cancer patients should be conducted. Another interesting consideration would be combining serological and immunological markers. As is partially the case in immunosignaturing (the protein array shows data from a variety of antibody reactivities), the use of multiple markers each with different sensitivity and specificity could result in an algorithm with improved combined diagnostic or prognostic potential; this could be successful assuming that decisions about priority, (e.g. which marker to consider more valid), mathematic methods and operational feasibility are in place. Larger clinical studies including more patients at different disease stages are required to identify and validate more reliable biomarkers in melanoma; these markers may include IgG_4. The effort to acquire such markers could improve the diagnosis, predict the risk of disease progression and guide the appropriate therapy decisions; these concepts fit into the frequently discussed model of personalised medicine and may help optimise the potential value of many therapies.

6.3 Extending the translational concept of Allergo-Oncology towards treating skin cancer

6.3.1 Rationale for improving effector functions by employing antibodies of the IgE class against tumours

Since the Fc domain of an antibody determines its interaction not only with complement, but also with relevant cell surface Fc receptors, it is evident that the class or subclass of an antibody critically influences its effector functions and efficacy. This discovery has stimulated the development of several antibody modifications, all aspiring to optimise the antibody-immune system interactions by enhancing Fc-mediated antibody functions and consequently the efficacy of the antibody as a therapeutic agent [Griggs and Zinkewich-Peotti, 2009, Jefferis, 2009]. The nascent field of Allergo-Oncology aims to harness the inflammatory response observed in allergy against cancer. The design of IgE passive immunotherapies is only one domain of the translational scope of this multidisciplinary field, which includes a wide range of methodologies utilising IgE against cancer: a) the utilisation of IgE as an adjuvant [Reali et al., 2001], b) the development of oral mimotope vaccination programs and IgE-coated cellular vaccines [Reali et al., 2001, Nigro et al., 2009, Nigro et al., 2012, Riemer et al., 2007], c) elucidating the roles of IgE effector cells in promoting tumour growth and strategies to deploy these cells against cancer [Dalton and Noelle, 2012, Gatault et al., 2012], d) IgE-mediated antigen uptake and cross-presentation to trigger immunoactivatory responses in cancer [Platzer et al., 2012], e) modulation of host IgE responses utilizing biological therapies [Bluth, 2012], f) induction of a more inflammatory Th_2 biased environment recruiting NKG2D cells to target tumours [Strid et al., 2008, Strid et al., 2011, Jensen-Jarolim and Pawelec, 2012], g) understanding differential associations between IgE, allergies and the incidence of a variety of cancer types and the immunological and pathological mechanisms behind these diverse findings, h) engineering therapeutic antibodies with IgE Fc regions to target cancer antigens. Moreover, investigating the presence of IgE antibodies against tumour antigens in healthy individuals and possibly in patients with cancer at different disease stages would provide evidence of the role of IgE in natural immune surveillance and improve our understanding of host immunity. The unique

features of IgE antibodies such as stimulating local immune activation in allergy and parasitic infections, include potent effector cell activation and target cell clearance -as in the case of protection from parasitic infections- and prolonged immune reaction at the site of antigen provocation, as in the case of allergen challenge. These properties provide the basis for the long-standing hypothesis that these mechanisms can be employed to reject cancer. Based on the above proposed advantages of IgE therapy in solid cancers, a few research groups developed techniques to produce recombinant IgE antibodies directed against tumour associated antigens aiming to elucidate the potency of IgE therapies against cancer [Nagy et al., 1991, Daniels et al., 2012, Karagiannis et al., 2012, Kershaw et al., 1996, Kershaw et al., 1998]. Several pre-clinical models propose that passive IgE immunotherapy is able to recruit Fcϵ receptor-bearing effector cells and to effectively direct their inflammatory immune reactions against solid tumours. [Karagiannis et al., 2012]. It is noteworthy that although IgE is present in the skin, the concept of IgE immunotherapy for solid tumours of the skin has not been tested until now. Melanoma with its large number of FcϵR bearing immune cells such as mast cells and macrophages and its origin in the skin may serve as an ideal candidate for IgE immunotherapy [Duncan et al., 1998, Erdag et al., 2012, Tth-Jakatics et al., 2000] and this research stream was conducted as part of this thesis. Investigating immune responses in cancer depends highly on the choice of antigen. CSPG4 represents an ideal target for a monoclonal antibody therapy since it is over-expressed on the surface of melanoma and other cancer cells [Campoli et al., 2010]. It was described that CSPG4 enhances the metastatic potential of tumour cells and that its blockade by the monoclonal antibody clone 225.28s leads to non-immunological mechanism-led tumour restriction [Price et al., 2011]. Further reports show that anti-CSPG4 225.28s restricts tumour growth in murine xenograft models *in vivo* [Hafner et al., 2005b, Hafner et al., 2005a]. By engineering an antibody of this specificity with human Fc regions, this clone derivative is herein armed with not only direct, but also effector cell-mediated tumour killing properties.

6.3.2 An anti-CSPG4 IgE antibody restricts tumour growth *in vitro* and *in vivo*

My colleague Amy Gilbert evaluated the chimeric anti-CSPG4 antibodies (IgE and IgG_1) Fab functions and demonstrated that these antibodies block melanoma cell adhesion and migration, thus targeting these known tumour-promoting advantages that CSPG4 expression provides for melanoma cells. This inhibition may be explained by the binding site of the antibody which recognises an epitope of the core glycoprotein component of CSPG4, a region that has been described to contain integrin and collagen binding sites, and it therefore contributes to adhesion and migration stimuli for melanoma cells [Wilson et al., 1981,Price et al., 2011,Kantor et al., 1986]. In addition to these findings, I evaluated the capability of the antibodies to restrict cell proliferation and to induce immune cell mediated responses (Chapter 5). IgE responses have been described against allergens and also as part of protective immunity against parasitic infections, through performing effector functions such as antibody dependent cell mediated cytotoxicity and antibody dependent cell-mediated phagocytosis. These effects were examined using the engineered anti-CSPG4 IgG_1 and IgE antibodies with human Fc regions, together with effector cells isolated from melanoma patients. Such Fc receptor mechanisms are described here for the first time with regards to this antibody clone, since the original clone, 225.28s, bears only murine Fc regions which are not able to effectively activate human immune cells (Bergman, Basse et al. 2000). The results of the *in vitro* studies demonstrate that anti-CSPG4 IgG_1 and IgE antibodies mediated tumour cell killing via ADCP or ADCC, triggered through the engagement of Fc receptors on human monocytes, which are known to express Fcγ and Fcϵ receptors [Maurer et al., 1994, Karagiannis et al., 2003]. Additionally, investigating the effects of antibodies *in vivo* is important, as several attributes of antibodies such as bioavailability cannot be mimicked *in vitro*. The anti-CSPG4 IgE antibody significantly restricted tumour growth when compared to its IgG1 counterpart in a humanised mouse model. In this model, anti-CSPG4 IgE recruited significant $CD68^+$ macrophage infiltration into the tumours, indicating that these cells might be altered towards an "activated" phenotype when engaged by a tumour-specific IgE antibody. This activation in the presence of IgE can result in anti-tumoural rather than tumour-promoting functions for these cells. Furthermore, enhanced overall survival of tumour-bearing animals was demonstrated in three tu-

mour transplants given to immunocompromised mice together with HLA-matched PBLs. These findings suggest that despite known immunosuppressive mechanisms at play in the circulation and in tumour microenvironments, the patient immune system has the capacity to be reactivated and redirected against autologous tumours by the use of tumour antigen-specific human/chimeric IgE antibodies. Thus, this latter model system contributes to the translational significance of this and perhaps other IgE antibody therapies. These findings complement data of previous investigations, which elucidate the effector functions of human, humanised and chimeric IgG and IgE antibodies recognizing different tumour associated antigens. These include research by our group on a trastuzumab IgE homologue recognising the Her2/neu antigen expressed on breast cancer cells [Karagiannis et al., 2009] and extensive studies on the chimeric IgG and IgE antibodies against the Folate Receptor α (FRα), another tumour-associated antigen expressed on ovarian cancer and mesothelioma tumour cells [Karagiannis et al., 2003, Karagiannis et al., 2012]. The latter antibody has shown significantly improved efficacy when directly compared to the corresponding IgG1 in three *in vivo* and numerous *in vitro* models of cancer. Collectively, these studies pave the way for the progression of CSPG4 IgE towards further pre-clinical testing and possibly future translation for clinical use.

6.3.3 Future work to extend the translational concept of Allergo-Oncology

The work presented in this thesis contributes to the nascent field of Allergo-Oncology, as here the efficacy of IgE antibodies against melanoma is demonstrated using a number of *in vitro* functional assays and two highly translational models of cancer *in vivo*. This data, together with on-going studies on MOv18 IgE against FRα-expressing tumours and with other IgE antibodies against a number of other tumour markers, indicate that IgE immunotherapy has a broad applicability across different solid tumours and can therefore be considered as an alternative treatment to IgG antibody class therapy. The applicability of IgE immunotherapy for cancer has been reported in a number of pre-clinical models of different malignant disease indications. These include several humanised xenograft models of ovarian cancer [Karagiannis et al., 2008, Karagiannis et al., 2007], human FcϵRIα transgenic mouse models of breast

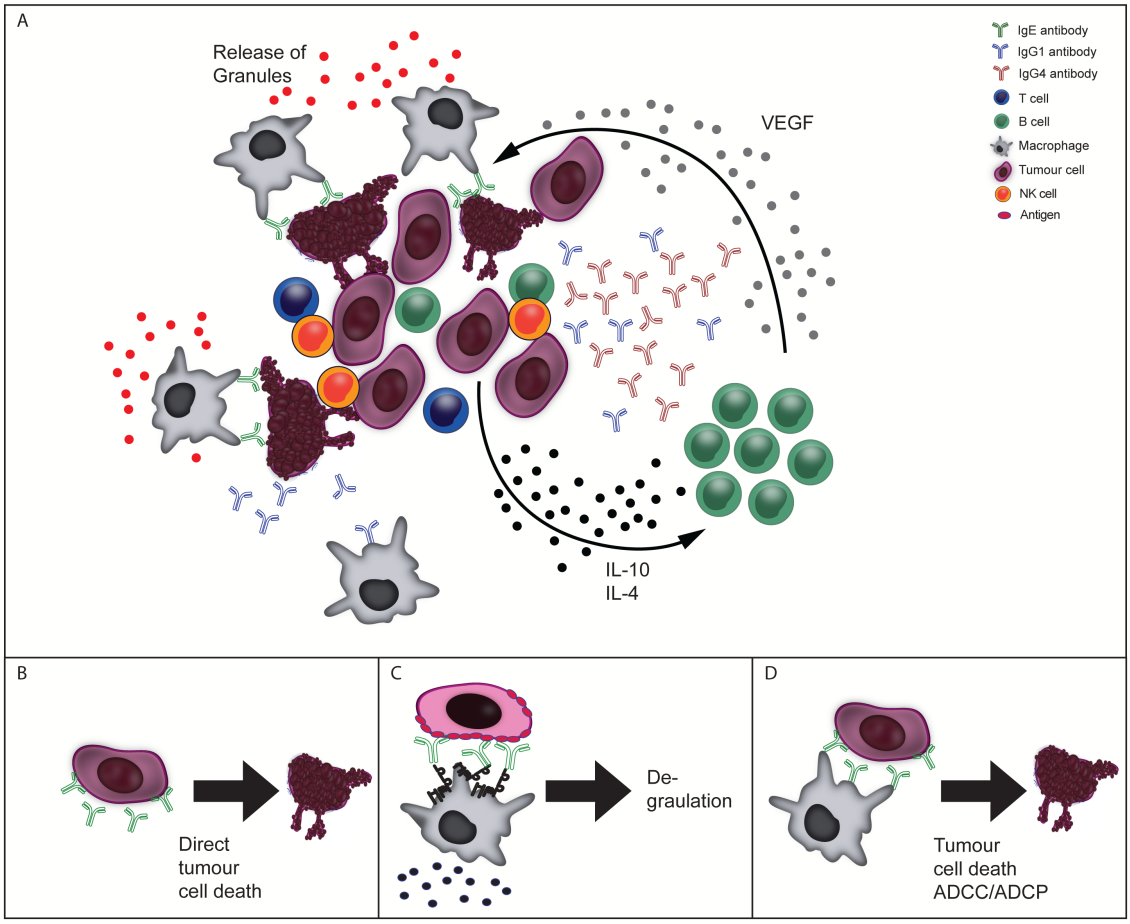

Figure 6.2: IgE immunotherapy induces tumour cell killing and may be less prone to IgG_4 effector cell impairment in the tumour microenviroment A) Tumour cells, aided by immune inflammatory and stromal cells in the tumour microenvironment, can polarise immune effector cells and inhibit their anti-tumour function. IgE loaded immune cells can mediate tumour cell death. B) Tumour specific IgE antibodies are directly inducing antibody-dependent tumour cell killing. C) IgE triggers degraulation upon cross-linking of FcϵRI on effector cells in the presence of antigen expressing cancer cells. D) Tumour specific IgE antibodies can mediate effective antibody-dependent tumour cell killing by immune effector cells (e.g. monocytes/macrophages) through activation of FcϵR signalling (by mechanisms such as ADCC and ADCP.

and prostate cancer [Daniels et al., 2012,Daniels-Wells et al., 2013], and an immunocompetent sygeneic rat model of colorectal adenocarcinoma grown as lung metastases (Debra H Josephs, PhD thesis, 2013, KCL). All those models have supported both the safety and efficacy for the applied IgE therapy and several of those models demonstrated superiority of IgE when compared directly with its IgG_1 counterpart.

Furthermore, key data by Rudman et al. provided evidence that a tumour antigen-specific IgE (MOv18 IgE) does not induce activation of effector cells that may contribute to the onset of type I hypersensitivity when this antibody is added to human blood. Two readouts were adopted in this study; these are normally used in the field of allergy to help predict and diagnose patient hypersensitivity to allergens or medicinal drugs. The findings support the prediction that i.v administration of a human cancer antigen-specific IgE would not be expected to induce early signs of Type I hypersensitivity reactions which may potentially lead to anaphylaxis. Additionally, my fellow PhD student Dr. Debra H. Josephs provided additional supporting evidence for the future clinical utility of IgE by demonstrating the safety and efficacy of MOv18 IgE in a dose escalating study using an immunocompetent rat model of a syngeneic FRα-expressing adenocarcinoma that grows as lung metastases in these animals. In support of IgE antibody therapeutic translation towards clinical use, Daniels and colleagues have reported administration of a tumour antigen-specific human IgE in a primate species (cynomolgus monkey) as part of a pharmacokinetic study. Despite cross-reactivity of human IgE Fc regions with primate Fcϵ receptors (Dr. Louise Saul, KCL, manuscript in preparation and personal communication), this systemic IgE administration did not yield any toxic effects in these animals. The combined efficacy and safety data collected using at least five *in vivo* models of cancer and numerous *in vitro* and *ex vivo* functional assays by our group alone, together with work independently conducted by others in a number of diverse model systems, underpin the case for clinical testing and applicability of this novel approach. Although a number of reports provide confidence that IgE antibodies are not likely to be associated with toxicity and might therefore be safe upon clinical application, the issue of safety should be considered when designing IgE therapeutics. While mediating potent immune reactions by IgE are well-desired within the tumour microenvironments in order to induce tumour eradication, it will always remain important to avoid designing an IgE antibody therapeutic that recognises repeat epitopes per tumour antigen and against antigens found at high levels in soluble multivalent form in patient circulation. This is because Type I hypersensitivity may be triggered by crosslinking FcϵRI on the surface of circulating basophils by soluble IgE complexes with multivalent but not monovalent antigens when found at high concentrations in blood. This concept is exemplified by *ex vivo* data which demonstrate no early signs of basophil or mast cell activation or degranulation in the presence of MOv18 and patient sera or blood, despite elevated levels of soluble target antigen FRα in the

circulation, reported by us and others. The antigenic target FRα is known to be shed in the circulation in a monovalent form, and because of its monovalent nature, it could not cross-link MOv18 IgE bound on circulating patient basophils. Thus, designing antibodies against antigens not shed at high levels in multivalent form in the circulation is expected to minimise the risk of any potential adverse events. In future, similar studies to those conducted by Rudman et al for MOv18 IgE should also be conducted for CSPG4 IgE and its target antigen, CSPG4, by interrogating *ex vivo* and *in vitro* functional assays using sera and whole blood specimens from patients with melanoma. These will provide some confidence that any shed circulating tumour antigen would not trigger basophil degranulation in patient circulation with systemic administration of CSPG4 IgE. An important aspect of translating IgE antibodies in cancer therapy would lie with dissecting the mechanisms associated with their superior efficacy in comparison to their IgG_1 counterparts. For instance:

1. Investigating pro-inflammatory cytokines as well as chemokines such as MCP-1 (Debra H Josephs, PhD thesis, 2013, KCL) released upon cross-linking of FcϵRs by IgE receptor-bearing cells in the tumour microenvironment are shown to correspond to increased macrophage infiltration and tumour clearance. These findings suggest important roles for IgE antibodies in recruiting and redirecting potent immune effector cells against cancer, providing novel insights into the mechanisms through which IgE antibodies may operate to destroy cancer cells.

2. Furthermore, recent findings demonstrated increased IgE secretion in sera of OVA-immunised mice associated with lymphoid stress. This increase in IgE antibodies was linked with increased levels of NKG2D-expressing cells such as NK and $\gamma\delta$T cells. Following from these findings, it is possible that tumour antigen-specific IgE antibodies may trigger immune activation in Th_2-biased environments which may trigger enhanced infiltration of cells bearing the natural killer cell activation receptor NKG2D, such as NK cells and $CD8^+$ T cells. Thus, IgE treatment would not only trigger tumour killing through mechanisms such as ADCC and ADCP directly mediated by the antibody itself, but it may additionally potentiate the recruitment of $NKG2D^+$ innate immune cells which can participate in further tumour cell clearance independently of IgE.

3. The possibility that IgE antibodies may or may not be subject to IgG_4 blockade in patients with melanoma requires further investigation. IgE antibodies

may be less prone to IgG_4 suppressive functions than IgG_1 antibodies because they activate immune effector cells through a different set of Fc receptors to IgG_1, which IgG_4 antibodies do not recognise. Thus, IgG_4 antibodies may not compete with IgE for recognition of FcϵRs in a way they compete with IgG_1 antibodies for recognition and activation of FcγRI. However, since Fcϵ and Fcγ receptors share the β subunit, it is possible that occupancy of FcγRs may impede FcϵR cell surface expression and therefore the effector functions of IgE antibodies. Furthermore, our findings that some IgG_4 antibodies in tumours and patient circulation recognise tumour cells may also constitute a mechanism by which IgG_4 antibodies could block tumour antigen-specific IgE antibodies from engaging and clearing tumour cells. This has been demonstrated in the context of allergy, as IgG_4 antibodies elevated in patients receiving allergen immunotherapies have been shown to partly inhibit allergen-specific IgE antibodies from recognising their specific epitopes on allergens [James et al., 2012]. Further mechanistic evaluations will be required to elucidate whether and to what extend IgE antibodies, either administered as therapeutics or naturally produced in response to tumour growth in patients, may be subject to IgG_4 blockade.

4. Future studies may focus on elucidating the recruitment of innate as well as adaptive immune cells following IgE treatment, and this could lead to the discovery of novel immune regulatory pathways, possibly including identification of new molecules which can activate effective anti-tumoural responses in the host independently of IgE therapeutics.

5. Investigation of the released cytokine-chemokine milieu in tumours might pave the way for drug-conjugated antibody immunotherapies aiming to modulate the tumour microenvironment in the context of tumour-induced immunoediting, making tumours susceptible to immune cell activation and attack.

The ensuing knowledge from explorations such as those mentioned above could lead to the design of better therapeutics with greater tumour eradication potential and to better clinical management of cancer patients.

6.4 Antibodies and Melanoma: Final remarks

Taken together the data presented in this thesis enhance our understanding of the interactions between the humoral response and tumours and present a translational interpretation of these findings by examining IgE antibody immunotherapy for cancer. The findings pave the way for further exploring novel mechanisms associated with immunoediting and irreversible immune escape in metastatic disease. Such knowledge could give rise to the design of novel therapies less prone to immune modulation which could prevent incurable malignant disease. Furthermore, these data point out that tumour-induced inflammatory conditions lead to secretion of serologically detectable proteins such as IgG_4, which may be directly involved in the pathogenesis of malignant disease and immune escape. These explorations may yield more robust disease-relevant biomarkers that can improve patient care at early stages of melanoma, where an unmet clinical need still exists to aid prognosis, stratification and early interventions. And finally, the efficacy of IgE as an emerging immunotherapeutic agent is evaluated and data presented here support previous findings with other IgE therapeutic approaches in a variety of tumour types, and indicate the superiority of the IgE antibody class compared to the conventional IgG in the treatment of solid tumours, including melanoma.

7 Abbreviations

ADCC	Antibody Dependent Cellular Cytotoxicity
ADCP	Antibody Dependent Cellular Phagocytosis
AKT	Protein Kinase B
APC	Antigen Presenting Cell
BCR	B Cell Receptor
CDC	Complement Dependent Cytotoxicity
CDR	Complementarity Determining Region
CFSE	Carboxy Fluorescein Diacetate Succinimidyl Ester
CSR	Class Switch Recombination
CTC	Circulating Tumour Cell
CTL	Cytotoxic T Lymphocyte
CTLA-4	Cytotoxic Lymphocyte Antigen 4
CXCL	CXC Chemokine Ligand
DAB	3,3'-Diaminobenzidine
DC	Dendritic Cell
dH_2O	distilled water
DNP	Dinitrophenyl
EDTA	Ethylenediaminetetraacetic acid
EGF	Epidermal Growth Factor
EGFR	Epidermal Growth Factor Receptor

EMA	European Medicines Agency
Fab	Fragment of Antigen Binding
FACS	Fluorescence-Activated Cell Sorting
Fc	Fragment Crystallisable
FcαR	Fc Alpha Receptor
FcγR	Fc Gamma Receptor
FcϵR	Fc Epsilon Receptor
FcR	Fc Receptor
FDA	Food and Drug Administration
FDR	Framework Determining Region
FRα	Folate Receptor Alpha
GPI	Glycophosphatidylinositol
HACA	Human Anti-Chimeric Antibody
HAHA	Human Anti-Human Antibody
HAMA	Human Anti-Mouse Antibody
HEK	Human Embryonic Kidney
HER2/neu	Human Epidermal Growth Factor Receptor 2
HMW	High Molecular Weight
HPLC	High Performance Liquid Chromatography
HRP	Horse radish peroxidase
IFNγ	Interferon Gamma
Ig	Immunoglobulin
IHC	Immunohistochemical
IL	Interleukin
iNOS	Inducible Nitric Oxide Synthase
ITAM	Immunoreceptor Tyrosine-Based Activation Motif
ITIM	Immunoreceptor Tyrosine-Based Inhibitory Motif
LMW	Low Molecular Weight
LN	Lymph Node
mAb	Monoclonal Antibody
MFI	Median Fluorescence Intensity
MHC	Major Histocompatibility Complex
MMTV	Mouse Mammary Tumour Virus
NHP	Non-Human Primate
NK	Natural Killer

NO	Nitric Oxide
NOD	Non-Obese Diabetic
OS	Overall Survival
PBL	Peripheral Blood Leukocyte
PBMC	Peripheral Blood Mononuclear Cell
PD-1	Programmed Death 1
PDL-1	Programmed Death Ligand 1
PI3K	Phosphatidylinositide 3-Kinase
PFS	Progression Free Survival
PTK2	Protein Tyrosine Kinase 2
PBS	Phosphate buffered saline
PMSF	phenylmethanesulfonylfluoride
RBL	Rat Basophilic Leukaemia
REC	Research Ethics Committee
RNA	Ribonucleic acid
RT	Room temperature
scFv	Single-Chain Fragments of the Variable Region
SCID	Severe Combined Immunodeficiency
SDS-PAGE	Sodium dodecyl sulphate polyacrylamide gel electrophoresis
TAA	Tumour-Associated Antigen
TAM	Tumour-Associated Macrophage
TATE	Tumour-Associated Tissue Eosinophilia
TGF	Transforming Growth Factor
Th1	T Helper Cell Subset 1
Th17	T Helper Cell Subset 17
Th2	T Helper Cell Subset 2
TME	Tumour Microenvironment
TNFα	Tumour Necrosis Factor Alpha
Treg	TRegulatory T Cell
UV	Ultraviolet
VDJ	Variable Diverse and Joining
VEGF	Vascular Endothelial Growth Factor

8 References

[Aalberse et al., 2009] Aalberse, R. C., Stapel, S. O., Schuurman, J. and Rispens, T. (2009). Immunoglobulin G4: an odd antibody. Clin Exp Allergy *39*, 469–477.

[Agarwal et al., 2006] Agarwal, A., Verma, S., Burra, U., Murthy, N. S., Mohanty, N. K. and Saxena, S. (2006). Flow cytometric analysis of Th1 and Th2 cytokines in PBMCs as a parameter of immunological dysfunction in patients of superficial transitional cell carcinoma of bladder. Cancer Immunol Immunother *55*, 734–743.

[Ali et al., 2012] Ali, N., Flutter, B., Sanchez Rodriguez, R., Sharif-Paghaleh, E., Barber, L. D., Lombardi, G. and Nestle, F. O. (2012). Xenogeneic graft-versus-host-disease in NOD-scid IL-2Rnull mice display a T-effector memory phenotype. PLoS One *7*.

[Aloulou et al., 2012] Aloulou, M., Ben Mkaddem, S., Biarnes-Pelicot, M., Boussetta, T., Souchet, H., Rossato, E., Benhamou, M., Crestani, B., Zhu, Z., Blank, U., Launay, P. and Monteiro, R. C. (2012). IgG1 and IVIg induce inhibitory ITAM signaling through FcγRIII controlling inflammatory responses. Blood *119*, 3084–3096.

[Altman et al., 2012] Altman, D. G., McShane, L. M., Sauerbrei, W. and Taube, S. E. (2012). Reporting Recommendations for Tumor Marker Prognostic Studies (REMARK): explanation and elaboration. PLoS Med *9*.

[Amur et al., 2008] Amur, S., Frueh, F. W., Lesko, L. J. and Huang, S. M. (2008). Integration and use of biomarkers in drug development, regulation and clinical practice: a US regulatory perspective. Biomark Med *2*, 305–311.

[Andreu et al., 2010] Andreu, P., Johansson, M., Affara, N. I., Pucci, F., Tan, T., Junankar, S., Korets, L., Lam, J., Tawfik, D., DeNardo, D. G., Naldini, L., de Visser, K. E., De Palma, M. and Coussens, L. M. (2010). FcRgamma activation regulates inflammation-associated squamous carcinogenesis. Cancer Cell *17*, 121–134.

[Angal et al., 1993] Angal, S., King, D. J., Bodmer, M. W., Turner, A., Lawson, A. D., Roberts, G., Pedley, B. and Adair, J. R. (1993). A single amino acid substitution abolishes the heterogeneity of chimeric mouse/human (IgG4) antibody. Mol Immunol *30*, 105–108.

[Angell and Galon, 2013] Angell, H. and Galon, J. (2013). From the immune contexture to the Immunoscore: the role of prognostic and predictive immune markers in cancer. Curr Opin Immunol *25*, 261–267.

[Armitage et al., 1993] Armitage, R. J., Macduff, B. M., Spriggs, M. K. and Fanslow, W. C. (1993). Human B cell proliferation and Ig secretion induced by recombinant CD40 ligand are modulated by soluble cytokines. J Immunol *150*, 3671–3680.

[Ascierto et al., 2011] Ascierto, P. A., Marincola, F. M. and Ribas, A. (2011). Anti-CTLA4 monoclonal antibodies: the past and the future in clinical application. J Transl Med *9*, 196–196.

[Aucouturier et al., 1984] Aucouturier, P., Danon, F., Daveau, M., Guillou, B., Sabbah, A., Besson, J. and Preud'homme, J. L. (1984). Measurement of serum IgG4 levels by a competitive immunoenzymatic assay with monoclonal antibodies. J Immunol Methods *74*, 151–162.

[Bakema et al., 2011] Bakema, J. E., Ganzevles, S. H., Fluitsma, D. M., Schilham, M. W., Beelen, R. H., Valerius, T., Lohse, S., Glennie, M. J., Medema, J. P. and van Egmond, M. (2011). Targeting FcaRI on polymorphonuclear cells induces tumor cell killing through autophagy. J Immunol *187*, 726–732.

[Baker, 2003] Baker, S. G. (2003). The central role of receiver operating characteristic (ROC) curves in evaluating tests for the early detection of cancer. J Natl Cancer Inst *95*, 511–515.

[Balch et al., 2009] Balch, C. M., Gershenwald, J. E., Soong, S. J., Thompson, J. F., Atkins, M. B., Byrd, D. R., Buzaid, A. C., Cochran, A. J., Coit, D. G., Ding, S., Eggermont, A. M., Flaherty, K. T., Gimotty, P. A., Kirkwood, J. M., McMasters, K. M., Mihm, M. C., Morton, D. L., Ross, M. I., Sober, A. J. and Sondak, V. K. (2009). Final version of 2009 AJCC melanoma staging and classification. J Clin Oncol *27*, 6199–6206.

[Balu et al., 2011] Balu, S., Reljic, R., Lewis, M. J., Pleass, R. J., McIntosh, R., van Kooten, C., van Egmond, M., Challacombe, S., Woof, J. M. and Ivanyi, J. (2011). A novel human IgA monoclonal antibody protects against tuberculosis. J Immunol *186*, 3113–3119.

[Banchereau et al., 1994] Banchereau, J., Brière, F., Liu, Y. J. and Rousset, F. (1994). Molecular control of B lymphocyte growth and differentiation. Stem Cells *12*, 278–288.

[Bassing et al., 2002] Bassing, C. H., Swat, W. and Alt, F. W. (2002). The mechanism and regulation of chromosomal V(D)J recombination. Cell *109 Suppl*, 45–55.

[Beatty et al., 2011] Beatty, G. L., Chiorean, E. G., Fishman, M. P., Saboury, B., Teitelbaum, U. R., Sun, W., Huhn, R. D., Song, W., Li, D., Sharp, L. L., Torigian, D. A., O'Dwyer, P. J. and Vonderheide, R. H. (2011). CD40 agonists alter tumor stroma and show efficacy against pancreatic carcinoma in mice and humans. Science *331*, 1612–1616.

[Beck et al., 2001] Beck, C., Schreiber, H. and Rowley, D. (2001). Role of TGF-beta in immune-evasion of cancer. Microsc Res Tech *52*, 387–395.

[Beck and Salant, 2010] Beck, L. H. and Salant, D. J. (2010). Membranous nephropathy: recent travels and new roads ahead. Kidney Int *77*, 765–770.

[Becker et al., 2009] Becker, M. R., Siegelin, M. D., Rompel, R., Enk, A. H. and Gaiser, T. (2009). COX-2 expression in malignant melanoma: a novel prognostic marker? Melanoma Res *19*, 8–16.

[Becker et al., 2010] Becker, P. D., Legrand, N., van Geelen, C. M., Noerder, M., Huntington, N. D., Lim, A., Yasuda, E., Diehl, S. A., Scheeren, F. A., Ott, M., Weijer, K., Wedemeyer, H., Di Santo, J. P., Beaumont, T., Guzman, C. A. and Spits, H. (2010). Generation of human antigen-specific monoclonal IgM antibodies using vaccinated "human immune system" mice. PLoS One *5*.

[Bender et al., 1997] Bender, H., Grapow, M., Schomburg, A., Reinhold, U. and Biersack, H. J. (1997). Effects of diagnostic application of monoclonal antibody on survival in melanoma patients. Hybridoma *16*, 65–68.

[Beyeler et al., 2006] Beyeler, M., Waldispuhl, S., Strobel, K., Joller-Jemelka, H. I., Burg, G. and Dummer, R. (2006). Detection of melanoma relapse: first comparative analysis on imaging techniques versus S100 protein. Dermatology *213*, 187–191.

[Biswas and Mantovani, 2010] Biswas, S. K. and Mantovani, A. (2010). Macrophage plasticity and interaction with lymphocyte subsets: cancer as a paradigm. Nat Immunol *11*, 889–896.

[Bloom et al., 1997] Bloom, J. W., Madanat, M. S., Marriott, D., Wong, T. and Chan, S. Y. (1997). Intrachain disulfide bond in the core hinge region of human IgG4. Protein Sci *6*, 407–415.

[Bluth, 2012] Bluth, M. H. (2012). IgE and chemotherapy. Cancer Immunol Immunother *61*, 1585–1590.

[Bodinier et al., 2008] Bodinier, M., Brossard, C., Triballeau, S., Morisset, M., Guérin-Marchand, C., Pineau, F., de Coppet, P., Moneret-Vautrin, D. A., Blank, U. and Denery-Papini, S. (2008). Evaluation of an in vitro mast cell degranulation test in the context of food allergy to wheat. Int Arch Allergy Immunol *146*, 307–320.

[Boon and van der Bruggen, 1996] Boon, T. and van der Bruggen, P. (1996). Human tumor antigens recognized by T lymphocytes. J Exp Med *183*, 725–729.

[Bosserhoff, 2006] Bosserhoff, A. K. (2006). Novel biomarkers in malignant melanoma. Clin Chim Acta *367*, 28–35.

[Bosserhoff et al., 2004] Bosserhoff, A. K., Küster, H. and Hein, R. (2004). Elevated MIA levels in the serum of pregnant women and of children. Clin Exp Dermatol *29*, 628–629.

[Bouwhuis et al., 2011] Bouwhuis, M. G., Suciu, S., Kruit, W., Salès, F., Stoitchkov, K., Patel, P., Cocquyt, V., Thomas, J., Liénard, D., Eggermont, A. M., Ghanem, G. and European Organisation for Research and Treatment of Cancer Melanoma Group (2011). Prognostic value of serial blood S100B determinations in stage IIB-III melanoma patients: a corollary study to EORTC trial 18952. Eur J Cancer *47*, 361–368.

[Bracher et al., 2007] Bracher, M., Gould, H. J., Sutton, B. J., Dombrowicz, D. and Karagiannis, S. N. (2007). Three-colour flow cytometric method to measure antibody-dependent tumour cell killing by cytotoxicity and phagocytosis. J Immunol Methods *323*, 160–171.

[Brahmer et al., 2010] Brahmer, J. R., Drake, C. G., Wollner, I., Powderly, J. D., Picus, J., Sharfman, W. H., Stankevich, E., Pons, A., Salay, T. M., McMiller, T. L., Gilson, M. M., Wang, C., Selby, M., Taube, J. M., Anders, R., Chen, L., Korman, A. J., Pardoll, D. M., Lowy, I. and Topalian, S. L. (2010). Phase I study of single-agent anti-programmed death-1 (MDX-1106) in refractory solid tumors: safety, clinical activity, pharmacodynamics, and immunologic correlates. J Clin Oncol *28*, 3167–3175.

[Brekke et al., 1994] Brekke, O. H., Michaelsen, T. E., Aase, A., Sandin, R. H. and Sandlie, I. (1994). Human IgG isotype-specific amino acid residues affecting complement-mediated cell lysis and phagocytosis. Eur J Immunol *24*, 2542–2547.

[Brown et al., 2012] Brown, E. R., Doig, T., Anderson, N., Brenn, T., Doherty, V., Xu, Y., Bartlett, J. M., Smyth, J. F. and Melton, D. W. (2012). Association of galectin-3 expression with melanoma progression and prognosis. Eur J Cancer *48*, 865–874.

[Brüggemann et al., 1987] Brüggemann, M., Williams, G. T., Bindon, C. I., Clark, M. R., Walker, M. R., Jefferis, R., Waldmann, H. and Neuberger, M. S. (1987). Comparison of the effector functions of human immunoglobulins using a matched set of chimeric antibodies. J Exp Med *166*, 1351–1361.

[Bruhns et al., 2009] Bruhns, P., Iannascoli, B., England, P., Mancardi, D. A., Fernandez, N., Jorieux, S. and Daëron, M. (2009). Specificity and affinity of human Fcgamma receptors and their polymorphic variants for human IgG subclasses. Blood *113*, 3716–3725.

[Buljan et al., 2011] Buljan, M., Situm, M., Tomas, D., Milosevic, M. and Kruslin, B. (2011). Prognostic value of galectin-3 in primary cutaneous melanoma. J Eur Acad Dermatol Venereol *25*, 1174–1181.

[Bunk et al., 2010] Bunk, S., Sigel, S., Metzdorf, D., Sharif, O., Triantafilou, K., Triantafilou, M., Hartung, T., Knapp, S. and von Aulock, S. (2010). Internalization and coreceptor expression are critical for TLR2-mediated recognition of lipoteichoic acid in human peripheral blood. J Immunol *185*, 3708–3717.

[Burmeister et al., 2012] Burmeister, B. H., Henderson, M. A., Ainslie, J., Fisher, R., Di Iulio, J., Smithers, B. M., Hong, A., Shannon, K., Scolyer, R. A., Carruthers, S., Coventry, B. J., Babington, S., Duprat, J., Hoekstra, H. J. and Thompson, J. F. (2012). Adjuvant radiotherapy versus observation alone for patients at risk of lymph-node field relapse after therapeutic lymphadenectomy for melanoma: a randomised trial. Lancet Oncol *13*, 589–597.

[Burns et al., 2010] Burns, W. R., Zhao, Y., Frankel, T. L., Hinrichs, C. S., Zheng, Z., Xu, H., Feldman, S. A., Ferrone, S., Rosenberg, S. A. and Morgan, R. A. (2010). A high molecular weight melanoma-associated antigen-specific chimeric antigen receptor redirects lymphocytes to target human melanomas. Cancer Res *70*, 3027–3033.

[Butler, 2008] Butler, M. S. (2008). Natural products to drugs: natural product-derived compounds in clinical trials. Nat Prod Rep *25*, 475–516.

[Cai et al., 2011] Cai, S. W., Yang, S. Z., Gao, J., Pan, K., Chen, J. Y., Wang, Y. L., Wei, L. X. and Dong, J. H. (2011). Prognostic significance of mast cell count following curative resection for pancreatic ductal adenocarcinoma. Surgery *149*, 576–584.

[Campoli et al., 2010] Campoli, M., Ferrone, S. and Wang, X. (2010). Functional and clinical relevance of chondroitin sulfate proteoglycan 4. Adv Cancer Res *109*, 73–121.

[Canfield and Morrison, 1991] Canfield, S. M. and Morrison, S. L. (1991). The binding affinity of human IgG for its high affinity Fc receptor is determined by multiple amino acids in the CH2 domain and is modulated by the hinge region. J Exp Med *173*, 1483–1491.

[Canonica et al., 2009] Canonica, G. W., Bousquet, J., Casale, T., Lockey, R. F., Baena-Cagnani, C. E., Pawankar, R., Potter, P. C., Bousquet, P. J., Cox, L. S., Durham, S. R., Nelson, H. S., Passalacqua, G., Ryan, D. P., Brozek, J. L., Compalati, E., Dahl, R., Delgado, L., van Wijk, R. G., Gower, R. G., Ledford, D. K., Filho, N. R., Valovirta, E. J., Yusuf, O. M., Zuberbier, T., Akhanda, W., Almarales, R. C., Ansotegui, I., Bonifazi, F., Ceuppens, J., Chivato, T., Dimova, D., Dumitrascu, D., Fontana, L., Katelaris, C. H., Kaulsay, R., Kuna, P., Larenas-Linnemann, D., Manoussakis, M., Nekam, K., Nunes, C., O'Hehir, R., Olaguibel, J. M., Onder, N. B., Park, J. W., Priftanji, A., Puy, R., Sarmiento, L., Scadding, G., Schmid-Grendelmeier, P., Seberova, E., Sepiashvili, R., Sol, D., Togias, A., Tomino, C., Toskala, E., Van Beever, H. and Vieths, S. (2009). Sub-lingual immunotherapy: World Allergy Organization Position Paper 2009. Allergy *64 Suppl 91*, 1–59.

[Carpenter et al., 2009] Carpenter, E. L., Mick, R., Rech, A. J., Beatty, G. L., Colligon, T. A., Rosenfeld, M. R., Kaplan, D. E., Chang, K. M., Domchek, S. M., Kanetsky, P. A., Fecher, L. A., Flaherty, K. T., Schuchter, L. M. and Vonderheide, R. H. (2009). Collapse of the CD27+ B-cell compartment associated with systemic plasmacytosis in patients with advanced melanoma and other cancers. Clin Cancer Res *15*, 4277–4287.

[Carter et al., 1992] Carter, P., Presta, L., Gorman, C. M., Ridgway, J. B., Henner, D., Wong, W. L., Rowland, A. M., Kotts, C., Carver, M. E. and Shepard, H. M. (1992). Humanization of an anti-p185HER2 antibody for human cancer therapy. Proc Natl Acad Sci U S A *89*, 4285–4289.

[Cassard et al., 2008] Cassard, L., Cohen-Solal, J. F., Fournier, E. M., Camilleri-Broët, S., Spatz, A., Chouaïb, S., Badoual, C., Varin, A., Fisson, S., Duvillard, P., Boix, C., Loncar, S. M., Sastre-Garau, X., Houghton, A. N., Avril, M. F., Gresser, I., Fridman, W. H. and Sautès-Fridman, C. (2008). Selective expression of inhibitory Fcgamma receptor by metastatic melanoma impairs tumor

susceptibility to IgG-dependent cellular response. Int J Cancer *123*, 2832–2839.

[Cazac and Roes, 2000] Cazac, B. B. and Roes, J. (2000). TGF-beta receptor controls B cell responsiveness and induction of IgA in vivo. Immunity *13*, 443–451.

[Cenci and Sitia, 2007] Cenci, S. and Sitia, R. (2007). Managing and exploiting stress in the antibody factory. FEBS Lett *581*, 3652–3657.

[Chapman et al., 2011] Chapman, P. B., Hauschild, A., Robert, C., Haanen, J. B., Ascierto, P., Larkin, J., Dummer, R., Garbe, C., Testori, A., Maio, M., Hogg, D., Lorigan, P., Lebbe, C., Jouary, T., Schadendorf, D., Ribas, A., O'Day, S. J., Sosman, J. A., Kirkwood, J. M., Eggermont, A. M., Dreno, B., Nolop, K., Li, J., Nelson, B., Hou, J., Lee, R. J., Flaherty, K. T., McArthur, G. A. and BRIM-3 Study Group (2011). Improved survival with vemurafenib in melanoma with BRAF V600E mutation. N Engl J Med *364*, 2507–2516.

[Chattopadhyay et al., 1991] Chattopadhyay, P., Kaveri, S. V., Byars, N., Starkey, J., Ferrone, S. and Raychaudhuri, S. (1991). Human high molecular weight-melanoma associated antigen mimicry by an anti-idiotypic antibody: characterization of the immunogenicity and the immune response to the mouse monoclonal antibody IMel-1. Cancer Res *51*, 6045–6051.

[Chekenya et al., 2008] Chekenya, M., Krakstad, C., Svendsen, A., Netland, I. A., Staalesen, V., Tysnes, B. B., Selheim, F., Wang, J., Sakariassen, P. Ø., Sandal, T., Lonning, P. E., Flatmark, T., Enger, P. Ø., Bjerkvig, R., Sioud, M. and Stallcup, W. B. (2008). The progenitor cell marker NG2/MPG promotes chemoresistance by activation of integrin-dependent PI3K/Akt signaling. Oncogene *27*, 5182–5194.

[Chen et al., 1994] Chen, Q., Daniel, V., Maher, D. W. and Hersey, P. (1994). Production of IL-10 by melanoma cells: examination of its role in immunosuppression mediated by melanoma. Int J Cancer *56*, 755–760.

[Cheson and Leonard, 2008] Cheson, B. D. and Leonard, J. P. (2008). Monoclonal antibody therapy for B-cell non-Hodgkin's lymphoma. N Engl J Med *359*, 613–626.

[Choi et al., 2007] Choi, E. K., Kim, M. H., Lee, T. Y., Kwon, S., Oh, H. C., Hwang, C. Y., Seo, D. W., Lee, S. S. and Lee, S. K. (2007). The sensitivity and specificity of serum immunoglobulin G and immunoglobulin G4 levels in the diagnosis of autoimmune chronic pancreatitis: Korean experience. Pancreas *35*, 156–161.

[Christiansen and Rajasekaran, 2004] Christiansen, J. and Rajasekaran, A. K. (2004). Biological impediments to monoclonal antibody-based cancer immunotherapy. Mol Cancer Ther *3*, 1493–1501.

[Chu et al., 2012] Chu, C. C., Ali, N., Karagiannis, P., Di Meglio, P., Skowera, A., Napolitano, L., Barinaga, G., Grys, K., Sharif-Paghaleh, E., Karagiannis, S. N., Peakman, M., Lombardi, G. and Nestle, F. O. (2012). Resident CD141 (BDCA3)+ dendritic cells in human skin produce IL-10 and induce regulatory T cells that suppress skin inflammation. J Exp Med *209*, 935–945.

[Clemente et al., 1996] Clemente, C. G., Mihm, M. C., Bufalino, R., Zurrida, S., Collini, P. and Cascinelli, N. (1996). Prognostic value of tumor infiltrating lymphocytes in the vertical growth phase of primary cutaneous melanoma. Cancer *77*, 1303–1310.

[Clynes et al., 2000] Clynes, R. A., Towers, T. L., Presta, L. G. and Ravetch, J. V. (2000). Inhibitory Fc receptors modulate in vivo cytotoxicity against tumor targets. Nat Med *6*, 443–446.

[Cooperman et al., 2004] Cooperman, J., Neely, R., Teachey, D. T., Grupp, S. and Choi, J. K. (2004). Cell division rates of primary human precursor B cells in culture reflect in vivo rates. Stem Cells *22*, 1111–1120.

[Cormier et al., 2006] Cormier, S. A., Taranova, A. G., Bedient, C., Nguyen, T., Protheroe, C., Pero, R., Dimina, D., Ochkur, S. I., O'Neill, K., Colbert, D., Lombari, T. R., Constant, S., McGarry, M. P., Lee, J. J. and Lee, N. A. (2006). Pivotal Advance: eosinophil infiltration of solid tumors is an early and persistent inflammatory host response. J Leukoc Biol *79*, 1131–1139.

[Cornell et al., 2007] Cornell, L. D., Chicano, S. L., Deshpande, V., Collins, A. B., Selig, M. K., Lauwers, G. Y., Barisoni, L. and Colvin, R. B. (2007).

Pseudotumors due to IgG4 immune-complex tubulointerstitial nephritis associated with autoimmune pancreatocentric disease. Am J Surg Pathol *31*, 1586–1597.

[Couper et al., 2008] Couper, K. N., Blount, D. G. and Riley, E. M. (2008). IL-10: the master regulator of immunity to infection. J Immunol *180*, 5771–5777.

[Coussens et al., 1999] Coussens, L. M., Raymond, W. W., Bergers, G., Laig-Webster, M., Behrendtsen, O., Werb, Z., Caughey, G. H. and Hanahan, D. (1999). Inflammatory mast cells up-regulate angiogenesis during squamous epithelial carcinogenesis. Genes Dev *13*, 1382–1397.

[Coussens et al., 2013] Coussens, L. M., Zitvogel, L. and Palucka, A. K. (2013). Neutralizing tumor-promoting chronic inflammation: a magic bullet? Science *339*, 286–291.

[CRUK, 2013] CRUK (2012 (accessed April 15, 2013)). Melanoma Incidence.

[Curran et al., 2010] Curran, M. A., Montalvo, W., Yagita, H. and Allison, J. P. (2010). PD-1 and CTLA-4 combination blockade expands infiltrating T cells and reduces regulatory T and myeloid cells within B16 melanoma tumors. Proc Natl Acad Sci U S A *107*, 4275–4280.

[Dai et al., 2010] Dai, F., Liu, L., Che, G., Yu, N., Pu, Q., Zhang, S., Ma, J., Ma, L. and You, Z. (2010). The number and microlocalization of tumor-associated immune cells are associated with patient's survival time in non-small cell lung cancer. BMC Cancer *10*, 220–220.

[Dalton and Noelle, 2012] Dalton, D. K. and Noelle, R. J. (2012). The roles of mast cells in anticancer immunity. Cancer Immunol Immunother *61*, 1511–1520.

[Daniels et al., 2012] Daniels, T. R., Leuchter, R. K., Quintero, R., Helguera, G., Rodríguez, J. A., Martínez-Maza, O., Schultes, B. C., Nicodemus, C. F. and Penichet, M. L. (2012). Targeting HER2/neu with a fully human IgE to harness the allergic reaction against cancer cells. Cancer Immunol Immunother *61*, 991–1003.

[Daniels-Wells et al., 2013] Daniels-Wells, T. R., Helguera, G., Leuchter, R. K., Quintero, R., Kozman, M., Rodríguez, J. A., Ortiz-Sánchez, E., Martínez-Maza, O., Schultes, B. C., Nicodemus, C. F. and Penichet, M. L. (2013). A novel IgE antibody targeting the prostate-specific antigen as a potential prostate cancer therapy. BMC Cancer *13*, 195–195.

[Darce et al., 2007a] Darce, J. R., Arendt, B. K., Chang, S. K. and Jelinek, D. F. (2007a). Divergent effects of BAFF on human memory B cell differentiation into Ig-secreting cells. J Immunol *178*, 5612–5622.

[Darce et al., 2007b] Darce, J. R., Arendt, B. K., Wu, X. and Jelinek, D. F. (2007b). Regulated expression of BAFF-binding receptors during human B cell differentiation. J Immunol *179*, 7276–7286.

[Daveau et al., 1977] Daveau, M., Pavie-Fischer, J., Rivat, L., Rivat, C., Ropartz, C., Peter, H. H., Cesarini, J. P. and Kourilsky, F. M. (1977). IgG4 subclass in malignant melanoma. J Natl Cancer Inst *58*, 189–192.

[Davey et al., 2000] Davey, G. E., Murmann, P., Hoechli, M., Tanaka, T. and Heizmann, C. W. (2000). Calcium-dependent translocation of S100A11 requires tubulin filaments. Biochim Biophys Acta *1498*, 220–232.

[Davies et al., 2013] Davies, A. M., Rispens, T., den Bleker, T. H., McDonnell, J. M., Gould, H. J., Aalberse, R. C. and Sutton, B. J. (2013). Crystal structure of the human IgG4 C(H)3 dimer reveals the role of Arg409 in the mechanism of Fab-arm exchange. Mol Immunol *54*, 1–7.

[Davies et al., 2002] Davies, H., Bignell, G. R., Cox, C., Stephens, P., Edkins, S., Clegg, S., Teague, J., Woffendin, H., Garnett, M. J., Bottomley, W., Davis, N., Dicks, E., Ewing, R., Floyd, Y., Gray, K., Hall, S., Hawes, R., Hughes, J., Kosmidou, V., Menzies, A., Mould, C., Parker, A., Stevens, C., Watt, S., Hooper, S., Wilson, R., Jayatilake, H., Gusterson, B. A., Cooper, C., Shipley, J., Hargrave, D., Pritchard-Jones, K., Maitland, N., Chenevix-Trench, G., Riggins, G. J., Bigner, D. D., Palmieri, G., Cossu, A., Flanagan, A., Nicholson, A., Ho, J. W., Leung, S. Y., Yuen, S. T., Weber, B. L., Seigler, H. F., Darrow, T. L., Paterson, H., Marais, R., Marshall, C. J., Wooster, R., Stratton, M. R. and Futreal, P. A. (2002). Mutations of the BRAF gene in human cancer. Nature *417*, 949–954.

[de Visser et al., 2005] de Visser, K. E., Korets, L. V. and Coussens, L. M. (2005). De novo carcinogenesis promoted by chronic inflammation is B lymphocyte dependent. Cancer Cell *7*, 411–423.

[de Vries et al., 2006] de Vries, M., Vonkeman, W. G., van Ginkel, R. J. and Hoekstra, H. J. (2006). Morbidity after inguinal sentinel lymph node biopsy and completion lymph node dissection in patients with cutaneous melanoma. Eur J Surg Oncol *32*, 785–789.

[de Vries et al., 2011] de Vries, V. C., Pino-Lagos, K., Nowak, E. C., Bennett, K. A., Oliva, C. and Noelle, R. J. (2011). Mast cells condition dendritic cells to mediate allograft tolerance. Immunity *35*, 550–561.

[de Vries et al., 2009] de Vries, V. C., Wasiuk, A., Bennett, K. A., Benson, M. J., Elgueta, R., Waldschmidt, T. J. and Noelle, R. J. (2009). Mast cell degranulation breaks peripheral tolerance. Am J Transplant *9*, 2270–2280.

[Del Vecchio et al., 2010] Del Vecchio, M., Mortarini, R., Canova, S., Di Guardo, L., Pimpinelli, N., Sertoli, M. R., Bedognetti, D., Queirolo, P., Morosini, P., Perrone, T., Bajetta, E. and Anichini, A. (2010). Bevacizumab plus fotemustine as first-line treatment in metastatic melanoma patients: clinical activity and modulation of angiogenesis and lymphangiogenesis factors. Clin Cancer Res *16*, 5862–5872.

[DeNardo et al., 2011] DeNardo, D. G., Brennan, D. J., Rexhepaj, E., Ruffell, B., Shiao, S. L., Madden, S. F., Gallagher, W. M., Wadhwani, N., Keil, S. D., Junaid, S. A., Rugo, H. S., Hwang, E. S., Jirström, K., West, B. L. and Coussens, L. M. (2011). Leukocyte complexity predicts breast cancer survival and functionally regulates response to chemotherapy. Cancer Discov *1*, 54–67.

[Depoil et al., 2008] Depoil, D., Fleire, S., Treanor, B. L., Weber, M., Harwood, N. E., Marchbank, K. L., Tybulewicz, V. L. and Batista, F. D. (2008). CD19 is essential for B cell activation by promoting B cell receptor-antigen microcluster formation in response to membrane-bound ligand. Nat Immunol *9*, 63–72.

[Deshpande et al., 2011] Deshpande, V., Gupta, R., Sainani, N., Sahani, D. V., Virk, R., Ferrone, C., Khosroshahi, A., Stone, J. H. and Lauwers, G. Y. (2011). Subclassification of autoimmune pancreatitis: a histologic classification with clinical significance. Am J Surg Pathol *35*, 26–35.

[Deshpande et al., 2012] Deshpande, V., Zen, Y., Chan, J. K., Yi, E. E., Sato, Y., Yoshino, T., Klöppel, G., Heathcote, J. G., Khosroshahi, A., Ferry, J. A., Aalberse, R. C., Bloch, D. B., Brugge, W. R., Bateman, A. C., Carruthers, M. N., Chari, S. T., Cheuk, W., Cornell, L. D., Fernandez-Del Castillo, C., Forcione, D. G., Hamilos, D. L., Kamisawa, T., Kasashima, S., Kawa, S., Kawano, M., Lauwers, G. Y., Masaki, Y., Nakanuma, Y., Notohara, K., Okazaki, K., Ryu, J. K., Saeki, T., Sahani, D. V., Smyrk, T. C., Stone, J. R., Takahira, M., Webster, G. J., Yamamoto, M., Zamboni, G., Umehara, H. and Stone, J. H. (2012). Consensus statement on the pathology of IgG4-related disease. Mod Pathol *25*, 1181–1192.

[Dhaliwal et al., 2012] Dhaliwal, B., Yuan, D., Pang, M. O., Henry, A. J., Cain, K., Oxbrow, A., Fabiane, S. M., Beavil, A. J., McDonnell, J. M., Gould, H. J. and Sutton, B. J. (2012). Crystal structure of IgE bound to its B-cell receptor CD23 reveals a mechanism of reciprocal allosteric inhibition with high affinity receptor FcεRI. Proc Natl Acad Sci U S A *109*, 12686–12691.

[Di Noia and Neuberger, 2007] Di Noia, J. M. and Neuberger, M. S. (2007). Molecular mechanisms of antibody somatic hypermutation. Annu Rev Biochem *76*, 1–22.

[Díaz-Lagares et al., 2011] Díaz-Lagares, A., Alegre, E., Arroyo, A., González-Cao, M., Zudaire, M. E., Viteri, S., Martín-Algarra, S. and González, A. (2011). Evaluation of multiple serum markers in advanced melanoma. Tumour Biol *32*, 1155–1161.

[DiSanto et al., 1993] DiSanto, J. P., Bonnefoy, J. Y., Gauchat, J. F., Fischer, A. and de Saint Basile, G. (1993). CD40 ligand mutations in x-linked immunodeficiency with hyper-IgM. Nature *361*, 541–543.

[Dong et al., 2002] Dong, H., Strome, S. E., Salomao, D. R., Tamura, H., Hirano, F., Flies, D. B., Roche, P. C., Lu, J., Zhu, G., Tamada, K., Lennon, V. A., Celis, E. and Chen, L. (2002). Tumor-associated B7-H1 promotes T-cell apoptosis: a potential mechanism of immune evasion. Nat Med *8*, 793–800.

[Dorta et al., 2002] Dorta, R. G., Landman, G., Kowalski, L. P., Lauris, J. R., Latorre, M. R. and Oliveira, D. T. (2002). Tumour-associated tissue eosinophilia

as a prognostic factor in oral squamous cell carcinomas. Histopathology *41*, 152–157.

[Downey et al., 2007] Downey, S. G., Klapper, J. A., Smith, F. O., Yang, J. C., Sherry, R. M., Royal, R. E., Kammula, U. S., Hughes, M. S., Allen, T. E., Levy, C. L., Yellin, M., Nichol, G., White, D. E., Steinberg, S. M. and Rosenberg, S. A. (2007). Prognostic factors related to clinical response in patients with metastatic melanoma treated by CTL-associated antigen-4 blockade. Clin Cancer Res *13*, 6681–6688.

[Dullaers et al., 2012] Dullaers, M., De Bruyne, R., Ramadani, F., Gould, H. J., Gevaert, P. and Lambrecht, B. N. (2012). The who, where, and when of IgE in allergic airway disease. J Allergy Clin Immunol *129*, 635–645.

[Dummer et al., 2011] Dummer, R., Guggenheim, M., Arnold, A. W., Braun, R., von Moos, R. and Project Group Melanoma of the Swiss Group for Clinical Cancer Research (2011). Updated Swiss guidelines for the treatment and follow-up of cutaneous melanoma. Swiss Med Wkly *141*.

[Dummer et al., 2012] Dummer, R., Hauschild, A., Guggenheim, M., Keilholz, U., Pentheroudakis, G. and ESMO Guidelines Working Group (2012). Cutaneous melanoma: ESMO Clinical Practice Guidelines for diagnosis, treatment and follow-up. Ann Oncol *23 Suppl 7*, 86–91.

[Duncan et al., 1998] Duncan, L. M., Richards, L. A. and Mihm, M. C. (1998). Increased mast cell density in invasive melanoma. J Cutan Pathol *25*, 11–15.

[Ebrahimnejad et al., 2004] Ebrahimnejad, A., Streichert, T., Nollau, P., Horst, A. K., Wagener, C., Bamberger, A. M. and Brümmer, J. (2004). CEACAM1 enhances invasion and migration of melanocytic and melanoma cells. Am J Pathol *165*, 1781–1787.

[Egberts et al., 2012] Egberts, F., Kotthoff, E. M., Gerdes, S., Egberts, J. H., Weichenthal, M. and Hauschild, A. (2012). Comparative study of YKL-40, S-100B and LDH as monitoring tools for Stage IV melanoma. Eur J Cancer *48*, 695–702.

[Eggermont et al., 2008] Eggermont, A. M., Suciu, S., Santinami, M., Testori, A., Kruit, W. H., Marsden, J., Punt, C. J., Salès, F., Gore, M., Mackie, R.,

Kusic, Z., Dummer, R., Hauschild, A., Musat, E., Spatz, A., Keilholz, U. and EORTC Melanoma Group (2008). Adjuvant therapy with pegylated interferon alfa-2b versus observation alone in resected stage III melanoma: final results of EORTC 18991, a randomised phase III trial. Lancet *372*, 117–126.

[Ehrlich, 1891] Ehrlich, P. (1891). Die Wertbemessung des Diphterieheilserums. Klinisches Jahrbuch 6.

[Emmerich et al., 2012] Emmerich, J., Mumm, J. B., Chan, I. H., LaFace, D., Truong, H., McClanahan, T., Gorman, D. M. and Oft, M. (2012). IL-10 directly activates and expands tumor-resident CD8(+) T cells without de novo infiltration from secondary lymphoid organs. Cancer Res *72*, 3570–3581.

[Erdag et al., 2012] Erdag, G., Schaefer, J. T., Smolkin, M. E., Deacon, D. H., Shea, S. M., Dengel, L. T., Patterson, J. W. and Slingluff, C. L. (2012). Immunotype and immunohistologic characteristics of tumor-infiltrating immune cells are associated with clinical outcome in metastatic melanoma. Cancer Res *72*, 1070–1080.

[Essler et al., 2011] Essler, M., Link, A., Belloni, B., Mirceva, V., Souvatzoglou, M., Thaler, M., Haller, B., Hein, R. and Krause, B. J. (2011). Prognostic value of [18F]-fluoro-deoxy-glucose PET/CT, S100 or MIA for assessment of cancer-associated mortality in patients with high risk melanoma. PLoS One *6*.

[Falchook et al., 2012] Falchook, G. S., Long, G. V., Kurzrock, R., Kim, K. B., Arkenau, T. H., Brown, M. P., Hamid, O., Infante, J. R., Millward, M., Pavlick, A. C., O'Day, S. J., Blackman, S. C., Curtis, C. M., Lebowitz, P., Ma, B., Ouellet, D. and Kefford, R. F. (2012). Dabrafenib in patients with melanoma, untreated brain metastases, and other solid tumours: a phase 1 dose-escalation trial. Lancet *379*, 1893–1901.

[FDA, 2013] FDA (2013 (accessed April 10, 2013)). Biomarkers.

[Fernández-Aceñero et al., 2000] Fernández-Aceñero, M. J., Galindo-Gallego, M., Sanz, J. and Aljama, A. (2000). Prognostic influence of tumor-associated eosinophilic infiltrate in colorectal carcinoma. Cancer *88*, 1544–1548.

[Ferrari et al., 2009] Ferrari, S., Mudde, G. C., Rieger, M., Veyradier, A., Kremer Hovinga, J. A. and Scheiflinger, F. (2009). IgG subclass distribution of anti-ADAMTS13 antibodies in patients with acquired thrombotic thrombocytopenic purpura. J Thromb Haemost *7*, 1703–1710.

[Ferrone et al., 1993] Ferrone, S., Kageshita, T. and Hirai, S. (1993). Active specific immunotherapy of malignant melanoma with anti-idiotypic monoclonal antibodies. J Dermatol *20*, 533–539.

[Fisher et al., 2005] Fisher, R. I., LeBlanc, M., Press, O. W., Maloney, D. G., Unger, J. M. and Miller, T. P. (2005). New treatment options have changed the survival of patients with follicular lymphoma. J Clin Oncol *23*, 8447–8452.

[Flaherty et al., 2014] Flaherty, K. T., Hennig, M., Lee, S. J., Ascierto, P. A., Dummer, R., Eggermont, A. M., Hauschild, A., Kefford, R., Kirkwood, J. M., Long, G. V., Lorigan, P., Mackensen, A., McArthur, G., O'Day, S., Patel, P. M., Robert, C. and Schadendorf, D. (2014). Surrogate endpoints for overall survival in metastatic melanoma: a meta-analysis of randomised controlled trials. Lancet Oncol *15*, 297–304.

[Flaherty et al., 2012] Flaherty, K. T., Infante, J. R., Daud, A., Gonzalez, R., Kefford, R. F., Sosman, J., Hamid, O., Schuchter, L., Cebon, J., Ibrahim, N., Kudchadkar, R., Burris, H. A., Falchook, G., Algazi, A., Lewis, K., Long, G. V., Puzanov, I., Lebowitz, P., Singh, A., Little, S., Sun, P., Allred, A., Ouellet, D., Kim, K. B., Patel, K. and Weber, J. (2012). Combined BRAF and MEK inhibition in melanoma with BRAF V600 mutations. N Engl J Med *367*, 1694–1703.

[Flaherty et al., 2010] Flaherty, K. T., Puzanov, I., Kim, K. B., Ribas, A., McArthur, G. A., Sosman, J. A., O'Dwyer, P. J., Lee, R. J., Grippo, J. F., Nolop, K. and Chapman, P. B. (2010). Inhibition of mutated, activated BRAF in metastatic melanoma. N Engl J Med *363*, 809–819.

[Forster and Rajewsky, 1990] Forster, I. and Rajewsky, K. (1990). The bulk of the peripheral B-cell pool in mice is stable and not rapidly renewed from the bone marrow. Proc Natl Acad Sci U S A *87*, 4781–4784.

[Franceschini et al., 2013] Franceschini, A., Szklarczyk, D., Frankild, S., Kuhn, M., Simonovic, M., Roth, A., Lin, J., Minguez, P., Bork, P., von Mering, C.

and Jensen, L. J. (2013). STRING v9.1: protein-protein interaction networks, with increased coverage and integration. Nucleic Acids Res *41*, 808–815.

[Francis et al., 2008] Francis, J. N., James, L. K., Paraskevopoulos, G., Wong, C., Calderon, M. A., Durham, S. R. and Till, S. J. (2008). Grass pollen immunotherapy: IL-10 induction and suppression of late responses precedes IgG4 inhibitory antibody activity. J Allergy Clin Immunol *121*, 1120–1125.

[Franzke et al., 1998] Franzke, A., Probst-Kepper, M., Buer, J., Duensing, S., Hoffmann, R., Wittke, F., Volkenandt, M., Ganser, A. and Atzpodien, J. (1998). Elevated pretreatment serum levels of soluble vascular cell adhesion molecule 1 and lactate dehydrogenase as predictors of survival in cutaneous metastatic malignant melanoma. Br J Cancer *78*, 40–45.

[French, 1986] French, M. (1986). Serum IgG subclasses in normal adults. Monogr Allergy *19*, 100–107.

[Fritsch, 2003] Fritsch, P. O. (2003). Dermatologie Venerologie. Springer.

[Galli et al., 1999] Galli, S. J., Maurer, M. and Lantz, C. S. (1999). Mast cells as sentinels of innate immunity. Curr Opin Immunol *11*, 53–59.

[Galon et al., 2006] Galon, J., Costes, A., Sanchez-Cabo, F., Kirilovsky, A., Mlecnik, B., Lagorce-Pagès, C., Tosolini, M., Camus, M., Berger, A., Wind, P., Zinzindohoué, F., Bruneval, P., Cugnenc, P. H., Trajanoski, Z., Fridman, W. H. and Pagès, F. (2006). Type, density, and location of immune cells within human colorectal tumors predict clinical outcome. Science *313*, 1960–1964.

[Garbe et al., 2003] Garbe, C., Leiter, U., Ellwanger, U., Blaheta, H. J., Meier, F., Rassner, G. and Schittek, B. (2003). Diagnostic value and prognostic significance of protein S-100beta, melanoma-inhibitory activity, and tyrosinase/MART-1 reverse transcription-polymerase chain reaction in the follow-up of high-risk melanoma patients. Cancer *97*, 1737–1745.

[Gatault et al., 2012] Gatault, S., Legrand, F., Delbeke, M., Loiseau, S. and Capron, M. (2012). Involvement of eosinophils in the anti-tumor response. Cancer Immunol Immunother *61*, 1527–1534.

[Geha et al., 1985] Geha, R. S., Helm, B. and Gould, H. (1985). Inhibition of the Prausnitz-Küstner reaction by an immunoglobulin epsilon-chain fragment synthesized in E. coli. Nature *315*, 577–578.

[Gerlini et al., 2004] Gerlini, G., Tun-Kyi, A., Dudli, C., Burg, G., Pimpinelli, N. and Nestle, F. O. (2004). Metastatic melanoma secreted IL-10 down-regulates CD1 molecules on dendritic cells in metastatic tumor lesions. Am J Pathol *165*, 1853–1863.

[Geyer et al., 2010] Geyer, J. T., Ferry, J. A., Harris, N. L., Stone, J. H., Zukerberg, L. R., Lauwers, G. Y., Pilch, B. Z. and Deshpande, V. (2010). Chronic sclerosing sialadenitis (Küttner tumor) is an IgG4-associated disease. Am J Surg Pathol *34*, 202–210.

[Ghazale et al., 2008] Ghazale, A. H., Chari, S. T. and Vege, S. S. (2008). Update on the diagnosis and treatment of autoimmune pancreatitis. Curr Gastroenterol Rep *10*, 115–121.

[Ghose et al., 1991] Ghose, T., Ferrone, S., Blair, A. H., Kralovec, Y., Temponi, M., Singh, M. and Mammen, M. (1991). Regression of human melanoma xenografts in nude mice injected with methotrexate linked to monoclonal antibody 225.28 to human high molecular weight-melanoma associated antigen. Cancer Immunol Immunother *34*, 90–96.

[Giacomini et al., 1984] Giacomini, P., Veglia, F., Cordiali Fei, P., Rehle, T., Natali, P. G. and Ferrone, S. (1984). Level of a membrane-bound high-molecular-weight melanoma-associated antigen and a cytoplasmic melanoma-associated antigen in surgically removed tissues and in sera from patients with melanoma. Cancer Res *44*, 1281–1287.

[Gilbert et al., 2011] Gilbert, A. E., Karagiannis, P., Dodev, T., Koers, A., Lacy, K., Josephs, D. H., Takhar, P., Geh, J. L., Healy, C., Harries, M., Acland, K. M., Rudman, S. M., Beavil, R. L., Blower, P. J., Beavil, A. J., Gould, H. J., Spicer, J., Nestle, F. O. and Karagiannis, S. N. (2011). Monitoring the systemic human memory B cell compartment of melanoma patients for anti-tumor IgG antibodies. PLoS One *6*.

[Globocan, 2013] Globocan (2012 (accessed April 15, 2013)). Melanoma Statistics.

[Gogas et al., 2009] Gogas, H., Eggermont, A. M., Hauschild, A., Hersey, P., Mohr, P., Schadendorf, D., Spatz, A. and Dummer, R. (2009). Biomarkers in melanoma. Ann Oncol *20 Suppl 6*, 8–13.

[Gould et al., 1999] Gould, H. J., Mackay, G. A., Karagiannis, S. N., O'Toole, C. M., Marsh, P. J., Daniel, B. E., Coney, L. R., Zurawski, V. R., Joseph, M., Capron, M., Gilbert, M., Murphy, G. F. and Korngold, R. (1999). Comparison of IgE and IgG antibody-dependent cytotoxicity in vitro and in a SCID mouse xenograft model of ovarian carcinoma. Eur J Immunol *29*, 3527–3537.

[Gould and Sutton, 2008] Gould, H. J. and Sutton, B. J. (2008). IgE in allergy and asthma today. Nat Rev Immunol *8*, 205–217.

[Gould et al., 2003] Gould, H. J., Sutton, B. J., Beavil, A. J., Beavil, R. L., McCloskey, N., Coker, H. A., Fear, D. and Smurthwaite, L. (2003). The biology of IGE and the basis of allergic disease. Annu Rev Immunol *21*, 579–628.

[Gounaris et al., 2007] Gounaris, E., Erdman, S. E., Restaino, C., Gurish, M. F., Friend, D. S., Gounari, F., Lee, D. M., Zhang, G., Glickman, J. N., Shin, K., Rao, V. P., Poutahidis, T., Weissleder, R., McNagny, K. M. and Khazaie, K. (2007). Mast cells are an essential hematopoietic component for polyp development. Proc Natl Acad Sci U S A *104*, 19977–19982.

[Greenwald et al., 2005] Greenwald, R. J., Freeman, G. J. and Sharpe, A. H. (2005). The B7 family revisited. Annu Rev Immunol *23*, 515–548.

[Griggs and Zinkewich-Peotti, 2009] Griggs, J. and Zinkewich-Peotti, K. (2009). The state of the art: immune-mediated mechanisms of monoclonal antibodies in cancer therapy. Br J Cancer *101*, 1807–1812.

[Gulubova and Vlaykova, 2009] Gulubova, M. and Vlaykova, T. (2009). Prognostic significance of mast cell number and microvascular density for the survival of patients with primary colorectal cancer. J Gastroenterol Hepatol *24*, 1265–1275.

[Hafner et al., 2005a] Hafner, C., Breiteneder, H., Ferrone, S., Thallinger, C., Wagner, S., Schmidt, W. M., Jasinska, J., Kundi, M., Wolff, K., Zielinski,

C. C., Scheiner, O., Wiedermann, U. and Pehamberger, H. (2005a). Suppression of human melanoma tumor growth in SCID mice by a human high molecular weight-melanoma associated antigen (HMW-MAA) specific monoclonal antibody. Int J Cancer *114*, 426–432.

[Hafner et al., 2005b] Hafner, C., Wagner, S., Allwardt, D., Riemer, A. B., Scheiner, O., Pehamberger, H. and Breiteneder, H. (2005b). Cross-reactivity of mimotopes with a monoclonal antibody against the high molecular weight melanoma-associated antigen (HMW-MAA) does not predict cross-reactive immunogenicity. Melanoma Res *15*, 111–117.

[Hamano et al., 2001] Hamano, H., Kawa, S., Horiuchi, A., Unno, H., Furuya, N., Akamatsu, T., Fukushima, M., Nikaido, T., Nakayama, K., Usuda, N. and Kiyosawa, K. (2001). High serum IgG4 concentrations in patients with sclerosing pancreatitis. N Engl J Med *344*, 732–738.

[Hamby et al., 1987] Hamby, C. V., Liao, S. K., Kanamaru, T. and Ferrone, S. (1987). Immunogenicity of human melanoma-associated antigens defined by murine monoclonal antibodies in allogeneic and xenogeneic hosts. Cancer Res *47*, 5284–5289.

[Hamid et al., 2013] Hamid, O., Robert, C., Daud, A., Hodi, F. S., Hwu, W. J., Kefford, R., Wolchok, J. D., Hersey, P., Joseph, R. W., Weber, J. S., Dronca, R., Gangadhar, T. C., Patnaik, A., Zarour, H., Joshua, A. M., Gergich, K., Elassaiss-Schaap, J., Algazi, A., Mateus, C., Boasberg, P., Tumeh, P. C., Chmielowski, B., Ebbinghaus, S. W., Li, X. N., Kang, S. P. and Ribas, A. (2013). Safety and Tumor Responses with Lambrolizumab (Anti-PD-1) in Melanoma. N Engl J Med .

[Harada et al., 2012] Harada, K., Shimoda, S., Kimura, Y., Sato, Y., Ikeda, H., Igarashi, S., Ren, X. S., Sato, H. and Nakanuma, Y. (2012). Significance of immunoglobulin G4 (IgG4)-positive cells in extrahepatic cholangiocarcinoma: molecular mechanism of IgG4 reaction in cancer tissue. Hepatology *56*, 157–164.

[Hauschild et al., 2012] Hauschild, A., Grob, J. J., Demidov, L. V., Jouary, T., Gutzmer, R., Millward, M., Rutkowski, P., Blank, C. U., Miller, W. H., Kaempgen, E., Martín-Algarra, S., Karaszewska, B., Mauch, C., Chiarion-Sileni, V.,

Martin, A. M., Swann, S., Haney, P., Mirakhur, B., Guckert, M. E., Goodman, V. and Chapman, P. B. (2012). Dabrafenib in BRAF-mutated metastatic melanoma: a multicentre, open-label, phase 3 randomised controlled trial. Lancet *380*, 358–365.

[Hellman, 2007] Hellman, L. (2007). Regulation of IgE homeostasis, and the identification of potential targets for therapeutic intervention. Biomed Pharmacother *61*, 34–49.

[Henry and Hayes, 2012] Henry, N. L. and Hayes, D. F. (2012). Cancer biomarkers. Mol Oncol *6*, 140–146.

[Hicklin and Ellis, 2005] Hicklin, D. J. and Ellis, L. M. (2005). Role of the vascular endothelial growth factor pathway in tumor growth and angiogenesis. J Clin Oncol *23*, 1011–1027.

[Hirai et al., 1997] Hirai, S., Kageshita, T., Kimura, T., Tsujisaki, M., Imai, K., Wakamatsu, K., Ito, S. and Ono, T. (1997). Serum levels of sICAM-1 and 5-S-cysteinyldopa as markers of melanoma progression. Melanoma Res *7*, 58–62.

[Hirano et al., 2006] Hirano, K., Kawabe, T., Yamamoto, N., Nakai, Y., Sasahira, N., Tsujino, T., Toda, N., Isayama, H., Tada, M. and Omata, M. (2006). Serum IgG4 concentrations in pancreatic and biliary diseases. Clin Chim Acta *367*, 181–184.

[Hodi et al., 2010] Hodi, F. S., O'Day, S. J., McDermott, D. F., Weber, R. W., Sosman, J. A., Haanen, J. B., Gonzalez, R., Robert, C., Schadendorf, D., Hassel, J. C., Akerley, W., van den Eertwegh, A. J., Lutzky, J., Lorigan, P., Vaubel, J. M., Linette, G. P., Hogg, D., Ottensmeier, C. H., Lebbé, C., Peschel, C., Quirt, I., Clark, J. I., Wolchok, J. D., Weber, J. S., Tian, J., Yellin, M. J., Nichol, G. M., Hoos, A. and Urba, W. J. (2010). Improved survival with ipilimumab in patients with metastatic melanoma. N Engl J Med *363*, 711–723.

[Hodi et al., 2002] Hodi, F. S., Schmollinger, J. C., Soiffer, R. J., Salgia, R., Lynch, T., Ritz, J., Alyea, E. P., Yang, J., Neuberg, D., Mihm, M. and Dranoff, G. (2002). ATP6S1 elicits potent humoral responses associated with immune-mediated tumor destruction. Proc Natl Acad Sci U S A *99*, 6919–6924.

[Hofmann et al., 2009] Hofmann, M. A., Gussmann, F., Fritsche, A., Biesold, S., Schicke, B., Küchler, I., Voit, C. and Trefzer, U. (2009). Diagnostic value of melanoma inhibitory activity serum marker in the follow-up of patients with stage I or II cutaneous melanoma. Melanoma Res *19*, 17–23.

[Hofmann et al., 2011] Hofmann, M. A., Schicke, B., Fritsch, A., Biesold, S., Gussmann, F., Küchler, I., Voit, C. and Trefzer, U. (2011). Impact of lymph node metastases on serum level of melanoma inhibitory activity in stage III melanoma patients. J Dermatol *38*, 880–886.

[Hong and Fogarty, 2012] Hong, A. and Fogarty, G. (2012). Role of radiation therapy in cutaneous melanoma. Cancer J *18*, 203–207.

[Honjo and Neuberger, 2004] Honjo, T. A. and Neuberger, F. W. (2004). Molecular biology of B cells. Elsevier.

[Hsieh et al., 2002] Hsieh, H. L., Schäfer, B. W., Cox, J. A. and Heizmann, C. W. (2002). S100A13 and S100A6 exhibit distinct translocation pathways in endothelial cells. J Cell Sci *115*, 3149–3158.

[Hudis, 2007] Hudis, C. (2007). Trastuzumab - Mechanism of action and use in clinical practice. New England Journal of Medicine *357*, 39–51.

[Hughes et al., 2012] Hughes, A. K., Cichacz, Z., Scheck, A., Coons, S. W., Johnston, S. A. and Stafford, P. (2012). Immunosignaturing can detect products from molecular markers in brain cancer. PLoS One *7*.

[Huland and Huland, 1992] Huland, E. and Huland, H. (1992). Tumor-associated eosinophilia in interleukin-2-treated patients: evidence of toxic eosinophil degranulation on bladder cancer cells. J Cancer Res Clin Oncol *118*, 463–467.

[Imai et al., 1983] Imai, K., Nakanishi, T., Noguchi, T., Yachi, A. and Ferrone, S. (1983). Selective in vitro toxicity of purothionin conjugated to the monoclonal antibody 225.28S to a human high-molecular-weight melanoma-associated antigen. Cancer Immunol Immunother *15*, 206–209.

[Ishibashi et al., 2006] Ishibashi, S., Ohashi, Y., Suzuki, T., Miyazaki, S., Moriya, T., Satomi, S. and Sasano, H. (2006). Tumor-associated tissue eosinophilia in human esophageal squamous cell carcinoma. Anticancer Res *26*, 1419–1424.

[Iwai et al., 2002] Iwai, Y., Ishida, M., Tanaka, Y., Okazaki, T., Honjo, T. and Minato, N. (2002). Involvement of PD-L1 on tumor cells in the escape from host immune system and tumor immunotherapy by PD-L1 blockade. Proc Natl Acad Sci U S A *99*, 12293–12297.

[Jacobs et al., 1972] Jacobs, D., Landon, J., Houri, M. and Merrett, T. G. (1972). Circulating levels of immunoglobulin E in patients with cancer. Lancet *2*, 1059–1061.

[Jakobovits et al., 2007] Jakobovits, A., Amado, R. G., Yang, X., Roskos, L. and Schwab, G. (2007). From XenoMouse technology to panitumumab, the first fully human antibody product from transgenic mice. Nat Biotechnol *25*, 1134–1143.

[James et al., 2012] James, L. K., Bowen, H., Calvert, R. A., Dodev, T. S., Shamji, M. H., Beavil, A. J., McDonnell, J. M., Durham, S. R. and Gould, H. J. (2012). Allergen specificity of IgG(4)-expressing B cells in patients with grass pollen allergy undergoing immunotherapy. J Allergy Clin Immunol *130*, 663–670.

[Jeannin et al., 1998] Jeannin, P., Lecoanet, S., Delneste, Y., Gauchat, J. F. and Bonnefoy, J. Y. (1998). IgE versus IgG4 production can be differentially regulated by IL-10. J Immunol *160*, 3555–3561.

[Jefferis, 2009] Jefferis, R. (2009). Glycosylation as a strategy to improve antibody-based therapeutics. Nat Rev Drug Discov *8*, 226–234.

[Jemal et al., 2010] Jemal, A., Siegel, R., Xu, J. and Ward, E. (2010). Cancer statistics, 2010. CA Cancer J Clin *60*, 277–300.

[Jensen-Jarolim et al., 2008] Jensen-Jarolim, E., Achatz, G., Turner, M. C., Karagiannis, S., Legrand, F., Capron, M., Penichet, M. L., Rodríguez, J. A., Siccardi, A. G., Vangelista, L., Riemer, A. B. and Gould, H. (2008). AllergoOncology: the role of IgE-mediated allergy in cancer. Allergy *63*, 1255–1266.

[Jensen-Jarolim and Pawelec, 2012] Jensen-Jarolim, E. and Pawelec, G. (2012). The nascent field of AllergoOncology. Cancer Immunol Immunother *61*, 1355–1357.

[Johansen, 2006] Johansen, J. S. (2006). Studies on serum YKL-40 as a biomarker in diseases with inflammation, tissue remodelling, fibroses and cancer. Dan Med Bull *53*, 172–209.

[Jones et al., 1986] Jones, P. T., Dear, P. H., Foote, J., Neuberger, M. S. and Winter, G. (1986). Replacing the complementarity-determining regions in a human antibody with those from a mouse. Nature *321*, 522–525.

[Jonker et al., 2007] Jonker, D. J., O'Callaghan, C. J., Karapetis, C. S., Zalcberg, J. R., Tu, D., Au, H. J., Berry, S. R., Krahn, M., Price, T., Simes, R. J., Tebbutt, N. C., van Hazel, G., Wierzbicki, R., Langer, C. and Moore, M. J. (2007). Cetuximab for the treatment of colorectal cancer. N Engl J Med *357*, 2040–2048.

[Juergensen et al., 2001] Juergensen, A., Holzapfel, U., Hein, R., Stolz, W., Buettner, R. and Bosserhoff, A. (2001). Comparison of two prognostic markers for malignant melanoma: MIA and S100 beta. Tumour Biol *22*, 54–58.

[Kamisawa et al., 2008] Kamisawa, T., Okazaki, K. and Kawa, S. (2008). Diagnostic criteria for autoimmune pancreatitis in Japan. World J Gastroenterol *14*, 4992–4994.

[Kaneko and Niwa, 2011] Kaneko, E. and Niwa, R. (2011). Optimizing therapeutic antibody function: progress with Fc domain engineering. BioDrugs *25*, 1–11.

[Kang et al., 2000] Kang, N., Hamilton, S., Odili, J., Wilson, G. and Kupsch, J. (2000). In vivo targeting of malignant melanoma by 125Iodine- and 99mTechnetium-labeled single-chain Fv fragments against high molecular weight melanoma-associated antigen. Clin Cancer Res *6*, 4921–4931.

[Kantor et al., 1986] Kantor, R. R., Albino, A. P., Ng, A. K. and Ferrone, S. (1986). Biosynthesis and intracellular processing of four human melanoma associated antigens. Cancer Res *46*, 5223–5228.

[Karagiannis et al., 2009] Karagiannis, P., Singer, J., Hunt, J., Gan, S. K., Rudman, S. M., Mechtcheriakova, D., Knittelfelder, R., Daniels, T. R., Hobson, P. S., Beavil, A. J., Spicer, J., Nestle, F. O., Penichet, M. L., Gould, H. J., Jensen-Jarolim, E. and Karagiannis, S. N. (2009). Characterisation of an

engineered trastuzumab IgE antibody and effector cell mechanisms targeting HER2/neu-positive tumour cells. Cancer Immunol Immunother *58*, 915–930.

[Karagiannis et al., 2008] Karagiannis, S. N., Bracher, M. G., Beavil, R. L., Beavil, A. J., Hunt, J., McCloskey, N., Thompson, R. G., East, N., Burke, F., Sutton, B. J., Dombrowicz, D., Balkwill, F. R. and Gould, H. J. (2008). Role of IgE receptors in IgE antibody-dependent cytotoxicity and phagocytosis of ovarian tumor cells by human monocytic cells. Cancer Immunol Immunother *57*, 247–263.

[Karagiannis et al., 2007] Karagiannis, S. N., Bracher, M. G., Hunt, J., McCloskey, N., Beavil, R. L., Beavil, A. J., Fear, D. J., Thompson, R. G., East, N., Burke, F., Moore, R. J., Dombrowicz, D. D., Balkwill, F. R. and Gould, H. J. (2007). IgE-antibody-dependent immunotherapy of solid tumors: cytotoxic and phagocytic mechanisms of eradication of ovarian cancer cells. J Immunol *179*, 2832–2843.

[Karagiannis et al., 2012] Karagiannis, S. N., Josephs, D. H., Karagiannis, P., Gilbert, A. E., Saul, L., Rudman, S. M., Dodev, T., Koers, A., Blower, P. J., Corrigan, C., Beavil, A. J., Spicer, J. F., Nestle, F. O. and Gould, H. J. (2012). Recombinant IgE antibodies for passive immunotherapy of solid tumours: from concept towards clinical application. Cancer Immunol Immunother *61*, 1547–1564.

[Karagiannis et al., 2003] Karagiannis, S. N., Wang, Q., East, N., Burke, F., Riffard, S., Bracher, M. G., Thompson, R. G., Durham, S. R., Schwartz, L. B., Balkwill, F. R. and Gould, H. J. (2003). Activity of human monocytes in IgE antibody-dependent surveillance and killing of ovarian tumor cells. Eur J Immunol *33*, 1030–1040.

[Karakousis et al., 2013] Karakousis, G., Yang, R. and Xu, X. (2013). Circulating melanoma cells as a predictive biomarker. J Invest Dermatol *133*, 1460–1462.

[Kasashima et al., 2008] Kasashima, S., Zen, Y., Kawashima, A., Konishi, K., Sasaki, H., Endo, M., Matsumoto, Y., Kawakami, K., Kasashima, F., Moriya, M., Kimura, K., Ohtake, H. and Nakanuma, Y. (2008). Inflammatory abdomi-

nal aortic aneurysm: close relationship to IgG4-related periaortitis. Am J Surg Pathol *32*, 197–204.

[Kawa et al., 2012] Kawa, S., Ito, T., Watanabe, T., Maruyama, M., Hamano, H., Maruyama, M., Muraki, T. and Arakura, N. (2012). The Utility of Serum IgG4 Concentrations as a Biomarker. Int J Rheumatol *2012*, 198314–198314.

[Kerkar and Restifo, 2012] Kerkar, S. P. and Restifo, N. P. (2012). Cellular constituents of immune escape within the tumor microenvironment. Cancer Res *72*, 3125–3130.

[Kershaw et al., 1998] Kershaw, M. H., Darcy, P. K., Trapani, J. A., MacGregor, D. and Smyth, M. J. (1998). Tumor-specific IgE-mediated inhibition of human colorectal carcinoma xenograft growth. Oncol Res *10*, 133–142.

[Kershaw et al., 1996] Kershaw, M. H., Darcy, P. K., Trapani, J. A. and Smyth, M. J. (1996). The use of chimeric human Fc(epsilon) receptor I to redirect cytotoxic T lymphocytes to tumors. J Leukoc Biol *60*, 721–728.

[Khattak et al., 2013a] Khattak, M., Fisher, R., Turajlic, S. and Larkin, J. (2013a). Targeted therapy and immunotherapy in advanced melanoma: an evolving paradigm. Ther Adv Med Oncol *5*, 105–118.

[Khattak et al., 2013b] Khattak, M. A., Fisher, R., Hughes, P., Gore, M. and Larkin, J. (2013b). Ipilimumab activity in advanced uveal melanoma. Melanoma Res *23*, 79–81.

[Kimura et al., 2012] Kimura, Y., Harada, K. and Nakanuma, Y. (2012). Pathologic significance of immunoglobulin G4-positive plasma cells in extrahepatic cholangiocarcinoma. Hum Pathol *43*, 2149–2156.

[Kircheis et al., 2012] Kircheis, R., Halanek, N., Koller, I., Jost, W., Schuster, M., Gorr, G., Hajszan, K. and Nechansky, A. (2012). Correlation of ADCC activity with cytokine release induced by the stably expressed, glyco-engineered humanized Lewis Y-specific monoclonal antibody MB314. MAbs *4*, 532–541.

[Kirkwood and Robinson, 1990] Kirkwood, J. M. and Robinson, J. E. (1990). Human IgG and IgM monoclonal antibodies against autologous melanoma produced by Epstein-Barr-virus-transformed B lymphocytes. Cancer Immunol Immunother *32*, 228–234.

[Kirkwood et al., 2008] Kirkwood, J. M., Tarhini, A. A., Panelli, M. C., Moschos, S. J., Zarour, H. M., Butterfield, L. H. and Gogas, H. J. (2008). Next generation of immunotherapy for melanoma. J Clin Oncol *26*, 3445–3455.

[Kleeberg et al., 2004] Kleeberg, U. R., Suciu, S., Bröcker, E. B., Ruiter, D. J., Chartier, C., Liénard, D., Marsden, J., Schadendorf, D., Eggermont, A. M. and EORTC Melanoma Group in cooperation with the German Cancer Society (DKG) (2004). Final results of the EORTC 18871/DKG 80-1 randomised phase III trial. rIFN-alpha2b versus rIFN-gamma versus ISCADOR M versus observation after surgery in melanoma patients with either high-risk primary (thickness ¿3 mm) or regional lymph node metastasis. Eur J Cancer *40*, 390–402.

[Kluger et al., 2011] Kluger, H. M., Hoyt, K., Bacchiocchi, A., Mayer, T., Kirsch, J., Kluger, Y., Sznol, M., Ariyan, S., Molinaro, A. and Halaban, R. (2011). Plasma markers for identifying patients with metastatic melanoma. Clin Cancer Res *17*, 2417–2425.

[Kopf et al., 1998] Kopf, M., Herren, S., Wiles, M. V., Pepys, M. B. and Kosco-Vilbois, M. H. (1998). Interleukin 6 influences germinal center development and antibody production via a contribution of C3 complement component. J Exp Med *188*, 1895–1906.

[Kraft and Kinet, 2007] Kraft, S. and Kinet, J. P. (2007). New developments in FcepsilonRI regulation, function and inhibition. Nat Rev Immunol *7*, 365–378.

[Krogh, 2013] Krogh (2010 (accessed May 16, 2013)). Prognostic value of serum YKL-40 in stage IIB-III melanoma patients receiving adjuvant interferon therapy.

[Kruijff et al., 2009] Kruijff, S., Bastiaannet, E., Kobold, A. C., van Ginkel, R. J., Suurmeijer, A. J. and Hoekstra, H. J. (2009). S-100B concentrations predict disease-free survival in stage III melanoma patients. Ann Surg Oncol *16*, 3455–3462.

[Kuzbicki et al., 2012] Kuzbicki, L., Lange, D., Straczynska-Niemiec, A. and Chwirot, B. W. (2012). The value of cyclooxygenase-2 expression in differentiating between early melanomas and histopathologically difficult types of benign human skin lesions. Melanoma Res *22*, 70–76.

[Kwakkenbos et al., 2010] Kwakkenbos, M. J., Diehl, S. A., Yasuda, E., Bakker, A. Q., van Geelen, C. M., Lukens, M. V., van Bleek, G. M., Widjojoatmodjo, M. N., Bogers, W. M., Mei, H., Radbruch, A., Scheeren, F. A., Spits, H. and Beaumont, T. (2010). Generation of stable monoclonal antibody-producing B cell receptor-positive human memory B cells by genetic programming. Nat Med *16*, 123–128.

[Labrijn et al., 2011] Labrijn, A. F., Rispens, T., Meesters, J., Rose, R. J., den Bleker, T. H., Loverix, S., van den Bremer, E. T., Neijssen, J., Vink, T., Lasters, I., Aalberse, R. C., Heck, A. J., van de Winkel, J. G., Schuurman, J. and Parren, P. W. (2011). Species-specific determinants in the IgG CH3 domain enable Fab-arm exchange by affecting the noncovalent CH3-CH3 interaction strength. J Immunol *187*, 3238–3246.

[Lacy et al., 2012] Lacy, K. E., Karagiannis, S. N. and Nestle, F. O. (2012). Advances in the treatment of melanoma. Clin Med *12*, 168–171.

[Ladányi et al., 2011] Ladányi, A., Kiss, J., Mohos, A., Somlai, B., Liszkay, G., Gilde, K., Fejös, Z., Gaudi, I., Dobos, J. and Tímár, J. (2011). Prognostic impact of B-cell density in cutaneous melanoma. Cancer Immunol Immunother *60*, 1729–1738.

[Lanzavecchia et al., 2006] Lanzavecchia, A., Bernasconi, N., Traggiai, E., Ruprecht, C. R., Corti, D. and Sallusto, F. (2006). Understanding and making use of human memory B cells. Immunol Rev *211*, 303–309.

[Lanzavecchia et al., 2007] Lanzavecchia, A., Corti, D. and Sallusto, F. (2007). Human monoclonal antibodies by immortalization of memory B cells. Curr Opin Biotechnol *18*, 523–528.

[Larson et al., 1985] Larson, S. M., Carrasquillo, J. A., McGuffin, R. W., Krohn, K. A., Ferens, J. M., Hill, L. D., Beaumier, P. L., Reynolds, J. C., Hellström, K. E. and Hellström, I. (1985). Use of I-131 labeled, murine Fab against a high molecular weight antigen of human melanoma: preliminary experience. Radiology *155*, 487–492.

[Lazar et al., 2006] Lazar, G. A., Dang, W., Karki, S., Vafa, O., Peng, J. S., Hyun, L., Chan, C., Chung, H. S., Eivazi, A., Yoder, S. C., Vielmetter, J.,

Carmichael, D. F., Hayes, R. J. and Dahiyat, B. I. (2006). Engineered antibody Fc variants with enhanced effector function. Proc Natl Acad Sci U S A *103*, 4005–4010.

[Le Gros et al., 1990] Le Gros, G., Ben-Sasson, S. Z., Seder, R., Finkelman, F. D. and Paul, W. E. (1990). Generation of interleukin 4 (IL-4)-producing cells in vivo and in vitro: IL-2 and IL-4 are required for in vitro generation of IL-4-producing cells. J Exp Med *172*, 921–929.

[Legrand et al., 2010] Legrand, F., Driss, V., Delbeke, M., Loiseau, S., Hermann, E., Dombrowicz, D. and Capron, M. (2010). Human eosinophils exert TNF-a and granzyme A-mediated tumoricidal activity toward colon carcinoma cells. J Immunol *185*, 7443–7451.

[Lens and Dawes, 2004] Lens, M. B. and Dawes, M. (2004). Global perspectives of contemporary epidemiological trends of cutaneous malignant melanoma. Br J Dermatol *150*, 179–185.

[Lin et al., 2012] Lin, C., Waller, L. and Lyles, R. (2012). The likelihood approach for the comparison of medical diagnostic system with multiple binary tests. Journal of Applied Statistics *39*, 1437–1454.

[Lin et al., 2007] Lin, E. Y., Li, J. F., Bricard, G., Wang, W., Deng, Y., Sellers, R., Porcelli, S. A. and Pollard, J. W. (2007). Vascular endothelial growth factor restores delayed tumor progression in tumors depleted of macrophages. Mol Oncol *1*, 288–302.

[Lin et al., 2004] Lin, S. C., Lo, S. S., Liu, C. J., Chung, M. Y., Huang, J. W. and Chang, K. W. (2004). Functional genotype in matrix metalloproteinases-2 promoter is a risk factor for oral carcinogenesis. J Oral Pathol Med *33*, 405–409.

[Lindner et al., 2013] Lindner, S., Dahlke, K., Sontheimer, K., Hagn, M., Kaltenmeier, C., Barth, T. F., Beyer, T., Reister, F., Fabricius, D., Lotfi, R., Lunov, O., Nienhaus, G. U., Simmet, T., Kreienberg, R., Möller, P., Schrezenmeier, H. and Jahrsdörfer, B. (2013). Interleukin 21-induced granzyme B-expressing B cells infiltrate tumors and regulate T cells. Cancer Res *73*, 2468–2479.

[Linko-Lopponen and Makinen, 1985] Linko-Lopponen, S. and Makinen, M. (1985). A microtiter plate assay for N-acetyl-beta-D-glucosaminidase using a fluorogenic substrate. Anal Biochem *148*, 50–53.

[Lipson and Drake, 2011] Lipson, E. J. and Drake, C. G. (2011). Ipilimumab: an anti-CTLA-4 antibody for metastatic melanoma. Clin Cancer Res *17*, 6958–6962.

[Lohse et al., 2011] Lohse, S., Derer, S., Beyer, T., Klausz, K., Peipp, M., Leusen, J. H., van de Winkel, J. G., Dechant, M. and Valerius, T. (2011). Recombinant dimeric IgA antibodies against the epidermal growth factor receptor mediate effective tumor cell killing. J Immunol *186*, 3770–3778.

[Long et al., 2011] Long, G. V., Menzies, A. M., Nagrial, A. M., Haydu, L. E., Hamilton, A. L., Mann, G. J., Hughes, T. M., Thompson, J. F., Scolyer, R. A. and Kefford, R. F. (2011). Prognostic and clinicopathologic associations of oncogenic BRAF in metastatic melanoma. J Clin Oncol *29*, 1239–1246.

[Long et al., 2013] Long, G. V., Wilmott, J. S., Haydu, L. E., Tembe, V., Sharma, R., Rizos, H., Thompson, J. F., Howle, J., Scolyer, R. A. and Kefford, R. F. (2013). Effects of BRAF inhibitors on human melanoma tissue before treatment, early during treatment, and on progression. Pigment Cell Melanoma Res *26*, 499–508.

[Lowe et al., 1981] Lowe, D., Jorizzo, J. and Hutt, M. S. (1981). Tumour-associated eosinophilia: a review. J Clin Pathol *34*, 1343–1348.

[Luo et al., 2005] Luo, W., Hsu, J. C., Tsao, C. Y., Ko, E., Wang, X. and Ferrone, S. (2005). Differential immunogenicity of two peptides isolated by high molecular weight-melanoma-associated antigen-specific monoclonal antibodies with different affinities. J Immunol *174*, 7104–7110.

[Ma et al., 2012] Ma, M. W., Medicherla, R. C., Qian, M., Vega-Saenz de Miera, E., Friedman, E. B., Berman, R. S., Shapiro, R. L., Pavlick, A. C., Ott, P. A., Bhardwaj, N., Shao, Y., Osman, I. and Darvishian, F. (2012). Immune response in melanoma: an in-depth analysis of the primary tumor and corresponding sentinel lymph node. Mod Pathol *25*, 1000–1010.

[Maecker et al., 2010] Maecker, H. T., McCoy, J. P., FOCIS Human Immunophenotyping Consortium, Amos, M., Elliott, J., Gaigalas, A., Wang, L., Aranda, R., Banchereau, J., Boshoff, C., Braun, J., Korin, Y., Reed, E., Cho, J., Hafler, D., Davis, M., Fathman, C. G., Robinson, W., Denny, T., Weinhold, K., Desai, B., Diamond, B., Gregersen, P., Di Meglio, P., DiMeglio, P., Nestle, F. O., Nestle, F., Peakman, M., Villanova, F., Villnova, F., Ferbas, J., Field, E., Kantor, A., Kawabata, T., Komocsar, W., Lotze, M., Nepom, J., Ochs, H., O'Lone, R., Phippard, D., Plevy, S., Rich, S., Roederer, M., Rotrosen, D. and Yeh, J. H. (2010). A model for harmonizing flow cytometry in clinical trials. Nat Immunol *11*, 975–978.

[Maehara et al., 2012] Maehara, T., Moriyama, M., Nakashima, H., Miyake, K., Hayashida, J. N., Tanaka, A., Shinozaki, S., Kubo, Y. and Nakamura, S. (2012). Interleukin-21 contributes to germinal centre formation and immunoglobulin G4 production in IgG4-related dacryoadenitis and sialoadenitis, so-called Mikulicz's disease. Ann Rheum Dis *71*, 2011–2019.

[Mahmoud et al., 2012] Mahmoud, S. M., Lee, A. H., Paish, E. C., Macmillan, R. D., Ellis, I. O. and Green, A. R. (2012). The prognostic significance of B lymphocytes in invasive carcinoma of the breast. Breast Cancer Res Treat *132*, 545–553.

[Maier et al., 2012] Maier, T., Laubender, R. P., Sturm, R. A., Klingenstein, A., Korting, H. C., Ruzicka, T. and Berking, C. (2012). Osteopontin expression in plasma of melanoma patients and in melanocytic tumours. J Eur Acad Dermatol Venereol *26*, 1084–1091.

[Maletzki et al., 2012] Maletzki, C., Jahnke, A., Ostwald, C., Klar, E., Prall, F. and Linnebacher, M. (2012). Ex-vivo clonally expanded B lymphocytes infiltrating colorectal carcinoma are of mature immunophenotype and produce functional IgG. PLoS One *7*.

[Mantovani et al., 2008] Mantovani, A., Allavena, P., Sica, A. and Balkwill, F. (2008). Cancer-related inflammation. Nature *454*, 436–444.

[Mantovani and Sica, 2010] Mantovani, A. and Sica, A. (2010). Macrophages, innate immunity and cancer: balance, tolerance, and diversity. Curr Opin Immunol *22*, 231–237.

[Mantovani et al., 2005] Mantovani, A., Sica, A. and Locati, M. (2005). Macrophage polarization comes of age. Immunity *23*, 344–346.

[Mao et al., 2013] Mao, M., Tian, F., Mariadason, J. M., Tsao, C. C., Lemos, R., Dayyani, F., Gopal, Y. N., Jiang, Z. Q., Wistuba, I. I., Tang, X. M., Bornman, W. G., Bollag, G., Mills, G. B., Powis, G., Desai, J., Gallick, G. E., Davies, M. A. and Kopetz, S. (2013). Resistance to BRAF inhibition in BRAF-mutant colon cancer can be overcome with PI3K inhibition or demethylating agents. Clin Cancer Res *19*, 657–667.

[Marcucci et al., 2013] Marcucci, F., Bellone, M., Rumio, C. and Corti, A. (2013). Approaches to improve tumor accumulation and interactions between monoclonal antibodies and immune cells. MAbs *5*, 34–46.

[Maurer et al., 1994] Maurer, D., Fiebiger, E., Reininger, B., Wolff-Winiski, B., Jouvin, M. H., Kilgus, O., Kinet, J. P. and Stingl, G. (1994). Expression of functional high affinity immunoglobulin E receptors (Fc epsilon RI) on monocytes of atopic individuals. J Exp Med *179*, 745–750.

[McAllister et al., 2008] McAllister, S. S., Gifford, A. M., Greiner, A. L., Kelleher, S. P., Saelzler, M. P., Ince, T. A., Reinhardt, F., Harris, L. N., Hylander, B. L., Repasky, E. A. and Weinberg, R. A. (2008). Systemic endocrine instigation of indolent tumor growth requires osteopontin. Cell *133*, 994–1005.

[McArthur and Ribas, 2013] McArthur, G. A. and Ribas, A. (2013). Targeting oncogenic drivers and the immune system in melanoma. J Clin Oncol *31*, 499–506.

[McIntosh and Pepe, 2002] McIntosh, M. W. and Pepe, M. S. (2002). Combining several screening tests: optimality of the risk score. Biometrics *58*, 657–664.

[McShane et al., 2005] McShane, L. M., Altman, D. G., Sauerbrei, W., Taube, S. E., Gion, M., Clark, G. M. and Statistics Subcommittee of the NCI-EORTC Working Group on Cancer Diagnostics (2005). Reporting recommendations for tumor marker prognostic studies. J Clin Oncol *23*, 9067–9072.

[Meyer et al., 2009] Meyer, S., Vogt, T., Landthaler, M., Berand, A., Reichle, A., Bataille, F., Marx, A. H., Menz, A., Hartmann, A., Kunz-Schughart, L. A. and

Wild, P. J. (2009). Cyclooxygenase 2 (COX2) and Peroxisome Proliferator-Activated Receptor Gamma (PPARG) Are Stage-Dependent Prognostic Markers of Malignant Melanoma. PPAR Res *2009*, 848645–848645.

[Michetti et al., 2012] Michetti, F., Corvino, V., Geloso, M. C., Lattanzi, W., Bernardini, C., Serpero, L. and Gazzolo, D. (2012). The S100B protein in biological fluids: more than a lifelong biomarker of brain distress. J Neurochem *120*, 644–659.

[Mittelman et al., 1990] Mittelman, A., Chen, Z. J., Kageshita, T., Yang, H., Yamada, M., Baskind, P., Goldberg, N., Puccio, C., Ahmed, T. and Arlin, Z. (1990). Active specific immunotherapy in patients with melanoma. A clinical trial with mouse antiidiotypic monoclonal antibodies elicited with syngeneic anti-high-molecular-weight-melanoma-associated antigen monoclonal antibodies. J Clin Invest *86*, 2136–2144.

[Mittelman et al., 1992] Mittelman, A., Chen, Z. J., Yang, H., Wong, G. Y. and Ferrone, S. (1992). Human high molecular weight melanoma-associated antigen (HMW-MAA) mimicry by mouse anti-idiotypic monoclonal antibody MK2-23: induction of humoral anti-HMW-MAA immunity and prolongation of survival in patients with stage IV melanoma. Proc Natl Acad Sci U S A *89*, 466–470.

[Mlecnik et al., 2011] Mlecnik, B., Tosolini, M., Kirilovsky, A., Berger, A., Bindea, G., Meatchi, T., Bruneval, P., Trajanoski, Z., Fridman, W. H., Pagès, F. and Galon, J. (2011). Histopathologic-based prognostic factors of colorectal cancers are associated with the state of the local immune reaction. J Clin Oncol *29*, 610–618.

[Mocellin et al., 2010] Mocellin, S., Pasquali, S., Rossi, C. R. and Nitti, D. (2010). Interferon alpha adjuvant therapy in patients with high-risk melanoma: a systematic review and meta-analysis. J Natl Cancer Inst *102*, 493–501.

[Molin et al., 2002] Molin, D., Edström, A., Glimelius, I., Glimelius, B., Nilsson, G., Sundström, C. and Enblad, G. (2002). Mast cell infiltration correlates with poor prognosis in Hodgkin's lymphoma. Br J Haematol *119*, 122–124.

[Molina et al., 2002] Molina, R., Navarro, J., Filella, X., Castel, T. and Ballesta, A. M. (2002). S-100 protein serum levels in patients with benign and malignant

diseases: false-positive results related to liver and renal function. Tumour Biol *23*, 39–44.

[Moore et al., 2010] Moore, G. L., Chen, H., Karki, S. and Lazar, G. A. (2010). Engineered Fc variant antibodies with enhanced ability to recruit complement and mediate effector functions. MAbs *2*, 181–189.

[Morton et al., 2006] Morton, D. L., Thompson, J. F., Cochran, A. J., Mozzillo, N., Elashoff, R., Essner, R., Nieweg, O. E., Roses, D. F., Hoekstra, H. J., Karakousis, C. P., Reintgen, D. S., Coventry, B. J., Glass, E. C., Wang, H. J. and MSLT Group (2006). Sentinel-node biopsy or nodal observation in melanoma. N Engl J Med *355*, 1307–1317.

[Mount et al., 1994] Mount, P. F., Sutton, V. R., Li, W., Burgess, J., McKEnzie, I. F., Pietersz, G. A. and Trapani, J. A. (1994). Chimeric (mouse/human) anti-colon cancer antibody c30.6 inhibits the growth of human colorectal cancer xenografts in scid/scid mice. Cancer Res *54*, 6160–6166.

[Movahedi et al., 2010] Movahedi, K., Laoui, D., Gysemans, C., Baeten, M., Stangé, G., Van den Bossche, J., Mack, M., Pipeleers, D., In't Veld, P., De Baetselier, P. and Van Ginderachter, J. A. (2010). Different tumor microenvironments contain functionally distinct subsets of macrophages derived from Ly6C(high) monocytes. Cancer Res *70*, 5728–5739.

[Munitz and Levi-Schaffer, 2004] Munitz, A. and Levi-Schaffer, F. (2004). Eosinophils: 'new' roles for 'old' cells. Allergy *59*, 268–275.

[Muramatsu et al., 2000] Muramatsu, M., Kinoshita, K., Fagarasan, S., Yamada, S., Shinkai, Y. and Honjo, T. (2000). Class switch recombination and hypermutation require activation-induced cytidine deaminase (AID), a potential RNA editing enzyme. Cell *102*, 553–563.

[Murphy and Walport, 2005] Murphy, K. M. and Walport, M. (2005). Janeway's Immunobiology, Vol. 6. Garland Science Publishing, NY.

[Murray et al., 2004] Murray, J. L., Gillogly, M., Kawano, K., Efferson, C. L., Lee, J. E., Ross, M., Wang, X., Ferrone, S. and Ioannides, C. G. (2004). Fine

specificity of high molecular weight-melanoma-associated antigen-specific cytotoxic T lymphocytes elicited by anti-idiotypic monoclonal antibodies in patients with melanoma. Cancer Res *64*, 5481–5488.

[Nagy et al., 1991] Nagy, E., Berczi, I. and Sehon, A. H. (1991). Growth inhibition of murine mammary carcinoma by monoclonal IgE antibodies specific for the mammary tumor virus. Cancer Immunol Immunother *34*, 63–69.

[Nahta and Esteva, 2007] Nahta, R. and Esteva, F. J. (2007). Trastuzumab: triumphs and tribulations. Oncogene *26*, 3637–3643.

[Neri et al., 1996] Neri, D., Natali, P. G., Petrul, H., Soldani, P., Nicotra, M. R., Vola, R., Rivella, A., Creighton, A. M., Neri, P. and Mariani, M. (1996). Recombinant anti-human melanoma antibodies are versatile molecules. J Invest Dermatol *107*, 164–170.

[Nestle, 2006] Nestle, F. O. (2006). A new lease on life for dendritic cell vaccines? Nat Biotechnol *24*, 1483–1484.

[Nevala et al., 2009] Nevala, W. K., Vachon, C. M., Leontovich, A. A., Scott, C. G., Thompson, M. A., Markovic, S. N. and Melanoma Study Group of the Mayo Clinic Cancer Center (2009). Evidence of systemic Th2-driven chronic inflammation in patients with metastatic melanoma. Clin Cancer Res *15*, 1931–1939.

[Ng et al., 1982] Ng, A. K., Giacomini, P., Kantor, R. and Ferrone, S. (1982). Molecular heterogeneity and shedding of a high-molecular-mass melanoma-associated antigen identified with monoclonal antibodies. Clin Chem *28*, 2347–2350.

[Nielsen et al., 2012] Nielsen, J. S., Sahota, R. A., Milne, K., Kost, S. E., Nesslinger, N. J., Watson, P. H. and Nelson, B. H. (2012). CD20+ tumor-infiltrating lymphocytes have an atypical CD27- memory phenotype and together with CD8+ T cells promote favorable prognosis in ovarian cancer. Clin Cancer Res *18*, 3281–3292.

[Nigro et al., 2009] Nigro, E. A., Brini, A. T., Soprana, E., Ambrosi, A., Dombrowicz, D., Siccardi, A. G. and Vangelista, L. (2009). Antitumor IgE adjuvanticity: key role of Fc epsilon RI. J Immunol *183*, 4530–4536.

[Nigro et al., 2012] Nigro, E. A., Soprana, E., Brini, A. T., Ambrosi, A., Yenagi, V. A., Dombrowicz, D., Siccardi, A. G. and Vangelista, L. (2012). An antitumor cellular vaccine based on a mini-membrane IgE. J Immunol *188*, 103–110.

[Nikkola et al., 2002] Nikkola, J., Vihinen, P., Vlaykova, T., Hahka-Kemppinen, M., Kähäri, V. M. and Pyrhönen, S. (2002). High expression levels of collagenase-1 and stromelysin-1 correlate with shorter disease-free survival in human metastatic melanoma. Int J Cancer *97*, 432–438.

[Nimmerjahn and Ravetch, 2008] Nimmerjahn, F. and Ravetch, J. V. (2008). Fcgamma receptors as regulators of immune responses. Nat Rev Immunol *8*, 34–47.

[Oberholzer et al., 2012] Oberholzer, P. A., Kee, D., Dziunycz, P., Sucker, A., Kamsukom, N., Jones, R., Roden, C., Chalk, C. J., Ardlie, K., Palescandolo, E., Piris, A., MacConaill, L. E., Robert, C., Hofbauer, G. F., McArthur, G. A., Schadendorf, D. and Garraway, L. A. (2012). RAS mutations are associated with the development of cutaneous squamous cell tumors in patients treated with RAF inhibitors. J Clin Oncol *30*, 316–321.

[Oberholzer et al., 2008] Oberholzer, P. A., Urosevic, M., Steinert, H. C. and Dummer, R. (2008). Baseline staging of melanoma with unknown primary site: the value of serum s100 protein and positron emission tomography. Dermatology *217*, 351–355.

[Oettinger et al., 1990] Oettinger, M. A., Schatz, D. G., Gorka, C. and Baltimore, D. (1990). RAG-1 and RAG-2, adjacent genes that synergistically activate V(D)J recombination. Science *248*, 1517–1523.

[Ojalvo et al., 2009] Ojalvo, L. S., King, W., Cox, D. and Pollard, J. W. (2009). High-density gene expression analysis of tumor-associated macrophages from mouse mammary tumors. Am J Pathol *174*, 1048–1064.

[Okazaki et al., 2004] Okazaki, A., Shoji-Hosaka, E., Nakamura, K., Wakitani, M., Uchida, K., Kakita, S., Tsumoto, K., Kumagai, I. and Shitara, K. (2004). Fucose depletion from human IgG1 oligosaccharide enhances binding enthalpy and association rate between IgG1 and FcgammaRIIIa. J Mol Biol *336*, 1239–1249.

[O'Keefe et al., 1999] O'Keefe, T. L., Williams, G. T., Batista, F. D. and Neuberger, M. S. (1999). Deficiency in CD22, a B cell-specific inhibitory receptor, is sufficient to predispose to development of high affinity autoantibodies. J Exp Med *189*, 1307–1313.

[Oseini et al., 2011] Oseini, A. M., Chaiteerakij, R., Shire, A. M., Ghazale, A., Kaiya, J., Moser, C. D., Aderca, I., Mettler, T. A., Therneau, T. M., Zhang, L., Takahashi, N., Chari, S. T. and Roberts, L. R. (2011). Utility of serum immunoglobulin G4 in distinguishing immunoglobulin G4-associated cholangitis from cholangiocarcinoma. Hepatology *54*, 940–948.

[Osella-Abate et al., 2002] Osella-Abate, S., Quaglino, P., Savoia, P., Leporati, C., Comessatti, A. and Bernengo, M. G. (2002). VEGF-165 serum levels and tyrosinase expression in melanoma patients: correlation with the clinical course. Melanoma Res *12*, 325–334.

[Ozaki et al., 2002] Ozaki, K., Spolski, R., Feng, C. G., Qi, C. F., Cheng, J., Sher, A., Morse, H. C., Liu, C., Schwartzberg, P. L. and Leonard, W. J. (2002). A critical role for IL-21 in regulating immunoglobulin production. Science *298*, 1630–1634.

[Pagès et al., 2009] Pagès, F., Kirilovsky, A., Mlecnik, B., Asslaber, M., Tosolini, M., Bindea, G., Lagorce, C., Wind, P., Marliot, F., Bruneval, P., Zatloukal, K., Trajanoski, Z., Berger, A., Fridman, W. H. and Galon, J. (2009). In situ cytotoxic and memory T cells predict outcome in patients with early-stage colorectal cancer. J Clin Oncol *27*, 5944–5951.

[Palmer et al., 2011] Palmer, S. R., Erickson, L. A., Ichetovkin, I., Knauer, D. J. and Markovic, S. N. (2011). Circulating serologic and molecular biomarkers in malignant melanoma. Mayo Clin Proc *86*, 981–990.

[Palucka et al., 2007] Palucka, A. K., Ueno, H., Fay, J. W. and Banchereau, J. (2007). Taming cancer by inducing immunity via dendritic cells. Immunol Rev *220*, 129–150.

[Passalacqua et al., 1999] Passalacqua, G., Albano, M., Riccio, A., Fregonese, L., Puccinelli, P., Parmiani, S. and Canonica, G. W. (1999). Clinical and immunologic effects of a rush sublingual immunotherapy to Parietaria species: A double-blind, placebo-controlled trial. J Allergy Clin Immunol *104*, 964–968.

[Pedicord et al., 2011] Pedicord, V. A., Montalvo, W., Leiner, I. M. and Allison, J. P. (2011). Single dose of anti-CTLA-4 enhances CD8+ T-cell memory formation, function, and maintenance. Proc Natl Acad Sci U S A *108*, 266–271.

[Pelletier et al., 2005] Pelletier, F., Bermont, L., Puzenat, E., Blanc, D., Cairey-Remonnay, S., Mougin, C., Laurent, R., Humbert, P. and Aubin, F. (2005). Circulating vascular endothelial growth factor in cutaneous malignant melanoma. Br J Dermatol *152*, 685–689.

[Perrotta et al., 2011] Perrotta, I., Russo, E., Camastra, C., Filice, G., Di Mizio, G., Colosimo, F., Ricci, P., Tripepi, S., Amorosi, A., Triumbari, F. and Donato, G. (2011). New evidence for a critical role of elastin in calcification of native heart valves: immunohistochemical and ultrastructural study with literature review. Histopathology *59*, 504–513.

[Petersson et al., 2009] Petersson, S., Shubbar, E., Enerbäck, L. and Enerbäck, C. (2009). Expression patterns of S100 proteins in melanocytes and melanocytic lesions. Melanoma Res *19*, 215–225.

[Petrella et al., 2007] Petrella, T., Quirt, I., Verma, S., Haynes, A. E., Charette, M., Bak, K. and Melanoma Disease Site Group of Cancer Care Ontario's Program in Evidence-based Care (2007). Single-agent interleukin-2 in the treatment of metastatic melanoma: a systematic review. Cancer Treat Rev *33*, 484–496.

[Pieper et al., 2013] Pieper, K., Grimbacher, B. and Eibel, H. (2013). B-cell biology and development. J Allergy Clin Immunol *131*, 959–971.

[Pietra et al., 2012] Pietra, G., Manzini, C., Rivara, S., Vitale, M., Cantoni, C., Petretto, A., Balsamo, M., Conte, R., Benelli, R., Minghelli, S., Solari, N., Gualco, M., Queirolo, P., Moretta, L. and Mingari, M. C. (2012). Melanoma cells inhibit natural killer cell function by modulating the expression of activating receptors and cytolytic activity. Cancer Res *72*, 1407–1415.

[Pilette et al., 2007] Pilette, C., Nouri-Aria, K. T., Jacobson, M. R., Wilcock, L. K., Detry, B., Walker, S. M., Francis, J. N. and Durham, S. R. (2007). Grass pollen immunotherapy induces an allergen-specific IgA2 antibody response associated with mucosal TGF-beta expression. J Immunol *178*, 4658–4666.

[Platts-Mills et al., 2004] Platts-Mills, T. A., Woodfolk, J. A., Erwin, E. A. and Aalberse, R. (2004). Mechanisms of tolerance to inhalant allergens: the relevance of a modified Th2 response to allergens from domestic animals. Springer Semin Immunopathol *25*, 271–279.

[Platzer et al., 2012] Platzer, B., Dehlink, E., Turley, S. J. and Fiebiger, E. (2012). How to connect an IgE-driven response with CTL activity? Cancer Immunol Immunother *61*, 1521–1525.

[Pollok et al., 1993] Pollok, K. E., Kim, Y. J., Zhou, Z., Hurtado, J., Kim, K. K., Pickard, R. T. and Kwon, B. S. (1993). Inducible T cell antigen 4-1BB. Analysis of expression and function. J Immunol *150*, 771–781.

[Poschke et al., 2011] Poschke, I., Mougiakakos, D. and Kiessling, R. (2011). Camouflage and sabotage: tumor escape from the immune system. Cancer Immunol Immunother *60*, 1161–1171.

[Price et al., 2011] Price, M. A., Colvin Wanshura, L. E., Yang, J., Carlson, J., Xiang, B., Li, G., Ferrone, S., Dudek, A. Z., Turley, E. A. and McCarthy, J. B. (2011). CSPG4, a potential therapeutic target, facilitates malignant progression of melanoma. Pigment Cell Melanoma Res *24*, 1148–1157.

[Prieto et al., 2012] Prieto, P. A., Yang, J. C., Sherry, R. M., Hughes, M. S., Kammula, U. S., White, D. E., Levy, C. L., Rosenberg, S. A. and Phan, G. Q. (2012). CTLA-4 blockade with ipilimumab: long-term follow-up of 177 patients with metastatic melanoma. Clin Cancer Res *18*, 2039–2047.

[Punt et al., 1994] Punt, C. J., Barbuto, J. A., Zhang, H., Grimes, W. J., Hatch, K. D. and Hersh, E. M. (1994). Anti-tumor antibody produced by human tumor-infiltrating and peripheral blood B lymphocytes. Cancer Immunol Immunother *38*, 225–232.

[Putnam, 1969] Putnam, F. W. (1969). Immunoglobulin structure: variability and homology. Science *163*, 633–644.

[Qian and Pollard, 2010] Qian, B. Z. and Pollard, J. W. (2010). Macrophage diversity enhances tumor progression and metastasis. Cell *141*, 39–51.

[Quaglino et al., 2007] Quaglino, P., Osella-Abate, S., Cappello, N., Ortoncelli, M., Nardò, T., Fierro, M. T., Cavallo, F., Savoia, P. and Bernengo, M. G.

(2007). Prognostic relevance of baseline and sequential peripheral blood tyrosinase expression in 200 consecutive advanced metastatic melanoma patients. Melanoma Res *17*, 75–82.

[Quintana et al., 2012] Quintana, E., Piskounova, E., Shackleton, M., Weinberg, D., Eskiocak, U., Fullen, D. R., Johnson, T. M. and Morrison, S. J. (2012). Human melanoma metastasis in NSG mice correlates with clinical outcome in patients. Sci Transl Med *4*, 159–159.

[Rabinovich et al., 2007] Rabinovich, G. A., Gabrilovich, D. and Sotomayor, E. M. (2007). Immunosuppressive strategies that are mediated by tumor cells. Annu Rev Immunol *25*, 267–296.

[Raina et al., 2008] Raina, A., Krasinskas, A. M., Greer, J. B., Lamb, J., Fink, E., Moser, A. J., Zeh, H. J., Slivka, A. and Whitcomb, D. C. (2008). Serum immunoglobulin G fraction 4 levels in pancreatic cancer: elevations not associated with autoimmune pancreatitis. Arch Pathol Lab Med *132*, 48–53.

[Ravetch and Kinet, 1991] Ravetch, J. V. and Kinet, J. P. (1991). Fc receptors. Annu Rev Immunol *9*, 457–492.

[Reali et al., 2001] Reali, E., Greiner, J. W., Corti, A., Gould, H. J., Bottazzoli, F., Paganelli, G., Schlom, J. and Siccardi, A. G. (2001). IgEs targeted on tumor cells: therapeutic activity and potential in the design of tumor vaccines. Cancer Res *61*, 5517–5522.

[Reichert, 2011] Reichert, J. M. (2011). Antibody-based therapeutics to watch in 2011. MAbs *3*, 76–99.

[Reichert and Dhimolea, 2012] Reichert, J. M. and Dhimolea, E. (2012). The future of antibodies as cancer drugs. Drug Discov Today *17*, 954–963.

[Reichert and Valge-Archer, 2007] Reichert, J. M. and Valge-Archer, V. E. (2007). Development trends for monoclonal antibody cancer therapeutics. Nat Rev Drug Discov *6*, 349–356.

[Reichert and Wenger, 2008] Reichert, J. M. and Wenger, J. B. (2008). Development trends for new cancer therapeutics and vaccines. Drug Discov Today *13*, 30–37.

[Reisfeld and Cheresh, 1987] Reisfeld, R. A. and Cheresh, D. A. (1987). Human tumor antigens. Adv Immunol *40*, 323–377.

[Restrepo et al., 2013] Restrepo, L., Stafford, P. and Johnston, S. A. (2013). Feasibility of an early Alzheimer's disease immunosignature diagnostic test. J Neuroimmunol *254*, 154–160.

[Revy et al., 2000] Revy, P., Muto, T., Levy, Y., Geissmann, F., Plebani, A., Sanal, O., Catalan, N., Forveille, M., Dufourcq-Labelouse, R., Gennery, A., Tezcan, I., Ersoy, F., Kayserili, H., Ugazio, A. G., Brousse, N., Muramatsu, M., Notarangelo, L. D., Kinoshita, K., Honjo, T., Fischer, A. and Durandy, A. (2000). Activation-induced cytidine deaminase (AID) deficiency causes the autosomal recessive form of the Hyper-IgM syndrome (HIGM2). Cell *102*, 565–575.

[Reynolds et al., 2006] Reynolds, S. R., Vergilis, I. J., Szarek, M., Ferrone, S. and Bystryn, J. C. (2006). Cytoplasmic melanoma-associated antigen (CYT-MAA) serum level in patients with melanoma: a potential marker of response to immunotherapy? Int J Cancer *119*, 157–161.

[Ribas et al., 2005] Ribas, A., Camacho, L. H., Lopez-Berestein, G., Pavlov, D., Bulanhagui, C. A., Millham, R., Comin-Anduix, B., Reuben, J. M., Seja, E., Parker, C. A., Sharma, A., Glaspy, J. A. and Gomez-Navarro, J. (2005). Antitumor activity in melanoma and anti-self responses in a phase I trial with the anti-cytotoxic T lymphocyte-associated antigen 4 monoclonal antibody CP-675,206. J Clin Oncol *23*, 8968–8977.

[Ribas et al., 2013] Ribas, A., Hodi, F. S., Callahan, M., Konto, C. and Wolchok, J. (2013). Hepatotoxicity with combination of vemurafenib and ipilimumab. N Engl J Med *368*, 1365–1366.

[Ribatti et al., 2003] Ribatti, D., Ennas, M. G., Vacca, A., Ferreli, F., Nico, B., Orru, S. and Sirigu, P. (2003). Tumor vascularity and tryptase-positive mast cells correlate with a poor prognosis in melanoma. Eur J Clin Invest *33*, 420–425.

[Riemer et al., 2007] Riemer, A. B., Untersmayr, E., Knittelfelder, R., Duschl, A., Pehamberger, H., Zielinski, C. C., Scheiner, O. and Jensen-Jarolim, E.

(2007). Active induction of tumor-specific IgE antibodies by oral mimotope vaccination. Cancer Res *67*, 3406–3411.

[Rivera et al., 2012] Rivera, Z., Ferrone, S., Wang, X., Jube, S., Yang, H., Pass, H. I., Kanodia, S., Gaudino, G. and Carbone, M. (2012). CSPG4 as a target of antibody-based immunotherapy for malignant mesothelioma. Clin Cancer Res *18*, 5352–5363.

[Robert et al., 2011] Robert, C., Thomas, L., Bondarenko, I., O'Day, S., M D, J. W., Garbe, C., Lebbe, C., Baurain, J. F., Testori, A., Grob, J. J., Davidson, N., Richards, J., Maio, M., Hauschild, A., Miller, W. H., Gascon, P., Lotem, M., Harmankaya, K., Ibrahim, R., Francis, S., Chen, T. T., Humphrey, R., Hoos, A. and Wolchok, J. D. (2011). Ipilimumab plus dacarbazine for previously untreated metastatic melanoma. N Engl J Med *364*, 2517–2526.

[Robinson et al., 2004] Robinson, D. S., Larché, M. and Durham, S. R. (2004). Tregs and allergic disease. J Clin Invest *114*, 1389–1397.

[Rock et al., 1989] Rock, B., Martins, C. R., Theofilopoulos, A. N., Balderas, R. S., Anhalt, G. J., Labib, R. S., Futamura, S., Rivitti, E. A. and Diaz, L. A. (1989). The pathogenic effect of IgG4 autoantibodies in endemic pemphigus foliaceus (fogo selvagem). N Engl J Med *320*, 1463–1469.

[Rose et al., 2011] Rose, R. J., Labrijn, A. F., van den Bremer, E. T., Loverix, S., Lasters, I., van Berkel, P. H., van de Winkel, J. G., Schuurman, J., Parren, P. W. and Heck, A. J. (2011). Quantitative analysis of the interaction strength and dynamics of human IgG4 half molecules by native mass spectrometry. Structure *19*, 1274–1282.

[Ross et al., 1983] Ross, A. H., Cossu, G., Herlyn, M., Bell, J. R., Steplewski, Z. and Koprowski, H. (1983). Isolation and chemical characterization of a melanoma-associated proteoglycan antigen. Arch Biochem Biophys *225*, 370–383.

[Rotte et al., 2012] Rotte, A., Martinka, M. and Li, G. (2012). MMP2 expression is a prognostic marker for primary melanoma patients. Cell Oncol (Dordr) *35*, 207–216.

[Rush et al., 2005] Rush, J. S., Liu, M., Odegard, V. H., Unniraman, S. and Schatz, D. G. (2005). Expression of activation-induced cytidine deaminase is regulated by cell division, providing a mechanistic basis for division-linked class switch recombination. Proc Natl Acad Sci U S A *102*, 13242–13247.

[Sahagan et al., 1986] Sahagan, B. G., Dorai, H., Saltzgaber-Muller, J., Toneguzzo, F., Guindon, C. A., Lilly, S. P., McDonald, K. W., Morrissey, D. V., Stone, B. A. and Davis, G. L. (1986). A genetically engineered murine/human chimeric antibody retains specificity for human tumor-associated antigen. J Immunol *137*, 1066–1074.

[Samija et al., 2010] Samija, I., Lukac, J., Mariae-Broziae, J., Buljan, M., Alajbeg, I., Kovaceviae, D., Situm, M. and Kusiae, Z. (2010). Prognostic value of microphthalmia-associated transcription factor and tyrosinase as markers for circulating tumor cells detection in patients with melanoma. Melanoma Res *20*, 293–302.

[Sapoznik et al., 2012] Sapoznik, S., Ortenberg, R., Schachter, J. and Markel, G. (2012). CEACAM1 in malignant melanoma: a diagnostic and therapeutic target. Curr Top Med Chem *12*, 3–10.

[Satoguina et al., 2008] Satoguina, J. S., Adjobimey, T., Arndts, K., Hoch, J., Oldenburg, J., Layland, L. E. and Hoerauf, A. (2008). Tr1 and naturally occurring regulatory T cells induce IgG4 in B cells through GITR/GITR-L interaction, IL-10 and TGF-beta. Eur J Immunol *38*, 3101–3113.

[Satoguina et al., 2005] Satoguina, J. S., Weyand, E., Larbi, J. and Hoerauf, A. (2005). T regulatory-1 cells induce IgG4 production by B cells: role of IL-10. J Immunol *174*, 4718–4726.

[Satyamoorthy et al., 2003] Satyamoorthy, K., Li, G., Gerrero, M. R., Brose, M. S., Volpe, P., Weber, B. L., Van Belle, P., Elder, D. E. and Herlyn, M. (2003). Constitutive mitogen-activated protein kinase activation in melanoma is mediated by both BRAF mutations and autocrine growth factor stimulation. Cancer Res *63*, 756–759.

[Scanlan et al., 2002] Scanlan, M. J., Gure, A. O., Jungbluth, A. A., Old, L. J. and Chen, Y. T. (2002). Cancer/testis antigens: an expanding family of targets for cancer immunotherapy. Immunol Rev *188*, 22–32.

[Schadendorf et al., 2006] Schadendorf, D., Ugurel, S., Schuler-Thurner, B., Nestle, F. O., Enk, A., Bröcker, E. B., Grabbe, S., Rittgen, W., Edler, L., Sucker, A., Zimpfer-Rechner, C., Berger, T., Kamarashev, J., Burg, G., Jonuleit, H., Tüttenberg, A., Becker, J. C., Keikavoussi, P., Kämpgen, E., Schuler, G. and DC study group of the DeCOG (2006). Dacarbazine (DTIC) versus vaccination with autologous peptide-pulsed dendritic cells (DC) in first-line treatment of patients with metastatic melanoma: a randomized phase III trial of the DC study group of the DeCOG. Ann Oncol *17*, 563–570.

[Schatz et al., 1989] Schatz, D. G., Oettinger, M. A. and Baltimore, D. (1989). The V(D)J recombination activating gene, RAG-1. Cell *59*, 1035–1048.

[Schioppa et al., 2011] Schioppa, T., Moore, R., Thompson, R. G., Rosser, E. C., Kulbe, H., Nedospasov, S., Mauri, C., Coussens, L. M. and Balkwill, F. R. (2011). B regulatory cells and the tumor-promoting actions of TNF-α during squamous carcinogenesis. Proc Natl Acad Sci U S A *108*, 10662–10667.

[Schmidt et al., 2006] Schmidt, H., Johansen, J. S., Gehl, J., Geertsen, P. F., Fode, K. and von der Maase, H. (2006). Elevated serum level of YKL-40 is an independent prognostic factor for poor survival in patients with metastatic melanoma. Cancer *106*, 1130–1139.

[Schmidt et al., 2005] Schmidt, H., Sorensen, B. S., Fode, K., Nexo, E. and von der Maase, H. (2005). Tyrosinase messenger RNA in peripheral blood is related to poor survival in patients with metastatic melanoma following interleukin-2-based immunotherapy. Melanoma Res *15*, 409–416.

[Schmidt et al., 2011] Schmidt, P., Kopecky, C., Hombach, A., Zigrino, P., Mauch, C. and Abken, H. (2011). Eradication of melanomas by targeted elimination of a minor subset of tumor cells. Proc Natl Acad Sci U S A *108*, 2474–2479.

[Schneeberger et al., 2000] Schneeberger, A., Goos, M., Stingl, G. and Wagner, S. N. (2000). Management of malignant melanoma: new developments in immune and gene therapy. Clin Exp Dermatol *25*, 509–519.

[Schreiber et al., 2011] Schreiber, R. D., Old, L. J. and Smyth, M. J. (2011). Cancer immunoediting: integrating immunity's roles in cancer suppression and promotion. Science *331*, 1565–1570.

[Schroff et al., 1985] Schroff, R. W., Woodhouse, C. S., Foon, K. A., Oldham, R. K., Farrell, M. M., Klein, R. A. and Morgan, A. C. (1985). Intratumor localization of monoclonal antibody in patients with melanoma treated with antibody to a 250,000-dalton melanoma-associated antigen. J Natl Cancer Inst *74*, 299–306.

[Schuurman et al., 2001] Schuurman, J., Perdok, G. J., Gorter, A. D. and Aalberse, R. C. (2001). The inter-heavy chain disulfide bonds of IgG4 are in equilibrium with intra-chain disulfide bonds. Mol Immunol *38*, 1–8.

[Scott et al., 2012] Scott, A. M., Wolchok, J. D. and Old, L. J. (2012). Antibody therapy of cancer. Nat Rev Cancer *12*, 278–287.

[Shamji et al., 2012] Shamji, M. H., Ljorring, C., Francis, J. N., Calderon, M. A., Larché, M., Kimber, I., Frew, A. J., Ipsen, H., Lund, K., Würtzen, P. A. and Durham, S. R. (2012). Functional rather than immunoreactive levels of IgG4 correlate closely with clinical response to grass pollen immunotherapy. Allergy *67*, 217–226.

[Sharpe et al., 2007] Sharpe, A. H., Wherry, E. J., Ahmed, R. and Freeman, G. J. (2007). The function of programmed cell death 1 and its ligands in regulating autoimmunity and infection. Nat Immunol *8*, 239–245.

[Sheu et al., 2001] Sheu, B. C., Lin, R. H., Lien, H. C., Ho, H. N., Hsu, S. M. and Huang, S. C. (2001). Predominant Th2/Tc2 polarity of tumor-infiltrating lymphocytes in human cervical cancer. J Immunol *167*, 2972–2978.

[Sica and Mantovani, 2012] Sica, A. and Mantovani, A. (2012). Macrophage plasticity and polarization: in vivo veritas. J Clin Invest *122*, 787–795.

[Siccardi et al., 1986] Siccardi, A. G., Buraggi, G. L., Callegaro, L., Mariani, G., Natali, P. G., Abbati, A., Bestagno, M., Caputo, V., Mansi, L. and Masi, R. (1986). Multicenter study of immunoscintigraphy with radiolabeled monoclonal antibodies in patients with melanoma. Cancer Res *46*, 4817–4822.

[Simson et al., 2007] Simson, L., Ellyard, J. I., Dent, L. A., Matthaei, K. I., Rothenberg, M. E., Foster, P. S., Smyth, M. J. and Parish, C. R. (2007). Regulation of carcinogenesis by IL-5 and CCL11: a potential role for eosinophils in tumor immune surveillance. J Immunol *178*, 4222–4229.

[Sittler et al., 2008] Sittler, T., Zhou, J., Park, J., Yuen, N. K., Sarantopoulos, S., Mollick, J., Salgia, R., Giobbie-Hurder, A., Dranoff, G. and Hodi, F. S. (2008). Concerted potent humoral immune responses to autoantigens are associated with tumor destruction and favorable clinical outcomes without autoimmunity. Clin Cancer Res *14*, 3896–3905.

[Sivan et al., 2012] Sivan, S., Suzan, F., Rona, O., Tamar, H., Vivian, B., Tamar, P., Jacob, S., Gal, M. and Michal, L. (2012). Serum CEACAM1 Correlates with Disease Progression and Survival in Malignant Melanoma Patients. Clin Dev Immunol *2012*, 290536–290536.

[Solassol et al., 2011] Solassol, J., Du-Thanh, A., Maudelonde, T. and Guillot, B. (2011). Serum proteomic profiling reveals potential biomarkers for cutaneous malignant melanoma. Int J Biol Markers *26*, 82–87.

[Sosman et al., 2012] Sosman, J. A., Kim, K. B., Schuchter, L., Gonzalez, R., Pavlick, A. C., Weber, J. S., McArthur, G. A., Hutson, T. E., Moschos, S. J., Flaherty, K. T., Hersey, P., Kefford, R., Lawrence, D., Puzanov, I., Lewis, K. D., Amaravadi, R. K., Chmielowski, B., Lawrence, H. J., Shyr, Y., Ye, F., Li, J., Nolop, K. B., Lee, R. J., Joe, A. K. and Ribas, A. (2012). Survival in BRAF V600-mutant advanced melanoma treated with vemurafenib. N Engl J Med *366*, 707–714.

[Soucek et al., 2007] Soucek, L., Lawlor, E. R., Soto, D., Shchors, K., Swigart, L. B. and Evan, G. I. (2007). Mast cells are required for angiogenesis and macroscopic expansion of Myc-induced pancreatic islet tumors. Nat Med *13*, 1211–1218.

[Spitler et al., 1987] Spitler, L. E., del Rio, M., Khentigan, A., Wedel, N. I., Brophy, N. A., Miller, L. L., Harkonen, W. S., Rosendorf, L. L., Lee, H. M. and Mischak, R. P. (1987). Therapy of patients with malignant melanoma using a monoclonal antimelanoma antibody-ricin A chain immunotoxin. Cancer Res *47*, 1717–1723.

[Spriggs et al., 1992] Spriggs, M. K., Armitage, R. J., Strockbine, L., Clifford, K. N., Macduff, B. M., Sato, T. A., Maliszewski, C. R. and Fanslow, W. C. (1992). Recombinant human CD40 ligand stimulates B cell proliferation and immunoglobulin E secretion. J Exp Med *176*, 1543–1550.

[Staerz et al., 1985] Staerz, U. D., Kanagawa, O. and Bevan, M. J. (1985). Hybrid antibodies can target sites for attack by T cells. Nature *314*, 628–631.

[Stamenkovic, 2003] Stamenkovic, I. (2003). Extracellular matrix remodelling: the role of matrix metalloproteinases. J Pathol *200*, 448–464.

[Stockert et al., 1998] Stockert, E., Jäger, E., Chen, Y. T., Scanlan, M. J., Gout, I., Karbach, J., Arand, M., Knuth, A. and Old, L. J. (1998). A survey of the humoral immune response of cancer patients to a panel of human tumor antigens. J Exp Med *187*, 1349–1354.

[Stone et al., 2012] Stone, J. H., Zen, Y. and Deshpande, V. (2012). IgG4-related disease. N Engl J Med *366*, 539–551.

[Strehl et al., 2011] Strehl, J. D., Hartmann, A. and Agaimy, A. (2011). Numerous IgG4-positive plasma cells are ubiquitous in diverse localised non-specific chronic inflammatory conditions and need to be distinguished from IgG4-related systemic disorders. J Clin Pathol *64*, 237–243.

[Strid et al., 2008] Strid, J., Roberts, S. J., Filler, R. B., Lewis, J. M., Kwong, B. Y., Schpero, W., Kaplan, D. H., Hayday, A. C. and Girardi, M. (2008). Acute upregulation of an NKG2D ligand promotes rapid reorganization of a local immune compartment with pleiotropic effects on carcinogenesis. Nat Immunol *9*, 146–154.

[Strid et al., 2011] Strid, J., Sobolev, O., Zafirova, B., Polic, B. and Hayday, A. (2011). The intraepithelial T cell response to NKG2D-ligands links lymphoid stress surveillance to atopy. Science *334*, 1293–1297.

[Su et al., 2012] Su, F., Viros, A., Milagre, C., Trunzer, K., Bollag, G., Spleiss, O., Reis-Filho, J. S., Kong, X., Koya, R. C., Flaherty, K. T., Chapman, P. B., Kim, M. J., Hayward, R., Martin, M., Yang, H., Wang, Q., Hilton, H., Hang, J. S., Noe, J., Lambros, M., Geyer, F., Dhomen, N., Niculescu-Duvaz, I., Zambon, A., Niculescu-Duvaz, D., Preece, N., Robert, L., Otte, N. J., Mok, S., Kee, D., Ma, Y., Zhang, C., Habets, G., Burton, E. A., Wong, B., Nguyen, H., Kockx, M., Andries, L., Lestini, B., Nolop, K. B., Lee, R. J., Joe, A. K., Troy, J. L., Gonzalez, R., Hutson, T. E., Puzanov, I., Chmielowski, B., Springer, C. J., McArthur, G. A., Sosman, J. A., Lo, R. S., Ribas, A. and Marais, R.

(2012). RAS mutations in cutaneous squamous-cell carcinomas in patients treated with BRAF inhibitors. N Engl J Med *366*, 207–215.

[Sulzer et al., 1994] Sulzer, B., Van Hemmen, J. L. and Behn, U. (1994). Central immune system, the self and autoimmunity. Bull Math Biol *56*, 1009–1040.

[Sumimoto et al., 2006] Sumimoto, H., Imabayashi, F., Iwata, T. and Kawakami, Y. (2006). The BRAF-MAPK signaling pathway is essential for cancer-immune evasion in human melanoma cells. J Exp Med *203*, 1651–1656.

[Sundström and Nilsson, 1976] Sundström, C. and Nilsson, K. (1976). Establishment and characterization of a human histiocytic lymphoma cell line (U-937). Int J Cancer *17*, 565–577.

[Swenson et al., 2005] Swenson, W. T., Wooldridge, J. E., Lynch, C. F., Forman-Hoffman, V. L., Chrischilles, E. and Link, B. K. (2005). Improved survival of follicular lymphoma patients in the United States. J Clin Oncol *23*, 5019–5026.

[Sykes et al., 2013] Sykes, K. F., Legutki, J. B. and Stafford, P. (2013). Immunosignaturing: a critical review. Trends Biotechnol *31*, 45–51.

[Takeda et al., 1996] Takeda, K., Tanaka, T., Shi, W., Matsumoto, M., Minami, M., Kashiwamura, S., Nakanishi, K., Yoshida, N., Kishimoto, T. and Akira, S. (1996). Essential role of Stat6 in IL-4 signalling. Nature *380*, 627–630.

[Tan and Coussens, 2007] Tan, T. T. and Coussens, L. M. (2007). Humoral immunity, inflammation and cancer. Curr Opin Immunol *19*, 209–216.

[Tanchot et al., 2012] Tanchot, C., Terme, M., Pere, H., Tran, T., Benhamouda, N., Strioga, M., Banissi, C., Galluzzi, L., Kroemer, G. and Tartour, E. (2012). Tumor-Infiltrating Regulatory T Cells: Phenotype, Role, Mechanism of Expansion In Situ and Clinical Significance. Cancer Microenviron .

[Tandler et al., 2012] Tandler, N., Mosch, B. and Pietzsch, J. (2012). Protein and non-protein biomarkers in melanoma: a critical update. Amino Acids *43*, 2203–2230.

[Tao et al., 1993] Tao, M. H., Smith, R. I. and Morrison, S. L. (1993). Structural features of human immunoglobulin G that determine isotype-specific differences in complement activation. J Exp Med *178*, 661–667.

[Teo et al., 2012] Teo, P. Z., Utz, P. J. and Mollick, J. A. (2012). Using the allergic immune system to target cancer: activity of IgE antibodies specific for human CD20 and MUC1. Cancer Immunol Immunother *61*, 2295–2309.

[Terabe et al., 2004] Terabe, M., Park, J. M. and Berzofsky, J. A. (2004). Role of IL-13 in regulation of anti-tumor immunity and tumor growth. Cancer Immunol Immunother *53*, 79–85.

[Thies et al., 2002] Thies, A., Moll, I., Berger, J., Wagener, C., Brümmer, J., Schulze, H. J., Brunner, G. and Schumacher, U. (2002). CEACAM1 expression in cutaneous malignant melanoma predicts the development of metastatic disease. J Clin Oncol *20*, 2530–2536.

[Thompson et al., 2005] Thompson, J. F., Scolyer, R. A. and Kefford, R. F. (2005). Cutaneous melanoma. Lancet *365*, 687–701.

[Topalian et al., 2012] Topalian, S. L., Hodi, F. S., Brahmer, J. R., Gettinger, S. N., Smith, D. C., McDermott, D. F., Powderly, J. D., Carvajal, R. D., Sosman, J. A., Atkins, M. B., Leming, P. D., Spigel, D. R., Antonia, S. J., Horn, L., Drake, C. G., Pardoll, D. M., Chen, L., Sharfman, W. H., Anders, R. A., Taube, J. M., McMiller, T. L., Xu, H., Korman, A. J., Jure-Kunkel, M., Agrawal, S., McDonald, D., Kollia, G. D., Gupta, A., Wigginton, J. M. and Sznol, M. (2012). Safety, activity, and immune correlates of anti-PD-1 antibody in cancer. N Engl J Med *366*, 2443–2454.

[Torisu-Itakura et al., 2007] Torisu-Itakura, H., Lee, J. H., Scheri, R. P., Huynh, Y., Ye, X., Essner, R. and Morton, D. L. (2007). Molecular characterization of inflammatory genes in sentinel and nonsentinel nodes in melanoma. Clin Cancer Res *13*, 3125–3132.

[Traggiai et al., 2004] Traggiai, E., Becker, S., Subbarao, K., Kolesnikova, L., Uematsu, Y., Gismondo, M. R., Murphy, B. R., Rappuoli, R. and Lanzavecchia, A. (2004). An efficient method to make human monoclonal antibodies from memory B cells: potent neutralization of SARS coronavirus. Nat Med *10*, 871–875.

[Trefzer et al., 2006] Trefzer, U., Hofmann, M., Reinke, S., Guo, Y. J., Audring, H., Spagnoli, G. and Sterry, W. (2006). Concordant loss of melanoma dif-

ferentiation antigens in synchronous and asynchronous melanoma metastases: implications for immunotherapy. Melanoma Res *16*, 137–145.

[Tsai et al., 2008] Tsai, J., Lee, J. T., Wang, W., Zhang, J., Cho, H., Mamo, S., Bremer, R., Gillette, S., Kong, J., Haass, N. K., Sproesser, K., Li, L., Smalley, K. S., Fong, D., Zhu, Y. L., Marimuthu, A., Nguyen, H., Lam, B., Liu, J., Cheung, I., Rice, J., Suzuki, Y., Luu, C., Settachatgul, C., Shellooe, R., Cantwell, J., Kim, S. H., Schlessinger, J., Zhang, K. Y., West, B. L., Powell, B., Habets, G., Zhang, C., Ibrahim, P. N., Hirth, P., Artis, D. R., Herlyn, M. and Bollag, G. (2008). Discovery of a selective inhibitor of oncogenic B-Raf kinase with potent antimelanoma activity. Proc Natl Acad Sci U S A *105*, 3041–3046.

[Tsoporis et al., 2011] Tsoporis, J. N., Mohammadzadeh, F. and Parker, T. G. (2011). S100B: a multifunctional role in cardiovascular pathophysiology. Amino Acids *41*, 843–847.

[Tth-Jakatics et al., 2000] Tth-Jakatics, R., Jimi, S., Takebayashi, S. and Kawamoto, N. (2000). Cutaneous malignant melanoma: correlation between neovascularization and peritumor accumulation of mast cells overexpressing vascular endothelial growth factor. Hum Pathol *31*, 955–960.

[Turajlic et al., 2013] Turajlic, S., Ali, Z., Yousaf, N. and Larkin, J. (2013). Phase I/II RAF kinase inhibitors in cancer therapy. Expert Opin Investig Drugs *22*, 739–749.

[Turner et al., 2006] Turner, M. C., Chen, Y., Krewski, D. and Ghadirian, P. (2006). An overview of the association between allergy and cancer. Int J Cancer *118*, 3124–3132.

[Ugurel et al., 2001] Ugurel, S., Rappl, G., Tilgen, W. and Reinhold, U. (2001). Increased serum concentration of angiogenic factors in malignant melanoma patients correlates with tumor progression and survival. J Clin Oncol *19*, 577–583.

[Untersmayr et al., 2010] Untersmayr, E., Bises, G., Starkl, P., Bevins, C. L., Scheiner, O., Boltz-Nitulescu, G., Wrba, F. and Jensen-Jarolim, E. (2010). The high affinity IgE receptor Fc epsilonRI is expressed by human intestinal epithelial cells. PLoS One *5*.

[Ure, 1969] Ure, D. M. (1969). Negative assoication between allergy and cancer. Scott Med J *14*, 51–54.

[Urosevic and Dummer, 2003] Urosevic, M. and Dummer, R. (2003). HLA-G and IL-10 expression in human cancer–different stories with the same message. Semin Cancer Biol *13*, 337–342.

[van de Veen et al., 2013] van de Veen, W., Stanic, B., Yaman, G., Wawrzyniak, M., Söllner, S., Akdis, D. G., Rückert, B., Akdis, C. A. and Akdis, M. (2013). IgG4 production is confined to human IL-10-producing regulatory B cells that suppress antigen-specific immune responses. J Allergy Clin Immunol *131*, 1204–1212.

[van der Neut Kolfschoten et al., 2007] van der Neut Kolfschoten, M., Schuurman, J., Losen, M., Bleeker, W. K., Martínez-Martínez, P., Vermeulen, E., den Bleker, T. H., Wiegman, L., Vink, T., Aarden, L. A., De Baets, M. H., van de Winkel, J. G., Aalberse, R. C. and Parren, P. W. (2007). Anti-inflammatory activity of human IgG4 antibodies by dynamic Fab arm exchange. Science *317*, 1554–1557.

[van der Zee et al., 1986] van der Zee, J. S., van Swieten, P. and Aalberse, R. C. (1986). Inhibition of complement activation by IgG4 antibodies. Clin Exp Immunol *64*, 415–422.

[Van Hemelrijck et al., 2010] Van Hemelrijck, M., Garmo, H., Binda, E., Hayday, A., Karagiannis, S. N., Hammar, N., Walldius, G., Lambe, M., Jungner, I. and Holmberg, L. (2010). Immunoglobulin E and cancer: a meta-analysis and a large Swedish cohort study. Cancer Causes Control *21*, 1657–1667.

[Vangelista et al., 2005] Vangelista, L., Soprana, E., Cesco-Gaspere, M., Mandiola, P., Di Lullo, G., Fucci, R. N., Codazzi, F., Palini, A., Paganelli, G., Burrone, O. R. and Siccardi, A. G. (2005). Membrane IgE binds and activates Fc epsilon RI in an antigen-independent manner. J Immunol *174*, 5602–5611.

[Verdecchia et al., 2009] Verdecchia, A., Guzzinati, S., Francisci, S., De Angelis, R., Bray, F., Allemani, C., Tavilla, A., Santaquilani, M., Sant, M. and EUROCARE Working Group (2009). Survival trends in European cancer patients diagnosed from 1988 to 1999. Eur J Cancer *45*, 1042–1066.

[Vereecken et al., 2012] Vereecken, P., Cornelis, F., Van Baren, N., Vandersleyen, V. and Baurain, J. F. (2012). A synopsis of serum biomarkers in cutaneous melanoma patients. Dermatol Res Pract *2012*, 260643–260643.

[Vergilis et al., 2005] Vergilis, I. J., Szarek, M., Ferrone, S. and Reynolds, S. R. (2005). Presence and prognostic significance of melanoma-associated antigens CYT-MAA and HMW-MAA in serum of patients with melanoma. J Invest Dermatol *125*, 526–531.

[Verma et al., 2012] Verma, S., Miles, D., Gianni, L., Krop, I. E., Welslau, M., Baselga, J., Pegram, M., Oh, D. Y., Diéras, V., Guardino, E., Fang, L., Lu, M. W., Olsen, S., Blackwell, K. and EMILIA Study Group (2012). Trastuzumab emtansine for HER2-positive advanced breast cancer. N Engl J Med *367*, 1783–1791.

[Vesely and Schreiber, 2013] Vesely, M. D. and Schreiber, R. D. (2013). Cancer immunoediting: antigens, mechanisms, and implications to cancer immunotherapy. Ann N Y Acad Sci *1284*, 1–5.

[Vial et al., 2000] Vial, D., Okazaki, H. and Siraganian, R. P. (2000). The NH2-terminal region of focal adhesion kinase reconstitutes high affinity IgE receptor-induced secretion in mast cells. J Biol Chem *275*, 28269–28275.

[Vihinen et al., 2007] Vihinen, P. P., Hilli, J., Vuoristo, M. S., Syrjänen, K. J., Kähäri, V. M. and Pyrhönen, S. O. (2007). Serum VEGF-C is associated with metastatic site in patients with malignant melanoma. Acta Oncol *46*, 678–684.

[Visús et al., 2007] Visús, C., Andres, R., Mayordomo, J. I., Martinez-Lorenzo, M. J., Murillo, L., Sáez-Gutiérrez, B., Diestre, C., Marcos, I., Astier, P., Godino, J., Carapeto-Marquez de Prado, F. J., Larrad, L. and Tres, A. (2007). Prognostic role of circulating melanoma cells detected by reverse transcriptase-polymerase chain reaction for tyrosinase mRNA in patients with melanoma. Melanoma Res *17*, 83–89.

[Volck et al., 1998] Volck, B., Price, P. A., Johansen, J. S., Sorensen, O., Benfield, T. L., Nielsen, H. J., Calafat, J. and Borregaard, N. (1998). YKL-40, a mammalian member of the chitinase family, is a matrix protein of specific granules in human neutrophils. Proc Assoc Am Physicians *110*, 351–360.

[vonWasielewski et al., 2000] vonWasielewski, R., Seth, S., Franklin, J., Fischer, R., Hubner, K., Hansmann, M. L., Diehl, V. and Georgii, A. (2000). Tissue eosinophilia correlates strongly with poor prognosis in nodular sclerosing Hodgkin's disease, allowing for known prognostic factors. Blood *95*, 1207–1213.

[Vouldoukis et al., 2011] Vouldoukis, I., Mazier, D., Moynet, D., Thiolat, D., Malvy, D. and Mossalayi, M. D. (2011). IgE mediates killing of intracellular Toxoplasma gondii by human macrophages through CD23-dependent, interleukin-10 sensitive pathway. PLoS One *6*.

[Wagner et al., 2005] Wagner, S., Hafner, C., Allwardt, D., Jasinska, J., Ferrone, S., Zielinski, C. C., Scheiner, O., Wiedermann, U., Pehamberger, H. and Breiteneder, H. (2005). Vaccination with a human high molecular weight melanoma-associated antigen mimotope induces a humoral response inhibiting melanoma cell growth in vitro. J Immunol *174*, 976–982.

[Wagner et al., 2008] Wagner, S., Krepler, C., Allwardt, D., Latzka, J., Strommer, S., Scheiner, O., Pehamberger, H., Wiedermann, U., Hafner, C. and Breiteneder, H. (2008). Reduction of human melanoma tumor growth in severe combined immunodeficient mice by passive transfer of antibodies induced by a high molecular weight melanoma-associated antigen mimotope vaccine. Clin Cancer Res *14*, 8178–8183.

[Waldmann, 2003] Waldmann, T. A. (2003). Immunotherapy: past, present and future. Nat Med *9*, 269–277.

[Waldmann and Morris, 2006] Waldmann, T. A. and Morris, J. C. (2006). Development of antibodies and chimeric molecules for cancer immunotherapy. Adv Immunol *90*, 83–131.

[Wang et al., 2010a] Wang, X., Osada, T., Wang, Y., Yu, L., Sakakura, K., Katayama, A., McCarthy, J. B., Brufsky, A., Chivukula, M., Khoury, T., Hsu, D. S., Barry, W. T., Lyerly, H. K., Clay, T. M. and Ferrone, S. (2010a). CSPG4 protein as a new target for the antibody-based immunotherapy of triple-negative breast cancer. J Natl Cancer Inst *102*, 1496–1512.

[Wang et al., 2010b] Wang, X., Wang, Y., Yu, L., Sakakura, K., Visus, C., Schwab, J. H., Ferrone, C. R., Favoino, E., Koya, Y., Campoli, M. R., McCarthy, J. B.,

DeLeo, A. B. and Ferrone, S. (2010b). CSPG4 in cancer: multiple roles. Curr Mol Med *10*, 419–429.

[Warren et al., 2003] Warren, S. J., Arteaga, L. A., Rivitti, E. A., Aoki, V., Hans-Filho, G., Qaqish, B. F., Lin, M. S., Giudice, G. J. and Diaz, L. A. (2003). The role of subclass switching in the pathogenesis of endemic pemphigus foliaceus. J Invest Dermatol *120*, 104–108.

[Watts, 2005] Watts, T. H. (2005). TNF/TNFR family members in costimulation of T cell responses. Annu Rev Immunol *23*, 23–68.

[Weber et al., 2008] Weber, J. S., O'Day, S., Urba, W., Powderly, J., Nichol, G., Yellin, M., Snively, J. and Hersh, E. (2008). Phase I/II study of ipilimumab for patients with metastatic melanoma. J Clin Oncol *26*, 5950–5956.

[Weinberg et al., 2000] Weinberg, A. D., Rivera, M. M., Prell, R., Morris, A., Ramstad, T., Vetto, J. T., Urba, W. J., Alvord, G., Bunce, C. and Shields, J. (2000). Engagement of the OX-40 receptor in vivo enhances antitumor immunity. J Immunol *164*, 2160–2169.

[Weiner et al., 2010] Weiner, L. M., Surana, R. and Wang, S. (2010). Monoclonal antibodies: versatile platforms for cancer immunotherapy. Nat Rev Immunol *10*, 317–327.

[Weng et al., 2004] Weng, W. K., Czerwinski, D., Timmerman, J., Hsu, F. J. and Levy, R. (2004). Clinical outcome of lymphoma patients after idiotype vaccination is correlated with humoral immune response and immunoglobulin G Fc receptor genotype. J Clin Oncol *22*, 4717–4724.

[Weng and Levy, 2003] Weng, W. K. and Levy, R. (2003). Two immunoglobulin G fragment C receptor polymorphisms independently predict response to rituximab in patients with follicular lymphoma. J Clin Oncol *21*, 3940–3947.

[WHO, 2013] WHO (2012 (accessed December 15, 2013)). Melanoma Skin Cancer.

[Wilson et al., 1981] Wilson, B. S., Imai, K., Natali, P. G. and Ferrone, S. (1981). Distribution and molecular characterization of a cell-surface and a cytoplasmic antigen detectable in human melanoma cells with monoclonal antibodies. Int J Cancer *28*, 293–300.

[Winter and Harris, 1993] Winter, G. and Harris, W. J. (1993). Humanized antibodies. Trends Pharmacol Sci *14*, 139–143.

[Wolchok et al., 2013] Wolchok, J. D., Kluger, H., Callahan, M. K., Postow, M. A., Rizvi, N. A., Lesokhin, A. M., Segal, N. H., Ariyan, C. E., Gordon, R. A., Reed, K., Burke, M. M., Caldwell, A., Kronenberg, S. A., Agunwamba, B. U., Zhang, X., Lowy, I., Inzunza, H. D., Feely, W., Horak, C. E., Hong, Q., Korman, A. J., Wigginton, J. M., Gupta, A. and Sznol, M. (2013). Nivolumab plus Ipilimumab in Advanced Melanoma. N Engl J Med .

[Wood et al., 2004] Wood, N., Bourque, K., Donaldson, D. D., Collins, M., Vercelli, D., Goldman, S. J. and Kasaian, M. T. (2004). IL-21 effects on human IgE production in response to IL-4 or IL-13. Cell Immunol *231*, 133–145.

[Woof, 2011] Woof (2011). The structure of IgA. Book *1*, 0–100.

[Woof, 2012] Woof, J. M. (2012). Insights from Fc receptor biology: a route to improved antibody reagents. MAbs *4*, 291–293.

[Wynn, 2003] Wynn, T. A. (2003). IL-13 effector functions. Annu Rev Immunol *21*, 425–456.

[Yamaguchi et al., 1987] Yamaguchi, H., Furukawa, K., Fortunato, S. R., Livingston, P. O., Lloyd, K. O., Oettgen, H. F. and Old, L. J. (1987). Cell-surface antigens of melanoma recognized by human monoclonal antibodies. Proc Natl Acad Sci U S A *84*, 2416–2420.

[Yang et al., 2009] Yang, J., Price, M. A., Li, G. Y., Bar-Eli, M., Salgia, R., Jagedeeswaran, R., Carlson, J. H., Ferrone, S., Turley, E. A. and McCarthy, J. B. (2009). Melanoma proteoglycan modifies gene expression to stimulate tumor cell motility, growth, and epithelial-to-mesenchymal transition. Cancer Res *69*, 7538–7547.

[Yang et al., 2004] Yang, J., Price, M. A., Neudauer, C. L., Wilson, C., Ferrone, S., Xia, H., Iida, J., Simpson, M. A. and McCarthy, J. B. (2004). Melanoma chondroitin sulfate proteoglycan enhances FAK and ERK activation by distinct mechanisms. J Cell Biol *165*, 881–891.

[Yeh and Bastian, 2009] Yeh, I. and Bastian, B. C. (2009). Genome-wide associations studies for melanoma and nevi. Pigment Cell Melanoma Res *22*, 527–528.

[YOUDEN, 1950] YOUDEN, W. J. (1950). Index for rating diagnostic tests. Cancer *3*, 32–35.

[Yu et al., 2011] Yu, L., Favoino, E., Wang, Y., Ma, Y., Deng, X. and Wang, X. (2011). The CSPG4-specific monoclonal antibody enhances and prolongs the effects of the BRAF inhibitor in melanoma cells. Immunol Res *50*, 294–302.

[Zen and Nakanuma, 2010] Zen, Y. and Nakanuma, Y. (2010). IgG4-related disease: a cross-sectional study of 114 cases. Am J Surg Pathol *34*, 1812–1819.

[Zhang et al., 2011] Zhang, H., Fu, T., McGettigan, S., Kumar, S., Liu, S., Speicher, D., Schuchter, L. and Xu, X. (2011). IL8 and Cathepsin B as Melanoma Serum Biomarkers. Int J Mol Sci *12*, 1505–1518.

[Ziai et al., 1987] Ziai, M. R., Imberti, L., Nicotra, M. R., Badaracco, G., Segatto, O., Natali, P. G. and Ferrone, S. (1987). Analysis with monoclonal antibodies of the molecular and cellular heterogeneity of human high molecular weight melanoma associated antigen. Cancer Res *47*, 2474–2480.

[Zimmer et al., 2012] Zimmer, L., Hillen, U., Livingstone, E., Lacouture, M. E., Busam, K., Carvajal, R. D., Egberts, F., Hauschild, A., Kashani-Sabet, M., Goldinger, S. M., Dummer, R., Long, G. V., McArthur, G., Scherag, A., Sucker, A. and Schadendorf, D. (2012). Atypical melanocytic proliferations and new primary melanomas in patients with advanced melanoma undergoing selective BRAF inhibition. J Clin Oncol *30*, 2375–2383.

[Zippelius et al., 2007] Zippelius, A., Gati, A., Bartnick, T., Walton, S., Odermatt, B., Jaeger, E., Dummer, R., Urosevic, M., Filonenko, V., Osanai, K., Moch, H., Chen, Y. T., Old, L. J., Knuth, A. and Jaeger, D. (2007). Melanocyte differentiation antigen RAB38/NY-MEL-1 induces frequent antibody responses exclusively in melanoma patients. Cancer Immunol Immunother *56*, 249–258.

9 List of Figures

10 List of Tables

11 APPENDIX

Published April 30, 2012

JEM

Brief Definitive Report

Resident CD141 (BDCA3)$^+$ dendritic cells in human skin produce IL-10 and induce regulatory T cells that suppress skin inflammation

Chung-Ching Chu,[1,4] Niwa Ali,[1,2] Panagiotis Karagiannis,[1] Paola Di Meglio,[1] Ania Skowera,[3] Luca Napolitano,[1] Guillermo Barinaga,[1] Katarzyna Grys,[1] Ehsan Sharif-Paghaleh,[2] Sophia N. Karagiannis,[1] Mark Peakman,[3] Giovanna Lombardi,[2] and Frank O. Nestle[1]

[1]St. John's Institute of Dermatology, [2]MRC Centre for Transplantation, and [3]Department of Immunology, King's College London and National Institutes for Health Research Biomedical Research Centre, SE1 9RT London, UK
[4]Shanghai Institute of Immunology, Institute of Medical Sciences, Shanghai Jiao Tong University School of Medicine, 200025 Shanghai, China

Human skin immune homeostasis, and its regulation by specialized subsets of tissue-residing immune sentinels, is poorly understood. In this study, we identify an immunoregulatory tissue-resident dendritic cell (DC) in the dermis of human skin that is characterized by surface expression of CD141, CD14, and constitutive IL-10 secretion (CD141$^+$ DDCs). CD141$^+$ DDCs possess lymph node migratory capacity, induce T cell hyporesponsiveness, cross-present self-antigens to autoreactive T cells, and induce potent regulatory T cells that inhibit skin inflammation. Vitamin D_3 (VitD3) promotes certain phenotypic and functional properties of tissue-resident CD141$^+$ DDCs from human blood DCs. These CD141$^+$ DDC-like cells can be generated in vitro and, once transferred in vivo, have the capacity to inhibit xeno-graft versus host disease and tumor alloimmunity. These findings suggest that CD141$^+$ DDCs play an essential role in the maintenance of skin homeostasis and in the regulation of both systemic and tumor alloimmunity. Finally, VitD3-induced CD141$^+$ DDC-like cells have potential clinical use for their capacity to induce immune tolerance.

CORRESPONDENCE
Frank Nestle:
frank.nestle@kcl.ac.uk

Abbreviations used: DDC, dermal DC; GvHD, graft versus host disease; ILT3, immunoglobulin-like transcript 3; MMR, macrophage mannose receptor; moDC, monocyte-derived DC; MST, median survival time; PPI, preproinsulin; T eff cell, effector T cell; TLR, Toll-like receptor; T reg cell, regulatory T cell; VitD3, vitamin D_3.

Efficient immunoregulation in peripheral tissues is essential to maintain tissue homeostasis (Swamy et al., 2010). This task is of significant importance to skin, a major first line immune defense organ that protects the body against pathogen-derived and environmental challenges (Nestle et al., 2009). In mice, several studies have highlighted the critical roles of DCs in the regulation of skin immunity and tissue homeostasis (Steinman et al., 2003; Reis e Sousa, 2006; Heath and Carbone, 2009; Merad and Manz, 2009). In human skin, studies have focused on the functional role of immunostimulatory DCs and their role during skin inflammation (Nestle et al., 2009); however, little is known about human tissue-resident DCs with regulatory properties. Human blood-derived immature DCs have been shown to induce IL-10–producing regulatory T (Tr1) cells or T cell hyporesponsiveness to antigenic stimulation (Jonuleit et al., 2000; Dhodapkar et al., 2001). It has also been reported that exposure to antiinflammatory or immunosuppressive agents can induce a regulatory DC phenotype (Adorini et al., 2004). Common features of human regulatory DCs include altered maturation status, reduced T cell stimulatory capacity, and induction of T regulatory cells (Penna et al., 2005).

In human skin, myeloid DCs that reside in the dermis represent a major subset of dermal DCs (DDCs) during tissue homeostasis (Nestle et al., 2009). Subpopulations of DDCs have been described under both normal and pathological

C.C. Chu and N. Ali contributed equally to this paper.
P. Karagiannis and P. Di Meglio contributed equally to this paper.

The Rockefeller University Press $30.00
J. Exp. Med. Vol. 209 No. 5 935-945
www.jem.org/cgi/doi/10.1084/jem.20112583

Published April 30, 2012

conditions. Classically, DDCs are CD1c$^+$ with a CD1a$^+$ and CD14$^+$ subpopulation (Lenz et al., 1993; Nestle et al., 1993). The functional roles of DDC subsets are only partly understood. Zaba et al. (2007) showed that CD1a$^+$ DDCs are potent inducers of allogeneic CD4$^+$ and CD8$^+$ T cell proliferation, whereas CD14$^+$ DDCs are less immunogenic and might have the potential to differentiate into Langerhans cells in response to TGF-β (Caux et al., 1996; Larregina et al., 2001; Klechevsky et al., 2008).

A genome-wide expression profiling study suggested that human blood CD141$^+$ DCs may correlate to mouse CD8α$^+$ DCs (Robbins et al., 2008) and are capable of cross-presentation. Although CD141$^+$ DCs are present only in small numbers in circulating blood, they are found in various lymphoid and nonlymphoid tissues (Demedts et al., 2005; Narbutt et al., 2006; Tsoumakidou et al., 2006; Zaba et al., 2007; Fiore et al., 2008; Jongbloed et al., 2010; Poulin et al., 2010). The functional specialization of CD141$^+$ DCs in human skin and other peripheral tissues remains elusive.

In this study, we show that CD141$^+$ DDCs are a major IL-10–producing skin-resident DC subset. They induce T cell hyporesponsiveness and CD25^{hi} regulatory T cells (T reg cells) that suppress skin inflammation. Vitamin D_3 (VitD3)–induced CD141$^+$ cells generated from blood DCs share phenotypic and functional features of skin-resident CD141$^+$ DDCs and are powerful regulators of alloimmunity. Adoptive transfer of these cells inhibits xeno-graft versus host disease (GvHD) and tumor alloimmunity in vivo. Collectively, our data suggest that CD141$^+$ DDCs are key immunoregulatory antigen-presenting cells playing a potentially important role in tissue homeostasis and for the induction of clinical tolerance.

RESULTS AND DISCUSSION

Identification and characterization of a skin-resident CD141$^+$ DDC population

Comprehensive profiling of human skin DCs identified a significant percentage of CD141$^+$ DDCs (Fig. 1 A) ranging from 14.13 to 53.36% (mean = 30%; SD = 12.08) within the viable lineage-negative FSC^{hi}SSC^{hi}CD45$^+$ migratory dermal cell population (Fig. S1). CD141$^+$ migratory DDCs expressed CD11c and CD1c at low levels, but lacked expression of CD1a (Fig. 1, A and B). Importantly, CD141$^+$ DDCs migrating from dermal explants coexpressed CD14 on the cell surface. They also expressed skin-relevant myeloid markers such as Factor XIIIa and CD163, but not CD103 or C-type lectin receptors such as CD209 (DC-SIGN), CD205 (DEC205), and CD207 (langerin; unpublished data). CD141$^+$HLA-DR$^+$ DDCs were located in a perivascular location in the upper dermis (Fig. 1 C). In agreement with the literature, CD141 expression was also detected on keratinocytes (Raife et al., 1994). Immunofluorescence staining for filamentous actin of flow cytometry–sorted CD141$^+$ DDCs demonstrated a typical DC morphology with multiple dendritic processes (Fig. 1 D). CD141$^+$ DDCs spontaneously migrated out from human dermis in tissue cultures and maintained a semimature phenotype, indicated by the absence of CD83, but expression of significant levels of co-stimulatory molecules, CD80 and CD86, and MHC class I and class II molecules (Fig. 1 E). This phenotype resembled the steady-state migratory (Kissenpfennig et al., 2005) and semimature tolerizing DCs (Lutz and Schuler, 2002) that have been described in mice. To address in vivo migratory capacity of CD141$^+$ DDCs, we established a humanized skin transplantation mouse model (Sagoo et al., 2011). Human CD45$^+$ leukocytes were detected in lymph nodes, but not in spleens, of mice that had received skin transplants (Fig. 1 F). Immunofluorescent staining showed both human CD3$^+$ and CD141$^+$ cells (Fig. 1 G). Detection of human CD141$^+$ transcript in skin-draining lymph nodes via PCR confirmed active migration of CD141$^+$ DDCs in vivo (Fig. 1 H). Together, human skin-resident CD141$^+$ cells express DC markers and display hallmarks of DCs, including dendritic morphology, nonplastic adherence, and migratory activity in vitro and in vivo.

An important aspect of maintaining tissue homeostasis is based on DC capacity to capture, process, and present tissue-derived self-antigens to self-reactive T cells via the MHC class I antigen presentation pathway under steady-state conditions (Liu et al., 2002). CD141$^+$ DDCs expressed markers associated with cross-presentation, including BATF3, Necl2, the C-type lectin CLEC9A, and XC chemokine receptor 1 (XCR1), in a pattern similar to human blood CD141$^+$ DCs and mouse CD8α$^+$ DCs (Bachem et al., 2010; Crozat et al., 2010; Jongbloed et al., 2010; Poulin et al., 2010; Fig. 1 I and Table S1). In particular, macrophage mannose receptor (MMR) and CLEC9A were selectively expressed by CD141$^+$ DDCs compared with CD1c$^+$ DDCs (Fig. 1, E and J), which may play an important role in the cross-presentation of soluble and cell-associated antigens (Burgdorf et al., 2006; Sancho et al., 2009). A distinctive feature of CD141$^+$ DDCs compared with CD141$^+$ blood DCs was the expression of Toll-like receptor (TLR) 4, 7, and 9 (unpublished data). To determine cross-presentation, CD1c$^+$ and CD141$^+$ DDCs pulsed with the model self-antigen preproinsulin (PPI) or control protein were co-cultured with a human autoreactive CD8$^+$ T cell clone specific for PPI (Skowera et al., 2008). PPI-pulsed CD141$^+$ DDCs induced significantly higher proliferation of the T cell clone than PPI-pulsed CD1c$^+$ DDCs (Fig. 1 K). Importantly, cross-presentation of PPI by CD141$^+$ DDCs occurred in the absence of proinflammatory stimuli such as poly(I:C), which was previously shown to be required for cross-presentation by CD141$^+$ blood DCs (Jongbloed et al., 2010; Poulin et al., 2010). This suggests an intrinsic and unique capacity of CD141$^+$ DDCs to cross-present self-antigens and may allow regulation of autoreactive CD8$^+$ T cell response under noninflammatory, steady-state conditions (Liu et al., 2002). Cross-presentation of tissue-associated self-antigens may significantly contribute to the maintenance of skin homeostasis.

CD141$^+$ DDCs produce IL-10 and induce CD25^{hi} T-regulatory cells

We next investigated the immunoregulatory properties of CD141$^+$ DDCs. They expressed high levels of the immunoregulatory

Published April 30, 2012

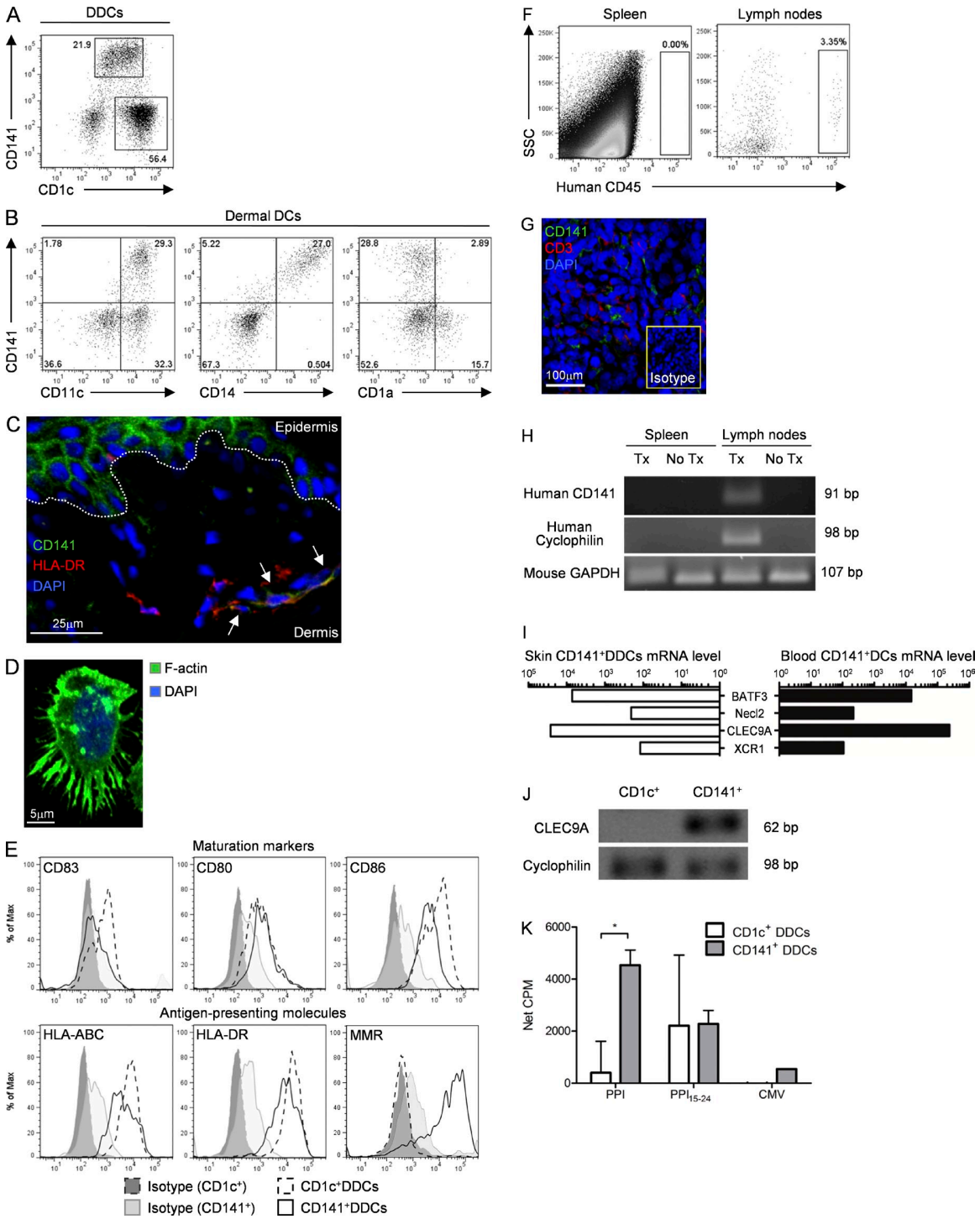

Figure 1. Identification and characterization of skin migratory CD141⁺ DDCs. (A and B) Healthy human skin DDCs were stained for CD1c, CD11c, CD14, and CD1a. (C) CD141⁺HLA-DR⁺ DDCs staining in the upper dermis of normal human skin (arrows). Dashed line indicates epidermal–dermal junction. (D) Filamentous actin (F-actin) staining of cell-sorted CD141⁺ DDCs. (E) CD141⁺ DDCs or CD1c⁺ DDCs stained for CD83, CD80, CD86, HLA-ABC, HLA-DR, and MMR. (F) Human CD45⁺ staining of lymph nodes and spleens of BALB/c Rag2$^{-/-}\gamma_c^{-/-}$ mice bearing human skin transplants (Tx). (G) Human CD141⁺ and CD3 staining in lymph nodes of Tx mice. (H) mRNA expression for human CD141, cyclophilin, and mouse GAPDH in spleens and lymph nodes of Tx mice. Blood and skin CD141⁺ DCs expression of BATF3, Necl2, CLEC9A, and XCR1 (I) and CD141⁺ DDCs expression of CLEC9A (J) as compared with CD1c⁺ DDCs. (K) CD141⁺ DDCs or CD1c⁺ DDCs pulsed with PPI were incubated with autoreactive CD8⁺ T cell clones and analyzed for proliferation. Net CPM represents proliferation of the clone in pulsed DDC co-culture minus nonpulsed DDC co-culture. Error bars indicate SEM. Results are representative of at least 30 (A), at least three (B–E), and two (F–K) independent experiments. Two-way ANOVA test; *, $P < 0.05$.

Published April 30, 2012

receptor immunoglobulin-like transcript 3 (ILT3; Chang et al., 2002) at the protein and mRNA levels in a consistently higher fashion than compared with CD1c$^+$ DDCs (Fig. 2 A). In keeping with their immunoregulatory phenotype, CD141$^+$ DDCs, but not CD1c$^+$ DDCs, constitutively secreted high levels of IL-10 that was significantly enhanced after CD40 cross-linking ($P < 0.05$; Fig. 2 B). After CD40L stimulation, IL-10 production became detectable in CD1c$^+$ DDCs and was boosted in CD141$^+$ DDCs. When co-cultured with allogeneic CD4$^+$ T cells, CD141$^+$ DDCs were less proficient than CD1c$^+$ DDCs in stimulating T cell proliferation (Fig. 2 C). This was not explained by significant differences in expression levels of MHC or co-stimulatory molecules (unpublished data). However, introducing a neutralizing anti–IL-10 receptor antibody significantly reversed the suppression of proliferation mediated by CD141$^+$ DDCs, whereas no effect was observed in CD1c$^+$ co-cultures (Fig. 2 D). During DC–T cell co-culture, alloreactive T cells became activated and up-regulated CD25 expression on the cell surface. Both CD141$^+$ and CD1c$^+$ DDCs induced a population of T cells that expressed high levels of CD25 (CD141 CD25^{hi} T cells and CD1c CD25^{hi} T cells, respectively). CD141$^+$ DDCs induced higher surface expression of cytotoxic T lymphocyte antigen-4 (CTLA-4) on CD25^{hi} T cells than CD1c$^+$ DDCs (Fig. 2 E). In addition, CD141 CD25^{hi} T cells, but not CD1c CD25^{hi} T cells, were unresponsive to secondary alloantigen restimulation (Fig. 2 F). Our previous work has demonstrated correlation of in vitro hyporesponsiveness and regulatory function of T cells (Lombardi et al., 1994). We then expanded the cells in the presence of IL-2 to obtain sufficient cell numbers for in vivo functional studies (Sagoo et al., 2011). After cell expansion, CD141 CD25^{hi} T cells and CD1c CD25^{hi} T cells maintained their expression of CD25 and Foxp3 (unpublished data). CD141 CD25^{hi} T cells were hyporesponsive to secondary TCR stimulation (Fig. 2 G) and suppressed CD4$^+$CD25$^-$ T effector (T eff) cell proliferation, whereas CD1c CD25^{hi} T cells enhanced T eff cell proliferation in a dose-dependent manner (Fig. 2 H).

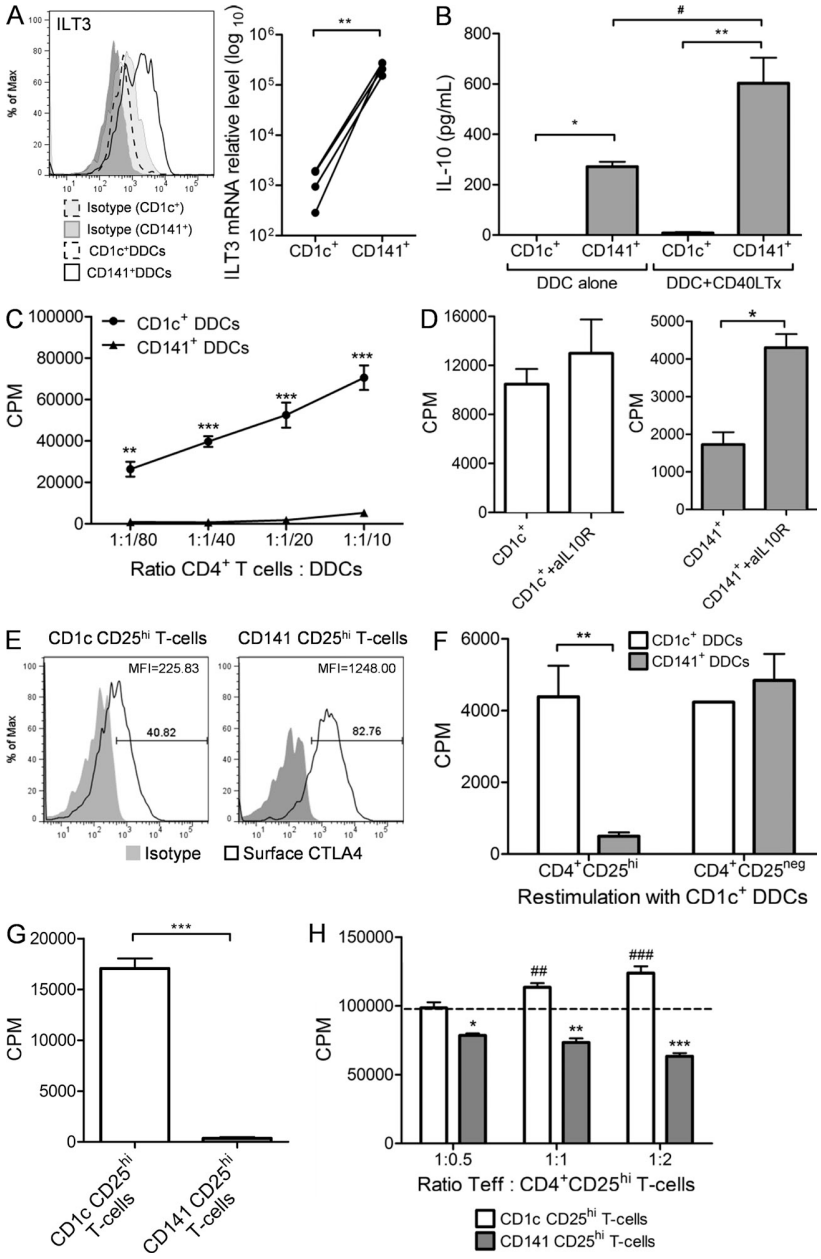

Figure 2. CD141$^+$ DDCs are immunoregulatory. (A) CD141$^+$ DDCs or CD1c$^+$ DDCs expression of ILT3 and (B) production of IL-10 in the absence or presence of CD40 ligand-transfected L cells (CD40L Tx). (C) CD141$^+$ DDCs or CD1c$^+$ DDCs stimulation of allogeneic CD4$^+$ T cell proliferation. (D) CD141$^+$ DDCs or CD1c$^+$ DDCs co-cultured with allogeneic CD4$^+$ T cells in the presence and absence of anti–IL-10 receptor antibody. CD4$^+$CD25^{hi} T cells induced by CD1c$^+$ DDCs (CD1c CD25^{hi} T cells) or CD141$^+$ DDCs (CD141 CD25^{hi} T cells) stained for surface CTLA-4 (E) and proliferation in response to alloantigen stimulation (F). (G) IL-2–expanded CD25^{hi} T cells proliferative response to secondary polyclonal stimulation and (H) suppression of CD4$^+$CD25$^-$ T eff cell proliferation. Error bars indicate SEM. Results are representative of five (A–C, E, and F) and two (D, G, and H) independent experiments. Wilcoxon matched pairs test (A), one-way ANOVA (B), two-way ANOVA (C, F, and H), or unpaired Student's *t* test (D, G). *, $P < 0.05$; **, $P < 0.01$; ***, $P < 0.001$; #, $P < 0.05$.

CD141$^+$ DDCs induce CD25^{hi} T reg cells that suppress alloimmune cell–mediated skin inflammation

We assessed the in vivo immunoregulatory function of DDC-induced CD25^{hi} T cells in

Published April 30, 2012

our recently described model of human alloimmune cell–mediated skin inflammation (Fig. 3 A; Sagoo et al., 2011). Skin grafts from animals receiving allogeneic PBMCs showed typical inflammatory skin pathology with increased numbers of epidermal T cells, proliferating keratinocytes in the basal epidermal layer, and loss of intact CD31$^+$ dermal microvasculature (Fig. 3, B–D).

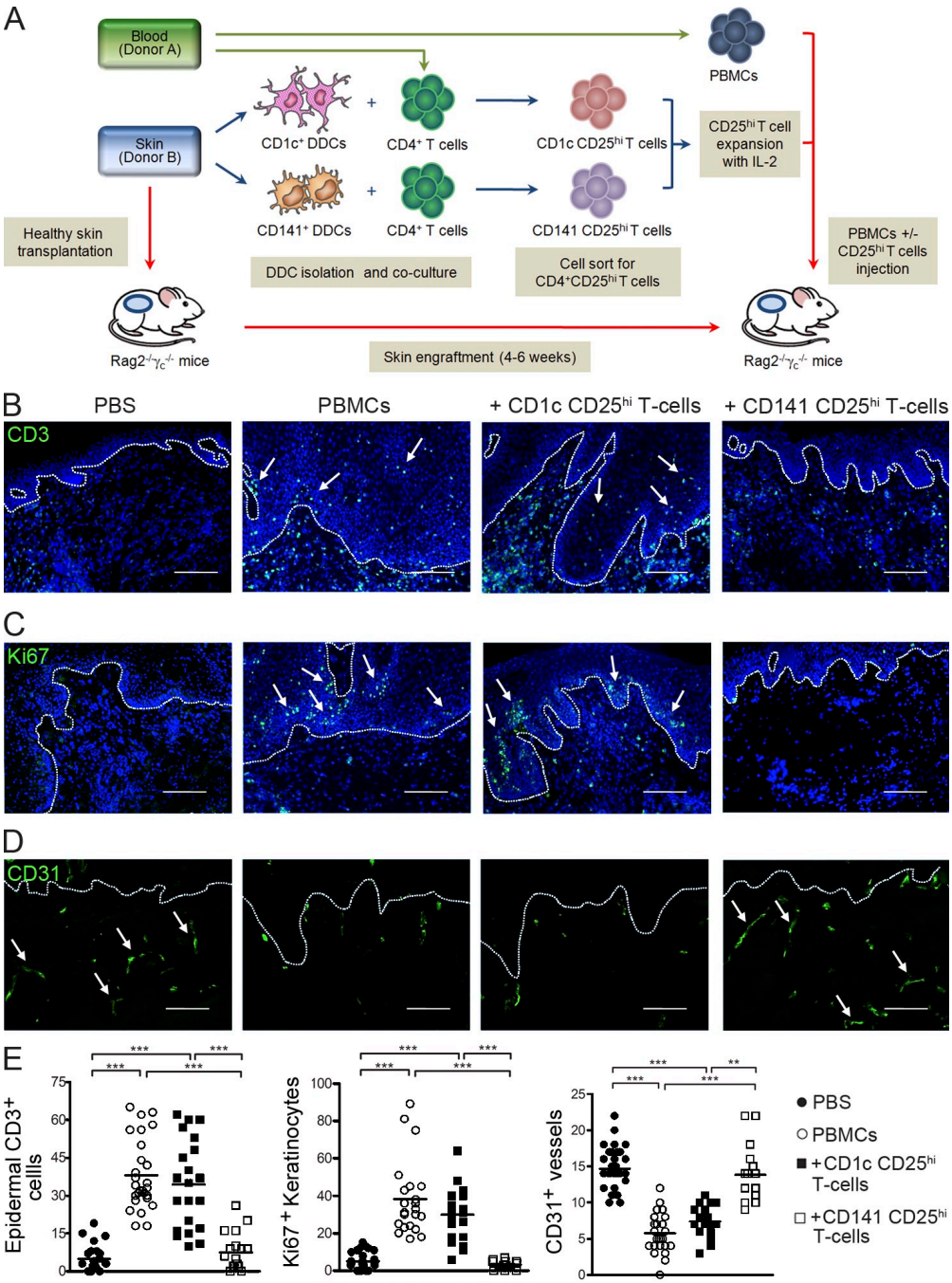

Figure 3. CD141$^+$ DDC-induced CD25^{hi} T reg cells inhibit human alloimmune cell–mediated skin inflammation. (A) Experimental strategy to assess CD25^{hi} T cell suppression. BALB/c Rag2$^{-/-}\gamma_c^{-/-}$ mice transplanted with human skin were injected with PBS, allogeneic PBMCs alone, or in combination with CD141 CD25^{hi} T cells or CD1c CD25^{hi} T cells. Representative fields from stained skin grafts for epidermal CD3$^+$ T cell infiltration (B, arrows), epidermal keratinocyte expression of the proliferation marker Ki67 (C, arrows), and intact human CD31 superficial dermal microvasculature (D, arrows). Dashed lines indicate epidermal–dermal junction. Nuclei are stained with DAPI (blue). Bars, 100 µm. (E) Quantitative histological analysis of at least three independent visual fields per skin graft. Lines represent the mean (n = 5–9 animals per treatment group). Results are combined data from three independent experiments. One-way ANOVA test; **, $P < 0.01$; ***, $P < 0.001$.

Published April 30, 2012

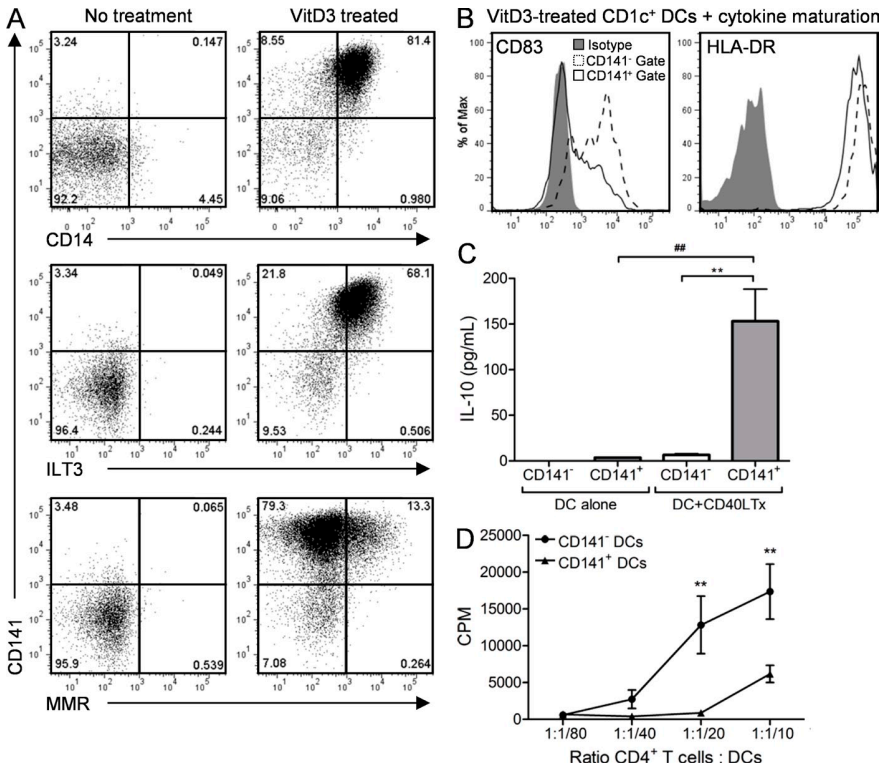

Figure 4. VitD3 induces CD141⁺ DDC-like phenotype in blood DCs. (A) VitD3-treated blood CD1c⁺ DC expression of CD141 with CD14, ILT3, and MMR. VitD3-induced CD141⁺ DCs or VitD3-induced CD141⁻ DCs were assessed for their expression of CD83 and HLA-DR in the presence of a cytokine maturation cocktail (B), production of IL-10 in the presence and absence of CD40L Tx stimulation (C), and ability to stimulate allogeneic CD4⁺ T cell proliferation (D). Results are representative of at least 12 (A) and 3 (B–D) independent experiments. One-way ANOVA (C) or two-way ANOVA (D); **, $P < 0.01$; ##, $P < 0.01$.

Co-transfer of CD141 CD25^{hi} T cells protected from the induction of skin pathology in a significant manner, restoring markers of pathology to levels observed in control grafts (Fig. 3 E), whereas no significant protective effect was seen in mice treated with CD1c CD25^{hi} T cells. Together, these data show that CD141⁺ DDCs display both phenotypic and functional characteristics of immunoregulatory DCs and induce T reg cells with immunosuppressive capability in vitro and in vivo.

VitD3 induces a CD141⁺ DDC-like phenotype and function in blood DCs

VitD3 has been linked to the immunosuppressive capacity of UV light, but human cellular effectors are ill defined (Schwarz and Schwarz, 2011). We addressed whether VitD3 could induce the unique immunoregulatory characteristics of CD141⁺ DDCs in blood DCs. Culture of CD141⁻CD1c⁺ blood DCs with the active form of VitD3, 1α,25-dihydroxyvitamin D_3 ($1,25[OH]_2D_3$), induced the coexpression of CD141, CD14, ILT3, and MMR (Fig. 4 A). A core module of molecular markers present in cross-presenting DCs including BATF3, CLEC9A, and Necl2 was also induced in CD141⁺ VitD3 blood DCs (Table S1). VitD3-induced CD141⁺ DCs had a stable CD83^{low} immature phenotype after exposure to a potent DC maturation cocktail consisting of TNF, IL-1β, IL-6, and prostaglandin E_2 (Fig. 4 B; Jonuleit et al., 1997). This was in contrast to VitD3-induced CD141⁻ DCs that readily up-regulated CD83 (Fig. 4 B). VitD3-induced CD141⁺ DCs produced significantly higher amounts of IL-10 than CD141⁻ DCs after CD40 cross-linking ($P < 0.01$; Fig. 4 C) and were weak stimulators of allogeneic CD4⁺ T cell proliferation (Fig. 4 D). VitD3-induced CD141⁺ DCs and CD141⁺ DDCs have many similarities, including CD14 and ILT3 co-expression, semimature phenotype, IL-10 production, and poor T cell stimulatory capacity. Our findings provide a potential cellular link between VitD3 production and skin immune regulation.

Adoptively transferred VitD3–induced CD141^{hi} DCs suppress alloimmunity in vivo

Establishment of a method to generate large numbers of cells with the immunoregulatory properties of CD141⁺ DDCs would allow the development of adoptive regulatory DC therapy in in vivo preclinical models and for development of therapeutic applications in patients. We thus investigated a source of DCs generated from blood monocytes after incubation with IL-4 and GM-CSF (moDCs). Incubation with VitD3 up-regulated CD141 expression on moDCs (VitD3 moDCs; unpublished data) and induced the expression of a molecular profile that resembles CD141⁺ DDCs (Table S1). VitD3 moDCs highly expressing CD141 (CD141^{hi} VitD3 moDCs) produced high levels of IL-10 after CD40 cross-linking and demonstrated a reduced T cell stimulatory capacity, as compared with CD141^{dim} VitD3 moDC or moDCs (unpublished data). PPI cross-presentation in the presence of poly(I:C) stimulation was enhanced in VitD3 moDCs compared with control moDCs (unpublished data). We assessed the in vivo regulatory capacity of CD141^{hi} VitD3 moDCs in a human xeno-GvHD model (King et al., 2009; Fig. 5 A). Injection of human PBMCs induced xeno-GvHD in NSG mice (median survival time [MST] = 32). Co-transfer of CD141^{hi} VitD3 moDCs with PBMCs significantly prolonged survival time ($P < 0.001$ versus PBMCs alone; MST = 62), whereas no significant protection was conferred by transfer of CD141^{dim} VitD3 moDCs (MST = 39; Fig. 5 B). We next assessed the immunoregulatory role of CD141^{hi} VitD3 moDCs in an alloimmune cell–dependent human melanoma

Published April 30, 2012

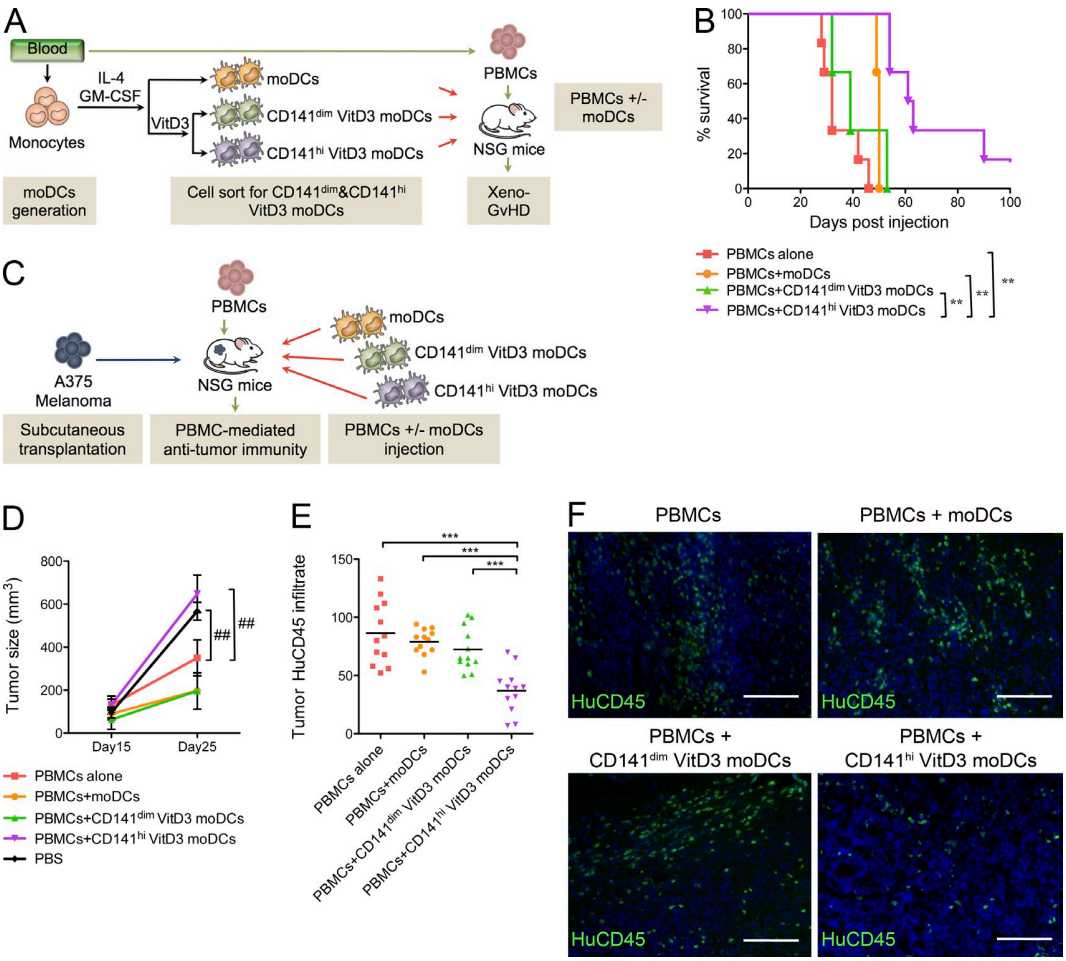

Figure 5. VitD3-induced CD141^{hi} DCs suppress xeno-GvHD and antitumor immunity. (A) Strategy for preclinical assessment of adoptive cell therapy in xeno-GvHD. (B) NSG mice were injected with either PBMCs alone or in combination with moDCs, CD141^{dim} VitD3 moDCs, or CD141^{hi} VitD3 moDCs to induce xeno-GVHD. Survival was monitored over time. (C) Strategy to determine regulation of antitumor alloimmunity. Tumor size (D) and CD45^{+} infiltration (E and F) were assessed in animals injected with PBMCs alone or in combination with moDCs, CD141^{dim} VitD3 moDCs or CD141^{hi} VitD3 moDCs to induce antitumor alloimmunity (E) Quantitative histological analysis of tumor CD45^{+} infiltration from at least three independent visual fields per skin graft. Lines represent the mean (n = 3–6 animals per treatment group). (F) Representative pictures of human CD45^{+} infiltrates in tumors. Nuclei are stained with DAPI (blue). Bars, 100 µm. Results are pooled from three independent experiments (n = 3–6 animals per treatment group). One-way ANOVA (E), two-way ANOVA (D), or Mantel-Cox (B) test; **, P < 0.01; ***, P < 0.001; ##, P < 0.01.

model (Fig. 5 C). Injection of PBMCs reduced tumor size significantly compared with PBS-injected mice. However, tumor size was significantly increased in mice co-injected with PBMCs and CD141^{hi} VitD3 moDCs, but not with CD141^{dim} VitD3 moDCs or moDCs (Fig. 5 D), suggesting suppression of tumor alloimmunity. In line with these findings, we observed a significantly reduced human CD45^{+} cell infiltrate in tumors recovered from CD141^{hi} VitD3 moDC–injected mice (Fig. 5, E and F). These results indicate that VitD3-induced CD141^{hi} blood DCs have the ability to suppress alloimmunity in vivo and are possible candidates for regulatory DC therapy approaches.

Immunoregulation at tissue sites is tightly regulated and involves key immune sentinels, such as DCs. Although major progress has been made in understanding the immunoregulatory role of DCs residing in mouse tissues, their human counterparts are less well characterized. In this study, we identify an immunoregulatory CD141^{+} DC population in dermis of healthy human skin and establish culture methods to generate sufficient numbers of such cells for future regulatory DC therapy.

CD141^{+} DDCs coexpressed CD14 with low CD1c expression, a phenotypically distinct profile from blood CD141^{+} DCs. Although CD14 is expressed on the cells of the monocyte/macrophage lineage in the blood, it is also considered a marker of skin DC subsets (Nestle et al., 1993; Larregina et al., 2001; Klechevsky et al., 2008). In future studies, it will be interesting to investigate whether CD141^{+} DDCs activate follicular helper T cells, as has been shown for CD14^{+} interstitial DDCs (Klechevsky et al., 2008). We propose that the coexpression of CD141 and CD14 may be

Published April 30, 2012

useful markers to define tissue-resident regulatory DC populations. DC populations with a similar phenotype have been identified in lung (Demedts et al., 2005), suggesting that our findings might extend to CD141$^+$ DCs residing in other peripheral tissue sites.

A population of CD103$^+$ DCs coexpressing CD207 has recently been identified in the dermis of murine skin as the primary migratory DDC subset capable of antigen capturing and (cross-)presentation (Bedoui et al., 2009; Henri et al., 2010). CD103$^+$CD207$^+$ DCs have been shown to mediate T cell tolerance, possibly in the context of their cross-presentation capability (Waithman et al., 2007) and their ability to induce T reg cells (Azukizawa et al., 2011). Given the skin origin, migratory capacity, cross-presentation ability, and immunoregulatory characteristics of the CD141$^+$ DDC population described here, they may be related to this migratory cross-presenting CD103$^+$ DC population. A population of CD26$^+$SIRPα^- DCs that shares transcriptomic and functional similarities with mouse CD8α^+ DCs has also been identified in sheep skin (Contreras et al., 2010). This suggests a unique functional specialization of skin DCs across mammalian species for the maintenance of skin tissue homeostasis.

One of the most striking findings was the potent in vivo regulatory function of CD141$^+$ DDCs and their induced T reg cells, as demonstrated in three independent human in vivo models of disease. A common denominator across these models was the efficient regulation of alloimmune-mediated pathology providing a framework for the future use of CD141$^+$ DDCs or their VitD3-induced functional counterparts in the context of GvHD in organ transplantation. On the other hand, specific blockade of CD141$^+$ DDCs might be beneficial in the cancer setting.

CD141$^+$ DDCs express various TLRs and CD14, which is thought to facilitate microbial clearance and to amplify cellular responses (Anas et al., 2010). It is possible that CD141$^+$ DDCs may exert antimicrobial or antiviral immunity when encountering viral/microbial products or under specific environmental conditions. TLR9 ligation was reported to reverse the regulatory function of CD8α^+ DCs and promote T cell immunity in mice (Rizzitelli et al., 2005). Thus, our study does not exclude the possibility that CD141$^+$ DDCs may be stimulatory in the context of viral/microbial infection and inflammatory skin pathology.

We identified VitD3 as a potent inducer of CD141$^+$ DDC phenotype and function. This allowed us to generate large numbers of CD141$^+$ DDC-like cells for future use in cell therapy applications. Collectively, our data identify a potent regulatory DC that is strategically positioned at epithelial tissue sites poised to play an important role in maintaining barrier immune homeostasis and to serve as a future therapeutic target in conditions of alloimmunity.

MATERIALS AND METHODS

Human samples. Human buffy coats were provided by the National Blood Transfusion Centre (South Thames, Tooting, England, UK). Discarded skin was obtained from routine plastic surgery of healthy individuals. Human studies were conducted in accordance with the Helsinki Declaration and approved by the Institutional Review Board of Guy's Hospital. Informed consent was obtained from all patients and healthy controls before enrollment into the study.

Isolation of DDCs. DDC isolation was performed as previously described (Nestle et al., 1993). Skin was sliced into long strips, followed by 5 mg/ml dispase digestion (StemCell) for 2 h at 37°C. Epidermis and loose connective tissues in the lower dermis was removed, and dermis was sliced into 1–2-mm-thick strips and cultured in RPMI 1640 supplemented with 50 IU/ml penicillin, 50 µg/ml streptomycin, 2 mM L-glutamine (complete RPMI medium, all from Invitrogen), and 10% human AB serum (HS; Sigma-Aldrich). Nonplastic adherent cells that had migrated out of dermis 48–72 h after culture were harvested for flow cytometric analysis. Cell sorting of DDC subsets was performed by staining dermal cells with CD45-PECy7 (eBioscience), CD1c/BDCA1-PE (Miltenyi Biotec), CD141/BDCA3-APC (Miltenyi Biotec), and DAPI (Invitrogen), followed by sorting with a FACSAria II cell sorter (BD).

Immunodeficient mice. Male and female NOD/scid/*IL-2R*$\gamma^{-/-}$ mice (NOD.cg-Prkdc^{scid}Il2rg^{tm1Wjl}/SzJ [NSG]; The Jackson Laboratory) and BALB/c RAG2$^{-/-}\gamma_c^{-/-}$ mice (provided by A. Hayday, The London Research Institute, Cancer Research UK, London, England, UK; and P. Gorer, Department of Immunobiology, King's College School of Medicine at Guy's Hospital, London, England, UK) were used between 8 and 12 wk of age. Mice were maintained under specific pathogen–free conditions and handled in accordance with the Institutional Committees on Animal Welfare of the UK Home Office (the Home Office Animals Scientific Procedures Act, 1986)

Humanized mouse model of skin DC lymph node migration. Human skin samples were first keratomed using a hand-held air-powered dermatome (Zimmer) to obtain 500–700-µm split-thickness explants consisting of the epidermis and superficial dermis. Explants were kept at 4°C in complete RPMI medium and subsequently cut into 1–1.5-cm^2 pieces and transplanted orthotopically onto the backs of BALB/c RAG2$^{-/-}\gamma_c^{-/-}$ mice, as previously described (Sagoo et al., 2011). Spleens and skin-draining lymph nodes were harvested 8–12 wk after transplantation for analysis of DDC migration. Cell suspensions were obtained by dissociating spleens and lymph nodes through 70-µm nylon mesh strainers (BD). Mouse spleens and lymph node cell suspensions were preincubated with Mouse Fc Block (BD), and then human leukocytes identified by co-staining with anti-human CD45-PECy7 (eBioscience) and mouse CD45-APC/eFluor780 (eBioscience).

Flow cytometry. The following antibodies were used in different combinations: CD1c-PE and CD141-APC (Miltenyi Biotec); CD45-PECy7 (eBioscience); CD11c-PerCp/Cy5.5 (BioLegend); CD14-FITC, CD80-PE, CD83-FITC, CD86-FITC, and HLA-DR-PE (Invitrogen); CD1a-PE, CD25-PE, CD45RO-PE, CD152/CTLA-4-APC, CD206/MMR-PECy5, and HLA-ABC-PE (BD); ILT3-PC5 (Beckman Coulter). Samples were acquired with a FACSCanto (BD), and data were analyzed by FlowJo (Tree Star) software.

Immunofluorescence staining. Laser confocal microscopy was performed (TCS SP2; Leica). The following antibodies were used to stain OCT-embedded cryosections: CD141 (AbD Serotec); CD3 (Dako); human CD45 (eBioscience); Ki-67 (Abcam); CD31 (Abcam); HLA-DR (BD); goat anti–mouse IgG Alexa Fluor 555 or 488 and goat anti–rabbit IgG Alexa Fluor 555 or 488 (Invitrogen). To determine DC morphology, sorted CD141$^+$ DDCs were immobilized on poly-L-lysine coated coverslips (BioCoat; BD) and stained with Fluorescent phallotoxins (Invitrogen) according to manufacturer's specification. ProLong Gold antifade reagent with DAPI (Invitrogen) was used for nuclear staining.

Blood DCs, monocyte-derived DCs (moDCs), T cell isolation, and culturing. PBMCs were isolated from buffy coats by density gradient centrifugation over Lymphocyte Separation Medium (PAA). To obtain CD1c$^+$

Published April 30, 2012

myeloid DCs, DC populations were enriched using Dynal DC-enrichment kit according to the manufacturer's specification (Invitrogen). $CD1c^+$ DCs were further purified by cell sorting of lineage (CD3, CD14, CD19, and CD56)-negative and CD1c-positive populations. Monocytes were isolated from PBMCs using CD14 microbeads (Miltenyi Biotec) according to the manufacturer's instructions, and cultured in complete RPMI medium supplemented with 1% single-donor plasma (NBS Totting), 500 IU/ml GM-CSF (PeproTech), and 500 IU/ml IL-4 (R&D Systems). Fresh GM-CSF and IL-4 were added on day 2 and 5 of a culture period of 7 d.

$CD141^+$ DDC-like DCs were induced by treatment of $CD1c^+$ blood DCs with 100 nM VitD3 for 2 d or on day 5 of moDC differentiation. In some cases, DCs were matured with TNF (10 ng/ml), IL-1β (10 ng/ml), IL-6 (1,000 IU/ml; all from R&D Systems), and prostaglandin E_2 (1 µg/ml; Sigma-Aldrich) 24 h before harvesting. Where indicated, VitD3-induced $CD141^{hi}$ and $CD141^{dim}$ DCs were cell sorted by methods described above.

To study the allostimulatory capacity of DCs, allogeneic $CD4^+$ T cells were prepared from buffy coats using RosetteSep human $CD4^+$ T cell enrichment cocktail (STEMCELL Technologies) according to the manufacturers' instructions. $CD4^+$ T cells were cultured in 96-well round-bottom plates (5×10^4 cells/well) with graded numbers of allogeneic $CD141^+$ and $CD1c^+$ DDCs, or VitD3-induced $CD141^{hi}$ and $CD141^{dim}$ DCs. Proliferation of alloreactive T cells was assessed by [H^3]thymidine incorporation (1 µCi/well; GE Healthcare) during the last 18 h of a 5-d culture. In some circumstances, because of limiting DDC numbers, responder T cells were scaled down accordingly resulting in lower thymidine counts. In some cultures, anti–IL-10R mAb (3F9; R&D Systems) was added. The optimal dose was determined to be 10 µg/ml. DDC-induced $CD4^+CD25^{hi}$ T cells were isolated by cell sorting $CD11c^-CD4^+CD25^{hi}$ T cells from DDC co-cultures, resting overnight, and restimulation with $CD1c^+$ DDCs derived from the primary allogeneic skin donor. To generate $CD4^+CD25^{hi}$ lines, $CD4^+CD25^{hi}$ T cells were cell-sorted directly into 96-well plates containing RPMI 10% HS and left to rest overnight. Subsequently, low dose IL-2 (R&D Systems) was added at 250 IU/ml and replenished every 2–3 d. After adequate expansion for a period of 4–5 wk, $CD25^{hi}$ T cells were harvested by cell sorting. To assess in vitro suppressive capacity, titrated numbers of $CD25^{hi}$ T cells were co-cultured with 5×10^4 autologous $CD4^+CD25^-$ effector T cells for 5 d in the presence of CD3/CD28 T cell Expander Dynal Beads (Invitrogen). Cell proliferation was measured as described above.

Humanized mouse model of alloimmune cell–mediated skin inflammation. BALB/c $RAG2^{-/-}\gamma_c^{-/-}$ mice bearing human skin transplants were allowed to engraft for 5–6 wk before adoptive transfer of human cells. For the total duration of these experiments, purified anti–mouse Gr1 mAb (100 µg; BioXell) was injected intraperitoneally every 4–5 d to deplete mouse granulocytes. Allogeneic (to the skin) PBMCs depleted of $CD25^+$ cells were then adoptively transferred intravenously via the tail vein to induce alloimmune skin inflammation, as previously described (Sagoo et al., 2011). The in vivo suppressive capacity of DDC induced $CD25^{hi}$ T cells was investigated by co-injecting CD141 $CD25^{hi}$ T cells or CD1c $CD25^{hi}$ T cells with PBMCs (autologous to the $CD25^{hi}$ T cells and allogeneic to the skin) depleted of $CD25^+$ cells at a ratio of 1:10 ($CD25^{hi}$ T cells:CD3 composition of PBMCs inoculum); typically 2.5×10^6 human PBMCs alone or in combination with 1.5×10^5 $CD25^{hi}$ T cells. Skin grafts were harvested 3–4 wk after transfer of human cells and assessed histologically for markers of skin inflammation.

Humanized mouse model of xeno-GvHD. GvHD was induced by intravenous transfer of 10×10^6 human PBMCs into adult NSG mice. Animals that developed clinical symptoms of GvHD (severe weight loss, hunched posture, fur loss, reduced mobility, and tachypnea) were sacrificed, and spleens were harvested for flow cytometric analysis of human cell engraftment. To assess the immunoregulatory potential of VitD3 moDCs in GvHD, human PBMCs were either injected alone or co-transferred with 5×10^5 cell-sorted $CD141^{hi}$ VitD3 moDCs, $CD141^{dim}$ VitD3 moDCs, or moDCs with an end point of survival recorded in all treatment groups.

Humanized mouse model of melanoma antitumor alloimmunity. To establish a xenograft melanoma model, 5×10^5 human A375 melanoma cells (American Type Culture Collection) were injected subcutaneously into the flank of adult NSG mice. 5 d after tumor xenografting, 10×10^6 human PBMCs were transferred intravenously via the tail vein. To determine immunoregulatory ability of VitD3 moDCs, human PBMCs were either injected alone or co-transferred with 5×10^5 cell sorted $CD141^{hi}$ VitD3 moDCs, $CD141^{dim}$ VitD3 moDCs, or moDCs. Tumor size was measured at day 15 and day 25 after adoptive transfer and calculated using the formula: $(\text{short diameter})^2 \times (\text{long diameter})/2$.

Determination of IL-10 production. 2×10^4 DCs were cultured in 96-well flat-bottom plates with 100 µl of complete RPMI medium containing 10% HS for 2 d in the absence or presence of CD40 ligand-transfected cells (CD40L Tx, 5×10^4 cells/well). IL-10 levels in the supernatant were assayed by using the MILLIPLEX MAP Human Cytokine kit (Millipore) and acquired on a Luminex 100 flow-based sorting and detection analyzer (Luminex Corporation).

RNA extraction and quantitative RT-PCR (qRT-PCR). RNA extraction was performed using NucleoSpin RNA XS kit (Macherey-Nagel GmbH and Co.) according to manufacturer's instructions and retrotranscribed into cDNA. Human CD141, CLEC9A, ILT3, BATF3, Necl2, and TLR9 expression was assessed by multiplex real-time quantitative RT-PCR using TaqMan assays (Applied Biosystems) according to manufacturer's instructions. For each sample, mRNA abundance was normalized to the amount of human cyclophilin. Data analysis was performed using the ΔΔCt method: results were expressed as relative mRNA levels in arbitrary units. Where indicated, qPCR products from singleplex assays were run on a 2% agarose gel followed by ethidium bromide.

Cross-presentation assays. 20 µg/ml of PPI protein, prepared in-house (Skowera et al., 2008), or recombinant CMV protein (Miltenyi Biotec) were added to the DDC containing dermal culture prepared from a HLA-A2 donor. After 48 h, $CD1c^+$ and $CD141^+$DDCs were isolated by cell sorting, rested overnight, and then co-cultured with $PPI_{15\text{-}24}$-specific $CD8^+$ T cell clone, clone 1E6, as previously described (Skowera et al., 2008).

DDCs pulsed with $PPI_{15\text{-}24}$ peptide 1 h before co-culture were used as positive control. Proliferation of clone 1E6 was assessed by [H^3]thymidine incorporation (1 µCi/well) during the last 18 h of 3-d culture.

Statistical analysis. Statistical analysis was performed using GraphPad Prism version 4.0 (GraphPad Software). Results were assessed for normal Gaussian distribution, and then analyzed by Mann-Whitney nonparametric Student's *t* test, Wilcoxon matched pairs test, one-way ANOVA test, two-way ANOVA, or Mantel-Cox as appropriate. For markers of skin inflammation quantification, at least one independent image was acquired from each individual, and every image was counted by two independent researchers blinded from treatment groups. Values of $P < 0.05$ were considered significant.

Online supplemental material. Fig. S1 shows the gating strategy of skin DDCs. Table S1 shows the expression of common molecular markers by $CD141^+$ DDCs and VitD3 induced blood DCs. Online supplemental material is available at http://www.jem.org/cgi/content/full/jem.20112583/DC1.

We thank Dr. Katie Lacy, Dr. Gayathri Perera, Dr. Rose Mak, Angela Clifford, Sharon Jones and Mrs. Jenny Geh and Mr. Ciaran Healy from plastic surgery for help with collecting clinical samples. In addition we thank Isabella Tosi for excellent management and coordination of our tissue bank. This work would not have been possible without the generous help of healthy volunteers and of patients from Guy's and St. Thomas' Hospital, London.

We acknowledge support by the following grant funding bodies: Wellcome Trust Program GR078173MA, Medical Research Council UK Program G0601387, Department of Health via the National Institute for Health Research (NIHR) comprehensive Biomedical Research Centre award to Guy's & St Thomas' NHS Foundation Trust in partnership with King's College London and King's College Hospital NHS Foundation Trust. C.C. Chu is supported by St. John's Institute of

Published April 30, 2012

JEM

Dermatology Studentship and Overseas Research Students Awards Scheme (ORSAS). N. Ali is supported by a PhD Studentship from the MRC Centre for Transplantation.

A patent application has been submitted by King's College London based on the findings presented in this study. The authors have no other competing financial interests.

Submitted: 6 December 2011
Accepted: 4 April 2012

REFERENCES

Adorini, L., N. Giarratana, and G. Penna. 2004. Pharmacological induction of tolerogenic dendritic cells and regulatory T cells. *Semin. Immunol.* 16:127–134. http://dx.doi.org/10.1016/j.smim.2003.12.008

Anas, A., T. van der Poll, and A.F. de Vos. 2010. Role of CD14 in lung inflammation and infection. *Crit. Care.* 14:209. http://dx.doi.org/10.1186/cc8850

Azukizawa, H., A. Döhler, N. Kanazawa, A. Nayak, M. Lipp, B. Malissen, I. Autenrieth, I. Katayama, M. Riemann, F. Weih, et al. 2011. Steady state migratory RelB+ langerin+ dermal dendritic cells mediate peripheral induction of antigen-specific CD4+ CD25+ Foxp3+ regulatory T cells. *Eur. J. Immunol.* 41:1420–1434. http://dx.doi.org/10.1002/eji.201040930

Bachem, A., S. Güttler, E. Hartung, F. Ebstein, M. Schaefer, A. Tannert, A. Salama, K. Movassaghi, C. Opitz, H.W. Mages, et al. 2010. Superior antigen cross-presentation and XCR1 expression define human CD11c+CD141+ cells as homologues of mouse CD8+ dendritic cells. *J. Exp. Med.* 207:1273–1281. http://dx.doi.org/10.1084/jem.20100348

Bedoui, S., P.G. Whitney, J. Waithman, L. Eidsmo, L. Wakim, I. Caminschi, R.S. Allan, M. Wojtasiak, K. Shortman, F.R. Carbone, et al. 2009. Cross-presentation of viral and self antigens by skin-derived CD103+ dendritic cells. *Nat. Immunol.* 10:488–495. http://dx.doi.org/10.1038/ni.1724

Burgdorf, S., V. Lukacs-Kornek, and C. Kurts. 2006. The mannose receptor mediates uptake of soluble but not of cell-associated antigen for cross-presentation. *J. Immunol.* 176:6770–6776.

Caux, C., B. Vanbervliet, C. Massacrier, C. Dezutter-Dambuyant, B. de Saint-Vis, C. Jacquet, K. Yoneda, S. Imamura, D. Schmitt, and J. Banchereau. 1996. CD34+ hematopoietic progenitors from human cord blood differentiate along two independent dendritic cell pathways in response to GM-CSF+TNF alpha. *J. Exp. Med.* 184:695–706. http://dx.doi.org/10.1084/jem.184.2.695

Chang, C.C., R. Ciubotariu, J.S. Manavalan, J. Yuan, A.I. Colovai, F. Piazza, S. Lederman, M. Colonna, R. Cortesini, R. Dalla-Favera, and N. Suciu-Foca. 2002. Tolerization of dendritic cells by T(S) cells: the crucial role of inhibitory receptors ILT3 and ILT4. *Nat. Immunol.* 3:237–243. http://dx.doi.org/10.1038/ni760

Contreras, V., C. Urien, R. Guiton, Y. Alexandre, T.P. Vu Manh, T. Andrieu, K. Crozat, L. Jouneau, N. Bertho, M. Epardaud, et al. 2010. Existence of CD8α-like dendritic cells with a conserved functional specialization and a common molecular signature in distant mammalian species. *J. Immunol.* 185:3313–3325. http://dx.doi.org/10.4049/jimmunol.1000824

Crozat, K., R. Guiton, V. Contreras, V. Feuillet, C.A. Dutertre, E. Ventre, T.P. Vu Manh, T. Baranek, A.K. Storset, J. Marvel, et al. 2010. The XC chemokine receptor 1 is a conserved selective marker of mammalian cells homologous to mouse CD8alpha+ dendritic cells. *J. Exp. Med.* 207:1283–1292. http://dx.doi.org/10.1084/jem.20100223

Demedts, I.K., G.G. Brusselle, K.Y. Vermaelen, and R.A. Pauwels. 2005. Identification and characterization of human pulmonary dendritic cells. *Am. J. Respir. Cell Mol. Biol.* 32:177–184. http://dx.doi.org/10.1165/rcmb.2004-0279OC

Dhodapkar, M.V., R.M. Steinman, J. Krasovsky, C. Munz, and N. Bhardwaj. 2001. Antigen-specific inhibition of effector T cell function in humans after injection of immature dendritic cells. *J. Exp. Med.* 193:233–238. http://dx.doi.org/10.1084/jem.193.2.233

Fiore, N., G. Castellano, A. Blasi, C. Capobianco, A. Loverre, V. Montinaro, S. Netti, D. Torres, C. Manno, G. Grandaliano, et al. 2008. Immature myeloid and plasmacytoid dendritic cells infiltrate renal tubulointerstitium in patients with lupus nephritis. *Mol. Immunol.* 45:259–265. http://dx.doi.org/10.1016/j.molimm.2007.04.029

Heath, W.R., and F.R. Carbone. 2009. Dendritic cell subsets in primary and secondary T cell responses at body surfaces. *Nat. Immunol.* 10:1237–1244. http://dx.doi.org/10.1038/ni.1822

Henri, S., L.F. Poulin, S. Tamoutounour, L. Ardouin, M. Guilliams, B. de Bovis, E. Devilard, C. Viret, H. Azukizawa, A. Kissenpfennig, and B. Malissen. 2010. CD207+ CD103+ dermal dendritic cells cross-present keratinocyte-derived antigens irrespective of the presence of Langerhans cells. *J. Exp. Med.* 207:189–206. http://dx.doi.org/10.1084/jem.20091964

Jongbloed, S.L., A.J. Kassianos, K.J. McDonald, G.J. Clark, X. Ju, C.E. Angel, C.J. Chen, P.R. Dunbar, R.B. Wadley, V. Jeet, et al. 2010. Human CD141+ (BDCA-3)+ dendritic cells (DCs) represent a unique myeloid DC subset that cross-presents necrotic cell antigens. *J. Exp. Med.* 207:1247–1260. http://dx.doi.org/10.1084/jem.20092140

Jonuleit, H., U. Kühn, G. Müller, K. Steinbrink, L. Paragnik, E. Schmitt, J. Knop, and A.H. Enk. 1997. Pro-inflammatory cytokines and prostaglandins induce maturation of potent immunostimulatory dendritic cells under fetal calf serum-free conditions. *Eur. J. Immunol.* 27:3135–3142. http://dx.doi.org/10.1002/eji.1830271209

Jonuleit, H., E. Schmitt, G. Schuler, J. Knop, and A.H. Enk. 2000. Induction of interleukin 10-producing, nonproliferating CD4(+) T cells with regulatory properties by repetitive stimulation with allogeneic immature human dendritic cells. *J. Exp. Med.* 192:1213–1222. http://dx.doi.org/10.1084/jem.192.9.1213

King, M.A., L. Covassin, M.A. Brehm, W. Racki, T. Pearson, J. Leif, J. Laning, W. Fodor, O. Foreman, L. Burzenski, et al. 2009. Human peripheral blood leucocyte non-obese diabetic-severe combined immunodeficiency interleukin-2 receptor gamma chain gene mouse model of xenogeneic graft-versus-host-like disease and the role of host major histocompatibility complex. *Clin. Exp. Immunol.* 157:104–118. http://dx.doi.org/10.1111/j.1365-2249.2009.03933.x

Kissenpfennig, A., S. Henri, B. Dubois, C. Laplace-Builhé, P. Perrin, N. Romani, C.H. Tripp, P. Douillard, L. Leserman, D. Kaiserlian, et al. 2005. Dynamics and function of Langerhans cells in vivo: dermal dendritic cells colonize lymph node areas distinct from slower migrating Langerhans cells. *Immunity.* 22:643–654. http://dx.doi.org/10.1016/j.immuni.2005.04.004

Klechevsky, E., R. Morita, M. Liu, Y. Cao, S. Coquery, L. Thompson-Snipes, F. Briere, D. Chaussabel, G. Zurawski, A.K. Palucka, et al. 2008. Functional specializations of human epidermal Langerhans cells and CD14+ dermal dendritic cells. *Immunity.* 29:497–510. http://dx.doi.org/10.1016/j.immuni.2008.07.013

Larregina, A.T., A.E. Morelli, L.A. Spencer, A.J. Logar, S.C. Watkins, A.W. Thomson, and L.D. Falo Jr. 2001. Dermal-resident CD14+ cells differentiate into Langerhans cells. *Nat. Immunol.* 2:1151–1158. http://dx.doi.org/10.1038/ni731

Lenz, A., M. Heine, G. Schuler, and N. Romani. 1993. Human and murine dermis contain dendritic cells. Isolation by means of a novel method and phenotypical and functional characterization. *J. Clin. Invest.* 92:2587–2596. http://dx.doi.org/10.1172/JCI116873

Liu, K., T. Iyoda, M. Saternus, Y. Kimura, K. Inaba, and R.M. Steinman. 2002. Immune tolerance after delivery of dying cells to dendritic cells in situ. *J. Exp. Med.* 196:1091–1097. http://dx.doi.org/10.1084/jem.20021215

Lombardi, G., S. Sidhu, R. Batchelor, and R. Lechler. 1994. Anergic T cells as suppressor cells in vitro. *Science.* 264:1587–1589. http://dx.doi.org/10.1126/science.8202711

Lutz, M.B., and G. Schuler. 2002. Immature, semi-mature and fully mature dendritic cells: which signals induce tolerance or immunity? *Trends Immunol.* 23:445–449. http://dx.doi.org/10.1016/S1471-4906(02)02281-0

Merad, M., and M.G. Manz. 2009. Dendritic cell homeostasis. *Blood.* 113:3418–3427. http://dx.doi.org/10.1182/blood-2008-12-180646

Narbutt, J., A. Lesiak, A. Sysa-Jedrzejowska, P. Smolewski, T. Robak, and A. Zalewska. 2006. The number and distribution of blood dendritic cells in the epidermis and dermis of healthy human subjects. *Folia Histochem. Cytobiol.* 44:61–63.

Nestle, F.O., X.G. Zheng, C.B. Thompson, L.A. Turka, and B.J. Nickoloff. 1993. Characterization of dermal dendritic cells obtained from normal human skin reveals phenotypic and functionally distinctive subsets. *J. Immunol.* 151:6535–6545.

Nestle, F.O., P. Di Meglio, J.Z. Qin, and B.J. Nickoloff. 2009. Skin immune sentinels in health and disease. *Nat. Rev. Immunol.* 9:679–691.

Published April 30, 2012

Penna, G., N. Giarratana, S. Amuchastegui, R. Mariani, K.C. Daniel, and L. Adorini. 2005. Manipulating dendritic cells to induce regulatory T cells. *Microbes Infect.* 7:1033–1039. http://dx.doi.org/10.1016/j.micinf.2005.03.025

Poulin, L.F., M. Salio, E. Griessinger, F. Anjos-Afonso, L. Craciun, J.L. Chen, A.M. Keller, O. Joffre, S. Zelenay, E. Nye, et al. 2010. Characterization of human DNGR-1+ BDCA3+ leukocytes as putative equivalents of mouse CD8alpha+ dendritic cells. *J. Exp. Med.* 207:1261–1271. http://dx.doi.org/10.1084/jem.20092618

Raife, T.J., D.J. Lager, K.C. Madison, W.W. Piette, E.J. Howard, M.T. Sturm, Y. Chen, and S.R. Lentz. 1994. Thrombomodulin expression by human keratinocytes. Induction of cofactor activity during epidermal differentiation. *J. Clin. Invest.* 93:1846–1851. http://dx.doi.org/10.1172/JCI117171

Reis e Sousa, C. 2006. Dendritic cells in a mature age. *Nat. Rev. Immunol.* 6:476–483. http://dx.doi.org/10.1038/nri1845

Rizzitelli, A., D. Vremec, J.A. Villadangos, N. Mavaddat, M.D. Wright, and K. Shortman. 2005. Switching from a restricted to an effective CD4 T cell response by activating CD8+ murine dendritic cells with a Toll-like receptor 9 ligand. *Eur. J. Immunol.* 35:3209–3220. http://dx.doi.org/10.1002/eji.200526231

Robbins, S.H., T. Walzer, D. Dembélé, C. Thibault, A. Defays, G. Bessou, H. Xu, E. Vivier, M. Sellars, P. Pierre, et al. 2008. Novel insights into the relationships between dendritic cell subsets in human and mouse revealed by genome-wide expression profiling. *Genome Biol.* 9:R17. http://dx.doi.org/10.1186/gb-2008-9-1-r17

Sagoo, P., N. Ali, G. Garg, F.O. Nestle, R.I. Lechler, and G. Lombardi. 2011. Human regulatory T cells with alloantigen specificity are more potent inhibitors of alloimmune skin graft damage than polyclonal regulatory T cells. *Sci. Transl. Med.* 3:ra42. http://dx.doi.org/10.1126/scitranslmed.3002076

Sancho, D., O.P. Joffre, A.M. Keller, N.C. Rogers, D. Martínez, P. Hernanz-Falcón, I. Rosewell, and C. Reis e Sousa. 2009. Identification of a dendritic cell receptor that couples sensing of necrosis to immunity. *Nature.* 458:899–903. http://dx.doi.org/10.1038/nature07750

Schwarz, T., and A. Schwarz. 2011. Molecular mechanisms of ultraviolet radiation-induced immunosuppression. *Eur. J. Cell Biol.* 90:560–564. http://dx.doi.org/10.1016/j.ejcb.2010.09.011

Skowera, A., R.J. Ellis, R. Varela-Calviño, S. Arif, G.C. Huang, C. Van-Krinks, A. Zaremba, C. Rackham, J.S. Allen, T.I. Tree, et al. 2008. CTLs are targeted to kill beta cells in patients with type 1 diabetes through recognition of a glucose-regulated preproinsulin epitope. *J. Clin. Invest.* 118:3390–3402.

Steinman, R.M., D. Hawiger, and M.C. Nussenzweig. 2003. Tolerogenic dendritic cells. *Annu. Rev. Immunol.* 21:685–711. http://dx.doi.org/10.1146/annurev.immunol.21.120601.141040

Swamy, M., C. Jamora, W. Havran, and A. Hayday. 2010. Epithelial decision makers: in search of the 'epimmunome'. *Nat. Immunol.* 11:656–665. http://dx.doi.org/10.1038/ni.1905

Tsoumakidou, M., N. Tzanakis, H.A. Papadaki, H. Koutala, and N.M. Siafakas. 2006. Isolation of myeloid and plasmacytoid dendritic cells from human bronchoalveolar lavage fluid. *Immunol. Cell Biol.* 84:267–273. http://dx.doi.org/10.1111/j.1440-1711.2006.01428.x

Waithman, J., R.S. Allan, H. Kosaka, H. Azukizawa, K. Shortman, M.B. Lutz, W.R. Heath, F.R. Carbone, and G.T. Belz. 2007. Skin-derived dendritic cells can mediate deletional tolerance of class I-restricted self-reactive T cells. *J. Immunol.* 179:4535–4541.

Zaba, L.C., J. Fuentes-Duculan, R.M. Steinman, J.G. Krueger, and M.A. Lowes. 2007. Normal human dermis contains distinct populations of CD11c+BDCA-1+ dendritic cells and CD163+FXIIIA+ macrophages. *J. Clin. Invest.* 117:2517–2525. http://dx.doi.org/10.1172/JCI32282

doi: 10.1111/j.1365-2222.2011.03770.x
Clinical & Experimental Allergy, **41**, 1400–1413

ORIGINAL ARTICLE **Basic Mechanisms in Allergic Disease**

Harnessing engineered antibodies of the IgE class to combat malignancy: initial assessment of FcεRI-mediated basophil activation by a tumour-specific IgE antibody to evaluate the risk of type I hypersensitivity

S. M. Rudman[1,2], D. H. Josephs[1,2], H. Cambrook[1], P. Karagiannis[1], A. E. Gilbert[1], T. Dodev[3,4], J. Hunt[3,4], A. Koers[5], A. Montes[6], L. Taams[7], S. Canevari[8], M. Figini[8], P. J. Blower[5], A. J. Beavil[3,4], C. F. Nicodemus[9], C. Corrigan[4], S. B. Kaye[10], F. O. Nestle[1], H. J. Gould[3,4], J. F. Spicer[2] and S. N. Karagiannis[1]

[1]NIHR Biomedical Research Centre at Guy's and St Thomas's Hospitals and King's College London, Cutaneous Medicine & Immunotherapy Unit, St John's Institute of Dermatology, Division of Genetics & Molecular Medicine, King's College London School of Medicine, Guy's Hospital, King's College London, London, UK, [2]Division of Cancer Studies, King's College London School of Medicine, Guy's Hospital, King's College London, London, UK, [3]Randall Division of Cell and Molecular Biophysics, King's College London, London, UK, [4]Division of Asthma, Allergy and Lung Biology, MRC and Asthma UK Centre for Allergic Mechanisms of Asthma, King's College London, London, UK, [5]Division of Imaging Sciences, King's College London, Rayne Institute, St Thomas' Hospital, London, UK, [6]Guy's and St Thomas' NHS Foundation Trust, London, UK, [7]Centre for Molecular & Cellular Biology of Inflammation, Division of Immunology, Infection and Inflammatory Diseases, King's College London, London, UK, [8]Unit of Molecular Therapies, Department of Experimental Oncology and Molecular Medicine, Fondazione IRCCS, Istituto Nazionale dei Tumouri, Milan, Italy, [9]Advanced Immune Therapeutics Inc., Charlestown, MA, USA and [10]Institute of Cancer Research and Royal Marsden NHS Foundation Trust, Sutton, Surrey, UK

Clinical & Experimental Allergy

Correspondence:
Dr Sophia N. Karagiannis, Division of Genetics and Molecular Medicine, St. John's Institute of Dermatology, King's College London, Guy's Hospital, Tower Wing 9th Floor, London SE1 9RT, UK.
E-mail: sophia.karagiannis@kcl.ac.uk
Cite this as: S. M. Rudman, D. H. Josephs, H. Cambrook, P. Karagiannis, A. E. Gilbert, T. Dodev, J. Hunt, A. Koers, A. Montes, L. Taams, S. Canevari, M. Figini, P. J. Blower, A. J. Beavil, C. F. Nicodemus, C. Corrigan, S. B. Kaye, F. O. Nestle, H. J. Gould, J. F. Spicer and S. N. Karagiannis, *Clinical & Experimental Allergy*, 2011 (41) 1400–1413.

Summary

Background IgE antibodies, sequestered into tissues and retained locally by the high-affinity IgE receptor, FcεRI, on powerful effector cells such as mast cells, macrophages and eosinophils, may offer improvements in the therapy of solid tumours. The chimeric antibody, MOv18 IgE, against the human ovarian carcinoma antigen, folate receptor α (FRα), is more effective than its IgG1 counterpart in xenograft models of ovarian cancer. Although MOv18 IgE binds to a single epitope on FRα and cannot cross-link IgE receptors on basophils, there remains a risk that components in the circulation of ovarian cancer patients might cross-link FRα-MOv18-IgE-receptor-FcεRI complexes on basophils to cause type I hypersensitivity.
Objective To assess the propensity for MOv18 used in a therapeutic setting to cause FcεRI-mediated type I hypersensitivity.
Methods As validated readouts of the potential for MOv18 to cause FcεRI-mediated type I hypersensitivity we measured release of a granule-stored mediator from a rat basophilic leukaemia cell line RBL SX-38 stably transfected with human tetrameric (αβγ2) FcεRI, and induction of CD63 on blood basophils from patients with ovarian carcinoma and healthy controls *ex vivo*.
Results Serum FRα levels were increased in ovarian cancer patients compared with healthy controls. MOv18 IgE alone, or in the presence of its antigen recombinant human FRα, or of healthy volunteer ($n = 14$) or ovarian carcinoma patient ($n = 32$) sera, did not induce RBL SX-38 cell degranulation. Exposure to FRα-expressing ovarian tumour cells at target-to-effector ratios expected within tumours induced degranulation. MOv18 IgE did not induce expression of CD63 in blood basophils from either healthy volunteers ($n = 6$), or cancer patients, despite detectable levels of circulating FRα ($n = 5$).
Conclusion and Clinical Relevance These encouraging data are compatible with the hypothesis that, when ovarian carcinoma patients are treated with MOv18, FcεRI-mediated activation of effector cells occurs within the tumour mass but not in the circulation mandating, with due caution, further pre-clinical studies.

Keywords anaphylaxis, basophil, cancer therapy, CD63, degranulation, FRα, tumour antigen-specific IgE, type I hypersensitivity
Submitted 3 February 2011; revised 11 March 2011; accepted 1 April 2011.

Introduction

Monoclonal antibodies have become an important treatment modality in the clinical management of both haematological and solid malignancies in the last 25 years [1]. Nevertheless, many solid tumours such as those of the ovary remain refractory to treatment, indicating a need to improve antibody therapeutics, with a particular emphasis on localization of the antibody and initiation of anti-tumour immunity within the tumour mass itself.

We have previously investigated means of improving antibody therapies for solid tumours, using antibodies of the IgE class [2–7]. Exploitation of the superior tissue bioavailability and higher Fc receptor affinity of IgE, compared with IgG antibodies may translate to improved anti-tumour efficacy. IgE-mediated immune responses play a role in allergic inflammation and in protection against parasitic infections [8, 9]. Previous studies have demonstrated that IgE-mediated immune responses may be harnessed against malignant cells in tissues [7, 10–14].

MOv18 IgE is a chimeric antibody directed against the tumour-associated antigen folate receptor α (FRα). We have shown that it has superior efficacy against solid ovarian tumours compared with its IgG1 counterpart *in vitro* and in two *in vivo* cancer models [2, 7]. This antibody may represent a novel paradigm for the treatment of solid malignancies. FRα, a glycosylphosphatidylinositol-anchored membrane protein that binds folic acid, is an emerging therapeutic target for ovarian cancers [15–17]. It is expressed in 90% of epithelial ovarian carcinomas and in other types of cancer, but has limited expression in normal tissues [18, 19]. Elevated FRα expression on ovarian cancer tumour cells correlates with more aggressive disease and a worse prognosis [18]. Thus FRα would appear to be a prime molecular target for ovarian carcinoma and this, together with the aforementioned data supporting the therapeutic efficacy of MOv18 IgE preclinically supports our enthusiasm for development of this antibody for clinical studies [2–5, 7].

IgE antibodies can exert anti-tumoural effects by activating potent FcεR-expressing effector cells within tumours. We have previously reported evidence suggesting that MOv18 IgE can direct monocytes and eosinophils to kill tumour cells by mechanisms such as antibody-mediated cytotoxicity and/or phagocytosis [2–4]. In general, however, the interactions between this IgE and potent IgE receptor-expressing immune effector cells, such as basophils (in the circulation and potentially within tumours) and mast cells (focused in tumour microenvironments), have not been extensively examined [5, 20–22].

To date, IgE has never been used as a therapeutic agent in patients, and the administration of IgE directed against a tumour antigen raises the theoretical possibility of induction of type I hypersensitivity through cross-linking of IgE molecules bound to FcεRI on mast cells and basophils. It is a requirement, however, that antigens capable of doing this have two or more IgE binding epitopes [23, 24] whereas MOv18 binds to only one single epitope on FRα [25, 26]. Consequently FRα, at least free and in solution, would not be expected to have the potential to cross-link surface-bound MOv18 bound to FcεRI although this could at least theoretically occur in the tumour cells expressing multiple surface FRα molecules within tumour islands.

In this study, we set out to investigate the capacity of FRα both in solution and expressed on ovarian carcinoma cells to activate basophils through MOv18 bound to human FcεRI. We adopted two assays used in the allergy field to examine sensitivity to a range of potential allergens in the presence of sera and blood of allergic individuals. We measured effector cell activation by functional degranulation with the humanized rat basophilic leukaemia (RBL) SX-38 cell line, and used the basophil activation test (BAT), based on detection of the activation marker, CD63, on basophils in the blood of healthy volunteers and ovarian carcinoma patients. With these experiments we account for any factors in blood that might recognize the tri-molecular complexes of FRα-MOv18 IgE-FcεRI on basophils, which could contribute to a risk of type I hypersensitivity in the proposed immunotherapy.

Methods

Human subjects and sera

Following written informed consent, sera from the peripheral blood of patients with stage III and IV ovarian cancer or healthy volunteers were collected and isolated by centrifugation of clotted blood at 1800 g for 15 min at room temperature. Sera were also collected from ovarian cancer patient peripheral blood as part of baseline studies before a clinical trial [27]. For the basophil activation assay (BAT), whole blood specimens of patients with stage III and IV ovarian cancer or healthy volunteers were freshly collected in 1.8 mg/mL K_2EDTA and assayed immediately.

Cell culture

Cells of the RBL SX-38 RBL cell line stably expressing the human tetrameric ($\alpha\beta\gamma_2$) high-affinity IgE receptor, FcεRI [28], (a kind gift from Prof. J-P. Kinet, Harvard University, Boston, MA) were cultured in EMEM, 10% FCS, 1.2 mg/mL Geneticin G418 (Gibco, Invitrogen, Paisley, UK). Human ovarian carcinoma IGROV-1 cells [3, 7], naturally over-expressing the human FRα, were cultured in RPMI 1640, 10% FCS and murine colon adenocarcinoma cells CT26 [6] in IMDM, 5% FCS. Cultures were maintained in a humidified incubator at 37 °C.

Flow cytometric assessments of MOv18 immunoglobulin E and antigen binding to effector cells

RBL SX-38 cells (2×10^5 cells per sample) were incubated with 0.5 μg/mL MOv18 IgE in 0.2 mL FACS buffer (PBS, 5% FCS, Invitrogen), followed by 3 μg/mL goat anti-human IgE-FITC (Vector Labs, Peterborough, UK) or 200 ng/mL human recombinant FRα [25], 3 μg/mL goat anti-human FRα (R&D Systems, Abingdon, UK) and donkey anti-goat-Ig-Alexa Fluor® 448, (all in FACS buffer). For MOv18 IgE binding to human basophils in unfractionated blood, 100 μL blood diluted 1 : 1 with FACS buffer was incubated with MOv18 IgE, anti-IgE-FITC and mouse anti-CD123-RPE-Cy5 (BD Biosciences, Oxford, UK) or isotypic control IgG1/RPE-Cy5 (1 μg/mL, Dako, Stockport, UK) for 30 min at 4 °C. Red blood cells were removed with 2 mL lysis buffer (155 mM NH_4Cl, 10 mM $KHCO_3$, 100 μM EDTA) for 10 min at room temperature. Cells were acquired on a dual laser FACSCanto (BD Biosciences) until at least 500 basophil ($SSC^{low}CD123^{high}$) events were recorded per sample.

Rat basophilic leukaemia SX-38 degranulation assays

We assessed degranulation of RBL SX-38 cells by measuring β-hexosaminidase release, as before [6, 28, 29]. Controls were: unstimulated cells; Triton X-100 lysed cells (to quantify 100% granule release); chimeric NIP IgE against the hapten 5-iodo-4-hydroxy-3-nitrophenyl (AbD Serotec, Kidlington, UK) with or without polyclonal antigen NIP-bovine serum albumin (BSA) [30]; NIP IgE plus polyclonal rabbit anti-IgE (Dako). Cells were seeded at 1×10^4 cells per well in culture medium overnight and sensitized with IgE (200 ng/mL), control antibody or medium alone. Samples were incubated at 37 °C for 1 h, washed 3× in stimulation buffer (HBSS, 1% BSA; Invitrogen) and stimulated for 30 min at 37 °C with 100 μL FRα [25], human sera (1 : 100 dilution), NIP-BSA, or rabbit anti-IgE (200 ng/mL). To detect β-hexosaminidase, 50 μL culture supernatants diluted 1 : 1 in stimulation buffer, were transferred onto black 96-well plates with 50 μL fluorogenic substrate per well (1 mM 4-nethylumbelliferyl *N*-acetyl-β-D-glucosaminide 0.1% DMSO, 0.1% Triton X-100, 200 mM citrate, pH 4.5) and incubated for 2 h in the dark. Reactions were quenched with 100 μL per well 0.5 M Tris and plates read with a Fluostar Omega microplate reader (350 nm excitation, 450 nm emission) (BMG Labtech, Offenburg, Germany). Degranulation was expressed as a percentage of Triton X-100 release, and compared with unstimulated cells (< 10%).

Enzyme-linked immunosorbent assay to detect circulating folate receptor α

To quantify circulating FRα in human sera, 96-well plates were coated overnight at 4 °C with 2 μg/mL mouse anti-human FRα (IgG1, R&D Systems) in 0.2 M carbonate-bicarbonate buffer, pH 9.4. Plates were given blocking buffer (SuperBlock buffer, 0.05% Tween-20; Perbio Science UK Ltd, Cramlington, UK) for 2 h at room temperature, washed 4× with PBS, 0.05% Tween-20 (washing buffer) and given recombinant FRα [25] or sera (1 : 5 in blocking buffer) and incubated for 2 h at room temperature. All conditions were tested in triplicate. Plates were washed 4×, incubated with 50 ng/mL goat anti-FRα-biotin in blocking buffer (R&D Systems) for 2 h at room temperature, washed again 4×, and given 50 ng/mL streptavidin-HRP (Pierce, Thermo Fisher Scientific, Cramlington, UK) in blocking buffer for 30 min at room temperature. Following five washes, samples were treated with 0.5 mg/mL *o*-phenylenediamine dihydrochloride substrate (Sigma-Aldrich, Gillingham, UK) in peroxide substrate buffer (Pierce) for 5 min at room temperature. Following addition of 50 μL per well stop solution (1 M HCl), plates were read at 492 nm (reference wavelength 650 nm) on a Fluostar Omega microplate reader. The lower limit of quantification of FRα in this assay was 1.25 ng/mL.

Enzyme-linked immunosorbent assay to detect circulating anti-folate receptor α immunoglobulin G autoantibodies

To quantify anti-FRα IgG autoantibodies in human sera, 96-well plates were coated overnight at 4 °C with 1 μg/mL recombinant human FRα (R&D Systems) in 0.2 M carbonate-bicarbonate buffer, pH 9.4. Plates were incubated in blocking buffer (SuperBlock buffer, 0.05% Tween-20; Perbio Science UK Ltd) for 2 h at room temperature, washed 4x with PBS, 0.05% Tween-20 (washing buffer) and incubated with MOv18 IgG or human sera (1 : 5 in blocking buffer) for 2 h at room temperature. All conditions were tested in triplicate. Plates were washed 4×, and incubated with 160 ng/mL $F(ab')_2$ goat anti-human Fcγ-HRP (Jackson ImmunoResearch, Stratech, Newmarket, UK) in blocking buffer (Stratech) for 45 min at room temperature. Following five washes, samples were treated with 0.5 mg/mL *o*-phenylenediamine dihydrochloride substrate (Sigma-Aldrich) in peroxide substrate buffer (Pierce) for 5 min at room temperature. Following addition of 50 μL per well stop solution (1 M HCl), plates were read at 492 nm (reference wavelength 540 nm) on a Fluostar Omega microplate reader. The lower limit of quantification of anti-FRα IgG in this assay was 2.5 ng/mL.

Whole blood basophil activation test

Activation of human basophils *ex vivo* was measured using a standard BAT, which measures up-regulation of CD63 on ($CCR3^{high}SSC^{low}$) basophils in whole human blood as described previously [31, 32]. Briefly, blood collected in 1.8 mg/mL K_2EDTA was assayed using a FLOW 2 CAST basophil activation kit (Bühlmann, Schönenbuch, Switzerland) and acquired within 4 h on a dual laser FACSCanto (BD Biosciences, Oxford, UK). To 100 μL blood were added 150 μL of stimulation buffer alone

(background), or 100 μL 'stimulus' with 50 μL stimulation buffer. Stimuli included positive controls, e.g. 1 μg/mL anti-human FcεR1 polyclonal or anti-human IgE polyclonal antibodies, or MOv18 IgE (ranges from 0.03 to ~10 μg/mL). Some blood samples pre-incubated with MOv18 IgE were given 100 μL human recombinant FRα solution (8–333 ng/mL) and incubation continued for a further 10 min. Samples were finally incubated with staining reagent (0.1 μg/mL mouse anti-human CCR3-PE and CD63-FITC antibodies) at 37 °C for 10 min before acquisition of at least 500 basophil ($CCR3^{high}SSC^{low}$) events per sample.

Live cell imaging

IGROV-1 tumour cells were seeded at 2×10^4 cells/well onto 12-well glass-bottomed plates (MatTek, Ashland, MA, USA) and labelled with 500 μL of 2 μM Calcein AM per well (Molecular Probes, Invitrogen) for 30 min, washed and resuspended in RPMI 1640 medium, with 10% FCS. RBL SX-38 cells (2×10^5/mL) were labelled for 30 min at 37 °C with 2 μg/mL Cholera Toxin B subunit Alexa Fluor® 647 (Invitrogen), which binds ganglioside 1 (GM1), and is a marker of granule cycling [33, 34]. Cells were washed and treated with MOv18 IgE or NIP IgE in medium for 30 min. The adherent labelled tumour cells and 4×10^4 RBL SX-38 cells/well were incubated for 30 min at 37 °C in a humidified chamber. Images were captured using a Zeiss AxiovertZ.1 microscope (Welwyn Garden City, UK) (with incorporated Calibri System) equipped with a Plan-Apochromat 63×/1.4 oil DIC objective, Axio CamMR3 camera and AxioVision software system (Carl Zeiss). Measurements of mean fluorescence intensity per cell (MFI±SD, five image fields per condition) were conducted using ImageJ version 1.4 image processing and analysis software (http://rsbweb.nih.gov/ij/index.html).

Statistical methods

A two-tailed Student's *t*-test was used to compare % RBL SX-38 cell degranulation and FRα concentrations in patient and healthy control sera (values $P<0.05$, were considered statistically significant). Linear regression analysis was used to assess correlation between degranulation with MOv18 IgE and FRα titres in patient serum samples. Statistical analyses were performed using GraphPad Prism version 5.03.

Results

MOv18 immunoglobulin E and soluble antigen do not trigger effector cell degranulation

We explored whether MOv18 IgE triggers FcεRI-mediated degranulation of RBL SX-38 cells, a validated model of human FcεRI cross-linking in the presence of specific IgE and polyvalent allergens (Fig. 1a) [28, 35, 36]. Flow cytometric analysis confirmed that MOv18 IgE bound to almost 100% of the human FcεRI-bearing cells, and that FRα in turn bound to virtually all of the IgE-primed cells (Fig. 1b). Cellular degranulation was measured by β-hexosaminidase release expressed as a percentage of that measured with Triton X-100 detergent (complete cell lysis). Unstimulated and NIP IgE-stimulated cells triggered background degranulation (<10% of Triton X-100, Fig. 1c). NIP IgE with its multivalent antigen NIP BSA or with polyclonal anti-IgE cross-linking FcεRI-bound IgE, triggered detectable degranulation (mean±SD, 34.5±4.1%, 25.4±2.9%, respectively, $n=3$) [37].

We then investigated whether MOv18 IgE alone or in the presence of soluble FRα can trigger degranulation. As with NIP IgE, MOv18 IgE alone did not induce degranulation (1.5±1.1%), but MOv18 IgE cross-linked by polyclonal anti-IgE antibody induced appreciable degranulation (37.6±6.7%). Degranulation was also triggered through cross-linking of cell surface MOv18 IgE-bound FRα by an anti-FRα polyclonal antibody (15.4±0.7%) to mimick the effect of a multimeric antigen or of tumour cells bearing multiple copies of the antigen. When cells were incubated with MOv18 IgE and increasing concentrations of recombinant FRα (1.9–1000 ng/mL) we measured background degranulation, even at supra-physiological concentrations (>100 ng/mL) and concentrations >10-fold (400–1000 ng/mL) in excess of those reported in ovarian cancer patient blood [39] (Fig. 1d).

MOv18 immunoglobulin E does not stimulate degranulation in the presence of sera from ovarian carcinoma patients or healthy volunteers, despite detectable circulating folate receptor α

We examined whether MOv18 IgE-primed RBL cells showed evidence of FcεRI-dependent activation in the presence of naturally shed, circulating FRα in sera from patients with ovarian carcinoma. Sera from 32 patients with stage III or IV disease caused minimal degranulation which was not statistically different to that observed in the presence of 14 normal control sera (2.45±1.53% vs. 3.05±2.40%, $P>0.05$; Table 1, Fig. 2a) despite the fact that the median FRα concentration in the patients' sera was clearly and significantly elevated compared with that measured in the normal sera ($P=0.006$, Fig. 2b). No significant differences in degranulation were measured in relation to disease stage: sera from patients with stage III disease ($n=20$) compared with sera from patients with stage IV ovarian carcinoma ($n=12$, $P>0.05$). We measured very low FRα levels in 14 healthy volunteer sera (1.73 ng/mL) and FRα titres above the mean in the healthy volunteer cohort in 19 out of 30 ovarian carcinoma patient sera (5.48 for stage III, 9.59 ng/mL for stage IV groups; total mean 7.1 ng/mL, Table 1). What little degranulation was observed in the presence of patient sera did not correlate with the disease stage or absolute serum concentration of FRα (Fig. 2c).

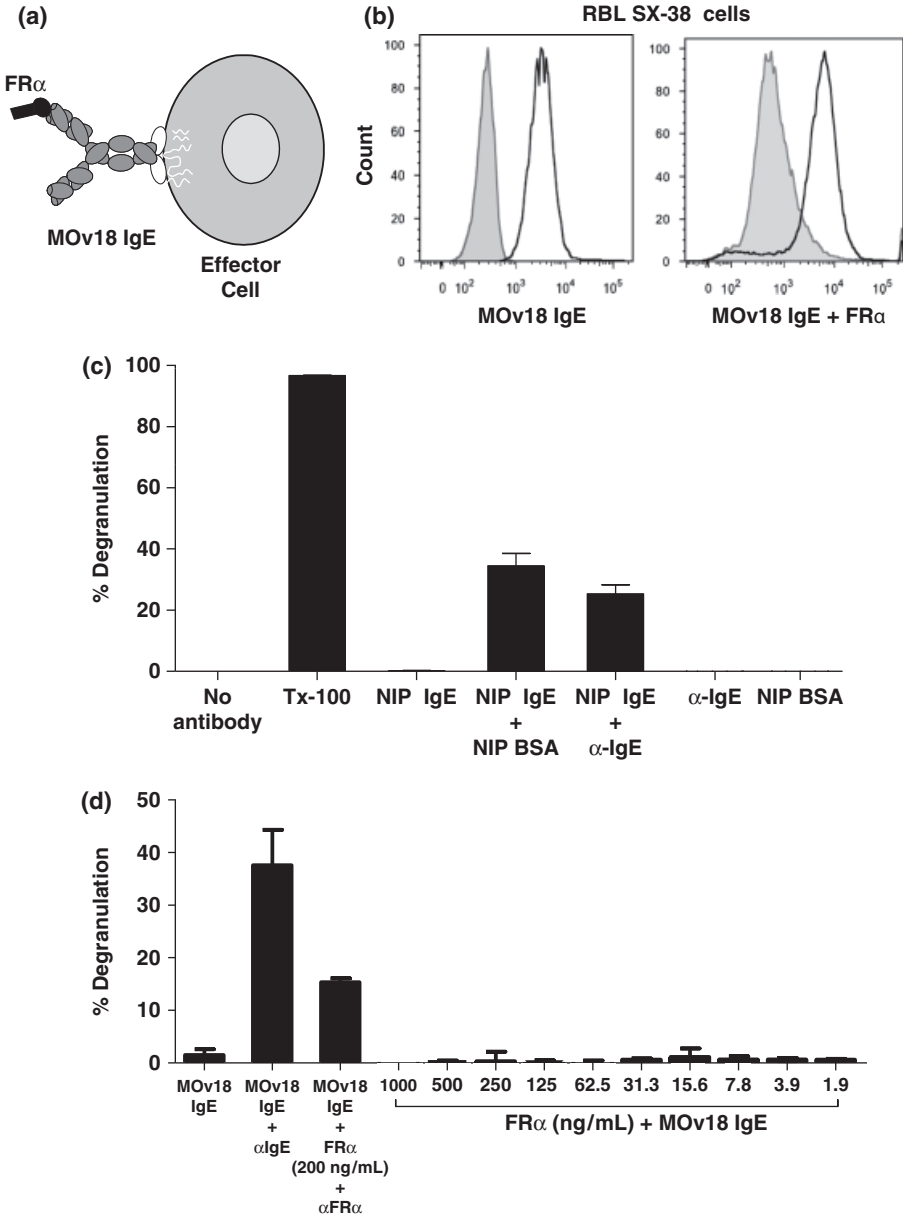

Fig. 1. MOv18 IgE and soluble FRα bind to RBL SX-38 cells and do not stimulate degranulation. (a) Schematic diagram of the monovalent interaction between shed FRα and MOv18 IgE on the surface of effector cells. (b) Flow cytometric assay demonstrating MOv18 IgE binding to RBL SX-38 cells (solid line histogram: MOv18 IgE; grey histogram: goat anti-IgE-FITC antibody control); and FRa binding to MOv18 IgE-primed RBL SX-38 cells (solid line histogram: MOv18 IgE+FRa+goat anti-human FRα+donkey anti-goat-Alexa Fluor® 448 antibodies; grey histogram: MOv18 IgE+goat anti-human FRα+donkey anti-goat-Alexa Fluor® 448 antibodies). (c) β-hexosaminidase release showing % degranulation relative to Triton X-100. Minimal degranulation was seen with cells alone, control antibody NIP IgE, its polyclonal ligand NIP-BSA, or polyclonal anti-IgE antibody alone. Significant degranulation is observed with samples given NIP IgE+NIP-BSA or NIP IgE+anti-IgE. (d) Degranulation with MOv18 IgE plus anti-IgE and minimal degranulation with MOv18 IgE alone and MOv18 IgE plus recombinant FRα (1.9–1000 ng/mL). Scale bars indicate mean values±standard deviation [38] of $n = 3$ experiments, all conditions were tested in triplicate. FRα, folate receptor α; RBL, rat basophilic leukaemia; BSA, bovine serum albumin.

Immunoglobulin E and tumour cells trigger degranulation in an antigen-dependent manner

A large proportion of ovarian carcinoma cells over-express FRα on their cell surface. MOv18 IgE may bridge effector and tumour cells, triggering FcεRI cross-linking through multiple copies of cell surface FRα (Fig. 3a). To explore the consequences of this interaction, RBL SX-38 cells were sensitized with MOv18 IgE and incubated with serially increasing numbers of FRα-expressing IGROV-1 ovarian carcinoma cells (Fig. 3b). We were able to detect significant degranulation at higher IGROV-1 : RBL SX-38 cell ratios ($> 15 : 10$), but not at the lower ratios ($< 8 : 10$) which one might expect to find in the peripheral blood of

Table 1. Percent RBL SX-38 cell degranulation in the presence of MOv18 IgE and measurement of serum FRα levels in human sera from (A) healthy volunteers and (B) ovarian carcinoma patients

Volunteer no.	Serum origin	% Degranulation	[FRα] (ng/mL)
(A) Healthy volunteers			
1	Healthy	2.68	ND
2	Healthy	0.99	2.30
3	Healthy	1.10	ND
4	Healthy	0.97	ND
5	Healthy	2.78	10.01
6	Healthy	1.66	ND
7	Healthy	2.13	2.74
8	Healthy	3.34	ND
9	Healthy	N/A	ND
10	Healthy	3.65	ND
11	Healthy	1.91	ND
12	Healthy	2.64	9.15
13	Healthy	9.43	ND
14	Healthy	6.38	ND
		Mean±SD	Mean [FRα]±SD
		3.05±2.40	1.73±3.45

Volunteer no.	Serum origin	Stage	Histological subtype	Primary treatment/relapse	% Degranulation	[FRα] (ng/mL)
(B) Ovarian carcinoma patients						
15	Patient	3	PD serous	Primary	1.44	5.18
16	Patient	3	Serous	Primary	3.27	ND
17	Patient	3	Serous	Primary	3.17	21.01
18	Patient	3	Papillary serous	Primary	3.92	N/A
19	Patient	3	Serous	Primary	1.27	8.27
20	Patient	3	PD serous	1st relapse	1.38	ND
21	Patient	3	Serous adeno	1st relapse	1.66	2.58
22	Patient	3	PD serous	1st relapse	1.40	5.62
23	Patient	3	Papillary serous	1st relapse	3.22	ND
24	Patient	3	Serous adeno	1st relapse	3.55	6.82
25	Patient	3	PD serous	1st relapse	1.29	5.50
26	Patient	3	WD serous	1st relapse	3.01	14.90
27	Patient	3	Serous adeno	1st relapse	3.14	1.60
28	Patient	3	Serous fallopian	1st relapse	1.85	15.85
29	Patient	3	Not known	1st relapse	1.68	ND
30	Patient	3	Primary Peritoneal	1st relapse	1.24	6.30
31	Patient	3	Not known	1st relapse	1.40	ND
32	Patient	3	Not known	1st relapse	2.24	1.53
33	Patient	3	PD serous	1st relapse	2.57	3.45
34	Patient	3	PD serous	1st relapse	2.41	N/A
					Mean±SD	Mean [FRα]±SD
					2.26±0.90	5.48±6.14
35	Patient	4	Clear cell	5th relapse	2.47	12.67
36	Patient	4	Serous	4th relapse	4.04	1.59
37	Patient	4	MD serous	1st relapse	0.0	14.26
38	Patient	4	PD adeno	5th relapse	8.70	ND
39	Patient	4	Adeno	2nd relapse	2.50	21.01
40	Patient	4	PD adeno	3rd relapse	2.40	2.50
41	Patient	4	Pap serous	Primary	1.60	ND
42	Patient	4	Serous	Primary	3.70	5.64*
43	Patient	4	Clear cell	1st relapse	2.76	34.45*
44	Patient	4	Serous	1st relapse	2.85	11.84*
45	Patient	4	Adeno	2nd relapse	2.14	9.67*
46	Patient	4	Clear cell	1st relapse	0.0	1.49*

Table 1. continued

Volunteer no.	Serum origin	Stage	Histological subtype	Primary treatment/relapse	% Degranulation	[FRα] (ng/mL)
					Mean±SD	Mean [FRα]±SD
					2.76±2.24	9.59±10.29
					Overall mean±SD	Overall mean [FRα]±SD
					2.45±1.53	7.12±8.15

*Patients tested in whole blood basophil activation assay (Fig. 5).
ND, not detected, depicting [FRα] values below 1.5 ng/mL; N/A, not analysed; PD, poorly differentiated; WD, well differentiated; MD, moderately differentiated; FRα, folate receptor α.

patients with ovarian cancer (equivalent to $<8\times10^3$ tumour cells/10^4 effector cells, typical basophil counts per mL blood) (Fig. 3b; supporting information Table S1) [34, 40–45]. Tumour cells that did not express FRα did not induce degranulation, even at high tumour : effector cell ratios (6 : 1), suggesting that the phenomenon is antigen-specific.

We confirmed that RBL SX-38 cells (red) were activated in the presence of MOv18 IgE and tumour cells using live cell imaging (Fig. 3c) to monitor membrane motility and exocytosis after labelling of cell membranes with cholera toxin B subunit [33, 34]. We observed enhanced mobilization of cytoplasmic granules (reduction of red cytoplasmic fluorescence) by RBL SX-38 cells incubated with MOv18 IgE after 15 and 30 min in culture (depicted by reduction in mean fluorescence intensity per cell, MFI±SD, measured at 58.3±26.4% and 36.6±17.2% of original after 15 and 30 min respectively, $n=5$) compared with samples treated with control NIP IgE antibody (91.4±15.5% and 77.5±14.9%, $n=5$, $P=0.028$).

Examination of early signals of blood basophil activation ex vivo *following administration of MOv18 immunoglobulin E by the basophil activation test assay*

To determine whether MOv18 IgE activates blood basophils from patients with ovarian carcinoma directly *ex vivo* we used the BAT using CD63 as a readout of basophil activation [31, 46]. Figure 4 summarizes a typical set of experiments in a healthy control. Human basophils ($CD123^{high}SSC^{low}$) bound MOv18 IgE ($CD123^{high}IgE^{+}$), and basophils ($CCR3^{high}SSC^{low}$) expressing CD63 ($CCR3^{high}CD63^{+}$) were detected in the presence of stimuli (Figs 4a and b). Only 2.3% of unstimulated basophils expressed CD63, in agreement with previous reports [32]. This increased to 81.48% and 89.58% following cross-linking of FcεRI with either polyclonal anti-FcεRI (Fig. 4b) or anti-IgE (Figs 4c and d) antibodies respectively. In contrast a range of concentrations of MOv18 alone (0.03–3.5 μg/mL) did not augment CD63 expression (Figs 4c and d).

We further investigated whether MOv18 IgE and soluble FRα can trigger basophil activation in whole human blood from healthy volunteers. In the presence of MOv18 IgE, addition of exogenous FRα even at concentrations 10-fold higher than those observed in patients (333 ng/mL, $n=6$) did not augment CD63 expression (Figs 5a and b). Similarly, addition of MOv18 IgE to blood of five patients with ovarian carcinoma did not result in detectable augmentation of CD63 expression (Figs 5c and d) despite the fact that all five patients had detectable circulating concentrations of FRα (Table 1). In contrast, cross-linking with anti-FcεRI or anti-IgE polyclonal antibodies clearly augmented CD63 expression (supporting information Figure S1).

We also examined sera from 24 patients in which we had detected the presence of circulating FRα antigen (Table 1) for the presence of anti-FRα IgG autoantibodies that might crosslink sFRα bound to MOv18 IgE-sensitized basophils. We found no detectable increase above background in sera from 18 of these patients. In the remaining six patients and we detected concentrations in the range of 3.23–42.64 ng/mL (supporting information Table S2). When tested in the RBL SX-38 assay, sera from these patients did not trigger any functional degranulation in the presence of MOv18 IgE. Further, in two patients with detectable autoantibodies, we could detect no increase in CD63 expression by the patients' blood basophils using the BAT.

Discussion

The human immune system uses five classes of antibodies to combat disease. Each antibody class operates in different anatomical compartments, and functions through unique Fc-receptors and immune effector cells. Understanding how antibody class influences the nature of the immune response harnessed against cancer cells may be key in the design of future effective antibody therapeutics. Research to-date has mostly focused on developing IgG antibodies, the most abundant circulating antibody class, and all antibodies currently licensed for cancer therapy are IgG. We have previously shown, using ovarian xenograft models in immunodeficient mice, that survival following treatment with the anti-FRα chimeric antibody MOv18 IgE with human PBMC as effector cells is superior to that with MOv18 IgG1 [2–5, 7]. This suggests that harnessing IgE as a therapy for human cancer may

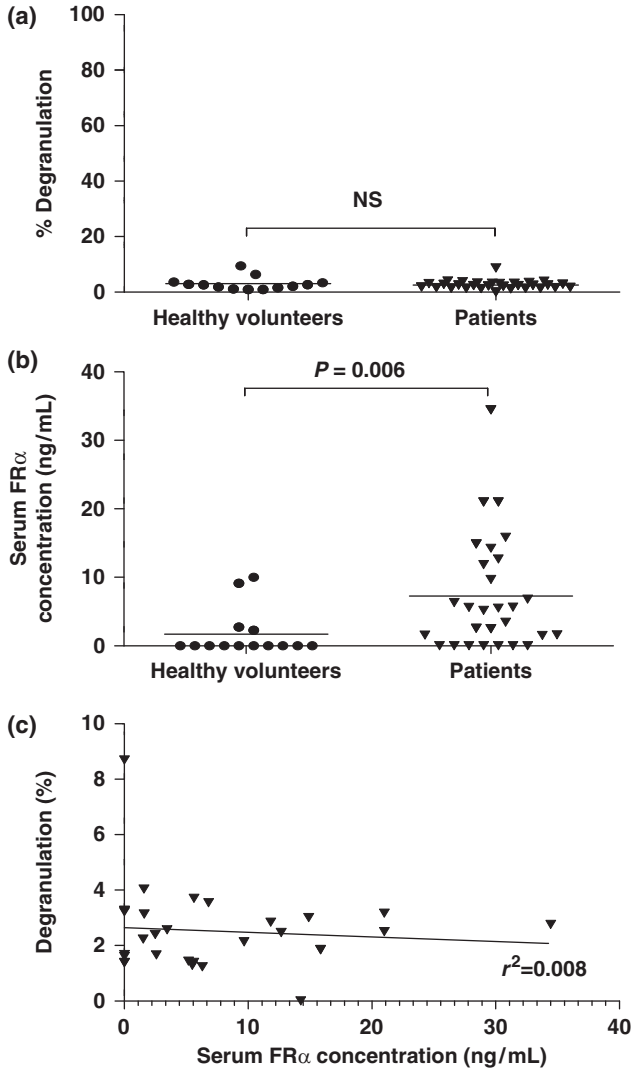

Fig. 2. Sera from ovarian carcinoma patients do not stimulate MOv18 IgE-primed RBL SX-38 cell degranulation despite elevated FRα concentrations. (a) β-hexosaminidase release assays performed with 14 healthy volunteer and 32 ovarian carcinoma patient sera; degranulation was minimal in both groups with no significant differences observed between groups ($P > 0.05$). (b) Serum samples from the above cohort were quantified by ELISA: [FRα] increased in ovarian carcinoma patients compared with healthy volunteers ($P = 0.006$). (c) No correlation ($r^2 = 0.008$) is seen between % degranulation and serum [FRα] in the ovarian carcinoma patient cohort. NS, not significant; FRα, folate receptor α; RBL, rat basophilic leukaemia.

provide increased efficacy compared with IgG-based therapies. However, before this hypothesis can be tested in patients, it is important to demonstrate that this approach is not likely to trigger type I hypersensitivity.

In the present study we made use of the RBL SX-38 cell line to examine human FcεRI-mediated effector activity through recognition of MOv18 IgE and its antigen FRα, excluding variability associated with the use of human mast cells and basophils. These are difficult to obtain in sufficient purity and numbers and have to be stripped of bound endogenous IgE, an aggressive procedure. In contrast, RBL cells express pristine, unoccupied, human tetrameric FcεRI which can be saturated with IgE antibodies of interest. While in theory RBL cells may differ physiologically from human cells, in practise they have shown high sensitivity and specificity for detecting the capacity of various allergens to induce type I hypersensitivity after sensitization by IgE from the serum of allergic human subjects using release of the granule protein β-hexosaminidase as a readout [28, 35, 48, 49].

We have shown that MOv18 IgE in the presence of recombinant FRα antigen does not trigger degranulation in this system, whereas cross-linking of FcεRI with an anti-FcεRI antibody or an antibody recognizing MOv18 IgE-bound FRα on the surface of RBL SX-38 cells does trigger degranulation. These data suggest that once cross-linked, MOv18 IgE-FRα complexes can mediate effector cell activation, while FRα is inactive in its monomeric form. To account for any effects on effector cell activation mediated by circulating FRα antigen released from tumour cells of patients, we measured serum concentrations of FRα by ELISA. In agreement with previous studies [39], we measured increased circulating antigen in patients compared with healthy volunteers. Nevertheless, MOv18 IgE did not trigger degranulation of the readout cells in the presence of sera from either cohort. These findings are consistent with the hypothesis that soluble FRα antigen binds to, but does not cross-link surface-bound MOv18 IgE. The presence of patient serum also takes some account of effects of other circulating agents that may potentially cross-link FcεRI such as endogenous anti-FRα autoantibodies, which we detected in sera of a subset of patients. Nevertheless, our admittedly somewhat limited data so far showed no evidence that these antibodies triggered activation of the relevant readout cells.

In an *ex vivo* setting, MOv18 IgE similarly did not induce early signs of basophil activation in the blood of patients with ovarian carcinoma, even at concentrations of 10 μg/mL, which we estimate as equivalent to a clinical therapeutic dose of 1 mg/kg. Here, we used the BAT tool, an emerging assay which has demonstrated sensitivity and specificity in the clinical diagnosis of type I hypersensitivity to a range of allergens including venom, latex, food allergens and drugs [31]. A caveat with these experiments is that the responder basophil FcεRI receptors are likely to be partly occupied with endogenous IgE *ex vivo*, allowing only partial occupancy by MOv18 IgE. On the other hand, these experiments take further account of any additional factors found in whole blood (but removed in the isolation of serum), that could trigger IgE-mediated basophil activation, such as circulating immune effector cells and, in cancer patients' blood, circulating tumour cells or fragments.

Although quantification of circulating tumour cells in patients with ovarian cancer is not standardized, figures in

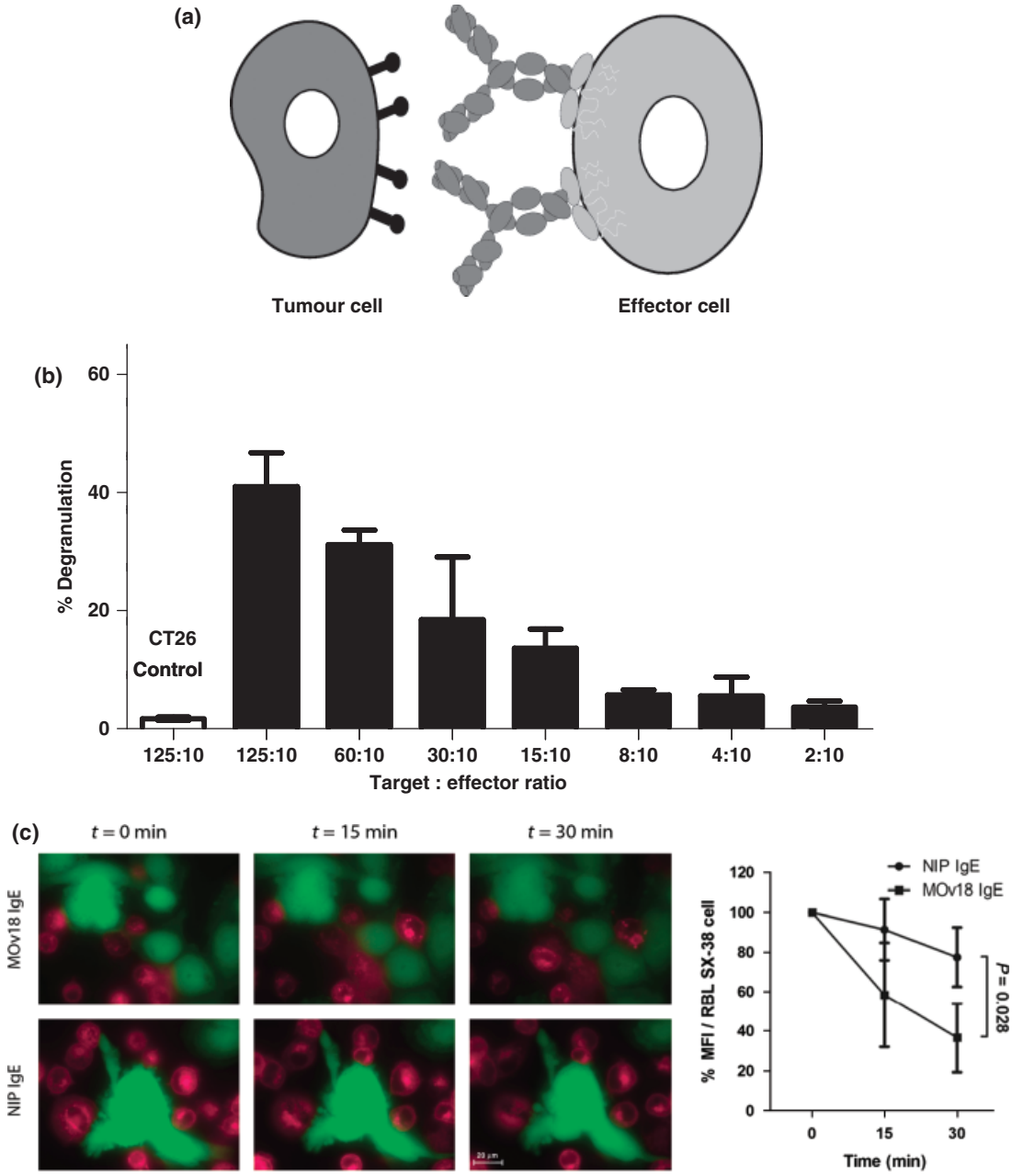

Fig. 3. MOv18 IgE stimulates RBL SX-38 cell degranulation in the presence of increasing numbers of IGROV-1 tumour cells. (a) Schematic diagram of FRα-expressing tumour cell cross-linking FcεRI-bound MOv18 IgE on mast cells. (b) Degranulation of RBL SX-38 mast cells treated with MOv18 IgE in the presence of increasing numbers of IGROV-1 tumour cells. Significant degranulation was detected with increasing Target:Effector cell ratios (> 15 : 10). Minimal degranulation is seen with non-FRα-expressing tumour cells (CT26). Scale bars indicate mean values±standard deviation [38] of $n = 3$ experiments, all conditions were tested in triplicate. (c) Left: Representative images of RBL SX-38 cell (labelled with Cholera Toxin subunit B, red) membrane mobilization in the presence of IGROV-1 tumour cells (labelled with Calcein AM, green) with MOv18 IgE (top panel) or control NIP IgE antibody (bottom panel) following 0, 15 and 30 min at 37 °C (magnification ×63/1.4 oil DIC objective, scale bars: 20 μm). Right: Quantitative assessments of % mean fluorescence intensity (MFI±SD) per cell for Cholera Toxin subunit B-labelled RBL SX-38 cells (red fluorescently labelled cells from left), measured after 15 and 30 min with either MOv18 IgE or control NIP IgE antibodies ($n = 5$), showing reduced % MFI for MOv18 IgE cells ($P = 0.028$), which depicts enhanced membrane mobilization in the presence of antigen-specific antibody and tumour cells. FRα, folate receptor α; RBL, rat basophilic leukaemia.

the range of 0–566 cells/mL have been reported [40, 41, 43–45], except for one report of a patient with as many as 3118 tumour cells/mL [42]. Our data show that even at a tumour cell burden of 4000 cells/mL (a density above any reported in cancer patient blood), MOv18 IgE induced minimal FcεRI-mediated activation of readout cells (Fig. 3), and did not augment CD63 expression on basophils in the patients' whole blood (Fig. 5). It is possible

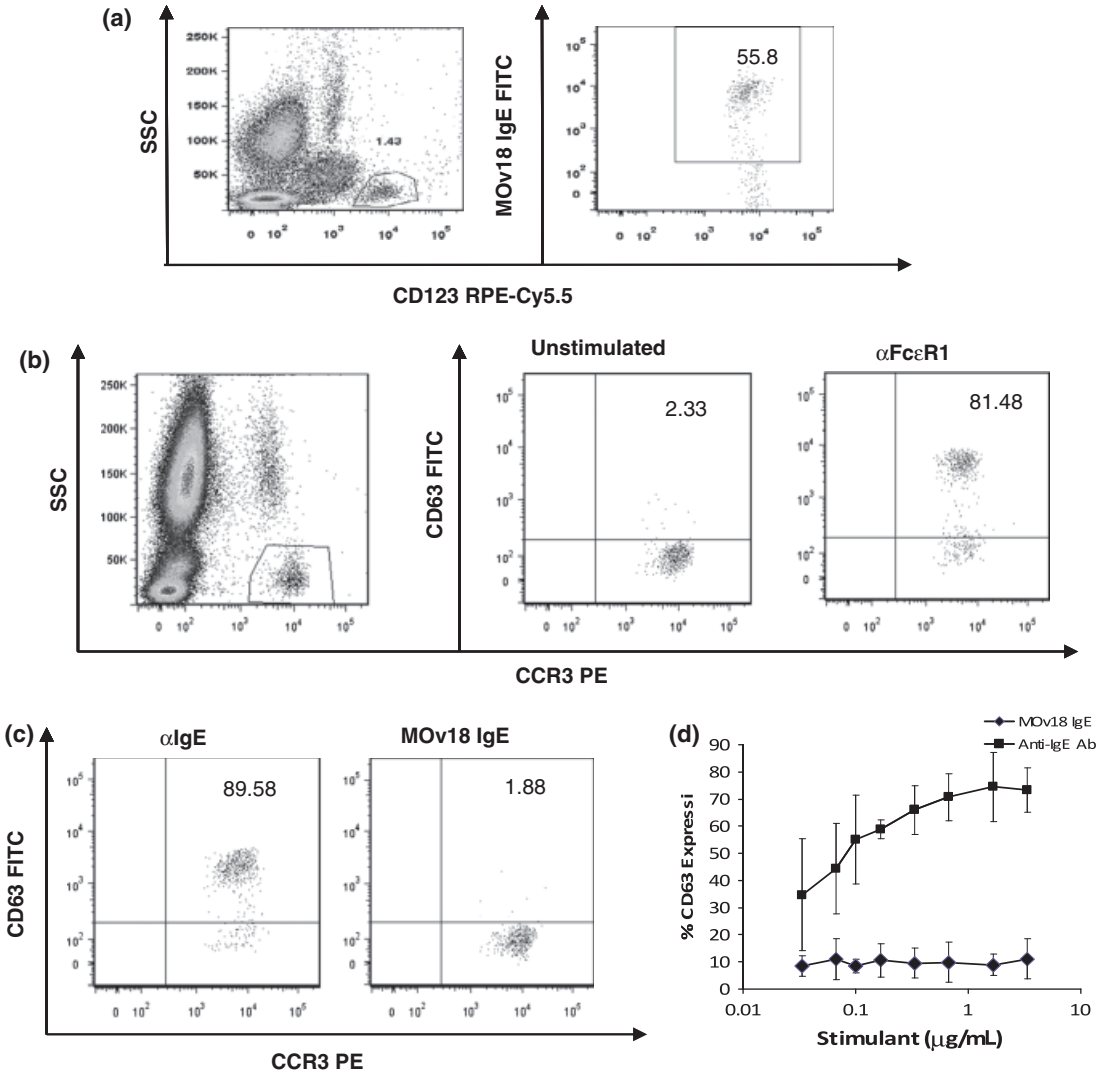

Fig. 4. MOv18 IgE does not trigger CD63 expression in whole human blood. (a) Flow cytometric dot plots identify basophils in whole blood ($CD123^{high}SSC^{low}$, left), and basophils bind MOv18 IgE ($CD123^{high}IgE^{+}$, right). Basophil activation assessments with representative two-colour dot plots of: (b) % $CCR3^{high}SSC^{low}$ basophils (gated, left) expressing CD63 in unstimulated blood ($CCR3^{high}CD63^{+}$, middle), and with anti-FcεRI polyclonal antibody [47]; (c) Increased % $CCR3^{high}CD63^{+}$ basophils with anti-IgE polyclonal antibody (left), but not with MOv18 IgE (0.7 μg/mL, right). (d) % $CCR3^{high}CD63^{+}$ basophils in whole blood titrated with either MOv18 IgE or anti-IgE polyclonal antibody (0.03–3.5 μg/mL). Scale bars indicate mean values±standard deviation [38] of $n = 5$ experiments, all conditions were tested in triplicate.

that, in some MOv18-treated patients antibody-induced tumour cell death could release fragments of tumour cells from lesions that might activate basophils in the periphery. On the other hand our previous studies [2–4] suggest that MOv18 IgE triggers not only cytotoxicity, but also substantial tumour cell infiltration and phago'cytosis by monocytes/macrophages that may limit their escape into the circulation. We will monitor this in patients treated with MOv18 IgE by repeated skin prick and intradermal testing with the antibody before each dosage by monitoring serum concentrations of FRα, β-tryptase and by repeated basophil activation testing with MOv18 in the patient's own whole blood.

At high tumour cell concentrations, where the density of epitope arrayed on the tumour cell surface may stimulate effector cells through IgE cross-linking, we did observe significant FcεRI-mediated activation of readout cells (Fig. 3). We speculate that this may resemble the situation where tumour deposits are infiltrated by effector cells. Infiltration of some tumours by mast cells is well described [20, 21]. This may trigger IgE-specific anti-tumour immune mechanisms in the resident mast cells and possibly infiltrating basophils, as we have previously observed for monocytes and eosinophils [2, 3, 6, 7]. We are aware that a number of studies with other cancers have suggested that the presence of mast cells and other

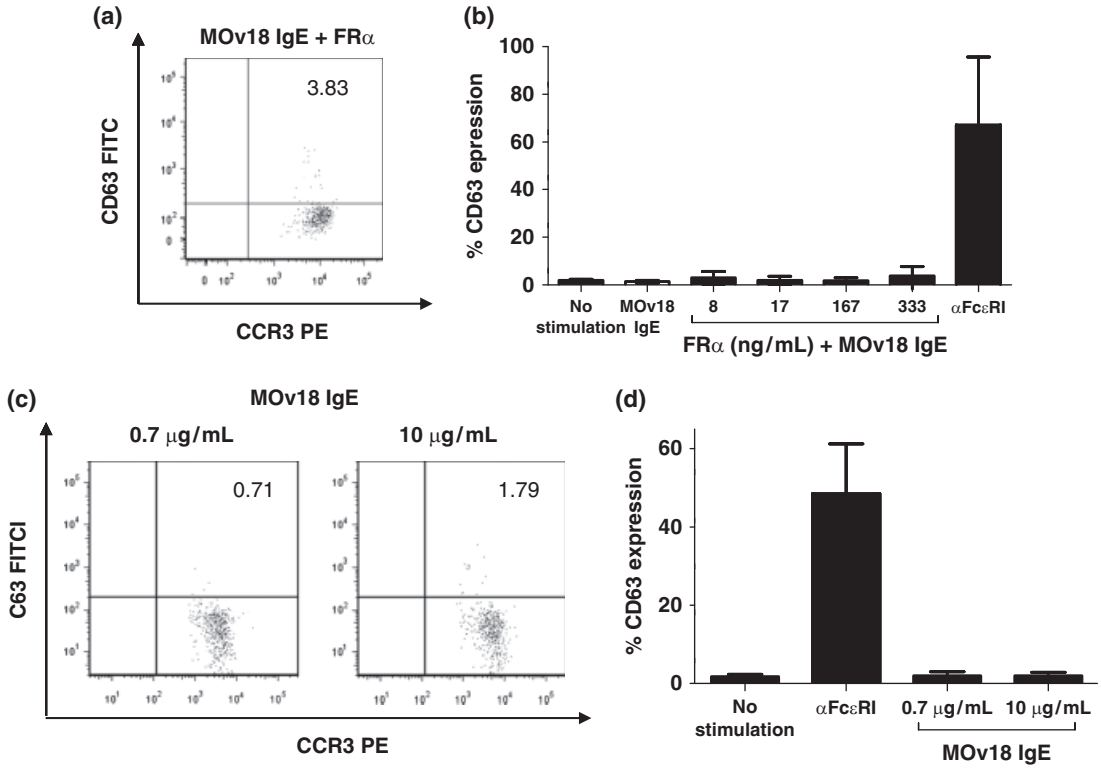

Fig. 5. MOv18 IgE does not trigger CD63 expression by blood basophils in the presence of soluble monomeric antigen or in the blood of patients with ovarian carcinoma. (a) Representative two-colour flow cytometric dot plot of % $CCR3^{high}CD63^{+}$ basophils exposed to MOv18 IgE and human FRα (17 ng/mL) showing background CD63 expression. (b) Basophil activation did not increase in blood from healthy volunteers treated with MOv18 IgE and increasing concentrations of FRα, but efficient activation occurs with anti-FcεRI control. Scale bars indicate mean values±standard deviation [38] of $n = 6$ experiments, all conditions were tested in triplicate. (c) Representative two-colour flow cytometric dot plots of % $CCR3^{high}CD63^{+}$ basophils in patient blood given MOv18 IgE (0.7 and 10 μg/mL). (d) % $CCR3^{high}CD63^{+}$ basophils in blood of a patient cohort ($n = 5$) with detectable serum FRα titre (indicated in Table 1), illustrating background expression with addition of MOv18 IgE compared with anti-FcεRI and no stimulation controls. Scale bars indicate mean values±standard deviation [38] of $n = 5$ experiments, all conditions were tested in triplicate. FRα, folate receptor α.

immune effector cells, such as monocytes, in tumours has been correlated with tumour progression [20, 21], and that activation of mast cells within a tumour mass may at least in theory trigger hypersensitivity *in situ*. Nevertheless the data we have so far concerning the effects of MOv18 IgE on tumour killing and progression in animal models suggest added benefits of MOv18 IgE over IgG antibodies and have not so far produced any evidence whatsoever of systemic adverse effects [2–4, 7].

Although we here report that circulating FRα in patients with ovarian cancer did not activate our readouts of hypersensitivity, another potentially detrimental effect of circulating FRα is that it might bind to MOv18 IgE bound to cytotoxic effector cells, blocking the ability of these cells to recognize tumour cell-associated FRα antigen. Our *in vitro* assays suggest that soluble FRα at 200 ng/mL may saturate cell surface-bound MOv18 IgE on cytotoxic effector cells, but this greatly exceeds concentrations we have so far observed in patients with advanced ovarian carcinoma (Fig. 2). Thus, we would expect that most of the cell-bound MOv18 IgE will be unoccupied and able to bind tumour cell surface-bound FRα in most, but perhaps not in all of the patients. This concern has been examined in the context of treatment with trastuzumab, where some patients with HER2/*neu*+ carcinomas have circulating serum soluble HER2 receptor concentrations exceeding 15 ng/mL, which was postulated potentially to reduce the efficacy of trastuzumab. Clinical experience with trastuzumab has however uncovered no clear correlation between serum HER2 concentrations and clinical responsiveness [50]. We will examine this question in future clinical studies with MOv18 IgE by measuring FcεRI-MOv18 IgE occupancy by circulating FRα on immune effector cells and by correlating serum FRα concentrations with clinical efficacy in dose escalation studies.

Despite being reassured by the fact that patient sera and whole blood did not activate our hypersensitivity readouts in the presence of MOv18 IgE we were intrigued by the possibility that these patients might make IgG autoantibodies against FRα and therefore developed an ELISA assay to measure these. We did indeed detect low concentrations of these autoantibodies in a small subset of our patients. Given, however that blood and sera from a

selection of these same patients did not activate our hypersensitivity readouts, and also the fact that IgG anti-folate receptor autoantibodies at similar or higher titres than those of our patients have been described in normal individuals and patients with a history of neural tube defect pregnancies, infertility and oral cleft defects [51], we are not sure of the pathophysiological significance, if any, of this observation. Obviously, because of the theoretical risk that such antibodies could cross-link MOv18 IgE-bound FRα on cells such as mast cells and basophils, we will be monitoring the prevalence and evolution of these antibodies in treated patients in addition to the precautions referred to above. We will also, as is routine in studies with biologicals, be monitoring possible antibody responses to MOv18 IgE itself.

Systemic anaphylaxis is the most extreme manifestation of FcεRI-mediated type I hypersensitivity. Very little is known about what predisposes IgE-sensitized individuals to systemic anaphylaxis. Conventional wisdom is that systemic anaphylaxis is caused by mast cell mediators because episodes are often accompanied by transient increases in serum histamine and beta-tryptase. There are however cases where histamine alone is elevated, interpreted by some to suggest that anaphylaxis may in some instances be caused primarily by basophil activation [52]. Insofar as no known test can predict or reliably exclude whether IgE-sensitized subjects will have systemic anaphylactic reactions to allergen exposure [53], none of the data described in the present study can address this question, although we find the lack of evidence of FcεRI-mediated effector cell activation in the presence of MOv18 IgE and its target antigen, and also in the presence of autoantibodies recognizing FRα in a subset of patients, very reassuring and sufficiently persuasive to proceed with further toxicity studies and eventual clinical studies of MOv18 therapy for ovarian carcinoma. The encouraging early safety and efficacy reports using the IgG anti-FRα antibody (farletuzumab; MORAb-003) and the chimeric MOv18 IgG1 anti-FRα antibody for ovarian carcinoma provide a strong case that FRα is a valid molecular target [15–17, 38, 54–57]. Our previous demonstration of superior efficacy of the FRα-specific antibody MOv18 IgE in comparison with its chimeric IgG1 counterpart [2, 3, 6, 7] encourages us to continue with our pre-clinical studies which may mark a new era of improved antibody therapy for solid tumours.

Clinical relevance

Despite the clinical successes of monoclonal antibodies in cancer therapy, many solid tumours remain unresponsive to treatment. Using MOv18, an antibody recognizing the tumour antigen FRα, we previously demonstrated that substituting the Fc region of the commonly used IgG antibody class with that of IgE results in superior responses against solid tumours. IgE antibodies play a role in the allergic response and the danger of triggering anaphylaxis during treatment for cancer is not yet fully elucidated. Using two readouts of the potential for type I hypersensitivity, however, we provide initial evaluations supporting the prediction that administration of a tumour antigen-specific IgE in human blood does not induce activation of effector cells that may contribute to the onset of type I hypersensitivity. These preliminary findings contribute to the safety profile of MOv18 IgE before clinical studies, adding weight to the promise of this novel approach.

Acknowledgements

The authors thank Mrs Angela Clifford for recruitment of volunteers and Ms Isabella Tosi for sample provision. We thank all patients and healthy volunteers who participated in this study. This manuscript is dedicated to the memory of Mrs Kate Kirwan. This work was supported by the Department of Health via the National Institute for Health Research (NIHR) comprehensive Biomedical Research Centre award to Guy's and St Thomas' NHS Foundation Trust in partnership with King's College London and King's College Hospital NHS Foundation Trust; Cancer Research UK (C30122/A11527); CR UK/EPSRC/MRC/NIHR KCL/UCL Comprehensive Cancer Imaging Centre (C1519/A10331); KCL Experimental Cancer Medicine Centre, jointly funded by Cancer Research UK, the National Institute for Health Research, Welsh Assembly Government, HSC R&D Office for Northern Ireland and Chief Scientist Office, Scotland; and the Overseas Research Students Award Scheme.

References

1 Weiner LM, Surana R, Wang S. Monoclonal antibodies: versatile platforms for cancer immunotherapy. *Nat Rev Immunol* 2010; **10**:317–27.

2 Karagiannis SN, Wang Q, East N *et al*. Activity of human monocytes in IgE antibody-dependent surveillance and killing of ovarian tumor cells. *Eur J Immunol* 2003; **33**:1030–40.

3 Karagiannis SN, Bracher MG, Hunt J *et al*. IgE-antibody-dependent immunotherapy of solid tumors: cytotoxic and phagocytic mechanisms of eradication of ovarian cancer cells. *J Immunol* 2007; **179**:2832–43.

4 Karagiannis SN, Bracher MG, Beavil RL *et al*. Role of IgE receptors in IgE antibody-dependent cytotoxicity and phagocytosis of ovarian tumor cells by human monocytic cells. *Cancer Immunol Immunother* 2008; **57**:247–63.

5 Karagiannis SN, Nestle FO, Gould HJ. IgE interacts with potent effector cells against tumours: ADCC and ADCP. In:

Penichet ML, Jensen-Jarolim E, eds. *Cancer and IgE: introducing the concept of allergooncology.* Berlin: Springer, 2010; 185–213.
6 Karagiannis P, Singer J, Hunt J *et al.* Characterisation of an engineered trastuzumab IgE antibody and effector cell mechanisms targeting HER2/neu-positive tumour cells. *Cancer Immunol Immunother* 2009; **58**:915–30.
7 Gould HJ, Mackay GA, Karagiannis SN *et al.* Comparison of IgE and IgG antibody-dependent cytotoxicity in vitro and in a SCID mouse xenograft model of ovarian carcinoma. *Eur J Immunol* 1999; **29**:3527–37.
8 Gould HJ, Sutton BJ, Beavil AJ *et al.* The biology of IGE and the basis of allergic disease. *Annu Rev Immunol* 2003; **21**: 579–628.
9 Gould HJ, Sutton BJ. IgE in allergy and asthma today. *Nat Rev Immunol* 2008; **8**:205–17.
10 Jensen-Jarolim E, Achatz G, Turner MC *et al.* AllergoOncology: the role of IgE-mediated allergy in cancer. *Allergy* 2008; **63**:1255–66.
11 Nigro EA, Brini AT, Soprana E *et al.* Antitumor IgE adjuvanticity: key role of Fc epsilon RI. *J Immunol* 2009; **183**: 4530–6.
12 Teng MW, Kershaw MH, Jackson JT, Smyth MJ, Darcy PK. Adoptive transfer of chimeric FcepsilonRI gene-modified human T cells for cancer immunotherapy. *Hum Gene Ther* 2006; **17**:1134–43.
13 Riemer AB, Untersmayr E, Knittelfelder R *et al.* Active induction of tumor-specific IgE antibodies by oral mimotope vaccination. *Cancer Res* 2007; **67**: 3406–11.
14 Reali E, Greiner JW, Corti A *et al.* IgEs targeted on tumor cells: therapeutic activity and potential in the design of tumor vaccines. *Cancer Res* 2001; **61**: 5517–22.
15 White AJ, Coleman RL, Armstrong DK, Glenn D. *et al.* Efficacy and safety of farletuzumab, a humanized monoclonal antibody to folate receptor alpha, in platinum-sensitive relapsed ovarian cancer subjects: final data from a multicenter phase II study. *J Clin Oncol* 2010; **28** (Suppl.); abstract 5001.
16 Molthoff CF, Prinssen HM, Kenemans P, van Hof AC, den Hollander W, Verheijen RH. Escalating protein doses of chimeric monoclonal antibody MOv18 immunoglobulin G in ovarian carcinoma patients: a phase I study. *Cancer* 1997; **80**:2712–20.
17 Macor P, Mezzanzanica D, Cossetti C *et al.* Complement activated by chimeric anti-folate receptor antibodies is an efficient effector system to control ovarian carcinoma. *Cancer Res* 2006; **66**: 3876–83.
18 Toffoli G, Russo A, Gallo A *et al.* Expression of folate binding protein as a prognostic factor for response to platinum-containing chemotherapy and survival in human ovarian cancer. *Int J Cancer* 1998; **79**:121–6.
19 Weitman SD, Weinberg AG, Coney LR, Zurawski VR, Jennings DS, Kamen BA. Cellular localization of the folate receptor: potential role in drug toxicity and folate homeostasis. *Cancer Res* 1992; **52**:6708–11.
20 Amini RM, Aaltonen K, Nevanlinna H *et al.* Mast cells and eosinophils in invasive breast carcinoma. *BMC Cancer* 2007; **7**:165.
21 Ch'ng S, Wallis RA, Yuan L, Davis PF, Tan ST. Mast cells and cutaneous malignancies. *Mod Pathol* 2006; **19**:149–59.
22 Wasiuk A, de Vries VC, Nowak EC, Noelle RJ. Mast cells in allergy and tumour disease. In: Penichet ML, Jensen-Jarolim E, eds. *Cancer and IgE: introducing the concept of allergooncology.* Berlin: Springer, 2010; 137–58.
23 Christensen LH, Holm J, Lund G, Riise E, Lund K. Several distinct properties of the IgE repertoire determine effector cell degranulation in response to allergen challenge. *J Allergy Clin Immunol* 2008; **122**:298–304.
24 Valenta R, Ferreira F, Focke-Tejkl M *et al.* From allergen genes to allergy vaccines. *Annu Rev Immunol* 2010; **28**:211–41.
25 Figini M, Martin F, Ferri R *et al.* Conversion of murine antibodies to human antibodies and their optimization for ovarian cancer therapy targeted to the folate receptor. *Cancer Immunol Immunother* 2009; **58**:531–46.
26 Luhrs CA, Pitiranggon P, da Costa M *et al.* Purified membrane and soluble folate binding proteins from cultured KB cells have similar amino acid compositions and molecular weights but differ in fatty acid acylation. *Proc Natl Acad Sci USA* 1987; **84**:6546–9.
27 Berek J, Taylor P, McGuire W, Smith LM, Schultes B, Nicodemus CF. Oregovomab maintenance monoimmunotherapy does not improve outcomes in advanced ovarian cancer. *J Clin Oncol* 2009; **27**:418–25.
28 Dibbern DA Jr, Palmer GW, Williams PB, Bock SA, Dreskin SC. RBL cells expressing human Fc epsilon RI are a sensitive tool for exploring functional IgE-allergen interactions: studies with sera from peanut-sensitive patients. *J Immunol Methods* 2003; **274**:37–45.
29 Wiegand TW, Williams PB, Dreskin SC, Jouvin MH, Kinet JP, Tasset D. High-affinity oligonucleotide ligands to human IgE inhibit binding to Fc epsilon receptor I. *J Immunol* 1996; **157**:221–30.
30 Karagiannis SN, Warrack JK, Jennings KH *et al.* Endocytosis and recycling of the complex between CD23 and HLA-DR in human B cells. *Immunology* 2001; **103**:319–31.
31 De Week AL, Sanz ML, Gamboa PM *et al.* Diagnostic tests based on human basophils: more potentials and perspectives than pitfalls. II. Technical issues. *J Investig Allergol Clin Immunol* 2008; **18**:143–55.
32 Boumiza R, Debard AL, Monneret G. The basophil activation test by flow cytometry: recent developments in clinical studies, standardization and emerging perspectives. *Clin Mol Allergy* 2005; **3**:9.
33 Naal RM, Holowka EP, Baird B, Holowka D. Antigen-stimulated trafficking from the recycling compartment to the plasma membrane in RBL mast cells. *Traffic* 2003; **4**:190–200.
34 Lisboa FA, Peng Z, Combs CA, Beaven MA. Phospholipase d promotes lipid microdomain-associated signaling events in mast cells. *J Immunol* 2009; **183**: 5104–12.
35 Bodinier M, Brossard C, Triballeau S *et al.* Evaluation of an in vitro mast cell degranulation test in the context of food allergy to wheat. *Int Arch Allergy Immunol* 2008; **146**:307–20.
36 Nakamura R, Uchida Y, Higuchi M, Tsuge I, Urisu A, Teshima R. A convenient and sensitive allergy test: IgE cross-linking-induced luciferase expression in cultured mast cells. *Allergy* 2010; **65**: 1266–73.
37 Knol EF. Requirements for effective IgE cross-linking on mast cells and basophils. *Mol Nutr Food Res* 2006; **50**:620–4.
38 van Zanten-Przybysz I, Molthoff C, Gebbinck JK *et al.* Cellular and humoral responses after multiple injections of unconjugated chimeric monoclonal antibody MOv18 in ovarian cancer

patients: a pilot study. *J Cancer Res Clin Oncol* 2002; **128**:484–92.
39 Basal E, Eghbali-Fatourechi GZ, Kalli KR *et al*. Functional folate receptor alpha is elevated in the blood of ovarian cancer patients. *PLoS One* 2009; **4**:e6292.
40 Ntouroupi TG, Ashraf SQ, McGregor SB *et al*. Detection of circulating tumour cells in peripheral blood with an automated scanning fluorescence microscope. *Br J Cancer* 2008; **99**:789–95.
41 Fan T, Zhao Q, Chen JJ, Chen WT, Pearl ML. Clinical significance of circulating tumor cells detected by an invasion assay in peripheral blood of patients with ovarian cancer. *Gynecol Oncol* 2009; **112**:185–91.
42 He W, Kularatne SA, Kalli KR *et al*. Quantitation of circulating tumor cells in blood samples from ovarian and prostate cancer patients using tumor-specific fluorescent ligands. *Int J Cancer* 2008; **123**:1968–73.
43 He W, Wang H, Hartmann LC, Cheng JX, Low PS. In vivo quantitation of rare circulating tumor cells by multiphoton intravital flow cytometry. *Proc Natl Acad Sci USA* 2007; **104**:11760–5.
44 Poveda A, Kaye SB, McCoramck RT, Wang S *et al*. Circulating tumour cells in a study of relapsed/recurrent advanced ovarian cancer: an exploratory analysis in the ova-301 phase III study of pegylated liposimal doxorubicin (PLD) compared with trabectadin and PLD. *J Clin Oncol* 2009; **27**: abstract 5551.
45 Kindelberger DDK, Kantoff E, Atkinson T *et al*. Predictive value of circulating tumour cells for response to therapy in women with recurrent epithelial ovarian cancer. *J Clin Oncol* 2010; **28**: abstract 5111.
46 Metzelaar MJ, Wijngaard PL, Peters PJ, Sixma JJ, Nieuwenhuis HK, Clevers HC. CD63 antigen. A novel lysosomal membrane glycoprotein, cloned by a screening procedure for intracellular antigens in eukaryotic cells. *J Biol Chem* 1991; **266**:3239–45.
47 Weisberg E, Manley PW, Breitenstein W *et al*. Characterization of AMN107, a selective inhibitor of native and mutant Bcr-Abl. *Cancer Cell* 2005; **7**:129–41.
48 Porterfield HS, Murray KS, Schlichting DG *et al*. Effector activity of peanut allergens: a critical role for Ara h 2, Ara h 6, and their variants. *Clin Exp Allergy* 2009; **39**:1099–108.
49 Blanc F, Adel-Patient K, Drumare MF, Paty E, Wal JM, Bernard H. Capacity of purified peanut allergens to induce degranulation in a functional in vitro assay: Ara h 2 and Ara h 6 are the most efficient elicitors. *Clin Exp Allergy* 2009; **39**:1277–85.
50 Lennon S, Barton C, Banken L *et al*. Utility of serum HER2 extracellular domain assessment in clinical decision making: pooled analysis of four trials of trastuzumab in metastatic breast cancer. *J Clin Oncol* 2009; **27**:1685–93.
51 Molloy AM, Quadros EV, Sequeira JM *et al*. Lack of association between folate-receptor autoantibodies and neural-tube defects. *N Engl J Med* 2009; **361**:152–60.
52 Lin RY, Schwartz LB, Curry A *et al*. Histamine and tryptase levels in patients with acute allergic reactions: an emergency department-based study. *J Allergy Clin Immunol* 2000; **106**:65–71.
53 Simons FE, Frew AJ, Ansotegui IJ *et al*. Risk assessment in anaphylaxis: current and future approaches. *J Allergy Clin Immunol* 2007; **120**:S2–S24.
54 Elit L, Konner JA, Armstrong DK, Buck M. *et al*. A randomized, double-blind, placebo-controlled phase II study of the efficacy and safety of farletuzumab (MORAb-003) in combination with weekly paclitaxel in subjects with platinum-resistant or refractory relapsed ovarian cancer. *J Clin Oncol* 2010; **28**: TPS255.
55 Konner JA, Bell-McGuinn KM, Sabbatini P *et al*. Farletuzumab, a humanized monoclonal antibody against folate receptor alpha, in epithelial ovarian cancer: a phase I study. *Clin Cancer Res* 2010; **16**:5288–95.
56 Zacchetti A, Coliva A, Luison E *et al*. (177)Lu- labeled MOv18 as compared to (131)I- or (90)Y-labeled MOv18 has the better therapeutic effect in eradication of alpha folate receptor-expressing tumor xenografts. *Nucl Med Biol* 2009; **36**: 759–70.
57 van Zanten-Przybysz I, Molthoff CF, Roos JC *et al*. Influence of the route of administration on targeting of ovarian cancer with the chimeric monoclonal antibody MOv18: i.v. vs. i.p.. *Int J Cancer* 2001; **92**:106–14.

Supporting Information

Additional Supporting Information may be found in the online version of this article:

Figure S1. Two-colour flow cytometric dot plots depicting % $CCR3^{high}$ basophils expressing CD63 in whole blood of patients with ovarian carcinoma. Examples of dot plots of % $CCR3^{high}CD63^{+}$ events in unstimulated blood (a), and in the presence of polyclonal α-FcεRI (b) and α-IgE (c) antibodies.

Table S1. Projected % effector cell degranulation in the presence of tumour cells and IgE, based on reports of circulating tumor cell quantification in the sera of ovarian cancer patients. Calculations were projected from % degranulation measurements in Fig. 3b.

Table S2. Levels of anti-FRα IgG auto-antibodies detected by ELISA in sera from 6 ovarian carcinoma patients from a 24 cohort with detectable circulating FRα. Measurements of % cell degranulation (shown in Table 1) and % basophils expressing CD63 (basophil activation tests in Fig. 5) in the presence of MOv18 IgE are from samples shown in Table 1.

Please note: Wiley-Blackwell is not responsible for the content or functionality of any supporting materials supplied by the authors. Any queries (other than missing material) should be directed to the corresponding author for the article.

OPEN ACCESS Freely available online

PLoS one

Monitoring the Systemic Human Memory B Cell Compartment of Melanoma Patients for Anti-Tumor IgG Antibodies

Amy E. Gilbert[1], Panagiotis Karagiannis[1], Tihomir Dodev[2], Alexander Koers[3], Katie Lacy[1], Debra H. Josephs[1], Pooja Takhar[2], Jenny L. C. Geh[4], Ciaran Healy[4], Mark Harries[5], Katharine M. Acland[4], Sarah M. Rudman[6], Rebecca L. Beavil[2], Philip J. Blower[3], Andrew J. Beavil[2], Hannah J. Gould[2], James Spicer[6], Frank O. Nestle[1]*, Sophia N. Karagiannis[1]*

1 Cutaneous Medicine and Immunotherapy Unit, Division of Genetics and Molecular Medicine, NIHR Biomedical Research Centre at Guy's and St. Thomas's Hospitals and King's College London, King's College London School of Medicine, St. John's Institute of Dermatology, Guy's Hospital, King's College London, London, United Kingdom, **2** Randall Division of Cell and Molecular Biophysics and Division of Asthma, Allergy and Lung Biology, MRC and Asthma UK Centre for Allergic Mechanisms of Asthma, King's College London, London, United Kingdom, **3** Division of Imaging Sciences, King's College London School of Medicine, Rayne Institute, St. Thomas's Hospital, King's College London, London, United Kingdom, **4** Skin Tumour Unit, Guy's and St. Thomas's NHS Trust, St. John's Institute of Dermatology, Guy's Hospital, London, United Kingdom, **5** Clinical Oncology, Guy's and St. Thomas's NHS Foundation Trust, London, United Kingdom, **6** Division of Cancer Studies, Department of Academic Oncology, King's College London, Guy's Hospital, London, United Kingdom

Abstract

Melanoma, a potentially lethal skin cancer, is widely thought to be immunogenic in nature. While there has been much focus on T cell-mediated immune responses, limited knowledge exists on the role of mature B cells. We describe an approach, including a cell-based ELISA, to evaluate mature IgG antibody responses to melanoma from human peripheral blood B cells. We observed a significant increase in antibody responses from melanoma patients (n = 10) to primary and metastatic melanoma cells compared to healthy volunteers (n = 10) ($P<0.0001$). Interestingly, we detected a significant reduction in antibody responses to melanoma with advancing disease stage in our patient cohort (n = 21) ($P<0.0001$). Overall, 28% of melanoma patient-derived B cell cultures (n = 1,800) compared to 2% of cultures from healthy controls (n = 600) produced antibodies that recognized melanoma cells. Lastly, a patient-derived melanoma-specific monoclonal antibody was selected for further study. This antibody effectively killed melanoma cells *in vitro* via antibody-mediated cellular cytotoxicity. These data demonstrate the presence of a mature systemic B cell response in melanoma patients, which is reduced with disease progression, adding to previous reports of tumor-reactive antibodies in patient sera, and suggesting the merit of future work to elucidate the clinical relevance of activating humoral immune responses to cancer.

Citation: Gilbert AE, Karagiannis P, Dodev T, Koers A, Lacy K, et al. (2011) Monitoring the Systemic Human Memory B Cell Compartment of Melanoma Patients for Anti-Tumor IgG Antibodies. PLoS ONE 6(4): e19330. doi:10.1371/journal.pone.0019330

Editor: Shan Lu, University of Massachusetts Medical Center, United States of America

Received January 29, 2011; **Accepted** March 26, 2011; **Published** April 29, 2011

Funding: This work was supported by the Department of Health via the National Institute for Health Research (NIHR) comprehensive Biomedical Research Centre award to Guy's, and St. Thomas's NHS Foundation Trust in partnership with King's College London and King's College Hospital NHS Foundation Trust, UK (AEG, PK, TD, AK, KL, PT, FON, SNK) (http://www.guysandstthomas.nhs.uk/healthprof/researchanddevelopment/biomedicalresearch/biomedhome.aspx); CR UK/EPSRC/MRC/NIHR KCL/UCL Comprehensive Cancer Imaging Centre (C1519/A10331) (DHJ, PJB, JS, SNK) (http://www.cancerimagingcentre.org.uk/); Cancer Research UK (C30122/A11527) (DHJ) (http://www.cancerresearchuk.org/); Mary Dunhill Trust (FON) (http://www.dunhillmedical.org.uk/page_viewer.asp?page = welcome&pid = 8); CR UK/NIHR in England/DoH for Scotland, Wales and Northern Ireland Experimental Cancer Medicine Centre (FON) (http://www.ecmcnetwork.org.uk/network-centres/london-kcl/); and the Overseas Research Students Award Scheme (AEG) (http://www.orsas.ac.uk/). The funders had no role in study design, data collection, analysis, decision to publish, or preparation of the manuscript.

Competing Interests: The authors have declared that no competing interests exist.

* E-mail: sophia.karagiannis@kcl.ac.uk (SNK); frank.nestle@kcl.ac.uk (FON)

Introduction

Malignant melanoma, the most fatal form of skin cancer, arises from malignantly-transformed melanocytes in the basal layer of the epidermis. The incidence of melanoma has been increasing at an accelerated rate in the past few decades amongst fair skinned populations [1] and advanced forms of the disease are highly resistant to treatment [2,3]. Thus, an urgent need exists for novel therapies and earlier diagnosis.

Melanoma is widely thought to be immunogenic, supported by clinical observations such as the frequency of spontaneous tumor regressions, the prevalence of melanoma in immunosuppressed patients, and the partial success of clinically-available immune modulatory therapies such as the polyclonal immune activating cytokines IFNα-2b and IL- 2 [4,5,6,7]. Host adaptive immune responses have been described in melanoma with a main focus on melanoma specific T cell responses [8,9], and supported by successful case scenarios using immunotherapeutic strategies such as dendritic cell vaccines, adoptive T cell therapies, and CTLA4 monoclonal antibodies [7,10,11,12,13].

Limited research has focused on B cells and the specificity of antibodies they produce in cancer. Promotion of cancer development by the creation of a pro-inflammatory environment [14,15] and anti-tumor functions by activating mature T cell

responses [16] have been proposed as potential roles for B cells in animal models of cancer. While there may be host immune responses to malignancy following immunization [17], a variety of mechanisms involved in tumor escape have been described and understanding this complex relationship between immunosurveillance and tumor escape in patients is key to the design of effective immunotherapies [18,19,20,21].

Despite well-characterized tumor-induced immunomodulation, immunotherapies such as monoclonal antibodies are emerging as key diagnostic and therapeutic modalities and are now standard of care for the treatment of various cancers. Antibodies for the treatment of melanoma aimed at enhancing key pathways of T cell activation (Cytotoxic T Lymphocyte-Associated Antigen 4, e.g. Ipilimumab), targeting tumor vasculature (e.g. Bevacizumab), or tumor-associated antigens (e.g. High Molecular Weight-Melanoma Associated Antigen, HMW-MAA) have demonstrated promise in clinical studies [13,22,23,24]. Antibodies therefore represent an attractive approach for the treatment of melanoma.

Reports of tumor-specific antibodies in the sera of melanoma patients date back over forty years [25] and have so far provided valuable insight into immune responses to cancer. Serological studies of individuals with melanoma have shown that patients expressing certain tumor-associated antigens have antibodies against these antigens, conversely, patients without the antibodies also lack the corresponding tumor antigens [26]. These studies have been restricted to few antibodies in sera against known tumor-associated antigens. Serological studies reported IgG antibodies recognizing intracellular melanocyte and melanoma-associated antigens such as tyrosinase, tyrosinase-related protein (TRP)-1, TRP-2, and melanoma-associated glycoprotein antigen family (gp100/pmel17) in patients with melanoma. Serum-resident antibodies to some of these antigens were enhanced following polyvalent melanoma cell vaccine immunization in patients with melanoma, suggesting that melanoma-associated antigens may be immunogenic and that humoral responses to melanocyte and melanoma antigens may constitute potential targets for immunotherapy [27]. New antigens, such as the NY-ESO-1, with restricted expression in normal tissues and wide distribution in various cancers including melanoma have been discovered using serological analysis of recombinant cDNA expression libraries (SEREX) techniques tested against tumor mRNA and autologous patient sera [28]. SEREX studies from human melanomas [29] and from one cell line [30] have led to the discovery of the human testis antigen HOM-MEL-40. Many of these antigens are primarily intracellular, making them less attractive targets as monoclonal antibodies. Furthermore, serological screens may also be limited by the temporal dynamics of sera antibodies. Evaluating the reactivity of antibodies secreted by circulating B cells may therefore provide additional insight to serological evaluations by interrogating the long-term memory anti-tumor systemic mature humoral response to cancer.

The production of tumor-specific antibodies in melanoma from patient-derived B cells in the peripheral blood and tumors has been reported and has yielded a few antibodies of the IgM and IgG class [31,32,33,34]. In the past, such studies have been limited by poor EBV transformation efficiency of human B cells, low production of immunoglobulin, evaluation of few patients, and lack of effective, reproducible methods to rapidly screen for tumor-specific antibodies. To address some of these limitations, we took advantage of recent advances in growing and immortalizing memory B cells in culture [35,36], increased the number of patients evaluated, and developed a novel screening tool to specifically detect tumor-reactive antibodies against cell surface antigens on melanoma cells. Our approach entails culture of patient-derived circulating B cells and screening of the antibodies they secrete for their reactivity and specificity to melanoma cells versus melanocytes. Our strategy does not screen for antibodies against known antigens or evaluate antibodies secreted or sequestered in the serum at discrete times, but rather uniquely, the aim here is to monitor tumor cell-reactive IgG antibodies produced by B cell cultures, elucidating the breadth of the long-term mature B cell repertoire recognizing melanoma antigens expressed on the surface of cancer cells.

In this study, we screen for tumor-reactive and tumor-specific IgG antibodies produced by patient and healthy individual B cell cultures. This allowed characterization, beyond phenotype, of the circulating B cell repertoire of individuals with melanoma and clinical correlations of mature humoral responses and disease progression. We also provide an example demonstrating that this screen may facilitate the identification of antibodies able to target cancer cells.

Results

Detection of Tumor-specific IgG Antibodies Using a Novel Cell-based ELISA

We developed and optimized a cell-based ELISA for specific detection of tumor-reactive antibodies in order to obtain a robust and optimized system for the detection of anti-tumor antibodies from patients (Figure S1). We first evaluated the sensitivity and specificity of an IgG antibody against a melanoma cell surface antigen (HMW-MAA), expressed on A-375 melanoma cells using immunocytochemistry (cytospins) and live cell flow cytometry. An anti-HMW-MAA antibody was observed to bind to A-375 cells, but not melanocytes over a range of concentrations as low as 20 ng/mL using both immunocytochemistry (Figure 1, A) and flow cytometry (Figure 1, B). Next, we compared the detection of this antibody bound to melanoma cells in our cell-based ELISA to the above methods.

Utilizing our novel ELISA, we detected tumor-specific antibodies at concentrations as low 10 ng/mL (Figure 1, C), demonstrating comparable sensitivity to flow cytometric or immunocytochemical methods. Additionally, we validated our ability to identify tumor-reactive antibodies from our patient cultures, compared to equal amounts of non-specific IgG and culture media (Figure 1, D). We also examined the potential applicability of this method to identify tumor-specific antibodies in other cancers using the mammary carcinoma cell line SK-BR-3, which highly expresses the cell surface tumor-associated antigen HER2/*neu* [37]. Trastuzumab (Herceptin^{TM}), a humanized antibody specific for HER2/*neu*, was specifically detected compared to an equal amount of a control IgG employing our method (Figure 1, D). Thus, we demonstrate that we can detect antibodies against tumor cell antigens in a sensitive, specific and reproducible manner.

Melanoma-reactive Antibodies are More Prevalent in Melanoma Patients than Healthy Volunteers

We first established B cell cultures from the peripheral blood of melanoma patients to study antibody responses to cancer (Figure S1). In agreement with a previously published report, we detected a reduced memory B cell subset in melanoma patients. Melanoma patient and healthy volunteer B cells were cultured with B cell purity greater than 90%. Following EBV transformation and activation with a TLR9 agonist, patient B cells were observed to proliferate in culture for over eight weeks and 80% of the cells in these cultures were IgG positive. B cell cultures derived from healthy volunteers (n = 5) and melanoma patients (n = 5) had

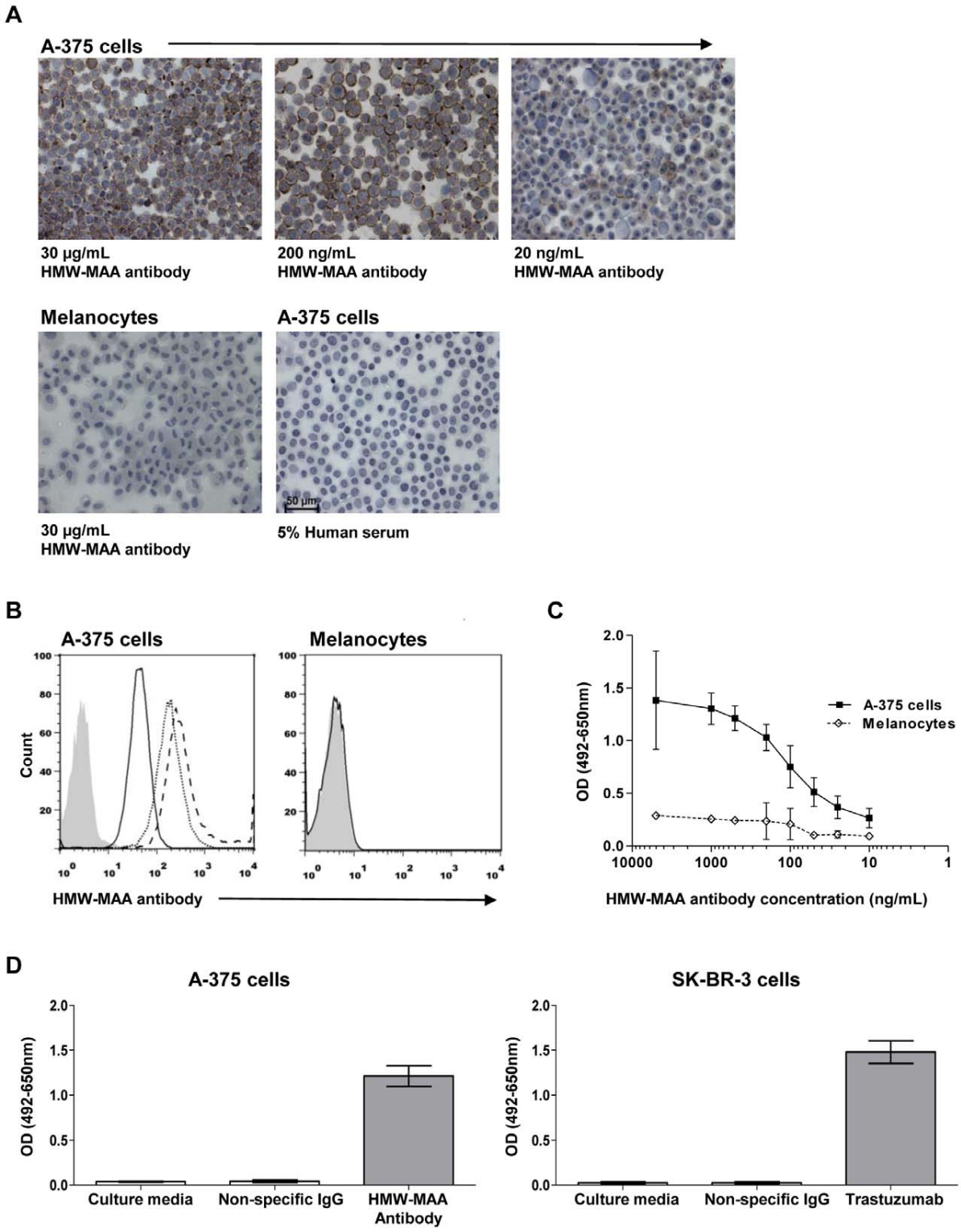

Figure 1. Development of a cell-based ELISA to detect tumor-specific antibodies. (**A**) Immunocytochemistry of cytospin preparations demonstrates that an antibody against the melanoma-associated antigen HMW-MAA, expressed on the surface of A-375 metastatic melanoma cells, can detect the antigen at 30 µg/mL (top left), 200 ng/mL (top middle) and 20 ng/mL (top right), while no binding to melanocytes was seen (bottom left). IgG from 5% human serum (bottom right) did not bind to A-375 cells. (**B**) Flow cytometry analysis demonstrates specific binding of the HMW-MAA antibody to A-375 cells (left) at 30 µg/mL (dashed line), 200 ng/mL (dotted line) and 20 ng/mL (solid line), but not to melanocytes (30 µg/mL HMW-MAA antibody). Isotype control is shown in shaded grey histogram. (**C**) Detection of anti-HMW-MAA antibody binding to melanoma cells over a range of antibody concentrations compared to melanocytes by cell-based ELISA. (**D**) Melanoma-specific antibody HMW-MAA binding to A-375 cells compared to an IgG isotype control or to culture media (left) utilizing the cell-based ELISA. Breast cancer-specific antibody Trastuzumab binding to SK_BR-3 cells compared to an IgG isotype control or to culture media (right). Error bars in figures represent 95% confidence intervals.
doi:10.1371/journal.pone.0019330.g001

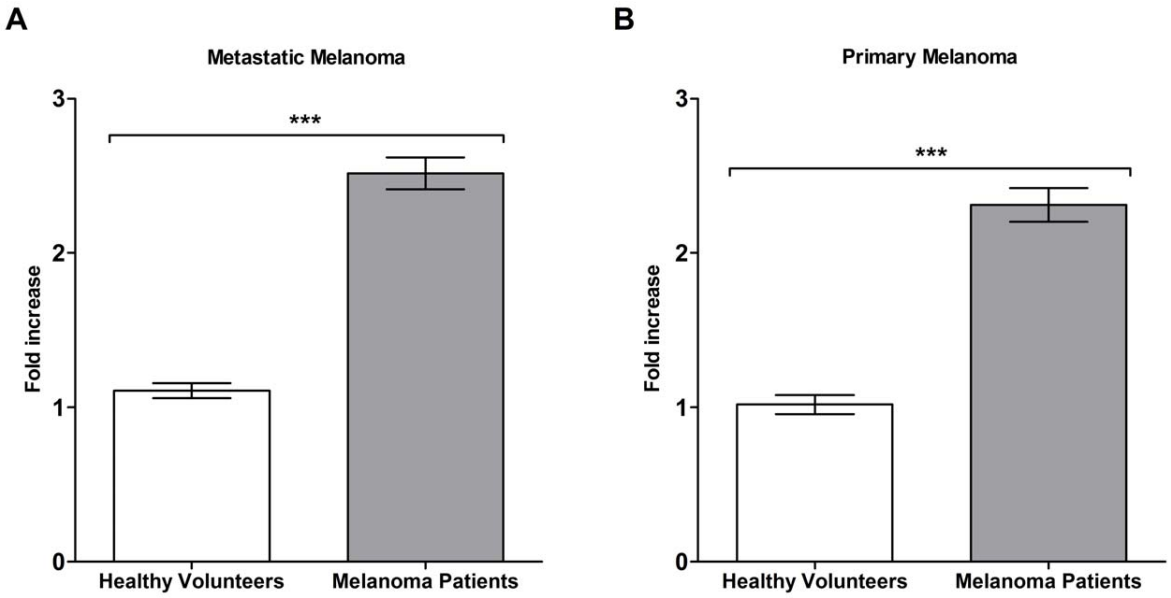

Figure 2. The reactivity of antibodies derived from melanoma patient B cells to primary and metastatic melanoma cells is compared to healthy volunteers. B cell cultures from melanoma patients secreted antibodies that were significantly more reactive against melanoma cell lines compared to healthy volunteers using the cell-based ELISA. Mean reactivity of antibody cultures (n = 600) from 10 melanoma patients to A-375 metastatic melanoma cells (A) and WM-115 primary melanoma cells (B), was compared to 10 healthy volunteer cultures (n = 600) ($P < 0.0001$). Fold increase values represent the optical density of each B cell culture relative to the mean optical density of a negative control human IgG antibody. *** = $P < 0.001$. Error bars in figures represent 95% confidence intervals.
doi:10.1371/journal.pone.0019330.g002

comparable mean antibody titers after 18 days, ranging from 1 to 7 μg from each individual, with an overall mean of 2.5 μg (95% CI = 2.3 to 2.7) per culture arising from 500 B cells per well. We therefore established antibody-secreting cultures from melanoma patients with comparable rates of IgG secretion to healthy volunteers.

We next investigated whether specific antibody responses to melanoma could be detected from circulating B cells of patients and healthy volunteers utilizing our cell-based ELISA. Antibody-secreting B cell cultures from 10 healthy volunteers and 10 patients (n = 4 stage II, n = 4 stage III, and n = 2 stage IV) were evaluated for reactivity to both metastatic and primary melanoma cells relative to non-specific human IgG control (calculated as fold increase above the non-specific human IgG control) employing our cell-based ELISA. We found a significant ($P<0.0001$) increase in the mean reactivity (fold increase) of patient-derived antibody cultures (n = 600) to metastatic melanoma cells (2.5 fold increase, 95% CI = 2.4 to 2.6) compared to antibody cultures (n = 600) derived from healthy volunteers (1.1 fold increase, 95% CI = 1.1 to 1.2) (Figure 2, A). A significant ($P<0.0001$) increase was also seen in the mean reactivity of patient-derived antibodies to primary melanoma cells (2.3 fold increase, 95% CI = 2.2 to 2.4) compared to antibodies from healthy volunteers (1.0 fold increase, 95% CI = 1.0 to 1.1) (Figure 2, B). From this patient cohort, we thus observed a significantly increased reactivity to primary and metastatic melanoma cells, compared to healthy volunteers.

Antibody Response to Melanoma Decreases with Disease Progression

To examine if antibody responses differ according to disease stage, we studied a cohort of 21 patients diagnosed with stage I, II, III and IV melanoma (Table 1) and evaluated the reactivity of antibody cultures (n = 1,800) from these patients to the metastatic melanoma cell line A-375 utilizing the cell-based ELISA. This patient cohort was almost exclusively Caucasian. Antibody reactivity against melanoma cells was quantified relative to a non-specific human IgG control and measured as fold increase above this negative control. Patients with local (non-metastatic, stages I and II) disease had a significantly ($P<0.0001$) higher mean antibody response (2.6 fold increase, 95% CI = 2.4 to 2.8) compared to those with confirmed metastatic disease (stages III and IV, 1.7 fold increase, 95% CI = 1.7 to 1.8) (Figure 3, A). We also found an overall significant reduction ($P<0.0001$) in the mean reactivity of antibodies secreted in B cell cultures against melanoma cells from stage II (2.8 fold increase, 95% CI = 2.6 to 3.0, n = 660) to stage III (1.9 fold increase, 95% CI = 1.8 to 2.0, n = 540) and to stage IV patients (1.5 fold increase, 95% CI 1.5 to 1.6, n = 480) (Figure 3, B). The stage I patient was not evaluated since samples from only one patient (n = 120 B cell cultures) from the cohort was available to include in this group. The highest mean antibody reactivity against melanoma cells was observed in Patients 5 and 6 diagnosed with stage II and III melanoma, respectively (Table 1). However, we observed variation in the antibody response among individual patients, with 19 out of 21 patients in our cohort having at least one antibody-producing culture with optical density values 2.5-fold above the negative IgG control (Table 1). These findings suggest that despite the significant reduction in the proportion of tumor-reactive antibody cultures as a function of disease progression, patients from each of stage groups had B cells with antibodies that recognized tumor cells.

Estimations of Melanoma-reactive Antibody Frequencies from Patient Peripheral Blood B Cell Cultures

We screened for tumor-reactive antibodies from patient B cell cultures and approximated frequency and specificity of selected

Table 1. Reactivity of patient-derived antibody-producing B cell cultures to A-375 metastatic melanoma cells.

Stage	Patient ID*	Age	Sex	Ethnicity	Mean fold increase over negative control†	95% CI of mean			Maximum fold increase over negative control	% Mean reactive cultures††
I	9	51	F	Caucasian	1.1	1	to	1	2.8	2
II	4	75	M	Caucasian	2.7	2.6	to	3	4.2	38
II	5	70	M	Caucasian	6.1	5.4	to	7	17	63
II	7	69	M	Caucasian	1.6	1.4	to	2	4.8	3
II	15	49	F	Caucasian	2.6	2.5	to	3	6.2	22
II	1	66	F	Caucasian	1.5	1.4	to	2	6.8	5
II	19	63	F	Caucasian	1.6	1.5	to	2	3.5	82
II	21	38	M	Caucasian	1.3	1.1	to	2	7.7	2
II	20	81	M	Caucasian	2	1.9	to	2	3.7	50
					2.4	2.2	to	3	6.7	33
III	6	67	M	Caucasian	3.2	3	to	3	5.8	14
III	10	54	M	Caucasian	1.8	1.6	to	2	3.6	13
III	16	77	M	Caucasian	1.8	1.6	to	2	3.8	97
III	17	88	M	Caucasian	1.8	1.7	to	2	2.8	40
III	18	68	M	Caucasian	1.3	1.2	to	1	2.8	6
III	8	23	M	Asian	1	0.8	to	1	2.9	8
					1.8	1.7	to	2	3.6	30
IV	11	77	F	Caucasian	1.7	1.5	to	2	3.3	92
IV	12	72	F	Caucasian	1	0.8	to	1	3.5	10
IV	2	66	M	Caucasian	1.8	1.7	to	2	3.1	19
IV	13	55	F	Caucasian	1.5	1.4	to	2	2.6	2
IV	3	51	M	Caucasian	1.8	1.7	to	2	2.7	8
IV	14	31	F	Caucasian	0.7	0.6	to	1	1.3	12
					Mean1.4	1.3	to	1.5		24

*Patient ID corresponds to patient number in all figures.
†Fold increases values were calculated by dividing the optical density of B cell culture supernatants by the optical density of a non-specific IgG negative control using a cell-based ELISA.
††% of cultures with absorbance values greater than 75% of a positive control antibody using a cell-based ELISA.
doi:10.1371/journal.pone.0019330.t001

cultures to tumor cells. For this we screened B cell culture supernatants against a stringent comparator using a positive control monoclonal antibody, Trastuzumab, that recognizes the HER2/*neu* tumor antigen, expressed on breast cancer cells and on some melanoma cells [38]. Trastuzumab was selected as a positive control because of comparable binding across melanoma cell lines and melanocytes, as shown by mean fluorescence intensities of antibody binding against a range of these cells (Figure 4, A). Previous studies screening for tumor-specific antibodies have selected wells greater than the mean negative control optical density (OD) + three standard deviations as criteria for positive tumor-reactive antibodies [39]. Due to the inherent variability of cell-based assays, and the potential identification of false positive cultures, we chose more stringent criteria for antibody screening, by comparing antibodies produced by B cells to a positive control antibody (> 75% OD of positive control). Based on this antibody selection criteria (>75% OD of positive control), we estimate that 28% of B cell cultures (n = 1,800) derived from 21 patients, each arising from 500 B cells, produced antibodies that recognized metastatic melanoma cells, compared to 2% (n = 600) of cultures derived from 10 healthy volunteers (Figure 4, B). From these 10 healthy volunteers, 2 individuals had one reactive culture (out of 60 cultures), 1 individual had 10 reactive cultures, and the rest of the cohort had no reactive cultures.

From our patient cohort, we can roughly estimate the frequency of B cells that produce an antibody that recognizes melanoma cells under the assumption that a reactive antibody culture, defined as having an OD >75% of the positive control, arises from only a single B cell (1 out of 500 plated per culture). By dividing the total number positive antibody cultures from the patient cohort by the total number of B cells evaluated from the patient cohort by the number of positive antibody cultures, we roughly approximate that from our patient cohort one out of 1,765 B cells produce an antibody that may recognize melanoma cells.

To estimate the frequency of melanoma-reactive antibody-producing B cells in melanoma patients we performed limiting dilution analysis. We selected a stage II patient, who, we predict, may have a high antibody response to melanoma, based on our findings that the antibody responses were highest in this group (Figure 3, B). For this stage II patient (Patient 15, see Table 1) from our limiting dilution analysis assays using the cell-based ELISA, we estimate that one out of 1,790 peripheral blood B cells produces antibodies that bind to A-375 melanoma cells (Figure 4, C). For this same patient, the frequency of B cells producing antibodies that react with melanocytes was also evaluated at the same B cell densities as melanoma cells. We did not observe a comparable patient antibody response to melanocytes as we did to melanoma cells, suggesting a much lower frequency of

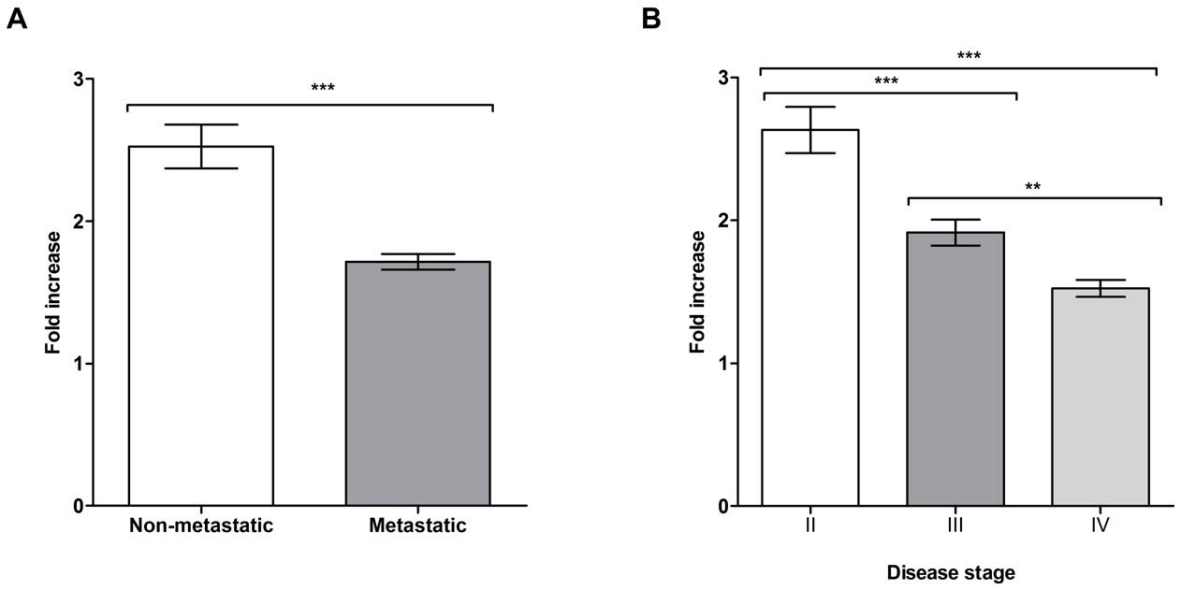

Figure 3. Prevalence of melanoma-reactive antibodies derived from melanoma patient B cell cultures is reduced in advanced disease stages. (A) Comparison of mean antibody culture reactivity to A-375 cells (fold increase relative to negative control human IgG antibody) for patients with localized (non-metastatic, n = 9) and metastatic (n = 12) disease, $P<0.0001$. (B) Mean reactivity to A-375 cells (fold increase relative to negative control antibody) of cultures from patients with stage II (n = 8), III (n = 6) and IV (n = 6) melanoma. Antibody reactivity was determined using a cell-based ELISA. Fold increase values in panels A and B were determined relative to the mean absorbance to a negative control human IgG antibody. ***$P<0.001$ and ** P = 0.001 to 0.01. Error bars in figures represent 95% confidence intervals.
doi:10.1371/journal.pone.0019330.g003

antibodies that bind to normal cells of the same origin (Figure 4, C left).

Limiting dilution analysis against two additional metastatic (SK-MEL-28, A-2058) and one primary (WM-115) melanoma cell lines for the same patient yielded different but comparable frequencies to A-375 for the metastatic cell lines (SK-MEL-28, 1 out of 1,650 B cells; A-2058, 1 out of 1,170 cells), and a much lower frequency of antibodies that bind to the primary melanoma line WM-115 which was similar to that observed with primary melanocytes (Figure 4, C right). For this patient, the data suggest detectable circulating B cell humoral response frequency against metastatic melanoma cells and lower frequency for normal human melanocytes or primary melanoma cells. To further confirm the frequency observations for the patient-derived circulating B cell repertoire, we performed additional limiting dilution assays for another stage II patient (Patient 21, Table 1). For Patient 21, we estimate 1 out of 2,430 B cells that produces antibodies bind to the same melanoma cell line tested for Patient 15 (Figure 4, D), suggesting lower but comparable frequency to those estimated for B cells from Patient 15. In summary, applying the above methodology, these results suggest that tumor-reactive antibodies from circulating B cells are more frequent in melanoma patients than healthy volunteers and more frequent against a range of metastatic melanoma cells compared to normal melanocytes.

Screening for Tumor-specific Antibodies and Selection of a Patient-derived Monoclonal Antibody with *In Vitro* Cytotoxicity against Melanoma Cells

We then selected patient-derived, tumor-specific antibodies in order to further evaluate their reactivity to melanoma cells, and conducted a preliminary assessment of the potential functional capabilities of a patient-derived antibody from this screen. B cell culture wells were selected based on stringent criteria (OD > 75% positive control antibody), using the cell-based ELISA. Tumor specificity of antibody cultures was evaluated by comparing binding of antibodies from these cultures against multiple melanoma cells (A-375, SK-MEL-2, WM-115) versus normal cells (Figure 5, A). We observed multiple antibody cultures with a higher degree of binding to some melanoma cells compared to melanocytes from the same patient (Patient 3, Figure 5, A; a selection of five of these cultures is shown on Figure 5, B). Similar results were obtained when we screened for tumor-specific cultures from different patients against melanoma cells and melanocytes. Positive cultures with different binding patterns against four melanoma cell lines (A-375, SK-MEL-2, SK-MEL-28, WM-115) and primary human melanocytes were detected (selected cultures derived from Patients 2, 3, 4 and 6 are shown as examples in Figure 5, C), reflecting specificity and reactivity of different antibodies to a range of antigens expressed at different levels in a number of melanoma cell lines, and some reactivity to antigens lowly expressed on human melanocytes. Selection of a tumor-positive antibody culture for sub-cloning and limiting dilution was based on degree of reactivity to melanoma cells relative to melanocytes (Figure 5, C).

One B cell culture from Patient 6 was selected for further evaluation since cell culture supernatants were observed to have a higher degree of binding to A-375 and SK-MEL-28 cells compared to melanocytes by ELISA (Figure 5, C; right). After limiting dilution of this melanoma-reactive B cell culture, a monoclonal antibody (6_2G3) was further assessed for specificity to 6 melanoma cell lines, melanocytes and fibroblasts by live cell flow cytometry (Figure 6). Since more antibody was available after monoclonal dilution, 2 additional melanoma cell lines along with dermal fibroblasts were evaluated. In concordance with the cell-based ELISA findings (Figure 5, C), the 6_2G3 clone bound to a range of melanoma cell lines, but not to melanocytes (Figure 6). The antibody had no reactivity against primary human dermal

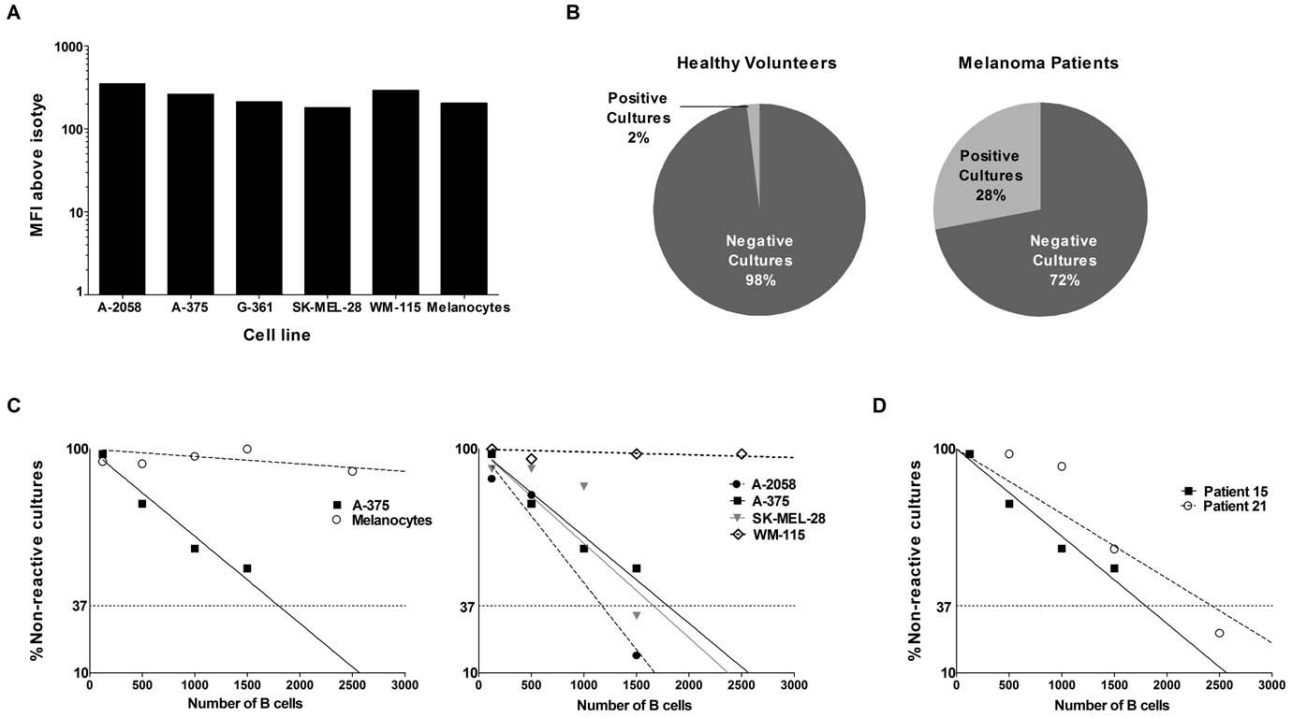

Figure 4. Estimations of the frequency of circulating B cells producing melanoma-reactive antibodies relative to a positive control antibody. (A) Binding of Trastuzumab is consistent across melanoma cell lines and primary human melanocytes evaluated by mean fluorescence intensity (MFI) above isotype control antibody binding for each cell line. (B) Proportion of B cell cultures (n = 1,800) from 21 melanoma patients arising from 500 B cells each that produced antibodies that reacted to metastatic melanoma cells compared to cultures (n = 600) from 10 healthy volunteers. (C) Frequency of B cells producing IgG antibodies able to bind to melanoma cells estimated by limiting dilution analysis for Patient 15 (see Table 1). The frequency of B cells producing antibodies reactive to the cells of interest was approximated according to Poisson distribution, the number of B cells at which 37% of the cultures were non-reactive (dotted horizontal line). Frequencies of tumor-reactive B cells against A-375 melanoma cells versus melanocytes evaluated at the same B cell densities (left) and against four melanoma cell lines (primary WM-115, and metastatic cell lines derived from different anatomic locations, right). (D) Comparison of the frequency of B cells that react to metastatic melanoma cells between two stage II patients, estimated by limiting dilution analysis. For these two patients, frequency was estimated to be 1 in 1,790 B cells (Patient 15) and 1 in 2,430 B cells (Patient 21).
doi:10.1371/journal.pone.0019330.g004

fibroblasts. In summary, by evaluating the specificity of antibodies to melanoma cells versus melanocytes and fibroblasts we could identify a melanoma-specific monoclonal antibody clone 6_2G3. While we had limited amounts of monoclonal antibodies our B cell culture supernatants after evaluating melanoma-cell specificity, we were able to conduct a limited functional investigation of this antibody.

Using clone 6_2G3, we wished to assess whether a patient-derived antibody has potential cytotoxic activity against tumor cells. We tested the tumor cell killing potential of this antibody using a real-time live-dead cell cytotoxicity assay using as targets metastatic melanoma cells recognized by this clone (Figure 7 & Supporting Videos S1 and S2). In these experiments, U-937 human monocytic cells which express Fcγ receptors served as effector cells [40] and A-375 melanoma cells were used as target cells to evaluate antibody-dependent cellular cytotoxicity (ADCC) of tumor cells mediated by patient-derived IgG antibodies. We tested two monoclonal antibodies, both derived from Patient 6 (Table 1): (1) the 6_2G3 antibody, which bound to A-375 cells and not melanocytes and (2) the 6_2D10 antibody, which did not bind to A-375 cells or melanocytes in the cell based ELISA prior to limiting dilution, which served as a non-tumor-reactive control (Figure 7).

After 2 hours in culture, 18% (95% CI = -5 to 41%) of tumor cells given the melanoma-specific antibody were viable, compared to 95% (95% CI = 86 to 104%) of the tumor cells given the non-melanoma specific antibody ($P<0.0001$) (Figure 7, A, left). Relative to tumor cell fluorescence at the start of the assay, mean green/live tumor cell fluorescent intensity was reduced to 64% for the non-tumor specific antibody (6_2D10) compared to 18% for the tumor-specific antibody (6_2G3) (Figure 7, A, right). These results highlight the potential of a patient derived tumor-specific antibody to kill tumor cells by antibody-dependent cell cytotoxicity (Figure 7, B and see Videos S1 and S2). For tumor cells treated with the tumor-specific 6_2G3 antibody, we also observed a significant ($P = 0.0002$) reduction in the movement of monocytic effector cells in contact with tumor (13 μm, 95% CI = 10 to 17 μm) compared to effector cells not in contact with tumor (26 μm, 95% CI = 21 to 31 μm) (Figure 7, C and D). Using the 6_2D10 non-specific antibody, no significant ($P = 0.3$) difference was observed for the movement of effector cells not in contact with tumor cells (20 μm, 95% CI = 15 to 25 μm) compared to those in contact with tumor cells (25 μm, 95% CI = 18 to 31). With this example, we demonstrate that a patient-derived tumor-specific antibody is capable of engaging immune effector cells in antibody-dependent cellular cytotoxicity against tumor cells. Taken together, these data suggest that systemic melanoma-specific mature B cell responses may be present in patients with melanoma and may harbor the potential to be activated against cancer cells.

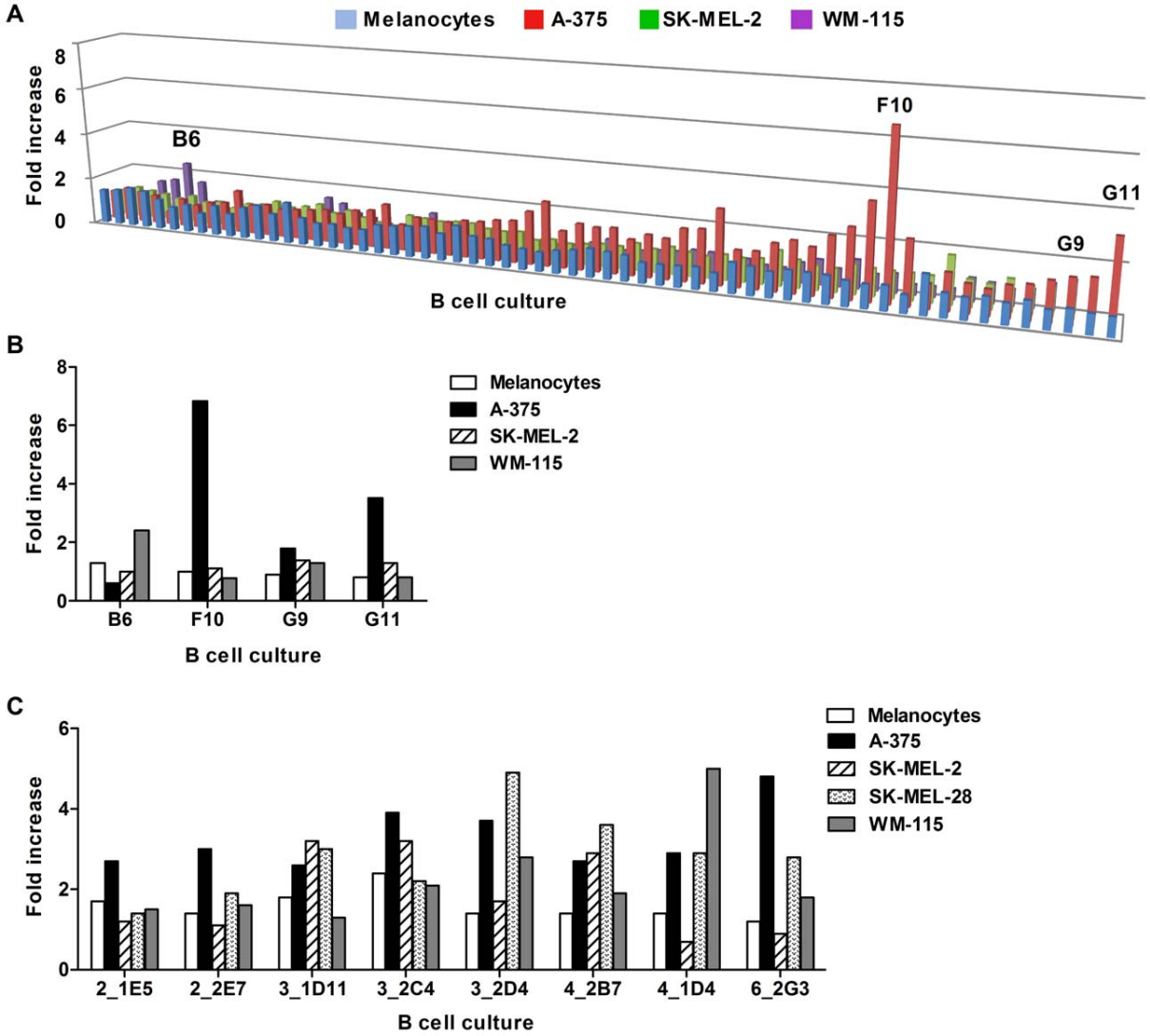

Figure 5. Selection of patient-derived antibodies that recognize melanoma cells. (A) Multiple antibody cultures from one patient (Patient 3, see Table 1) were screened against 3 melanoma cell lines (A-375, SK-MEL-2 and WM-115) and primary melanocytes using the cell-based ELISA. Fold increase values represent optical density (OD) values relative to a negative control antibody. (B) Selected cultures from Patient 3 evaluated in A, which secreted antibodies that bound to the above tumor cell lines are compared to melanocytes. (C) Selected cultures derived from 4 patients were evaluated against 4 melanoma cells lines and compared to melanocytes.
doi:10.1371/journal.pone.0019330.g005

Discussion

We describe an approach to study the circulating B cell-derived humoral immune response to cancer and apply this to detect tumor-specific IgG antibodies from melanoma patient B cells. This strategy has the potential to be applied to any type of cancer. Findings presented herein complement previous serological studies, providing added insight into the mature systemic B cell response to melanoma.

As a first step to evaluate the tumor reactivity and specificity of patient B cell-derived IgG antibodies, we developed a medium-throughput cell-based ELISA with melanoma cells to detect antibodies against tumor cell surface antigens (Figure 1). Cells were allowed to grow and adhere on to 96-well plates prior to being preserved by a light fixative (0.5% formaldehyde). While preserving the cells and allowing for storage and access to multiple plates at any one time, light fixation with formalin allows preservation of potentially-antigenic epitopes on the surface of target cells. Previous studies have reported cell-based ELISA methods to identify tumor-specific antibodies in melanoma [39,41], where tumor cells were preserved using strong fixatives such as glutaraldehyde, known to potentially mask antigenic epitopes, thus compromising the recognition of antigens by antibodies [42]. Furthermore, the specificity and sensitivity of such methods has not been reported using antibodies against known cell surface antigens. Although many intracellular melanoma associated antigens have been described (tyrosinase, TRP-1, TRP-2, gp100/pmel17), most are also expressed by normal melanocytes, only a few defined cell surface antigens such as the High Molecular Weight Melanoma-Associated Antigen (HMW-MAA) are reported to be expressed on the surface of melanoma cells, and other antigens show heterogeneous expression among

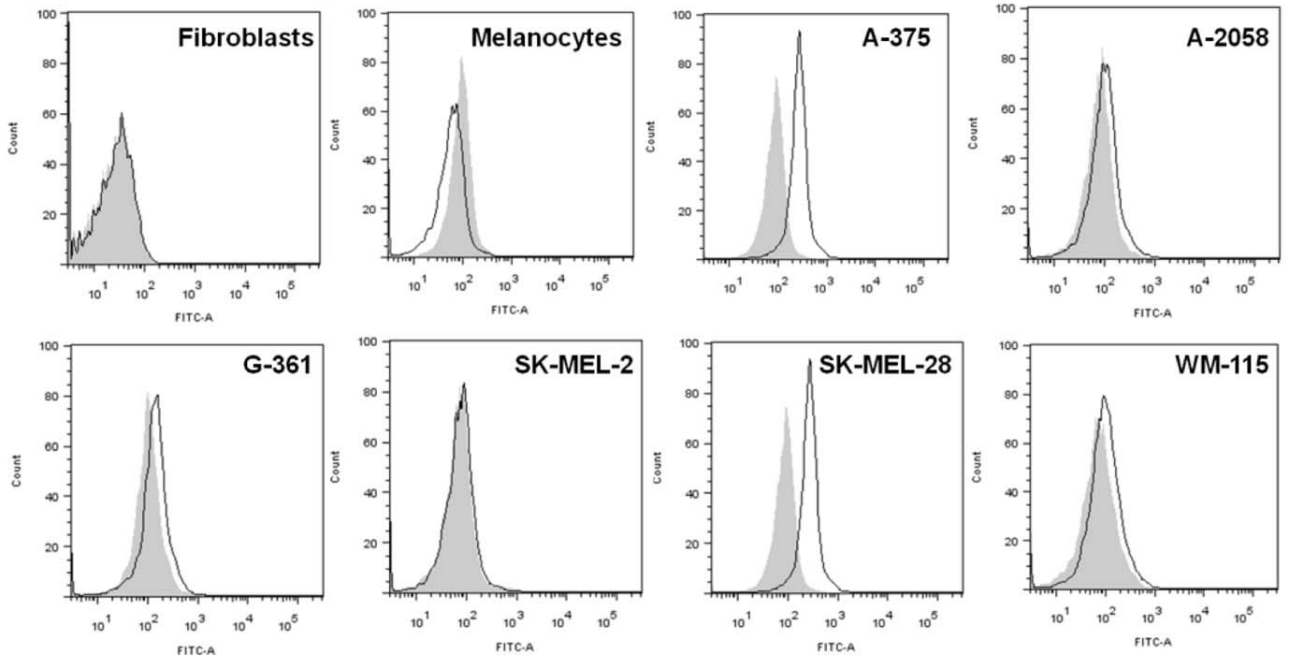

Figure 6. Selection of a patient derived B antibody that recognizes melanoma cells but not melanocytes. A selected tumor-reactive culture from a stage III patient (Patient 6) which secreted antibodies that bound to tumor cell lines and compared to melanocytes by ELISA (Figure 5, C) was sub-cloned, and a monoclonal antibody 6_2G3 was selected and evaluated on live cells by flow cytometry (solid black line histograms) for reactivity to fibroblasts, melanocytes, and 6 melanoma cell lines. IgG isotype controls are shown in shaded grey histograms.
doi:10.1371/journal.pone.0019330.g006

patients [43,44]. Thus, this ELISA constitutes an attractive tool to evaluate broad responses to any naturally-expressed antigens on the surface of melanoma cells and melanocytes in this context. This screening methodology has additional potential advantages. Unlike assays screening against a single recombinant antigen or antigenic epitope, our method enables the evaluation of antibody repertoires of patients against a multitude of cell surface antigens in their native confirmation on the surface of both primary and metastatic melanoma cells and also melanocytes, providing more comprehensive information on the broad prevalence of tumor-reactive and tumor-specific antibodies. Previous studies have shown concordance of cell line-associated antigens with antigens expressed on corresponding tumors, making them a suitable platform for tumor-reactive antibody screening [26,45]. Thus, cell lines provide a promising alternative source of multiple tumor antigens in the absence of multiple well-defined, highly expressed, and readily available recombinant antigens. Unlike flow cytometric evaluations, the cell-based ELISA does not require the use of proteolytic enzymes such as trypsin, therefore better preserving cell surface antigens. Plates of target cells can be prepared, fixed and frozen in batches, thus allowing for higher throughput screening for tumor cell-reactive antibodies. It can be applied to evaluate $>$ 300 culture supernatants against cell lines within a few hours. In principle, numerous ELISA plates for screening a range of cell lines with multiple supernatant samples can be processed simultaneously. Additionally, this methodology may be a potential tool for immunomonitoring tumor-specific humoral responses to therapies; selecting patients most likely to benefit from immunotherapy; or as a prognostic factor in linking tumor-reactive humoral responses to clinical outcomes. This assay may also be utilized to detect surface antigens in a range of cell types, and thus may be adapted to monitor the B cell-derived antibody repertoire in different disease contexts.

In agreement with a recent report [46], we also observed a reduction in the peripheral blood memory B cell compartment of metastatic melanoma patients. We measured a reduction of the CD27+ subset of memory B cells in patients with both metastatic and non-metastatic melanoma compared to healthy volunteers (Figure S2). Despite the reduction of circulating memory B cells in our cohort, patient-derived B cells were capable of secreting high amounts of IgG antibodies when activated *in vitro* with a TLR 9 agonist, with comparable antibody production to B cells from healthy individuals, and a high percentage of patient- and healthy volunteer-derived B cells expressed IgG antibodies within a few days in culture (80% of B cells from three patients with melanoma, Figure S2). Thus, while a reduced memory B compartment has been reported in cancer patients, we show that a melanoma-reactive portion of this compartment remains in our patient cohort.

We demonstrated a high prevalence of melanoma patient-derived antibodies produced by circulating B cells in cancer patients that recognize melanoma cell lines (Figure 2). We observed that B cell culture supernatants from different patients displayed differential binding to each cell line, which reflects specificity and reactivity of different antibodies to a range of antigens expressed at different levels in a number of melanoma cell lines; these may also reflect binding to some antigens lowly expressed on human melanocytes (Figure 4 and Table 1). Melanoma patients had a high percentage of melanoma-reactive antibody-producing B cell cultures, significantly higher than those from healthy volunteer-derived B cell cultures (Figure 2), with 28% of melanoma patient-derived B cell cultures recognizing melanoma cells, compared to 2% of cultures from healthy volunteers (Figure 4). Limiting dilution analyses of reactivity against melanoma cells versus normal melanocytes provided further evidence in support of the presence and frequency of tumor-reactive B cells in

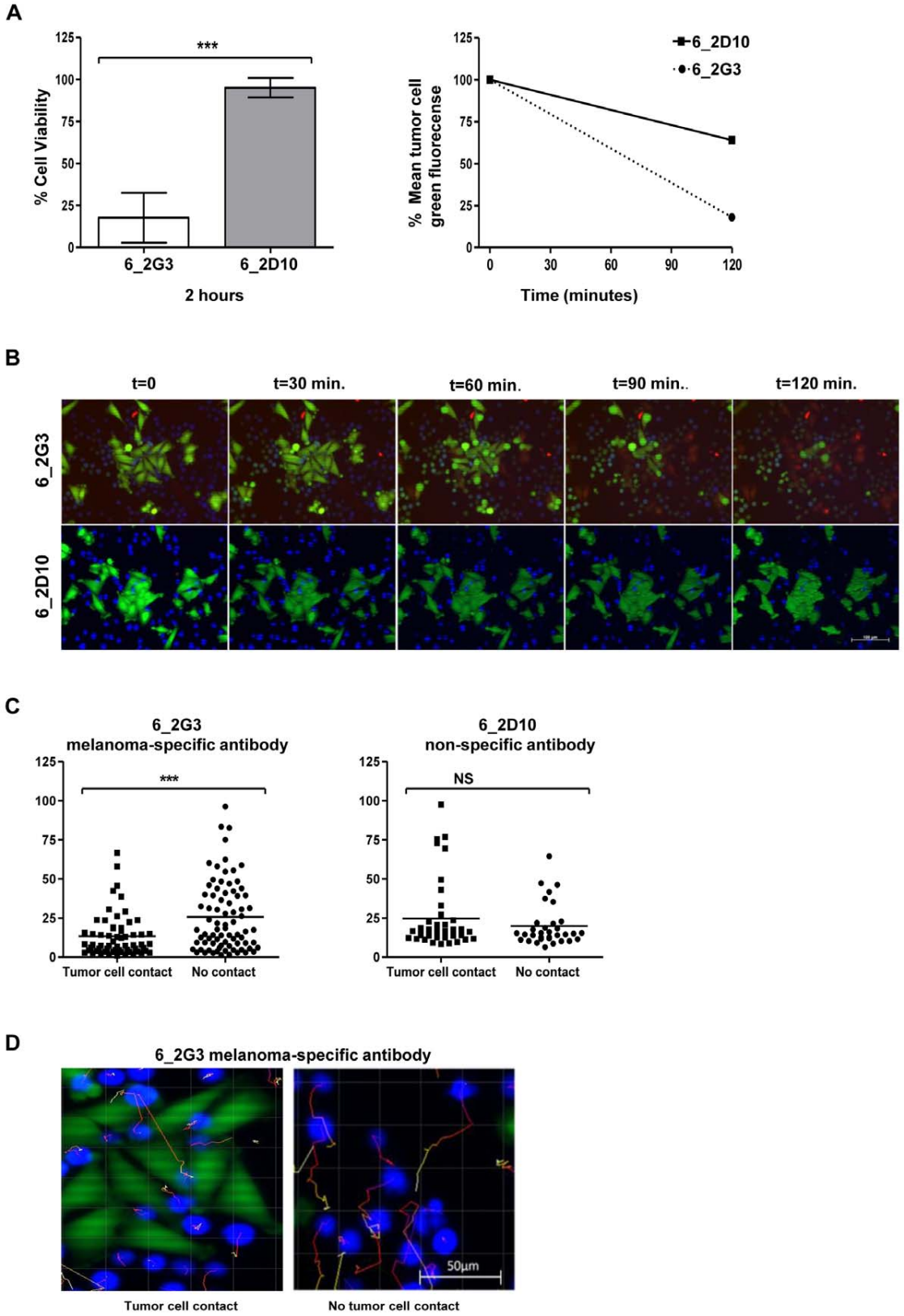

Figure 7. A tumor-specific antibody derived from a patient with melanoma is able to induce tumor cell cytotoxicity. Two monoclonal antibodies were evaluated *in vitro* using a live cell imaging assay: 6_2G3 clone bound to A-375 cells compared to melanocytes; and 6_2D10, a clone also from Patient 6 did not, and served as a negative control antibody for these experiments. (A) Cell viability of A-375 melanoma cells incubated with

human U-937 monocytic cells was compared between samples treated with 6_2G3 or 6_2D10 antibody after 2 hours at 37°C (*** = $P<0.001$) (left). Error bars represent 95% confidence intervals. Mean fluorescence intensity of A-375 tumor cells pre-labeled with the live cell dye Calcein AM, and incubated with U-937 cells and antibody 6_2G3 or 6_2D10 was measured at 0 and 120 min time points (right). (B) Fluorescent images of the live cell cytotoxicity assays at 30 minute intervals. Live Calcein AM-labeled melanoma tumor cells (green) were incubated with 6_2G3 or 6_2D10 antibody and U-937 cells (blue) and cell death was evaluated (red). Incorporation of Ethidium homodimer-1 (incorporation of red into tumor cells) was observed with 6_2G3 but not 6_2D10 (magnification 20x, Scale bar: 100 μm). (C) Movement of U-937 cells tracked and measured over two hours was compared for cells in contact and those not in contact with tumor cells (*** = $P<0.001$for 6_2G3 and $P=0.3$ for 6_2D10 antibody) (upper panel). (D) Images of U-937 movement in tumor cell cultures treated with 6_2G3, tracked for cells in contact (left) and cells not in contact with tumor cells (right). Movement is indicated by tracking lines (red to yellow) from the original position of U-937 cells at t = 0 to t = 2 hours (magnification 20x, Scale bar: 50 μm).
doi:10.1371/journal.pone.0019330.g007

patient blood (Figure 4). For one stage II patient evaluated, the data indicate that metastatic melanoma cells are recognized by a higher proportion of B cells (estimated on average ~ 1 in 2,000 mature B cells) compared to primary melanoma cells or melanocytes, although in a cohort of 10 patients we measured reactivity of B cell cultures to both metastatic and primary melanoma cell lines (Figure 2). Taking into consideration the expected variability in immune responses among patients, and the array of tumor antigens these patients may be exposed to, the observations that B cells from two patients with stage II melanoma yielded comparable reactivity to metastatic melanoma cells (estimated 1 in 1,790 for Patient 15, and 1 in 2,430 B cells for Patient 21) indicate the presence and support the prevalence of a circulating melanoma-reactive B cell compartment.

While tumor-reactive antibodies were detected from most melanoma patients studied, antibody responses derived from circulating B cells against melanoma cells decreased with more advanced disease stages (Figure 3). Previous serological studies report serum-resident antibodies against tumor cells in melanoma patients, with some evidence that serum antibodies are diminished in patients with advanced disease [25,47]. It was unclear whether this was a consequence of the sequestering of antibodies into tumors with increasing tumor burden in these patients. Our findings provide further insight by demonstrating the presence of a circulating long-term mature B cell response to cancer at all disease stages, against a broad range of naturally expressed antigens on the surface of primary and metastatic tumor cells. We also report decreased frequency of tumor-reactive antibody-producing B cells with advanced disease, thus supporting the premise that mechanisms of immune tolerance rather than adsorption of antibodies into tumors in advanced disease setting may also explain these reductions. One limitation may arise from screening for antibodies against mostly metastatic melanoma cells. It is possible that our observations may reflect reactivity to antigens present in primary disease, which may be preserved or upregulated in advanced disease setting. While our findings may not account for reactivity to tumor antigens that are lost with disease progression, this reduced reactivity to melanoma we observed may imply weakened immune responses to a subset of antigens on the surface of melanoma cells. Another explanation for these observations may be that with advanced disease, mature circulating B cells home into increasing tumor sites, thus reducing the circulating tumor-reactive B cell compartment in these patients. Future studies aimed at monitoring local B cell responses in tumors may provide further clues into the dynamics of mature B cell responses at the systemic and local levels in cancer. Thus, despite well-known weakened host immune response with disease progression [48], we were able to detect melanoma-reactive antibodies from patient circulating B cells, implying that although mature humoral immune responses are weakened, responses in the form of mature memory B cells may persist. However, further work elucidating potential immunomodulatory roles of B cells and other immune cells in cancer, including the production of IL-10 by B cell population subsets [49], merits consideration.

Although we report the presence of anti-tumor antibodies produced by patient memory B cells, and these cells were stimulated *ex vivo* to secrete antibodies, it is not clear whether tumor antigen-reactive B cells are activated in patients to secrete antibodies or whether these humoral responses are capable of exerting any beneficial anti-tumoral activities in the same patients *in vivo*. In the 21 patient cohort at different disease stages in this study, we were not able to draw any conclusions regarding the relationship between tumor cell reactivity and clinical disease progression in the short term (6 months to 2 year follow up) or associations with any particular disease treatment regimes. However, monitoring mature memory B cells and their antibody repertoires together with clinical outcomes in patients over a long period of time may help identify any correlations between melanoma-reactive mature memory B cell responses and disease progression. Additionally, future studies may help identify particular components of the humoral response which may hold clinical relevance, and elucidate the potential merits of monitoring these responses in relation to therapies, or of evaluating humoral responses as a prognostic factor to clinical outcomes.

An important question therefore relates to whether patient-derived mature B cell responses have any functional capability to potently activate immune effector cells against cancer. For this, we measured the capacity of one antibody clone to kill tumor cells. Antibody clone 6_2G3 derived from a patient with stage III disease (Patient 6, Table 1) was not observed to bind to fibroblasts or melanocytes, but bound to a proportion of melanoma cell lines tested (Figure 5). Antibodies against tumor-associated antigens can attack tumor cells via a number of mechanisms including induction of apoptosis in tumor cells and engaging Fc receptors on immune cells [50,51,52,53]. Antibodies approved for the treatment of cancer have been shown to function through one or more of these mechanisms [54,55]. While our strategy yields fully human monoclonal antibodies in a matter of a few months, we were limited in the amount of antibody we could produce from the B cells to perform functional studies and evaluate reactivity to patient-derived melanoma tumors. However, we had sufficient quantity to evaluate whether a patient-derived melanoma tumor-specific monoclonal antibody could mediate antibody dependent cellular cytotoxicity (ADCC) in the presence of monocytic effector cells and tumor cells using a real-time live cell imaging assay. We show that the tumor-specific 6_2G3 clone is capable of mediating ADCC *in vitro* and additionally measured the restricted movement of monocytic effector cells once in contact with tumor-specific antibody-coated tumor cells, providing further evidence of ADCC (Figure 6). These preliminary assessments provide a promising clue that a potentially active mature B cell response against melanoma may be present in patients. An example of this possibility was recently reported by Yuan et al. who demonstrated that administration of the anti-CTLA-4 antibody ipilimumab led to serological enhancement of antibodies to the testis antigen NY

-ESO-1 in patients who responded to the antibody therapy [56]. It is therefore conceivable that the mature B cell compartment could be enhanced with immunotherapeutic approaches, and that monitoring humoral responses to therapeutics may have clinical relevance.

Harnessing the cancer-specific antibody repertoire of cancer patients using the methodology described herein may also potentially offer an alternate strategy to yield IgG antibodies against cancer antigens. Recent advances reported by Traggiai et al., evaluating monoclonal antibodies from human memory B cells have yielded fully-human virus-neutralizing antibodies of therapeutic relevance for infectious diseases and have contributed to the dissection of humoral memory responses to vaccinations [35,57,58]. Here, we focus on B cells from cancer patients such as melanoma patients, analyze systemic humoral responses to cancer and demonstrate the presence of tumor-reactive and tumor-specific antibodies. This approach may offer an advantage over other approaches such as phage display in that it yields *in vivo* affinity-matured human antibodies with naturally paired heavy and light chains. The patient-derived monoclonal antibody 6_2G3 bound to 2 out of 6 of the melanoma cell lines evaluated compared to melanocytes, suggesting that this antibody may be against a protein over-expressed or mutated on the surface of cancer cells. In light of the efficacy of Trastuzumab, against the HER2/*neu* antigen expressed on 20–30% of breast cancers, as a clinically-validated therapeutic tool for the treatment of an equivalent proportion of breast cancer patients [59], selection of antibodies that bind to a portion of cell lines may merit further characterization. Although the clinical significance of mature memory B cells expressing antibodies that recognize tumor cells in patients remains to be elucidated, antibodies derived from these cells, introduced by passive immunotherapy in therapeutically-relevant doses, such as those used for Trastuzumab to patients with breast cancer, merit investigation for any potential relevance in melanoma. Other potential future benefits of screening patient-derived B cells from tumor-reactive antibodies may be identification of novel cell surface tumor antigens. Future evaluations of clone 6_2G3 will include sequence analysis and expression cloning to allow for further analyses of specificity to melanoma tumors, antigen identification, and for thorough functional assessments.

These data provide additional understanding of the mature B cell response to melanoma by evaluating antibodies derived from circulating B cells of cancer patients. The prevalence of mature humoral responses against cancer cells in patients, as well as the capacity of a patient-derived antibody to activate effector cells against melanoma cells indicate the potential functional significance of the humoral immune response against cancer.

Materials and Methods

Ethics Statement

Specimens from patients and healthy volunteers were collected with informed written consent. The work was conducted in strict accordance with study design approved by the Guy's Research Ethics Committee, St. Thomas' Hospital, London, UK.

Study Subjects and Isolation and Culture of Peripheral Blood Human B Cells

After obtaining informed consent, peripheral blood was isolated from healthy volunteers (n = 10) and from patients with melanoma (n = 21). Patients were staged and classified according to the American Joint Committee on Cancer Melanoma Staging and Classification criteria [60]. B cells were isolated by negative selection using RosetteSep® B cell enrichment cocktail (Stem Cell Technologies, Vancouver, Canada) according to the manufacturer's instructions. B cell purity was assessed by flow cytometry by staining for mature B cells (CD22), T cells (CD3), monocytes (CD14) and plasmacytoid dendritic cells (BDCA3) using fluorescently-labeled monoclonal antibodies, all from BD Biosciences, Oxford, UK (Figure S1). Flow cytometry experiments were conducted with either the FACSAria or FACSCanto (BD Biosciences) and flow cytometric data were analyzed using Flow Jo (Tree Star, Ashland, OR).

B cells were plated at 500 cells per well on 96 well U-bottom microplates (Nunc, Rochester, NY) along with $3x10^4$ cells per well of irradiated (30 Gy) autologous PBMCs, obtained by Ficoll centrifugation, as feeder cells. B cells were grown in RPMI-1640 medium obtained from Gibco (Invitrogen, Carlsbad, CA) supplemented with 10% fetal calf serum, 1% penicillin-streptomycin, 2.5 ng/mL TLR9 ligand CpG 2006 ODN (Operon, Ebersberg, Germany), and 30% supernatant of Epstein Barr Virus (EBV) producing B95-8 cells [35]. For each patient evaluated, 60-120 B cell cultures originating from 500 B cells each were established, and cultures were grown in 200 µL per well volumes. After 18 days, supernatant (40 µL) from each culture well was screened individually for tumor-specific antibodies and selected B cultures were sub-cloned by limiting dilution to derive monoclonal cultures. We plated B cells at 1 cell/well in the presence of $3x10^4$ autologous 30 Gy irradiated autologous PBMC stimulated with 2.5 ng/mL CpG 2006 ODN.

Cell Lines and Culture

Human dermal fibroblasts were a gift from Dr. Christian Hundhausen, King's College London, UK. All other cell lines used were obtained from the American Type Culture Collection [ATCC] (Manassas, VA). Cell lines were used to identify tumor-reactive antibodies and to test for cytotoxic activity of antibodies. Media used for cell lines A-375 (CRL-1619), A-2058 (CRL-11147), G-361 (CRL-1424), SK-MEL-2 (HTB-68), SK-MEL-28 (HTB-72), SK-BR-3 (HTB-30), U-937 (CRL-1593.2) and WM-115 (CRL-1675) were obtained from Gibco and supplemented with 10% fetal calf serum and 1% penicillin-streptomycin. The human metastatic melanoma cell lines A-375 and A-2058 were grown in Dulbecco's Modified Eagle's Medium. The human melanoma cell line derived from primary melanoma tissue, WM-115, and the metastatic melanoma cell lines SK-MEL-2 and SK-MEL-28 were grown in Eagle's Minimum Essential Medium. The human metastatic melanoma cell line G-361, and the human mammary carcinoma cell line SK-BR-3, which expresses the Human Epidermal Growth Factor Receptor 2 (HER2/*neu*), were grown in McCoy's medium. The Fc receptor-expressing monocytic-like U-937 cell line was grown in RMPI-1640 medium. Primary human melanocytes (ATCC, PCS-2000-012) were grown in Dermal Cell Basal Medium (ATCC) and supplemented with the Melanocyte Growth Kit (ATCC). Human fibroblasts were grown in Medium 106 (Invitrogen) and supplemented with Low Serum Growth Supplement (Invitrogen).

Detection of Antibodies Bound to Tumor Cell Surface Proteins by Immunocytochemistry and Flow Cytometry

Qualitative detection of tumor-specific antibodies by immunocytochemistry was performed by centrifugation of 2×10^5 cells at 300g using a Shandon Cytospin® 4 Cytocentrifuge (Thermo Fisher Scientific, Waltham, MA) onto glass slides. Cells were fixed in 0.5% formalin and antibodies, such as those recognizing the human High Molecular Weight Melanoma-Associated Antigen (anti-HMW-MAA clone LHM2, Invitrogen, Carlsbad, CA), were incubated overnight at 4°C and detected following a 2 hour

incubation at 4°C with a horseradish peroxidase-conjugated anti-IgG Fc-specific antibody (1:100 dilution in Tris Buffered Saline, Sigma, Dorset, UK). Slides were stained with DAB chromogenic substrate (DAKO, Ely, UK) for 5 minutes, washed and counterstained with Mayer's hematoxlin (Merck, Darmstadt, Germany) for one minute, dehydrated and mounted in DPX mountant (Sigma) prior to assessments.

Antibodies bound to cell surface antigens were also detected on live cells by flow cytometry. Adherent cells were detached using StemPro® Accutase® cell disassociation solution (Gibco) and incubated at 2×10^5 cells per sample with antibody, isotype control or cell culture supernatants for 30 minutes at 4°C. Antibodies bound to cells were detected using a FITC-conjugated anti-IgG Fc-specific antibody (Jackson ImmunoResearch). The binding of tumor-specific antibodies to cells was compared to an excess of isotype control IgG_1 antibody (Jackson ImmunoResearch). Binding of Trastuzumab across melanoma cell lines and primary human melanocytes was evaluated by subtracting the mean fluorescence intensity (MFI) values of equal amounts of isotype control. Evaluations are representative of three experiments.

Development of a Cell-based ELISA to Detect Tumor-specific Antibodies

We developed and employed a novel cell-based ELISA to identify melanoma-reactive antibodies. Adherent cells of interest were plated at 3×10^5 cells per in 200 μL of appropriate media well on 96-well flat bottom tissue culture plates (Corning, Corning, NY) and were grown in a monolayer at 37°C and 5% CO_2 to 80-100% confluence. Cells were then lightly fixed in 0.5% formaldehyde/Hank's Buffered Salt Solution. Plates were then wrapped in foil and placed in a -80°C freezer until the day of the assay. On the day of the assay, plates were thawed for 30 minutes, washed 3 times with PBS and then blocked with a 5% non-fat milk/PBS solution for 2 hours. After removal of the blocking solution, 50 μL of culture supernatants or tumor-specific antibodies were diluted 1:2 in 1% non-fat milk/PBS solution and then added to each well, and plates were incubated for 90 minutes at room temperature on an orbital shaker. Plates were then washed 4 times with PBS/0.05%Tween (PBS-T). The binding of antibodies to cell surface proteins was detected following a 45 minute incubation with a goat anti-human horseradish peroxidase-labeled $F(ab')_2$ Fc-specific antibody (Jackson ImmunoResearch, West Grove, PA) diluted 1:250 in 1% milk/PBS-T at room temperature on an orbital shaker. Wells were then washed 4 times with PBS-T. The color reaction was developed for 15 minutes with OPD (Sigma) and OD was measured in an ELISA reader (BMG Labtech, Offenbury, Germany) at 492 nm (reference wavelength, 650 nm). Each plate contained triplicate wells of a positive control antibody, Trastuzumab (Genentech, South San Francisco, CA), and a negative control antibody, non-specific human IgG_1 (Jackson Immunoresearch) at a concentration of 250 ng/mL both diluted in RPMI-1640 media supplemented with 10% fetal calf serum. Binding of Trastuzumab to cells and background OD values for the negative non-specific human IgG control antibody formed the criteria for inclusion of readouts in the study. Since we were limited by the volume of culture supernatants for each culture, assays were repeated only when sufficient culture supernatants were available to confirm reproducibility of readouts.

Criteria for Evaluating Antibody Responses to Melanoma Using the Cell-based ELISA

Patient and healthy volunteer antibody responses were assessed using the cell-based ELISA. We evaluated the reactivity of the supernatant from each B cell culture to tumor cells relative to negative and positive control antibodies. In order to compare anti-tumor antibody responses to metastatic and primary melanoma cells between patients and healthy volunteers, and among patient groups, optical densities (OD) were normalized using the following formula:

$$\text{Fold increase} = \frac{\text{Optical density of B cell culture supernatant}}{\text{Mean optical density of non}-\text{specific IgG}_1}$$

Additionally, this calculation was used to normalize ELISA results among multiple melanoma cell lines and primary melanocytes in order to evaluate the tumor specificity of antibodies.

To evaluate the presence and estimate the frequency of tumor-reactive antibodies, we selected wells with OD values above 75% of the OD of the positive control antibody. To compare the percentage of positive cultures across patients, OD values were normalized against the positive control. For these evaluations, the mean positive control OD was assigned a relative absorbance of 1 for each plate and B cell cultures were converted from OD units to relative absorbance, and culture wells with relative absorbance values greater than 0.75 to melanoma cells but not melanocytes were selected. These criteria were also applied in limiting dilution assays to estimate the percentage of non-reactive B cell culture well. In these limiting dilution assays, B cells were plated at different densities (ranging from 125 to 2,500 B cells) and the percentage of non-reactive cultures was calculated for different patients and cell lines as a way to approximate the frequency of B cells producing melanoma-reactive antibodies using Poisson distribution.

Live Cell Imaging Assays to Measure Antibody-Dependent Cellular Cytotoxicity

The tumor-killing potential of 2 patient-derived monoclonal antibodies was assessed: one tumor-specific antibody (6_2G3), and another antibody that did not recognize tumor cells (6_2D10), both derived from the same patient (Patient 6). Both antibodies were simultaneously evaluated using a three-color fluorescent live cell imaging cytotoxicity assay. A-375 cells were plated overnight at $2x10^5$ cells per well on 6-well culture plates (Corning). Using a LIVE/DEAD® Viability/Cytotoxicity kit (Molecular Probes, Eugene, OR) live tumor cells were labeled with 2μM of Calcein AM 30 minutes prior to cytotoxicity assays, washed in RPMI 1640 supplemented with 10% FCS and 1% penicillin streptomycin, and re-suspended in media containing 4 μM Ethidium homodimer-1. Ethidium homodimer-1 incorporates into the DNA of dead cells and served as a label for cell death in this assay. U-937 monocytic cells expressing Fcγ receptors were used as immune effector cells at a ratio of 3:1 (effectors: tumor cells) [40]. U-937 monocytes were incubated with the 6_2G3 or 6_2D10 antibody for 30 minutes, stained with the CellTracker™ Blue dye (4-chloromethyl-7-hydroxycoumarin) (Molecular Probes), washed and added to the Calcein AM-labelled tumor cell cultures containing Ethidium homodimer-1. Samples were incubated and images were captured every 5 minutes for two hours in a humidified temperature controlled chamber using a Zeiss Axiovert microscope equipped with a LD-Plan-Neofluar 20x/0.4 Korr/Ph2 objective and AxioVision software system (Carl Zeiss, Jena, Germany). Following incubation, fluorescent intensities of Calcein AM-positive live tumor cells, as well as incorporation of Ethidium homodimer-1 into cells were measured and cell death was assessed with NIS-Elements BR 3 software (Nikon). The movement of effector cells in the cultures was tracked and analyzed using IMARIS software (Bitplane, Zurich, Switzerland).

Statistical Methods

Descriptive statistics were generated to examine the distribution of melanoma-reactive B cell cultures from each patient including the mean, 95% confidence interval and maximum reactivity to melanoma cells. A two-sided Student's *t* test was used to compare the mean reactivity of antibody cultures derived from melanoma patients to healthy volunteers to primary or metastatic melanoma cell lines and to compare antibody responses between patients with non-metastatic and metastatic disease. A one-way ANOVA was used to compare antibody reactivity to a metastatic melanoma cell line among B cell cultures derived from patients with stage II, III and IV disease with a Tukey's post hoc comparison test. A two-sided Student's *t* test was used to compare antibody-mediated tumor cell killing between tumor-specific and non-specific monoclonal antibodies derived from the same patient. A two-sided Student's *t* test was also employed to compare the movement of immune effector cells, pre-incubated with antibodies, in contact with tumor cells to the movement of immune cells not in contact with tumor cells. All statistical analyses were performed using GraphPad Prism software (version 5.03, GraphPad, San Diego, CA) and error bars in all figures represent 95% confidence intervals.

Supporting Information

Figure S1 Schematic of cell-based ELISA used to detect antibodies against tumor cell antigens.
(TIF)

Figure S2 Secretion of IgG antibodies from peripheral blood B cells derived from patients and healthy volunteers.
(TIF)

Video S1 Real-time live-cell cytotoxicity assay for the 6_2G3 melanoma-specific antibody.
(AVI)

Video S2 Real-time live-cell cytotoxicity assay for the 6_2D10 non-melanoma-specific antibody (negative control).
(AVI)

Videos S1 and S2

These video files show our real-time cytotoxic assays. Video S1 shows real-time functional data of the 6_2G3 melanoma-specific patient derived antibody which was observed to kill melanoma cells. Video S2 shows the identical assays shown in Video S1 using a non-melanoma specific antibody derived from the same patient, as a negative control. In these assays, live tumor cells are labeled in green (live cell dye), U-937 monocytic cells are labeled in blue, and cell death is indicated by the incorporation of red (Ethidium homodimer-1 incorporation). Frames from these videos are also displayed in Figure 7, B.

Acknowledgments

The authors thank Mrs. Angela Clifford and Mrs. Sharon Jones for recruitment of volunteers, Ms. Isabella Tosi and Ms. Katazryna Grys for sample provision and Mrs. Lynda Miles for critical comments. We thank all patients and healthy volunteers who participated in this study. This manuscript is dedicated to the memory of Mrs. Kate Kirwan and Mr. David King.

Author Contributions

Conceived and designed the experiments: AEG PK SNK FON. Performed the experiments: AEG PK. Analyzed the data: AEG PK SNK FON. Contributed reagents/materials/analysis tools: DHJ KL TD PT RLB AJB HJG SMR JS MH JLCG CH KMA AK PJB. Wrote the paper: AEG PK SNK FON DHJ KL TD PT RLB AJB HJG SMR JS MH JLCG KMA AK PJB.

References

1. Lens MB, Dawes M (2004) Global perspectives of contemporary epidemiological trends of cutaneous malignant melanoma. British Journal of Dermatology 150: 179–185.
2. Cummins DL, Cummins JM, Pantle H, Silverman MA, Leonard AL, et al. (2006) Cutaneous Malignant Melanoma. Mayo Clinic Proceedings 81: 500–507.
3. Nestle FO, Halpern AC (2007) Melanoma. In: JL B, JL J, RP R, eds. Dermatology. 2 ed. St. Louis: Mosby Elsevier.
4. Kalialis LV, Drzewiecki KT, Klyver H (2009) Spontaneous regression of metastases from melanoma: review of the literature. [Review]. Melanoma Research October 19: 275–282.
5. Schadendorf D, Algarra SM, Bastholt L, Cinat G, Dreno B, et al. (2009) Immunotherapy of distant metastatic disease. Annals of Oncology 20: vi41–vi50.
6. Vajdic CM, van Leeuwen MT, Webster AC, McCredie MRE, Stewart JH, et al. (2009) Cutaneous Melanoma Is Related to Immune Suppression in Kidney Transplant Recipients. Cancer Epidemiology Biomarkers & Prevention 18: 2297–2303.
7. Kirkwood JM, Tarhini AA, Panelli MC, Moschos SJ, Zarour HM, et al. (2008) Next Generation of Immunotherapy for Melanoma. J Clin Oncol 26: 3445–3455.
8. Lee PP, Yee C, Savage PA, Fong L, Brockstedt D, et al. (1999) Characterization of circulating T cells specific for tumor-associated antigens in melanoma patients. Nat Med 5: 677–685.
9. Vence L, Palucka AK, Fay JW, Ito T, Liu Y-J, et al. (2007) Circulating tumor antigen-specific regulatory T cells in patients with metastatic melanoma. Proceedings of the National Academy of Sciences 104: 20884–20889.
10. Rosenberg SA, Restifo NP, Yang JC, Morgan RA, Dudley ME (2008) Adoptive cell transfer: a clinical path to effective cancer immunotherapy. Nat Rev Cancer 8: 299–308.
11. Schadendorf D, Ugurel S, Schuler-Thurner B, Nestle FO, Enk A, et al. (2006) Dacarbazine (DTIC) versus vaccination with autologous peptide-pulsed dendritic cells (DC) in first-line treatment of patients with metastatic melanoma: a randomized phase III trial of the DC study group of the DeCOG. Annals of Oncology 17: 563–570.
12. Besser MJ, Shapira-Frommer R, Treves AJ, Zippel D, Itzhaki O, et al. (2010) Clinical Responses in a Phase II Study Using Adoptive Transfer of Short-term Cultured Tumor Infiltration Lymphocytes in Metastatic Melanoma Patients. Clinical Cancer Research 16: 2646–2655.
13. Hodi FS, O'Day SJ, McDermott DF, Weber RW, Sosman JA, et al. Improved Survival with Ipilimumab in Patients with Metastatic Melanoma. N Engl J Med 363(8): 711–723.
14. Andreu P, Johansson M, Affara NI, Pucci F, Tan T, et al. (2010) FcR[gamma] Activation Regulates Inflammation-Associated Squamous Carcinogenesis. Cancer Cell 17: 121–134.
15. Qin Z, Richter G, Schuler T, Ibe S, Cao X, et al. (1998) B cells inhibit induction of T cell-dependent tumor immunity. Nat Med 4: 627–630.
16. DiLillo DJ, Yanaba K, Tedder TF (2010) B Cells Are Required for Optimal CD4+ and CD8+ T Cell Tumor Immunity: Therapeutic B Cell Depletion Enhances B16 Melanoma Growth in Mice. J Immunol 184: 4006–4016.
17. Takahashi T, Johnson TD, Nishinaka Y, Morton DL, Irie RF (1999) IgM Anti-Ganglioside Antibodies Induced by Melanoma Cell Vaccine Correlate with Survival of Melanoma Patients. 112: 205–209.
18. Restifo NP, Marincola FM, Kawakami Y, Taubenberger J, Yannelli JR, et al. (1996) Loss of Functional Beta2-Microglobulin in Metastatic Melanomas From Five Patients Receiving Immunotherapy. J Natl Cancer Inst 88: 100–108.
19. Dunn GP, Bruce AT, Ikeda H, Old LJ, Schreiber RD (2002) Cancer immunoediting: from immunosurveillance to tumor escape. Nat Immunol 3: 991–998.
20. Houghton AN, Gold JS, Blachere NE (2001) Immunity against cancer: lessons learned from melanoma. Current Opinion in Immunology 13: 134–140.
21. Marincola FM, Wang E, Herlyn M, Seliger B, Ferrone S (2003) Tumors as elusive targets of T-cell-based active immunotherapy. Trends in Immunology 24: 334–341.
22. Kirkwood JM, Lorigan P, Hersey P, Hauschild A, Robert C, et al. Phase II Trial of Tremelimumab (CP-675,206) in Patients with Advanced Refractory or Relapsed Melanoma. Clinical Cancer Research 16: 1042–1048.
23. Mittelman A, Chen ZJ, Yang H, Wong GY, Ferrone S (1992) Human high molecular weight melanoma-associated antigen (HMW-MAA) mimicry by mouse anti-idiotypic monoclonal antibody MK2-23: induction of humoral anti-HMW-MAA immunity and prolongation of survival in patients with stage IV melanoma. Proceedings of the National Academy of Sciences of the United States of America 89: 466–470.

24. Perez DG, Suman VJ, Fitch TR, III TA, Morton RF, et al. (2009) Phase 2 trial of carboplatin, weekly paclitaxel, and biweekly bevacizumab in patients with unresectable stage IV melanoma. Cancer 115: 119–127.
25. Lewis MG, Ikonopisov RL, Nairn RC, Phillips TM, Fairley GH, et al. (1969) Tumour-specific Antibodies in Human Malignant Melanoma and their Relationship to the Extent of the Disease. Br Med J 3: 547–552.
26. Stockert E, Jager E, Chen Y-T, Scanlan MJ, Gout I, et al. (1998) A Survey of the Humoral Immune Response of Cancer Patients to a Panel of Human Tumor Antigens. J Exp Med 187: 1349–1354.
27. Huang SKS, Okamoto T, Morton DL, Hoon DSB (1998) Antibody Responses to Melanoma//Melanocyte Autoantigens in Melanoma Patients. 111: 662–667.
28. Chen Y-T, Scanlan MJ, Sahin U, Türeci Ö, Gure AO, et al. (1997) A testicular antigen aberrantly expressed in human cancers detected by autologous antibody screening. Proceedings of the National Academy of Sciences 94: 1914–1918.
29. Sahin U, Türeci O, Schmitt H, Cochlovius B, Johannes T, et al. (1995) Human neoplasms elicit multiple specific immune responses in the autologous host. Proceedings of the National Academy of Sciences of the United States of America 92: 11810–11813.
30. Chen Y-T, Gure AO, Tsang S, Stockert E, Jäger E, et al. (1998) Identification of multiple cancer/testis antigens by allogeneic antibody screening of a melanoma cell line library. Proceedings of the National Academy of Sciences of the United States of America 95: 6919–6923.
31. Yamaguchi H, Furukawa K, Fortunato SR, Livingston PO, Lloyd KO, et al. (1987) Cell-surface antigens of melanoma recognized by human monoclonal antibodies. Proceedings of the National Academy of Sciences of the United States of America 84: 2416–2420.
32. Kirkwood JM, Robinson JE (1990) Human IgG and IgM monoclonal antibodies against autologous melanoma produced by Epstein-Barr-virus-transformed B lymphocytes. Cancer Immunology, Immunotherapy 32: 228–234.
33. Yeilding NM, Gerstner C, Kirkwood JM (1992) Analysis of two human monoclonal antibodies against melanoma. International Journal of Cancer 52: 967–973.
34. Punt CJA, Barbuto JAM, Zhang H, Grimes WJ, Hatch KD, et al. (1994) Anti-tumor antibody produced by human tumor-infiltrating and peripheral blood B lymphocytes. Cancer Immunology, Immunotherapy 38: 225–232.
35. Traggiai E, Becker S, Subbarao K, Kolesnikova L, Uematsu Y, et al. (2004) An efficient method to make human monoclonal antibodies from memory B cells: potent neutralization of SARS coronavirus. Nat Med 10: 871–875.
36. Lanzavecchia A, Corti D, Sallusto F (2007) Human monoclonal antibodies by immortalization of memory B cells. Current Opinion in Biotechnology 18: 523–528.
37. Gril B, Palmieri D, Bronder JL, Herring JM, Vega-Valle E, et al. (2008) Effect of Lapatinib on the Outgrowth of Metastatic Breast Cancer Cells to the Brain. J Natl Cancer Inst 100: 1092–1103.
38. Stove C, Stove V, Derycke L, Van Marck V, Mareel M, et al. (2003) The Heregulin//Human Epidermal Growth Factor Receptor as a New Growth Factor System in Melanoma with Multiple Ways of Deregulation. 121: 802–812.
39. Zhang H, Lake DF, Barbuto JAM, Bernstein RM, Grimes WJ, et al. (1995) A Human Monoclonal Antimelanoma Single-Chain Fv Antibody Derived from Tumor-infiltrating Lymphocytes. Cancer Res 55: 3584–3591.
40. Karagiannis P, Singer J, Hunt J, Gan S, Rudman S, et al. (2009) Characterisation of an engineered trastuzumab IgE antibody and effector cell mechanisms targeting HER2/ neu -positive tumour cells. Cancer Immunology, Immunotherapy 58: 915–930.
41. Cai X, Garen A (1995) Anti-melanoma antibodies from melanoma patients immunized with genetically modified autologous tumor cells: selection of specific antibodies from single-chain Fv fusion phage libraries. Proceedings of the National Academy of Sciences of the United States of America 92: 6537–6541.
42. Wewetzer K, Heiniger C, Seilheimer B (1996) An improved cell-ELISA for the differential screening of antibodies against cell surface molecules of viable adherent Schwann cells. Journal of Immunological Methods 191: 171–178.
43. Hodi FS (2006) Well-Defined Melanoma Antigens as Progression Markers for Melanoma: Insights into Differential Expression and Host Response Based on Stage. Clinical Cancer Research 12: 673–678.
44. Campoli MR, Chang C-C, Kageshita T, Wang X, McCarthy JB, et al. (2004) Human High Molecular Weight-Melanoma-Associated Antigen (HMW-MAA): A Melanoma Cell Surface Chondroitin Sulfate Proteoglycan (MSCP) with Biological and Clinical Significance. Critical Reviews Immunology 24: 30.
45. Wistuba II, DavidBryant, Behrens C, Milchgrub S, Virmani AK, et al. (1999) Comparison of Features of Human Lung Cancer Cell Lines and Their Corresponding Tumors. Clinical Cancer Research 5: 991–1000.
46. Carpenter EL, Mick R, Rech AJ, Beatty GL, Colligon TA, et al. (2009) Collapse of the CD27+ B-cell compartment associated with systemic plasmacytosis in patients with advanced melanoma and other cancers. Clin Cancer Res 15: 4277–4287.
47. Shimbo T, Tanemura A, Yamazaki T, Tamai K, Katayama I, et al. (2010) Serum Anti-BPAG1 Auto-Antibody Is a Novel Marker for Human Melanoma. PLoS One 5: e10566.
48. Swann JB, Smyth MJ (2007) Immune surveillance of tumors. The Journal of Clinical Investigation 117: 1137–1146.
49. Bouaziz J-D, Calbo S, Maho-Vaillant M, Saussine A, Bagot M, et al. IL-10 produced by activated human B cells regulates CD4+ T-cell activation in vitro. European Journal of Immunology 40: 2686–2691.
50. Weiner LM, Surana R, Wang S (2010) Monoclonal antibodies: versatile platforms for cancer immunotherapy. Nat Rev Immunol 10: 317–327.
51. Clynes R, Towers T, Presta L, Ravetch J (2000) Inhibitory Fc receptors modulate in vivo cytoxicity against tumor targets. Nature Med 6: 443–446.
52. Karagiannis SN, Bracher MG, Hunt J, McCloskey N, Beavil RL, et al. (2007) IgE-Antibody-Dependent Immunotherapy of Solid Tumors: Cytotoxic and Phagocytic Mechanisms of Eradication of Ovarian Cancer Cells. J Immunol 179: 2832–2843.
53. Karagiannis Sophia N, Wang Q, East N, Burke F, Riffard S, et al. (2003) Activity of human monocytes in IgE antibody-dependent surveillance and killing of ovarian tumor cells. European Journal of Immunology 33: 1030–1040.
54. Hudis CA (2007) Trastuzumab -- Mechanism of Action and Use in Clinical Practice. N Engl J Med 357: 39–51.
55. Glennie MJ, French RR, Cragg MS, Taylor RP (2007) Mechanisms of killing by anti-CD20 monoclonal antibodies. Molecular Immunology 44: 3823–3837.
56. Yuan J, Gnjatic S, Li H, Powel S, Gallardo HF, et al. (2008) CTLA-4 blockade enhances polyfunctional NY-ESO-1 specific T cell responses in metastatic melanoma patients with clinical benefit. Proceedings of the National Academy of Sciences 105: 20410–20415.
57. DeboraPinna, DavideCorti, DavidJarrossay, FedericaSallusto, Lanzavecchia A (2009) Clonal dissection of the human memory B-cell repertoire following infection and vaccination. European Journal of Immunology 39: 1260–1270.
58. Kwakkenbos MJ, Diehl SA, Yasuda E, Bakker AQ, van Geelen CMM, et al. Generation of stable monoclonal antibody-producing B cell receptor-positive human memory B cells by genetic programming. Nat Med 16: 123–128.
59. Slamon D, Clark G, Wong S, Levin W, Ullrich A, et al. (1987) Human breast cancer: correlation of relapse and survival with amplification of the HER-2/neu oncogene. Science 235: 177–182.
60. Balch CM, Gershenwald JE, Soong S-J, Thompson JF, Atkins MB, et al. (2009) Final Version of 2009 AJCC Melanoma Staging and Classification. J Clin Oncol 27: 6199–6206.

Cancer Immunol Immunother (2009) 58:915–930
DOI 10.1007/s00262-008-0607-1

ORIGINAL ARTICLE

Characterisation of an engineered trastuzumab IgE antibody and effector cell mechanisms targeting HER2/*neu*-positive tumour cells

Panagiotis Karagiannis · Josef Singer · James Hunt · Samuel K. E. Gan · Sarah M. Rudman · Diana Mechtcheriakova · Regina Knittelfelder · Tracy R. Daniels · Philip S. Hobson · Andrew J. Beavil · James Spicer · Frank O. Nestle · Manuel L. Penichet · Hannah J. Gould · Erika Jensen-Jarolim · Sophia N. Karagiannis

Received: 20 June 2008 / Accepted: 26 September 2008 / Published online: 22 October 2008

Abstract Trastuzumab (Herceptin®), a humanized IgG1 antibody raised against the human epidermal growth factor receptor 2 (HER2/*neu*), is the main antibody in clinical use against breast cancer. Pre-clinical evidence and clinical studies indicate that trastuzumab employs several anti-tumour mechanisms that most likely contribute to enhanced survival of patients with HER2/*neu*-positive breast carcinomas. New strategies are aimed at improving antibody-based therapeutics like trastuzumab, e.g. by enhancing antibody-mediated effector function mechanisms. Based on our previous findings that a chimaeric ovarian tumour antigen-specific IgE antibody showed greater efficacy in tumour cell killing, compared to the corresponding IgG1 antibody, we have produced an IgE homologue of trastuzumab. Trastuzumab IgE was engineered with the same light- and heavy-chain variable-regions as trastuzumab, but with an epsilon in place of the gamma-1 heavy-chain constant region. We describe the physical characterisation and ligand binding properties of the trastuzumab IgE and elucidate its potential anti-tumour activities in functional assays. Both trastuzumab and trastuzumab IgE can activate monocytic cells to kill tumour cells, but they operate by different mechanisms: trastuzumab functions in antibody-dependent cell-mediated phagocytosis (ADCP), whereas trastuzumab IgE functions in antibody-dependent cell-mediated cytotoxicity (ADCC). Trastuzumab IgE, incubated with mast cells

Panagiotis Karagiannis and Josef Singer contributed equally to this work.

Electronic supplementary material The online version of this article (doi:10.1007/s00262-008-0607-1) contains supplementary material, which is available to authorized users.

P. Karagiannis · F. O. Nestle · S. N. Karagiannis (✉)
Cutaneous Medicine and Immunotherapy Unit,
St. John's Institute of Dermatology,
Division of Genetics and Molecular Medicine,
King's College London School of Medicine, 9th Floor,
Guy's Tower, Guy's Hospital, London SE1 9RT, UK
e-mail: sophia.karagiannis@kcl.ac.uk

J. Hunt · S. K. E. Gan · P. S. Hobson · A. J. Beavil · H. J. Gould
Randall Division of Cell and Molecular Biophysics,
King's College London, 3rd Floor, New Hunt's House,
Guy's Campus, London SE1 1UL, UK

S. M. Rudman · J. Spicer
Department of Academic Oncology, King's College London,
3rd Floor, Bermondsey Wing, Guy's Hospital,
London SE1 9RT, UK

T. R. Daniels · M. L. Penichet
Division of Surgical Oncology, Department of Surgery,
David Geffen School of Medicine, University of California,
Los Angeles, USA

M. L. Penichet
Departments of Microbiology, Immunology,
and Molecular Genetics, David Geffen School of Medicine,
University of California, Los Angeles, USA

M. L. Penichet
The Jonsson Comprehensive Cancer Center,
David Geffen School of Medicine, University of California,
Los Angeles, USA

P. Karagiannis · J. Singer · D. Mechtcheriakova · R. Knittelfelder · E. Jensen-Jarolim
IPP, Department of Pathophysiology, Center of Physiology,
Pathophysiology and Immunology,
Medical University Vienna, Waehringer G. 18,
1090 Vienna, Austria

and HER2/*neu*-expressing tumour cells, triggers mast cell degranulation, recruiting against cancer cells a potent immune response, characteristic of allergic reactions. Finally, in viability assays both antibodies mediate comparable levels of tumour cell growth arrest. These functional characteristics of trastuzumab IgE, some distinct from those of trastuzumab, indicate its potential to complement or improve upon the existing clinical benefits of trastuzumab.

Keywords HER2/*neu* · Trastuzumab · IgE · Monocytes · Mast cells · Tumour immunity

Abbreviations

HER2/*neu*	Human epidermal growth factor receptor 2
ADCC	Antibody-dependent cell-mediated cytotoxicity
ADCP	Antibody-dependent cell-mediated phagocytosis
FBP	Folate binding protein
sFcεRIα	Soluble FcεRI α-chain
ECD^{HER2}	HER2 protein extracellular domain
CM	Complete medium
PI	Propidium iodide
CFSE	Carboxy-fluorescein diacetate, succinimidyl ester
NIP	4-Hydroxy-3-nitro-phenacetyl
PI3K	Phosphoinositide 3-kinase
TGF-a	Tumour growth factor α
VEGF	Vascular endothelial growth factor
TNF-α	Tumour necrosis factor-α
MTS	3-(4,5-Dimethylthiazol-2-yl)-5-(3-carboxymethoxyphenyl)-2-(4-sulfophenyl)-2H-tetrazolium inner salt)
PMS	Phenazine methosulfate

Introduction

HER2/*neu* (c-erb-B2) is a 185 kDa protein that belongs to the human epidermal growth factor receptor family. Its functions include engendering cell signalling and regulating cell growth, proliferation, differentiation and motility [1]. Approximately 30% of breast carcinomas as well as other cancers, such as those of the ovary, endometrium, bladder, prostate and lung, over-express HER2/*neu*, whilst its expression in normal tissues is low [2]. Its expression in breast cancer is thought to play a vital role in the pathogenesis of breast tumours and is linked to poor clinical outcomes [3]. This antigen is now a validated target for cancer therapeutics.

Trastuzumab (Herceptin®) is an IgG1 antibody raised against the extracellular domain (ECD) of HER2/*neu* and is the main antibody in clinical use for the treatment of HER2-positive breast cancers [4–6]. Trastuzumab was approved by the FDA in 1998 for the treatment of metastatic HER2/*neu* over-expressing breast cancer and is now also used as adjuvant therapy for early breast cancers. The success of trastuzumab in breast cancer therapy has renewed interest in antibody therapies and provoked further research into the development of therapeutic antibodies. However, only a subset of patients treated with trastuzumab show significant responses and thus there is scope for additional modalities designed to improve clinical outcomes [7].

Trastuzumab is thought to exert anti-tumour effects by a number of mechanisms. The best-defined mechanism is the blocking of the hetero-dimerization of HER2/*neu* receptors with other HER family members (HER1, HER3) on the surface of breast cancer cells thereby switching off vital tumour cell growth signals [8, 9]. Trastuzumab inhibits metalloproteinase activity and interferes with signalling via phosphoinositide 3-kinase (PI3 K) pathways, promoting apoptosis and cell cycle arrest during the G1 phase. Another mechanism is thought to be blocking angiogenesis by inducing expression of anti-angiogenic factors such as thrombospondin-1 and suppression of pro-angiogenic factors such as TGF-α, VEGF, angiopoietin-1, and plasminogen-activator inhibitor-1 [10]. Clinical and pre-clinical studies suggest that trastuzumab may also enlist immune effector cells to attack and kill tumour cells by cytotoxicity (ADCC) and phagocytosis (ADCP), and by augmenting chemotherapy-induced cytotoxicity [11–14]. Studies are now focusing on strategies aimed at improving the significant but circumscribed success of trastuzumab. These include optimising antigen specificity or affinity and enhancing antibody-mediated effector cell functions targeted against tumour cells.

Although there are five antibody classes in man, each with distinctive functions in the immune system, trastuzumab, but essentially all monoclonal antibodies approved for clinical use are IgG1 s. Antibodies of the IgG class function most effectively in the circulation [15]. There are many reasons why IgE antibodies might be more effective against tumours that develop in tissues and are therefore inaccessible to IgGs [16]. The concentration of IgE in the serum of normal individuals is minute (<150 ng/mL, 1/10,000 the concentration of IgG) because IgE is sequestered in solid tissues, where it is bound with high-affinity to receptors on its effector and antigen-presenting cells [17]. The affinity of IgE for FcεRI (Ka $\sim 10^{11}$ M^{-1}) is 10^2–10^5 times higher than those of IgGs for their receptors, making IgE the only antibody strongly retained by effector cells in the absence of antigen [17, 18]. The half-life of IgE in tissues (measured in the skin ~2 weeks) is longer than that of IgG (2–3 days) [18, 19]. IgE saturates FcεRI at nM concentrations, but only 10% of the receptors need be occupied by IgE and antigen for full mast cell activation and effector cell

recruitment to the site of antigen challenge in tissues [17, 20]. IgE antibodies on the surface of tissue mast cells are cross-linked by antigens to induce the release of histamines, leukotrienes, proteases, and, importantly, Th2 cell-type cytokines (IL-3, IL-4, IL-5, IL-6, IL-9, IL-13, TNF-α) at the site of antigen challenge. This results in activation of the resident immune effector cells, but also elicits further recruitment and persistence of an inflammatory cell infiltrate, comprising Th2 cells, monocytes, eosinophils and basophils, from the circulation, which enhances and maintains the local immune response [17]. IgE antibodies directed against a tumour-associated antigen would therefore trigger an immediate local effector cell response against tumour cells and stimulate a cascade of inflammation targeted to the tumour cells in situ. These activities could possibly be highly effective in immune rejection of tumours embedded in solid tissues.

Several studies support the ideas IgE antibodies may be highly effective tools in cancer therapy [21–28]. We have previously shown that an antibody of the IgE class is superior to the corresponding IgG1 antibody against folate binding protein (FBP) in prolonging survival of mice in two xenograft models of ovarian cancer [29–32]. Ours and other studies [23, 27, 33–35] have contributed to the suggestion that the antibody class may influence the nature as well as the potency of the immune responses elicited against tumour cells.

In order to examine the mechanisms by which an IgE version of trastuzumab may act in tumour cell killing, we have engineered a humanised trastuzumab IgE. Here, we report the physical characterisation and functional properties of the engineered trastuzumab IgE, and show that these properties are distinct from those of trastuzumab (IgG1). Our data suggests that trastuzumab IgE may potentiate tumour killing by mechanisms and pathways that might be highly effective in cancer therapy.

Materials and methods

Antibodies and reagents

Chimaeric mAbs MOv18 IgE and MOv18 IgG (IgG1 isotype) against the human folate binding protein (FBP), NIP IgE specific for the hapten 4-hydroxy-3-nitro-phenacetyl (NIP) and the recombinant IgE receptor FcεRI alpha (sFcεRIα) were prepared as before [29, 36, 37]. ECD^{HER2}, the soluble human HER2 protein comprising the HER2/*neu* extracellular domain (ECD) (90 kDa) was prepared as previously described [38]. Trastuzumab (Herceptin®) was from Genentech (San Francisco, CA, USA), goat anti-human IgE-FITC was from VECTOR Laboratories Ltd. (Peterborough, UK) and anti-CD89-PE and anti-CD33-APC mAbs were from BD Biosciences (Oxford, UK). Antibodies to Fcε and Fcγ receptors, human IgG isotype-matched control and goat anti-mouse-Ig-FITC Abs were from Dako (Glostrup, Denmark). PI, CFSE, and tissue culture reagents were from Invitrogen (Paisley, UK).

Generation of trastuzumab IgE antibody

The cDNA derived from the protein sequences of the heavy and light chains of the trastuzumab variable regions was synthesised (Gene Art AG, Regensburg, Germany) based on the published protein sequence of trastuzumab (source: http://www.pdb.org; 1n8z) [39]. This cDNA was then cloned into two vectors based on a pTT vector backbone, one containing the epsilon heavy chain of IgE (humighae2, accession no: L00022; Kenten et al. 1982), the other containing the human kappa light chain constant region cDNA (IGKC, accession no: BC110394) [40, 41] (Fig. 1). For full amino acid sequences for trastuzumab IgE see Supplementary Table I (Supplementary Data). For transfection into compatible HEK293 cells, vector DNA was produced using the HiSpeed Plasmid Maxi Kit® (Qiagen®), according to the manufacturer's instructions. HEK293 cells were harvested and seeded at 4×10^5 cells/mL and allowed to adhere before being transfected with 1 μg of DNA with the aid of 2 μg of PEI (Polyethenylenimine, MW: 25 kDa; Polysciences Inc., Warrington, PA, USA) per 4×10^7 cells [40]. Supernatants were harvested 2–4 weeks later and antibodies were purified by affinity chromatography as previously described [29]. Antibody purity was confirmed by HPLC analysis.

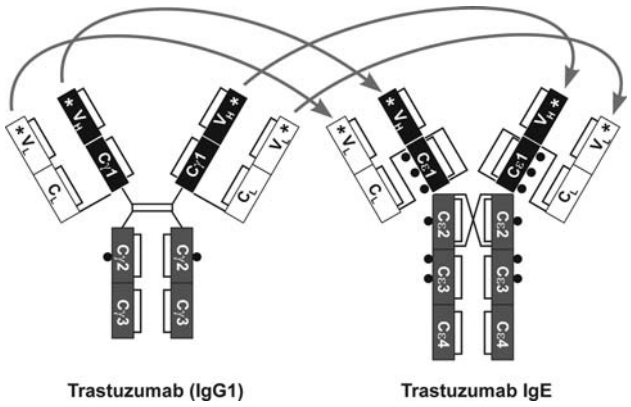

Fig. 1 Schematic representation of the design of trastuzumab IgE antibody. To engineer trastuzumab IgE, the variable heavy and light chains of trastuzumab (IgG1, *left*; regions indicated with *stars*) were inserted into the epsilon heavy chain regions of IgE and the epsilon heavy chain was combined with the kappa light chain to produce the corresponding trastuzumab IgE antibody (*right*). The resulting engineered IgE molecule should recognise the HER2/*neu* antigen and IgE receptors (see Supplementary Table I, Supplementary Data for full sequence). Glycosylation sites are depicted by *black circles*

Kinetic assays of antibody binding to HER2 and FcεRI

Kinetic studies were performed using surface plasmon resonance (SPR) analysis to examine the specificities and binding affinities of trastuzumab (IgG1) and trastuzumab IgE antibodies to the soluble ECD^{HER2} protein and to the soluble high-affinity IgE receptor alpha subunit (sFcεRIα), each immobilised on the biosensor surface. Kinetics of trastuzumab IgE binding to immobilised FcεRIα on the biosensor surface were compared to the well-characterised chimaeric antibody NIP IgE. All experiments were performed at 24°C on a Biacore 3000 instrument (Biacore Int. SA, Switzerland). Methods and kinetic analysis have been described previously [36, 42, 43]. In these experiments, antibodies were tested at a concentration range of 125–7.8 nM, coupling density was typically restricted to 200RU, flow rate 20 μL/min, and exposure time to analyte 360 s.

Cell culture

The human monocytic cell line U937 [44] (kindly provided by Prof. J.-P. Kinet, Harvard University, Boston, MA, USA) was grown in RPMI 1640 medium, 10% FCS, 2 mM l-glutamine, penicillin (5,000 U/mL) and streptomycin (100 μg/mL). The murine colon adenocarcinoma cell lines CT26 [45, 46] and CT26-HER2/*neu*$^{Her2+}$ transfected with the HER2/*neu* antigen [47] were grown in Iscove's medium (IMDM), 5% FCS, 2 mM l-glutamine, penicillin (5,000 U/mL) and streptomycin (100 μg/mL). The human breast adenocarcinoma cell line SKBR3 (ATCC, No. HTB-30), that naturally expresses the HER2/*neu* antigen, was grown in DMEM, 10% FCS, 2 mM l-glutamine, penicillin (5,000 U/mL) and streptomycin (100 μg/mL). The rat basophilic leukaemia mast cell line RBL-SX38 [48] (Prof. J.-P. Kinet, Harvard University, Boston, MA, USA) expresses the human form of the FcεRI receptor and was maintained in MEM supplemented with 10% FCS, 250 μg/mL Geneticin, 2 mM l-glutamine, penicillin (5,000 U/mL) and streptomycin (100 μg/mL). All cells were maintained at 37°C in 5% CO_2.

Flow cytometric assessments of antibody binding to receptors on cells

For flow cytometric assessments of antibody binding to the tumour-associated antigens FBP and HER2/*neu* and to Fcε (IgE) and Fcγ (IgG) receptors on receptor-expressing cells, cells were incubated with 0.5 μg/mL mAbs for 30 min at 4°C, followed by two washes in FACS buffer (PBS, 5% normal goat serum). Cells were then given anti-human IgE-FITC or anti-human IgG-FITC (10 μg/mL) for 30 min at 4°C, washed in FACS buffer and fixed in 1% paraformaldehyde-FACS buffer prior to acquisition and analysis on a dual laser FACSCalibur™ (BD Biosciences). For quantitative assessments of Fcε and Fcγ cell surface receptors, 2×10^5 U937 cells/sample were stained with mouse mAbs by indirect immunofluorescence using the QIFIKIT® (Dako). U937 cells, setup beads and calibration beads were given goat anti-mouse IgG-FITC, followed by two washes in FACS buffer and analysis by flow cytometry on a FACSAria II flow system (BD Biosciences). The numbers of receptors per cell were calculated against fluorescent calibrating bead standards using linear regression.

Flow cytometric ADCC/ADCP assay

Treatment of tumour cells

We employed our previously described novel three-colour flow cytometric assay to simultaneously measure tumour cell cytotoxicity (ADCC) and phagocytosis (ADCP) of HER2/*neu*-positive tumour cells by human effector cells [30, 31, 49]. CT26-HER2/*neu* or SKBR3 cells were stained 24 h prior to assays with 7.5 μM CFSE in PBS for 10 min at 37°C, washed in RPMI 1640 medium, 10% FCS, 2 mM L-glutamine, and returned to normal culture conditions. The following day, CFSE-labelled tumour cells were washed, mixed with unstained effector cells at E:T ratio of 2:1 with or without antibodies, followed by incubation for 2.5 h at 37°C. Antibodies were tested at concentrations of 0.05, 0.5 and 5 μg/mL.

Three-colour flow cytometric assay setup

CFSE-labelled tumour cells were detected in FL1 (530/30 nm band pass filter), PE-labelled monocytic effector cells in FL2 (582/42 nm band pass filter) and PI^+ dead cells in FL3 (670 nm LP band pass filter) channels, whilst control samples were set for compensation adjustments between fluorochromes. Two dual colour flow cytometric dot plots were generated to calculate ADCC and ADCP as previously described [30, 31, 49]. Briefly, one dot plot depicted CFSE + tumour cells and PI + cells, allowing quantitation of tumour targets killed externally by effector cells (ADCC, cytotoxicity) (CFSE +/PI + cells). The second dot plot depicted CFSE + tumour cells and CD89-PE + effector cells in order to quantitate total CFSE + tumour cells and the number of tumour cells present within PE + effector cells, depicting phagocytosis (ADCP) by effector cells (CFSE +/PE + cells) [49]. This dot plot would also indicate any non-specific uptake of CFSE fluorescence by PE + U937 effector cells.

Confocal imaging of cell contact and antibody-mediated tumour cell phagocytosis

U937 monocytes, which served as effector cells, were incubated on Lab-Tec II glass chamber slides (SLS Ltd,

Manchester, UK) with CFSE-labelled CT26-HER2/*neu* tumour cells at an original E:T ratio of 2:1. Treatments were performed as above. Mixed cell cultures were incubated for 3 h with MOv18 IgG, MOv18 IgE, trastuzumab (IgG1) or trastuzumab IgE antibodies. At the end of the incubations, cells were then given anti-CD33-APC for 40 min at 4°C, to label monocytic cells. Cells were then washed, fixed in 4% paraformaldehyde-FACS buffer and mounted with fluorescence preserver (Dako). Fluorescence microscopy was performed on a Zeiss Axiovert 200 confocal microscope (63 × oil immersion objective). Acquisition and analysis was performed with UltraView software (PerkinElmer, Waltham, MA, USA).

In vitro degranulation assays

The ability of the engineered trastuzumab IgE to trigger degranulation was measured in vitro using the rat basophilic mast cell line RBL-SX38. This cell line expresses the human form of the FcεRI receptor as a $\alpha\beta\gamma_2$ tetramer, the form naturally expressed on the surface of human mast cells [48, 50, 51]. For degranulation experiments cells were plated at 2×10^4 per well in 100 µL in 96 well flat-bottomed tissue culture plates and incubated overnight at 37°C in a humidified CO_2 incubator. The following day, cells were sensitised with IgE diluted in culture medium at 100 ng/mL, incubated for two hours at 37°C and washed twice with HBSS, 1% BSA (wash buffer). Cell degranulation was triggered for 30 min either with 100 µL of anti-human IgE polyclonal rabbit mAb (Dako) (final concentration: 100 ng/mL), or HER2/*neu*-expressing CT26 cells added at different concentrations (1×10^3 to 5×10^5 per well) in wash buffer at 37ºC. Degranulation was terminated by placing the cells on ice and the supernatants removed for quantification of mediator release. Control supernatants were either from individual or mixed cell populations alone treated with no antigen for background release, or wash buffer plus 0.1% Triton-X-100 (Tx) for total release. Degranulation was measured by quantification of β-hexosaminidase release, assayed using a fluorogenic substrate (4-methylumbelliferyl-*N*-acetyl-β-D-glucosaminide) prepared according to a standard protocol [51, 52]. Supernatants were incubated in black 96 well plates with an equal volume of substrate at 37°C for 2 h and quenched with 0.5 M Tris. Fluorescence was measured using a Thermo Fluoskan II fitted with a 350 nm excitation and a 450 nm emission filters. All measurements were made in triplicate for each concentration and release was expressed as a percentage of total content determined by treatment with 0.1% Triton-X-100 solution in HBSS, 1% BSA. Background release, subtracted from all values, was always <10% of total release.

Cell viability assay

Tumour cell viability was analysed by the MTS assay (tetrazolium compound 3-(4,5-dimethylthiazol-2-yl)-5-(3-carboxymethoxyphenyl)-2-(4-sulfophenyl)-2H-tetrazolium inner salt) using phenazine methosulfate (PMS) as a reducing agent (CellTiter 96® AQueous One Solution Cell Proliferation Assay kit, Promega, Southampton, UK). Cells were seeded in 96-well plates at 4×10^4 cells per well and allowed to adhere overnight under standard culture conditions prior to assays. Cells were exposed to 0.5 µg/mL trastuzumab, trastuzumab IgE, MOv18 IgG or MOv18 IgE antibodies over a period of 4, 24, and 48 h. Control groups received media alone, or 0.9% v/v Triton-X-100 for 30 min prior to addition of MTS. Following treatments, MTS/PMS solution prepared according to the manufacturer's instructions were added at 20 µL per well and cells were incubated for a further 1 h prior to recording absorbance at 490 nm with a 96-well plate reader. The quantity of formazan product as measured by the amount of 490 nm absorbance is directly proportional to the number of living cells in culture.

Data handling and statistical analysis

In surface plasmon resonance assays, mean values ±SD were calculated from three measurements. Flow cytometry experiments of receptor binding and blocking were repeated at least three times. In vitro ADCC/ADCP assays were performed in triplicate and data are shown as mean ADCC ± SD and ADCP ± SD of a number (n) of independent experiments (see Supplementary Table II in Supplementary Data). Statistical analyses of in vitro ADCC/ADCP assays and microscopic measurements of effector-tumour cell interactions were performed by means of the unpaired two-tailed Student's t test, and significance was accepted at $P < 0.05$.

Results

Binding of trastuzumab IgE to antigen and FcεRI

We have compared the kinetics of binding of the engineered trastuzumab IgE and trastuzumab (IgG1) to HER2/*neu* ECD^{HER2} immobilised on a biosensor surface by surface plasmon resonance (Fig. 2a; Table 1). The two antibodies exhibited similar rates of association and dissociation from their complexes with ECD^{HER2} (k_a, k_d, mean ± SD, Table 1). These data demonstrate that trastuzumab IgE exhibits the expected interaction with ECD^{HER2}, and the calculated affinity values of both trastuzumab IgE and IgG1 (Ka of 10^{10}) are similar to those

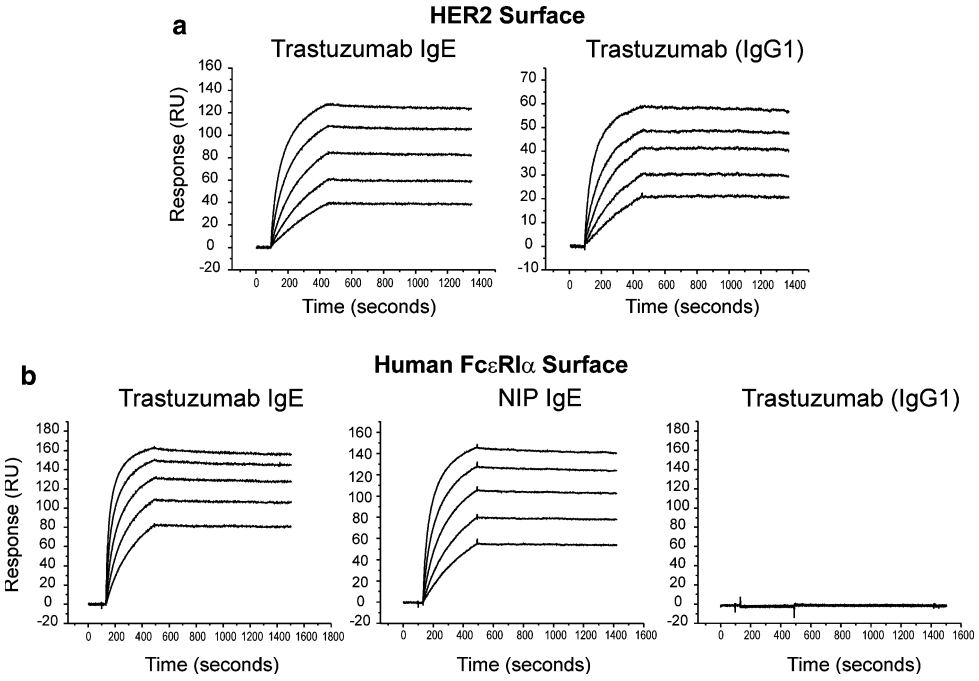

Fig. 2 Comparative SPR analysis of trastuzumab IgE and trastuzumab (IgG1) kinetics of binding to immobilised HER2 receptor ECD^{HER2} (**a**) and to immobilised FcεRIα (**b**). Data were recorded using a Biacore 3000 (flow rate 20 μL/min). Antibodies were tested at concentrations ranging from 125 to 7.8 nM. All values derived from the fitting procedures are given in Table 1

Table 1 Calculated kinetic values of trastuzumab IgE binding to HER2 and FcεRI

Constant	ECD^{HER2} surface		sFcεRIα surface	
	Trastuzumab IgE	Trastuzumab (IgG1)	Trastuzumab IgE	NIP IgE
k_a (M^{-1} s^{-1})	$(3.5 \pm 1.4) \times 10^5$	$(7.3 \pm 3.5) \times 10^5$	$(4.8 \pm 2.3) \times 10^5$	$(2.3 \pm 1.1) \times 10^5$
k_d (s^{-1})	$(2.4 \pm 0.3) \times 10^{-5}$	$(1.8 \pm 0.9) \times 10^{-5}$	$(2.3 \pm 0.5) \times 10^{-5}$	$(2.6 \pm 0.5) \times 10^{-5}$
Ka (M^{-1})	1.5×10^{10}	4.2×10^{10}	2.1×10^{10}	1.0×10^{10}

Kinetic parameters and affinity constants derived from the SPR analysis of NIP IgE and trastuzumab IgE binding to immobilised sFcεRIα and trastuzumab (IgG1) and trastuzumab IgE binding to immobilised ECD^{HER2}. Both IgEs and trastuzumab were analysed using a 1:1 model of association from which association and dissociation constants were derived for each component (shown ± SD for at least five determinations in the concentration range 125–7.8 nM)

previously reported for the IgG1 [6, 53]. Comparison of sensograms representing binding of trastuzumab IgE and the chimaeric NIP IgE to the immobilised soluble alpha-chain of FcεRI (sFcεRIα) demonstrates that both antibodies bind to the high-affinity IgE receptor with the expected kinetics and affinity (k_a, k_d, mean ± SD; Fig. 2b; Table 1). In particular, both antibodies demonstrate the documented slow dissociation rate that is characteristic of the complex of IgE with FcεRI (Fig. 2b) [36, 42, 43]. As expected, trastuzumab (IgG1) did not bind to the IgE receptor (Fig. 2b, right panel).

Trastuzumab interaction with receptors on monocytic effector and tumour cells

Flow cytometric assessments of trastuzumab and trastuzumab IgE interactions with HER2/*neu* and Ig (Fcγ and Fcε) receptors on the surface of cells served two purposes. The first was to confirm that the antibodies recognise their native receptors as presented on cell surfaces. The second was to explore the mechanisms employed by trastuzumab and trastuzumab IgE together with human monocytic cells to target and kill HER2/*neu* receptor-expressing tumour cells. For this, we analysed the interactions of these antibodies with U937 monocytic cells, which served as effector cells, and with the CT26 cells transfected to express the human HER2/*neu* receptor on the cell surface (CT26-HER2/*neu*) [46], used as target cells.

The expression of IgG receptors FcγRI, FcγRII and FcγRIII and of IgE receptors FcεRI and CD23 on U937 cells were also measured (Table 2). U937 monocytes express FcγRI (~12,000 molecules per cell) and FcγRII (~19,000 molecules per cell) but very low levels of FcγRIII (~700 molecules per cell). In agreement with our previously published data [30], we measured approximately 22,000 molecules of FcεRI are expressed per cell, whilst the expression of CD23 was low (~2,200 molecules/cell).

Consistent with the abundant expression of Fcγ receptors on the surface of U937 cells, trastuzumab bound to Fcγ receptors expressed on the surface of 99.8% of U937 mono-

Table 2 Quantification of IgE and IgG Receptors on U937 Monocytes

Surface antigen	Number of molecules per cell (mean ± SD) ($n = 9$)
CD23	$2.2 \times 10^3 \pm 1.3 \times 10^3$
FcεRI	$21.8 \times 10^3 \pm 4.8 \times 10^3$
FcγRI	$12.1 \times 10^3 \pm 3.9 \times 10^3$
FcγRII	$19.0 \times 10^3 \pm 3.9 \times 10^3$
FcγRIII	$0.7 \times 10^3 \pm 0.4 \times 10^3$

cytic cells (Fig. 3a, upper left), as did the chimaeric antibody MOv18 IgG, specific for the ovarian tumour antigen FBP, used as positive control (Fig. 3a, upper right). Trastuzumab also bound to 79.8% of CT26-HER2/*neu* cells (Fig. 3a, bottom left), whilst only background binding of the MOv18 IgG was detected (5.2%) (Fig. 3a, bottom right). These data confirm the specificity of the antibody for the human HER2/*neu* antigen expressed on the surface of tumour cells as well as to the Fcγ receptors expressed by monocytic cells.

Trastuzumab-mediated killing of tumour cells

We employed our previously developed three-colour flow cytometric assay to simultaneously measure trastuzumab ADCC and ADCP of HER2/*neu*-expressing tumour cells [49] (Fig. 3b, c). The CT26-HER2/*neu* cells were used as tumour targets and human U937 monocytes were employed to provide effector cells. The green-fluorescent dye CFSE was used to stain live CT26-HER2/*neu* cells prior to incubation with U937 monocytes and, after the incubation, U937 cells were stained with anti-CD89-PE and dead cells with propidium iodide (PI). Two colour flow cytometric dot plots show that after 2.5 h in culture, U937 cells mixed with trastuzumab and CT26-HER2/*neu* mediated little ADCC above that seen with samples incubated with the MOv18 IgG (5.3 vs. 4.8%; Fig. 3b, top panels, top right boxes for double positive CFSE +/PI + cells). Two-colour flow cytometric dot plots also showed that incubation with trastuzumab induced appreciable tumour cell ADCP compared to control MOv18 IgG (30.6 vs. 4.9%; Fig. 3b, bottom panels; top right boxes for double positive CFSE +/PE + cells). Flow cytometric ADCC/ADCP assay measurements confirmed that trastuzumab at an optimal concentration of 0.5 μg/mL mediated significant levels of ADCP of CT26-HER2/*neu* tumour cells by monocytic cells. Levels of ADCP increased ~10% above those of the MOv18 IgG and no antibody controls (Fig. 3c and Supplementary Table II, Supplementary Data). Statistically significant levels of ADCC were not measured with any of the conditions tested here (Supplementary Table II, Supplementary Data). These data suggest that trastuzumab-IgG1 mediates ADCP, but not ADCC of tumour cells by monocytic cells.

Cell viability assays demonstrated that CT26-HER2/*neu* tumour cells were susceptible to the anti-proliferative effects of trastuzumab (IgG1). These effects were detected after 24 h (89 vs. 96.6% cell viability for trastuzumab and MOv18 IgG, respectively) and 48 h incubation (87.5 vs. 104.5% cell viability for trastuzumab and MOv18 IgG, respectively). No cell growth arrest was detected with trastuzumab after exposure to antibody for 4 h (104.6 and 100% viability for trastuzumab and MOv18 IgG, respectively (Supplementary Fig. 1, Supplementary Data). This confirmed that tumour cell death measured with the ADCC/ADCP assays after 3 h exposure to antibodies was not the result of receptor hetero-dimerisation blocking by trastuzumab alone. Thus, the rapid cell death detected by the ADCC/ADCP assay was most likely mediated by Fcγ receptors on U937 monocytes in combination with trastuzumab.

The tumour-targeting and phagocytic activities of trastuzumab measured in the ADCC/ADCP assays were confirmed by confocal microscopical imaging (Fig. 3d). CT26-HER2/*neu* cells were pre-labelled with CFSE (green), incubated with U937 cells at and E:T ratio of 2:1, combined with antibodies, incubated for 3 h on glass chamber slides, and U937 cells were labelled with anti-CD33-APC mAb (red). In samples incubated with trastuzumab, enhanced contact between CT26-HER2/*neu* tumour cells (green) and U937 monocytic cells (red) was evident, and in many instances two or more monocytic cells were observed in contact with a single tumour cell (Fig. 3d, left, white arrows). We also observed phagocytosis of tumour cells, clearly visible in the merged image of the green tumour cells inside the red U937 cells: most monocytic cells in contact with tumour cells appeared to contain tumour cell material (Fig. 3d, left; white arrows). In contrast to these observations, neither contact nor phagocytosis were observed in samples given MOv18 IgG examined after 3 h in the same culture conditions (Fig. 3d, right). To confirm the microscopic observations, the frequency of interactions between effector and target cells were measured (Table 3). Incubation with trastuzumab led to enhanced contact (24.5% of tumour cells) between tumour and U937 monocytes after 3 h compared to 7.9% contact observed in samples incubated with MOv18 IgG. Most of the U937 monocytes in contact with tumour cells contained tumour cell material (20.4% of tumour cells), suggesting tumour cell phagocytosis, rarely seen with MOv18 IgG (3.5%). Findings from microscopic observations and measurements of cell-cell interactions are in agreement with our ADCC/ADCP assays suggesting that trastuzumab mediated tumour cell killing by phagocytosis.

Trastuzumab IgE interaction with HER2/*neu* and IgE receptors on monocytic effector cells and tumour cells

We analysed the interactions of trastuzumab IgE with its Fcε receptors on U937 monocytic cells and with human

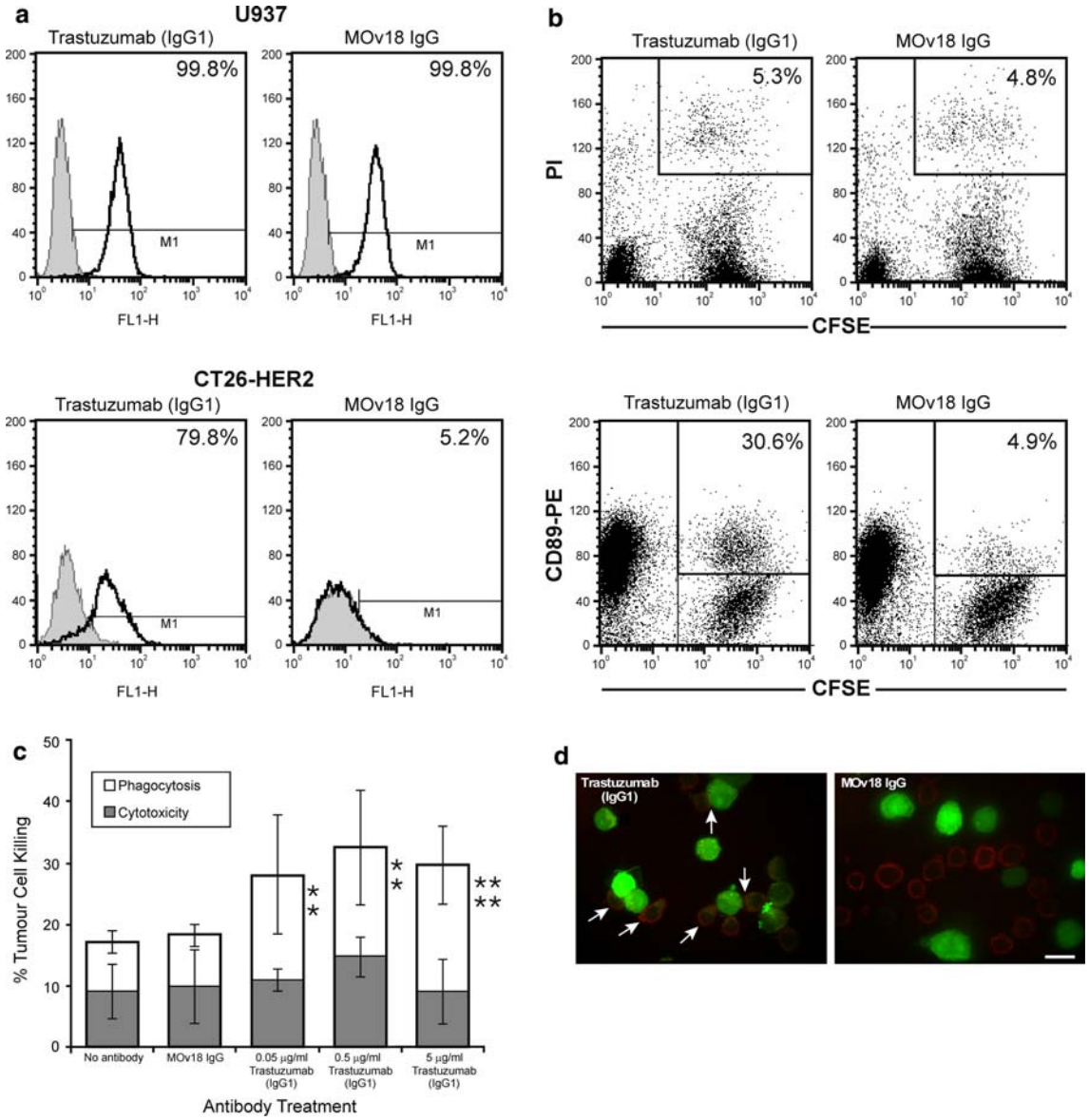

Fig. 3 **a** Flow cytometric analysis of binding to Fcγ receptor-expressing U937 monocytic cells for trastuzumab (IgG1) (*top left*) and the chimaeric MOv18 IgG antibody against the ovarian cancer antigen FBP (*top right*). Flow cytometric analysis of binding to the HER2/*neu* antigen on the surface of CT26-HER2/*neu* cells for trastuzumab (*bottom left*) and the chimaeric MOv18 IgG antibody against FBP (*bottom right*) (Monoclonal antibodies: *solid lines*; secondary antibody controls: *grey histograms*). **b** Trastuzumab-mediated killing of CT26-HER2/*neu* tumour cells by U937 monocytes: two-colour flow cytometric dot plots detected no ADCC but appreciable ADCP after 2.5 h in culture. CFSE-labelled tumour cells (*x*-axis) and dead tumour cells labelled with Propidium Iodide (PI) (*y*-axis), double-positive cells depict tumour cells killed by ADCC ($CFSE^+/PI^+$, *upper right boxes*, values are % ADCC) (*top*). CFSE-labelled tumour cells phagocytosed by U937 cells labelled with CD89-PE mAb (*y*-axis, *upper left*), double positive cells, $CFSE^+/PE^+$ (*upper right boxes*, values are % ADCP) (*bottom*). **c** Quantification of trastuzumab-mediated CT26-HER2/*neu* tumour cell killing by U937 monocytes after 2.5 h using the ADCC/ADCP assay. Cytotoxicity: *black bars*; phagocytosis: *white bars*. Results are means ± SD of six independent experiments. Significance of values compared to samples given MOv18 IgG (*top*) or no antibody (*bottom*) by the Student's *t* test: $^{n/s}P > 0.05$, $^{*}P < 0.05$, $^{**}P < 0.005$, $^{***}P < 0.0005$. **d** Representative confocal fluorescence images of CT26-HER2/*neu*-U937 interactions potentiated by trastuzumab. CFSE-stained CT26-HER2/*neu* tumour cells (*green*) and CD33-APC labelled U937 cells (*red*) combined at an original E:T ratio of 2:1 and incubated for 3 h in culture. U937 cells (*red*) given trastuzumab IgG (*left*) showed enhanced contact with tumour cells (*green*) and phagocytosis of tumour cells (*green* CFSE inside U937 monocytes, *white arrows*). Neither effector-target cell contact nor phagocytosis was observed when cells were incubated with control MOv18 IgG antibody (*right*). Original magnification ×63 (*scale bar* 15 μm)

HER2/*neu* on the surface of CT26-HER2/*neu* cells. Trastuzumab IgE bound to Fcε receptors expressed on the surface of U937 monocytic cells (53.6% of cells) (Fig. 4a, upper left), in a manner indistinguishable from the positive control MOv18 IgE (60.6% of cells) (Fig. 4a, upper right). Lower levels of trastuzumab IgE binding to Fcε receptors,

Table 3 Microscopic Measurements of CT26-HER2/*neu*: U937 Cell Interactions

Antibody	E:T contact (mean ± SD) (%)	CT26-HER2/*neu* phagocytosis (mean ± SD) (%)
Trastuzumab (IgG1)	24.5 ± 10.5**	20.43 ± 9.2***
MOv18 IgG	7.9 ± 11.2	3.5 ± 5.9
Trastuzumab IgE	29.2 ± 13.9***	4.7 ± 5.8 $^{n/s}$
MOv18 IgE	5.1 ± 5.2	2.2 ± 5.1

Data were collected by counting effector: target cell contact or target cell phagocytosis per microscopic field at a magnification of 40× and percentage values were calculated. Mean values were calculated from ten microscopic fields for each condition and are shown ± SD. Student's *t* test was used to generate significance of values compared to samples given the corresponding MOv18

$^{n/s}$ $P > 0.05$; * $P < 0.05$; ** $P < 0.005$; *** $P < 0.0005$

compared to binding of trastuzumab binding to Fcγ receptors, are consistent with lower expression of IgE receptors on U937 cells (Table 2) and our previous findings that MOv18 IgE bound to only a fraction of FcεRI receptors on these cells [30]. Trastuzumab IgE also recognised the HER2/*neu* receptor since it bound to 89.3% of CT26-HER2/*neu* cells (Fig. 4a, bottom left), similarly, to trastuzumab (91.5% cells, Fig. 4a, bottom middle), whilst only background binding of trastuzumab IgE was detected in untransfected CT26 cells, which do not express the HER2/*neu* receptor (5.2%) (Fig. 4a, bottom right). These data confirm the specificity of the engineered IgE antibody for the human HER2/*neu* antigen as well as for the Fcε receptors expressed on the surface of the monocytic cells.

Assessments of the functional properties of trastuzumab IgE

Monocytic cells and IgE-mediated tumour cell killing

We wished to assess whether our engineered trastuzumab IgE was biologically active and thus sought to characterise its biological properties using two functional assays. One related to the ability of this antibody to mediate tumour cell targeting and killing by human effector cells and was assessed using our three-colour flow cytometric ADCC/ADCP assay. As done above for trastuzumab, the CT26-HER2/*neu* cells were used as tumour targets and human U937 monocytes were employed to provide effector cells. Using this method, we observed that incubation of CT26-HER2/*neu* and U937 cells with trastuzumab IgE was associated with increased tumour cell death by cytotoxicity (ADCC) (Fig. 4b, c). This was evident by the increased population of CFSE +/PI + tumour cells in samples incubated with trastuzumab IgE (Fig. 4b, upper right, top right boxes for CFSE +/PI + tumour cells), compared to those with the control MOv18 IgE (18.7 vs. 4.6%; Fig. 4b, upper left). In contrast to trastuzumab, the neither the trastuzumab nor the MOv18 IgE enhanced the phagocytosis of tumour cells, as seen in the double positive CFSE +/PE + cell population (4.7 vs. 4.3%; Fig. 4b, bottom panel, top right boxes for CFSE +/PE + tumour cells). These results also confirmed that phagocytic killing by trastuzumab and U937 monocytes, measured by the ADCC/ADCP assays (Fig. 3), were a result of Fcγ receptor functions of this antibody rather than non-specific uptake of killed tumour cells.

Therefore, flow cytometric ADCC/ADCP assay measurements confirmed that trastuzumab IgE, at an optimal concentration of 0.5 μg/mL mediated significant levels of ADCC of CT26-HER2/*neu* cells by the monocytic cells (Fig. 4c). Levels of ADCC increased by ~10% above those of the MOv18 IgE, tested at the same concentrations, and the no antibody controls (Fig. 4c and Supplementary Table II, Supplementary Data). Statistically significant levels of ADCP were not measured in this assay system ($P > 0.05$; Supplementary Table II, Supplementary Data). These data suggest that trastuzumab IgE mediates tumour killing by a mechanism different from trastuzumab, directing monocytes to act in ADCC instead of ADCP against the tumour cells.

Interestingly, the antibody concentration (0.5 μg/mL) required to achieve maximum tumour cell killing by monocytes in these assays was the same for IgG and IgE (Fig. 3c, Fig. 4c and Supplementary Table II, Supplementary Data). Furthermore, when compared directly in ADCC/ADCP assays, the two IgE antibodies mediated similar levels of total tumour cell killing (35% of tumour cells by IgE vs. 36% of tumour cells by IgG; Table 4). Our data show that IgE is as effective as IgG in recruiting monocytes to kill tumour cells in vitro and warrant further studies to compare the anti-tumour effector cell functions of these antibodies in vivo.

Trastuzumab IgE-mediated interactions of monocytic and tumour cells

The tumour-targeting activities of trastuzumab IgE measured in the ADCC/ADCP assays were studied by confocal microscopical imaging (Fig. 4d). CT26-HER2/*neu* cells were pre-labelled with CFSE (green), incubated with U937 cells, combined with antibodies for 3 h on glass chamber slides, and U937 cells were labelled with anti-CD33-APC (red). In samples incubated with trastuzumab IgE, contact between CT26-HER2/*neu* tumour cells and U937 monocytic cells, was clearly evident, and two or more monocytic cells were frequently observed in contact with or in close proximity to a single tumour cell (Fig. 4d, left; white arrows). However, in contrast to our observations with

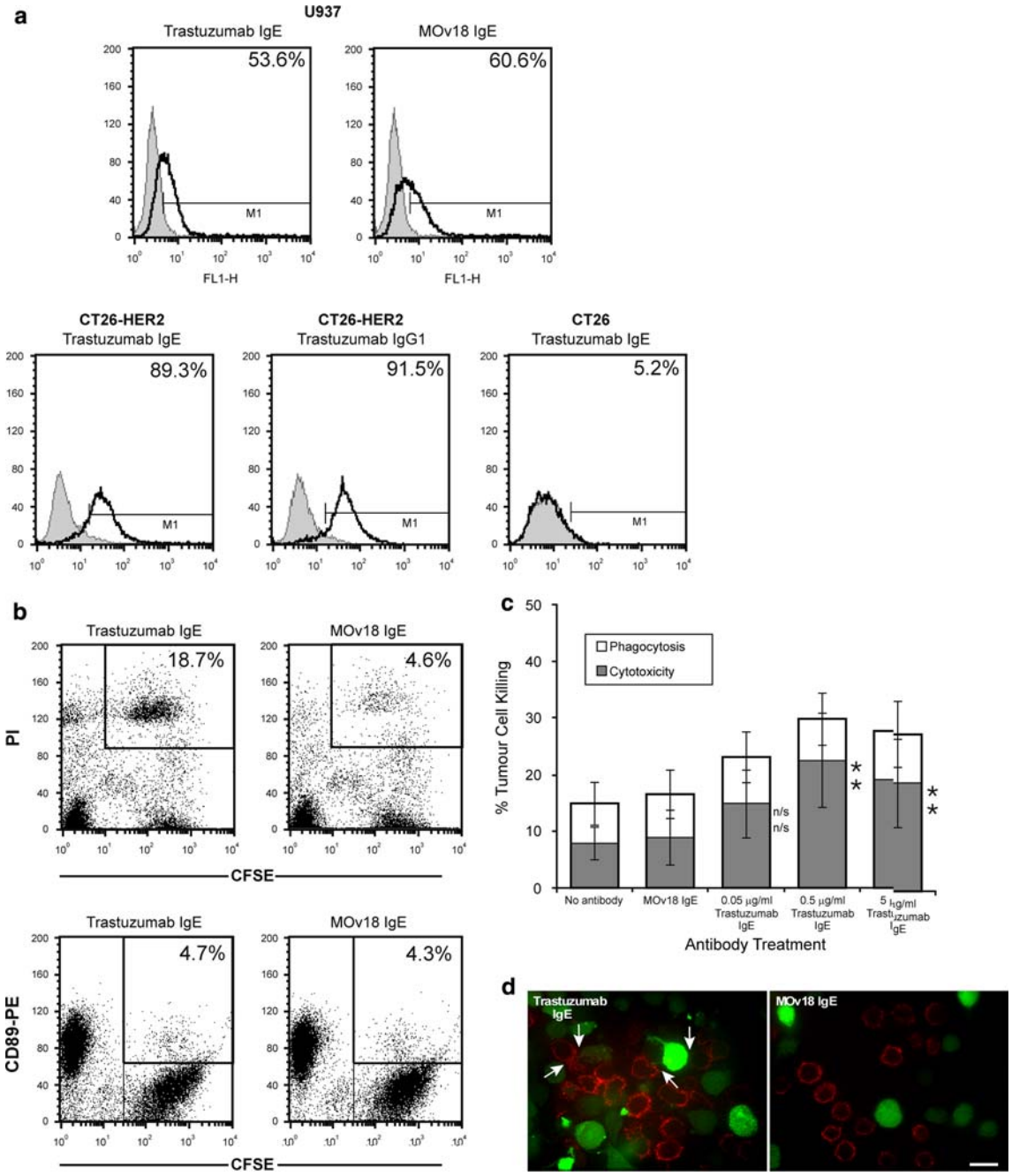

Fig. 4 **a** Flow cytometric analysis of binding to IgE receptor-expressing U937 monocytic cells for trastuzumab IgE (*top left*) and the chimaeric MOv18 IgE antibody against the ovarian cancer antigen FBP (*top right*). Flow cytometric analysis of trastuzumab IgE (*bottom left*) and trastuzumab (IgG1) antibody (*bottom middle*) binding to the HER2/*neu* antigen on the surface of HER2/*neu*-expressing CT26-HER2/*neu* cells, and lack of trastuzumab IgE binding to HER2/*neu*-negative CT26 tumour cells (*bottom right*). (Monoclonal antibodies: *solid lines*; secondary antibody controls: *grey histograms*). **b** Trastuzumab IgE-mediated killing of CT26-HER2/*neu* tumour cells by U937 monocytes: two-colour flow cytometric dot plots detected ADCC but no ADCP after 2.5 h in culture. CFSE-labelled tumour cells (*x*-axis) and dead tumour cells labelled with Propidium Iodide (PI) (*y*-axis), double-positive cells depict tumour cells killed by ADCC ($CFSE^+/PI^+$, *upper right boxes*, values are % ADCC) (*top*). CFSE-labelled tumour cells phagocytosed by U937 cells labelled with CD89-PE mAb (*y*-axis) are double positive $CFSE^+/PE^+$ cells (*upper right boxes*, values are % ADCP) (*bottom*). **c** Quantitation of trastuzumab IgE-mediated CT26-HER2/*neu* tumour cell killing by U937 monocytes after 2.5 h using the ADCC/ADCP assay, at different antibody concentrations. Cytotoxicity: *black bars*; phagocytosis: *white bars*. Results are mean ± SD of five independent experiments. Significance of values compared to samples given MOv18 IgE (*top*) or no antibody (*bottom*) by the Student's *t* test: $^{n/s}P > 0.05$, $^{*}P < 0.05$, $^{**}P < 0.005$, $^{***}P < 0.0005$. **d** Typical confocal fluorescence images of CT26-HER2/*neu*-U937 interactions potentiated by trastuzumab IgE. CFSE-stained CT26-HER2/*neu* tumour cells (*green*) and anti-CD33-APC labelled U937 cells (*red*) combined at an original E:T ratio of 2:1 and incubated for 3 h in culture. U937 cells (*red*) given trastuzumab IgE (*left*) exhibited enhanced contact with tumour cells (*green*) but no phagocytosis of tumour cells was observed (no *green* CFSE fluorescence detected inside U937 cells; *white arrows*). No effector-target cell contact was observed when cells were incubated with control MOv18 IgE antibody (*right*). Original magnification ×63 (*scale bar* 15 µm)

Table 4 % Total tumour cell death by U937 monocytes and antibodies

Antibody	Tumour cell death ± SD ($n = 6$) (%)
No ab	12.5 ± 3.1
MOv18 IgG	18.5 ± 6.6
Trastuzumab (IgG1) 0.5 μg/mL	36.1 ± 2.2 (***)(***)
MOv18 IgE	19.8 ± 3.2
Trastuzumab IgE 0.5 μg/mL	34.8 ± 3.5 (***)(***)(n/s)

Significance comparing trastuzumab (IgG1) and trastuzumab IgE to samples given no antibody (left brackets), MOv18 IgG/IgE (middle brackets) and significance comparing trastuzumab (IgG1) to trastuzumab IgE (right bracket)

Comparisons by the Student's t test: (n/s)$P > 0.05$; (*)$P < 0.05$; (**)$P < 0.005$; (***)$P < 0.0005$

trastuzumab, trastuzumab IgE did not appear to enhance phagocytosis, since no green tumour material was observed inside the red U937 cells (Fig. 4d, left). As expected, rare contact was observed with the control antibody MOv18 IgE, examined in the same culture conditions (Fig. 4d, right). Measurements of interactions between effector and target cells (Table 3) showed that trastuzumab IgE mediated enhanced effector: target cell contact (29.2% of tumour cells) after 3 h, compared to 5.1% contact in samples given MOv18 IgG. A very small proportion of the U937 monocytes in contact with tumour cells contained tumour cell material (4.7% of tumour cells), suggesting little tumour cell phagocytosis was mediated by trastuzumab IgE. Microscopic observations and measurements of effector: tumour cell interactions are in agreement with our ADCC/ADCP assays and are consistent with a role for trastuzumab IgE in mediating tumour cell death by cytotoxicity.

Trastuzumab IgE activity in mast cell degranulation assays

The second functional assay examined the capacity of trastuzumab IgE to stimulate mast cells by way of the high-affinity IgE receptor FcεRI, and trigger their degranulation. This is a test of the potency of IgE to activate these effector cells, and occurs only following cross-linking of FcεRI-bound IgE by multivalent antigen, by anti-human IgE polyclonal antibodies or by antigen-expressing target cells. We used a previously established system, designed to evaluate the functional activities of IgE antibodies [48]. The assay utilises the rat basophilic mast cell line RBL-SX38, transfected to express all four subunits ($\alpha\beta\gamma_2$) of human FcεRI [48]. Flow cytometric evaluations confirmed that trastuzumab IgE bound to cell surface FcεRI of the RBL-SX38 cells (45.3% of cells), similar to the previously characterised chimaeric MOv18 IgE (Fig. 5a). To assess the ability of trastuzumab IgE to cause degranulation of RBL-SX38 cells, we measured β-hexosaminidase release upon cell stimulation and cross-linking by tumour cells (Fig. 5b). Mast cells alone and mast cells stimulated with trastuzumab IgE in the absence of cross-linking by anti-IgE antibody, triggered minimal mast cell degranulation [54]. Mast cells stimulated with trastuzumab IgE in the presence of anti-IgE antibody triggered a strong degranulation response (~40%), compared to negligible degranulation measured with controls.

We also examined whether the engineered trastuzumab IgE cross-linked by HER2/*neu*–expressing tumour cells was capable of stimulating mast cells in an antigen-dependent manner. Trastuzumab IgE induced strong degranulation of RBL-SX38 cells following stimulation with CT26-HER2/*neu* cells, which express HER2/*neu,* whilst untransfected CT26, which do not express HER2/*neu*, did not potentiate β-hexosaminidase release (Fig. 5b). Furthermore, CT26-HER2/*neu* tumour cells with trastuzumab IgE potentiated significant β-hexosaminidase release that was decreased proportionally to the decreasing number of tumour cells per sample. These results clearly demonstrate the functional activity of trastuzumab IgE-CT26-HER2/*neu* cells in triggering mast cell activation and mediator release, and confirm that the IgE possesses biological activities that could be specifically directed against HER2/*neu*-expressing tumour cells in cancer patients.

Trastuzumab IgE targeting of SKBR3 breast cancer cells

ADCC/ADCP assays using the human breast adenocarcinoma cell line SKBR3, which naturally express the HER2/*neu* antigen, confirm that trastuzumab and trastuzumab IgE can focus U937 effector cells to kill SKBR3 cells (Fig. 6). As with CT26-HER2/*neu* cells (Figs. 3, 4), trastuzumab acted in ADCP of tumour cells (Fig. 6a) whilst trastuzumab IgE killed by ADCC (Fig. 3b). These findings demonstrate the functional properties of trastuzumab IgE focusing effector cell functions against native HER2/*neu*-expressing breast tumour cells.

Since trastuzumab (IgG1) can potentiate anti-tumour effects by blocking hetero-dimerisation of HER2/*neu* receptors with other HER family members on the surface of breast cancer cells, switching off tumour cell growth signals [8, 9], the anti-proliferative properties of the engineered trastuzumab IgE were examined using the MTS cell viability assay (Fig. 6c). Neither trastuzumab nor trastuzumab IgE had any anti-tumour growth effects after 4 h incubation with SKBR3 cells (99.3 and 98.6% viability for IgG and IgE, respectively). Decreased tumour cell viability was measured after 24 h (88.3 and 83.6% for IgG and IgE, respectively) and more prominent effects were measured after 48 h exposure of tumour cells to the antibodies (72.2 and 64.0% for IgG and IgE, respectively). Control MOv18 IgG and MOv18 IgE antibodies did not affect SKBR3 cell viability (mean values ranging from 93.0 to 103.8% viability).

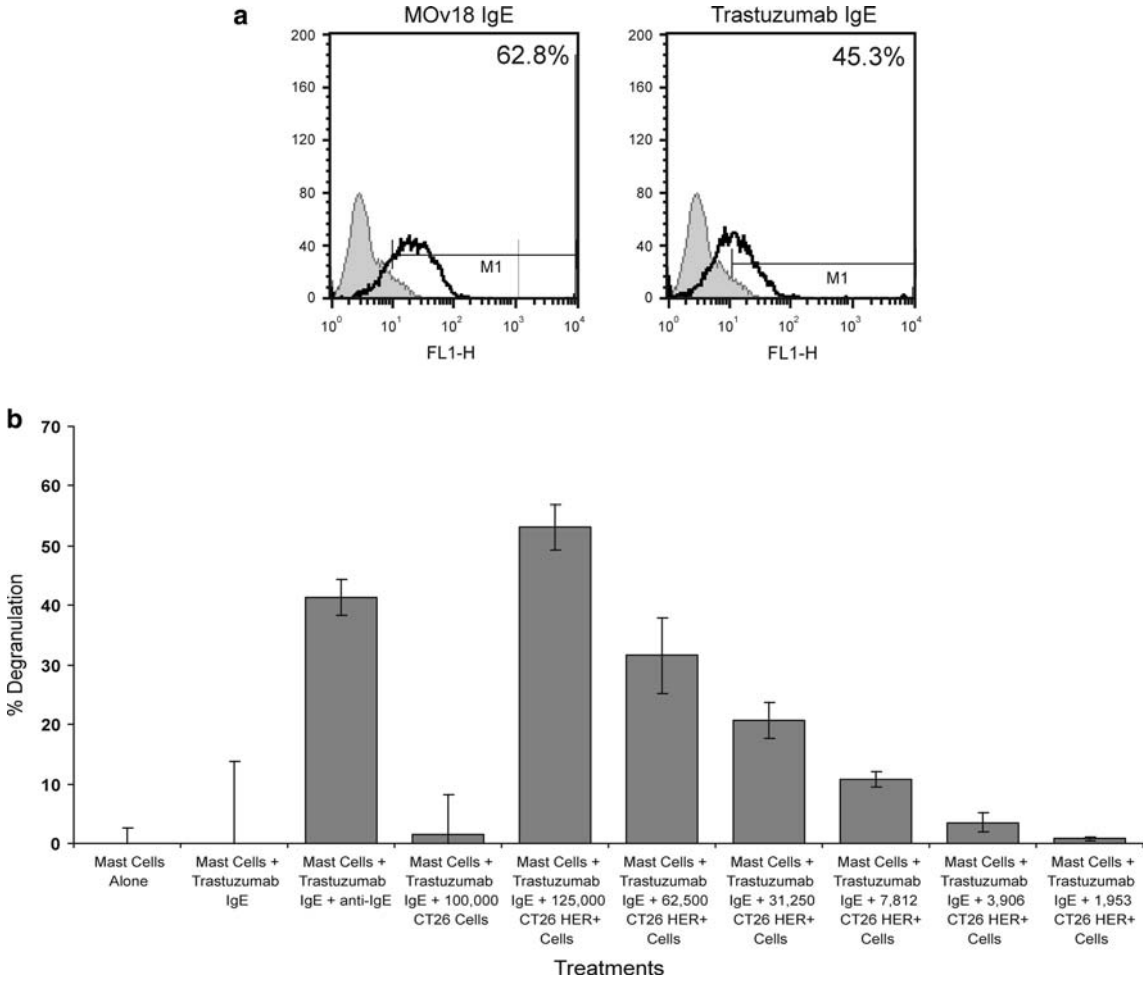

Fig. 5 **a** Flow cytometric analysis of MOv18 IgE (*left*) and trastuzumab IgE (*right*) binding to human FcεRI receptor-expressing RBL-SX38 cells. (Monoclonal antibodies: *solid lines*; secondary antibody controls: *grey histograms*). **b** Effects of trastuzumab IgE cross-linking on mast cell degranulation. Cells alone or sensitised with trastuzumab IgE, CT26 tumour cells or CT26-HER2/*neu* tumour cells at different concentrations. Trastuzumab IgE was cross-linked with anti-IgE polyclonal antibody to confirm its mast cell degranulation activity. Degranulation was monitored by β-hexosaminidase activity released into culture supernatants in all experiments. Data are mean ± SD of three measurements in a representative of three different experiments with similar results

These data strongly suggest that trastuzumab IgE possesses similar properties to trastuzumab in blocking tumour growth after 24 and 48 h in culture.

Discussion

In our previous studies, we reported the anti-tumour activities of MOv18 IgE, a chimaeric antibody against the ovarian tumour-associated antigen FBP, compared to the corresponding antibody of the IgG class [29–32, 49]. Our studies now form part of a growing body of evidence suggesting that IgE antibodies may have a role in cancer therapy [21–23, 27, 28, 33–35, 55]. The emergence of the human epidermal growth factor receptor HER2/*neu* as a well-validated target for cancer therapeutics [1–4] and the well-documented but circumscribed success of the humanised anti-HER2/*neu* IgG1 antibody trastuzumab, approved for the treatment of breast cancer [5–7], rendered the proposition to produce an IgE equivalent moiety timely and relevant in the field of biological therapeutics for cancer. For this, we have engineered a humanised trastuzumab IgE antibody and here we describe the binding characteristics and biological properties of this molecule.

The kinetics of antigen binding and cell binding data suggest that trastuzumab IgE possesses HER2/*neu* binding properties that are similar to those observed and measured for trastuzumab (Table 1; Figs. 2, 3, 4). Similar to other well-characterised IgE antibodies (MOv18 IgE and NIP IgE), trastuzumab IgE bound to its high-affinity receptor FcεRI as expected (Table 1; Figs. 2, 4). Furthermore, using functional assays, this study demonstrates the biological activity of trastuzumab IgE antibody in directing effector cells to target tumour cells in a tumour antigen-specific manner (Figs. 4, 5).

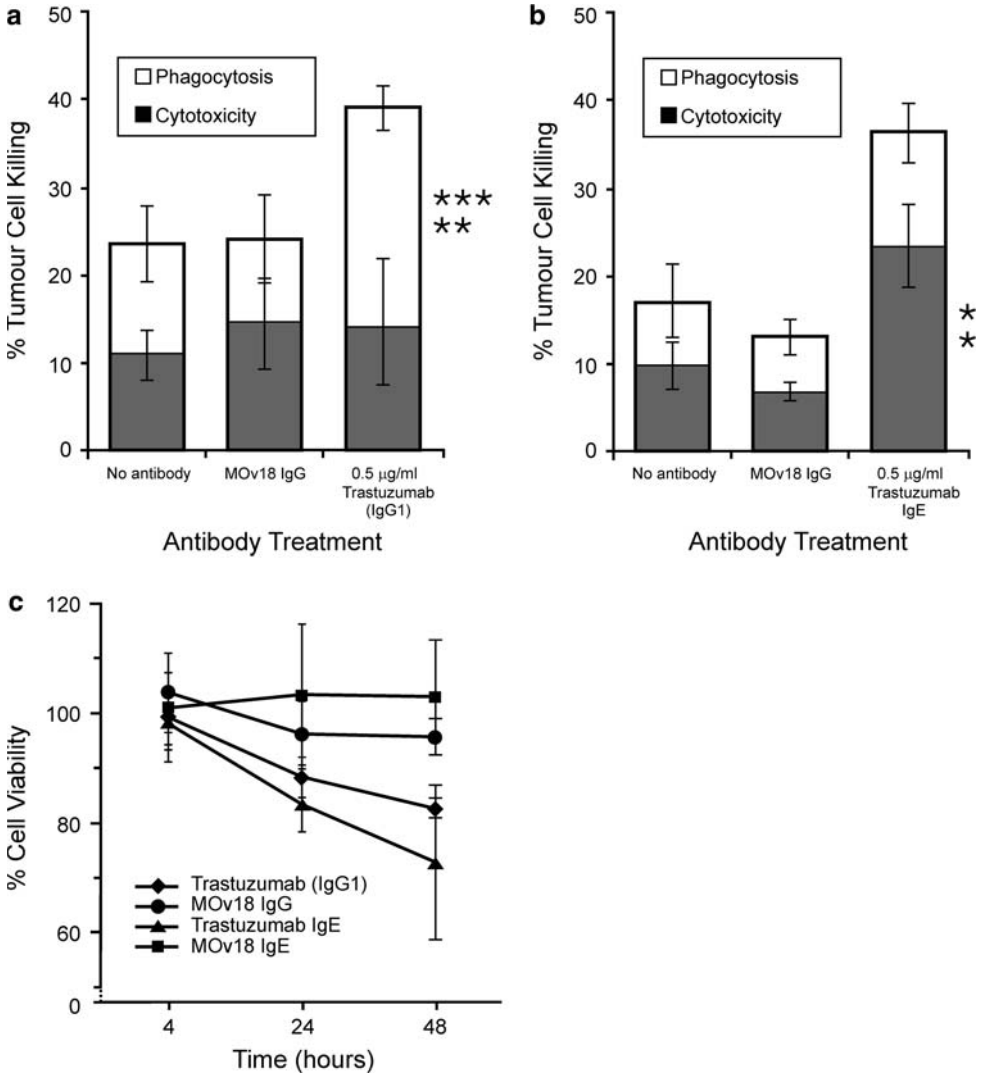

Fig. 6 **a** Quantitation of trastuzumab (IgG1)-mediated tumour cell killing of SKBR3 human breast tumour cells by U937 monocytes after 2.5 h using the ADCC/ADCP assay. **b** Quantitation of trastuzumab IgE-mediated tumour cell killing of SKBR3 human breast tumour cells by U937 monocytes after 2.5 h using the ADCC/ADCP assay. Cytotoxicity: *black bars*; phagocytosis: *white bars*. Results are means ± SD of 5 independent experiments. Significance of values compared to samples given MOv18 IgG/IgE (*top*) or no antibody (*bottom*) by the Student's *t* test: $^{n/s}P > 0.05$, $^{*}P < 0.05$, $^{**}P < 0.005$, $^{***}P < 0.0005$. **c** Cell viability assays (MTS) demonstrating levels of susceptibility of SKBR3 breast cancer cells to trastuzumab (IgG1), trastuzumab IgE, MOv18 IgG and MOv18 IgE antibodies at 4, 24 and 48 h in culture. Each data point represents mean % cell viability ± SD ($n = 4$)

Using our ADCC/ADCP assays and microscopic images, we made a number of observations relating to the effector functions of trastuzumab (IgG1) and trastuzumab IgE. Trastuzumab triggered appreciable levels of monocyte-mediated tumour cell phagocytosis by human monocytic cells (Figs. 3b, c, 6a), also clearly observed in confocal images by the presence of tumour cell material ingested by monocytic cells in contact with tumour cells (Fig. 3d; Table 3). Whilst the signalling and tumour growth arrest activities of trastuzumab and their role in its clinical efficacy have been the subject of many studies, the anti-tumour mechanisms relating to effector cell functions of trastuzumab have been less extensively investigated [7, 8, 10–14]. ADCC is a known anti-tumour mechanism of trastuzumab [11, 13, 14]. ADCP is not a widely described function attributed to trastuzumab, but our data are consistent with ADCP as a potential anti-tumour mechanism for trastuzumab with human macrophages, as reported by Lazar et al. [12].

Surprisingly, no trastuzumab-dependent monocyte-mediated cytotoxicity (ADCC) of tumour cells was detected above that seen in the controls in our ADCC/ADCP assays. Using our ADCC/ADCP assay to simultaneously measure the contributions of ADCC and ADCP [30, 31, 49], we detected only ADCP killing of tumour cells by trastuzumab. There are several possible explanations for the discrepancy between the present results and earlier reports. (1) Previous assays on the effector cell functions of trastuzumab, in combination with either unfractionated or purified human effector cell populations, did not assess the contributions of ADCP in the death of tumour cells [11–14]. It is therefore possible that ADCP-mediated tumour cell death may have been scored as ADCC if the assays measured total loss of tumour cells; (2) U937 monocytes express FcγRI and FcγRII, but very low levels of FcγRIII (Table 2), and thus it is possible that the absence of appreciable levels of FcγRIII may result in low levels of ADCC [18]; (3) The previously reported tumour cell trastuzumab ADCC

may have been mediated by other IgG receptor-bearing effector cells in peripheral blood lymphocytes, such as NK cells and neutrophils, as previously shown [11–14].

When compared to the FBP-specific MOv18 IgE antibody in the same assay, trastuzumab IgE activated monocytic effector cells to exhibit significantly enhanced contact with tumour cells and to effectively kill HER2/*neu*-expressing tumour cells (Fig. 4d; Table 3). Trastuzumab IgE directed monocytes to kill HER2/*neu*-transfected tumour cells and also tumour cells naturally-expressing the HER2/*neu* antigen by ADCC (cytotoxicity), a mechanism clearly different from that of the anti-tumour mechanism employed by trastuzumab in the same assay system (Figs. 3, 4, 6). This may reflect the specific binding of trastuzumab IgE to the high-affinity receptor FcεRI. Evidence presented in our previous studies on the mechanism of MOv18 IgE monocyte-mediated tumour cell killing, suggested that binding of IgE to its high-affinity receptor FcεRI on monocytes triggered tumour cell death by a cytotoxic mechanism, whilst binding to the low-affinity receptor CD23 resulted in tumour cell death by ADCP. U937 monocytes express low levels of CD23 (~2,200 molecules/cell, Table 2) and, as observed in our studies with MOv18 IgE, these receptor levels are too low to mediate ADCP of tumour cells [30]. The function of trastuzumab IgE effected through CD23 remains to be explored and may reveal additional tumour cell killing properties of the trastuzumab IgE.

Our assays clearly indicated that the levels of tumour cell killing mediated by trastuzumab IgE were equivalent to those by trastuzumab (IgG) at the same optimal doses and in the same assay system (Figs. 3, 4, Table 4). This was true despite the relatively low levels of IgE binding on the surface of U937 cells, compared to IgG (Figs. 3a, 4a), in agreement with previous findings [30] suggesting the potency of IgE-mediated effector functions [20–23, 27, 28, 35, 56]. IgE has much higher affinity for FcεRI ($Ka = 10^{10}\ M^{-1}$) than IgG1 has for any of its three Fcγ receptors, especially for FcγRIII ($Ka = 10^{5}\ M^{-1}$), the main receptor associated with tumour cell killing [17, 18, 57]. The relatively high affinities of the IgE-FcεRI interaction may compensate for the lower binding of IgE on U937 monocytes, resulting in comparable levels of tumour cell killing. These data clearly indicate the biological function of trastuzumab IgE in focusing monocytic cells to kill HER2/*neu*-expressing tumour cells as effectively as, but through a mechanism different from, trastuzumab.

The antibody concentration (0.5 μg/mL) required to achieve maximum tumour cell killing by ADCC/ADCP was the same for IgG and IgE in our in vitro assays (Figs. 3, 4). In addition, our cell viability data clearly show that trastuzumab IgE, at concentrations found optimal for effector cell responses (0.5 μg/mL), maintains the ability to mediate tumour cell growth arrest over a period of 48 h in culture and at levels similar to those measured for trastuzumab (Fig. 6c). The concentration found optimal for the in vitro effector cell functions of trastuzumab IgE was tenfold lower than our previously reported optimal concentrations required for MOv18 IgG and IgE-mediated (5 μg/mL) killing of ovarian tumour cells in equivalent in vitro assays [30–32]. This may suggest that lower levels of trastuzumab IgE may be required for in vivo activities compared to those used for MOv18 IgG and MOv18 IgE studies. The IgE responses measured and observed in our assays support the conclusion that trastuzumab IgE functions with similar potency, but through mechanisms different from those of trastuzumab in vitro, warranting further exploration of this engineered antibody in more clinically relevant models. It is possible, however, that trastuzumab IgE may be more effective than trastuzumab (IgG1) in vivo for the reasons cited in the Introduction or that a combination of trastuzumab and trastuzumab IgE could have potential synergistic anti-tumour effects.

We also assessed the potential of the engineered trastuzumab IgE to activate other potent IgE receptor-bearing effector cells. For this, we have utilised a functional assay that exemplifies the unique properties of IgE to generate and enhance immune effector functions that can be targeted against cancer cells. Trastuzumab IgE bound to the human FcεRI $\alpha\beta\gamma 2$ receptor on the surface of mast cells can be cross-linked by HER2/*neu*-expressing tumour cells to trigger mast cell degranulation in an antigen-specific manner (Fig. 5). Tissue mast cell degranulation is a known biological property of the IgE antibody class. Mediators released by degranulated mast cells initiate and potentiate effector cell recruitment to the site of tumour antigen challenge, which can be expected to lead to activation and stimulation of recruited and locally present effector cells to act in the ADCC and ADCP of tumour cells. Mast cell activation by IgE may thus serve as a potential trigger of a strong, local, tumour antigen-specific IgE immune response against cancer.

This is the first study describing the properties of an engineered trastuzumab IgE. Based on the considerable evidence pointing to a number of advantages that IgE may have in tumour cell surveillance and killing, compared to IgG, our work points to the importance and value of further research to investigate the efficacy and mechanisms of action of tumour antigen-specific antibodies of different classes, in particular IgE and may help to realise the full potential of antibodies for immunotherapy of cancer.

Acknowledgments This work was generously supported by the the National Institute for Health Research (NIHR) Biomedical Research Centre (BRC) at Guy's and St. Thomas' NHS Foundation Trust/King's College London, United Kingdom; the Austrian Science Fund (FWF) (P-18238-B13); the European Molecular Biology Organisation (EMBO) (fellowship ASTF258.00-2008); Hans und

Blanca Moser Stiftung (AP00326OFF), Austria; NIH/NCI R01 supplement CA107023-02S1, Susan G. Komen Breast Cancer Foundation grant (BCTR0706771) and the 2007–2008 University of California Cancer Research Coordinating Committee seed grant, USA. We thank Dr. Rebecca Beavil, Dr. Pooja Takhar and Mr. Richard Brunner for their helpful comments and Ms. Kate Kirwan for expert assistance with the figures. We are grateful to Dr. Jean-Pierre Kinet and to Dr. Silvana Canevari for the generous provision of advice and materials.

References

1. Rubin I, Yarden Y (2001) The basic biology of HER2. Ann Oncol 12(Suppl 1):S3–S8
2. Kaptain S, Tan LK, Chen B (2001) Her-2/neu and breast cancer. Diagn Mol Pathol 10:139–152
3. Yarden Y (2001) Biology of HER2 and its importance in breast cancer. Oncology 61(Suppl 2):1–13
4. Landgraf R (2007) HER2 therapy. HER2 (ERBB2): functional diversity from structurally conserved building blocks. Breast Cancer Res 9:202
5. Hortobagyi GN (2005) Trastuzumab in the treatment of breast cancer. N Engl J Med 353:1734–1736
6. Carter P, Presta L, Gorman CM, Ridgway JB, Henner D, Wong WL, Rowland AM, Kotts C, Carver ME, Shepard HM (1992) Humanization of an anti-p185HER2 antibody for human cancer therapy. Proc Natl Acad Sci USA 89:4285–4289
7. Gonzalez-Angulo AM, Morales-Vasquez F, Hortobagyi GN (2007) Overview of resistance to systemic therapy in patients with breast cancer. Adv Exp Med Biol 608:1–22
8. Hudis CA (2007) Trastuzumab—mechanism of action and use in clinical practice. N Engl J Med 357:39–51
9. Lee-Hoeflich ST, Crocker L, Yao E, Pham T, Munroe X, Hoeflich KP, Sliwkowski MX, Stern HM (2008) A central role for HER3 in HER2-amplified breast cancer: implications for targeted therapy. Cancer Res 68:5878–5887
10. Izumi Y, Xu L, di Tomaso E, Fukumura D, Jain RK (2002) Tumour biology: herceptin acts as an anti-angiogenic cocktail. Nature 416:279–280
11. Barok M, Isola J, Palyi-Krekk Z, Nagy P, Juhasz I, Vereb G, Kauraniemi P, Kapanen A, Tanner M, Szollosi J (2007) Trastuzumab causes antibody-dependent cellular cytotoxicity-mediated growth inhibition of submacroscopic JIMT—1 breast cancer xenografts despite intrinsic drug resistance. Mol Cancer Ther 6:2065–2072
12. Lazar GA, Dang W, Karki S, Vafa O, Peng JS, Hyun L, Chan C, Chung HS, Eivazi A, Yoder SC et al (2006) Engineered antibody Fc variants with enhanced effector function. Proc Natl Acad Sci U S A 103:4005–4010
13. Gennari R, Menard S, Fagnoni F, Ponchio L, Scelsi M, Tagliabue E, Castiglioni F, Villani L, Magalotti C, Gibelli N et al (2004) Pilot study of the mechanism of action of preoperative trastuzumab in patients with primary operable breast tumors overexpressing HER2. Clin Cancer Res 10:5650–5655
14. Sliwkowski MX, Lofgren JA, Lewis GD, Hotaling TE, Fendly BM, Fox JA (1999) Nonclinical studies addressing the mechanism of action of trastuzumab (Herceptin). Semin Oncol 26:60–70
15. Riethmuller G, Johnson JP (1992) Monoclonal antibodies in the detection and therapy of micrometastatic epithelial cancers. Curr Opin Immunol 4:647–655
16. Gould HJ, Takhar P, Harries HE, Durham SR, Corrigan CJ (2006) Germinal-centre reactions in allergic inflammation. Trends Immunol 27:446–452
17. Gould HJ, Sutton BJ, Beavil AJ, Beavil RL, McCloskey N, Coker HA, Fear D, Smurthwaite L (2003) The biology of IGE and the basis of allergic disease. Annu Rev Immunol 21:579–628
18. Clynes RA, Towers TL, Presta LG, Ravetch JV (2000) Inhibitory Fc receptors modulate in vivo cytoxicity against tumor targets. Nat Med 6:443–446
19. Geha RS, Helm B, Gould H (1985) Inhibition of the Prausnitz-Kustner reaction by an immunoglobulin epsilon-chain fragment synthesised in E. coli. Nature 315:577–578
20. Gonzalez-Espinosa C, Odom S, Olivera A, Hobson JP, Martinez ME, Oliveira-Dos-Santos A, Barra L, Spiegel S, Penninger JM, Rivera J (2003) Preferential signalling and induction of allergy-promoting lymphokines upon weak stimulation of the high affinity IgE receptor on mast cells. J Exp Med 197:1453–1465
21. Riemer AB, Untersmayr E, Knittelfelder R, Duschl A, Pehamberger H, Zielinski CC, Scheiner O, Jensen-Jarolim E (2007) Active induction of tumor-specific IgE antibodies by oral mimotope vaccination. Cancer Res 67:3406–3411
22. Jensen-Jarolim E, Achatz G, Turner MC, Karagiannis S, Legrand F, Capron M, Penichet ML, Rodriguez JA, Siccardi AG, Vangelista L et al (2008) AllergoOncology: the role of IgE-mediated allergy in cancer. Allergy 63:1255–1266
23. Reali E, Greiner JW, Corti A, Gould HJ, Bottazzoli F, Paganelli G, Schlom J, Siccardi AG (2001) IgEs targeted on tumor cells: therapeutic activity and potential in the design of tumor vaccines. Cancer Res 61:5517–5522
24. Turner MC, Chen Y, Krewski D, Ghadirian P (2006) An overview of the association between allergy and cancer. Int J Cancer 118:3124–3132
25. Turner MC, Chen Y, Krewski D, Ghadirian P, Thun MJ, Calle EE (2005) Cancer mortality among US men and women with asthma and hay fever. Am J Epidemiol 162:212–221
26. Nagy E, Berczi I, Sehon AH (1991) Growth inhibition of murine mammary carcinoma by monoclonal IgE antibodies specific for the mammary tumor virus. Cancer Immunol Immunother 34:63–69
27. Kershaw MH, Darcy PK, Trapani JA, MacGregor D, Smyth MJ (1998) Tumor-specific IgE-mediated inhibition of human colourectal carcinoma xenograft growth. Oncol Res 10:133–142
28. Riemer AB, Klinger M, Wagner S, Bernhaus A, Mazzucchelli L, Pehamberger H, Scheiner O, Zielinski CC, Jensen-Jarolim E (2004) Generation of peptide mimics of the epitope recognized by trastuzumab on the oncogenic protein Her-2/neu. J Immunol 173:394–401
29. Gould HJ, Mackay GA, Karagiannis SN, O'Toole CM, Marsh PJ, Daniel BE, Coney LR, Zurawski VR Jr, Joseph M, Capron M et al (1999) Comparison of IgE and IgG antibody-dependent cytotoxicity in vitro and in a SCID mouse xenograft model of ovarian carcinoma. Eur J Immunol 29:3527–3537
30. Karagiannis SN, Bracher MG, Beavil RL, Beavil AJ, Hunt J, McCloskey N, Thompson RG, East N, Burke F, Sutton BJ et al (2008) Role of IgE receptors in IgE antibody-dependent cytotoxicity and phagocytosis of ovarian tumor cells by human monocytic cells. Cancer Immunol Immunother 57:247–263
31. Karagiannis SN, Bracher MG, Hunt J, McCloskey N, Beavil RL, Beavil AJ, Fear DJ, Thompson RG, East N, Burke F et al (2007) IgE-antibody-dependent immunotherapy of solid tumors: cytotoxic and phagocytic mechanisms of eradication of ovarian cancer cells. J Immunol 179:2832–2843
32. Karagiannis SN, Wang Q, East N, Burke F, Riffard S, Bracher MG, Thompson RG, Durham SR, Schwartz LB, Balkwill FR et al (2003) Activity of human monocytes in IgE antibody-dependent surveillance and killing of ovarian tumor cells. Eur J Immunol 33:1030–1040
33. Luiten RM, Fleuren GJ, Warnaar SO, Litvinov SV (1996) Target-specific activation of mast cells by immunoglobulin E reactive

with a renal cell carcinoma-associated antigen. Lab Invest 74:467–475
34. Luiten RM, Warnaar SO, Schuurman J, Pasmans SG, Latour S, Daeron M, Fleuren GJ, Litvinov SV (1997) Chimeric immunoglobulin E reactive with tumor-associated antigen activates human Fc epsilon RI bearing cells. Hum Antibodies 8:169–180
35. Teng MW, Kershaw MH, Jackson JT, Smyth MJ, Darcy PK (2006) Adoptive transfer of chimeric FcepsilonRI gene-modified human T cells for cancer immunotherapy. Hum Gene Ther 17:1134–1143
36. Cook JP, Henry AJ, McDonnell JM, Owens RJ, Sutton BJ, Gould HJ (1997) Identification of contact residues in the IgE binding site of human FcepsilonRIalpha. Biochemistry 36:15579–15588
37. Neuberger MS, Williams GT, Mitchell EB, Jouhal SS, Flanagan JG, Rabbitts TH (1985) A hapten-specific chimaeric IgE antibody with human physiological effector function. Nature 314:268–270
38. Dela Cruz JS, Lau SY, Ramirez EM, De Giovanni C, Forni G, Morrison SL, Penichet ML (2003) Protein vaccination with the HER2/neu extracellular domain plus anti-HER2/neu antibody-cytokine fusion proteins induces a protective anti-HER2/neu immune response in mice. Vaccine 21:1317–1326
39. Cho HS, Mason K, Ramyar KX, Stanley AM, Gabelli SB, Denney DW Jr, Leahy DJ (2003) Structure of the extracellular region of HER2 alone and in complex with the Herceptin Fab. Nature 421:756–760
40. Durocher Y, Perret S, Kamen A (2002) High-level and high-throughput recombinant protein production by transient transfection of suspension-growing human 293-EBNA1 cells. Nucleic Acids Res 30:E9
41. Gan SK, Hunt J, Beavil AJ, Marsh PJ, Harries HE (2008) The design and optimisation of a transient expression system for the rapid expression of human immunoglobulin E. Example cited in GB patent application 61/060,239
42. McDonnell JM, Calvert R, Beavil RL, Beavil AJ, Henry AJ, Sutton BJ, Gould HJ, Cowburn D (2001) The structure of the IgE Cepsilon2 domain and its role in stabilizing the complex with its high-affinity receptor FcepsilonRIalpha. Nat Struct Biol 8:437–441
43. Henry AJ, Cook JP, McDonnell JM, Mackay GA, Shi J, Sutton BJ, Gould HJ (1997) Participation of the N-terminal region of Cepsilon3 in the binding of human IgE to its high-affinity receptor FcepsilonRI. Biochemistry 36:15568–15578
44. Sundstrom C, Nilsson K (1976) Establishment and characterization of a human histiocytic lymphoma cell line (U-937). Int J Cancer 17:565–577
45. Corbett TH, Griswold DP Jr, Roberts BJ, Peckham JC, Schabel FM Jr (1975) Tumor induction relationships in development of transplantable cancers of the colon in mice for chemotherapy assays, with a note on carcinogen structure. Cancer Res 35:2434–2439
46. Griswold DP, Corbett TH (1975) A colon tumor model for anticancer agent evaluation. Cancer 36:2441–2444
47. Penichet ML, Challita PM, Shin SU, Sampogna SL, Rosenblatt JD, Morrison SL (1999) In vivo properties of three human HER2/neu-expressing murine cell lines in immunocompetent mice. Lab Anim Sci 49:179–188
48. Wiegand TW, Williams PB, Dreskin SC, Jouvin MH, Kinet JP, Tasset D (1996) High-affinity oligonucleotide ligands to human IgE inhibit binding to Fc epsilon receptor I. J Immunol 157:221–230
49. Bracher M, Gould HJ, Sutton BJ, Dombrowicz D, Karagiannis SN (2007) Three-colour flow cytometric method to measure antibody-dependent tumour cell killing by cytotoxicity and phagocytosis. J Immunol Methods 323:160–171
50. Bodinier M, Brossard C, Triballeau S, Morisset M, Guerin-Marchand C, Pineau F, de Coppet P, Moneret-Vautrin DA, Blank U, Denery-Papini S (2008) Evaluation of an in vitro mast cell degranulation test in the context of food allergy to wheat. Int Arch Allergy Immunol 146:307–320
51. Linko-Lopponen S, Makinen M (1985) A microtiter plate assay for N-acetyl-beta-D-glucosaminidase using a fluorogenic substrate. Anal Biochem 148:50–53
52. Casal JA, Chabas A, Tutor JC (2003) Thermodynamic determination of beta-hexosaminidase isoenzymes in mononuclear and polymorphonuclear leukocyte populations. Am J Med Genet A 116A:229–233
53. Gerstner RB, Carter P, Lowman HB (2002) Sequence plasticity in the antigen-binding site of a therapeutic anti-HER2 antibody. J Mol Biol 321:851–862
54. Posner RG, Geng D, Haymore S, Bogert J, Pecht I, Licht A, Savage PB (2007) Trivalent antigens for degranulation of mast cells. Org Lett 9:3551–3554
55. Riemer AB, Jensen-Jarolim E (2007) Mimotope vaccines: epitope mimics induce anti-cancer antibodies. Immunol Lett 113:1–5
56. Bramswig KH, Knittelfelder R, Gruber S, Untersmayr E, Riemer AB, Szalai K, Horvat R, Kammerer R, Zimmermann W, Zielinski CC et al (2007) Immunization with mimotopes prevents growth of carcinoembryonic antigen positive tumors in BALB/c mice. Clin Cancer Res 13:6501–6508
57. Ravetch JV, Kinet JP (1991) Fc receptors. Annu Rev Immunol 9:457–492

Primers	Sequence	Comany
Cg2	AGGTCTAGAGACSGATGGGCCCTTGGTGGA	eurofins mwg operon
VH2F	GTCTTGTCCCAGGTCAACTTAAGGGAGTCTT	eurofins mwg operon
VH4F	CAGGTGCAGCTGCAGGAGTCGG	eurofins mwg operon
VH5F	GAGGTGCAGCTGCTGCAGTCTG	eurofins mwg operon
VH6F	CTGTCACAGGTACAGCTGCAGCAGTCAG	eurofins mwg operon
VH1L	CCATGGACTGGACCTGGA	eurofins mwg operon
VH2L	CAGATGGACATACTTTGTTCCAC	eurofins mwg operon
VH3L	CCATGGAGTTTGGGCTGAGC	eurofins mwg operon
VH4L	CGATGAAACACCTGTGGTTCTT	eurofins mwg operon
VH5L	ATGGGGTCAACCGCCATCCT	eurofins mwg operon
VH6L	GATGTCTGTCTCCTTCCTCAT	eurofins mwg operon
Cg1	GCCAGGGGGAAGACSCATG	eurofins mwg operon
VH1F	CAGGTGCAGCTGGTGCAGTCTG	eurofins mwg operon
VH3F	GAGGTGCAGCTGGTGGAGTCTG	eurofins mwg operon
L-Vk1/2	ATGAGGGTCCCCGCTCAGCTGCTGG	eurofins mwg operon
L-Vk3	CTCTTCCTCCTGCTACTCTGGCTCCCAG	eurofins mwg operon
L-Vk4	ATTTCTCTGTTGCTCTGGATCTCTG	eurofins mwg operon
Ck 543-566	GTTTCTCGTAGTCTGCTTTGCTCA	eurofins mwg operon
Pan-Vk	ATGACCCAGACTCCATCCACCCTG	eurofins mwg operon
Ck 494-516	GTGCTGTCCTTGCTGTCCTGCT	eurofins mwg operon
L-lambda 1 for	GGTCCTGGGCCCAGTCTGTGCTG	eurofins mwg operon
L-lambda 2 for	GGTCCTGGGCCCAGTCTGCCCTG	eurofins mwg operon
L-lambda 3 for	GCTCTGTGACCTCCTATGAGCTG	eurofins mwg operon
L-lambda 4/5 for	GGTCTCTCTCGCAGCCTGTGCTG	eurofins mwg operon
L-lambda 6 for	GTTCTTGGGCCAATTTTATGCTG	eurofins mwg operon
L-lambda 7 for	GGTCCAATTCCCAGGCTGTGGTG	eurofins mwg operon
L-lambda 8 for	GAGTGGATTCTCAGACTGTGGTG	eurofins mwg operon
C lambda rev	CACCAGTGTGGCCTTGTTGGCTTG	eurofins mwg operon
F-lambda1	CAGTCTGTGTTGACGCAGCC	eurofins mwg operon
F-lambda2	CAGTCTGCCCTGACTCAGCC	eurofins mwg operon
F-lambda3	TCTTATGAGCTGACACAGCCAC	eurofins mwg operon
F-lambda3l	TCTTCTGAGCTGACTCAGGACCC	eurofins mwg operon
F-lambda4ab	CAGCTTGTGCTGACTCAATC	eurofins mwg operon
F-lambda4c	CTGCCTGTGCTGACTCAGC	eurofins mwg operon
F-lambda5/9	CAGCCTGTGCTGACTCAGC	eurofins mwg operon
F-lambda6	AATTTTATGCTGACTCAGCCCCACT	eurofins mwg operon
F-lambda7/8	CAGACTGTGGTGACCCAGGAG	eurofins mwg operon
F-lambda10	CAGGCAGGGCTGACTCAG	eurofins mwg operon
C lambda-2	GGGTGGGAACAGAGTGACC	eurofins mwg operon
J segment F	ACCCTGGTCACCGTCTCCTCA	Applied Biosytems
Mature IgG R	TTCTGGAAGTAGTCCTTGACCA	Applied Biosytems
Mature IgE R	TGCAGCAGCGGGTCAAG	Applied Biosytems

Sample ID	RNA yield	260/280 Ratio
LNM1	407.2	2.04
LN1	257	2.11
LN2	619.9	2.08
LN3	306.3	2.03
LN4	452.9	2.1
LN5	1953.2	1.97
LNM2	1344.9	1.99
LNM3	1275.6	2
LNM4	1242.4	1.99
LNM5	857.5	2
LNM6	1578.3	1.97
LN6	439.8	2.07
LN7	169.4	2.1
LN8	349.7	<1.8
LN9	1095.3	<1.8
LN10	126.5	<1.8
LN11	451.2	<1.8
LNM7	76.7	2.13
LNM8	231	2.07
LNM9	225	2.08
LNM10	80.8	2.09
LNM11	567.2	2.01
LN12	96.5	2.05
LNM12	702.3	2.07
LNM13	609.5	2.07
LN13	1643	1.99
LN14	558.3	2.07
LN15	405.2	2.05
LN16	246.5	2.07
LNM14	319.3	2.06
LN17	186.3	2.06
LNM15	326.1	2.05
LN18	329.6	1.95
LNM16	439.1	1.93
LN19	231.5	2.05
LN20	1539.7	1.91
LN21	131.7	2.06
LNM17	354.7	2.07
M128	255	2.05
M129	137.4	2.06
M171	132.2	2.08
M72	594.2	2.09
M147	63.3	2.02
M173	412.6	2.07
WM115	104	2.08
M78	90.6	2.04
M80	148.2	2.05

Sample ID	RNA yield	260/280 Ratio
LRTAN1	1075.9	2.07
LRTAN2	1069.5	2.06
N63	454.54	2
N73	461.7	2.02
N101	330.3	2.06
N131	447.78	2.2
N144	346.3	1.99
N148	429.5	2.03
M269	458.89	2.08
M254	362.35	2.01
M245	502.42	2.01
M221	189.72	1.89
M215	213.34	1.96
M81	21.8	1.92
M91	1	1.57
M92	290.5	2.06
M103	330.6	2.03

Taqman Probes	**Sequence**	**Catalogue No.**
Mature IgG	6-FAM-CTCAGCCAGGACCAAG-MGB	(Custom-made)
Mature IgE	FAM-TCACAGCTCCACACAGAG-MGB	(Custom-made)
β2-Microglobulin	VIC----MGB	Hs00984230_m1
CD22	FAM----MGB	HS0023533_m1
GAPDH	VIC----MGB	HS4310884_m1
VEGF	FAM----MGB	HS00174379_m1
IFN-γ	FAM----MGB	HS00174379_m1
IL-4	FAM----MGB	HS00174379_m1
Il-10	FAM----MGB	HS00174379_m1